University of KwaZulu-Natal

Designed, Synthesis, and antibacterial evolution of Piperazine Hybrids

By

Pankaj Sanjay Girase

219075062

2023

Designed, Synthesis, and antibacterial evolution of Piperazine Hybrids

A Thesis

Submitted in fulfilment for the requirements

for the award of the degree of

Doctor of Philosophy

in the

Department of Pharmaceutical Chemistry

Discipline of Pharmaceutical Science

College of Health Science,

By

Pankaj Sanjay Girase

2023

Supervisor: Prof. Rajshekhar Karpoormath

Designed, Synthesis, and antibacterial evolution of Piperazine Hybrids

by

Pankaj Sanjay Girase

219075062

2023

A thesis submitted to the School of Health Science, Discipline of Pharmaceutical science, Department of Pharmaceutical Chemistry, University of KwaZulu-Natal, Westville, for the degree of Doctor of Philosophy.

This thesis has been prepared according to **Format 4** (Thesis by publications) as outlined in the guidelines of College of Health Sciences, University of KwaZulu-Natal. The chapters consist of an overall introduction, chapters in discrete research papers and a final discussion. Two chapters have been published and the remaining chapters revision have been submitted in peer-reviewed internationally accepted journals.

As the candidate's supervisor, I have approved this thesis for examination/submission.

Supervisor: Prof Rajshekhar Karpoormath

Signed: ……

Date: 29-05-2023

// Shree Ganeshaya Namah: //

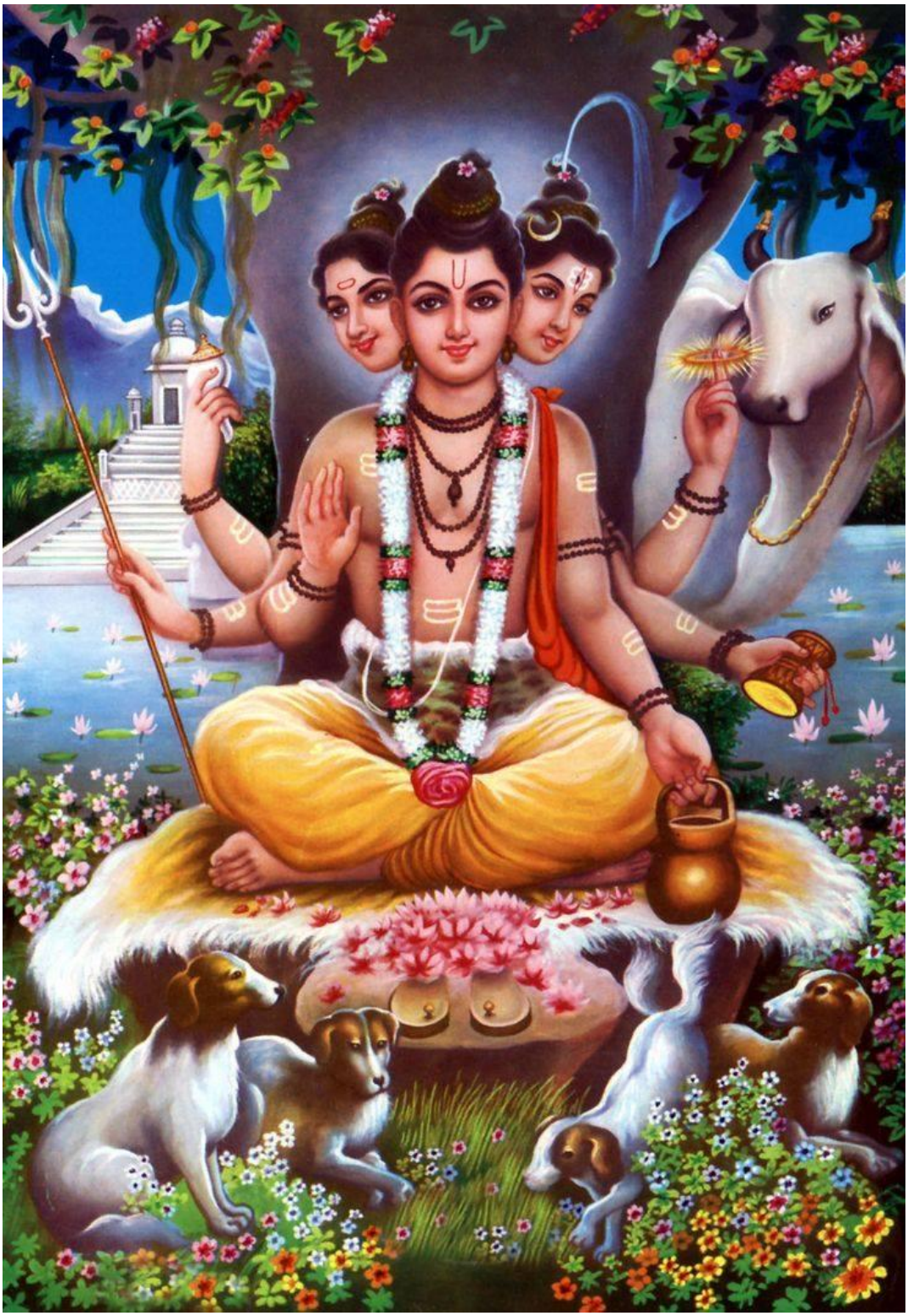

//हरिॐतत्सत्जयगुरुदत्त//

Preface

I hereby declare that the thesis entitled "**Designed, Synthesis, and antibacterial evolution of Piperazine Hybrids**" submitted to the University of KwaZulu-Natal for the award of the degree of Doctor of Philosophy in Pharmaceutical Chemistry under the supervision of Prof. R. Karpoormath represents original work by the author and has not been submitted in full or part for any degree or diploma at this or any other University.

Where use was made of the work of others it has been duly acknowledged in the text. This work was carried out in the School of Health Science, Discipline of Pharmaceutical science, Department of Pharmaceutical Chemistry, University of KwaZulu-Natal, Westville Campus, Durban, South Africa.

Signed: 

Date: 29-05-2023

Pankaj Sanjay Girase

As the candidate's supervisors, we have approved this dissertation for submission.

Signed:

Dated: 29-05-2023

Prof. Rajshekhar Karpoormath

(**Supervisor**)

Abstract

Piperazine is a kind of azacycloalkane that has two nitrogen atoms at1-4 places on a six-membered ring. It is well known that molecules with the piperazine ring, a key component of the N-heterocyclicfamily of bioactive natural products, are often prevalent in biologically active substances. There are many antitumor, antibacterial, antiinflammatory, antipsychotic, antifungal, and anti-diabetic compounds based on the piperazine scaffold, which has been recognized as an active structure in drug discovery. Piperazine hybrids with different moieties such as isoniazid, coumarin, benzothiazinones, isoquinoline, triazole,pyrrole, and oxazolidinone showed good activity against mycobacterium tuberculosis and microbial strains. In this thesis we have demonstrated the synthesis of piperazine hybrid with hydrazides, hydrazines, and coumarines and tested their activity against mycobacterium tuberculosis, gram positive and gram negative microbial strains.

In Chapter 2, we have covered topics related to the analogues of piperazine that have anti-tubercular efficacy. This chapter we have published as a review article in **European Journal of Medicinal Chemistry**. In this review, we have made a concerted effort to trace the development of anti-mycobacterial compounds during the past 50 years (1971-2019), focusing on instances where piperazine has been utilized as a key building block. In depth discussion of the design, rationale, and structure-activity relationship (SAR) of the reported potent piperazine-based anti-TB molecules will help medicinal chemists fill in the blanks, capitalize on the reported strategies, and create more effective, selective, and less hazardous anti-mycobacterial drugs.

In **chapter 3**, we have developed and synthesized a new class of hybrids between phenylpiperazine and hydrazides (c1-c15). During the synthesis of phenyl piperazines, the formylation of piperazine was observed, a phenomenon on which we have developed a different methodology discussed in **chapter 5.** All of the derivatives have been tested in vitro against $H_{37}Rv$, a strain of mycobacterium. In addition, we have analysed the zone of inhibition against eight different bacterial strains, including both gram-positive (methicillin resistant staphylococcus aureus (MRSA), Streptococcus pyrogens, Bacillus subtilis, Enterococcus faecium, and Staphylococcus aureus), and gram-negative

(Enterobacter hormaechei, Pseudomonas aeruginosa, and Escherichia coli) bacteria. Among the derivatives tested, only compound c8 showed action against the mycobacterium strain *$H_{37}Rv$* (MIC value of 0.39-0.78 g/ml). No zone of inhibition was seen for any of the microbiological strains when exposed to any of the synthesized compounds.

The hybrids between phenylpiperazine sulphonamide and phenyl hydrazide (E1-E6) and phenylpiperazine sulphonamide and phenyl hydrazine (F7-F19) were proposed and synthesized in **chapter 4**. All substances were evaluated against mycobacterium tuberculosis, five gram-positive and three gram-negative bacterial strains in vitro. Derivatives E1 and E2 with an isoniazid moiety were the most effective in inhibiting the growth of the *$H_{37}Rv$* strain of tuberculosis, with an IC50 value of 3.125 M. Of the derivatives tested, F10 showed significant action against the gram-positive bacteria Enterococcus faecium (7.81 μg/mL), whereas the others (E2, E6, F7, F9, F14) were only moderately active (250-62.5 μg/mL).

Using a the molecular hybridization strategy, we were enabled to create novel analogues of coumarin-(phenylsulfonyl)piperazine and 4-methyl coumarin-(phenylsulfonyl)piperazine in **chapter 5**.All synthesised compounds were evaluated for their in vitro anti-mycobacterial and antimicrobial activity against *$H_{37}Rv$*and a variety of antimicrobial gram-positive and gram-negative strains.The Compounds 6G, 6H, 10D and 10E displayed moderate inhibition against gram positive and gram negative strains with MIC values in the range of 62.5-250 (table 1) against MRSA, Bacillus subtilis, and Enterococcus faecium, and gram negative strains Enterobacter hormaechei, Pseudomonas aeruginosa, and Escherichia coli.In addition, the Structure-Activity Relationship (SAR) analysis showed that phenyl ring substituents could enhance antibacterial activity.

Chapter 6 came from the process of synthesizing phenyl piperazine in **chapter 1**. This chapter disclosed a method for efficient synthesis of transamidation in the presence of Iodine and $NH_2OH.HCl$ which published in **Chemistry Select**. This method is efficient for a broad range of primary, secondary, and tertiary amides, and it enables the formylation, acylation, and benzoylation of a number of different amines. The key benefits of the present technique are that it is easy to follow,

quick, does not need a metal catalyst, uses a starting material that is inexpensive, and has a low effect on the environment when the synthesis process is carried out. All of the chapters in this thesis are written in thesis by publication style, rather than the conventional style.

Declaration 1: plagiarism

I, **Pankaj Sanjay Girase**, declare that

i. The research reported in this dissertation, except where otherwise indicated, is my original work.

ii. This dissertation has not been submitted for any degree or examination at any other university.

iii. This dissertation does not contain other persons' data, pictures, graphs or other information, unless specifically acknowledged as being sourced from other persons**.**

iv. This dissertation does not contain other persons' writing, unless specifically acknowledged as being sourced from other researchers. Where other written sources have been quoted, then:

a. their words have been re-written but the general information attributed to them has been referenced;

b. where their exact words have been used, their writing has been placed inside quotation marks, and referenced.

v. Where I have reproduced a publication of which I am an author, co-author or editor, I have indicated in detail which part of the publication was actually written by myself alone and have fully referenced such publications.

vi. This dissertation does not contain text, graphics or tables copied and pasted from the Internet, unless

specifically acknowledged, and the source being detailed in the dissertation and in the References sections.

Signed: 

Date: 29-05-2023

Declaration 2: publications

DETAILS OF CONTRIBUTION TO PUBLICATIONS that form part and/or include research presented in this thesis (include publications in preparation, submitted, *in the press* and published and give details of the contributions of each author to the experimental work and writing of each publication).

First Author Publications

1.**Pankaj Sanjay Girase**, Sanjeev Dhawan, Vishal Kumar, Suraj Raosaheb Shinde, Mahesh B. Palkar, Rajshekhar Karpoormath.**An appraisal of anti-mycobacterial activity with structure-activity relationship of Piperazine and its analogues: A review**

Contributions: Under the direction of Prof. Rajshekhar Karpoormath, I conducted the literature review and written the article. The other co-authors helped me with improvisation, writing up, and summarising the literature review.

2. **Pankaj Sanjay Girase**, Sanjeev Dhawan, Vishal Kumar, Suraj Raosaheb Shinde,Mahesh B. Palkar, Rajshekhar Karpoormath;**An appraisal of anti-mycobacterial activity with structure-activity relationship of Piperazine and its analogues: A review**. *European Journal of Medicinal Chemistry*. ***2021***, *210, 112967***.**

Contributions: Under the direction of Prof. Rajshekhar Karpoormath, I came up with the idea, completed all the experiments and characterizations, and wrote up the report. The co-authors helped me write up the data, talk about the target compounds, and design them.

Signed: 

Date: 29-05-2022

Other Publications

1. Vishal Kumar, Sanjeev Dhawan, Renu Bala, **Pankaj Sanjay Girase,** Parvesh Singh and Rajshekhar Karpoormath; **Metal-free direct annulation of 2-aminophenols and 2-aminothiophenols with unactivated amides through transamidation: Access to polysubstituted benzoxazole and benzothiazole derivatives**. *Tetrahedron*, 2022.

2. Vishal Kumar, Sanjeev Dhawan, Renu Bala, **Pankaj S. Girase,** Parvesh Singh, Rajshekhar Karpoormath; **Recent Advances in Transamidation of Unactivated Amides**. *Manuscript.*

3.Sanjeev Dhawan, Vishal Kumar,**Pankaj S. Girase**, Sithabile Mokoena, andRajshekhar Karpoormath;**Recent Progress in Iodine-Catalysed C-O/C-N Bond Formation of 1,3-Oxazoles: A Comprehensive Review**. *ChemistrySelect*,***2021***, 6, 754-787.*

4. Sanjeev Dhawan, **Pankaj Sanjay Girase**, **Vishal Kumar**& RajshekharKarpoormath; **HCl-mediated transamidation of unactivated formamides using aromatic amines in aqueous media**. *Synthetic Communications, **2021**, 51(24), 3729-3739.*

5. Suraj R. Shinde, **Pankaj Girase**, Sanjeev Dhawan, Shaukatali N. Inamdar,Vishal Kumar,Chandrakant Pawar, Mahesh B. Palkar, Mahadev Shinde &Rajshekhar Karpoormath; **A systematic appraisal on catalytic synthesis of 1,3-oxazole derivatives: A mechanistic review on metal dependent synthesis**. *Synthetic Communications, **2022**, 52(1), 1-36.*

6. Rajeshwar Reddy Aleti, Srinivasulu Cherukupalli, Sanjeev Dhawan, Vishal Kumar,**Pankaj S Girase**, Sachin Mohite, Rajshekhar Karpoormath; **A Metal-free Approach for in-situ Regioselective Synthesis of Isoxazoles *via* 1,3 Dipolar Cycloaddition Reaction of Nitrile Oxide with Propargyl bromide**. *Chemical papers, **2022**, 76, 3005-3010.*

Signed: [redacted] **Date**: 29-05-2022

Dedicated

This thesis is dedicated To My beloved Wife, Mother, Father, Sister, and Brother

Acknowledgements

I thank God and my family for helping me finish my thesis. I want to honour everyone who helped me finish my thesis. Thank you so much to my PhD supervisor, ***Prof. Rajshekhar Karpoormath****, for making this project a reality. Thanks to his guidance, I was able to accomplish everything I set out to do.*

I would also like to extend my gratitude to my wife, mother, father, brother, and sister for their constant encouragement and understanding while I conducted research and wrote my project. Your prayers have brought me to this point.

Prof. Shubhangi Soman*,* ***Dr. Rina Soni,****and* ***Dr. Sanjeev Dhawan*** *who provided academic support for this research and encouragement to complete my research, have my sincere gratitude. I am extremely appreciative for this.*

I would like to thank ***Dr. Ramandeep Singh*** *and* ***Sithabile Mokoena*** *for conducting biological activity.*

I would also like to thank ***Mr Yogesh Aher****,* ***Dr.Durga Prasad****,* ***Vuyisa Mzozoyana****,* ***Sanket shete****,* ***Tushar Pattebahadur, Ganesh Shinde*** *and****Chetan Girase,*** *for analytical support.*

Especially to all the lab colleagues, ***Vishal Kumar, Suraj Shinde, Narva Deshwar kushwaha****,* ***Ruchika Chauhan****,****BabitaKushwaha, Srinivas Meragu****,* ***Ashish Sharma****, and all* ***SMCRG*** *members whom I've had the pleasure to work with during all these years, for all the good times we've had together.*

I also thankful to ***Sachin MohiteShaik Baji Baba*** *and* ***Srinivas****for their help.*

My humble gratitude to the University of KwaZulu-Natal, South Africa, for granting approval for my research proposal and providing all the necessary facilities to carry it out successfully. My sincere thanks and appreciation for all the supporting staff at Discipline of Pharmaceutical Sciences College of Health Sciences.

My special thanks go to the Indian community at the University of KwaZulu-Natal. I am also indebted to all my friends for their invaluable support, day in and day out, during all these years.

I extend my gratitude to my previous teachers, lecturers and professors who shaped me to reach this position

Lastly, I would like to thank God for allowing me to overcome all obstacles. I have daily experienced your guidance. You made it possible for me to complete my degree. I will continue to rely on you for my future.

Ethical Clearance Certificate

Mr Pankaj Sanjay Girase (219075062)
School Of Health Sciences
Westville

Dear Mr Pankaj Sanjay Girase,

Original application number: 00021280
Project title: Designed, Synthesis, and antibacterial evolution of Piperazine Hybrids

Exemption from Ethics Review

In response to your application received on , your school has indicated that the protocol has been granted **EXEMPTION FROM ETHICS REVIEW.**

Any alteration/s to the exempted research protocol, e.g., Title of the Project, Location of the Study, Research Approach and Methods must be reviewed and approved through an amendment/modification prior to its implementation. The original exemption number must be cited.

For any changes that could result in potential risk, an ethics application including the proposed amendments must be submitted to the relevant UKZN Research Ethics Committee. The original exemption number must be cited.

In case you have further queries, please quote the above reference number.

PLEASE NOTE:
Research data should be securely stored in the discipline/department for a period of 5 years.

I take this opportunity of wishing you everything of the best with your study.

Yours sincerely,

[redacted]

Prof Khathutshelo Percy Mashige
Academic Leader Research
School Of Health Sciences

List of abbreviations

µg/ml:	Micro gram per millilitre
µM:	Micro molar
13C-NMR:	Carbon (C-13) nuclear magnetic resonance spectroscopy
1H-NMR:	proton (H-1) nuclear magnetic resonance spectroscopy
Ac:	Acetate
Aq:	Aqueous
ATR:	Attenuated total reflection
CDCl3:	Deuterated chloroform
Comp:	Compound
Conc.:	Concentration
d:	doublet
d:	doublet
DCM:	Dichloromethane
dd:	double of doublets
DEPT:	Distortionless enhancement by polarization transfer
DMF:	Dimethylformamide
DMSO-d6:	Deuterated dimethyl sulfoxide
EAA:	Ethyl acetoacetate
EDC:	1-Ethyl-3-(3-dimethylaminopropyl)carbodiimide
EIMS:	Electron impact mass spectroscopy
Equiv:	Equivalent
EtOAc:	Ethyl acetate
EtOH:	ethanol
FTIR:	Fourier transform infrared

H2SO4:	Sulphuric acid
HCl:	hydrochloric acid
HOBt:	1-Hydroxybenzotriazole
Hrs:	Hour
Hz:	hertz
INH:	Isoniazid
LCMS:	Liquid chromatography–mass spectrometry
m:	multiplet
MDR:	Multi-drug resistant
Me:	Methyl
MeOH:	Methanol
MIC:	Minimum inhibitory concentration
Min:	Minute
Mmol:	millimole
MS:	mass spectroscopy
MTB:	Mycobacterium tuberculosis
ND:	Not determined
ppm:	Parts per million
RIF:	Rifampicin
Rpm:	revolution per minute
rt:	Room temperature
s:	singlet
SAR:	Structure activity relation
t:	triplet
TB:	Tuberculosis
td:	triplet of doublets

TEA:	Triethyl amine
TLC:	thin layer chromatography
UV:	ultraviolet
Vol:	volume
WHO:	World Health Organization
XDR:	Extensively drug resistant

Table of Contents

List of Figures

Chapter 1

Chapter 2

Chapter 3

Chapter 4

Chapter 5

Chapter 6

List of Tables

List of Schemes

Chapter 1:

Nil

Chapter 2:

Nil

Chapter 3:

Chapter 4:

Chapter 5:

Chapter 6:

Chapter 7:

Nil

Chapter 1

General Introduction

Mycobacterium species such as *M. tuberculosis, M. caprae, M. canettii, M. bovis, M. pinnipedii, M. africanum,* and *M. microtiv* can cause tuberculosis (TB), which has the potential to become a devastating pandemic. The most prevalent pathogenic strain among them is *Mycobacterium tuberculosis* (MTB), which may affect not just the lungs but also the other part of organ[1]. South Africa has the highest TB infections occurrence rate worldwide, at 834 per 100,000, surpassing even Lesotho. There has been a dramatic increase in the number of deaths caused by tuberculosis and human immunodeficiency virus (HIV) infection throughout Africa. Poor therapeutic medication, medication toxicity, and efflux pumps are the issues harming the present TB treatment regimen. [2, 3].

Due to limitations with existing treatments, poor patient compliance, co-infections, inadequate therapeutic regimen and the emergence of resistant strains such as extensively drug resistant-TB (XDR-TB, strains that are resistant to rifampicin (RIF) and isoniazid (INH), as well as any fluoroquinolone and at least one of three injectable second-line drugs, viz: capreomycin, kanamycin, or amikacin), multi-drug resistant[4]. **Fig 1** illustrate type of Drug resistance TB[5].

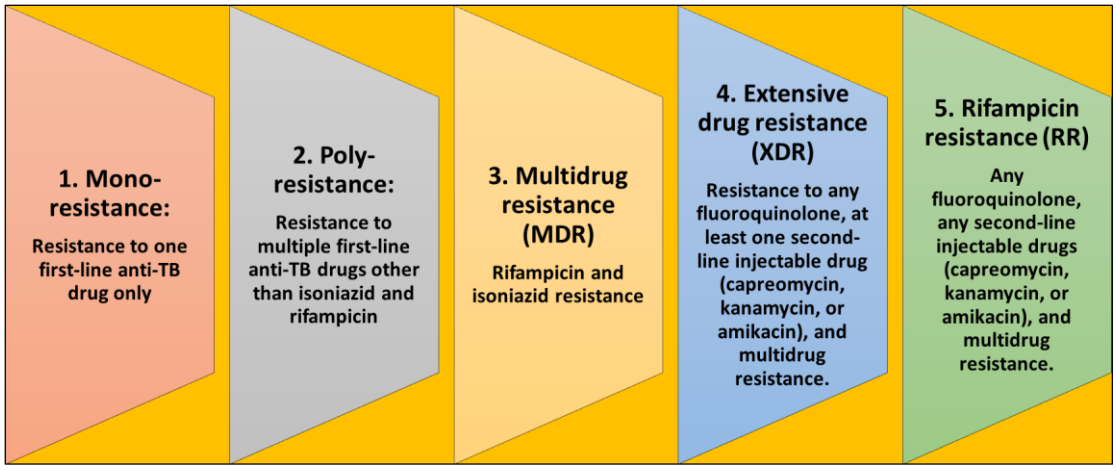

Figure 1 Type of drug resistance TB

Similarly, The rising hostility between humans and the microbiome has led to a global health crisis known as antimicrobial resistance (AMR)[6]. Human health is increasingly at danger from the problem of microbial antibiotic resistance. Antibiotic resistance has been steadily increasing worldwide with

the launch of each new bacterial treatment during the past several decades[7]. Human wellness is also seriously impacted by bacteria including *Methicillin-resistant Staphylococcus aureus* (MRSA), *Enterococcus*, *Streptococcus pyrogens*, and *Pseudomonas aeruginosa*[8]. The bacteria and their respective drug resistances are listed in **Fig. 2**[9].

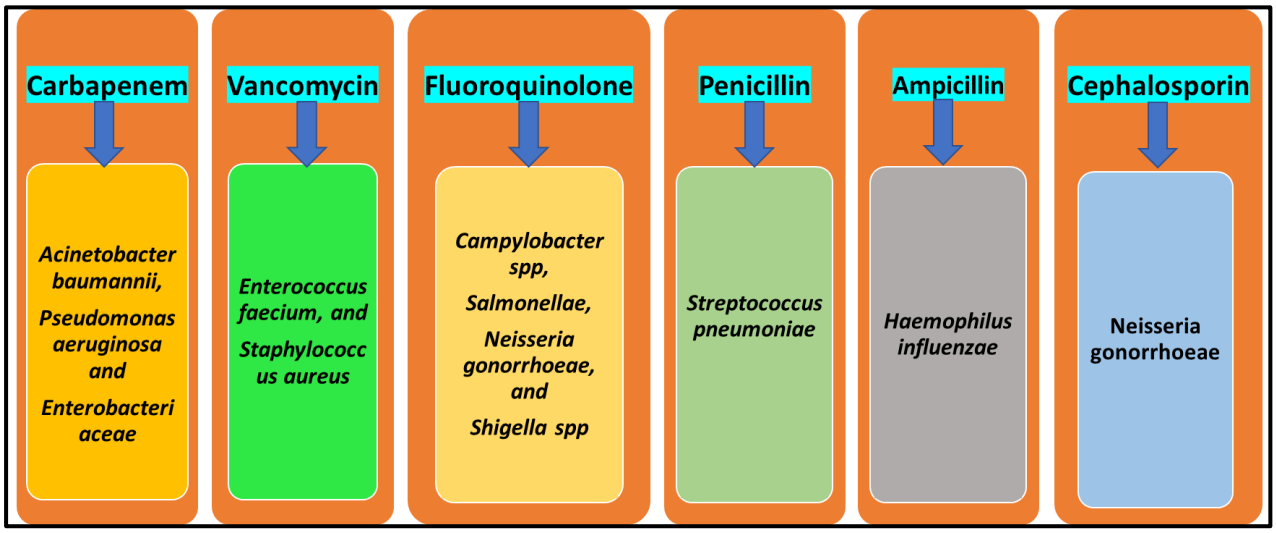

Figure 2 Drugs with resistance bacteria

Numerous N-containing heterocycles have been important in the pharmaceutical industry for decades. Due to thier extensive pharmacological action, piperazine has attracted the attention of medicinal chemists[10]. Therapeutically, various piperazine derivatives demonstrate a wide variety of effects, such as those againstantioxidative[11], antipsychotic[12], antidepressant[13], anticancer[14], antibacterial[15], antifungal[16], antimalarial[17], anticonvulsant[18], and antimycobacterial[19]. In light of this, we have generated numerous hybrids of piperazine by combining it with a variety of bioactive chemical moieties such as isoniazid, phenyl hydrazides, phenyl hydrazines, and coumarins. These hybrids were then examined for their anti-microbial and anti-tubercular activities.

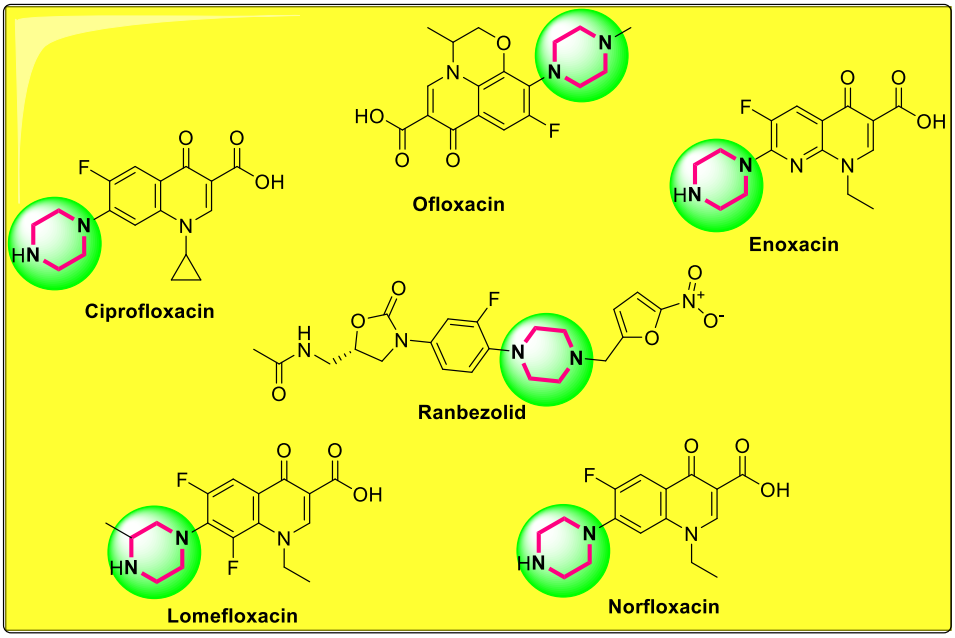

Figure 3 Piperazine containing antibacterial drugs

The objective of the present research

1. This study establishes an effective approach for the synthesis of piperazine hybrids
2. Evaluate the enhancement in efficacy against mycobacterium and antimicrobial strains.
3. To overcome the power of medication resistance possessed by mycobacterium and antimicrobial diseases.

References

[1] A. Koch, V. Mizrahi, Mycobacterium tuberculosis, Trends Microbiol. (2018). https://doi.org/10.1016/j.tim.2018.02.012.

[2] E. Pontali, M.C. Raviglione, G.B. Migliori, O.W. Akkerman, J.W. Alffenaar, F.X. Blanc, S. Borisov, D.M. Cirillo, M. Dalcolmo, K. Dheda, A.L. Kritski, C. Lienhardt, P. Olliaro, M. Tadolini, S. Tiberi, Z. Udwadia, Regimens to treat multidrug-resistant tuberculosis: Past, present and future perspectives, Eur. Respir. Rev. (2019). https://doi.org/10.1183/16000617.0035-2019.

[3] C.M. Rumende, Risk Factors for Multidrug-resistant Tuberculosis, Acta Med. Indones. (2018). https://doi.org/10.3126/ijasbt.v5i4.18771.

[4] Z. Xu, C. Gao, Q.C. Ren, X.F. Song, L.S. Feng, Z.S. Lv, Recent advances of pyrazole-containing derivatives as anti-tubercular agents, Eur. J. Med. Chem. (2017). https://doi.org/10.1016/j.ejmech.2017.07.059.

[5] https://www.who.int/teams/global-tuberculosis-programme/diagnosis-treatment/treatment-of- drug-resistant-tb/types-of-tb-drug-resistance

[6] Bitla, S., Gayatri, A.A., Puchakayala, M.R., Bhukya, V.K., Vannada, J., Dhanavath, R., Kuthati, B., Kothula, D., Sagurthi, S.R. and Atcha, K.R., 2021. Design and synthesis, biological evaluation of bis-(1, 2, 3-and 1, 2, 4)-triazole derivatives as potential antimicrobial and antifungal agents. Bioorganic & Medicinal Chemistry Letters, 41, p.128004.

[7] Prestinaci, F., Pezzotti, P. and Pantosti, A., 2015. Antimicrobial resistance: a global multifaceted phenomenon. Pathogens and global health, 109(7), pp.309-318.

[8] Ahmed, M.H., Ibrahim, M.A., Zhang, J., Melek, F.R., El-Hawary, S.S., Jacob, M.R. and Muhammad, I., 2014. Methicillin-resistant Staphylococcus aureus, Vancomycin-resistant Enterococcus faecalis and Enterococcus faecium active Dimeric Isobutyrylphloroglucinol from Ivesiagordonii. Natural product communications, 9(2), p.1934578X1400900223.

[9] Ventola, C.L., 2015. The antibiotic resistance crisis: part 1: causes and threats. Pharmacy and therapeutics, 40(4), p.277.

[10] A.K. Rathi, R. Syed, H.S. Shin, R. V. Patel, Piperazine derivatives for therapeutic use: A patent review (2010-present), Expert Opin. Ther. Pat. (2016). https://doi.org/10.1080/13543776.2016.1189902.

[11] Patel, R.V., Mistry, B., Syed, R., Rathi, A.K., Lee, Y.J., Sung, J.S., Shinf, H.S. and Keum, Y.S., 2016. Chrysin-piperazine conjugates as antioxidant and anticancer agents. European Journal of Pharmaceutical Sciences, 88, pp.166-177.

[12] Brito, A.F., Moreira, L.K., Menegatti, R. and Costa, E.A., 2019. Piperazine derivatives with central pharmacological activity used as therapeutic tools. Fundamental & clinical pharmacology, 33(1), pp.13-24.

[13] Kumar, R.R., Sahu, B., Pathania, S., Singh, P.K., Akhtar, M.J. and Kumar, B., 2021. Piperazine, a Key Substructure for Antidepressants: Its Role in Developments and Structure-Activity Relationships. ChemMedChem, 16(12), pp.1878-1901.

[14] Walayat, K., MOHSIN, N.U.A., Aslam, S. and Ahmad, M., 2019. An insight into the therapeutic potential of piperazine-based anticancer agents. Turkish Journal of Chemistry, 43(1), pp.1-23.

[15] Patil, M., Poyil, A.N., Joshi, S.D., Patil, S.A., Patil, S.A. and Bugarin, A., 2019. Design, synthesis, and molecular docking study of new piperazine derivative as potential antimicrobial agents. Bioorganic chemistry, 92, p.103217.

[16] Thamban Chandrika, N., Shrestha, S.K., Ngo, H.X., Tsodikov, O.V., Howard, K.C. and Garneau-Tsodikova, S., 2018. Alkylated piperazines and piperazine-azole hybrids as antifungal agents. Journal of medicinal chemistry, 61(1), pp.158-173.

[18] Tiwari, H.K., Kumar, P., Jatana, N., Kumar, K., Garg, S., Narayanan, L., Sijwali, P.S., Pandey, K.C., Gorobets, N.Y., Dunn, B.M. and Parmar, V.S., 2017. In Vitro Antimalarial Evaluation of Piperidine-and Piperazine-Based Chalcones: Inhibition of Falcipain-2 and Plasmepsin II Hemoglobinases Activities from Plasmodium falciparum. ChemistrySelect, 2(25), pp.7684-7690.

[19] Archana, A., 2021. Synthesis of Novel Triazolyl/Oxadiazolyl/Thiadiazolyl-Piperazine as Potential Anticonvulsant Agents. Drug Research, 71(04), pp.199-203.

[20] Zhao, S.J., Lv, Z.S., Deng, J.L., Zhang, G.D. and Xu, Z., 2018. Pyrrolidine-containing or Piperazine-containing Nitrofuranylamides: Design, Synthesis, and In Vitro Anti-mycobacterial Activities. Journal of Heterocyclic Chemistry, 55(12), pp.2996-3000.

Chapter 2

An appraisal of anti-mycobacterial activity with structure-activity relationship of Piperazine and its analogues: A review

Published: European Journal of Medicinal Chemistry (doi.org/10.1016/j.ejmech.2020.112967)

Graphical Abstract

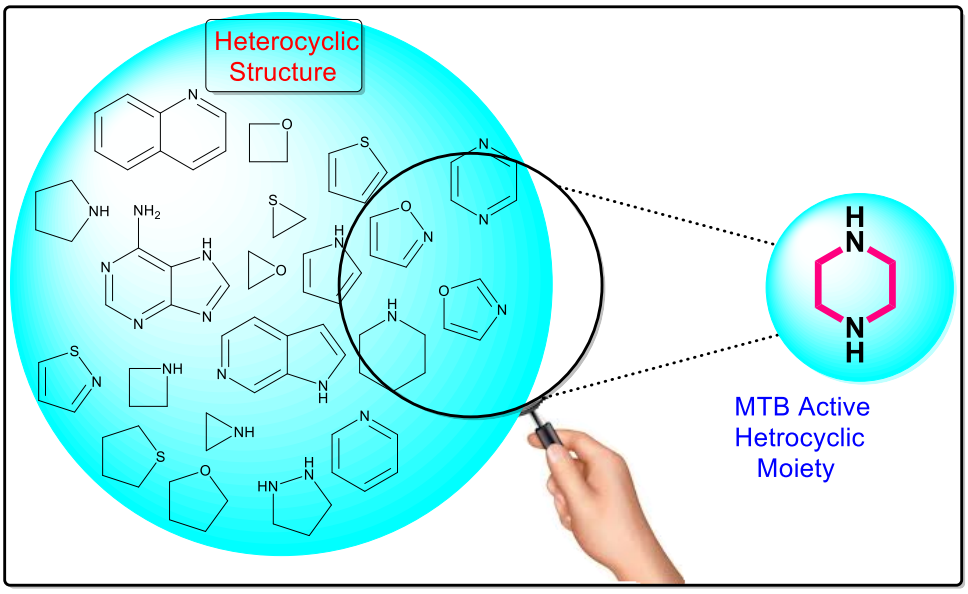

Abstract

Piperazine, is privileged six membered nitrogen containing heterocyclic ring also known as 1,4-Diazacyclohexane. Consequently, piperazine is a versatile medicinally important scaffold and is an essential core in numerous marketed drugs with diverse pharmacological activities. In recent years several potent molecules containing piperazine as an essential subunit of the structural frame have been reported, especially against *Mycobacterium tuberculosis* (MTB). Remarkably, a good number of these reported molecules also displayed potential activity against *multidrug-resistant* (MDR), and *extremely drug-resistant* (XDR) strains of MTB. In this review, we have made a concerted effort to retrace anti-mycobacterial compounds for the past five decades (1971-2019) specifically where piperazine has been used as a vital building block. This review will benefit medicinal chemists as it elaborates on the design, rationale and structure-activity relationship (SAR) of the reported potent

piperazine based anti-TB molecules, which in turn will assist them in addressing the gaps, exploiting the reported strategies and developing safer, selective, and cost-effective anti-mycobacterial agents.

Keywords: Piperazine, *Mycobacterium tuberculosis*, Structure-Activity Relationship, Anti-mycobacterial agent

Table of content

1. Introduction

Tuberculosis (TB) is potentially a catastrophic pandemic caused by *Mycobacterium* species such as *Mycobacterium tuberculosis* (MTB), *M. caprae, M. canettii, M. bovis, M. pinnipedii, M. africanum,* and *M. microtiv*. Among these, primarily MTB is the most common pathogenic strain and can cause TB of the lungs (pulmonary-TB) apart from other vital organs[1]. The World Health Organization (WHO) has speculated that quarter of the world's population is diagnosed with MTB, with 10.0 million of the new cases in 2018 alone. Presently, TB is one among the top ten leading causes of mortality globally [2]. China, India, Russian Federation, and South Africa have almost ~63% of the world's active cases of TB. Apart from Lesotho, South Africa tops the list of incident rates with 834 cases per 100,000 people. TB, together with human immunodeficiency virus (HIV) infection, has become a lethal combination and covers the principal ascent of the diseases responsible for the highest mortality in Africa. The current TB treatment regimen has several drawbacks, such as poor therapeutic efficacy, drug toxicity, and efflux pumps [3,4]. Besides, the non-compliance of patients due

to the relatively long duration and complexity has contributed to the emergence of drug-resistant strains. Efforts to eliminate, TB have remained as a major challenge because of limitations with existing treatments, poor patient compliance, co-infections, inadequate therapeutic regimen and the emergence of resistant strains such as extensively drug resistant-TB (XDR-TB, strains that are resistant to rifampicin (RIF) and isoniazid (INH), as well as any fluoro-quinolone and at least one of three injectable second-line drugs, *viz:* capreomycin, kanamycin, or amikacin), multi-drug resistant-TB (MDR-TB, resistant to at least two front-line anti-TB agents *viz*: RIF and INH, drug resistant-TB (DR-TB,resistant to at least one anti-TB drug), and recent incidents of total drug-resistant (TDR, resistant to all first-line and second-line anti-TB drugs) is a serious threat to mankind[5]. These facts clearly indicate that there is still a major challenge to medicinal chemists to control as well as manage TB worldwide[6].

In the past few decades, several natural products, as well as synthetic compounds, have been reported to display potent activity against resistant MTB strains. However, most of them failed either in pre-phase I or Phase I clinical trials. Thus in the last 50 years, only a small number of drugs have been successfully registered for the TB therapy. The current anti-mycobacterial agents causes several side effects, mainly due to the long treatment regimen, which has created an immediate need to design new and safer chemotherapeutic agents for effective therapy[7].

In recent years, the concept of molecular hybridization (MH) has become quite popular among the medicinal chemists, which is based on the combination/conjugation of different or more related pharmacophore moieties into a single framework to give a desired pharmacological activity, consequently boosting therapeutic efficacy and enhancing the physiochemical profile. This comprehensive approach contributed to many novel chemicals moieties with enhanced anti-TB activity[8].

In past decades, many N-containing heterocycles played a significant role in drug design. Piperazine has gained attention in medicinal chemistry due to its wide pharmacological activity [9]. Many piperazine derivatives typically exhibit an interesting range of therapeutic activities including

anti-mycobacterial, anti-bacterial, anti-virus, anti-fungal, anti-tumor, anti-analgesic, anticonvulsant activities[10,11]

Further, piperazine skeleton has recognized as a valuable pharmacophore against mycobacterial infections with aforementioned beneficial profiles[12]. In quest of exploring novel anti-TB hybrids, numerous piperazine-containing analogues were synthesized and evaluated for their anti-TB activity with enhanced hydrogen bonding capability, dipole moment, stability and rigidity under *in vivo* conditions[13]. These properties have attributed to their improved pharmacological activities. Besides that, the piperazine derivatives were also identified as a promising class of possible anti-TB drug candidates[14].

The broad range of pharmacological activities and efficient utilization of piperazine containing drugs in the healthcare setups inspires even more aggressive research that enables to design of a huge proportion of structurally diverse analogues of piperazine[10,11,15,16]. In recent times, several attempts have been made to develop piperazine derivatives as novel effective anti-TB agents (**Fig. 5**). So, in this review, we have summarized by systematically presenting significant advancements of piperazine-based molecular-hybrids as novel anti-mycobacterial agents. We also attempted to derive some useful SAR of successful piperazine analogues that could be further investigated in order to design and develop potential anti-mycobacterial drug candidates.

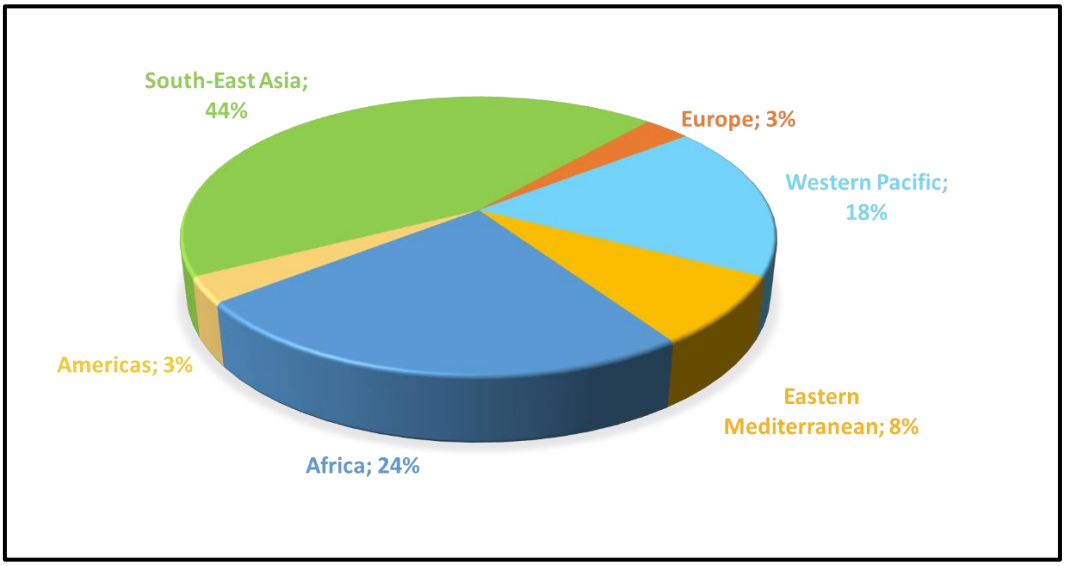

Figure 1 Estimated percentage of TB-deaths worldwide.

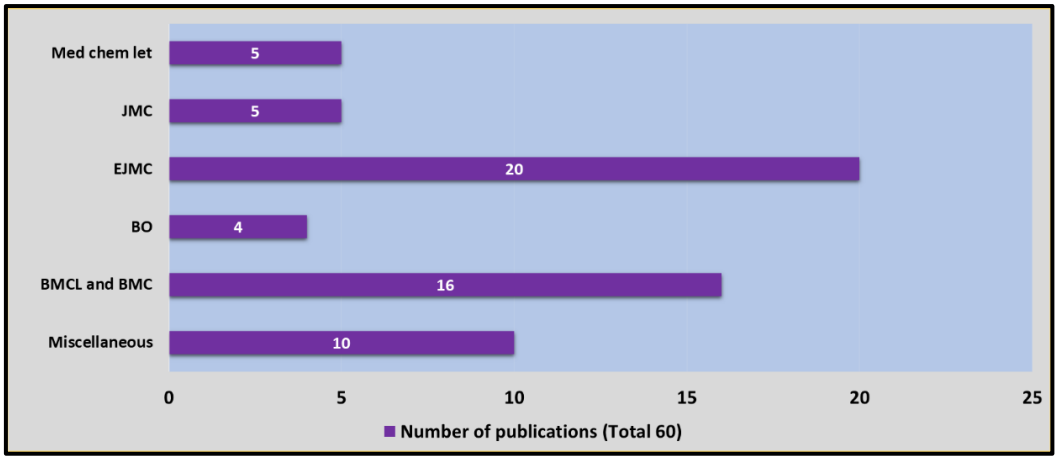

Figure 2 Publisher wise publications on piperazine based anti-mycobacterial agents (1971-2019).

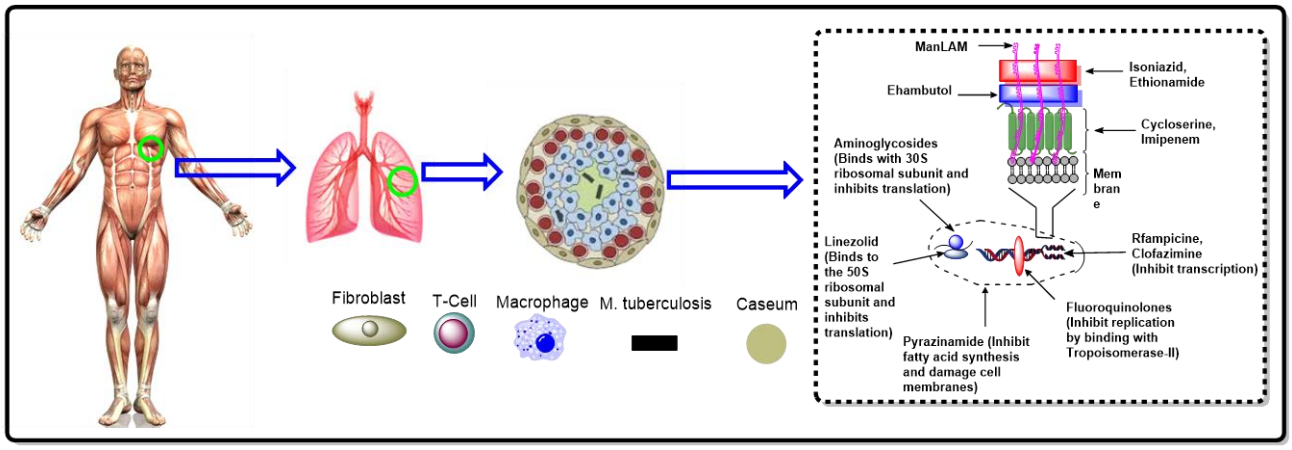

Figure 3 Drug targets for different agents in mycobacterial chemotherapy.

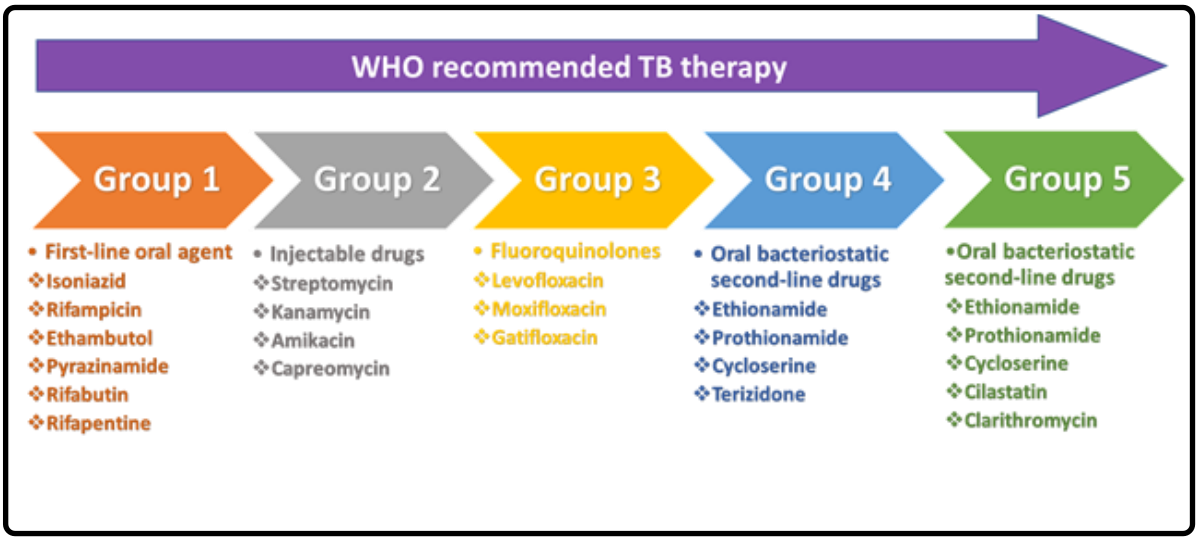

Figure 4 Classes of drugs used in mycobacterial chemotherapy.

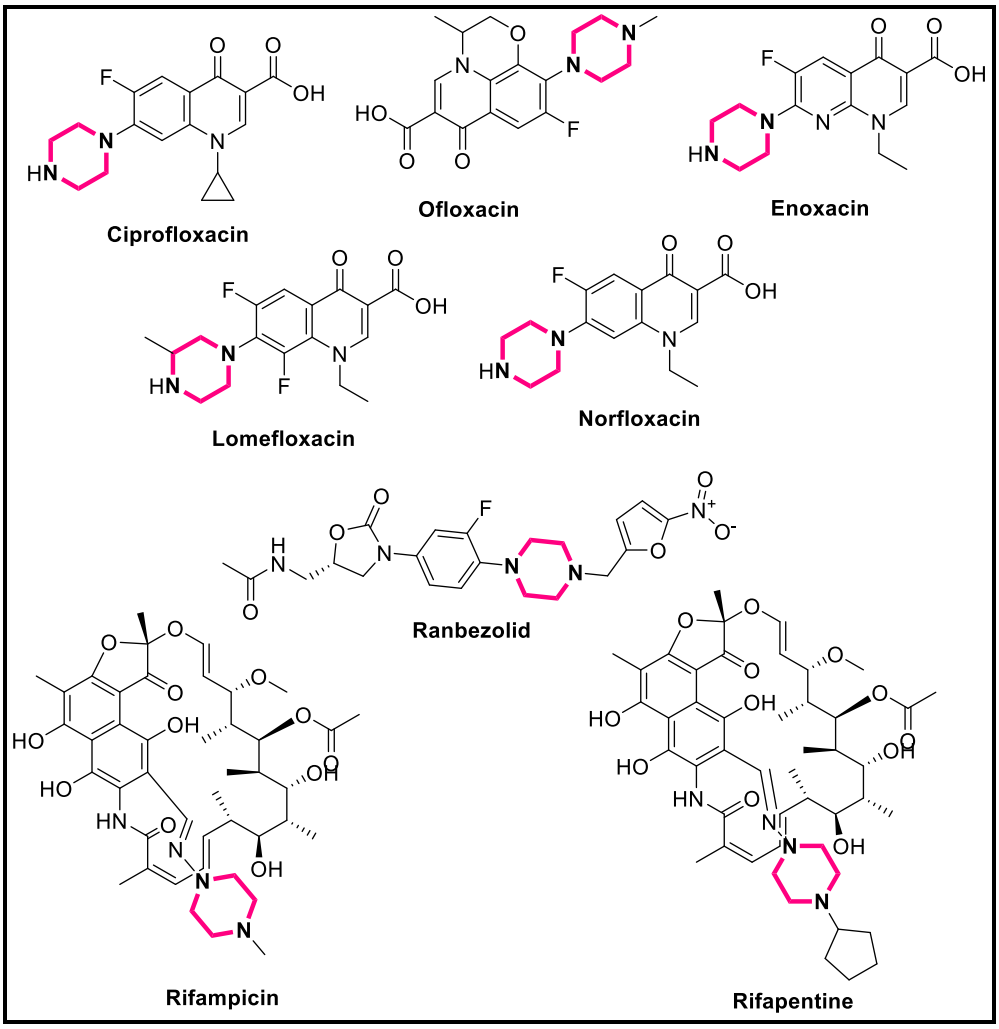

Figure 5 Piperazine containing anti-mycobacterial agents.

2. Data sources, background study and data extraction process

Throughout the data search process, we used various resources such as Scifinder, PubMed, PubChem, and Google Scholar for literature quest, while the espacenet, and world intellectual property organisation (WIPO) used for patent search. Among these, Scifinder, PubMed and WIPO were considered useful for collecting the related literatures and patents. The literature search strategy is outlined in the **Fig. 6**.

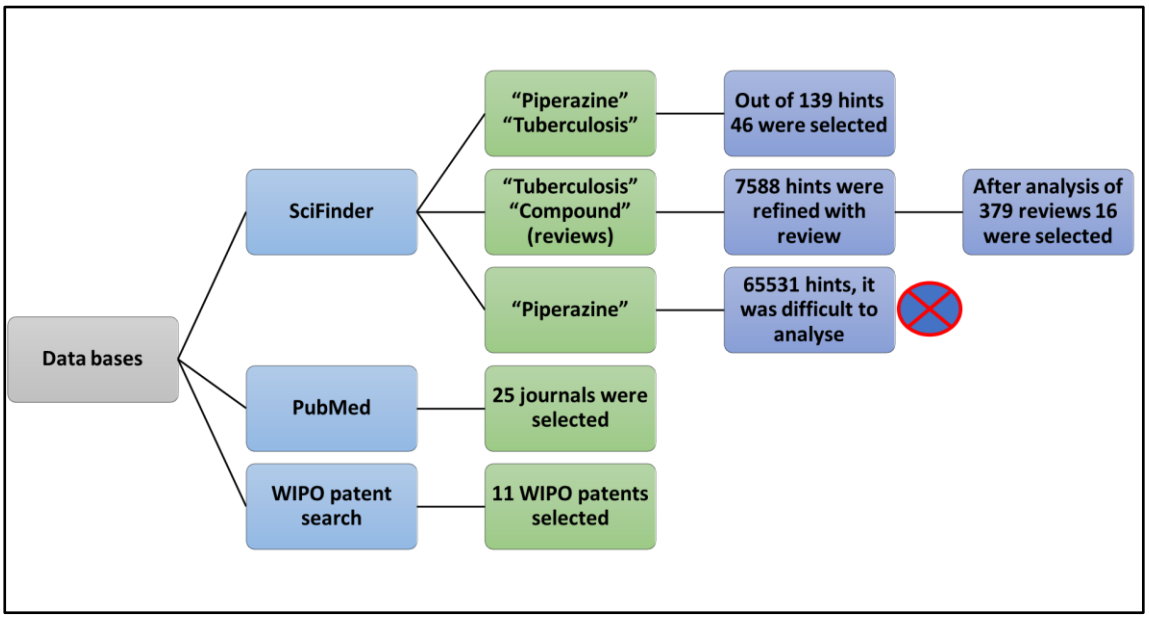

Figure 6 Flow diagram used for data collection during literature review.

Another unique feature of this review is that we have established few important SAR parameters that correlates the chemical structure and the biological activity of the compounds. **Fig. 7** describes the scheme and the various signs/shapes employed for generation SAR data.

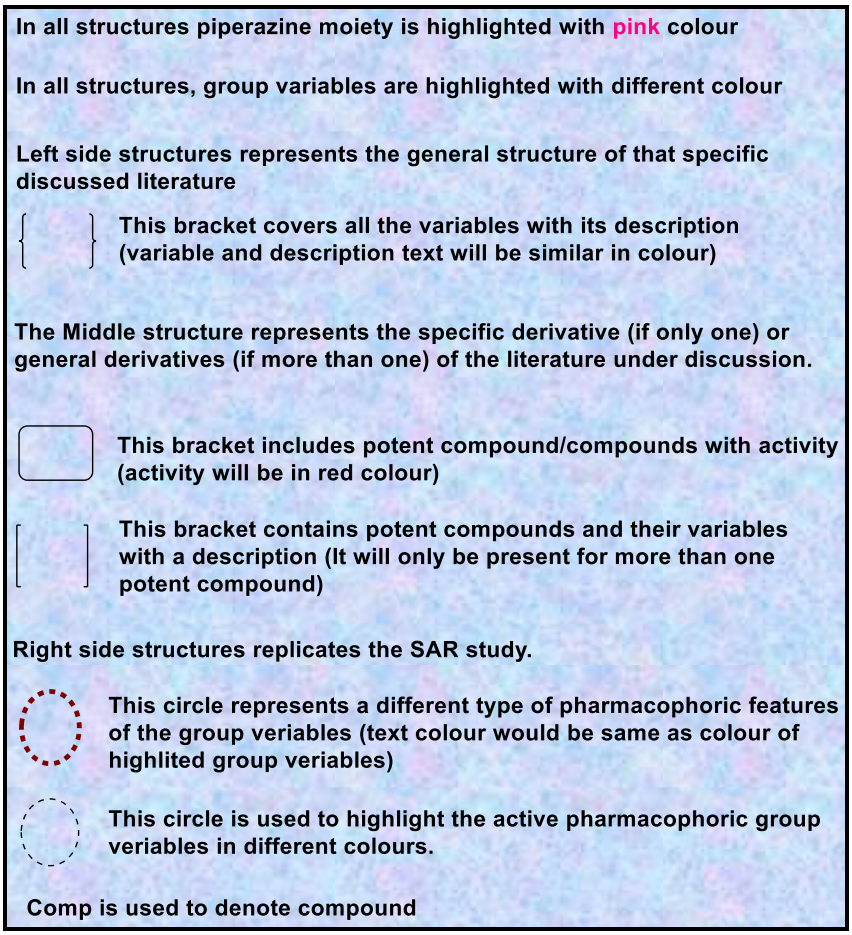

Figure 7 The scheme and the various signs/shapes used for SAR-studies explanation.

3. Literature study

The incorporation of piperazine moiety into anti-TB compounds elicited a significant impact on their biological activities, with improved pharmacological and toxicological properties[9,11].

Based on the molecular docking studies, Simons et al. [17]have synthesized three series of azole-piperazine derivatives (**1a-c,Fig. 8**)as MTBdicyclotyrosine (cYY)[18] mimic agents. Their*in vitro* anti-TB activity was evaluated against MTB *$H_{37}Rv$* strain by using REMA method (Resazurin Microtiter Assay) [19,20]. By exploring **1c** analogues,they identified that compounds **1ca**, and **1cb** displayed moderateinhibitory activity with minimum inhibitory concentration (MIC) value of 26.79 and 144.31 µM, compared with the standard drug Fluconazole and Clotrimazole (MIC = >326.50 and 0.29 µM), respectively. Further, SAR study (**Fig. 8**) revealed that the pyrazole ring with piperazine enhanced the inhibitory activity against MTB-*$H_{37}Rv$* due to their haem iron binding.

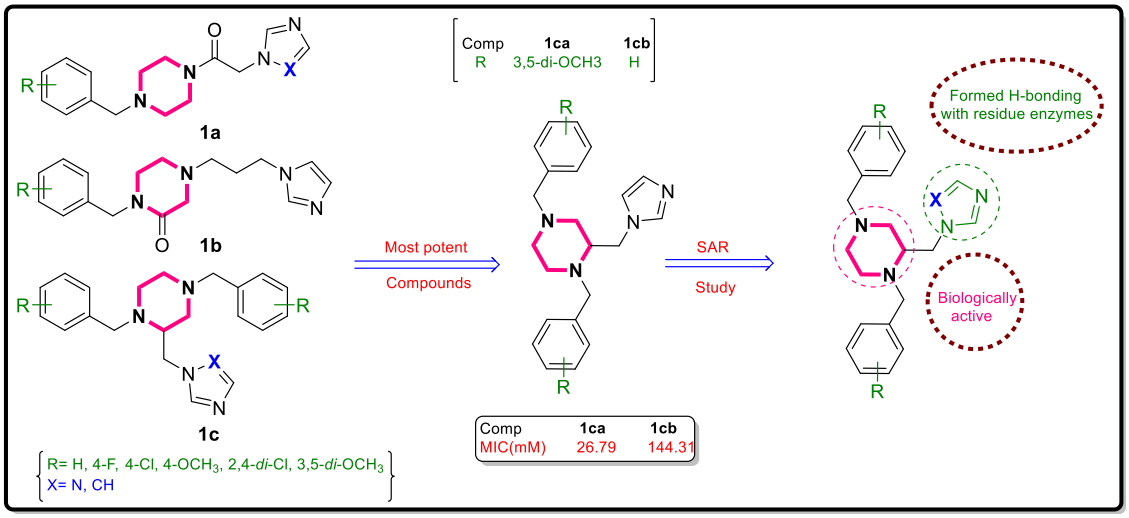

Figure 8 Azole-piperazine analogues (1a, 1b and 1c) with potent compounds (1ca and 1cb) and SAR study

Gonec et al.[21] have designed and synthesized a series of aryl-piperazine analogues (**2, Fig. 9**)with considerable lipophilic character. All analogues were evaluated for their anti-TB activity against MT *My 331/88 ($H_{37}Rv$), MK My 235/80, MK 6 509/96, MA My 330/88* as well as *CIT11/06, CIT03, ATCC 13950,* and *CIT10/08* strains. Their results have shown that the analogue **2a** was identified as the most potent against *$H_{37}Rv$* strain with MIC value of 8.0 µM, compared to reference drugs Ofloxacin and Ethambutol (EMB) (MIC= 1.0 and 1.1 µM). Further, SAR study (**Fig. 9**) correlates the impact of anti-TB activity with the lipophilicity and substitutions on the N-aryl piperazine ring.

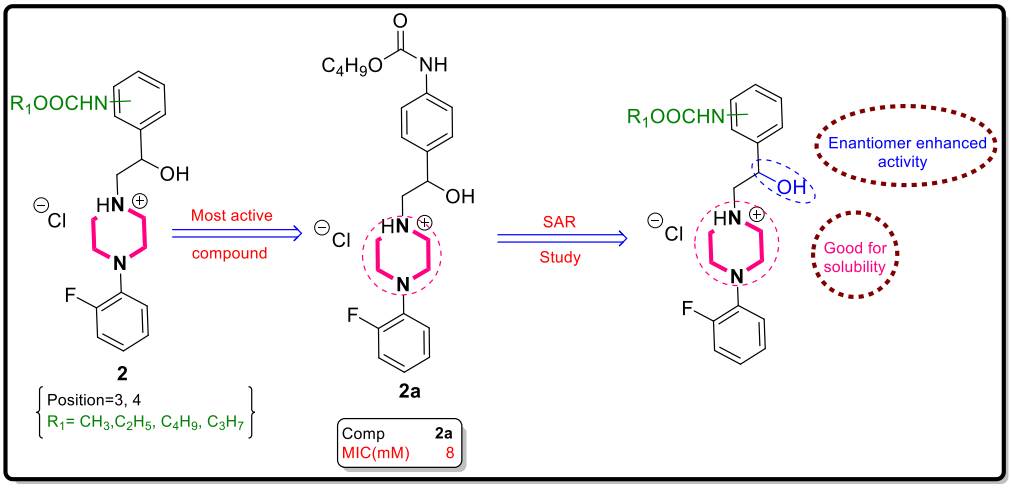

Figure 9 Aryl-piperazine hybrids (2) with potent analogue (2a) and SAR study

Roh et al.[22] explored four different sequences of 3,5-dinitrophenyl tetrazoleand oxadiazole derivatives (**3a-d, Fig. 10**), and resolved solubility issues of the previous study by preparing piperazine hydrochloride salt. In this study it was revealed that the solubility had great impact on the inhibitory profile of N-benzyl piperazine derivatives **3ba**, **3ca**, and **3da** with enhancedMIC value of 1.0, 1.0 and 0.125 µM against MTB, *CNCTC, My 331/88* (*$H_{37}Rv$*) strains. However, the **3da** compound showed better activity (MIC= 0.125 µM) than standard drug isoniazid (INH) and rifampicin (RIF) (MIC=0.5 and 0.25 µM). The SAR report explained that the piperazine pharmacophoric structural feature showed the highest MTB activity than other heterocyclic groups (**Fig. 10**).

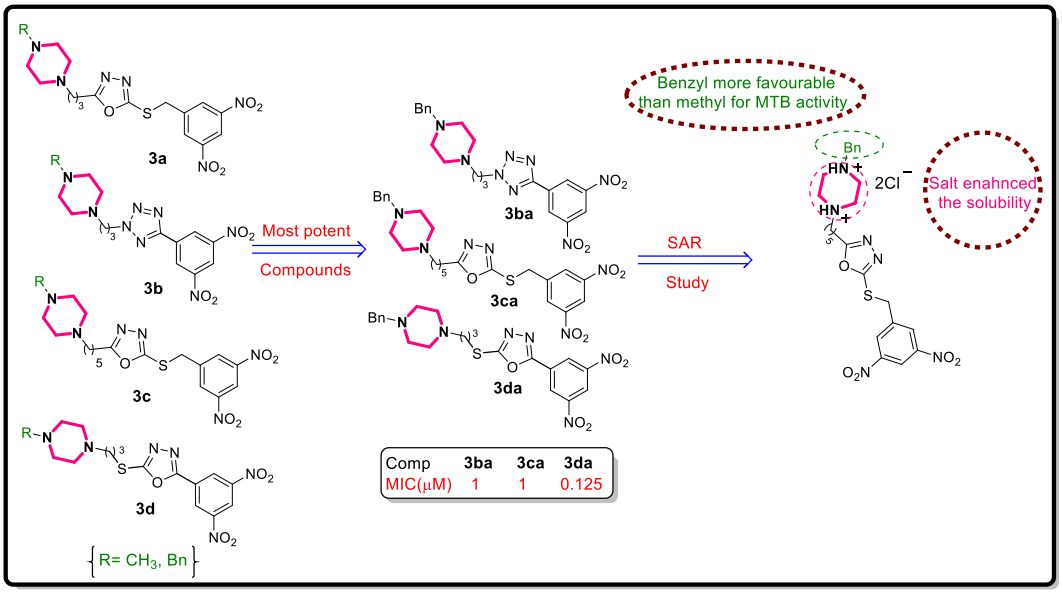

Figure 10 3,5-dinitrophenyl tetrazole and oxadiazole derivatives (3a-d)with potent derivative (3da)and SAR study

Patel and co-workers[23] have synthesized a series of 2-(4-cyano-3-trifluoromethyl-phenylamino)-4-(quinoline-4-yloxy)-6-(piperazinyl/piperidinyl)-s-triazine hybrids (**4, Fig. 11**) and evaluated them for anti-TB, anti-bacterial, and anti-fungal activities. The preliminary *in vitro* studies showed their anti-TB activity at the concentration of 9.01-12.71 µM in BACTEC MGIT system. Further, they identified most potent analogues **4a-c** that has shown inhibition against MTB *$H_{37}Rv$* strain at MIC of 19.61, 42.62, and 72.14 µM, as compared to the reference drug pyrazinamide (PZA).

The brief SAR analysis (**Fig. 11**) has indicated that the anti-TB activity is depended on halogen substitutions of phenyl-piperazine rings.

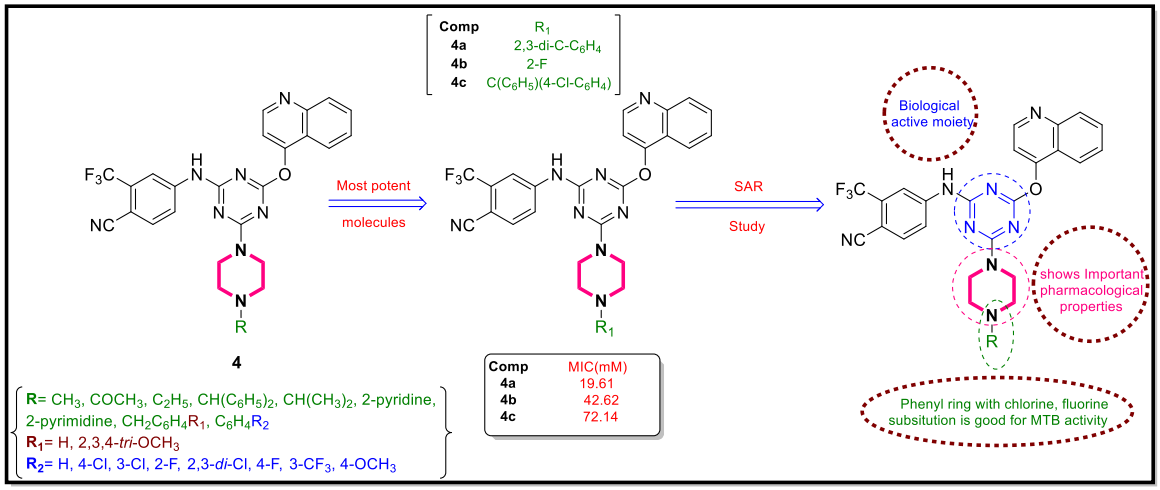

Figure 11 Piperazine substituted Triazines (4) with potent hybrids(4a-c)and SAR study.

Luo-Ting et al.[24] have synthesized and evaluated benzothiazinone analogues (**5, Fig. 12**)as novel decaprenylphosphoryl-b-D-ribose-epimerase (*DprE1*) inhibitors. They have synthesized a wide range of 4-carbonyl piperazine substituted 1,3-benzothiazin-4-one analogues tested *in vitro* against MTB $H_{37}Rv$ strain using PBTZ169 as standard[25,26]. The SAR studies (**Fig. 12**)revealed that anti-TB activity is depending on the 4-carbonyl piperazine substitution on benzo-thiazinone ring. The most potent compound **5a** (MIC = 0.008 µM) of this series showed inhibition against $H_{37}Rv$ strain and found non-cytotoxic to VERO cells.

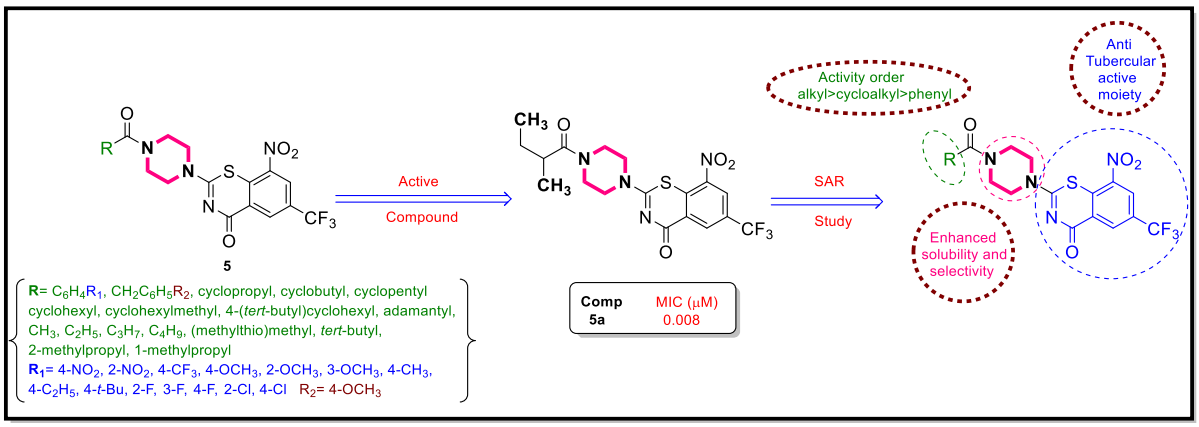

Figure 12 Piperazine substituted benzothiazinones (5) with potent hybrid (5a) and SAR study.

Marvadi and co-workers[27] synthesized a novel series of 2-(thiophen-2-yl) dihydro-quinoline conjugates (**6, Fig. 13**) by fusing dihydro-quinoline moiety and nitrogen containing substituents *viz*: morpholine, thiomorpholine and piperazine. These compounds were evaluated for anti-TB activity against MTB *$H_{37}Rv$* strain using microplate alamar blue assay (MABA) technique [28,29]. Six compounds displayed acceptable activity half maximal inhibitory concentration (MIC) <18.01 µM, while, the compounds **6a** and **6b** have emerged as the most potent conjugates with each MIC value of 3.58 µM against standard reference Ciprofloxacine (Cf) with less toxicity and enhanced solubility profile. A SAR study (**Fig. 13)** demonstrated the positive influence of piperazine, N-substituted benzyl and pyridine ring on the MTB activity.

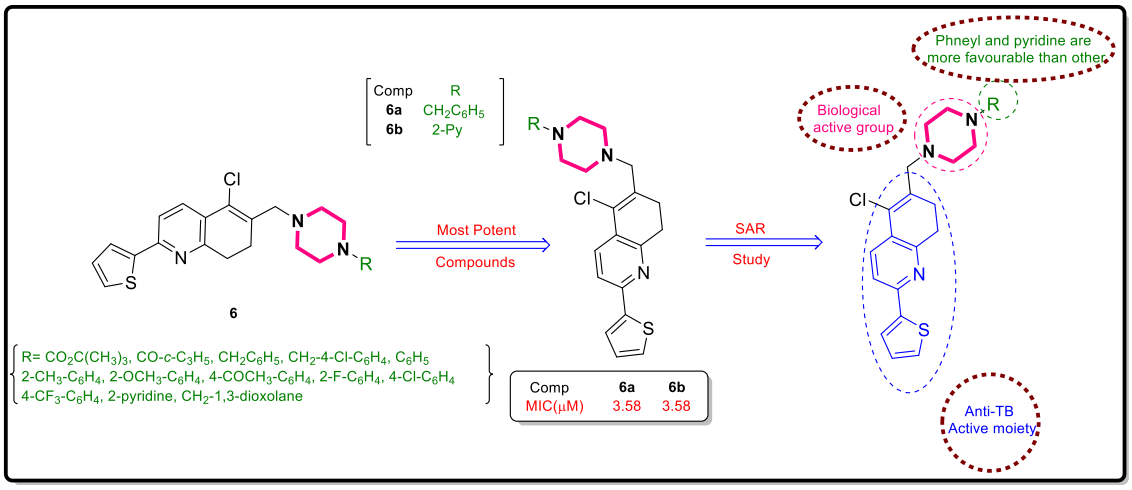

Figure 13 Piperazine substituted 2-(thiophen-2-yl)dihydroquinoline conjugates (6) with potent compounds (6a and 6b) and SAR study.

Zhi Xu et al.[30] have performed the *in vitro* MTB activity on the synthesized nitro-ferricyanides pyrrolidine and piperazine analogues (**7, Fig. 14**) against different TB-strains MTB *$H_{37}Rv$*, *MDR-MTB 16833* and *MDR-MTB 16995* strains (using MABA). From the results it was identified that some promising compounds (**7a-c)** exhibited most potent activity with MIC value range of <0.04 to > 9.2 µM while reference drugs INH and RIF showed a MIC of 0.06, and >48.61 µM, respectively. Further, the SAR study identifies the importance of piperazine ring in anti-TB activity of these hybrids, as its absence significantly reduced the activity.

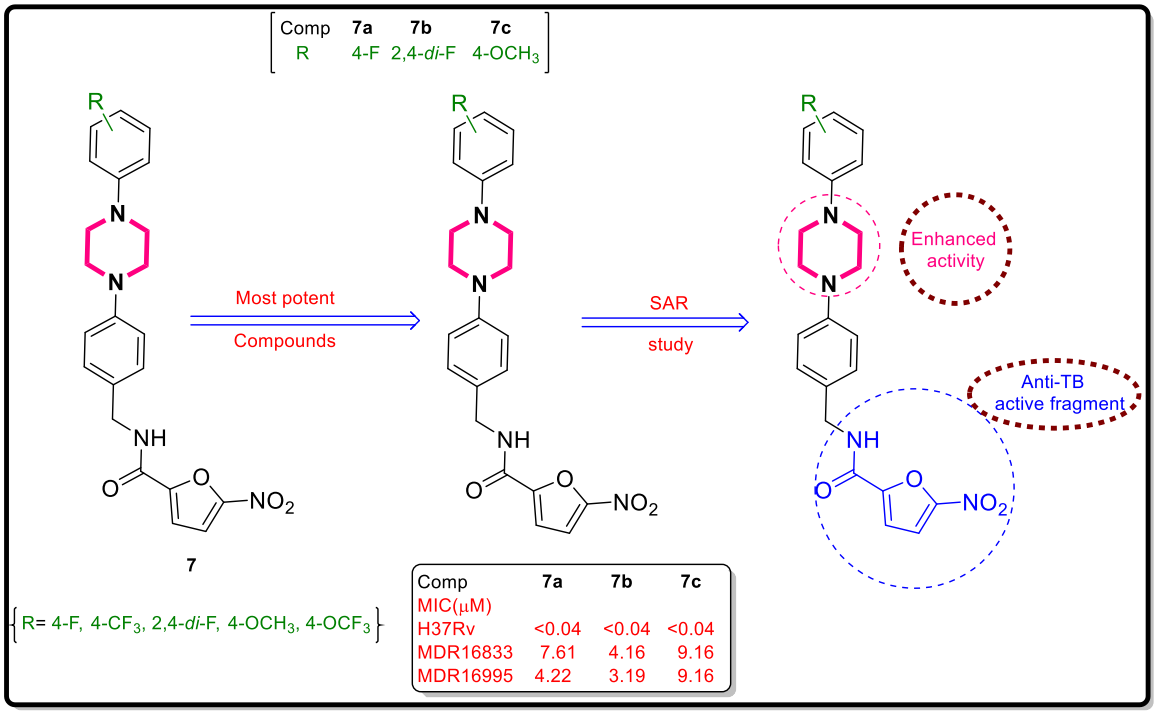

Figure 14 Nitro-ferricyanides piperazine hybrids (7) with potent derivatives (7a, 7b and 7c) and SAR study.

NARD and co-workers[31] have reported the synthesis of a verity of substituted 5-nitro-2-furaldehyde piperazinoacyl hydrazone derivatives (**8, Fig. 15**) and compounds were screened *in vitro* against 10 different microbial strains *viz*: *E. coli* 100, *Salmonella typhimurium* 1090, *Pseudomonas aeruginosa* H2, *Proteue vulgaris* OX, *Micrococcus p yogenes* SG511, *Streptococcus pyogenes* ASS, *Bacillus subtilis* ATCC 9466, *Trichophyton mentagrophytes* 1236, and *Candida albicans* 28 including MTB H_{37}Ra, respectively. Among them, Compound **8a** showed most potent *in vitro* activity against the tested strains. Moreover, the active analogues did not show any activity in their *in vivo* studies. Their SAR studies revealed that the long-chain alkyl groups attached to N-atom of piperazine were important for anti-TB activity.

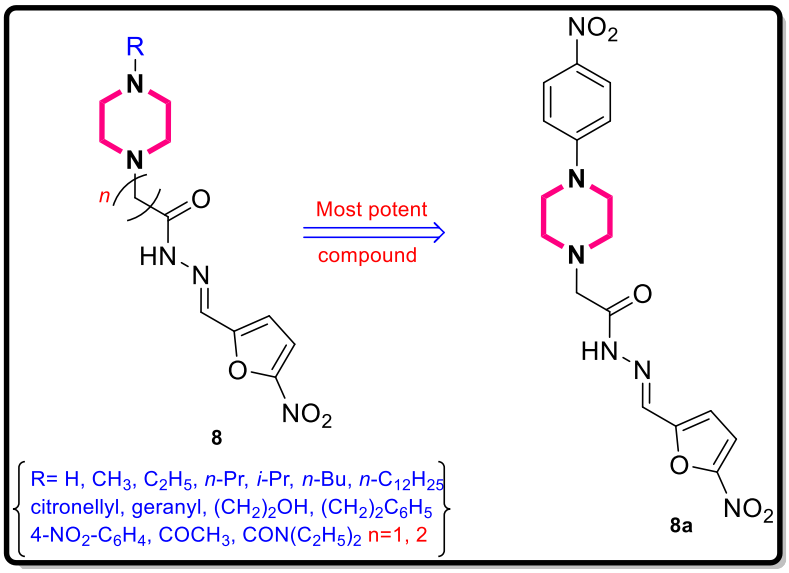

Figure 15 5-Nitro-2-furaldehyde piperazinoacyl hydrazones(8)and active derivative (8a)

Piperazine and oxime containing benzo-thiazinones (BTZs) (**9, Fig. 16**) were incorporated into a single framework to check their *in vitro* MTB activity, by Wang and co-workers[32]. These analogues exhibited high selectivity and potency towards MTB $H_{37}Rv$ strain (MIC range <0.03-0.913 μM) using MABA. The most potent conjugates **9a** and **9b** exhibited excellent anti-TB activity with MIC value of <0.03 μM and lower toxicity to mammalian VERO cells, in comparison RIF, INH and PBTZ169 positive control drugs exhibited lower activity and more toxicity. Further, these potent compounds **9a** and **9b** were examined through *in vivo* studies on mice, MTB $H_{37}Rv$ infected murine strain model and evaluated *Pyruvate kinase* (PK) activity in the Institute of Cancer Research (ICR). Both the tested compounds showed excellent anti-TB activity, and compound **9a** displayed significantly higher PK profile than PBTZ169 at the same oral doses in Sprague Dawley (SD) rat's model.

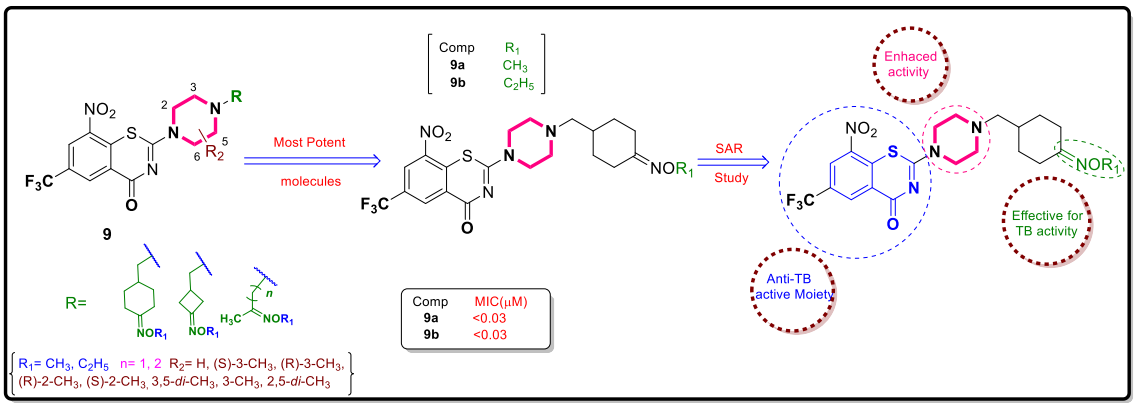

Figure 16 Piperazine and oxime containing BTZs (9) with potent analogues (9a and 9b) and SAR study.

Singh et al.[12] reported the SAR study for some novel 1-(5-isoquinolinesulfonyl)piperazine derivatives (**10, Fig. 17)** with promising inosine-5'-monophosphate dehydrogenase (IMPDH) enzyme inhibition [33,34] in anti-TB activity. These activities were screened respectively with a mutant SRMV2.6 and wild-type MTB. The analogues with piperazine iso-quinoline and cyclohexyl ring have shown their mild to excellent MTB inhibitory activity. Further, SAR study (**Fig. 17**) showed that the activity of this series heavily depends on the distance between sulfonyl and carbonyl group, indicating these compounds have specific targets to bind.

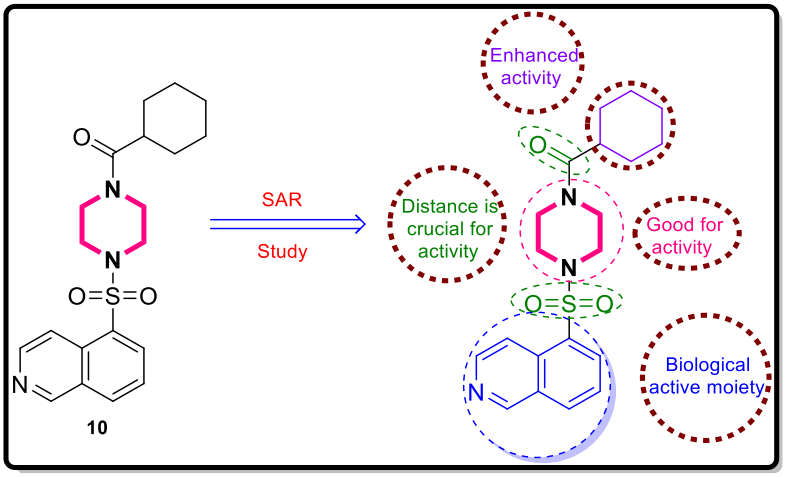

Figure 17 1-(5-isoquinolinesulfonyl)piperazine derivative (10) and SAR study

Heather and the team[35] synthesized and evaluated a new series of 1,2,4-trisubstituted piperazine derivatives (**11, Fig. 18**) and studied for their anti-TB activity against *$H_{37}Rv$* strain. Notable, compound **11a** showed excellent activity than standard anti-TB drugs Fluoroquinolone (FQ),

RIF, and INH against TB strain under aerobic conditions. Besides, they showed moderate potential against replicating MTB, indicating their potential as a safe anti-TB therapeutic agent.

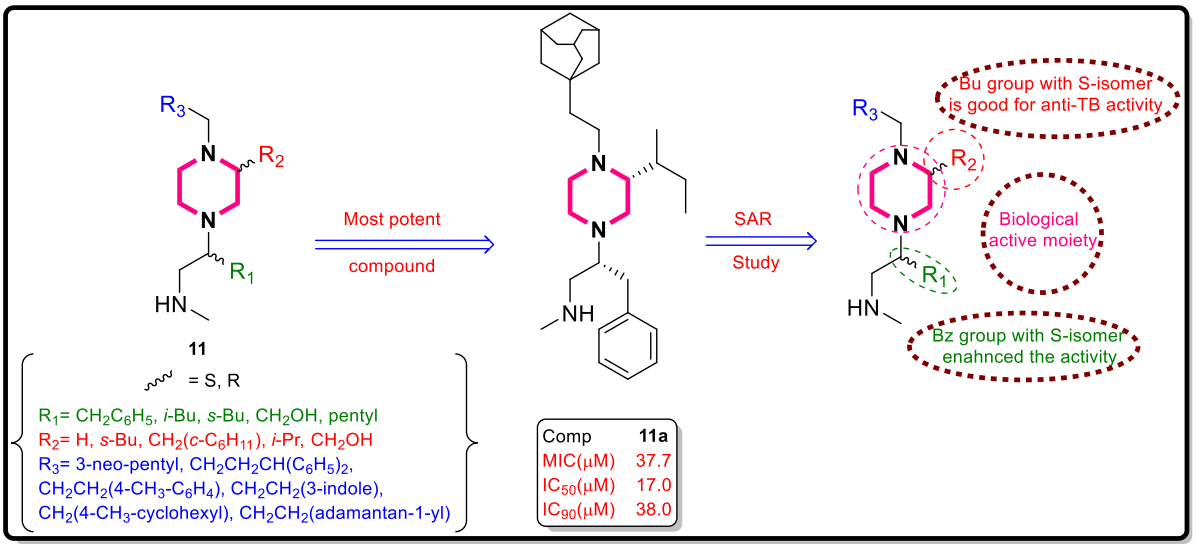

Figure 18 1,2,4-trisubstituted piperazine hybrids (11) with potent derivative (11a) and SAR study

Kantevaria et al.[36] designed and synthesized two novel series of dibenzo[b,d] thiophene and imidazo[1,2-a]pyridine-3-carboxamides hybrids (**12, Fig. 19**) by hybridizing two bioactive molecules and evaluated for their *in vitro* anti-TB activity. Compound **12a** (MIC = 2.48 μM) displayed excellent anti-TB activity compared to the standard drugs EMB and PZA (MIC = 15.32 and 406.13 μM) respectively. The results revealed that 4-chlorophenyl piperazine derivative **12a** emerged as most potent compound and less toxic than 4-benzyl piperidine analogues. Further, the SAR study (**Fig. 19**) revealed the impact of substitutions on benzyl amines for the anti-TB activity.

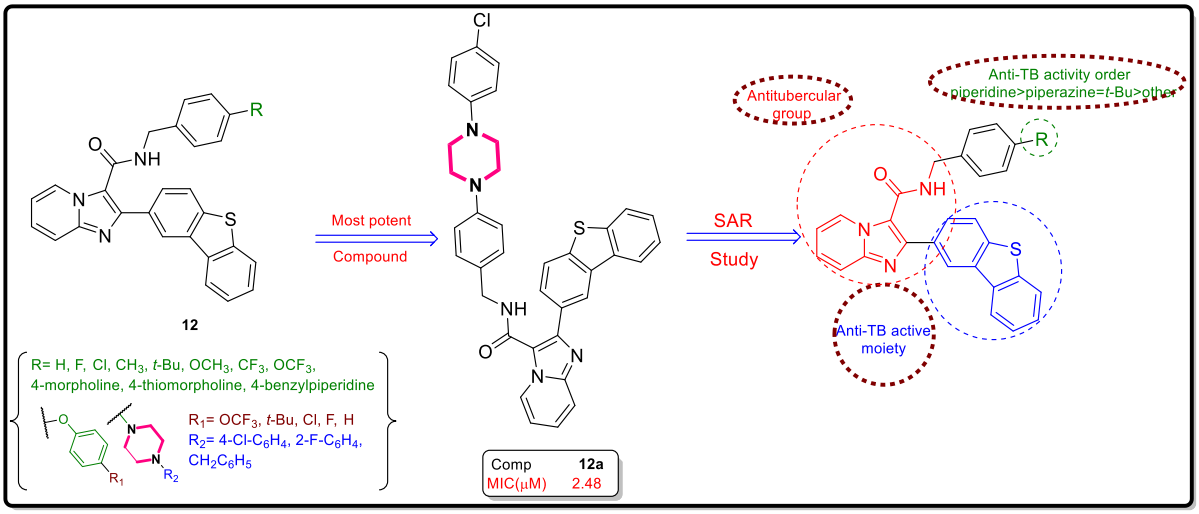

Figure 19 dibenzo[b,d]thiophene and imidazo[1,2-a]pyridine-3-carboxamides analogues (12) with potent derivative (12a) and SAR study

Kalaga et al.[37] synthesized a series of indole and triazole tethered piperazin-1-yl/1,4-diazepan-1-yl)benzo[d]isoxazole conjugates (**13a** and **13b, Fig. 20**) to find potent anti-TB candidates. The authors also demonstrated favourable *in silico* binding of **13ba** and **13bb** with pantothenate-synthetase enzyme. Among tested compounds, **13ba** and **13bb** showed the highest activity with MIC value of 29.19 and 6,16 μM against $H_{37}Rv$ strain as compared to iso-nicotinic acid hydrazide (MIC = 91.14 μM). The SAR studies (**Fig. 20**) revealed the importance of electron-withdrawing groups (EWG) on phenyl-piperazine ring to enhance anti-TB activity these analogues.

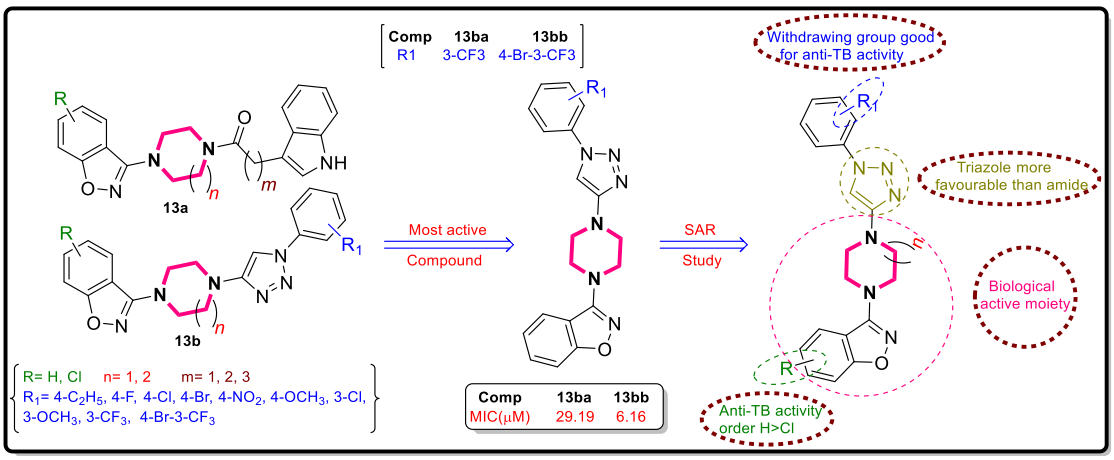

Figure 20 Indole and triazole tethered piperazin-1-yl/1,4-diazepan-1-yl)benzo[d]isoxazole conjugates (13a and 13b) with potent derivative (13ba and 13bb) and SAR study

In 2016, Miller and his team[38] designed and synthesized a novel series of imidazo[2,1-b]thiazole-5-carboxamides **(14, Fig. 21)** as potential anti-TB agents. These analogues inhibited MTB by arresting *QcrB* genes in MTB *$H_{37}Rv$* and *ATCC 25618* strains. Compared with biaryl ether aniline derivatives, compounds with pyrazine and piperazine subunits displayed better anti-TB activity with MIC of < 10 nM against replicating and drug-resistant MTB strain. These analogues were also exhibited less cytotoxicity in VERO cells line. Furthermore, most potent hybrid **14a** screened for QcrB mutants to target the bc1 complex and chosen for further study in *ex vivo* macrophages infected with the Erdman MTB strain. These active analogues have shown their potential against Gram-positive and four Gram-positive strains.

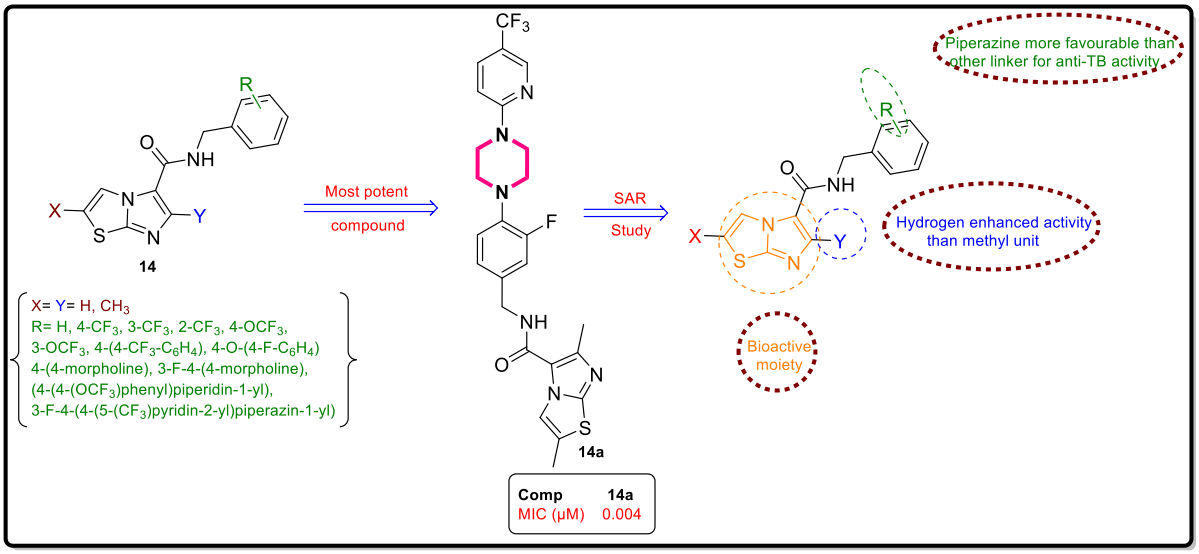

Figure 21 dibenzo[b, d]thiophene and imidazo[1,2-a]pyridine-3-carboxamides analogues (14) with potent derivative (14a) and SAR study

Based on rational drug design for anti-TB agents, Marvin J. Miller[39] synthesized a novel series of piperazino-1,3-benzothiazine-4-ones (pBTZ's) hybrids (**15, Fig. 22**) by incorporating imidazo-pyridine and cephalosporins in a single molecular framework. Compound **15a** exhibited the highest potency against the MTB *$H_{37}Rv$* strain in MABA[40]. Further, their evaluation in two specific 7H12, and GAS mycobacterial growth media, the hybrid **15a** exhibited good activity with the MIC value of 2.03 and 1.51 μM respectively, compared with first-line drug RIF (MIC = 0.05 and 0.04 μM) respectively. SAR studies (**Fig. 22**) indicated that acid protection affects the activity of cephalosporin-pBTZ pharmacophore. Moreover, these hybrids were found effective against Gram-positive bacteria with MICs of 0.2 μM and <0.003 μM against *M. vaccae* and *B. subtilis*, respectively.

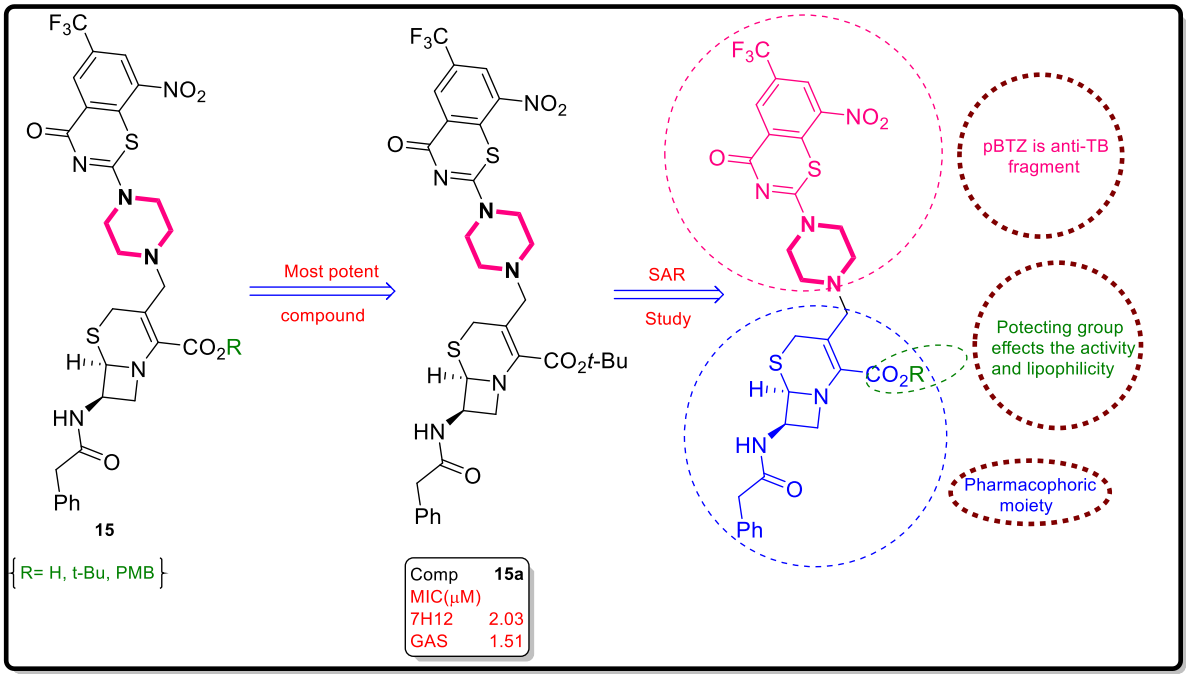

Figure 22 pBTZ's hybrids (15) with potent anti-TB molecule (15a) and SAR study

Using Asinex and Zinc collections, Vita et al.[41] developed a novel anti-TB pharmacophore model and selected 60 molecules through virtual screening to build an in-house library. All analogues displayed their *in vitro* anti-TB potential (MIC range of 5.46-133.6 µM) against MTB $H_{37}Ra$ strain using agar dilution method[42]. The results revealed that azole analogue **16a** exhibited significant inhibition with MIC value of 8.34 µM, and displayed high metabolic stability with the mixture of unmodified parent drug metabolites. SAR studies (**16, Fig. 23**) showed that the anti-TB activity largely depends on the position of chloro substitutions on phenyl piperazine ring. Additionally, the imidazole rings with phenyl and pyrrole substitutions have a negative impact on the anti-TB potency.

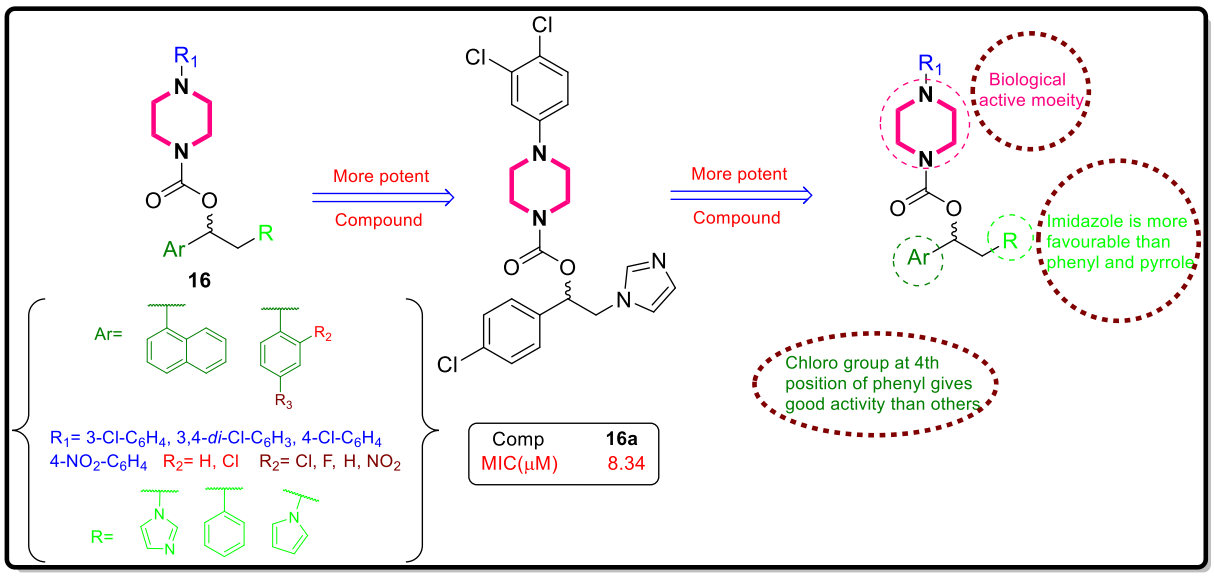

Figure 23 Piperazine analogues (16) with potent compound (16a) and SAR study

DNA gyrase and ATPase are the two crucial enzymes in MTB, and the fluoro-quinolones reported as anti-TB gyrase inhibitors against drug-resistant MTB strains[43,44]. Sriram et al.[45]designed and synthesized a series of quinolone and piperazine derivatives **(17, Fig. 24)**. The synthesized analogues were screened against MTB *$H_{37}Ra$* strain, *RAW 264.7* cells by using MTB DNA supercoiling and gyrase B assay[46]. Their*in vitro* data revealed that compound **17a** as a lead candidate with MIC and IC_{50} value of 3.45 µM and 0.29 µM against MTB H_{37}Ra strain, DNA gyrase enzyme supercoiling, respectively. Among these compounds, except nitro bearing once were found non-toxic against RAW 264.7 cell lines. SAR study (**Fig. 24**) revealed that thiourea linker and quinolone enhanced the MTB activity.

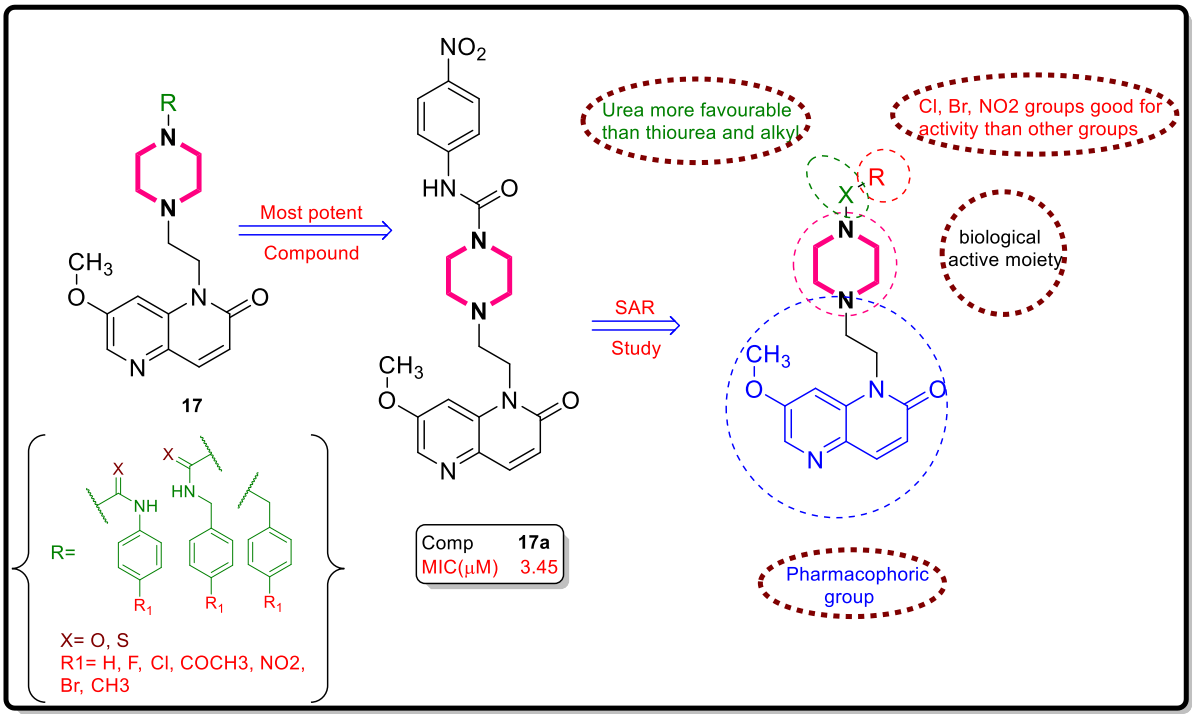

Figure 24 Quinolone and piperazine derivatives (17) with potent compound (17a) and SAR study

Castagnolo et al.[47] synthesized a novel series of pyrrole tethered piperazine and oxime/*sec*-amine derivatives as hybrids of BM212[48] and SQ109[49] with common topological distribution (**18a** and **18b**, **Fig. 25**). The substituted piperazine unit resulted in various potent analogues against *M. smegmatis*, *M. bovis* BCG and *M. aurum* strains and further tested against mc27000, MTB H_{37}Rav, MDR1 and MDR2 strains. The authors concluded that series is **18b** much active than series **18a**, with MIC value 1.58 μM against *mc27000* strain, 0.63, 1.58 μM against *H_{37}Rv* and MDR-1 TB respectively (**18ba**).

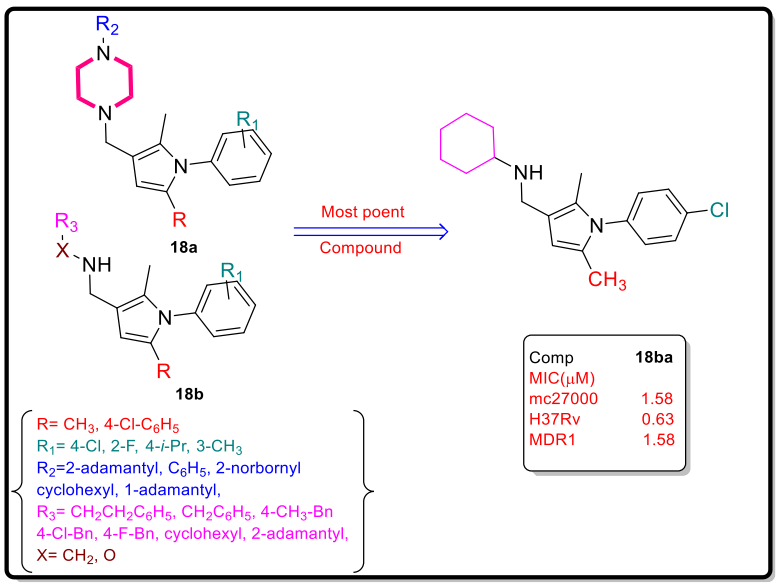

Figure 25 Pyrrole with piperazine and oxime/sec aminederivatives (18a and 18b) with potent compound (18ba) and SAR study

Oxazolidinone constituted an essential structure for various potent anti-TB agents, along with linezolid (anti-TB drug) and inspired Wang et al.[50], to synthesize and evaluate the anti-TB activity of its derivatives (**19, Fig. 26**) against MTB *$H_{37}Rv$ (ATCC 27294)* strain with piperazine moiety. The tested analogues showed potent anti-TB activity with the MIC range of 1.01–15.5 µM. Two compound **19a** and **19b** of the series revealed the most potent activity with 99 % growth inhibition against *MTB $H_{37}Rv$ (ATCC 27294)* strain at MIC 1.1 and 1.03 µM. The activities of both compounds were observed consistent with standard line olid drug. The SAR (**Fig. 26**) study defined the impact of piperazine substitution on anti-TB activity. Results revealed that the anti-TB activity of these derivatives enhanced with non-polar substitutions on piperazine.

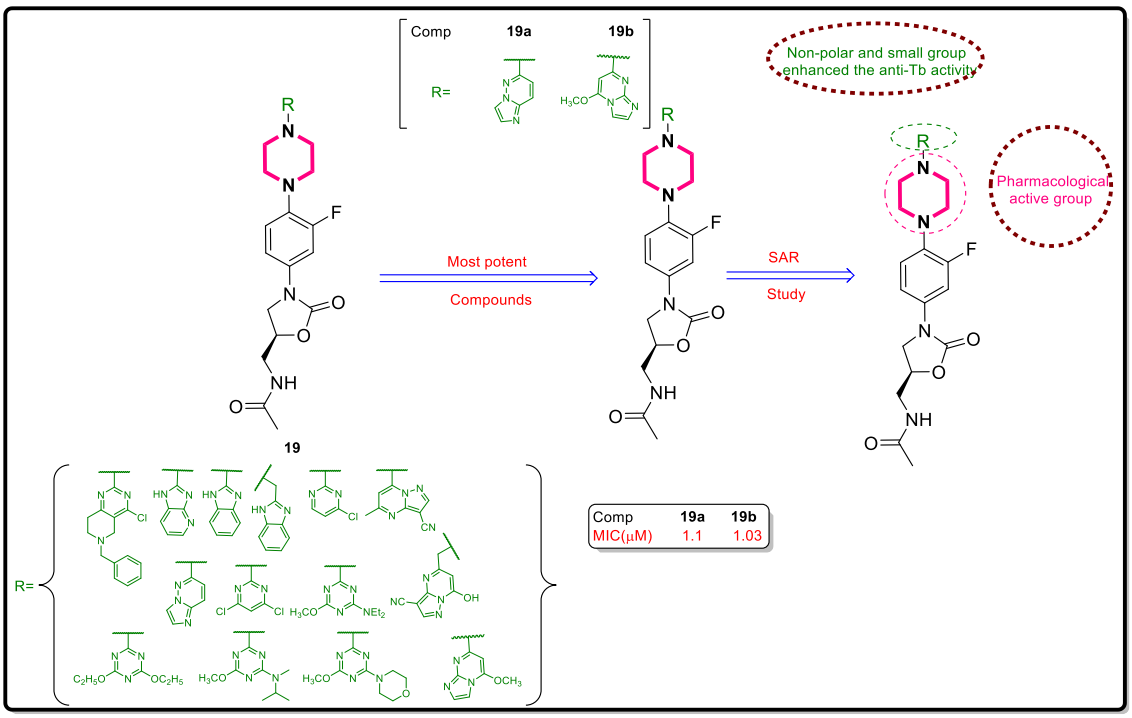

Figure 26 Oxazolidinone-piperazine derivatives (19) with potent compounds (19a and 19b) and SAR study

Similarly, inspired by diverse pharmacological properties of FQ[51], Suresh and colleagues[52]reported the synthesis and anti-TB activity of quinolone tagged piperazine analogues (**20, Fig. 27**) connected by a carbonyl linker. The result revealed that compound **20a** emerged as a most potent anti-TB agent against *MTB* $H_{37}Rv$ with MIC value of 7.32 μM, which was comparatively less than the standard drug RIF (MIC = 0.14 μM). SAR study (**Fig. 27**) concluded that the combination of branching at α-position of alkyl with piperazine appears to affect the anti-TB activity profile. Furthermore, alkyl substitutions on piperazine have a positive impact on anti-TB activity. Besides, these compounds were also found to exhibit better anti-bacterial activity against *S. aureus* and *E.coli* bacterial strains.

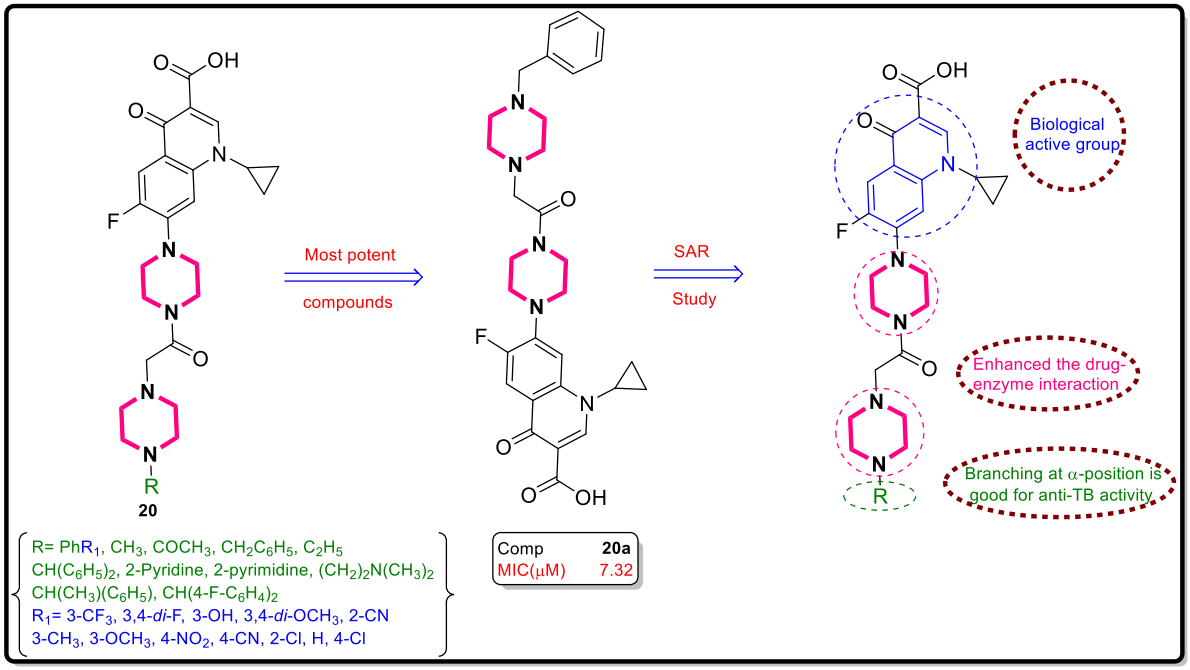

Figure 27 Quinolone-piperazine analogues (20) with most active derivative 20a and SAR study

Reddy et al.[53] reported the synthesis and anti-TB activity for the two series of benzofuran and benzo[d]isothiazole analogues (**21a and 21b, Fig. 28**) against *M. smegmatis* (MS), *M. tuberculosis* (MTB) strains using GyrB ATPase and DNA gyrase supercoiling assay. Most of the analogues displayed around 70% of the DNA supercoiling inhibition at MIC of 50 µM. However, compound **21ba** have exhibited the highest activity with IC_{50} and MIC value of 0.42 and 3.44 µM using EMB as a positive control (MIC = 0.66 µM). The presence of urea as a linker and chloro on the *o*-position of thiazole-phenyl ring generally found to enhance the anti-TB activity. The representative analogue (**21ba**) of this series displayed low toxicity with 20.2 % inhibition against mouse macrophage *RAW 264.7* cell line.

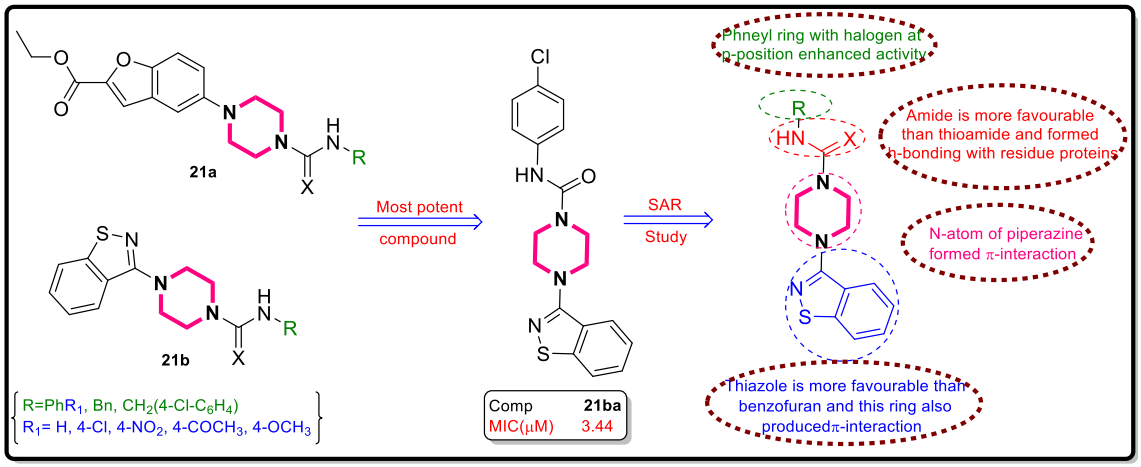

Figure 28 Benzofuran and benzo[d]isothiazole analogues (21a and 21b) with most active derivative (21ba) and SAR study

The anti-TB potential of piperazine ring was further improved by its coupling with substituted cinnamic acid and yielded novel analogues (**22, Fig. 29**) with MIC value of 6.28 μM[54]. The *in vitro* evaluation was performed against MTB *$H_{37}Rv$* strain using REMA plate assay and INH (MIC=2.84 μM) was used as reference drug. The results revealed that the role of cinnamic acid conjugation with piperazine in anti-TB activity improvement was established. The analogue **22a** bearing trifluoro-methane on phenyl piperazine ring exhibited less toxicity in a mammalian VERO cell line with selective index (SI) >10**.**

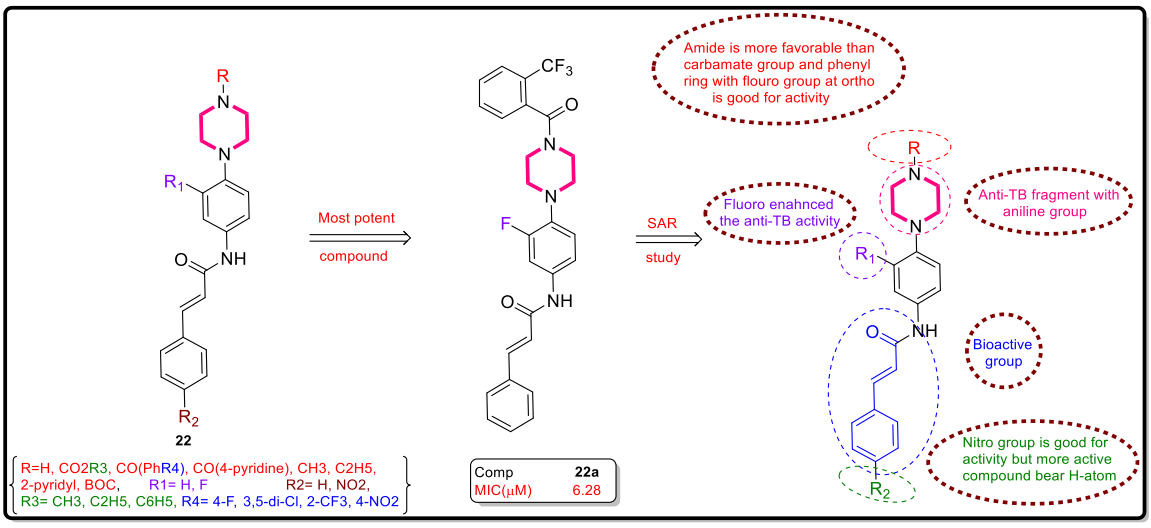

Figure 29 Cinnamic acid and piperazine analogues (22) with most active derivative (22a) and SAR study

Efforts conducted to evaluate the ability of piperazine as anti-TB agents by their integration with isoxazole nucleus weren't promising as most of the isoxazole-piperazine analogues **(23, Fig. 30)** demonstrated IC_{50} values >59 µM against MTB *$H_{37}Rv$* strain[55]. The most potent analogue **23a**, however, exhibited MIC value of 9.1 µM against MTB *$H_{37}Rv$* strain and INH (MIC= 2.62 µM) as reference standard using the MABA. Furthermore, compound **23a** demonstrated low toxicity with good SI against mouse macrophage cell lines (RAW264.7). SAR studies (**Fig. 30**) showed that the sulfonyl linker integrating phenyl and piperazine group exhibited considerable enhancement in the activity.

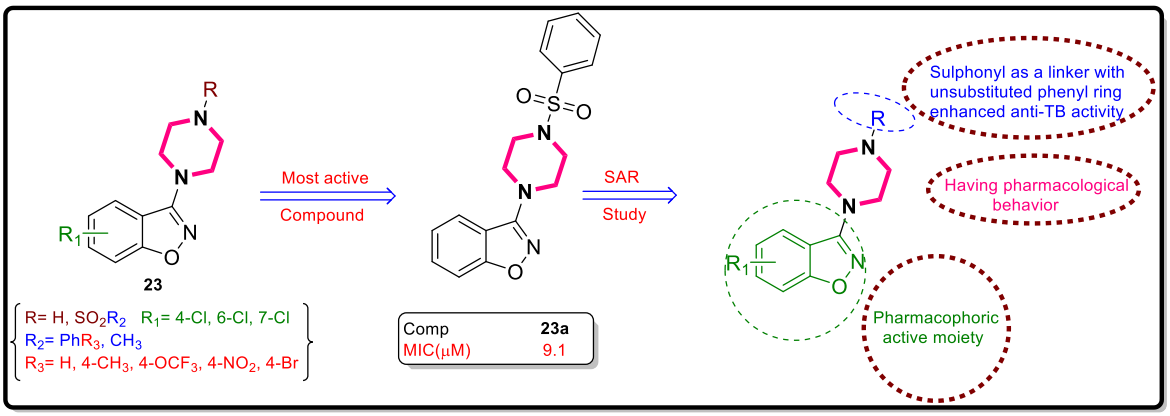

Figure 30 Isoxazole-piperazine derivatives (23)with most active analogue (23a) and SAR study

A novel series of thiazole-di-piperazine analogues (**24, Fig. 31**) as anti-TB agents were synthesized by Nagesh and co-workers[56]. The activity of this series against MTB *$H_{37}Rv$* strain was investigated using the MABA method. All active compounds displayed lower cytotoxicity profiles against *RAW 264.7* cell lines. The *in vitro* analysis revealed that the reported analogues displayed MIC range of 2.62 – 11.66 µM as compared to the standard reference drug INH (MIC =0.36 µM). SAR study (**Fig. 31**) represents the influence of the benzhydryl group in forming strong hydrogen bonding with specific targets. The prototype analogue **24a** bearing an N-methylthiazol-2-amine attached through propyl to benzhydryl piperazine exhibited superior activity with a MIC value of 2.62 µM.

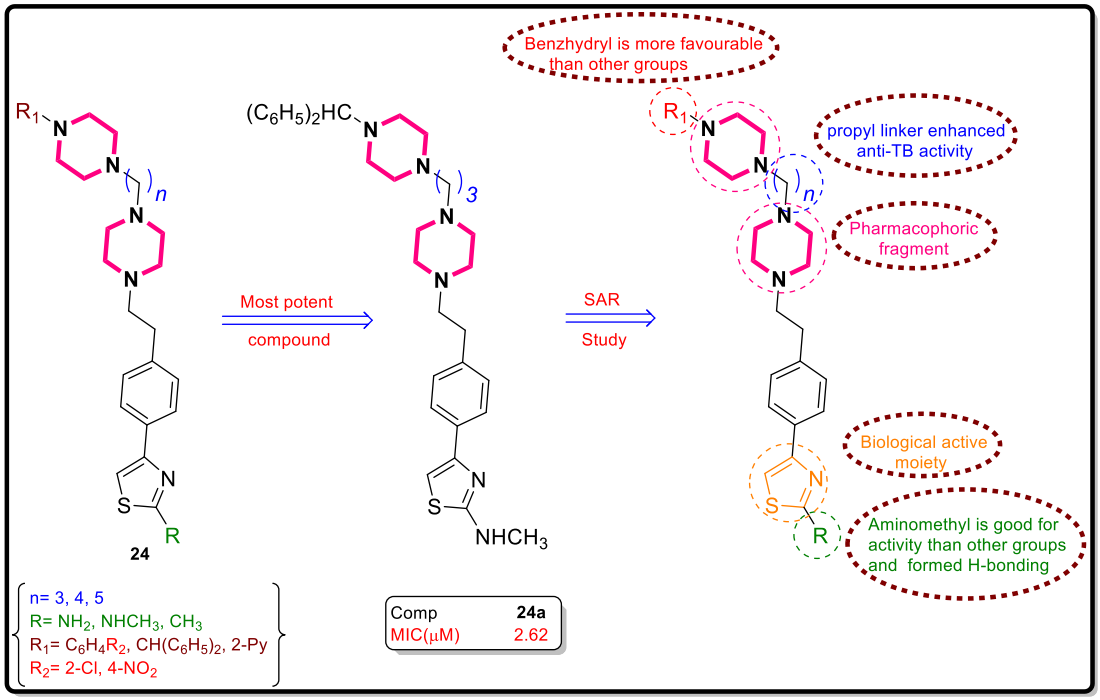

Figure 31 Thiazole-di-piperazine analogues (24)with most active derivative (24a) and SAR study

Makarov and his team[57] evaluated the anti-TB potential of Benzothiazinone derivatives (BTZ043) (**25, Fig. 32**) as cellular enzyme *DprE1* inhibitor[58] that has displayed superior activities against XDR and MDR strains of MTB. All the tested compounds showed anti-TB activity against MTB *$H_{37}Rv$* strain with the MIC range of 0.0004 to 0.66 µM using REMA assay. Majority of derivatives with cyclohexyl methyl substitutions on piperazine enhanced the anti-TB activity (**Fig. 32**). Compound **25a** emerged as the most potent molecule with potent anti-TB activity (MIC <0.42 µM) and low cytotoxicity in a murine model. Besides, the cytotoxicity study showed that most of the compounds were found non-toxic against the *HepG2* human cell line.

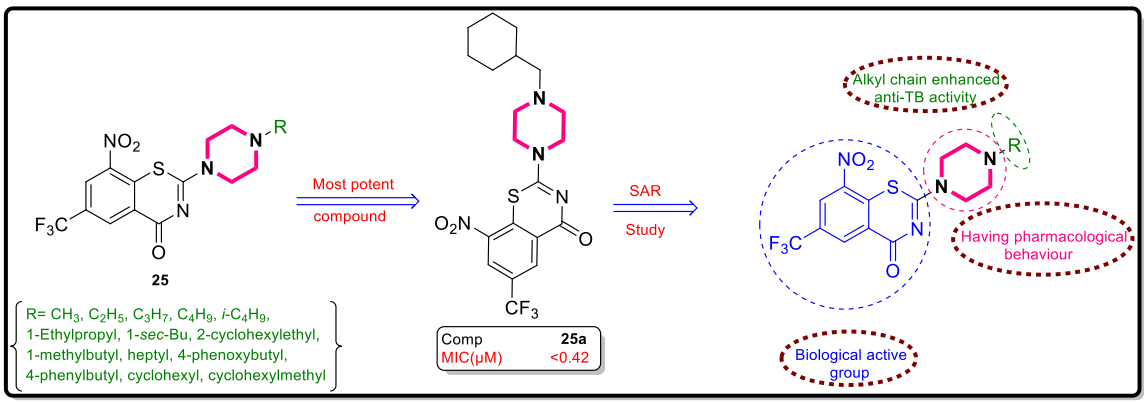

Figure 32 Benzothiazinone analogues (25)with most active derivative (25a) and SAR study

Kantevari et al.[59] designed and synthesized various piperazine analogues by coupling it with thio-semicarbazone in a single pharmacophore (**26, Fig. 33**). These analogues were biologically evaluated for their *in vitro* MTB activity against $H_{37}Rv$ strain using the agar dilution method. The *in vitro* analysis showed that all analogues exhibited moderate anti-TB activity with MIC value range of 6.36-58.23 μM, compared with the standard INH (MIC = 0.73 μM). Compounds **26a** and **26b** showed good activity among all the tested compounds with MIC value of 6.57 and 6.36 μM against *$H_{37}Rv$* strain. Further, the active analogues showed 31% cytotoxicity toxicity against *HEK-293* T cell. SAR studies (**Fig. 33**) concluded the positive influence of electron-donating groups on the phenyl ring of piperazine that remarkably enhances the anti-TB activity.

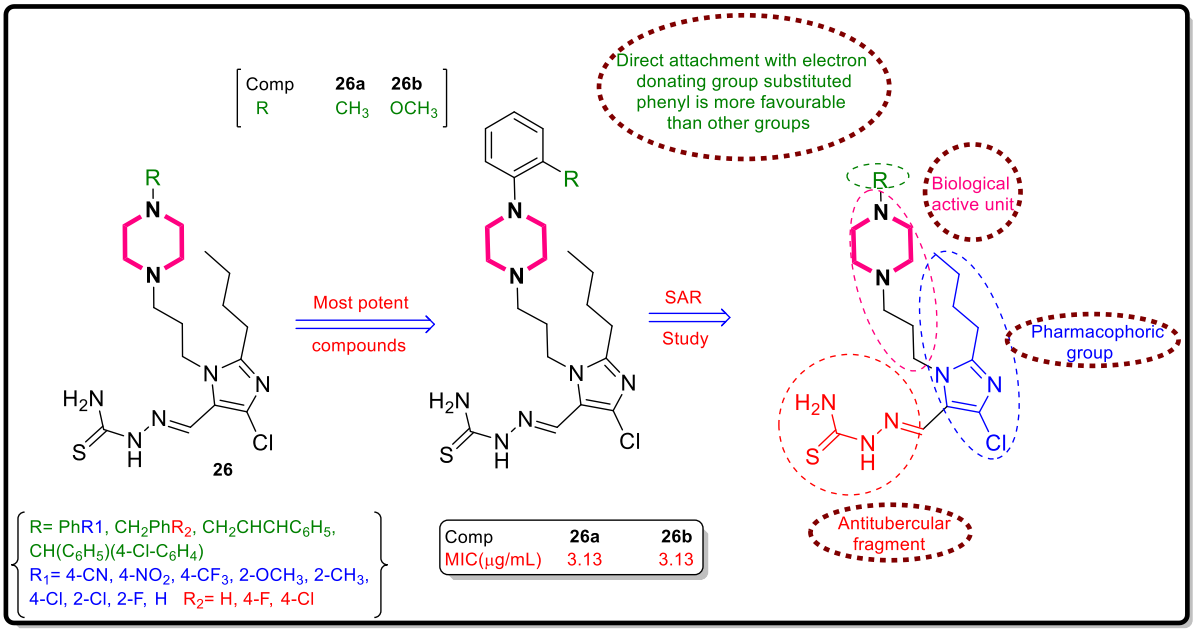

Figure 33 Thiosemicarbazone–piperazine analogues (26)with most active derivatives (26a and 26b) and SAR study

Thiazolone-tetrazole analogues (**27, Fig. 34**) synthesized by Chauhan and his colleagues[60] exhibited good to excellent anti-TB activity against MTB *$H_{37}Rv$* strain. Compounds **27a-d** of this series, displayed much potent anti-TB activity (MIC = 3.08, 3.01, 2.62 and 2.51 µM) against MTB *$H_{37}Rv$* strain as compared to the EMB (MIC = 9.78 µM), respectively. Further, all these active compounds considered to be safe as they showed non-cytotoxicity against *VERO* cells. SAR studies demonstrated that ferrocene and para-substituted phenyl derivatives showed better anti-TB activity than aryl or hetero aryl-substituted derivatives, as shown in **Fig. 34**.

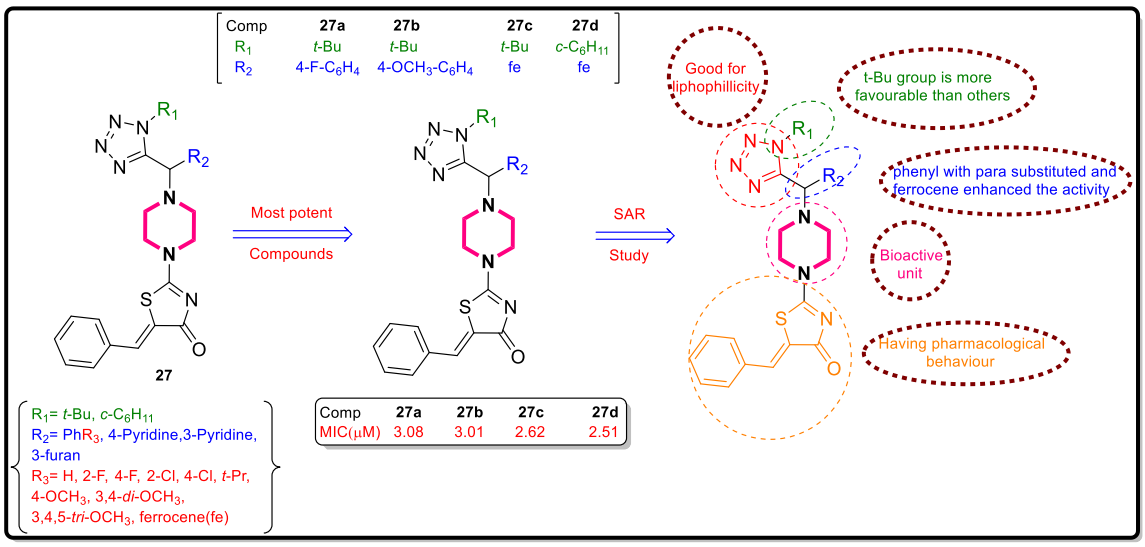

Figure 34 Thiazolone-tetrazole analogues (27)with active derivatives (27a-d) and SAR study

Rotta et al.[61]designed and synthesized a series of piperazine analogues (**28, Fig. 35**) and screened them to evaluate their IC_{50} value against *MtInhA* strain[62]. Compound **28a** with electron-rich substitutions on benzyl ring exhibited good *MtInhA* inhibition (IC_{50} of 0.22 μM), as compared to electron-deficient substituent analogue, respectively. The effect of different substitution revealed the basicity enhancement on carbonyl group and maintaining the hydrophobic environment around the benzyl ring. The methyl substituent at 4th position in Compound **28a** is more preferred over 3rd position. Moreover, docking studies demonstrated that substitution at 2nd position hindered in the cavity of *Met103, Tyr158, and Met161* which residues of *MtInhA*. Among all screened compound **28a** with some active analogues were further screened against MTB *$H_{37}Rv$* strain.

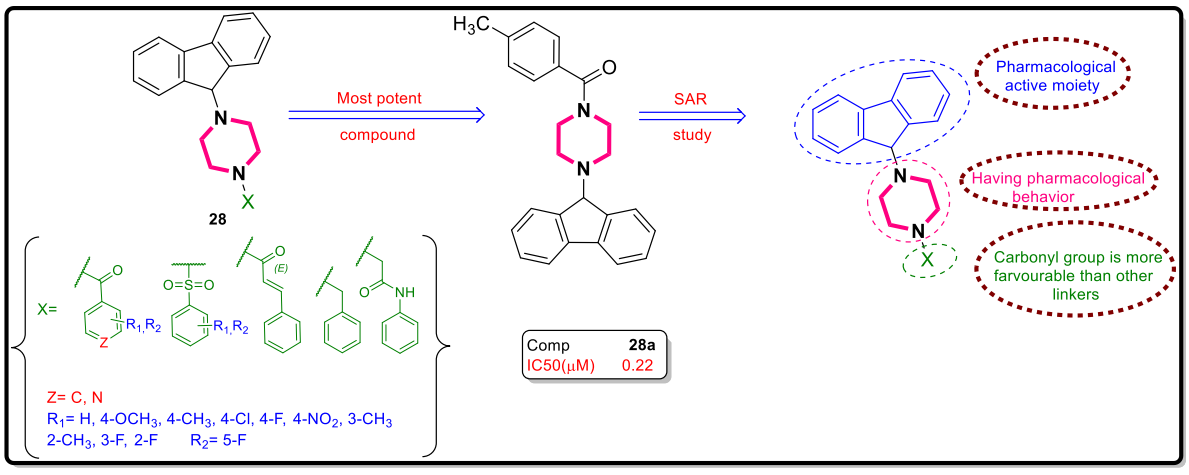

Figure 35 Piperazine derivatives (28)with most active derivative (28a) and SAR study

Singh et al.[63] reported the synthesis and anti-TB activity of nitrothiophene/nitrofuran tethered piperazine moiety and the resulted compounds **(29a** and **29b, Fig. 36**) were evaluated against MTB *H37Rv* strain using micro-broth dilution method. The anti-TB activity of these analogues was tested against resistant (RIF and MDR) and non-replicating (NRP) strains of MTB. The results revealed that compound **29aa** displayed the most potent activity against MTB *H37Rv* with (MIC = 0.0072 µM), MDR RIF (MIC = 0.072 µM) and (MIC = 0.029 µM), respectively. Further compound **29ba** exhibited more potent activity against NRP compared to the standard drug RIF. SAR study (**Fig. 36**) demonstrated that the sulfonyl group with bulky substitutions on the *p*- position of phenyl ring are most favourable to enhance the anti-TB activity. However, the replacement of piperazine with morpholine or piperidine ring negatively affects the activity.

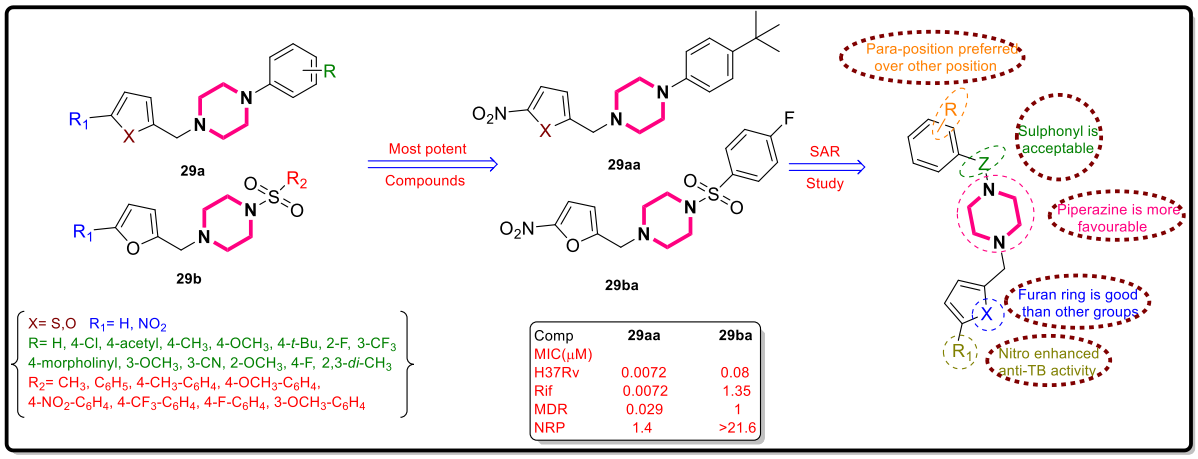

Figure 36 Piperazine with nitrothiophene/nitrofurany analogues (29a and 29b)with active derivatives (29aa and 29ba) and SAR study

Penta and co-workers[8] reported the synthesis and the anti-TB activity of newly synthesized pyridol[3,4-b]indole-piperazine derivatives, modified by coupling of indole and piperazine moieties (**30, Fig. 37**). The withdrawing groups like chloro (-Cl) substitutions on *o*- and *m*-positions were favourable and displayed the highest anti-TB activity with an excellent selective index. Further, the phenyl ring replacement with pyridine or benzyl moieties also enhances the anti-TB activity to a certain extent. Compounds with MIC value less than 10.1 µM were further evaluated for their *in vitro* analysis against MTB *H37Rv* strain using MABA. The results revealed that compound **30a**

demonstrated potent inhibitory activity with MIC of 2.99 µM, good SI (>33.3) and less toxic against *VERO* cell lines (CC_{50}> 99.72 µM).

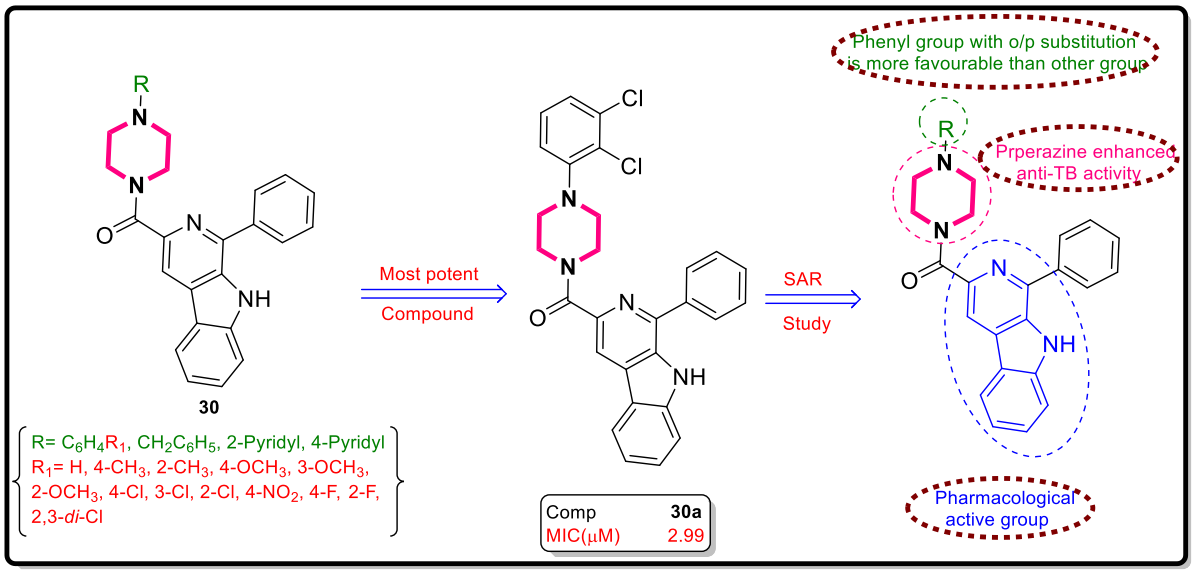

Figure 37 Pyridol[3,4-b]indole-piperazine derivatives (30)with most active derivative (30a) and SAR study

In literature, phenanthridine-piperazine analogues were previously reported as anti-TB agents inspired from that Naidu et al.[64] reported the discovery of phenanthridine-piperazine compounds (**31a** and **31b, Fig. 38**) as anti-TB agents. All synthesized analogous showed their MTB activity with a range of MIC value of 3.39-111.48 µM against MTB *$H_{37}Rv$* strain using MABA. Compounds **31aa, 31ab, and 31ba** demonstrated promising anti-TB activity with MIC value of 4.23, 3.48 and 3.39 µM, without showing *in vitro* toxicity against R*AW264-7* cells. Further, the SAR study (**Fig. 38**) revealed that sulphonamides with phenyl substitutions are positively influenced anti-TB activity.

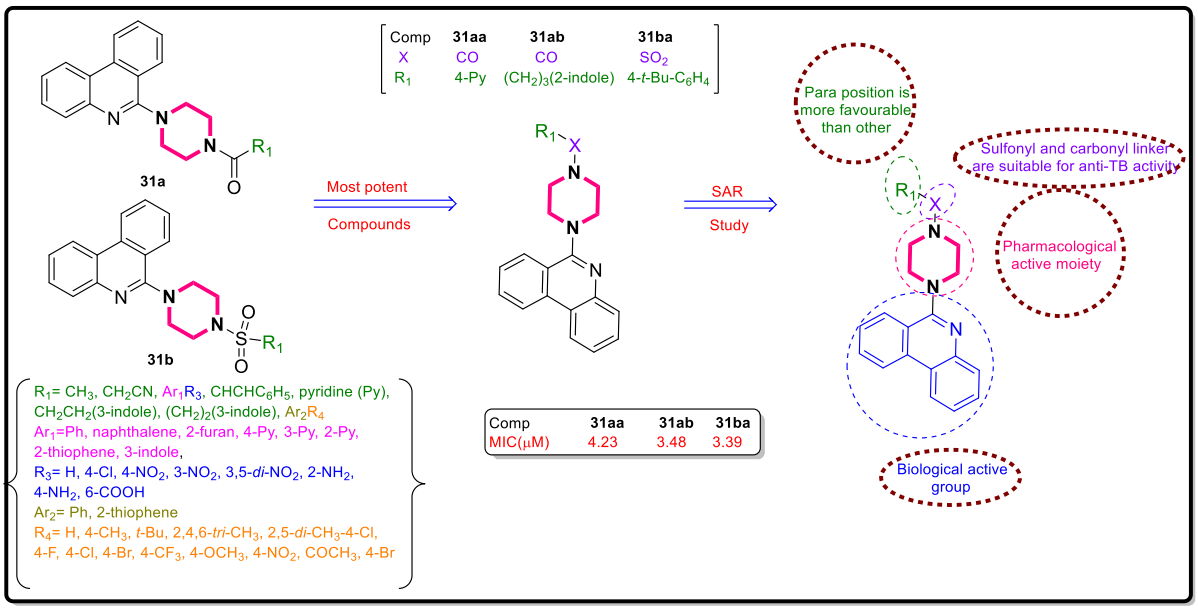

Figure 38 Phenanthridine-piperazine analogues (31a and 31b) with active derivatives (31aa, 31ab, and 31ba) and SAR study

In another interesting study, Chollet et al.[65]synthesized a series of the Genz-10850 compounds with piperazine, amide, aryl substitutions on fluorene ring (**32, Fig. 39**). The synthesized analogues were studied for their anti-TB activity against MTB $H_{37}Rv$ strain using MABA technique[66]. Compound **32a** was found to be the most potent compound with MIC value of 11.0 μM compared to the positive control INH (MIC= 0.4 μM). Further, SAR study (**Fig. 39**) revealed that the amide group on piperazine significantly enhanced the activity by forming hydrophobic interactions with receptor sites. The analogue with hexyloxy chain substituent on fluorene moiety showed good anti-TB activity. *In silico* studies revealed the potent interactions of these compounds with InhA enzyme.

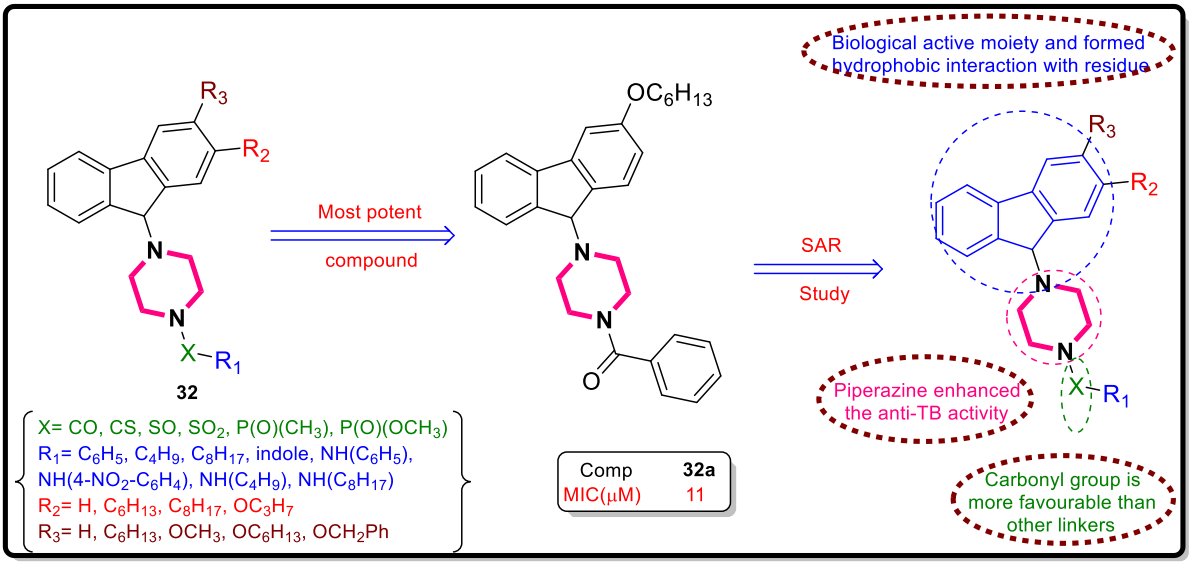

Figure 39 Piperazine-fluorene hybrids (32) with most active derivative (32a) and SAR study

Medapi et al.[67] reported piperazine and 4-aminoquinoline in a single pharmacophore, and the resultant derivatives (**33, Fig. 40**) were evaluated for their anti-TB activity. The synthesized analogues were screened for *in vitro* study against *RAW 264.7* cell lines, *GyrB*, *DNA gyrase supercoiling*, MTB *$H_{37}Rv$* strain, and cytotoxicity. Compounds **33a-c** have shown GyrB inhibition with IC_{50} values of <1 μM. From the results, compound **33c** considered as a lead compound of this series with MIC value of 0.86, 3.3 μM against mycobacterial *GyrB* and MTB *$H_{37}Rv$* strain. SAR study (**Fig. 40**) proved the positive impact ethyl piperazine ring on the anti-TB activity. Further, computational studies proved the molecular interaction responsible for their potent inhibitory activity.

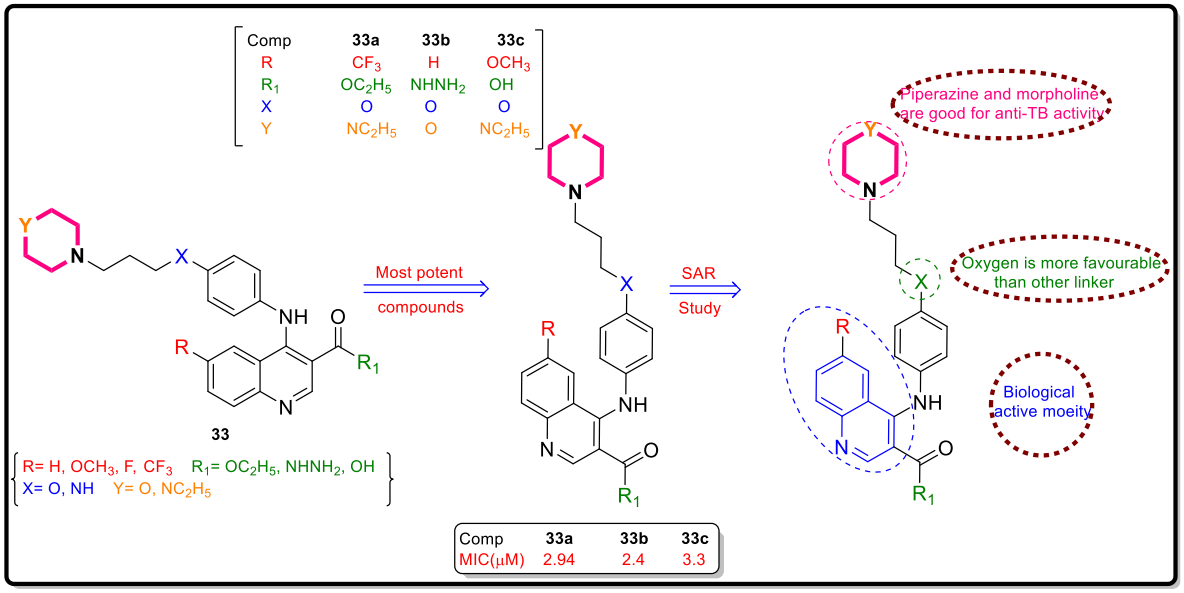

Figure 40 Piperazine-4-aminoquinoline analogue (33) with active derivatives (33a-c) and SAR study

In 2015, Nair et al.[68] synthesized a series of novel compounds and evaluated anti-TB activity against MDR-TB strain using middlebrow 7H10 agar solid growth medium. The results revealed that the compound **34** (**Fig. 41)** exhibited potent inhibitory activity with MIC of 2.39 μM against the tested strains. Compound **34** was subsequently tested in conjunction with PA-824 (mycolic acid synthesis inhibitor), and combination therapy displayed superior efficacy against MDR-MTB. The SAR study showed that the anti-TB activity was decreased with fluorine substitution on phenyl ring. Furthermore, the analogue with pyrazole substituent showed better results compared to their pyrrole (MIC = 9.6 μM).

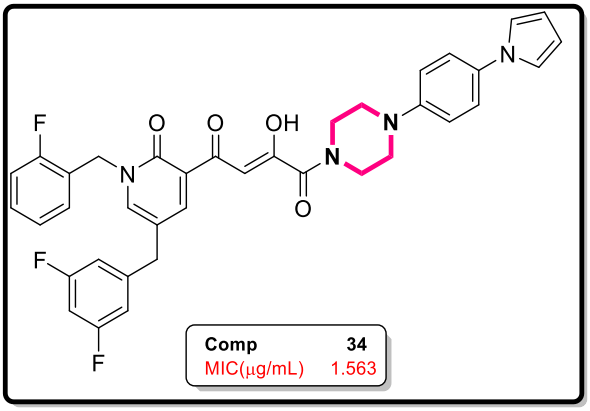

Figure 41 Potent compound (34) with MTB activity

Wang et al.[69] disclosed the synthesis of a series of Cf derivatives with N-substituted piperazine (**35, Fig. 42**) as anti-bacterial and anti-TB agents. They evaluated these analogues for their *in vitro* anti-TB and anti-bacterial activity against MTB $H_{37}Rv$ and Gram-positive and Gram-negative strains using MABA method. Among all, compound **35a** with a *para*-substituted methoxy group was the most potent compound with MIC value of 2.2 μM, as compared to the positive control Cf (MIC= 1.5 μM). In addition, the active compound has also displayed potent inhibitory activity against MRSA and *P. aeruginosa* with MIC range of 0.13–0.07 μM, respectively. The SAR study (**Fig. 42**) showed that the presence of *p*-methoxy substitution at the benzyl group which in turn connected with piperazine is responsible for enhanced the anti-TB activity.

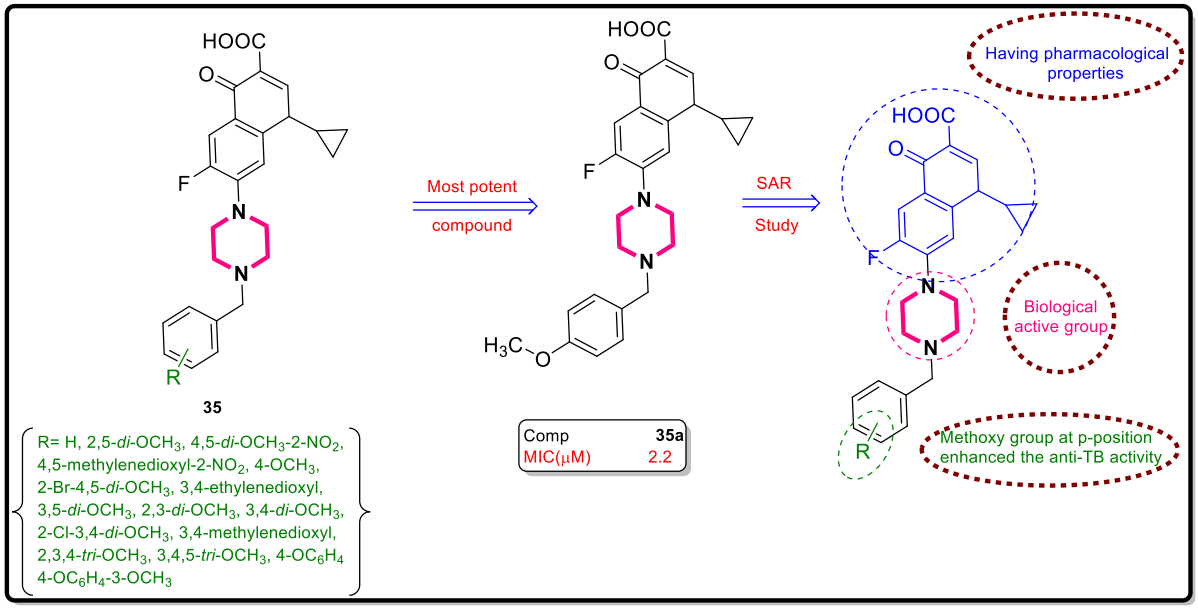

Figure 42 CPFX analogues with N-substituted piperazine (35) with most active derivative (35a) and SAR study

Patel and co-workers[70] synthesized a series of s-triazines-quinazoline hybrids by conjugating *s*-triazine, quinazoline, and piperazines or piperidines (**36, Fig. 43**) in a single molecular framework and evaluated their anti-TB potential against MTB *H37Rv* strain. Among the series tested, compound **36a** showed excellent anti-TB activity with MIC value of >9.79 µM, as compared with PZA (MIC= 50.76 µM) using BACTEC MGIT and L. J. agar dilution method. The SAR study (**Fig. 43**) revealed that the EWG substituent enhanced the anti-TB activity as compared to other substituent and the heterocyclic piperazine group positively influence the anti-TB activity.

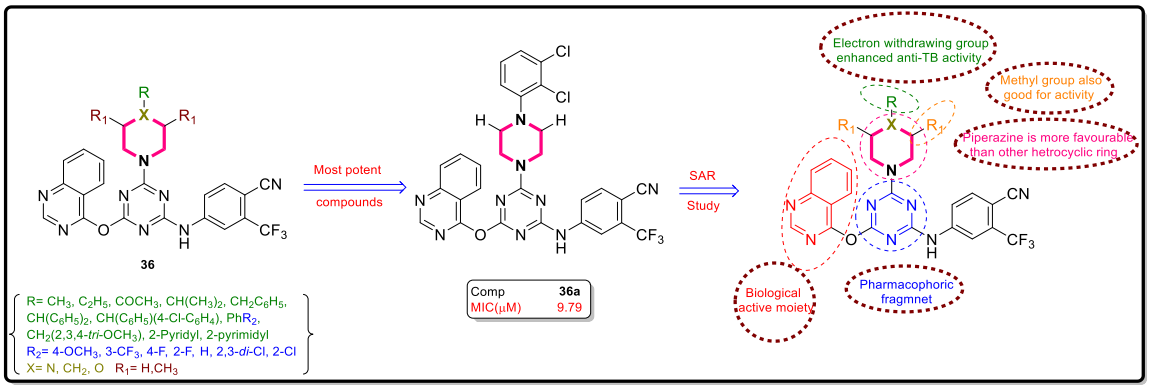

Figure 43 s-triazines-quinazoline-piperazine/piperidines (36) with active derivative (36a) and SAR study

Another example containing pharmacophoric synthesis of benzoylmethylenethio-1,3,4-thiadiazole (**37, Fig. 44**) with anti-bacterial active quinolone moiety. Agrawal et al.[71] synthesized a new class of quinolone-thiadiazole analogues and evaluated them for anti-TB activity *in vitro* good to moderate inhibitory activity with MIC value range of 0.82-16.73 µM, compared to the INH (MIC= 10.93 µM). Compounds **37a-c** have shown maximum inhibition against MTB *H37Rv* strain with MIC value of 1.67, 0.82 and 1.68 µM respectively, with low cytotoxicity. Furthermore, these active compounds reported good gram-positive and poor gram-negative activity than Cf and norfloxacin (NRFX). The SAR study (**Fig. 44**) described that electron-withdrawing substituents at phenyl ring are preferable over electron-donating groups (EDG) at phenyl ring to inhibiting the MTB strain.

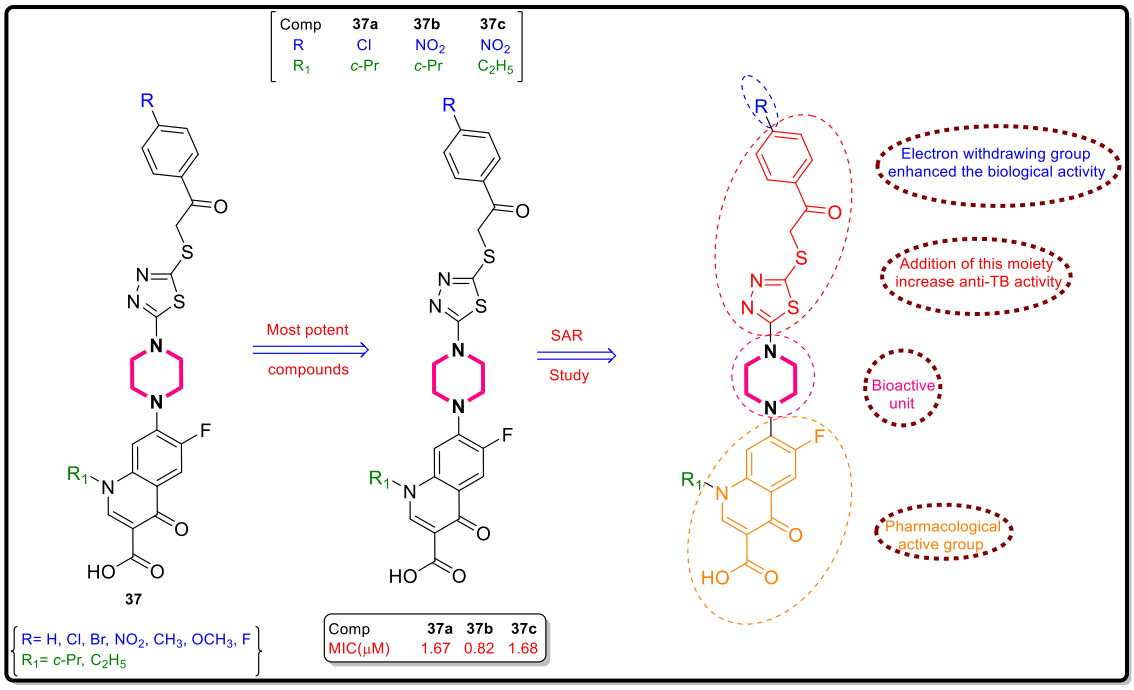

Figure 44 Benzoylmethylenethio-1,3,4-thiadiazolen analogues (37) with active derivatives (37a-c) and SAR study

A novel series of phenanthridine tagged piperazine (**38, Fig. 45**) and substituted triazoles were synthesized and evaluated for their biological activities by Nagesh et al.[72]. The synthesized conjugates were evaluated as anti-TB agents against MTB *H37Rv* strain using the MABA method[73]. Compound **38a**, a prototype of the series, exhibited good *in vitro* anti-TB activity (MIC = 3.22 µM) against MTB *H37Rv* strain, comparable to the standard drug INH (MIC = 2.62 µM), respectively.

Besides, active analogues showed non toxicity against *RAW264.7* cell line (MIC = < 11 µM). The SAR study (**Fig. 45**) revealed that the presence of sulfonyl substitution on triazole connected to piperazine ring displayed considerably higher potency than that of unsubstituted phenyl-triazoles.

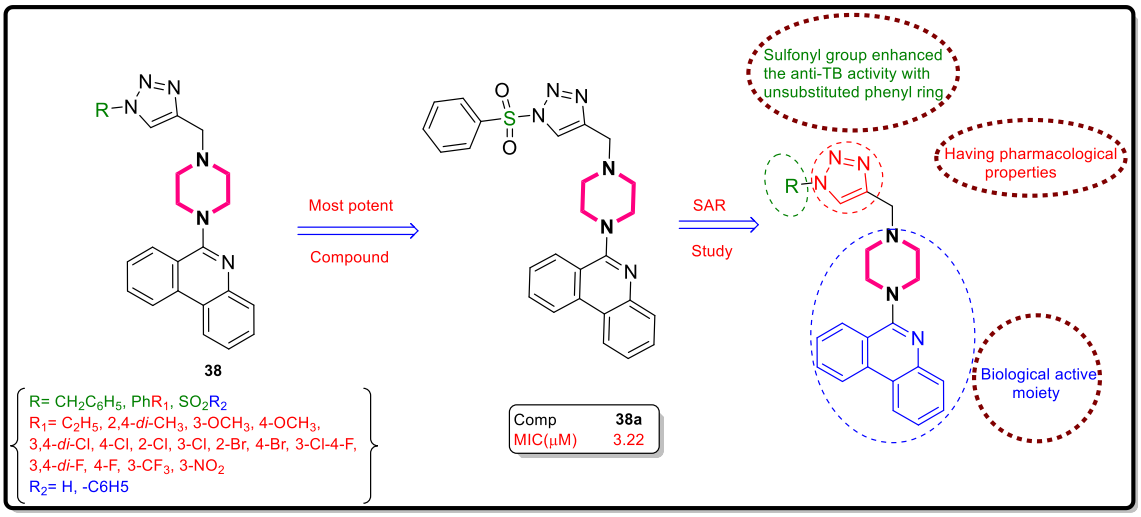

Figure 45 Phenanthridine-piperazine and triazole analogues (38) with most active derivative (38a) and SAR study

Further, extending the scope of the anti-TB potential of BM212, linezolid, and PH-027, Kamal et al.[74] synthesized two series of hybrid (**39a** and **39b**, **Fig. 46**) molecules by fusing all these three active scaffolds into a single molecular framework. All these analogues were evaluated for their *in vitro* study, against MTB $H_{37}Rv$, MTB, *RifR* and MTB XDR using MABA technique. The evaluated hybrids showed potent anti-TB activity with the ranges from 2.84 to > 8.61 µM that was comparable to the positive control linezolid (2.3 µM). Among all, the compound **39ba** has shown the highest activity with MIC value of 2.84, 5.68 and 11.37 µM against MTB $H_{37}Rv$, MTB *RifR* and MTB XDR-1 respectively. From SAR analysis (**Fig. 46**) it was found that the pyridyl/1-methyl-1H-imidazol-5-yl group substituted triazole hybrids at the 4th position displayed excellent activity in contrast to other groups.

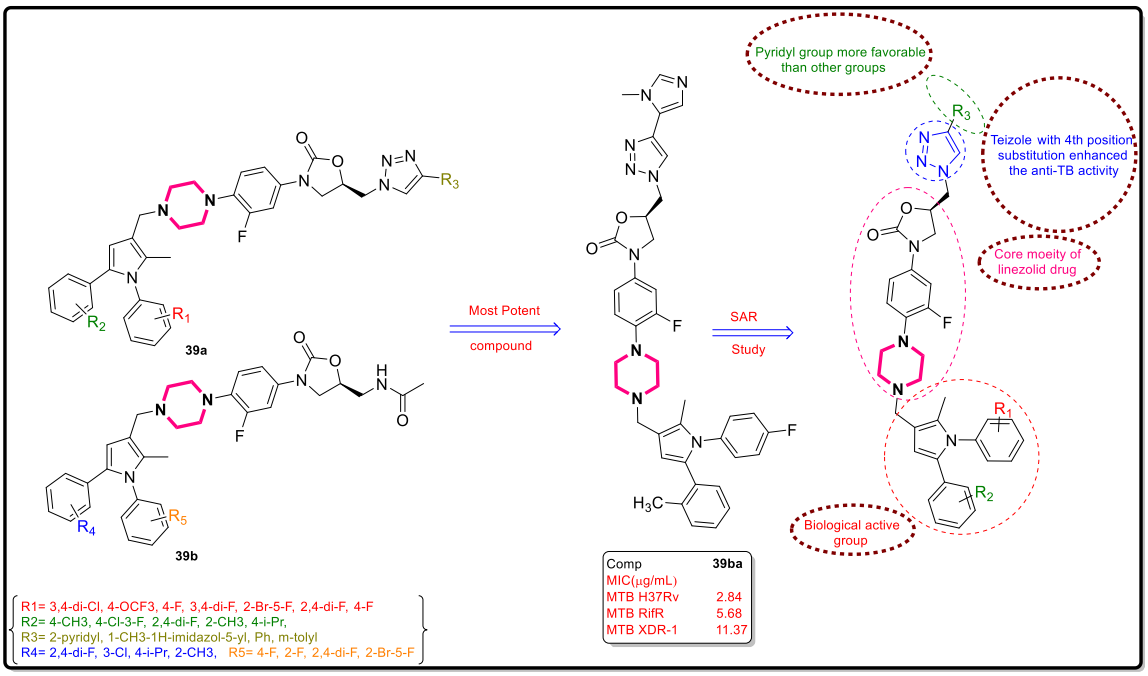

Figure 46 Active piperazine analogues (39) with most active derivative (39a) and SAR study

Sheu et al.[75] developed a library of FQ derivatives (**40, Fig. 47**) and investigated their anti-TB activity against MTB growth. All derivatives were assessed for their *in vitro* evaluation at a concentration of 11.4-15.9 µM; some of the compounds showed 100% MTB inhibition. The *in vitro* study revealed that the compound **40a** showed higher potency against MTB $H_{37}Rv$ strain with MIC, EC90 value of 3.9, 14.3 µM and selective index (SI)>40. The active analogues were found non-cytotoxic against *VERO* cell line. The SAR studies (**Fig. 47**) suggest that the hydroxy (-OH) substitution greatly influence anti-TB activity rather than other ethoxy and amine groups.

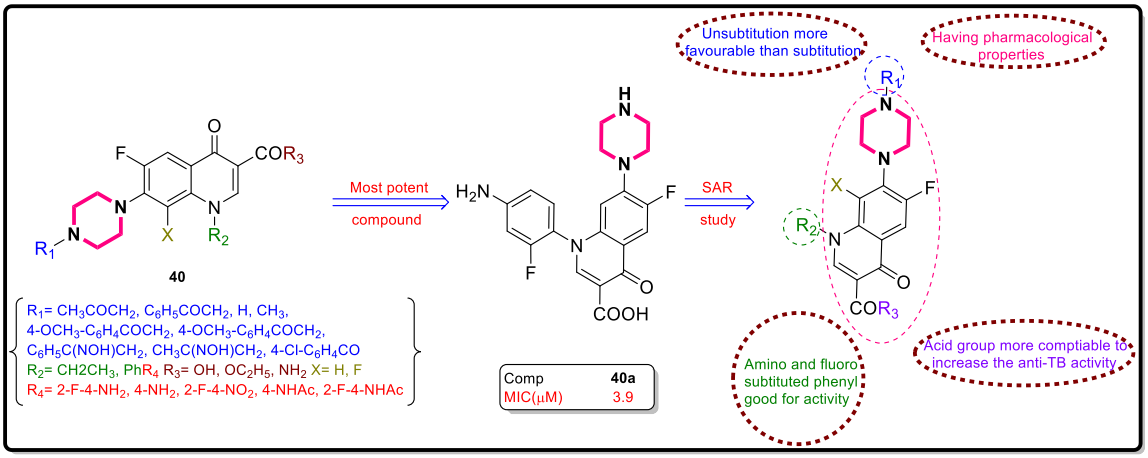

Figure 47 FQs (40) with most active derivative (40a) and SAR study

Sriram and colleagues[76]designed and synthesized a series of mannich-based isatin tagged piperazine hybrids (**41, Fig. 48**) and discussed their anti-HIV, anti-HCV, and anti-TB activities. The results suggested that compound **41a** showed most prominent activity (MIC= 1.91 µM) against MTB *$H_{37}Rv$ ATCC 27294* strain using the MABA method as compared to standard Cf. Other piperazine hybrids displayed the encouraging activity against *MT-4* and *CEM* cell lines with a good half maximal effective concentration (EC_{50}) value of 11.50 µM. The SAR study (**Fig. 48**) revealed that piperazine substituted isatin derivative shown promising anti-TB activity.

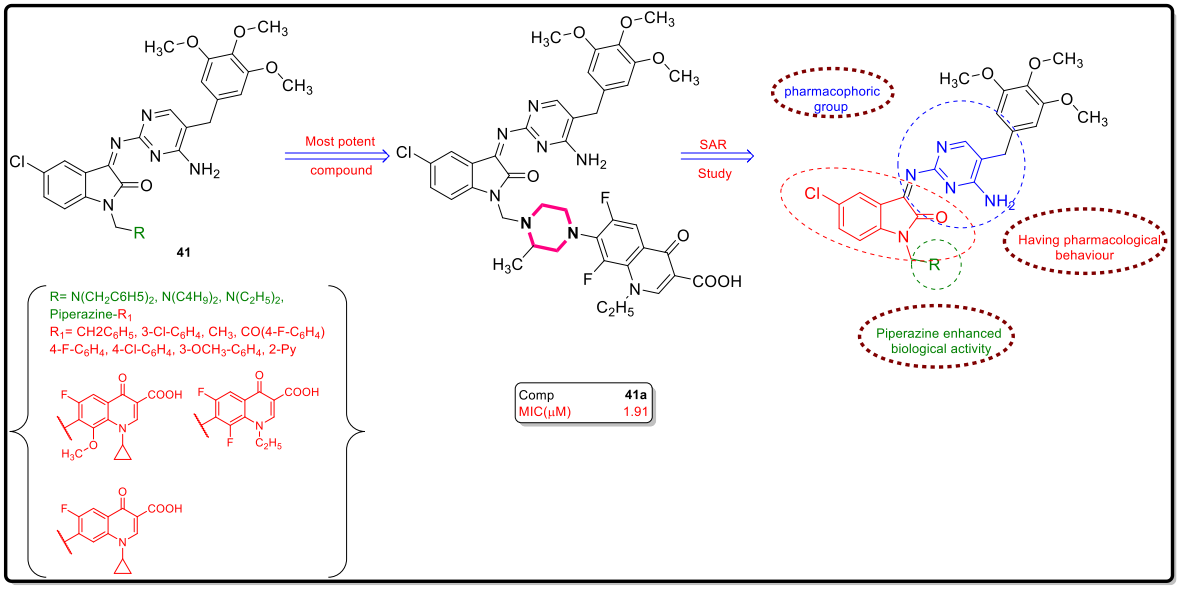

Figure 48 Isatin-piperazine hybrid derivatives (41) with most active derivative (41a) and SAR study

Patel and group[77] reported the synthesis of a series of novel 2-(4-cyano-3 trifluoromethylphenylamino)-4-(quinoline-4-yloxy)-6-(piperazinyl/piperidinyl)-s-triazine derivatives (**42, Fig. 49**) by modifying quinolone and phenyl ring. The synthesized compounds were evaluated for anti-TB activity against eight bacterial, four fungal and one MTB strain. Among the tested compounds, **49a-e** exhibited 99% of inhibition against MTB *$H_{37}Rv$* strain at MIC of 4.56, 17.75, 38.55, and 83.68 µM, respectively. Further, the SAR study (**Fig. 49**) has evidenced that the anti-TB activity has been depended on dimethyl, alkoxy, and halogen substitutions at piperazine/phenyl piperazine rings. Moreover, these compounds have displayed potent anticancer activity against prostate (*DU-145*) cancer cells.

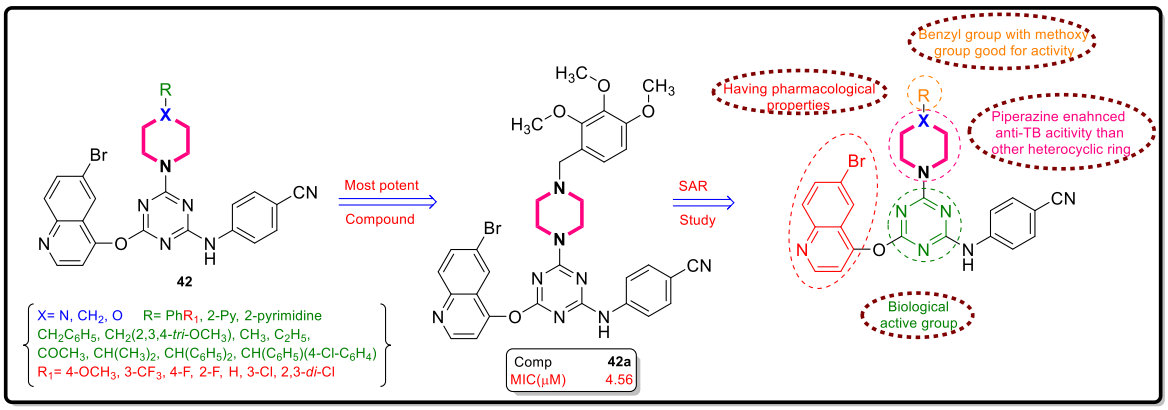

Figure 49 Piperazine/piperidine-triazine analogues (42) with most active derivative (42a) and SAR study

Shindikar et al.[78] synthesized a series of FQ based derivatives (**43, Fig. 50**) evaluated *in-vivo* anti-TB activity against MTB *$H_{37}Rv$* infected swiss albino mice. The animals were monitored for survival rate by considering spleen weights, gross lung lesions, and colony-forming units (CFUs), using sparfloxacin as positive control drug. Among the series tested, compound **43a** showed 100% survival, lack of lung lesions and the most effective 75% inhibition of CFUs. The SAR study (**Fig. 50**) explained that amide linker connected to piperazine ring enhanced the anti-TB activity as compared to Schiff base linker and unsubstituted piperazine suitable for activity.

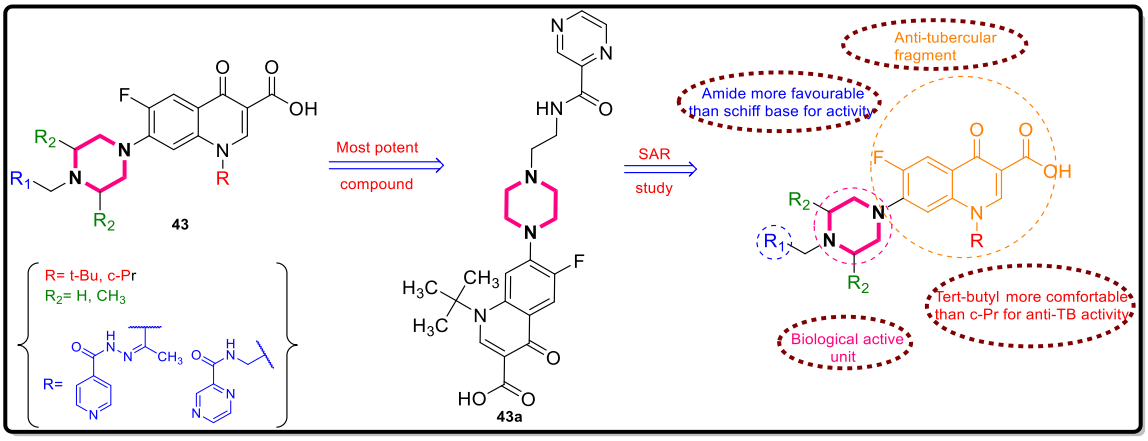

Figure 50 FQ-piperazine derivatives (43) with most active derivative (43a) and SAR study

Phenazines class of compounds (Clofazimine, B746 and B4157) have been reported as promising anti-TB agents. Kamal and his colleagues[79] designed and synthesized a series of a novel phenazine conjugates connected phthalimido and naphthalimido moieties through piperazine (**44, Fig.**

51). The synthesized analogues were analysed for their *in vitro* anti-TB activity against *$H_{37}Rv$ ATCC 27294, avium ATCC 49601, intracellular ATCC 13950* and clinical isolate MTB strains by diffusion assay. Compounds **44a** and **44b** from phthalimide–phenazine series have shown highest activity against all MTB strains along with potent inhibition against clinical resistant isolates of MTB as compared to the reference drug INH (MIC= 1.82 μM). The SAR studies (**Fig. 51**) demonstrated that phthalimide–phenazine conjugate with an increase in alkyl spacer chain to five and six shown improved activity compare to phthalimide–naphthalimido and which are connected through piperazine linker to improve its solubility.

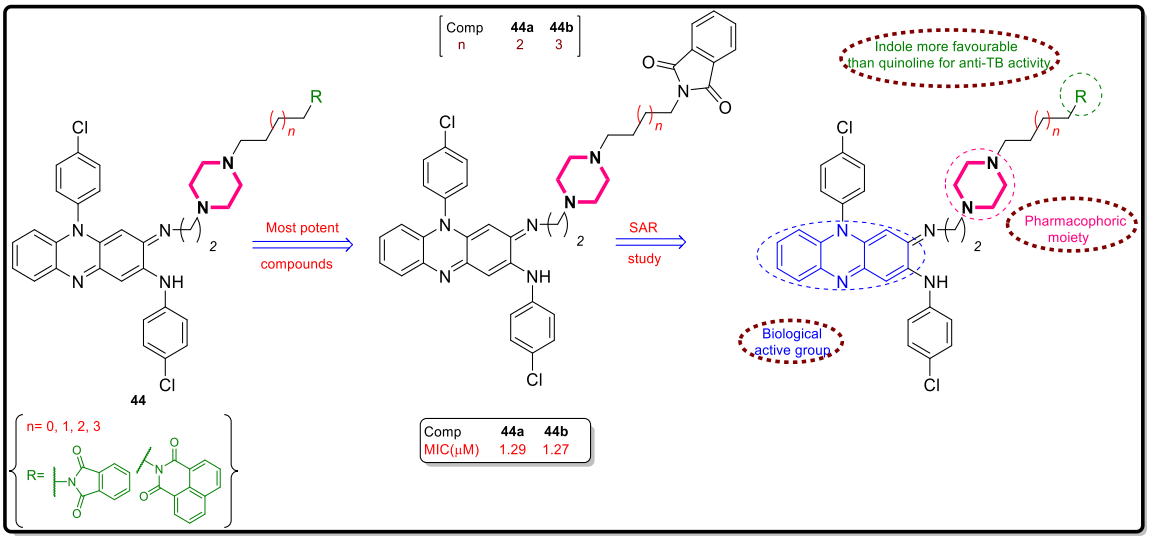

Figure 51 Phthalimido-piperazine-naphthalimido conjugates (44) with active derivatives (44a and 44b) and SAR study

Mannangatty and co-workers[80] screened piperazine containing 2,6-diarylpiperidin-4-one derivatives (**45, Fig. 52**) against MTB *ATCC-27294 $H_{37}Rv$* strain, five bacterial and fungal strains. Compounds **45a–e** showed better *in vitro* activity for the MTB *ATCC-27294 $H_{37}Rv$* strain using the BACTEC method[81]. The results explained that two alkyl substituents on the piperazine ring showed good MTB activity. Moreover, the anti-bacterial activity of compound **45f** has displayed excellent activity against *E. coli* and*K. pneumonia*, wherein analogue **45d** showed good activity against *S. aureus.*

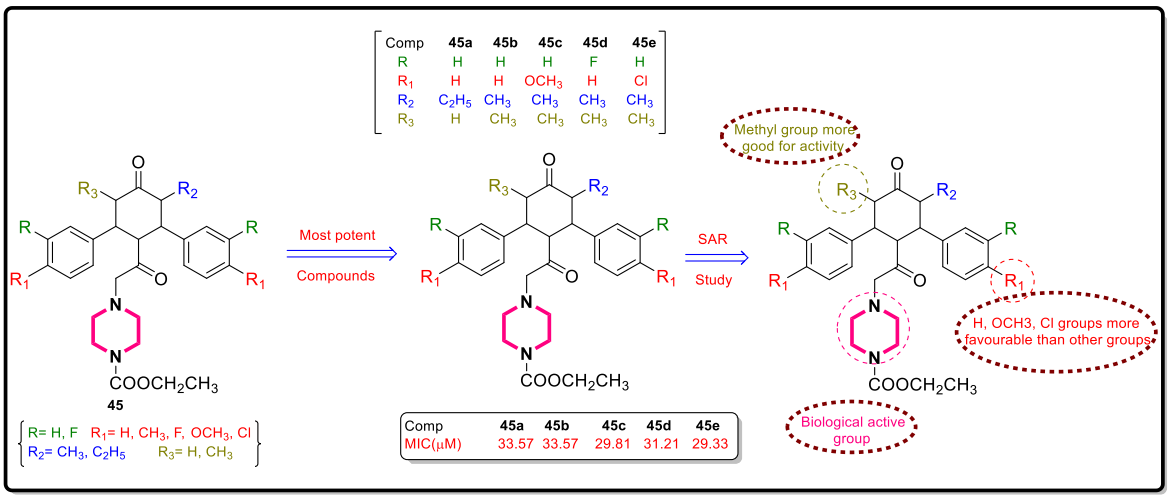

Figure 52 2,6-diarylpiperidin-4-one-piperazine analogues (45) with active derivatives (45a-e) and SAR study

Nitro-furan containing molecules (5-nitrofuran-2-carboxylic acid 3,4-dimethoxybenzylamide) were identified as the most promising anti-TB agents. However, their poor aqueous solubility negatively influences their*in vivo* bioavailability in animal models. In an attempt to improve solubility Tangallapally et al.[82] synthesized two series of cyclic secondary amine substituted phenyl nitrofuranyl amides substituted with cyclic amines, piperazine, pyrazine, morpholine and thiomorpholine heterocycles (**46a and 46b, Fig. 53**). Their preliminary *in vitro* studies were performed against MTB *$H_{37}Rv$* strain using micro broth dilution method. Compound **46ba** bearing benzyl substituent on piperazine of phenyl nitro-furanyl amides showed the most potent activity with MIC90 of 0.03 μM against MTB *$H_{37}Rv$* strain.The SAR study (**Fig. 53**) revealed that benzyl nitro-furanyl amides with *para*-substitutions of piperazines, pyrazine, morpholine and thiomorpholine enhances anti-TB activity than phenyl nitro-furanyl amides.

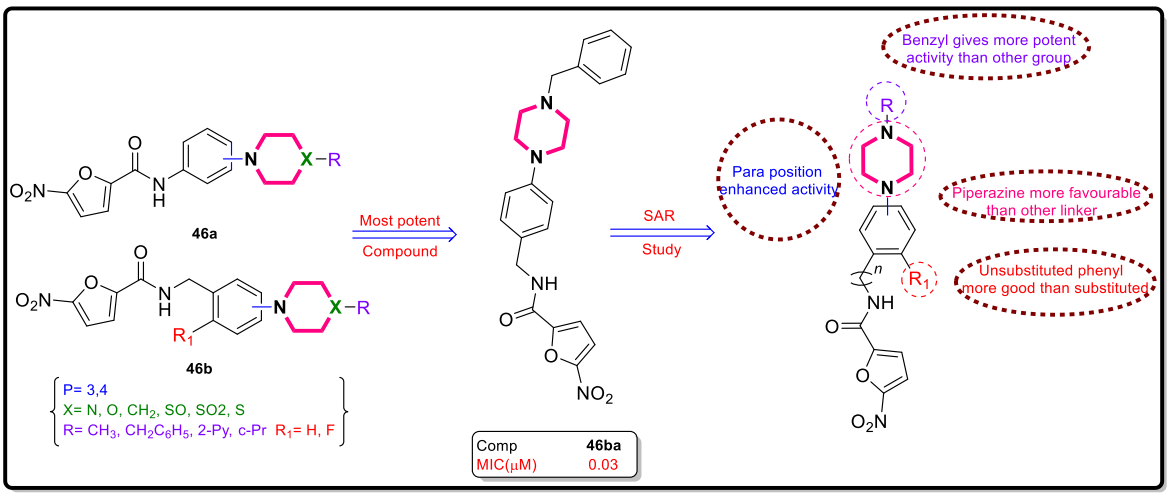

Figure 53 Nitro-furanyl amides (46a and 46b) with active derivative (46ba) and SAR study

Xin and his colleagues[83] developed a new series of pyrrolidine carboxamides and aryl-amides derivatives (**47, Fig. 54**) as *InhA* inhibitors. From the anti-TB activity data it was observed that compound **47a** demonstrated the best IC_{50} value of 0.99 μM. The SAR results (**Fig. 54**) identified the pharmacophoric properties that compounds with Cl or -CF_3 substituted aryl ring groups next to a carbonyl group, CH_3 group on another ring and that both rings connected by piperazine rather than pyrazine showed improved activity, clearly suggesting that piperazine scaffold improved InhA inhibition activity.

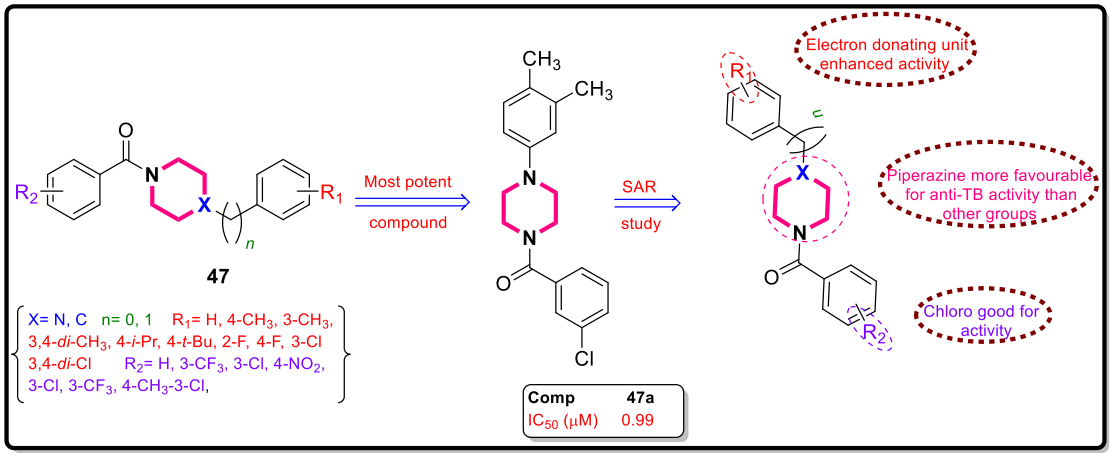

Figure 54 Aryl amide-piperazine analogues (47) with active derivative (47a) and SAR study

Tangallapally et al.[84] synthesized two series of nitro-furanylisoxazolines derivatives (**48a** and **48b**, **Fig. 55**) and screened for anti-TB activity against MTB strain. The compounds displayed highly

potent anti-TB activity with MIC value range of 0.0001-0.0045 µM. The synthesized analogues demonstrated their high protein binding with low volume distribution, poor solubility and low free drug concentration at the infection site. They further modified and synthesized another series by replacing nitro-furanyl group with other substituents of highly potent series **48b** as shown in **Fig. 55**. From the newly generated series, compound **48ba** ethyl ester group found an active candidate with MIC value of 3.96 µM against MTB with good solubility than nitro-furans.

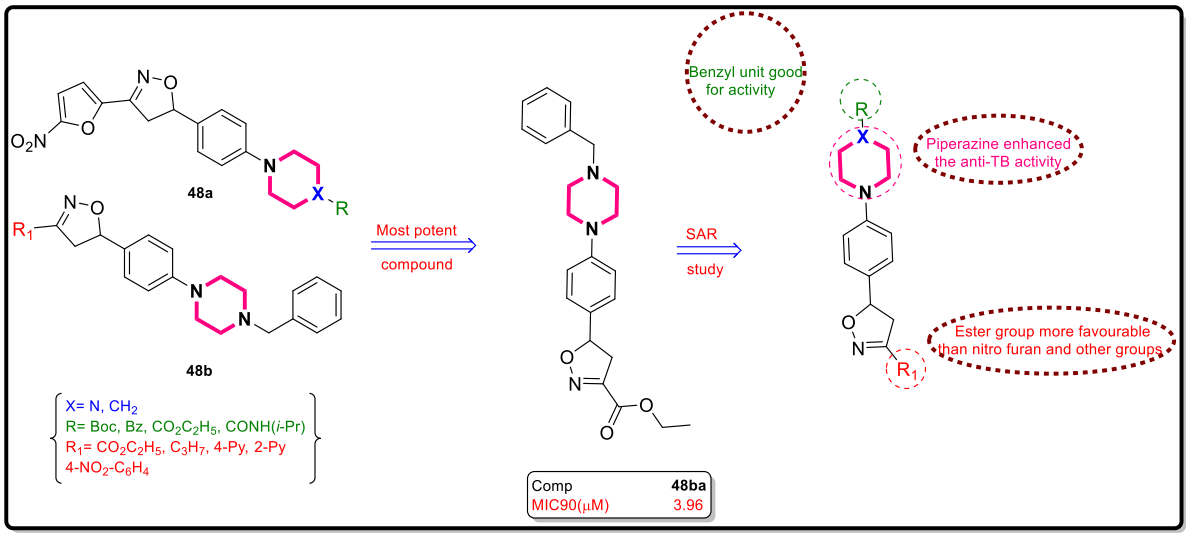

Figure 55 Nitro-furanylisoxazolines (48a and 48b) with active derivative (48ba) and SAR study

Zhao and colleagues[75] designed FQ analogues (**Fig. 56**) as anti-TB agents. They synthesized, two series of FQ, (**49a**) 1-aryl FQ derivatives, and (**49b**) bi-functional FQ-hydroxyl-quinoline derivatives connected as a linker *via* piperazine. All derivatives were screened against MTB growth and determined the inhibition percentage at 13.63 µM. Compounds **49aa** and **49ab** exhibited most effective activity against MTB and showed 97% and 98% of inhibition, respectively. SAR studies **(Fig. 56**) revealed that piperazine as a linker displayed promising anti-TB activity.

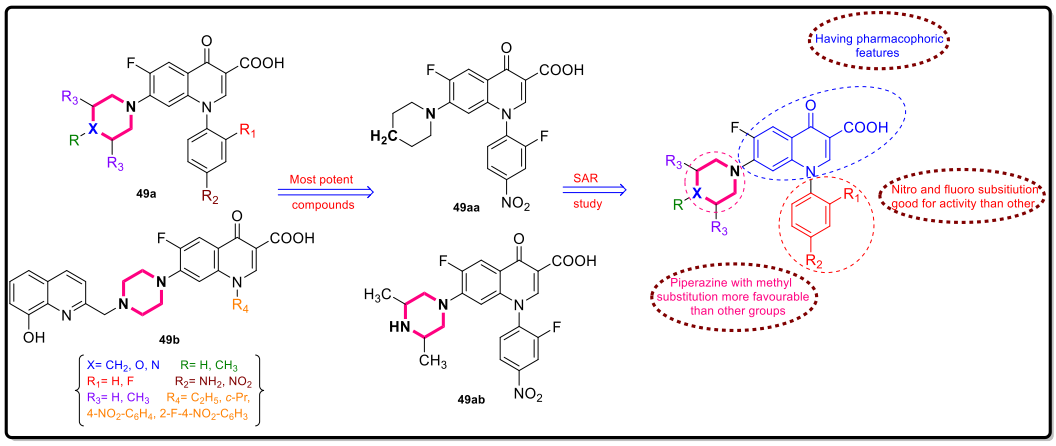

Figure 56 FQ analogue (49a and 49b) with active derivatives (49aa and 49ab) and SAR study

Bogatcheva et al.[85] synthesized some series of novel substituted diamine derivatives (**50, Fig. 57**) and screened against MTB and *HepG2* cell line using broth micro-dilution and MTS assay [86] to assess their safety profile. The author identified piperazine and homo-piperazine compound (**50a** and **50b)** (**Fig. 57**) as low cytotoxic active compounds. Additionally, compounds **50b** and **50a** studied against mice model for *in vivo* analysis. Both compounds resulted in a loss of 12 and 21% of their initial body weight. The *in vitro* and *in vivo* data revealed that homo-piperazine and piperazine substituted with benzyl group have shown promising anti-TB activity.

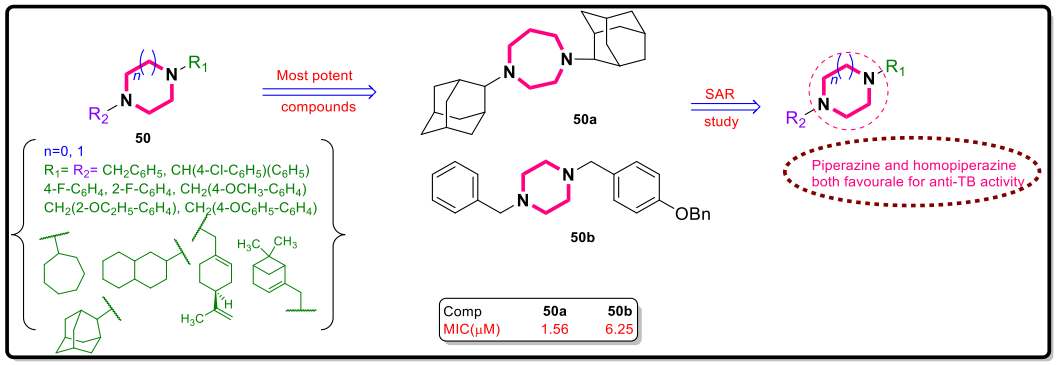

Figure 57 Diamine derivatives (50) with active compounds (50a and 50b) and SAR study

Upadhayaya et al.[87] designed newer 2-pyridyl-piperazine based conjugates (**51a-c, Fig. 58**). All derivatives were screened for anti-TB activity against MTB *$H_{37}Rv$* strain by MABA method. From the anti-TB data, analogues of series **51a** and **51b** showed good activity. Compounds of series **51b** displayed more promising activity the MIC value range 0.43-3.065 μM.

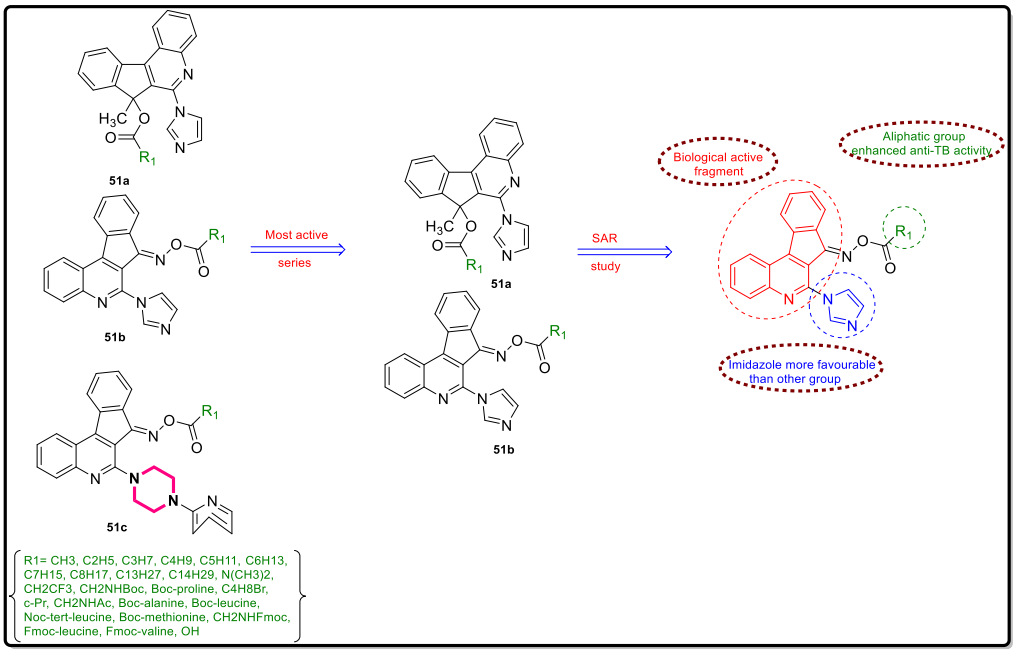

Figure 58 Indeno[2,1-c]quinoline derivatives (51a-c) and SAR study

Sriram et al.[88]developed a series of PZA Mannich-bases bearing a piperazine moiety with various substituents (**52, Fig. 59**) as an anti-TB agent. All analogues were evaluated *in vitro* against MTB $H_{37}Rv$ and MTB MDR strains using an agar dilution method[42]. Most compounds showed decent potency against MTB-strains with low cytotoxicity. Compound **52a** displayed the highest potency, with MIC value of 0.76 and 0.40 µM against MTB $H_{37}Rv$ and MTB MDR strains with 90% inhibition, respectively. Further, compound **52a** elicited *in vivo* anti-TB potential against MTB *ATCC 35801* by mitigating bacterial infection in lung and spleen. The SAR study (**Fig. 59**) concluded that methoxy and cyclo-propyl substituted quinolone analogues claimed as a good candidate against the anti-TB activity and low cytotoxicity.

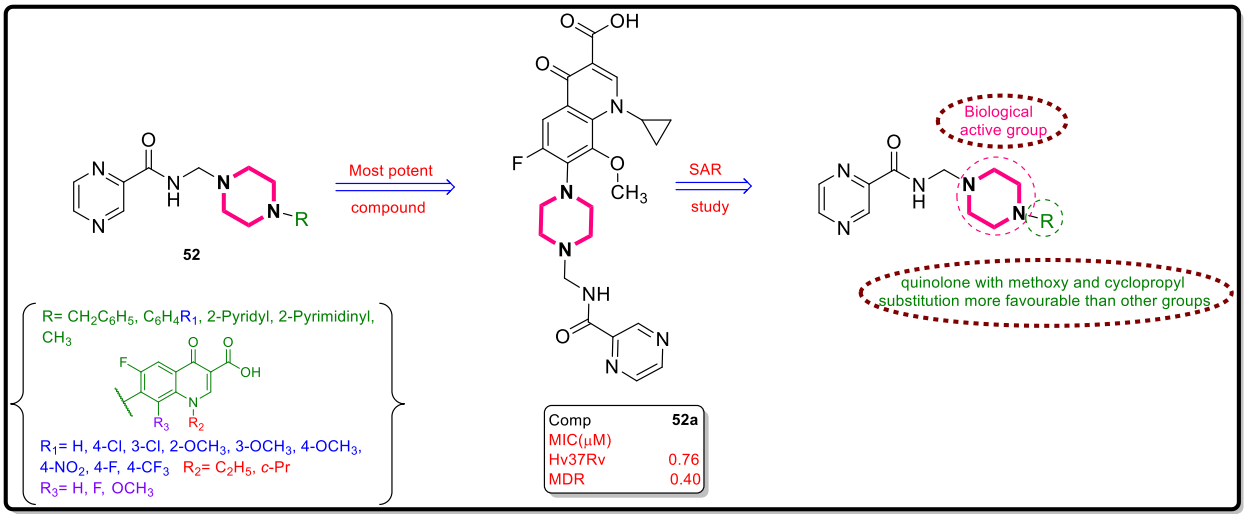

Figure 59 PZA Mannich-bases bearing piperazine derivatives (52) with active derivative (52a) and SAR study

Three novel series of quinolin-4-yl-1,2,3-triazoles derivatives were designed and synthesized using amides, sulphonamides and amido-piperazines (**53a-c, Fig. 60**) as a linker and evaluated for their anti-TB activity by Thomas and his colleague[89]. The synthesized compounds were screened against MTB $H_{37}Rv$, *M. smegmatis* (ATCC 19420) and *M. fortuitum* (ATCC 19542), respectively. Compounds from series **53a** showed more potent activity than standard reference drug INH. The *in vitro* study revealed that compounds **53ca-cd** belongs to quinolin-4-yl-1,2,3-triazole amido-piperazine family (**Fig. 60**) displayed the percentage of inhibition of 90-95% at the concentration of 2.63, 2.17, 2.17 and 2.48 μM, against MTB *$H_{37}Rv$*. The SAR (**Fig. 60**) studies revealed that amido-piperazine derivatives with acetyl, fluoro, methoxy substituents positively influence the anti-TB activity.

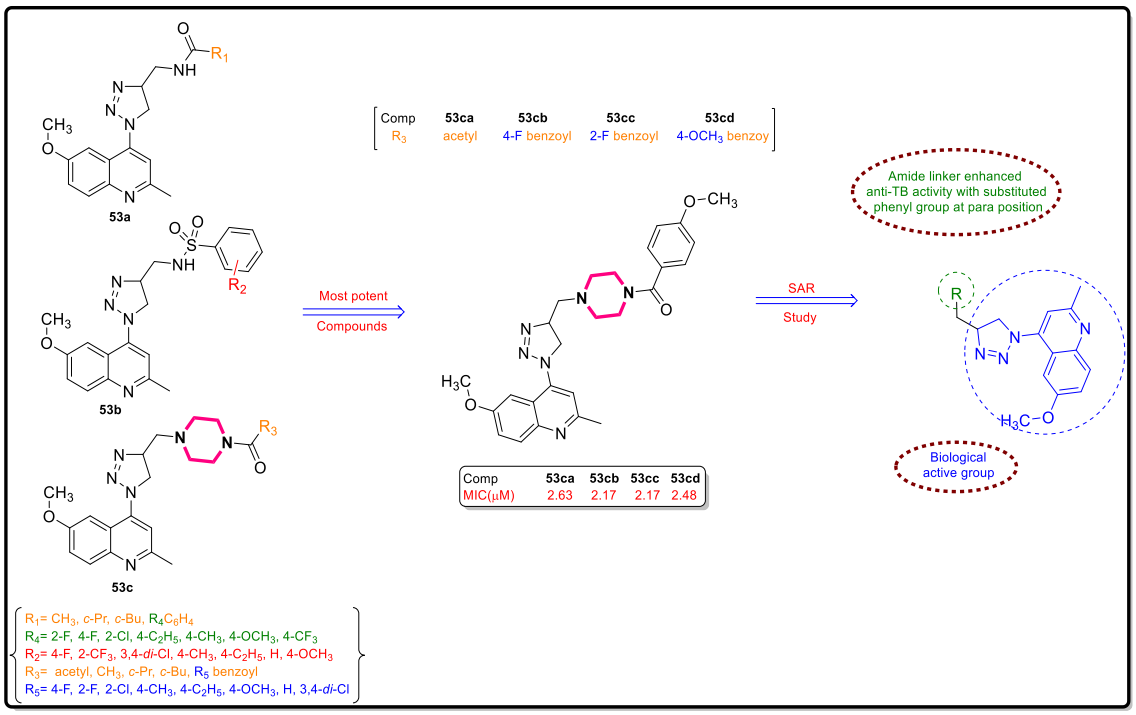

Figure 60 Quinolin-4-yl-1,2,3-triazoles analogues (53a-c) with active derivatives (53ca-cd) and SAR study

Recently, Talath et al.[90] reported the application of quinolone tagged thiadiazole ring with sulfoxide piperazine linker as anti-TB agents. They synthesized 7-[4-(5-amino-[1,3,4]thiadiazole-2-sulfonyl)-piperazin-1-yl]fluoro quinolonic analogues (**54, Fig. 61**) and screened for anti-TB activity against MTB *H37Rv* strain using broth dilution assay[91]. Among series tested, compounds **54a** and **54b** showed the most promising anti-TB activity with MIC value of 20.72 and 20.22 μM. Compounds **54a** and **54b** have shown better potency than reference drugs Cf, NRFX, sparfloxacin, and gatifloxacin against Gram-positive bacteria and less potent against Gram-negative strains. SAR studies (**Fig. 61**) showed that the anti-TB activity largely depends on the alkyl substitutions on phenyl quinolone ring.

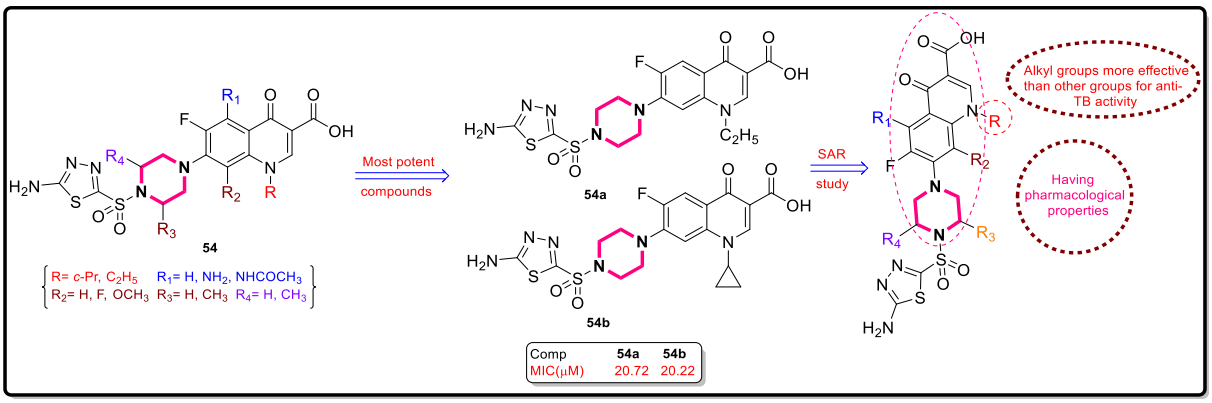

Figure 61 Thiazole-piperazine-fluoro-quinoloic analogues (54) with active derivatives (54a and 54b) and SAR study

Kamal et al.[92] synthesized four series of novel oxazolidinone conjugated aryl-sulfonamido-piperazine derivatives (**55a-d, Fig. 62**) and tested their anti-TB activity against MTB *$H_{37}Rv$* strain by employing broth micro-dilution assay method. Compounds **55aa** and **55ab** showed potent MTB inhibitory activity with MIC value of 1.88 and 1.84 μM as compared to the standard drug Linezolid with MIC value 5.9 μM. The pharmacophoric structure has shown that piperazine works effectively for linking and improves anti-TB activity as compared to other binders and groups. The SAR studies (**Fig. 62**) revealed the importance of alkyl groups on sulfonamido-piperazine ring to enhance anti-TB activity of these analogues.

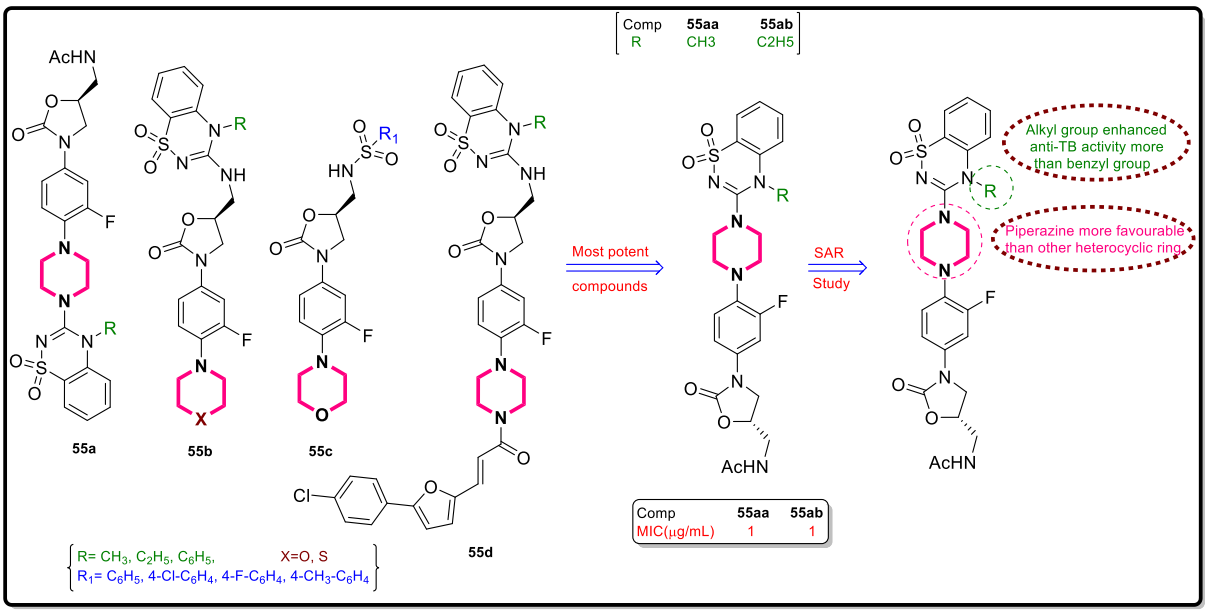

Figure 62 Oxazolidinone-conjugated aryl-sulfonamido-piperazine analogues (55a-d) with active derivatives (55aa and 55ab) and SAR study

Qiang Guo and his research team[93] designed and synthesized some novel series of piperazine tagged coumarin hybrids (**56, Fig. 63**) with a FQ (Gatifloxacin, Ciprofloxacin and 8-OCH_3 ciprofloxacin) and evaluated for their anti-TB activity. All derivatives were screened using a rapid direct susceptibility test technique [94] against *M. smegmatis* CMCC 93202 and MTB $H_{37}Rv$ strain. The *in vitro* results revealed that all hybrids displayed less inhibitory activities toward *M. smegmatis* (CMCC 93202) than key starting 8-OCH_3-CPFX, CPFX, MXFX and GTFX. The SAR study (**Fig. 63**) indicated that amide linker with methoxy substituted hybrid **56a** showed most promising inhibition with MIC value of 0.43 μM against MTB $H_{37}Rv$ as compared to reference drug gatifloxacin (MIC= 0.66 μM). Further, the SAR (**Fig. 63**) study identifies the importance of coumarin ring in anti-TB activity of these hybrids, as its absence significantly reduced the activity.

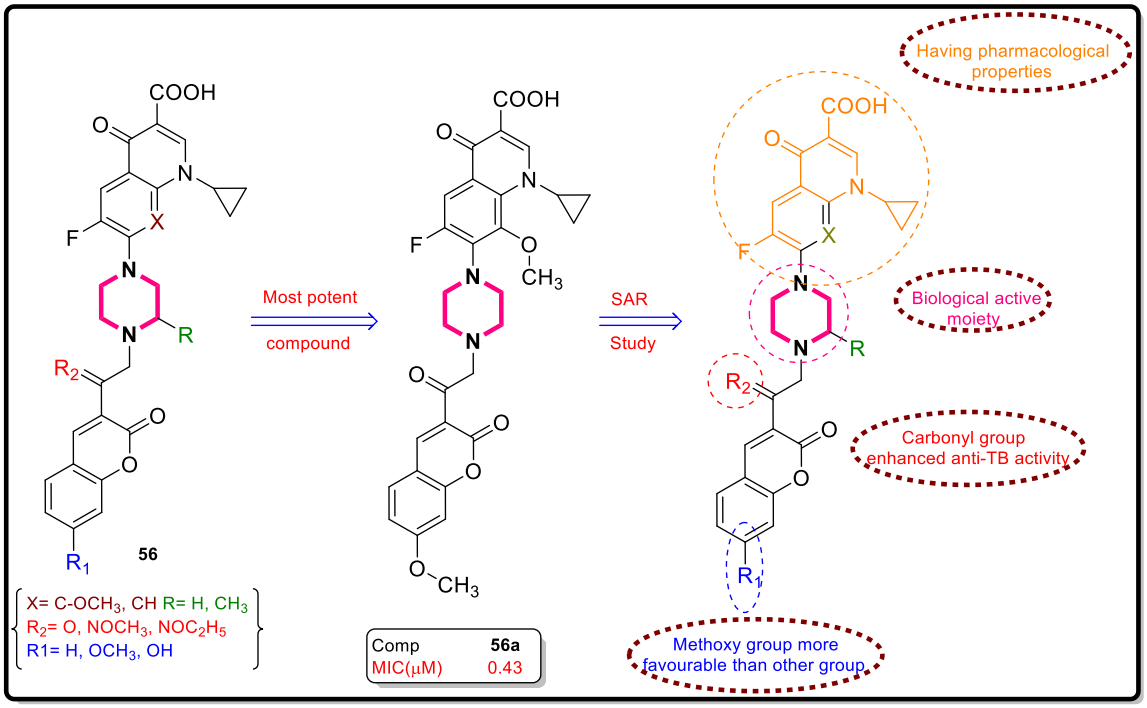

Figure 63 Oxazolidinone-conjugated aryl-sulfonamido-piperazine derivatives (56) with most active derivative (56a) and SAR study

Varghese's team[95] systematically evaluated the anti-TB activity of series of 4N-acylpiperazinyl oxazolidinones, 4-N-arylcarbonyl and 4-N-arylsulfonyl-piperazinyl oxazolidinones (**57a** and **57b**, **Fig. 64**). Most of the compounds from 4-N-acylpiperazinyl (**57b**) series shown potent activity against MTB *H*$_{37}$*Rv* strain with IC_{90} value of <0.53–1 μM, respectively. Two compounds **57ba** and **57bb** from 4-N-arylcarbonyl and analogue **57bc** from 4-N-arylsulfonyl series have displayed highest anti-TB activity with IC_{90} value <0.47 μM. The SAR report explained that the morpholine pharmacophoric structural feature showed the highest anti-TB activity than other heterocyclic groups (**Fig. 64**).

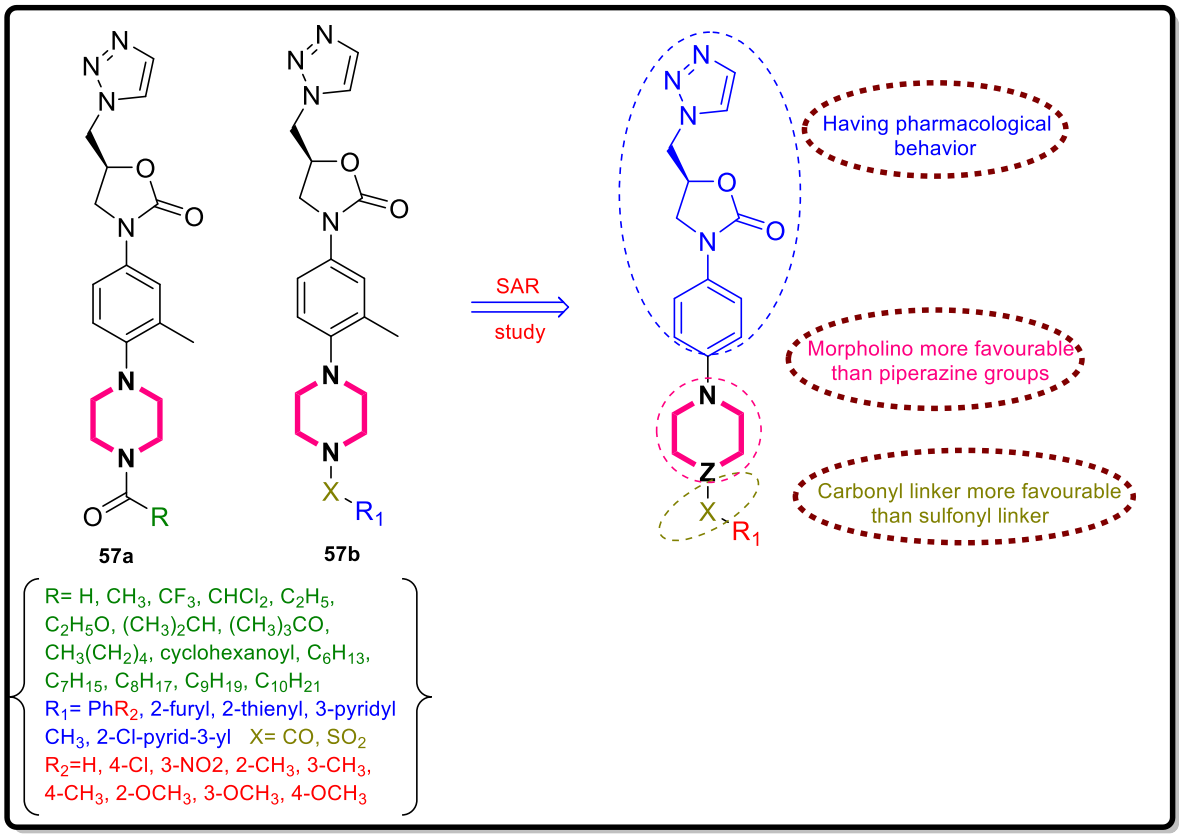

Figure 64 Oxazolidinones-piperazine analogues (57a and 57b) with SAR study

Gill and co-workers[96] designed three benz-oxazinorifamycin derivatives using the change in three-dimensional structures of rifamycins bound to RNA polymerase (RNAP) and human pregnane X receptor (hPXR). All three derivatives shown inhibition of wild-type MTB RNAP in the nano-molar range. These analogues were also screened for their anti-TB activity against MTB *$H_{37}Rv$* in aerobic and anaerobic conditions. All the compound exhibited good inhibitory activity with MIC_{90} value range of 0.022−0.77, 0.33−0.38 µM and under aerobic and anaerobic conditions, compared to Rif-resistant mutants of the MTB RNAP[97].

Tzeng's group[98] designed and synthesized some novel series of piperazine arylsulfonyl and arylcarbonyl derivatives of ofloxacin (**58, Fig. 65**) as promising anti-TB agents for effective inhibition of MTB. Among the tested molecules, compound **58a** displayed more than 90% of inhibition at MIC of 11.7-17.9 µM. The SAR study (**Fig. 65**) revealed that the substitution of aryl-sulfonyl group at C-7 piperazin-4-yl of N-demethyl ofloxacin exhibited considerable enhancement in the activity.

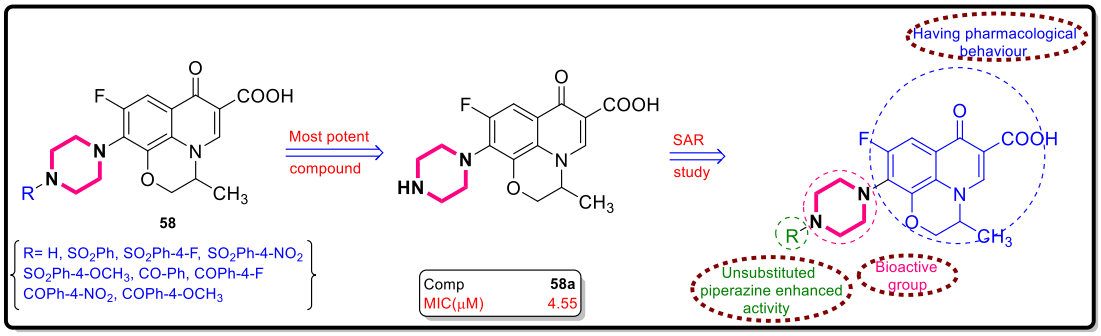

Figure 65 Arylsulfonyl and arylcarbonyl derivatives of ofloxacin (58) with active derivative (58a) and SAR study

Sriram et al.[99] designed and synthesized a series of chloro-quinoline and piperazine derivatives (**59, Fig. 66**)and screened for anti-TB activity against MTB $H_{37}Ra$ strain by using MTB DNA supercoiling and gyrase B assay. The anti-TB data revealed that compound **59a** emerged as a lead candidate with MIC and IC_{50} value of 7.8, 2.5 and 2.7 μM against MTB *$H_{37}Ra$* strain, *gyrase B* and MTB *DNA supercoiling*, respectively. Among these compounds, except nitro bearing once were found non-toxic against *RAW 264.7* cell lines. SAR study (**Fig. 66**) revealed that thiourea linker and choro-quinoline enhanced the MTB activity.

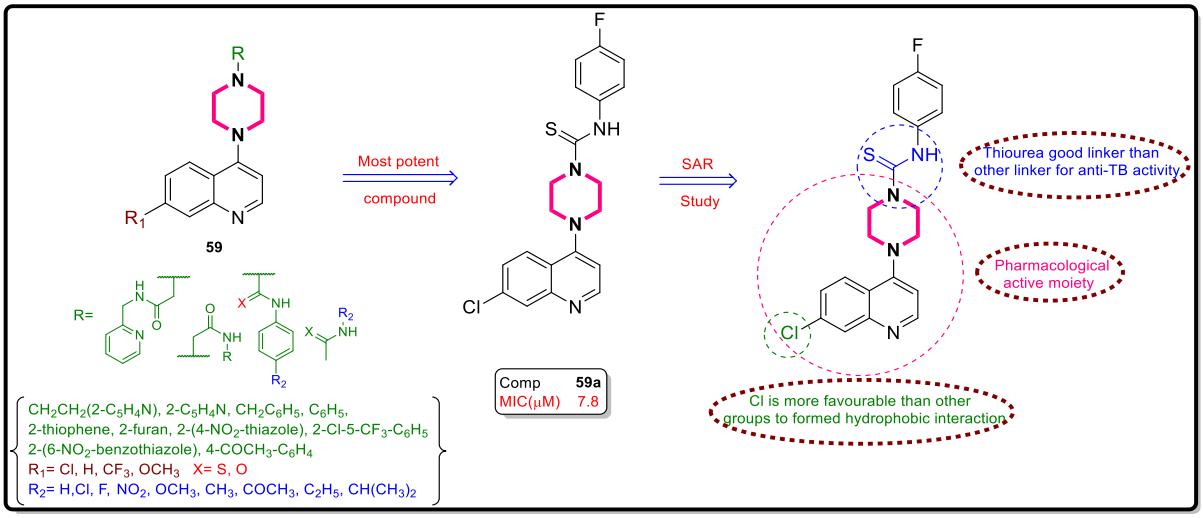

Figure 66 Chloro-quinoline and piperazine analogues (59) with most active analogue (59a) and SAR study

In an interesting study, Stewart and his team[100] attempted to enhance the solubility and bioavailability of MCZ scaffold by synthesizing a new series of 2-sulphonylpiperazin 8-nitro 6-trifluoromethyl 1,3-benzothiazin-4-one (sPBTZ) derivatives (**60, Fig. 67**). *In vitro* studies, the sulfonylated analogues with piperazine and cyclohexyl moieties exhibited less anti-TB against MTB $H_{37}Rv$ strain with MIC range of 0.001-0.02 µg/mL, than PBTZ169 (MIC = 0.0002 µg/mL), but with enhanced solubility and stability in microsomal assays. Compound **60a** (**Fig. 67**) emerged as ideal molecule with potent anti-TB activity (MIC = 0.0064 µM) and 90-fold better solubility (7.2 µg/mL) than PBTZ169. SAR studies demonstrated that benzothiazin-4-one and sulphonyl-piperazine showed better anti-TB activity with enhanced solubility and bioavailability, as shown in **Fig. 67**.

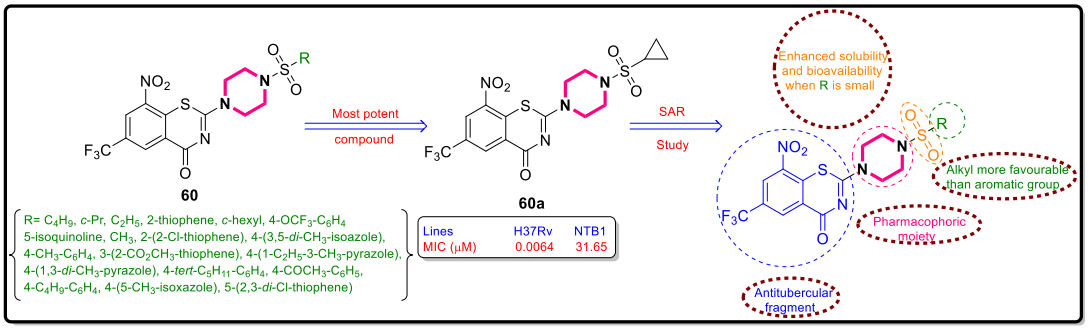

Figure 67 sPBTZ derivatives (**60**) with potent derivative (**60a**) and SAR study.

4. List of Patents

The piperazine hybrids from natural and synthetic origin have gained an ample attention and focus due to their multifaceted pharmacological properties. Various patents on piperazine analogues as anti-TB agents have substantially found in each database.

Table 1: List of patent publications and with piperazine containing active anti-TB molecules

Sr. no.	Patent Publication Number	Date of publication	Application number	Markus structure and active compounds with MIC/IC_{50} value	Ref

1	WO2013148174	03-Oct-2013	PCT/US2013/030687	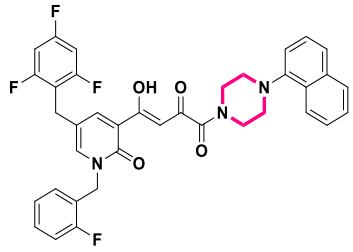 MIC=<1.5 µM (MDR TB)	[101]
2	WO2019243971	26-Dec-2019	PCT/IB2019/054978	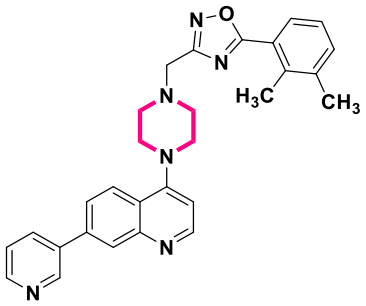 MIC=0.52µM (H_{37}RvMtb stains)	[102]
3	WO2011089456	28-Jul-2011	PCT/HU2011/000008	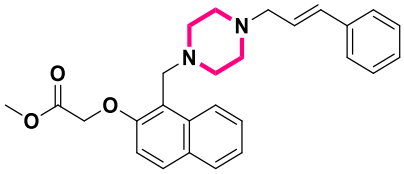 MIC=9.2 µM (MTB H_{37}Rv)	[102]
4	WO2005007625	27-Jan-2005	PCT/US2004/022491	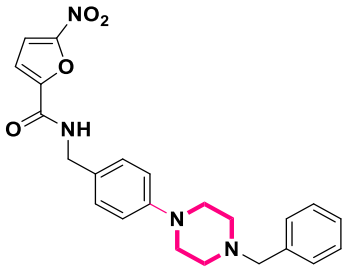 MIC=0.014 µM (MTB H37Ra)	[103]

5	WO2012066518	24-May-2012	PCT/IB2011/055209	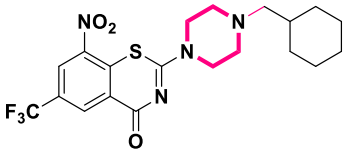 MIC<0.41×10-6 µM (MTB $H_{37}Rv$)	[104]
6	WO2001056974	09-Aug-2001	PCT/US2001/040045	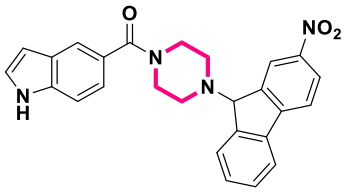 INHA IC-50 = 0.27µM	[105]
7	WO2007014885	08-Feb-2007	PCT/EP2006/064656	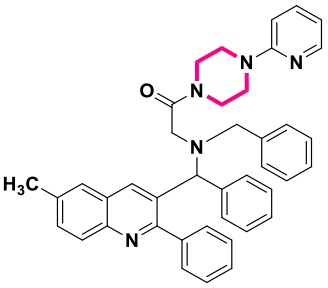 MTB pIC50 = 5.4	[106]
8	WO2012141338	18-Oct-2012	PCT/JP2012/060645	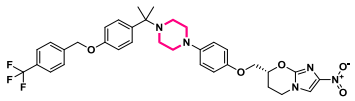 MIC=0.001 µM (MTB kurono)	[107]
9	WO2006109323	19-Oct-2006	PCT/IN2006/000115	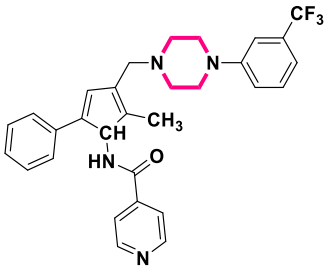	[108]

				MDR TB active compound	
10	WO2015193454	23-Dec-2015	PCT/EP2015/063752	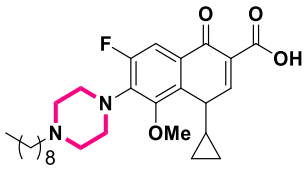 MIC=0.25 μM (MTB H_{37}Rv stains)	[109]
11	WO2013072903	23-May-2013	PCT/IB2012/056546	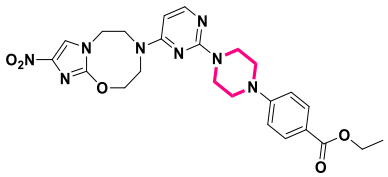 MIC MABA = 22 >100 μM MTB H_{37}Rv	[110]

5. Conclusion

Tuberculosis (TB), an infectious diseases is one of the greatest threat to human kind. With the emergence of MDR-TB, XDR-TB, DR-TB, and TDR-TB, has further complicated the treatment and management of TB. This has encouraged the researchers worldwide for the development of novel, fast-acting, potent, anti-TB agents. In this review, we have focused on piperazine-based MTB agents reported over the past five decades and have made a systematic attempt to compile a literature review focusing on their therapeutic aspects in detail. Majority of piperazine hybrids displayed excellent *in vitro* activity against MDR-TB and drug-susceptible TB, signifying its importance as a scaffold with a novel mode of action, which could be further exploited my medicinal chemist in designing potent MTB drugs. In addition, there are several piperazine containing drug molecules that are either already in market or in clinical trials. This compilation of literature review (from 1971-2019) will definitely be update as well as significantly useful to the scientific community especially for the researchers

involved in anti-TB drug discovery, for successful and fast development of novel molecules with enhanced chemotherapeutic benefits.

References

[1] A. Koch, V. Mizrahi, Mycobacterium tuberculosis, Trends Microbiol. (2018). https://doi.org/10.1016/j.tim.2018.02.012.

[2] WHO, Global Tuberculosis Report 2018. Geneva: World Health Organization; 2018., 2018. https://doi.org/WHO/HTM/TB/2017.23.

[3] E. Pontali, M.C. Raviglione, G.B. Migliori, O.W. Akkerman, J.W. Alffenaar, F.X. Blanc, S. Borisov, D.M. Cirillo, M. Dalcolmo, K. Dheda, A.L. Kritski, C. Lienhardt, P. Olliaro, M. Tadolini, S. Tiberi, Z. Udwadia, Regimens to treat multidrug-resistant tuberculosis: Past, present and future perspectives, Eur. Respir. Rev. (2019). https://doi.org/10.1183/16000617.0035-2019.

[4] C.M. Rumende, Risk Factors for Multidrug-resistant Tuberculosis, Acta Med. Indones. (2018). https://doi.org/10.3126/ijasbt.v5i4.18771.

[5] Z. Xu, C. Gao, Q.C. Ren, X.F. Song, L.S. Feng, Z.S. Lv, Recent advances of pyrazole-containing derivatives as anti-tubercular agents, Eur. J. Med. Chem. (2017). https://doi.org/10.1016/j.ejmech.2017.07.059.

[6] S. Sarkar, A. Ganguly, Current Overview of Anti-Tuberculosis Drugs: Metabolism and Toxicities, Mycobact. Dis. (2016). https://doi.org/10.4172/2161-1068.1000209.

[7] G.J. Fox, C.C. Dobler, B.J. Marais, J.T. Denholm, Preventive therapy for latent tuberculosis infection—the promise and the challenges, Int. J. Infect. Dis. (2017). https://doi.org/10.1016/j.ijid.2016.11.006.

[8] A. Penta, S. Franzblau, B. Wan, S. Murugesan, Design, synthesis and evaluation of

diarylpiperazine derivatives as potent anti-tubercular agents, Eur. J. Med. Chem. 105 (2015) 238–244. https://doi.org/10.1016/j.ejmech.2015.10.024.

[9] A.K. Rathi, R. Syed, H.S. Shin, R. V. Patel, Piperazine derivatives for therapeutic use: A patent review (2010-present), Expert Opin. Ther. Pat. (2016). https://doi.org/10.1080/13543776.2016.1189902.

[10] M. Shaquiquzzaman, G. Verma, A. Marella, M. Akhter, W. Akhtar, M.F. Khan, S. Tasneem, M.M. Alam, Piperazine scaffold: A remarkable tool in generation of diverse pharmacological agents, Eur. J. Med. Chem. (2015). https://doi.org/10.1016/j.ejmech.2015.07.026.

[11] M. Al-Ghorbani, A. Bushra Begum, Z. Zabiulla, S. V. Mamatha, S.A. Khanum, Piperazine and morpholine: Synthetic preview and pharmaceutical applications, Res. J. Pharm. Technol. (2015). https://doi.org/10.5958/0974-360X.2015.00100.6.

[12] V. Singh, A. Pacitto, S. Donini, D.M. Ferraris, S. Boros, E. Illyés, B. Szokol, M. Rizzi, T.L. Blundell, D.B. Ascher, J. Pato, V. Mizrahi, Synthesis and Structure–Activity relationship of 1-(5-isoquinolinesulfonyl)piperazine analogues as inhibitors of Mycobacterium tuberculosis IMPDH, Eur. J. Med. Chem. 174 (2019) 309–329. https://doi.org/10.1016/j.ejmech.2019.04.027.

[13] Y.Q. Hu, S. Zhang, F. Zhao, C. Gao, L.S. Feng, Z.S. Lv, Z. Xu, X. Wu, Isoniazid derivatives and their anti-tubercular activity, Eur. J. Med. Chem. (2017). https://doi.org/10.1016/j.ejmech.2017.04.002.

[14] M. Chandran, J. Renuka, J.P. Sridevi, G.S. Pedgaonkar, V. Asmitha, P. Yogeeswari, D. Sriram, Benzothiazinone-piperazine derivatives as efficient Mycobacterium tuberculosis DNA gyrase inhibitors, Int. J. Mycobacteriology. (2015). https://doi.org/10.1016/j.ijmyco.2015.02.002.

[15] M. Asif, Piperazine and Pyrazine containing molecules and their diverse pharmacological

activities, Int. J. Adv. Sci. Res. (2015). https://doi.org/10.7439/ijasr.v1i1.1766.

[16] R. Kharb, K. Bansal, A.K. Sharma, A valuable insight into recent advances on antimicrobial activity of piperazine derivatives, Der Pharma Chem. (2012).

[17] H.A.A.A. El-wahab, M. Accietto, L.B. Marino, K.J. McLean, C.W. Levy, H.M. Abdel-Rahman, M.A. El-Gendy, A.W. Munro, A.S. Aboraia, C. Simons, Design, synthesis and evaluation against Mycobacterium tuberculosis of azole piperazine derivatives as dicyclotyrosine (cYY) mimics, Bioorganic Med. Chem. 26 (2018) 161–176. https://doi.org/10.1016/j.bmc.2017.11.030.

[18] S.M. Kishk, K.J. McLean, S. Sood, M.A. Helal, M.S. Gomaa, I. Salama, S.M. Mostafa, L.P.S. de Carvalho, A.W. Munro, C. Simons, Synthesis and biological evaluation of novel cYY analogues targeting Mycobacterium tuberculosis CYP121A1, Bioorganic Med. Chem. (2019). https://doi.org/10.1016/j.bmc.2019.02.051.

[19] R.A. Khalifa, M.S. Nasser, A.A. Gomaa, N.M. Osman, H.M. Salem, Resazurin Microtiter Assay Plate method for detection of susceptibility of multidrug resistant Mycobacterium tuberculosis to second-line anti-tuberculous drugs, Egypt. J. Chest Dis. Tuberc. (2013). https://doi.org/10.1016/j.ejcdt.2013.05.008.

[20] J.C. Palomino, A. Martin, M. Camacho, H. Guerra, J. Swings, F. Portaels, Resazurin microtiter assay plate: Simple and inexpensive method for detection of drug resistance in Mycobacterium tuberculosis, Antimicrob. Agents Chemother. (2002). https://doi.org/10.1128/AAC.46.8.2720-2722.2002.

[21] T. Gonec, I. Malík, J. Csöllei, J. Jampílek, J. Stolaríková, I. Solovic, P. Miku, S. Keltoová, P. Kollár, J. O'Mahony, A. Coffey, Synthesis and in vitro antimycobacterial activity of novel n-arylpiperazines containing an ethane-1,2-diyl connecting chain, Molecules. 22 (2017). https://doi.org/10.3390/molecules22122100.

[22] J. Roh, G. Karabanovich, H. Vlčková, A. Carazo, J. Němeček, P. Sychra, L. Valášková, O. Pavliš, J. Stolaříková, V. Klimešová, K. Vávrová, P. Pávek, A. Hrabálek, Development of water-soluble 3,5-dinitrophenyl tetrazole and oxadiazole antitubercular agents, Bioorganic Med. Chem. 25 (2017) 5468–5476. https://doi.org/10.1016/j.bmc.2017.08.010.

[23] R. V. Patel, P. Kumari, D.P. Rajani, K.H. Chikhalia, A new class of 2-(4-cyanophenyl amino)-4-(6-bromo-4-quinolinyloxy)-6- piperazinyl (piperidinyl)-1,3,5-triazine analogues with antimicrobial/ antimycobacterial activity, J. Enzyme Inhib. Med. Chem. 27 (2012) 370–379. https://doi.org/10.3109/14756366.2011.592491.

[24] C.T. Peng, C. Gao, N.Y. Wang, X.Y. You, L.D. Zhang, Y.X. Zhu, Y. Xv, W.Q. Zuo, K. Ran, H.X. Deng, Q. Lei, K.J. Xiao, L.T. Yu, Synthesis and antitubercular evaluation of 4-carbonyl piperazine substituted 1,3-benzothiazin-4-one derivatives, Bioorganic Med. Chem. Lett. 25 (2015) 1373–1376. https://doi.org/10.1016/j.bmcl.2015.02.061.

[25] J. Shi, J. Lu, S. Wen, Z. Zong, F. Huo, J. Luo, Q. Liang, Y. Li, H. Huang, Y. Pang, In vitro activity of PBTZ169 against multiple Mycobacterium species, Antimicrob. Agents Chemother. (2018). https://doi.org/10.1128/AAC.01314-18.

[26] L. Li, K. Lv, Y. Yang, J. Sun, Z. Tao, A. Wang, B. Wang, H. Wang, Y. Geng, M. Liu, H. Guo, Y. Lu, Identification of N-Benzyl 3,5-Dinitrobenzamides Derived from PBTZ169 as Antitubercular Agents, ACS Med. Chem. Lett. (2018). https://doi.org/10.1021/acsmedchemlett.8b00177.

[27] S.K. Marvadi, V.S. Krishna, D. Sriram, S. Kantevari, Synthesis of novel morpholine, thiomorpholine and N-substituted piperazine coupled 2-(thiophen-2-yl)dihydroquinolines as potent inhibitors of Mycobacterium tuberculosis, Eur. J. Med. Chem. 164 (2019) 171–178. https://doi.org/10.1016/j.ejmech.2018.12.043.

[28] L.T.E. Fdd, Alamar Blue Assay, 2010. https://doi.org/776-3425.

[29] G. Li, L.L. Lian, L. Wan, J. Zhang, X. Zhao, Y. Jiang, L.L. Zhao, H. Liu, K. Wan, Antimicrobial susceptibility of standard strains of nontuberculous mycobacteria by microplate Alamar Blue assay, PLoS One. (2013). https://doi.org/10.1371/journal.pone.0084065.

[30] S.J. Zhao, Z.S. Lv, J.L. Deng, G. De Zhang, Z. Xu, Pyrrolidine-containing or Piperazine-containing Nitrofuranylamides: Design, Synthesis, and In Vitro Anti-mycobacterial Activities, J. Heterocycl. Chem. 55 (2018) 2996–3000. https://doi.org/10.1002/jhet.3340.

[31] A. Tajana, -x-"-ht, 3100 (1971) 6–9.

[32] W. Yan, C. Xiangyu, L. Ya, W. Yu, X. Feng, An orally antitumor chalcone hybrid inhibited HepG2 cells growth and migration as the tubulin binding agent, Invest. New Drugs. 37 (2019) 784–790. https://doi.org/10.1007/s10637-019-00737-z.

[33] C.R. Chong, D.Z. Qian, F. Pan, Y. Wei, R. Pili, D.J. Sullivan, J.O. Liu, Identification of type 1 inosine monophosphate dehydrogenase as an antiangiogenic drug target, J. Med. Chem. (2006). https://doi.org/10.1021/jm051225t.

[34] A. Trapero, A. Pacitto, V. Singh, M. Sabbah, A.G. Coyne, V. Mizrahi, T.L. Blundell, D.B. Ascher, C. Abell, Fragment-Based Approach to Targeting Inosine-5′-monophosphate Dehydrogenase (IMPDH) from Mycobacterium tuberculosis, J. Med. Chem. (2018). https://doi.org/10.1021/acs.jmedchem.7b01622.

[35] K.H. Rohde, H.A. Michaels, A. Nefzi, Synthesis and antitubercular activity of 1,2,4-trisubstitued piperazines, Bioorganic Med. Chem. Lett. 26 (2016) 2206–2209. https://doi.org/10.1016/j.bmcl.2016.03.063.

[36] L. Pulipati, J.P. Sridevi, P. Yogeeswari, D. Sriram, S. Kantevari, Synthesis and antitubercular evaluation of novel dibenzo[b,d]thiophene tethered imidazo[1,2-a]pyridine-3-carboxamides, Bioorganic Med. Chem. Lett. 26 (2016) 3135–3140. https://doi.org/10.1016/j.bmcl.2016.04.088.

[37] K.M. Naidu, S. Srinivasarao, N. Agnieszka, A.K. Ewa, M.M.K. Kumar, K.V.G. Chandra Sekhar, Seeking potent anti-tubercular agents: Design, synthesis, anti-tubercular activity and docking study of various ((triazoles/indole)-piperazin-1-yl/1,4-diazepan-1-yl)benzo[d]isoxazole derivatives, Bioorganic Med. Chem. Lett. 26 (2016) 2245–2250. https://doi.org/10.1016/j.bmcl.2016.03.059.

[38] G.C. Moraski, N. Seeger, P.A. Miller, A.G. Oliver, H.I. Boshoff, S. Cho, S. Mulugeta, J.R. Anderson, S.G. Franzblau, M.J. Miller, Arrival of imidazo[2,1-b]thiazole-5-carboxamides: Potent anti-tuberculosis agents that target QcrB, ACS Infect. Dis. 2 (2016) 393–398. https://doi.org/10.1021/acsinfecdis.5b00154.

[39] M.W. Majewski, R. Tiwari, P.A. Miller, S. Cho, S.G. Franzblau, M.J. Miller, Design, syntheses, and anti-tuberculosis activities of conjugates of piperazino-1,3-benzothiazin-4-ones (pBTZs) with 2,7-dimethylimidazo [1,2-a]pyridine-3-carboxylic acids and 7-phenylacetyl cephalosporins, Bioorganic Med. Chem. Lett. 26 (2016) 2068–2071. https://doi.org/10.1016/j.bmcl.2016.02.076.

[40] S. Cho, H.S. Lee, S. Franzblau, Microplate alamar blue assay (MABA) and Low oxygen recovery assay (LORA) for Mycobacterium tuberculosis, Methods Mol. Biol. (2015). https://doi.org/10.1007/978-1-4939-2450-9_17.

[41] D. De Vita, F. Pandolfi, R. Cirilli, L. Scipione, R. Di Santo, L. Friggeri, M. Mori, D. Fiorucci, G. Maccari, R.S.A. Christopher, C. Zamperini, V. Pau, A. De Logu, S. Tortorella, M. Botta, Discovery of in vitro antitubercular agents through in silico ligand-based approaches, Eur. J. Med. Chem. 121 (2016) 169–180. https://doi.org/10.1016/j.ejmech.2016.05.032.

[42] A. Ben-David, C.E. Davidson, Estimation method for serial dilution experiments, J. Microbiol. Methods. (2014). https://doi.org/10.1016/j.mimet.2014.08.023.

[43] K.J. Aldred, R.J. Kerns, N. Osheroff, Mechanism of quinolone action and resistance, Biochemistry. (2014). https://doi.org/10.1021/bi5000564.

[44] P. Miotto, Y. Zhang, D.M. Cirillo, W.C. Yam, Drug resistance mechanisms and drug susceptibility testing for tuberculosis, Respirology. (2018). https://doi.org/10.1111/resp.13393.

[45] K.A. Bobesh, J. Renuka, R.R. Srilakshmi, S. Yellanki, P. Kulkarni, P. Yogeeswari, D. Sriram, Replacement of cardiotoxic aminopiperidine linker with piperazine moiety reduces cardiotoxicity? Mycobacterium tuberculosis novel bacterial topoisomerase inhibitors, Bioorganic Med. Chem. 24 (2016) 42–52. https://doi.org/10.1016/j.bmc.2015.11.039.

[46] S. Chopra, K. Matsuyama, T. Tran, J.P. Malerich, B. Wan, S.G. Franzblau, S. Lun, H. Guo, M.C. Maiga, W.R. Bishai, P.B. Madrid, Evaluation of gyrase B as a drug target in Mycobacterium tuberculosis, J. Antimicrob. Chemother. (2012). https://doi.org/10.1093/jac/dkr449.

[47] S. Bhakta, N. Scalacci, A. Maitra, A.K. Brown, S. Dasugari, D. Evangelopoulos, T.D. McHugh, P.N. Mortazavi, A. Twist, E. Petricci, F. Manetti, D. Castagnolo, Design and Synthesis of 1-((1,5-Bis(4-chlorophenyl)-2-methyl-1H-pyrrol-3-yl)methyl)-4-methylpiperazine (BM212) and N-Adamantan-2-yl-N′-((E)-3,7-dimethylocta-2,6-dienyl)ethane-1,2-diamine (SQ109) Pyrrole Hybrid Derivatives: Discovery of Potent Antitubercul, J. Med. Chem. (2016). https://doi.org/10.1021/acs.jmedchem.6b00031.

[48] D. Deidda, G. Lampis, R. Fioravanti, M. Biava, G.C. Porretta, S. Zanetti, R. Pompei, Bactericidal activities of the pyrrole derivative BM212 against multidrug-resistant and intramacrophagic Mycobacterium tuberculosis strains, Antimicrob. Agents Chemother. (1998). https://doi.org/10.1128/aac.42.11.3035.

[49] L. Jia, J.E. Tomaszewski, C. Hanrahan, L. Coward, P. Noker, G. Gorman, B. Nikonenko, M. Protopopova, Pharmacodynamics and pharmacokinetics of SQ109, a new diamine-based antitubercular drug, Br. J. Pharmacol. (2005). https://doi.org/10.1038/sj.bjp.0705984.

[50] D. Wang, Y. Zhao, Z. Liu, H. Lei, M. Dong, P. Gong, In vitro and intracellular activity of 4-substituted piperazinyl phenyl oxazolidinone analogues against Mycobacterium tuberculosis, J.

Antimicrob. Chemother. 69 (2014) 1711–1714. https://doi.org/10.1093/jac/dkt539.

[51] J. Sarathy, L. Blanc, N. Alvarez-Cabrera, P. O'Brien, I. Dias-Freedman, M. Mina, M. Zimmerman, F. Kaya, H.P.H. Liang, B. Prideaux, J. Dietzold, P. Salgame, R.M. Savic, J. Linderman, D. Kirschner, E. Pienaar, V. Dartois, Fluoroquinolone efficacy against tuberculosis is driven by penetration into lesions and activity against resident bacterial populations, Antimicrob. Agents Chemother. (2019). https://doi.org/10.1128/AAC.02516-18.

[52] N. Suresh, H.N. Nagesh, J. Renuka, V. Rajput, R. Sharma, I.A. Khan, C.S. Kondapalli Venkata Gowri, Synthesis and evaluation of 1-cyclopropyl-6-fluoro-1,4-dihydro-4-oxo-7-(4-(2-(4-substitutedpiperazin-1-yl)acetyl)piperazin-1-yl)quinoline-3-carboxylic acid derivatives as anti-tubercular and antibacterial agents, Eur. J. Med. Chem. 71 (2014) 324–332. https://doi.org/10.1016/j.ejmech.2013.10.055.

[53] K.I. Reddy, K. Srihari, J. Renuka, K.S. Sree, A. Chuppala, V.U. Jeankumar, J.P. Sridevi, K.S. Babu, P. Yogeeswari, D. Sriram, An efficient synthesis and biological screening of benzofuran and benzo[d]isothiazole derivatives for Mycobacterium tuberculosis DNA GyrB inhibition, Bioorganic Med. Chem. 22 (2014) 6552–6563. https://doi.org/10.1016/j.bmc.2014.10.016.

[54] K.N. Patel, V.N. Telvekar, Design, synthesis and antitubercular evaluation of novel series of N-[4-(piperazin-1-yl)phenyl]cinnamamide derivatives, Eur. J. Med. Chem. 75 (2014) 43–56. https://doi.org/10.1016/j.ejmech.2014.01.024.

[55] K.M. Naidu, A. Suresh, J. Subbalakshmi, D. Sriram, P. Yogeeswari, P. Raghavaiah, K.V.G. Chandra Sekhar, Design, synthesis and antimycobacterial activity of various 3-(4-(substitutedsulfonyl)piperazin-1-yl)benzo[d[isoxazole derivatives, Eur. J. Med. Chem. 87 (2014) 71–78. https://doi.org/10.1016/j.ejmech.2014.09.043.

[56] H.N. Nagesh, A. Suresh, S.D.S.S. Sairam, D. Sriram, P. Yogeeswari, K.V.G. Chandra Sekhar, Design, synthesis and antimycobacterial evaluation of 1-(4-(2- substitutedthiazol-4-yl)phenethyl)-4-(3-(4-substitutedpiperazin-1-yl)alkyl) piperazine hybrid analogues, Eur. J.

Med. Chem. 84 (2014) 605–613. https://doi.org/10.1016/j.ejmech.2014.07.067.

[57] V. Makarov, B. Lechartier, M. Zhang, J. Neres, A.M. van der Sar, S.A. Raadsen, R.C. Hartkoorn, O.B. Ryabova, A. Vocat, L.A. Decosterd, N. Widmer, T. Buclin, W. Bitter, K. Andries, F. Pojer, P.J. Dyson, S.T. Cole, Towards a new combination therapy for tuberculosis with next generation benzothiazinones, EMBO Mol. Med. 6 (2014) 372–383. https://doi.org/10.1002/emmm.201303575.

[58] R. Manjunatha, R. Shandil, M. Panda, C. Sadler, A. Ambady, V. Panduga, N. Kumar, J. Mahadevaswamy, M. Sreenivasaiah, A. Narayan, S. Guptha, S. Sharma, V.K. Sambandamurthy, V. Ramachandran, M. Mallya, C. Cooper, K. Mdluli, S. Butler, R. Tommasi, P.S. Iyer, S. Narayanan, M. Chatterji, P.S. Shirude, Scaffold Morphing To Identify Novel DprE1 Inhibitors with Antimycobacterial Activity, ACS Med. Chem. Lett. (2019). https://doi.org/10.1021/acsmedchemlett.9b00343.

[59] A. Jallapally, D. Addla, P. Yogeeswari, D. Sriram, S. Kantevari, 2-Butyl-4-chloroimidazole based substituted piperazine-thiosemicarbazone hybrids as potent inhibitors of Mycobacterium tuberculosis, Bioorganic Med. Chem. Lett. 24 (2014) 5520–5524. https://doi.org/10.1016/j.bmcl.2014.09.084.

[60] K. Chauhan, M. Sharma, P. Trivedi, V. Chaturvedi, P.M.S. Chauhan, New class of methyl tetrazole based hybrid of (Z)-5-benzylidene-2- (piperazin-1-yl)thiazol-4(%H)-one as potent antitubercular agents, Bioorganic Med. Chem. Lett. 24 (2014) 4166–4170. https://doi.org/10.1016/j.bmcl.2014.07.061.

[61] M. Rotta, K. Pissinate, A.D. Villela, D.F. Back, L.F.S.M. Timmers, J.F.R. Bachega, O.N. De Souza, D.S. Santos, L.A. Basso, P. Machado, Piperazine derivatives: Synthesis, inhibition of the Mycobacterium tuberculosis enoyl-acyl carrier protein reductase and SAR studies, Eur. J. Med. Chem. 90 (2015) 436–447. https://doi.org/10.1016/j.ejmech.2014.11.034.

[62] H. Kanetaka, Y. Koseki, J. Taira, T. Umei, H. Komatsu, H. Sakamoto, G. Gulten, J.C.

Sacchettini, M. Kitamura, S. Aoki, Discovery of InhA inhibitors with anti-mycobacterial activity through a matched molecular pair approach, Eur. J. Med. Chem. (2015). https://doi.org/10.1016/j.ejmech.2015.02.062.

[63] K.R. Yempalla, G. Munagala, S. Singh, A. Magotra, S. Kumar, V.S. Rajput, S.S. Bharate, M. Tikoo, G.D. Singh, I.A. Khan, R.A. Vishwakarma, P.P. Singh, Nitrofuranyl Methyl Piperazines as New Anti-TB Agents: Identification, Validation, Medicinal Chemistry, and PK Studies, ACS Med. Chem. Lett. 6 (2015) 1041–1046. https://doi.org/10.1021/acsmedchemlett.5b00141.

[64] K.M. Naidu, R.N. Gajanan, K.V.G. Chandra Sekhar, Design, synthesis and biological evaluation of 5-(2-(4-(substituted benzo[d]isoxazol-3-yl)piperazin-1-yl)acetyl)indolin-2-one and 5-(2-(4-substitutedpiperazin-1-yl)acetyl)indolin-2-one analogues as novel anti-tubercular agents, Arab. J. Chem. 12 (2019) 2418–2429. https://doi.org/10.1016/j.arabjc.2015.02.025.

[65] A. Chollet, G. Mori, C. Menendez, F. Rodriguez, I. Fabing, M.R. Pasca, J. Madacki, J. Korduláková, P. Constant, A. Quémard, V. Bernardes-Génisson, C. Lherbet, M. Baltas, Design, synthesis and evaluation of new GEQ derivatives as inhibitors of InhA enzyme and Mycobacterium tuberculosis growth, Eur. J. Med. Chem. 101 (2015) 218–235. https://doi.org/10.1016/j.ejmech.2015.06.035.

[66] F. Bonnier, M.E. Keating, T.P. Wróbel, K. Majzner, M. Baranska, A. Garcia-Munoz, A. Blanco, H.J. Byrne, Cell viability assessment using the Alamar blue assay: A comparison of 2D and 3D cell culture models, Toxicol. Vitr. (2015). https://doi.org/10.1016/j.tiv.2014.09.014.

[67] B. Medapi, P. Suryadevara, J. Renuka, J.P. Sridevi, P. Yogeeswari, D. Sriram, 4-Aminoquinoline derivatives as novel Mycobacterium tuberculosis GyrB inhibitors: Structural optimization, synthesis and biological evaluation, Eur. J. Med. Chem. 103 (2015) 1–16. https://doi.org/10.1016/j.ejmech.2015.06.032.

[68] V. Nair, M.O. Okello, N.K. Mangu, B.I. Seo, M.G. Gund, A novel molecule with notable activity against multi-drug resistant tuberculosis, Bioorganic Med. Chem. Lett. 25 (2015) 1269–1273. https://doi.org/10.1016/j.bmcl.2015.01.050.

[69] S. Wang, X.D. Jia, M.L. Liu, Y. Lu, H.Y. Guo, Synthesis, antimycobacterial and antibacterial activity of ciprofloxacin derivatives containing a N-substituted benzyl moiety, Bioorganic Med. Chem. Lett. 22 (2012) 5971–5975. https://doi.org/10.1016/j.bmcl.2012.07.040.

[70] R. V. Patel, P. Kumari, D.P. Rajani, K.H. Chikhalia, Discovery of 2-(4-cyano-3-trifluoromethylphenyl amino)-4-(4-quinazolinyloxy)-6-piperazinyl(piperidinyl)-s-triazines as potential antibacterial agents, Med. Chem. Res. 21 (2012) 4177–4192. https://doi.org/10.1007/s00044-011-9950-4.

[71] K.M. Agrawal, G.S. Talele, Synthesis and antibacterial, antimycobacterial and docking studies of novel N-piperazinyl fluoroquinolones, Med. Chem. Res. 22 (2013) 818–831. https://doi.org/10.1007/s00044-012-0074-2.

[72] H.N. Nagesh, K.M. Naidu, D.H. Rao, J.P. Sridevi, D. Sriram, P. Yogeeswari, K.V.G. Chandra Sekhar, Design, synthesis and evaluation of 6-(4-((substituted-1H-1,2,3-triazol-4-yl)methyl)piperazin-1-yl)phenanthridine analogues as antimycobacterial agents, Bioorganic Med. Chem. Lett. 23 (2013) 6805–6810. https://doi.org/10.1016/j.bmcl.2013.10.016.

[73] Y. Hu, X. Wu, J. Luo, Y. Fu, L. Zhao, Y. Ma, Y. Li, Q. Liang, Y. Shang, H. Huang, Detection of pyrazinamide resistance of Mycobacterium tuberculosis using nicotinamide as a surrogate, Clin. Microbiol. Infect. (2017). https://doi.org/10.1016/j.cmi.2017.03.028.

[74] A. Kamal, P. Swapna, R.V.C.R.N.C. Shetti, A.B. Shaik, M.P. Narasimha Rao, F. Sultana, I.A. Khan, S. Sharma, N.P. Kalia, S. Kumar, B. Chandrakant, Anti-tubercular agents. Part 7: A new class of diarylpyrrole-oxazolidinone conjugates as antimycobacterial agents, Eur. J. Med. Chem. 64 (2013) 239–251. https://doi.org/10.1016/j.ejmech.2013.03.027.

[75] Y.L. Zhao, Y.L. Chen, J.Y. Sheu, I.L. Chen, T.C. Wang, C.C. Tzeng, Synthesis and antimycobacterial evaluation of certain fluoroquinolone derivatives, Bioorganic Med. Chem. 13 (2005) 3921–3926. https://doi.org/10.1016/j.bmc.2005.04.005.

[76] D. Sriram, T.R. Bal, P. Yogeeswari, Synthesis, antiviral and antibacterial activities of isatin mannich bases, Med. Chem. Res. 14 (2005) 211–228. https://doi.org/10.1007/s00044-005-0135-x.

[77] R. V. Patel, P. Kumari, D.P. Rajani, K.H. Chikhalia, Synthesis and studies of novel 2-(4-cyano-3-trifluoromethylphenyl amino)-4-(quinoline-4-yloxy)-6-(piperazinyl/piperidinyl)-s-triazines as potential antimicrobial, antimycobacterial and anticancer agents, Eur. J. Med. Chem. 46 (2011) 4354–4365. https://doi.org/10.1016/j.ejmech.2011.07.006.

[78] A. V. Shindikar, C.L. Viswanathan, Novel fluoroquinolones: Design, synthesis, and in vivo activity in mice against Mycobacterium tuberculosis H37Rv, Bioorganic Med. Chem. Lett. 15 (2005) 1803–1806. https://doi.org/10.1016/j.bmcl.2005.02.037.

[79] A. Kamal, A.H. Babu, A.V. Ramana, R. Sinha, J.S. Yadav, S.K. Arora, Antitubercular agents. Part 1: Synthesis of phthalimido- and naphthalimido-linked phenazines as new prototype antitubercular agents, Bioorganic Med. Chem. Lett. 15 (2005) 1923–1926. https://doi.org/10.1016/j.bmcl.2005.01.085.

[80] M. Rani, P. Parthiban, R. Ramachandran, S. Kabilan, Design and synthesis of novel piperazine unit condensed 2,6-diarylpiperidin-4-one derivatives as antituberculosis and antimicrobial agents, Med. Chem. Res. 21 (2012) 653–662. https://doi.org/10.1007/s00044-011-9573-9.

[81] R. Ganeswrie, C.S. Chui, S. Balan, S.D. Puthucheary, Comparison of BACTEC MGIT 960 system and BACTEC 460 TB system for growth and detection of Mycobacteria from clinical specimens., Malays. J. Pathol. (2004).

[82] R.P. Tangallapally, R. Yendapally, R.E. Lee, A.J.M. Lenaerts, R.E. Lee, Synthesis and

evaluation of cyclic secondary amine substituted phenyl and benzyl nitrofuranyl amides as novel antituberculosis agents, J. Med. Chem. 48 (2005) 8261–8269. https://doi.org/10.1021/jm050765n.

[83] X. He, A. Alian, P.R. Ortiz de Montellano, Inhibition of the Mycobacterium tuberculosis enoyl acyl carrier protein reductase InhA by arylamides, Bioorganic Med. Chem. 15 (2007) 6649–6658. https://doi.org/10.1016/j.bmc.2007.08.013.

[84] R. Tangallapally, R. Yendapally, A. Daniels, R. Lee, R. Lee, Nitrofurans as Novel Anti-tuberculosis Agents: Identification, Development and Evaluation, Curr. Top. Med. Chem. 7 (2007) 509–526. https://doi.org/10.2174/156802607780059772.

[85] E. Bogatcheva, C. Hanrahan, B. Nikonenko, R. Samala, P. Chen, J. Gearhart, F. Barbosa, L. Einck, C.A. Nacy, M. Protopopova, Identification of new diamine scaffolds with activity against Mycobacterium tuberculosis, J. Med. Chem. 49 (2006) 3045–3048. https://doi.org/10.1021/jm050948+.

[86] N. Patil, H. Saba, A. Marco, R. Samant, L. Mukasa, Initial experience with GeneXpert MTB/RIF assay in the Arkansas tuberculosis control program, Australas. Med. J. (2014). https://doi.org/10.4066/amj.2014.1905.

[87] R.S. Upadhayaya, P.D. Shinde, S.A. Kadam, A.N. Bawane, A.Y. Sayyed, R.A. Kardile, P.N. Gitay, S. V. Lahore, S.S. Dixit, A. Földesi, J. Chattopadhyaya, Synthesis and antimycobacterial activity of prodrugs of indeno[2,1-c]quinoline derivatives, Eur. J. Med. Chem. 46 (2011) 1306–1324. https://doi.org/10.1016/j.ejmech.2011.01.053.

[88] D. Sriram, P. Yogeeswari, S.P. Reddy, Synthesis of pyrazinamide Mannich bases and its antitubercular properties, Bioorganic Med. Chem. Lett. 16 (2006) 2113–2116. https://doi.org/10.1016/j.bmcl.2006.01.064.

[89] K.D. Thomas, A.V. Adhikari, I.H. Chowdhury, E. Sumesh, N.K. Pal, New quinolin-4-yl-1,2,3-

triazoles carrying amides, sulphonamides and amidopiperazines as potential antitubercular agents, Eur. J. Med. Chem. 46 (2011) 2503–2512. https://doi.org/10.1016/j.ejmech.2011.03.039.

[90] S. Talath, A.K. Gadad, Synthesis, antibacterial and antitubercular activities of some 7-[4-(5-amino-[1,3,4]thiadiazole-2-sulfonyl)-piperazin -1-yl] fluoroquinolonic derivatives, Eur. J. Med. Chem. 41 (2006) 918–924. https://doi.org/10.1016/j.ejmech.2006.03.027.

[91] Y. Nakamura, R. Kano, T. Murai, S. Watanabe, A. Hasegawa, Susceptibility testing of Malassezia species using the urea broth microdilution method, Antimicrob. Agents Chemother. (2000). https://doi.org/10.1128/AAC.44.8.2185-2186.2000.

[92] A. Kamal, R.V.C.R.N.C. Shetti, S. Azeeza, P. Swapna, M.N.A. Khan, I.A. Khan, S. Sharma, S.T. Abdullah, Anti-tubercular agents. Part 6: Synthesis and antimycobacterial activity of novel arylsulfonamido conjugated oxazolidinones, Eur. J. Med. Chem. 46 (2011) 893–900. https://doi.org/10.1016/j.ejmech.2010.12.028.

[93] Q. Guo, M.L. Liu, L.S. Feng, K. Lv, Y. Guan, H.Y. Guo, C.L. Xiao, Synthesis and in-vitro antimycobacterial activity of fluoroquinolone derivatives containing a coumarin moiety, Arch. Pharm. (Weinheim). 344 (2011) 802–809. https://doi.org/10.1002/ardp.201000256.

[94] J. Choi, H.Y. Jeong, G.Y. Lee, S. Han, S. Han, B. Jin, T. Lim, S. Kim, D.Y. Kim, H.C. Kim, E.C. Kim, S.H. Song, T.S. Kim, S. Kwon, Direct, rapid antimicrobial susceptibility test from positive blood cultures based on microscopic imaging analysis, Sci. Rep. (2017). https://doi.org/10.1038/s41598-017-01278-2.

[95] O.A. Phillips, E.E. Udo, R. Varghese, Antimycobacterial Activities of Novel 5-(1H-1,2,3-Triazolyl)Methyl Oxazolidinones, Tuberc. Res. Treat. 2012 (2012) 1–7. https://doi.org/10.1155/2012/289136.

[96] S.K. Gill, H. Xu, P.D. Kirchhoff, T. Cierpicki, A.J. Turbiak, B. Wan, N. Zhang, K.W. Peng,

S.G. Franzblau, G.A. Garcia, H.D.H. Showalter, Structure-based design of novel benzoxazinorifamycins with potent binding affinity to wild-type and rifampin-resistant mutant Mycobacterium tuberculosis RNA polymerases, J. Med. Chem. 55 (2012) 3814–3826. https://doi.org/10.1021/jm201716n.

[97] V. Molodtsov, N.T. Scharf, M.A. Stefan, G.A. Garcia, K.S. Murakami, Structural basis for rifamycin resistance of bacterial RNA polymerase by the three most clinically important RpoB mutations found in Mycobacterium tuberculosis, Mol. Microbiol. (2017). https://doi.org/10.1111/mmi.13606.

[98] Y.L. Chen, Y.W. Chen, W.F. Lo, C.L. Kao, Y.S. Liu, C.W. Yao, C.C. Tzeng, Synthesis and antimycobacterial evaluation on arylsulfonyl and arylcarbonyl derivatives of ofloxacin, J. Chinese Chem. Soc. 56 (2009) 374–380. https://doi.org/10.1002/jccs.200900054.

[99] V.U. Jeankumar, R.S. Reshma, R. Vats, R. Janupally, S. Saxena, P. Yogeeswari, D. Sriram, Engineering another class of anti-tubercular lead: Hit to lead optimization of an intriguing class of gyrase ATPase inhibitors, Eur. J. Med. Chem. 122 (2016) 216–231. https://doi.org/10.1016/j.ejmech.2016.06.042.

[100] J. Piton, A. Vocat, A. Lupien, C.S. Foo, O. Riabov, V. Makarov, S.T. Cole, Structure-based drug design and characterization of sulfonyl-piperazine benzothiazinone inhibitors of DprE1 from mycobacterium tuberculosis, Antimicrob. Agents Chemother. 62 (2018). https://doi.org/10.1128/AAC.00681-18.

[101] WO2013148174A1.pdf, (n.d.).

[102] WO2019243971A1.pdf, (n.d.).

[103] WO2005007625A2.pdf, (n.d.).

[104] WO2012066518A1.pdf, (n.d.).

[105] WO2001056974A2.pdf, (n.d.).

[106] WO2007014885A1.pdf, (n.d.).

[107] WO2012141338A1.pdf, (n.d.).

[108] WO2006109323A1.pdf, (n.d.).

[109] WO2015193454A1.pdf, (n.d.).

[110] WO2013072903A1.pdf, (n.d.).

Chapter3

Design, Synthesis and Antibacterial Activity of Novel Piperazine-Hydrazide Hybrids

(Ready to communicate)

Graphical Abstract

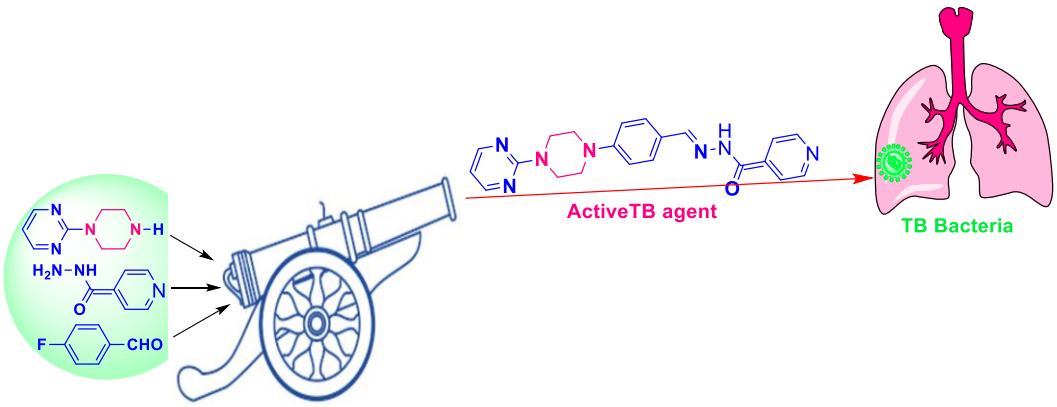

Abstract

A series of piperazine-hydrazide hybrids (**c1-c15**) have been designed and synthesised. The *in vitro* study of all the derivatives has been performed against the *mycobacterium tuberculosis* (MTB) strain *H37Rv* strain. We have also studied the zone of inhibition against eight microbial strains, including gram-positive (*methicillin-resistant staphylococcus aureus (MRSA), Streptococcus pyrogens, Bacillus subtilis, Enterococcus faecium,* and *Staphylococcus aureus)* and gram-negative (*Enterobacter hormaechei, Pseudomonas aeruginosa,* and *Escherichia coli*) strains. Compound **c8** displayed the best activity against mycobacterium strain $H_{37}Rv$ with a MIC value of **0.39-0.78µg/ml**,whereas other derivatives failed to show their activity against $H_{37}Rv$. None of the synthesised derivatives has displayed an effective inhibition zone against any microbial strain.

1. Introduction

Tuberculosis is a life-threatening infectious disease caused by the mycobacterium tuberculosis bacteria. According to the 2021 report by WHO, tuberculosis is the 13th leading cause of death and reported 10 million TB-infected cases globally[1]. Furthermore, bacteria in some TB patients

develop resistance to first-line TB drugs and convert the disease into MDR-TB. Also, few bacterial strains develop resistance to second-line drugs, resulting in drug-resistant TB (XDR TB). As a result, curing it is getting increasingly difficult because of TB's resistance to the reported drugs. Consequently, novel antitubercular agents must be developed to treat MDR and XDR TB. Similarly, researchers are hard at work developing new anti-TB drugs based on various types of moieties and their combinations.

The compound bearing piperazine moiety shows pharmacological activity towards different pharmacological targets, including antioxidative[2], antipsychotic[3], antidepressant[4], anticancer[5], antibacterial[6], antifungal[7], antimalarial[8], anticonvulsant[9], and antimycobacterial[10] (EJMC review). There are some potential anti-TB agents under clinical development, such as Bedaquiline, Delamanid, Rifapentine, Clofazimine, Rifampicin, Telacebec, BTZ-043, Macozinone, OPC-167832, GSK-286, TBI-223, TBA-7371, TBAJ-876 Diarylquinoline, TBI-166, etc. among these drug molecules, most of them are having piperazine moiety , which motivates researchers to design molecular hybrids of piperazine moiety. In many antitubercular agents, the piperazine unit connected to the phenyl ring has shown high potency towards mycobacterium strain *$H_{37}Rv$*. **Fig 1** displayed phenylpiperazine with different heteroaromatic hybrids with potent anti-TB activity[10,11,12, 13].

Schiff base of isoniazid, thiazoles as a hydrazide have also displayed good pharmacological efficacy towards the MTB [14,15,16], Molecular hybrid of N-phenylpiperazine with Imidazo[2,1-b]thiazolealso showed excellent potency towards the *Mycobacterium* strain[17]. The hybrid structure of Phenylsulfonyl-piperazine with 2-nitrofuran showed good antitubercular activity[18].Our research into the related earlier arts led us to build a novel series ofPhenylsulfonyl-piperazine **c** and phenyl-piperazine **e**. Hybrids via Schiff base formation with aryl hydrazides as shown in **scheme:1** and **2,** respectively. All the synthesised compounds have been tested for their anti-mycobacterial and antibacterial properties under *in vitro* study.

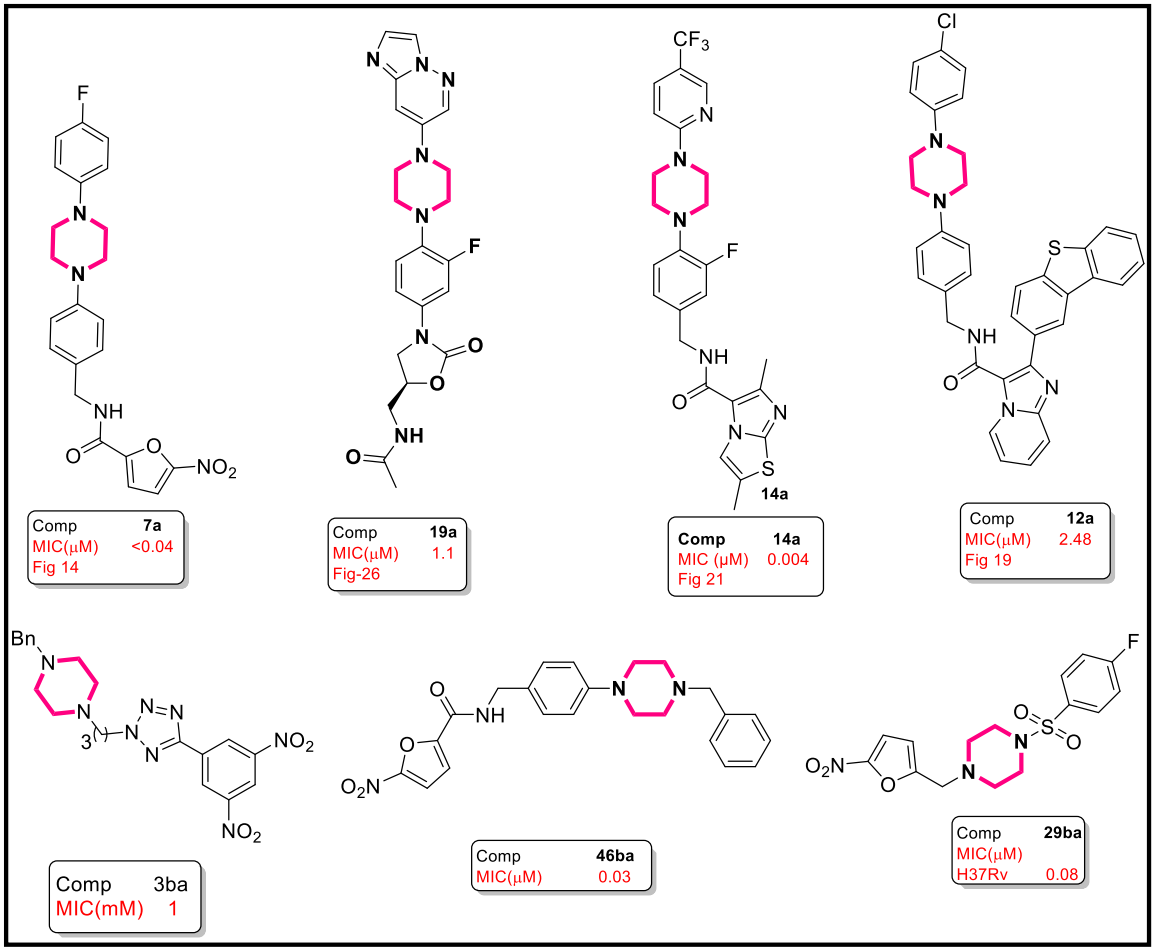

Figure 1 Phenyl piperazine derivatives with their antitubercular activity

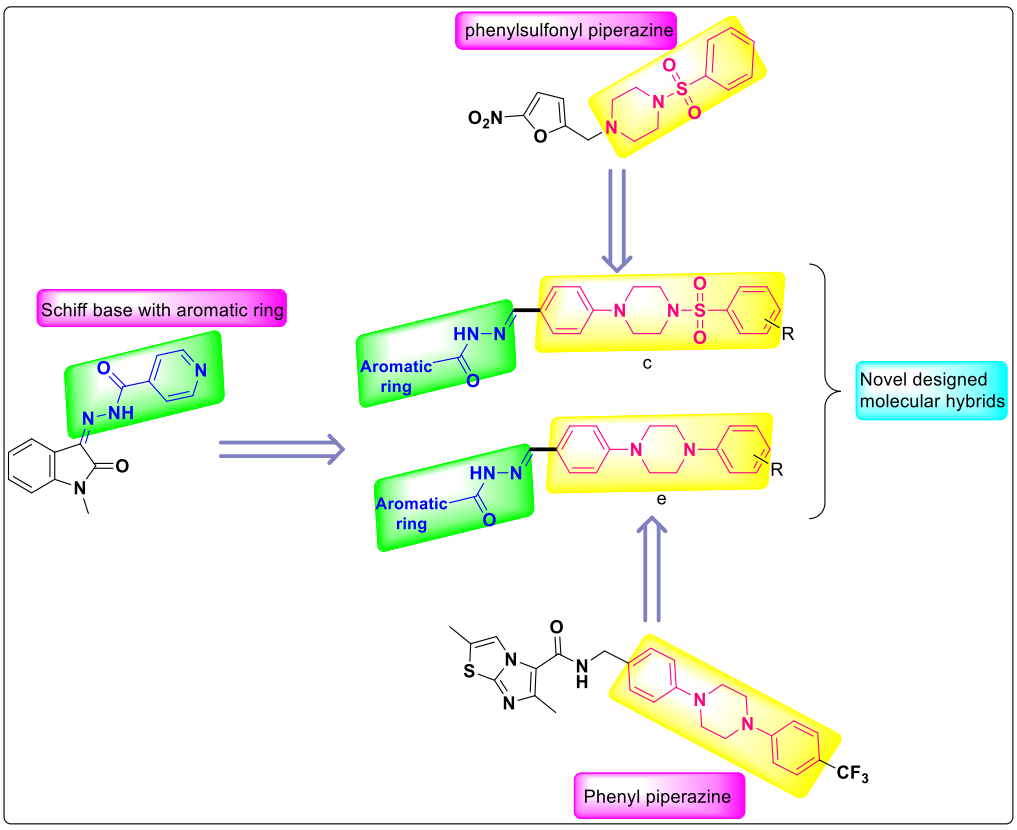

Figure 2 Design strategy for the synthesis of Piperazine-Hydrazide Hybrids

2. Result and discussion

2a. Chemistry

All the compounds were synthesised from relatively low-cost precursors except phenyl piperazines. As per the synthetic strategy, phenyl hydrazides A (**scheme 1**) were first required to form a Schiff base(**step iii**, **scheme 2**). Phenyl hydrazides were obtained by refluxing phenyl benzoate and hydrazine in ethanol, as shown in **scheme 1**. Next, we have synthesised the final derivatives, as illustrated in **Scheme 2**. Intermediate **a**was obtained by reaction of phenyl sulphonyl chloride and piperazine. To avoid substitution at both nitrogen and piperazine, we have used excess piperazine (10 equivalents) (**scheme 2, step i)**. Intermediate **b** obtained by aromatic nucleophilic subtitution of intermediate **a** on 4-fluorobenzaldehyde (**step ii**). Final **step iii** involved a Schiff base formation between intermediate**b** and phenyl hydrazides under reflux in ethanol and in the presence of the catalytic amount of glacial acetic acid.

We also tried to synthesise phenyl piperazines **R_3** using the commercially available, low-cost precursors aniline and bis(2-chloroethyl)amine hydrochloride salt (**Scheme 3**). This reaction was carried out at 140°C in base K_2CO_3 under DMF to obtain the expected compound **R_3.** Additionaly, we observed 35% of amide compound **R_4** due to the incorporation of the formyl group of the solvent DMF**.** This amide was refluxed under ethanol in the presence of base NaOH **to** get **R_3.** Though we obtained the desired compound **R_3**, the relative yield was relatively low due to the harsh reaction conditions and the need for two steps.

For this reason, we tried a variety of solvents and temperatures (including toluene, xylene, and dimethyl sulfoxide) at 100°C, 120°C, 140°C, and 160°C, but we were unable to get compound **R_3**. We also tried this reaction under different bases, such as $KHCO_3$, NaHCO3, NaOH, and KOH, but the reaction failed in the presence of these bases. Based on this study, we have developed and published a methodology on transamidation, "Facile Synthesis of Amides Through TransamidationWith Iodine Under Neat Conditions" [19].Hence, we procure commercially available phenyl piperazine derivatives **R_3** and synthesised **c5-c15** using the same procedure for the synthesis of c in **scheme 2** (steps **ii** and **iii)**. The synthetic route of derivatives **e5-e15**is illustrated in **scheme 5.**

1. Synthesis of hydrazides **A1-A5**

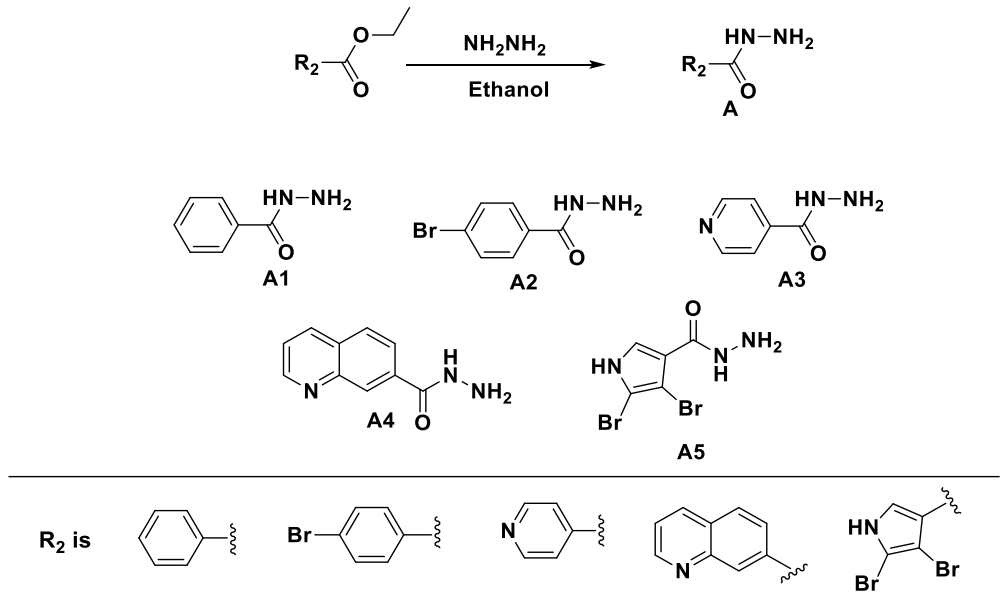

Reaction conditions: Hydrazine, ethanol, 80°C, 5hrs

Scheme 1

2. Synthesis of compound **c1-c15**

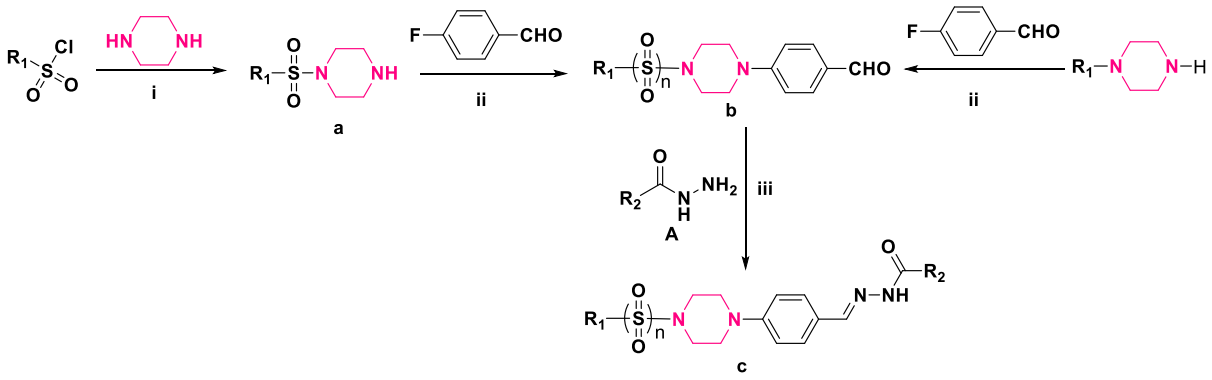

Comp no.	n	R_1	R_2	Comp no.	n	R_1	R_2
c1	1	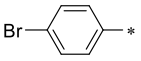		c9	0		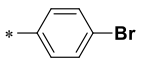
c2	1	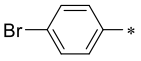	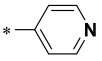	c10	0		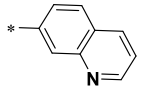
c3	1	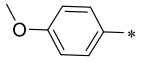		c11	0	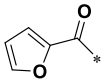	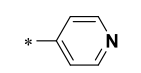
c4	1	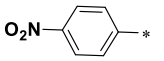	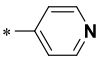	c12	0	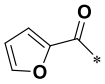	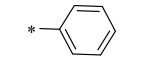
c5	0	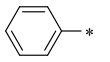	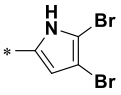	c13	0	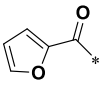	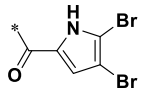
c6	0	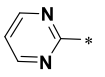	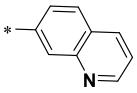	c14	0		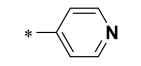
c7	0	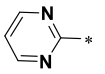	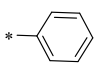	c15	0		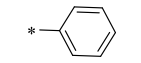
c8	0	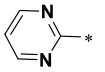	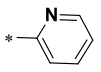				

Reaction conditions: i) Piperazine, DCM, 0°C-rt, 30 min, ii) K_2CO_3, DMF, 120°C, 16hrs, iii) Glacial acetic acid, ethanol, 80°C, 2hrs

Scheme 2

3. Synthesis of phenyl piperazines

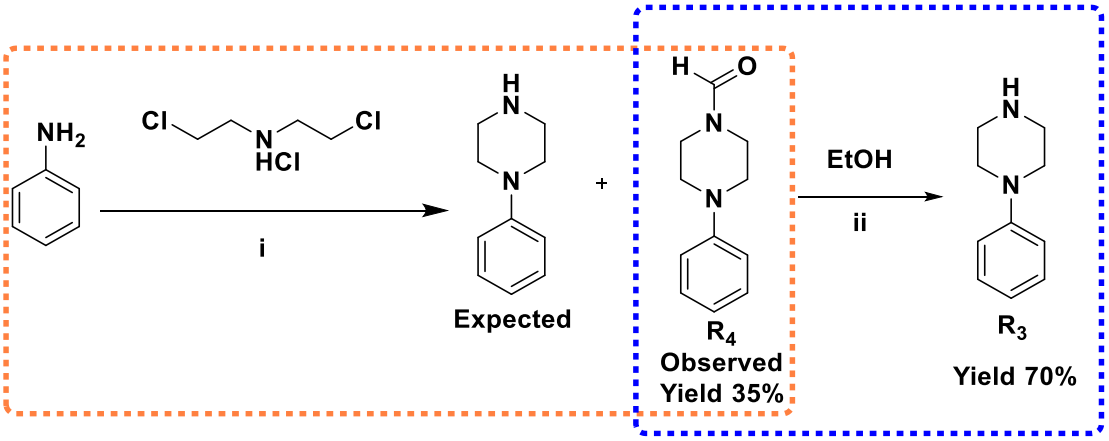

Reaction conditions: ii) K_2CO_3, DMF, 140°C, 18hrs, iii) NaOH, ethanol, 80°C, 2hrs

Scheme 3

NMR data discussion

(E)-N'-(4-(4-((4-bromophenyl)sulfonyl)piperazin-1-yl)benzylidene)isonicotinohydrazide (c2)

^{1}H NMR

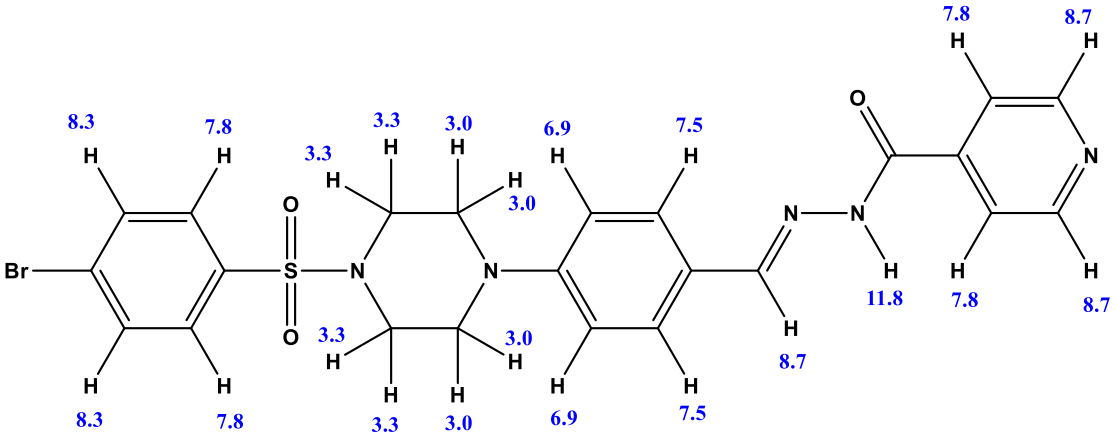

The amide proton is highly deshielded and it displayed delta value at 11.8 ppm due to the resonance with the adjacent carbonyl group. The proton on the sp^2 carbon attached to the hydrazide group is deshielded and showed delta value at 8.7 ppm. Similarly, the aromatic protons adjacent to nitrogen in the pyridine ring and the aromatic protons adjacent to bromine substituent are deshielded and showed the delta value at 8.7 and 8.3 ppm respectively. The other aromatic protons appeared between 7.8 to

6.9 ppm. Due to the difference in the chemical environment, the piperazine ring showed two sets of protons with the delta value 3.33 and 3.0 ppm respectively.

^{13}C NMR

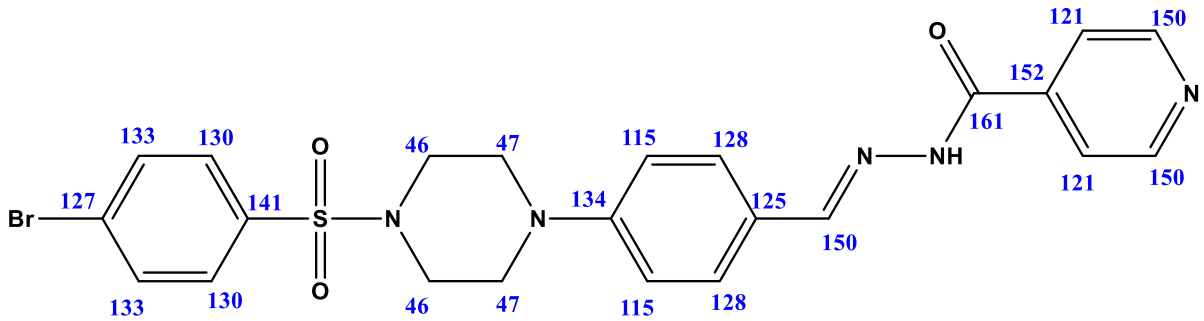

In C^{13} NMR, carbonyl carbons exhibit delta values between 180 and 220 ppm. However, due to the conjugation between the lone pair electrons of the amide nitrogen and the carbonyl carbon, the delta value of the amide carbonyl carbon is shifted to up field at 161 ppm in the present compound. The carbons next to the nitrogen in the pyridyl ring are deshielded, and showed a delta value of 150 ppm. Similarly, the carbon next to the amide carbonyl and the carbon next to the sufonyl group showed delta values at152 and 141 ppm, respectively. The other aromatic sp^2 carbons showed peaks ranging from 115 to 134 ppm. The delta value of the piperazine ring's sp3 carbons was 46 and 47 ppm.

(E)-N'-(4-(4-(pyrimidin-2-yl)piperazin-1-yl)benzylidene)picolinohydrazide (c8)

^{1}H NMR

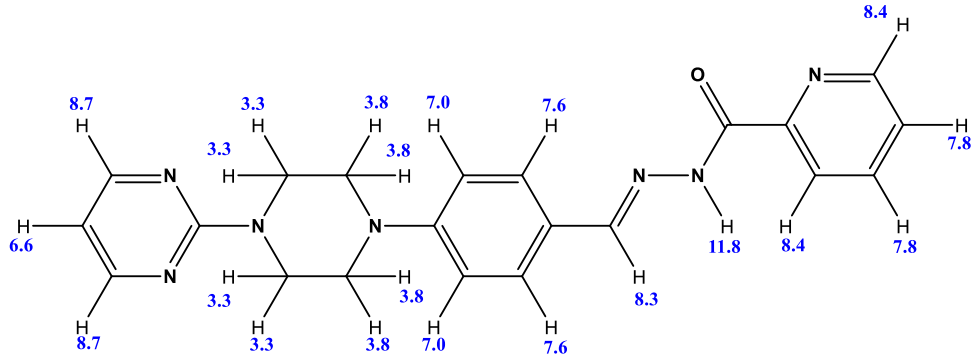

The amide proton is highly deshielded and it displayed delta value at 11.8 ppm because of the resonance with the adjacent carbonyl carbon. The protons on thesp^2carbonattached to the hydrazide

group is deshielded and showed a delta value at 8.3 ppm. Similarly, the protons adjacent to the nitrogen in the pyridine and the pyrimidine ring are deshielded and these protons showed the delta value at 8.4 and 8.7 ppm respectively. The protons of the middle phenyl ring showed the delta value ranging from 6.6 to 7.8 ppm. Due to the difference in the chemical environment, the piperazine showed two sets of protons with the delta value 3.8 and 3.3 ppm respectively.

^{13}C NMR

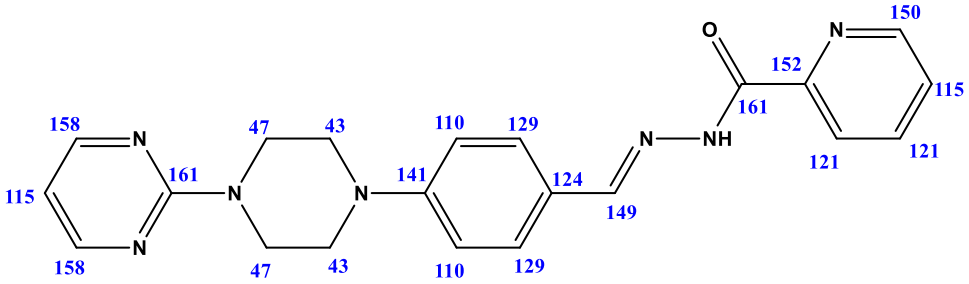

In C^{13} NMR, carbonyl carbons generally exhibit delta values between 180 and 220 ppm. However, due to the conjugation between nitrogen's lone pair and the carbonyl carbon, the delta value of amide carbonyl carbon is shifted to up field at 161 ppm in this structure. The sp^2carbon atoms next to nitrogen in the pyridine and pyrimidine ring are deshielded and showed the delta value at150, 158 and 158 ppm respectively. The sp^2carbon atom that is attached to the pyrimidine ring and the piperazine ring showed delta value at 161 ppm. Similarly, the carbon atom next to the hydrazine groups showed a peak at 149 ppm. The other aromatic sp2 carbons of the middle phenyl ring, the pyridine and the pyrimidine ring showed delta values ranging from 115 to 130 ppm. The delta value of the piperazine ring's sp3 carbon was 47 and 43 ppm.

2b. Biological evaluation

1. *Mycobacterium* activity

We performed the in vitro assessment against the *$H_{37}Rv$* mycobacterium strain based on the design of novel piperazine-hydrazone derivatives. The combination of Phenyl sulphonamide piperazines with isoniazid and phenylhydrazone (**c1-c4**) did not show a good effect. The combination of the furan-piperazine amide with various hydrazones (**c11-c13**) could not demonstrate any activity. Next, we linked pyrazine with phenyl piperazine and incorporated different hydrazones on the other end (**c6-**

c9); compounds with simple phenyl hydrazone and 4-bromo phenyl hydrazone (**c7** and **c9**) showed no activity up to 50µg/ml while the replacement of phenyl hydrazone by isoniazid (**c8**) showed surprising inhibition of $H_{37}Rv$ strain as it displayed its potency as 0.39-0.78 µg/ml. We also incorporated quinoline hydrazones with pyrazine and 2-chloro phenyl-piperazine and (**c6** and **c10**), but none showed expected inhibition.

Table 1: Antimicobacterium activities of synthesized derivatives (c1-c15) against growth of $H_{37}Rv$ strain.

Compound No.	**$H_{37}R_V$[a]MIC(µM)**
c1	>50
c2	>50
c3	>50
c4	>50
c5	>50
c6	>50
c7	>50
c8	**0.39-0.78**
c9	>50
c10	>50
c11	>50
c12	>50
c13	>50
c14	>50

c15	>50
NIH	**0.053**

[a]Minimal inhibitory concentration (MIC µM).*

2. Antimicrobial activity

In the subsequent biological evaluation, we tested these compounds against different microorganisms consisting of Gram-positive bacterial strains *(Methicillin Resistant Staphylococcus aureus (MRSA), Streptococcus pyrogens, Bacillus subtilis, Enterococcus faecium, Staphylococcus aureus),* and Gram-negative bacterial strains (*Enterobacter hormaechei, Pseudomonas aeruginosa, Escherichia coli*) illustrated in Table. We checked the zone of inhibition of all the synthesised compounds at 1000µg/ml and compared their activity with standard reference Ciprofloxacin and Vancomycin. Both the reference drugs showed a 100% inhibition zone, whereas all synthesised compounds failed to show a zone of inhibition against all the bacterial strains.

3. Experimental

3a. Bioassays

1. Material and method

a. M. tuberculosis

MIC determination assays

At 37°C with shaking (200 rpm), Middlebrook 7H9 broth (MB broth) supplemented with 0.05% Tween-80, 0.2% glycerol and 1x albumin dextrose-saline (ADS) was used to culture mycobacterium tuberculosis $H_{37}Rv$ (*M. tuberculosis*). The compounds were prepared as 1000 µg/ml stocks in DMSO and evaluated MIC of antimycobacterial activity at concentrations ranging from 50 to 0.39 µg/ml[20]

b. Antimicrobial

Method used: i) Agar diffusion assay[21] , ii) Broth Microdilution assay[22]

Concentration of compounds: Stock solution [1000 µg/ml] of each compound was prepared in DMSO. Agar diffusion is carried out by taking 5 micro liters from stock solution. Broth micro dilution Assay carried out by 2-fold serial dilution of 100 microliters from stock solution.

Media used:i) Microbiological media used for bacteria is Mueller Hinton Agar (M-H Agar) Composition (gL-1): Beef infusion solids 2.0; starch 1.5; Casein hydrolysate 17.5; Agar 17.0; Final pH (at 25°C) 7.3 ± 0.2. ii) Microbiological media used for bacteria is Mueller Hinton Broth (M-H Broth) Composition (gL-1): Beef infusion solids 2.0; starch 1.5; Casein hydrolysate 17.5; Final pH (at 25°C) 7.4 ± 0.2

3b. Chemistry

1. Material and method

All reactions were conducted under standard operating conditions without any stringent conditions. All chemicals were obtained from Aldrich Chemical Co., Alfa Aesar, and used as received without additional purification. Lab reagent (LR) grade solvents were used for extraction. The reaction progress was monitored on Merck TLC Silica gel 60 F254 plates. The spots were visualized under ultraviolet (UV) light, followed by iodine or ninhydrin staining solution, followed by heating.

NMR spectra were recorded on 400 and 100 MHz NMR spectrometers using $CDCl_3$ and DMSO as solvents unless otherwise stated. MS were made employing ESI (Electron spray ionization). Unless otherwise specified, all reagents were weighed and handled in air.

2. Synthetic procedure

1. Synthesis of compound **A1-A5**

1. Preparation of benzohydrazide **(compound A1)**

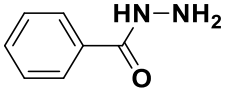

2 mmol of Hydrazine was added to the solution of ethyl benzoate (1 mmol) in 10 volumes of ethanol.The reaction mixture was refluxed for 5 hrs at 80° C[23]. After the reaction completion, the consumption of both the starting materials was confirmed by TLC. The solution was poured into ice-

cold water on completion of the reaction to give a brown crystalline solid. The solid was filtered, washed with water, and recrystallised from ethanol to give **compound A1** (Yield: 73%).

Similarly, compounds**A2** to **A5** were produced using the method described to prepare compound **A1** as illustrated in **scheme 1**.

1. Synthesis of compound **c1-c15**

Preparation of 1-((4-bromophenyl)sulfonyl)piperazine **(compound a)**

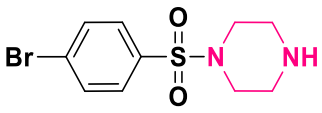

At 0°C with vigorous stirring, 1.0 mmol of benzenesulfonyl chloride was added to a solution containing 10.0 mmol of piperazine dissolved in 50 volumes of DCM. The reaction mixture was stirred for 30 min at rt. After the reaction completion, the consumption of starting materials was confirmed by TLC. The reaction mixture was washed with water (3×40 mL), dried over anhydrous Na2SO4, and DCM evaporated in a vacuum[24] (Yield: 88%).

Preparation of 4-(4-((4-bromophenyl)sulfonyl)piperazin-1-yl)benzaldehyde **(compound b)**

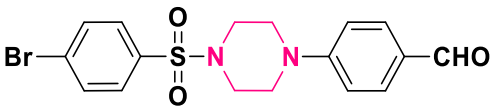

A mixture of 1.0 mmol of 1-((4-bromophenyl)sulfonyl)piperazine, 1.0 mmol of 4-fluorobenzaldehyde and 2.0 mmol of K_2CO_3 was stirred in 5 volumes of DMF at 120°C for 16 hrs. After the reaction completion, the consumption of both the starting materials was confirmed by TLC. The reaction mixture was poured into ice-cold water. The solid separated was filtered and washed with water, and dried. The crude product was purified using column chromatography (silica gel, Ethyl acetate (EtOAc)/Hexane) to obtain a pure product[25](Yield: 62%).

Preparation of (E)-N'-(4-(4-((4-bromophenyl)sulfonyl)piperazin-1-yl)benzylidene)benzohydrazide**(compound c1)**

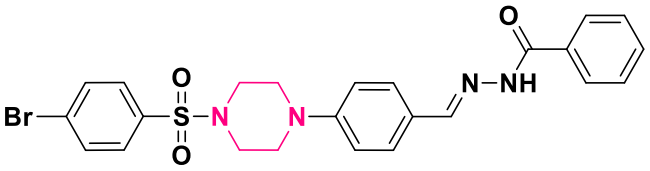

A catalytic amount of glacial acetic acid was added to the solution of 1.0 mmol of 1-(phenylsulfonyl)piperazine and 1.1 mmol of benzo hydrazide in ethanol rt, and the resultant reaction mixture was stirred at 80°C for 2 hrs. The reaction mixture was poured into ice-cold water. The separated solid was filtered and washed with water and diethyl ether and dried under reduced pressure. Similarly, the rest of the derivatives,**c2-c4,** were prepared per the procedure given for **c1**[26] (Yield: 72%).

Similarly, compounds**c2** to **c15** were produced using the method described to prepare compound 1, as illustrated in **Scheme 2**.

3. Experimental data

(E)-N'-(4-(4-((4-bromophenyl)sulfonyl)piperazin-1-yl)benzylidene)benzohydrazide (c1)

White Solid, Yield: 72%, M.P: 264-266°C, FTIR (ATR, Vmax, cm-1): 3299, 2964, 1674, 1444, 1222, 1150, 821.^{1}H NMR (400 MHz, DMSO-d_6) δ 11.6 (s, 1H), 8.33 (s, 1H), 7.9 (t, J=7.5Hz, 4H), 7.7 (d, J=8.4Hz, 2H), 7.5 (m, 5H), 6.9 (d, J=8.5Hz, 2H), 3.3 (s, 4H), 3.0 (s, 4H)ppm. ^{13}C NMR (125 MHz, DMSO-d_6) δ 163.3, 151.8, 148.4, 134.5, 134.1, 133.0, 132.0, 130.0, 128.8, 128.7, 127.9, 127.9, 125.4, 115.7, 47.4, 46.0ppm. LCMS (m/z): $[M+H]^+$ Calculated for $C_{24}H_{23}BrN_4O_3S$ is 527.07; Observed. = 527.67

(E)-N'-(4-(4-((4-bromophenyl)sulfonyl)piperazin-1-yl)benzylidene)isonicotinohydrazide (c2)

White Solid, Yield: 78%, M.P: 230-234°C, FTIR (ATR, Vmax, cm-1): 3497, 2825, 1661, 1384, 1229, 1116, 757. ^{1}H NMR (400 MHz, DMSO-d_6) δ 11.8 (s, 1H), 8.7 (d, J=2.7Hz, 2H), 8.3 (s, 1H), 7.8 (d, J=4.2Hz, 2H), 7.8 (d, J=2.3Hz, 2H), 7.7 (d, J=4.2Hz, 2H), 7.5 (d, J=4.3Hz, 2H), 6.9 (d, J=4.4Hz, 2H), 3.3 (s, 4H), 3.0 (s, 4H) ppm. ^{13}C NMR (125 MHz, DMSO-d_6) δ 161.7, 152.0, 150.7, 149.6, 141.1,

134.5, 133.0, 130.3, 128.9, 127.9, 125.0, 121.9, 115.6, 47.3, 46.0 ppm. LCMS (m/z): $[M+H]^+$ Calculated for $C_{23}H_{22}BrN_5O_3S$ is 528.85; Observed. = 528.06.

(E)-N'-(4-(4-((4-methoxyphenyl)sulfonyl)piperazin-1-yl)benzylidene)benzohydrazide (c3)

White Solid, Yield: 68%, M.P: 244-249°C, FTIR (ATR, Vmax, cm-1): 3744, 3013, 1741, 1478, 1254, 1116, 752.^{1}H NMR (400 MHz, DMSO-d_6) δ 11.6 (s, 1H), 8.3 (s, 1H), 7.9 (t, J=7.5Hz, 4H), 7.7 (d, J=8.8Hz, 2H), 7.6-7.4 (m, 5H), 7.1 (d, J=8.6Hz, 2H), 7.1 (d, J=8.8v, 1H), 6.9 (d, J=8.8Hz, 1H), 3.8 (s, 3H), 3.3 (s, 4H), 2.9 (s, 4H). ^{13}C NMR (125 MHz, DMSO-d_6) δ 163.3, 163.2, 153.1, 151.8, 148.3, 134.1, 132.0, 130.3, 130.2, 130.0, 128.8, 128.7, 127.9, 127.0, 126.5, 125.3, 115.6, 115.0, 115.0, 52.2, 47.3, 46.0, 45.9, 45.3 ppm. LCMS (m/z): $[M+H]^+$ Calculated for $C_{25}H_{26}N_4O_4S$ is 479.17; Observed. = 479.00

(E)-N'-(4-(4-((4-nitrophenyl)sulfonyl)piperazin-1-yl)benzylidene)isonicotinohydrazide (c4)

White solid, Yield: 84%, M.P: 258-263°C, FTIR (ATR, Vmax, cm-1): 3212, 2821, 1653, 1447, 1218, 1060, 746.^{1}H NMR (400 MHz, DMSO-d_6) δ 11.8(s, 1H), 8.7 (d, J=2.3Hz, 2H), 8.5 (1H, J=4.1Hz, d), 8.4 (1H, s), 8.3 (s, 1H), 8.2 (s, J=3.8Hz, 1H), 7.9 (t, J=7.9Hz, 1H), 7.8 (d, J=2.3Hz, 2H), 7.5 (d, J=4.1Hz, 2H), 6.9 (d, J=4.18Hz, 2H), 3.3 (s, 4H), 3.1 (s, 4H) ppm. ^{13}C NMR (125 MHz, DMSO-d_6) δ161.7, 151.9, 150.7, 149.5, 148.6, 141.1, 136.9, 133.9, 132.0, 128.9, 128.4, 125.0, 122.6, 121.9, 115.6, 47.2, 46.0 ppm.LCMS (m/z): $[M+H]^+$ Calculated for $C_{23}H_{22}N_6O_5S$ is 495.14; Observed. = 495.05.

(E)-4,5-dibromo-N'-(4-(4-phenylpiperazin-1-yl)benzylidene)-1H-pyrrole-2-carbohydrazide (c5)

Yellow solid, Yield: 82%, M.P: 248-255°C, FTIR (ATR, Vmax, cm-1): 3743, 3148, 1654, 1431, 1229, 1072, 737.^{1}H NMR (400 MHz, DMSO-d_6) δ 12.9 (s, 1H), 11.3 (s, 1H), 8.2 (s, 1H), 7.5 (d, J=8.0Hz, 2H), 7.2 (t, J=8.1Hz, 2H), 7.0 (d, J=4.3Hz, 3H), 7.0 (d, J=8.1Hz, 2H), 6.8 (t, J=7.1Hz, 1H), 3.4 (t, J=4.7Hz, 4H), 3.2 (t, J=4.2Hz, 4H) ppm. ^{13}C NMR (125 MHz, DMSO-d_6) δ 165.2, 152.3, 151.3, 147.4, 129.4, 128.7, 124.7, 119.6, 116.1, 115.2, 48.6, 47.7 ppm. LCMS (m/z): $[M+H]^+$ Calculated for $C_{22}H_{21}Br_2N_5O$ is 531.61; Observed. = 530.01.

(E)-N'-(4-(4-(pyrimidin-2-yl)piperazin-1-yl)benzylidene)quinoline-7-carbohydrazide (c6)

Yellow sold, Yield: 75%, M.P: 222-228°C, FTIR (ATR, Vmax, cm-1): 3744, 3191, 1741, 1478, 1254, 1034, 752.^{1}H NMR (400 MHz, DMSO-d_6) δ 11.9 (s, 1H), 8.6 (m, 2H), 8.4 (d, J=4.6Hz, 2H), 8.2 (d, J=8.4Hz, 2H), 8.1 (d, J=8.7Hz, 1H), 7.9 (t, J=7.5Hz, 1H), 7.7 (t, J=7.5Hz, 1H), 7.6 (d, J=8.5Hz, 2H), 7.0 (d, J=8.5Hz, 2H), 6.6 (t, J=4.6Hz, 2H), 3.8 (t, J=4.6Hz, 4H), 3.3 (t, J=8.2Hz, 4H) ppm. ^{13}C NMR (125 MHz, DMSO-d_6) 161.6, 160.7, 158.4, 152.5, 150.5, 150.1, 146.4, 138.4, 131.0, 129.6, 129.3, 129.0, 128.7, 128.6, 124.7, 119.5, 115.2, 110.8, 47.5, 43.4 ppm. LCMS (m/z): $[M+H]^+$ Calculated for $C_{25}H_{23}N_7O$ is 465.10; Observed. = 465.10

(E)-N'-(4-(4-(pyrimidin-2-yl)piperazin-1-yl)benzylidene)benzohydrazide (c7)

White Solid, Yield: 66%, M.P: 260-265°C, FTIR (ATR, Vmax, cm-1): 3247, 2832, 1650, 1446, 1223, 961, 793.^{1}H NMR (400 MHz, DMSO-d_6) δ 11,6 (s, 1H), 8.4 (d, J=4.6Hz, 2H), 8.3 (s, 1H), 7.9 (d, J=3.7Hz, 2H), 7.6-7.5 (m, 5H), 7.0(d, J=4.3Hz, 2H), 6,6 (t, J=4.6Hz, 1H), 3.9 (t, J=4.8Hz, 4H), 3.3 (t, J=4.8Hz, 4H) ppm. ^{13}C NMR (125 MHz, DMSO-d_6) δ 163.2, 161.6, 158.4, 152.4, 148.5, 134.1, 132.0, 128.9, 128.8, 128.0, 124.8, 115.2, 110.8, 47.5, 43.4 ppm. LCMS (m/z): $[M+H]^+$ Calculated for $C_{22}H_{22}N_6O$ is 387.19; Observed. = 387.19.

(E)-N'-(4-(4-(pyrimidin-2-yl)piperazin-1-yl)benzylidene)picolinohydrazide (c8)

Yellow solid, Yield: 79%, M.P: 273-278°C, FTIR (ATR, Vmax, cm-1): 3198, 2817, 1649, 1443, 1292, 1058, 765.^{1}H NMR (400 MHz, DMSO-d_6) δ 11.8 (s, 1H), 8.7 (d, J=2.8Hz, 2H), 8.4 (d, J=2.4Hz, 2H), 8.35 (s, 1H), 7.8 (d, J=2.8Hz, 2H), 7.6 (d, J=4.8Hz, 2H), 7.0 (d, J=4.4Hz, 2H), 6.6 (t, J=4.8Hz, 1H), 3.88 (t, J=5.1Hz, 4H), 3.3 (t, J=5.3Hz, 4H) ppm. ^{13}C NMR (125 MHz, DMSO-d_6) δ 161.6, 158.4, 152.6, 150.7, 148.8, 141.2, 129.0, 124.3, 121.9, 115.1, 110.8, 47.45, 43.46 ppm. LCMS (m/z): $[M+H]^+$ Calculated for $C_{21}H_{21}N_7O$ is 388.18; Observed. = 388.18.

(E)-4-bromo-N'-(4-(4-(pyrimidin-2-yl)piperazin-1-yl)benzylidene)benzohydrazide (c9)

Yellow solid, Yield: 71%, M.P: 230-236°C, FTIR (ATR, Vmax, cm-1): 3247, 2839, 1650, 1437, 1224, 1090, 812.^{1}H NMR (400 MHz, DMSO-d_6) δ 10.2 (s, 1H), 8.4 (d, J=4.7Hz, 2H), 7.8 (s, 1H), 7.5

(d, J=8.5Hz, 2H), 7.3 (d, J=8.6Hz, 2H), 6.9 (t, J=8.2Hz, 4H), 6.6 (t, J=4.7Hz, 1H), 3.8 (t, J=4.8Hz, 4H), 3.2 (t, J=4.9Hz, 4H) ppm. ^{13}C NMR (125 MHz, DMSO-d_6) δ 161.6, 158.4, 151.3, 145.4, 138.5, 132.1, 127.3, 126.7, 115.8, 114.1, 110.8, 109.2, 48.1, 43.5 ppm. LCMS (m/z): $[M+H]^+$ Calculated for $C_{22}H_{21}BrN_6O$ is 456.10; Observed. = 465.10

(E)-N'-(4-(4-(2-chlorophenyl)piperazin-1-yl)benzylidene)quinoline-7-carbohydrazide (c10)

Yellow Solid,Yield: 85%, M.P: 207-212°C, FTIR (ATR, Vmax, cm-1): 3299, 2818, 1674, 1444, 1222, 1035, 821.^{1}H NMR (400 MHz, $CDCl_3$) δ 11.6 (s, 1H), 8.4 (d, J=8.5Hz, 1H), 8.3 (m, 2H), 8.1 (d, J=8.5Hz, 1H), 7.8 (d, J=8.2Hz, 1H), 7.7 (m, 3H), 7.6 (t, J=7.5Hz, 1H), 7.3 (d, J=7.8Hz, 1H), 7.2 (t, J=7.3Hz, 1H), 7.0 (d, J=7.9Hz, 1H), 6.9 (m, 3H), 3.4 (t, J=4.5Hz, 4H), 3.1 (t, J=4.4Hz, 4H) ppm. ^{13}C NMR (125 MHz, $CDCl_3$) δ 159.9, 152.7, 149.3, 149.1, 148.9, 146.3, 137.7, 130.7, 130.3, 129.8, 129.6, 129.5, 129.3, 128.8, 128.1, 127.8, 127.6, 124.3, 124.0, 120.3, 119.1, 114.9 ppm. LCMS (m/z): $[M+H]^+$ Calculated for $C_{25}H_{23}N_7O$ is 470.17; Observed. = 417.17

(E)-N'-(4-(4-(furan-2-carbonyl)piperazin-1-yl)benzylidene)isonicotinohydrazide (c11)

Yellow solid, Yield: 89%, M.P: 255-261°C, FTIR (ATR, Vmax, cm-1): 3248, 2818, 1675, 1440, 1225, 1037, 725.^{1}H NMR (400 MHz, DMSO-d_6) δ 11.86 (s, 1H), 8,7 (d, J=2.5Hz, 2H), 8.3 (s, 1H), 7.87 (s, 1H), 7,82 (d, J=2.6Hz, 2H), 7.63 (d, J=4.2Hz, 2H), 7.0 (m, 3H), 6.6 (s, 1H), 3.83 (t, 4H), 3.37 (t, 4H) ppm. ^{13}C NMR (125 MHz, DMSO-d_6) δ 161.7, 158.8, 150.7, 149.7, 147.4, 145.3, 141.2, 129.0, 124.5, 121.9, 116.2, 115.1, 111.8, 47.7, 40.6 ppm. LCMS (m/z): $[M+H]^+$ Calculated for $C_{22}H_{21}N_5O_3$ is 404.17; Observed. = 404.16.

(E)-N'-(4-(4-(furan-2-carbonyl)piperazin-1-yl)benzylidene)benzohydrazide (c12)

White Solid,Yield: 76%, M.P: 233-237°C, FTIR (ATR, Vmax, cm-1): 3274, 2813, 1675, 1435, 1279, 1074, 747.^{1}H NMR (400 MHz, DMSO-d_6) δ 11.8 (s, 1H), 8.7 (d, J=2.7Hz, 2H), 8.3 (s, 1H), 7.8 (d, J=4.2Hz, 2H), 7.8 (d, J=2.3Hz, 2H), 7.7 (d, J=4.2Hz, 2H), 7.5 (d, J=4.3Hz, 2H), 6.9 (d, J=4.4Hz, 2H), 3.3 (s, 4H), 3.0 (s, 4H) ppm. ^{13}C NMR (125 MHz, DMSO-d_6) δ 161.7, 152.0, 150.7, 149.6, 141.1, 134.5, 133.0, 130.3, 128.9, 127.9, 125.0, 121.9, 115.6, 47.3, 46.0 ppm. LCMS (m/z): $[M+H]^+$ Calculated for $C_{23}H_{22}BrN_5O_3S$ is 528.85; Observed. = 528.06.

(E)-4,5-dibromo-N'-(4-(4-(furan-2-carbonyl)piperazin-1-yl)benzylidene)-1H-pyrrole-2-carbohydrazide (c13)

White solid, Yield: 63%, M.P: 257-260°C, FTIR (ATR, Vmax, cm-1): 3198, 2826, 1644, 1413, 1231, 1055, 754.^{1}H NMR (400 MHz, DMSO-d_6) δ 12.9 (s, 1H), 11.3 (s, 1H), 8.2 (s, 1H), 7.8(s, 1H), 7.5 (d, J=7.6Hz, 2H), 7.2(t, J=7.7Hz, 2H), 7.08 (d, J=8Hz, 2H) 7.0(d, J=8.3Hz, 2H), 6.8 (t, J=7.0Hz, 1H), 3.4 (t, J=4.5Hz, 4H), 3.3(t, J=4.5Hz, 4H) ppm. ^{13}C NMR (125 MHz, DMSO-d_6) δ 158.8, 155.5, 152.0, 147.6, 147.45, 145.3, 128.9, 128.7, 127.3, 124.9, 116.2, 115.2, 113.7, 111.8, 106.2, 98.5, 47.8 ppm. LCMS (m/z): $[M-H]^+$ Calculated for $C_{21}H_{19}Br_2N_5O_3$ is 547.99; Observed. = 547.75.

(E)-N'-(4-(4-(2-chlorophenyl)piperazin-1-yl)benzylidene)isonicotinohydrazide (c14)

White solid, Yield: 83%, M.P: 235-240°C, FTIR (ATR, Vmax, cm-1): 3277, 2828, 1672, 1449, 1224, 959, 722.^{1}H NMR (400 MHz, DMSO-d_6) δ 11.8 (s, 1H), 8.7 (d, J=5.6Hz, 2H), 8.3 (s, 1H), 7.8 (d, J=5.7Hz, 2H), 7.6 (d, J=8.6Hz, 2H), 7.4 (d, J=7.8Hz, 1H), 7.3 (t, J=7.7Hz, 1H), 7.2 (d, J=7.7Hz, 1H), 7.0 (m, 3H), 3.4(t, J=4.5Hz, 4H), 3.1(t, J=4.2Hz, 4H)ppm. ^{13}C NMR (125 MHz, DMSO-d_6) δ 161.6, 152.7, 150.7, 149.8, 149.2, 141.2, 130.8, 129.0, 128.6, 128.1, 124.6, 124.4, 121.9, 121.3, 115.1, 51.1, 47.9ppm. LCMS (m/z): $[M+H]^+$ Calculated for C23H22ClN5O is 420.15; Observed. = 479.00

(E)-N'-(4-(4-(2-chlorophenyl)piperazin-1-yl)benzylidene)benzohydrazide (c15)

White solid, Yield: 65%, M.P: 235-239°C, FTIR (ATR, Vmax, cm-1): 3294, 2848, 1598, 1481, 1166, 946, 754.^{1}H NMR (400 MHz, DMSO-d_6) δ 11.6 (s, 1H), 8.3 (s, 1H), 7.9 (d, J=7.3Hz, 2H), 7.5 (m, 5H), 7.4 (d, J=7.8Hz, 1H), 7.3(t, J=7.5Hz, 1H), 7.2 (d, J=7.7Hz, 1H), 7.0 (t, J=7.0Hz, 3H), 3.4 (s, 4H). 3.1 (s, 4H). ^{13}C NMR (125 MHz, DMSO-d_6) δ 163.2, 152.5, 149.2, 148.5, 134.1, 131.9, 130.8, 128.8, 128.8, 128.8, 128.1, 127.9, 124.4, 124.6, 121.3, 115.2, 51.1, 48.0 ppm. LCMS (m/z): $[M-H]^+$ Calculated for $C_{24}H_{23}ClN_4O$ is 417.16; Observed. = 416.95

4. Conclusion

In conclusion, the mycobacterium activity of compound **e8** demonstrated a synergistic effect with respect to the combination of isoniazid with pyrazine phenyl-piperazine and was found to be the most potent compound in comparison to all other synthesised derivatives that could not inhibit

mycobacterium strain $H_{37}Rv$. In an antibacterial study, none of the compounds shown reponse against either Gram positive or Gram negative bacterial strains.

5. Acknowledgement

The authors are thankful to the Discipline of Pharmaceutical Sciences, College of Health Sciences, University of Kwa-Zulu Natal (UKZN), Durban, South Africa, for providing all the necessary facilities and Institute of Translational Health Science Technology, Faridabad, India R.K. gratefully acknowledges National Research Foundation-South Africa for funding this project (Grant Nos.103728 and 112079). The biological activities (anti mycobacterial and anti microbial activities) are not performed by student

6. Conflict of interest

Authors hereby declare that there are no financial/commercial conflicts of interest.

References

[1] https://www.who.int/news-room/fact-sheets/detail/tuberculosis (World health organisation report(Tuberculosis))

[2] Patel, R.V., Mistry, B., Syed, R., Rathi, A.K., Lee, Y.J., Sung, J.S., Shinf, H.S. and Keum, Y.S., 2016. Chrysin-piperazine conjugates as antioxidant and anticancer agents. European Journal of Pharmaceutical Sciences, 88, pp.166-177.

[3] Brito, A.F., Moreira, L.K., Menegatti, R. and Costa, E.A., 2019. Piperazine derivatives with central pharmacological activity used as therapeutic tools. Fundamental & clinical pharmacology, 33(1), pp.13-24.

[4] Kumar, R.R., Sahu, B., Pathania, S., Singh, P.K., Akhtar, M.J. and Kumar, B., 2021. Piperazine, a Key Substructure for Antidepressants: Its Role in Developments and Structure-Activity Relationships. ChemMedChem, 16(12), pp.1878-1901.

[5] Walayat, K., MOHSIN, N.U.A., Aslam, S. and Ahmad, M., 2019. An insight into the therapeutic potential of piperazine-based anticancer agents. Turkish Journal of Chemistry, 43(1), pp.1-23.

[6] Patil, M., Poyil, A.N., Joshi, S.D., Patil, S.A., Patil, S.A. and Bugarin, A., 2019. Design, synthesis, and molecular docking study of new piperazine derivative as potential antimicrobial agents. Bioorganic chemistry, 92, p.103217.

[7] Thamban Chandrika, N., Shrestha, S.K., Ngo, H.X., Tsodikov, O.V., Howard, K.C. and Garneau-Tsodikova, S., 2018. Alkylated piperazines and piperazine-azole hybrids as antifungal agents. Journal of medicinal chemistry, 61(1), pp.158-173.

[8] Tiwari, H.K., Kumar, P., Jatana, N., Kumar, K., Garg, S., Narayanan, L., Sijwali, P.S., Pandey, K.C., Gorobets, N.Y., Dunn, B.M. and Parmar, V.S., 2017. In Vitro Antimalarial Evaluation of Piperidine-and Piperazine-Based Chalcones: Inhibition of Falcipain-2 and Plasmepsin II Hemoglobinases Activities from Plasmodium falciparum. ChemistrySelect, 2(25), pp.7684-7690.

[9] Archana, A., 2021. Synthesis of Novel Triazolyl/Oxadiazolyl/Thiadiazolyl-Piperazine as Potential Anticonvulsant Agents. Drug Research, 71(04), pp.199-203.

[10] Zhao, S.J., Lv, Z.S., Deng, J.L., Zhang, G.D. and Xu, Z., 2018. Pyrrolidine-containing or Piperazine-containing Nitrofuranylamides: Design, Synthesis, and In Vitro Anti-mycobacterial Activities. Journal of Heterocyclic Chemistry, 55(12), pp.2996-3000.

[11] Moraski, G.C., Seeger, N., Miller, P.A., Oliver, A.G., Boshoff, H.I., Cho, S., Mulugeta, S., Anderson, J.R., Franzblau, S.G. and Miller, M.J., 2016. Arrival of imidazo [2, 1-b] thiazole-5-carboxamides: potent anti-tuberculosis agents that target QcrB. ACS Infectious Diseases, 2(6), pp.393-398.

[12] Pulipati, L., Sridevi, J.P., Yogeeswari, P., Sriram, D. and Kantevari, S., 2016. Synthesis and antitubercular evaluation of novel dibenzo [b, d] thiophene tethered imidazo [1, 2-a] pyridine-3-carboxamides. Bioorganic & Medicinal Chemistry Letters, 26(13), pp.3135-3140.

[13] Wang, D., Zhao, Y., Liu, Z., Lei, H., Dong, M. and Gong, P., 2014. In vitro and intracellular activity of 4-substituted piperazinyl phenyl oxazolidinone analogues against Mycobacterium tuberculosis. Journal of Antimicrobial Chemotherapy, 69(6), pp.1711-1714.

[14] Girase, P.S., Dhawan, S., Kumar, V., Shinde, S.R., Palkar, M.B. and Karpoormath, R., 2021. An appraisal of anti-mycobacterial activity with structure-activity relationship of piperazine and its analogues: A review. European Journal of Medicinal Chemistry, 210, p.112967.

[15] Cordeiro, R. and Kachroo, M., 2020. Synthesis and biological evaluation of anti-tubercular activity of Schiff bases of 2-Amino thiazoles. Bioorganic & Medicinal Chemistry Letters, 30(24), p.127655.

[16] Sivakumar, K.K. and Rajasekaran, A., 2013. Synthesis, in-vitro antimicrobial and antitubercular screening of Schiff bases of 3-amino-1-phenyl-4-[2-(4-phenyl-1, 3-thiazol-2-yl) hydrazin-1-ylidene]-4, 5-dihydro-1H-pyrazol-5-one. Journal of Pharmacy &Bioallied Sciences, 5(2), p.126.

[17] Moraski, G.C., Seeger, N., Miller, P.A., Oliver, A.G., Boshoff, H.I., Cho, S., Mulugeta, S., Anderson, J.R., Franzblau, S.G. and Miller, M.J., 2016. Arrival of imidazo [2, 1-b] thiazole-5-carboxamides: potent anti-tuberculosis agents that target QcrB. ACS Infectious Diseases, 2(6), pp.393-398.

[18] Yempalla, K.R., Munagala, G., Singh, S., Magotra, A., Kumar, S., Rajput, V.S., Bharate, S.S., Tikoo, M., Singh, G.D., Khan, I.A. and Vishwakarma, R.A., 2015. Nitrofuranyl methyl piperazines as new anti-TB agents: identification, validation, medicinal chemistry, and PK studies. ACS medicinal chemistry letters, 6(10), pp.1041-1046.

[19] Girase, P.S., Kumar, V., Dhawan, S. and Karpoormath, R., 2022. Facile Synthesis of Amides through Transamidation with Iodine under Neat Conditions. ChemistrySelect, 7(6), p.e202103237.

[20] Meena, C.L., Singh, P., Shaliwal, R.P., Kumar, V., Kumar, A., Tiwari, A.K., Asthana, S., Singh, R. and Mahajan, D., 2020. Synthesis and evaluation of thiophene based small molecules as potent inhibitors of Mycobacterium tuberculosis. European Journal of Medicinal Chemistry, 208, p.112772.

[21] Govender, H., Mocktar, C. and Koorbanally, N.A., 2018. Synthesis and Bioactivity of Quinoline-3-carboxamide Derivatives. Journal of Heterocyclic Chemistry, 55(4), pp.1002-1009.

[22] S Aremu, O., Gopaul, K., Kadam, P., Singh, M., Mocktar, C., Singh, P. and A Koorbanally, N., 2017. Synthesis, characterization, anticancer and antibacterial activity of some novel pyrano [2, 3-d] pyrimidinone carbonitrile derivatives. Anti-Cancer Agents in Medicinal Chemistry (Formerly Current Medicinal Chemistry-Anti-Cancer Agents), 17(5), pp.719-725.

[23] Okawa, T., Aramaki, Y., Yamamoto, M., Kobayashi, T., Fukumoto, S., Toyoda, Y., Henta, T., Hata, A., Ikeda, S., Kaneko, M. and Hoffman, I.D., 2017. Design, synthesis, and evaluation of the highly selective and potent G-protein-coupled receptor kinase 2 (GRK2) inhibitor for the potential treatment of heart failure. Journal of medicinal chemistry, 60(16), pp.6942-6990.

[24] Akbar, A., McNeil, N.M., Albert, M.R., Ta, V., Adhikary, G., Bourgeois, K., Eckert, R.L. and Keillor, J.W., 2017. Structure–activity relationships of potent, targeted covalent inhibitors that abolish both the transamidation and GTP binding activities of human tissue transglutaminase. Journal of medicinal chemistry, 60(18), pp.7910-7927.

[25] Koshio, H., Hirayama, F., Ishihara, T., Kaizawa, H., Shigenaga, T., Taniuchi, Y., Sato, K., Moritani, Y., Iwatsuki, Y., Uemura, T. and Kaku, S., 2004. Orally active factor Xa inhibitor: synthesis and biological activity of masked amidines as prodrugs of novel 1, 4-diazepane derivatives. Bioorganic & medicinal chemistry, 12(20), pp.5415-5426.

[26] Mishra, C.B., Kumari, S., Angeli, A., Bua, S., Buonanno, M., Monti, S.M., Tiwari, M. and Supuran, C.T., 2018. Discovery of potent anti-convulsant carbonic anhydrase inhibitors: design, synthesis, in vitro and in vivo appraisal. European Journal of Medicinal Chemistry, 156, pp.430-443.

Chapter 4

New Piperazine-Sulfonamide-Hydrazide and Hydrazine Hybrids: Design, Synthesis, and Antibacterial Activity Evaluation

(Ready to communicate)

Abstract

A series of novel phenylpiperazine sulphonamide and phenyl hydrazide (**E1-E6**) and Phenylpiperazine sulphonamide and phenyl hydrazine (**F7-F19**) hybrids were designed and synthesised. All compounds were screened *in vitro* against *mycobacterium tuberculosis* (MTB), five gram positive and three gram negative bacterial strains. Among tested derivatives isoniazid moiety containing derivatives **E1** and **E2** demonstrated significant anti tuberculosis (TB) activity (3.125 µM) against the $H_{37}Rv$ strain of tuberculosis. **F10** displayed better result (7.81 µg/mL) against *Enterococcus faecium* of gram positive bacteria, the other derivatives **E2, E6, F7, F9-F14** had moderate activity in the range of 250-62.5 µg/mL.

1. Introduction

Tuberculosis (TB), an infectious illness caused by the bacteria Mycobacterium tuberculosis(M.TB), is one of the oldest leading causes of death in the world. Patients with HIV infection and an impaired immune system are more likely to get tuberculosis[1]. Similarly the other bacterias such as Methicillin-resistant *Staphylococcus aureus (MRSA)*, *Enterococcus*, *Streptococcus pyrogens*, and *Pseudomonasaerugenosa* also significantly affect public health[2]. For the treatment of this bacterial infection a good number of antibiotics have been developed by researchers, but some of the bacteria including, Methicillin-resistant *Staphylococcus aureus (MRSA)*, Vancomycin-resistant Enterococcus (VRE), Carbapenem-resistant Enterobacteriaceae (CRE) gut bacteria, and multi-drug-resistant M.TB (MDR-TB) have developed a resistance to almost all of the antibiotics that are readily available in market[3]. Due to this drug-resistance of bacteria, it is necessary to design new antibacterial agents.

The sulphonamides play a crucial role in antibacterial activity, hence it is used as essential constituent in antibiotics[4]. Derivatives of 1-benzhydryl-piperazine sulfonamide have shown antibacterial activity against gram positive and gram negative bacterial strains[5]. Ravindra R. Shinde et.al have developed a series of Sulfonyl-piperazine derivatives showed good activity against gram positive, negative bacterial and anti-fungal strains[6]. In addition to this, we found that Schiff bases are widely used for inhibiting bacterial strains[7-8]. Piperazine is an essential component in wide verity of anti-TB agents[9]. Also, there are well known marketed pharmaceutical drugs including ofloxacin[10-12], gatifloxacin[13], norfloxacin[14], levofloxacin[15], sparfloxacin[16], lomefloxacin[17], ciprofloxacin[18], pipemidic acid[19], and grepafloxacin[20] containing piperazine unit**.** In conclusion we have incorporated piperazine, sulphonamide and Schiff base in our design as illustrated in **fig 1** and synthesised a novel phenylpiperazine sulphonamide and phenyl hydrazide (**E1-E6**) as well as phenylpiperazine sulphonamide and phenyl hydrazine (**F7-F19**) hybrids (**Scheme 1** and **2**) and investigated their activity against Gram positive, Gram negative and mycobacterium bacterial strains (**table 1**).

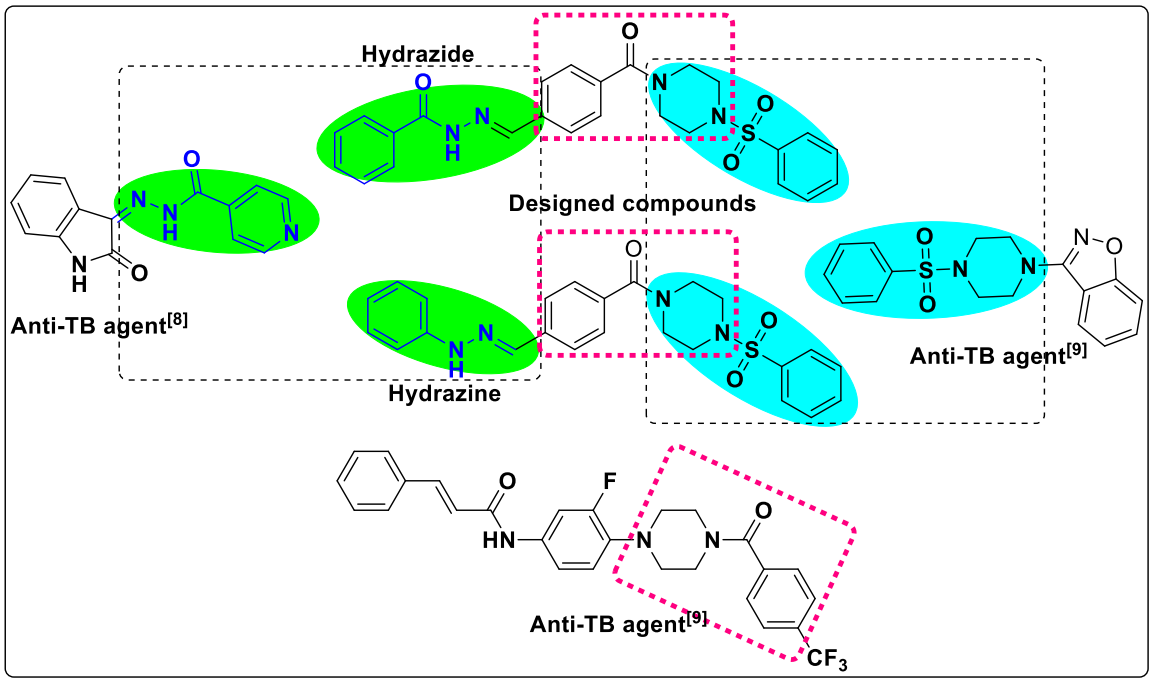

Figure 1 Design strategy for the synthesis of phenylpiperazine sulphonamide and hydrazide/hydrazine hybrids

2. Result and discussion

2a. Chemistry

The novel designed compounds (**E1-E6** and **F7-F19**) have been synthesised from commercially available precursors at an affordable cost. Based on this synthetic strategy (**scheme 2**), phenyl hydrazides were prepared first (**scheme 1**), which were needed at final step **iii** to attempt **E** category of compounds (**E1-E6**, **scheme 2**), whereas **F** category of compounds required commercially available phenyl hydrazines (**F7-F19, scheme 2**). **Scheme 1** describes the method used to synthesise phenyl hydrazides by refluxing phenyl esters with hydrazine in ethanol. The reaction of phenyl sulphonyl chloride with piperazine was not under control, hence disubstituted piperazines were produced. To resolve di-substitution, 10 equivalents of piperazine was used in DCM followed by sulphonyl chloride addition under cooling condition to yield **C (step i, scheme 2).** To get **D**, acid-amine coupling between **C** and 4-formyl benzoic acid was done in the presence of 1-ethyl-3-(3-dimethylaminopropyl)carbodiimide (EDC) and hydroxybenzotriazole (HOBT) under base triethyl amine **(step ii, scheme 2)**. In the final step **iii**, **E** and **F** were created by forming a Schiff base between aldehyde group of **D** with **A** and**B**.

1.Synthesis of hydrazides A1-A5

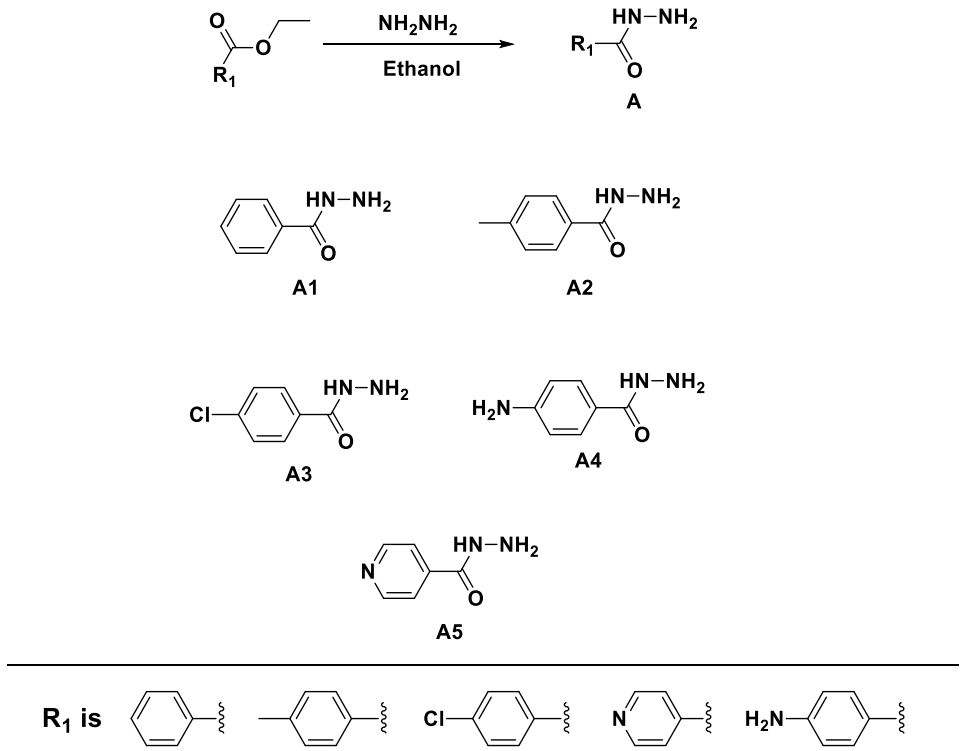

Reaction conditions: Hydrazine, ethanol, 80°C, 5hrs

Scheme 1

2. Synthesis of compound**E1–E6** and **F7–F19**

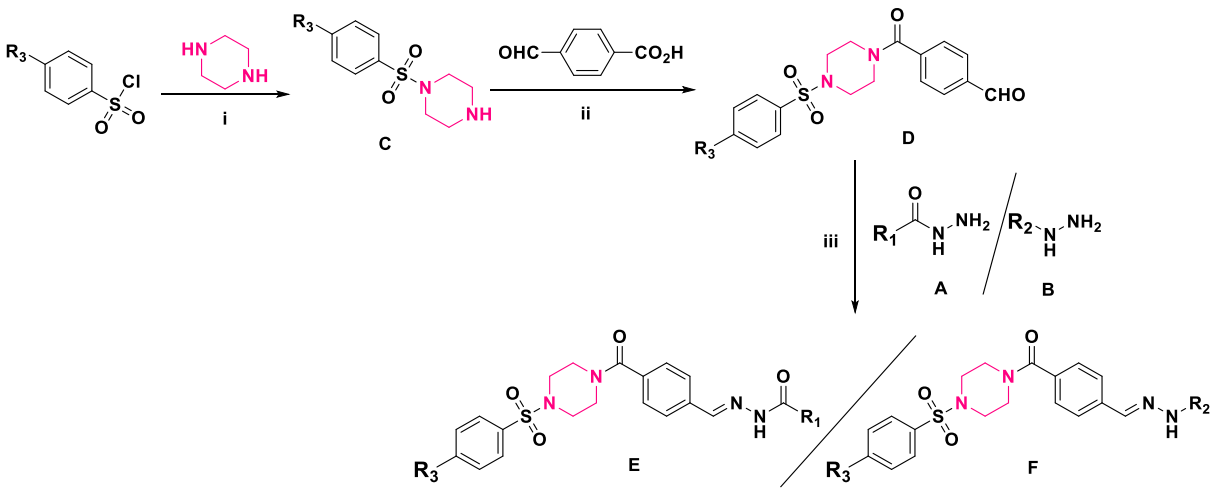

Comp no.	R_3	R_1	Comp no.	R_3	R_2
E1	—Cl	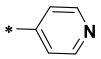	F11	—H	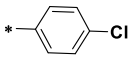
E2	—CH_3	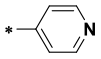	F12	—H	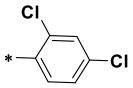
E3	—CH_3	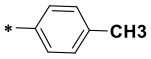	E13	—NO_2	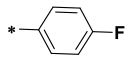
E4	—CH_3	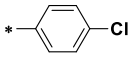	F14	—NO_2	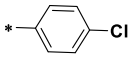
E5	—CH_3	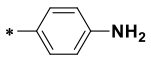	E15	—NO_2	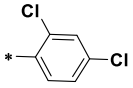
E6	—H		F16	—Cl	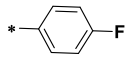
F7	—CH_3		E17	—CH_3	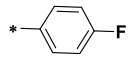
F8	—NO_2		F18	—CH_3	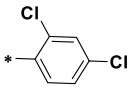
E9	—H		F19	—Cl	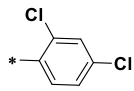
F10	—H	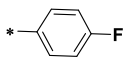			

Reaction conditions: (i) Piperazine, DCM, 0°C 30min, (ii) EDC, HOBT, Triethyl amine, DCM, rt 16hrs, (iii) Glacial acetic acid, Ethanol, 80°C 16hrs.

Scheme 2

NMR data discussion

4-chloro-N'-(4-(4-tosylpiperazine-1-carbonyl)benzylidene)benzohydrazide (E4)

^{1}H NMR

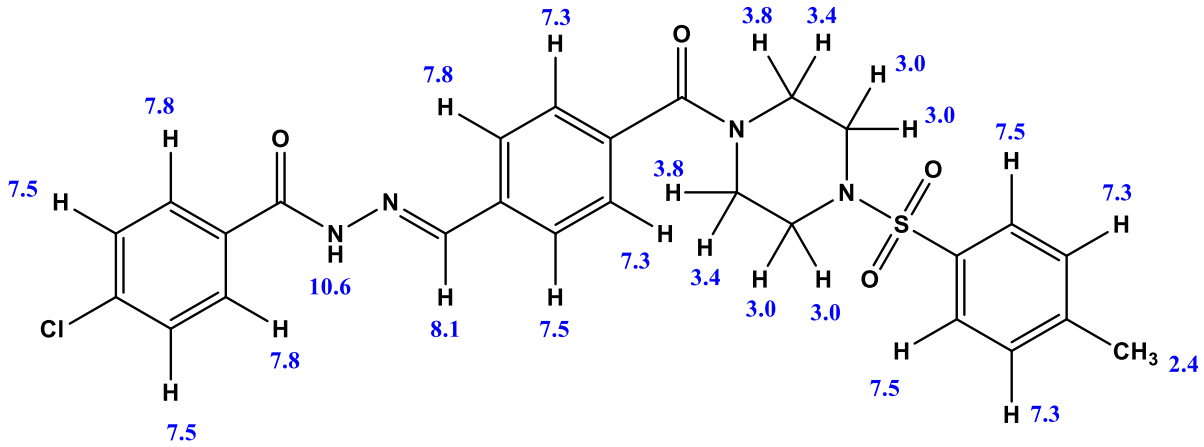

The amide proton is highly deshielded and it displayed adelta value at 10.6 ppm because of the resonance with the adjacent carbonyl carbon. The proton on the sp^2proton attached to the hydrazide group is deshielded and showed a delta value at 8.1 ppm. The protons of the phenyl rings displayed the delta value ranging from 7.8 to 7.3 ppm. Due to the difference in the chemical environment, the piperazine ring showed two sets of protons with the delta value 3.4 and 2.0 ppm respectively. The methyl protons of the tolyl group are highly deshielded in this structure and showed a delta value of 2.4 ppm.

^{13}C NMR

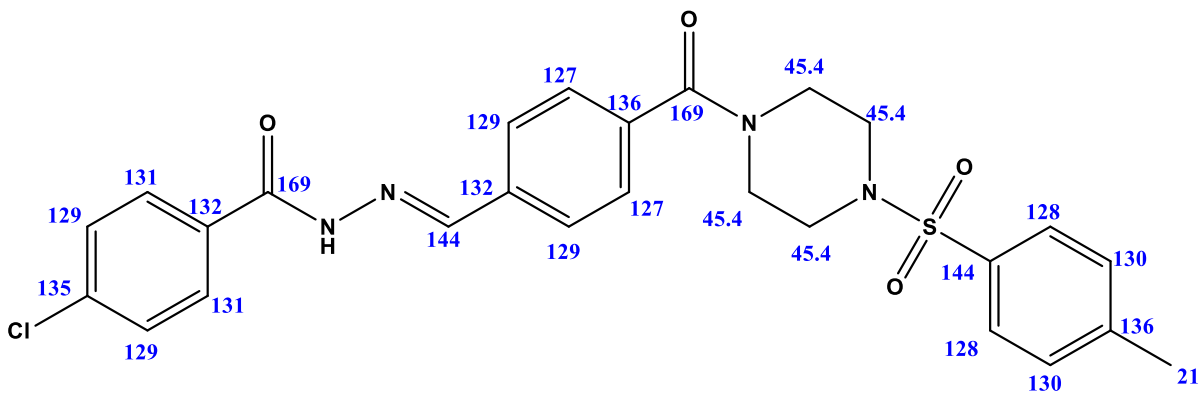

In C^{13} NMR, carbonyl carbons generally exhibit delta values between 180 and 220 ppm. However, the delta value of the amide carbonyl carbons in this structure has moved to up field at 169 ppm because of the conjugation between nitrogen's lone pair electrons and the carbonyl carbon. The sp^2 carbon atom adjacent to the hydrazine group is deshielded, and it showed a delta value at 144 ppm. Similarly, the carbon next to the sulfonyl group showed a delta value of 144 ppm. The other carbons of the phenyl rings displayed delta values ranging from 130 to 140 ppm. The delta value of the piperazine ring's carbons was 45 ppm. The methyl carbon of the tolyl group displayed delta value at 21 ppm.

(4-((2-phenylhydrazono)methyl)phenyl)(4-tosylpiperazin-1-yl)methanone) (F7)

^{1}H NMR

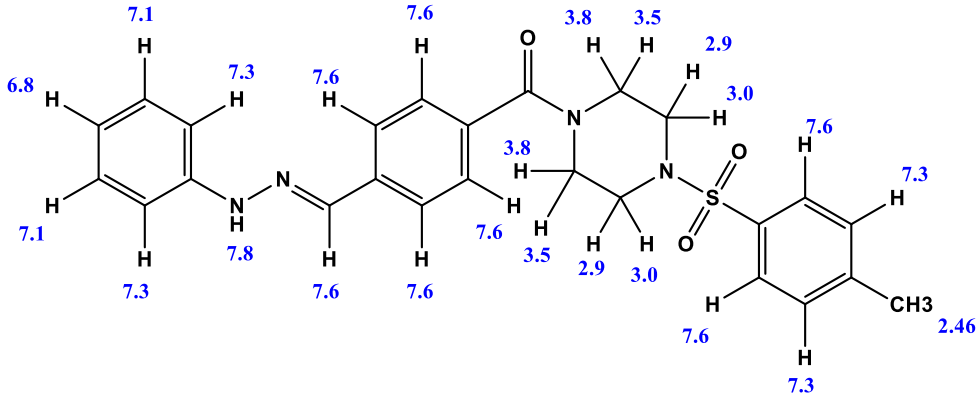

The protons attached to the heteroatom are exchangeable protons. Hence, these protons are deshielded in the H^1 NMR spectrum. Accordingly, the N-H proton in thisstructure displayed a delta value at 7.8 ppm. The proton on the sp^2carbon attached to the hydrazine group is also deshielded and showed a delta value at 8.1 ppm. The protons of the phenyl rings displayed the delta value ranging from 7.6 to 6.8 ppm. Due to the difference in the chemical environment, and different conformational structures of piperazine, the four sets of protons of the piperazine ring appeared at3.8, 3.5, 3.0 and 2.9 ppm respectively. The aromatic methyl protons showed a delta value at 2.4 ppm.

^{13}C NMR

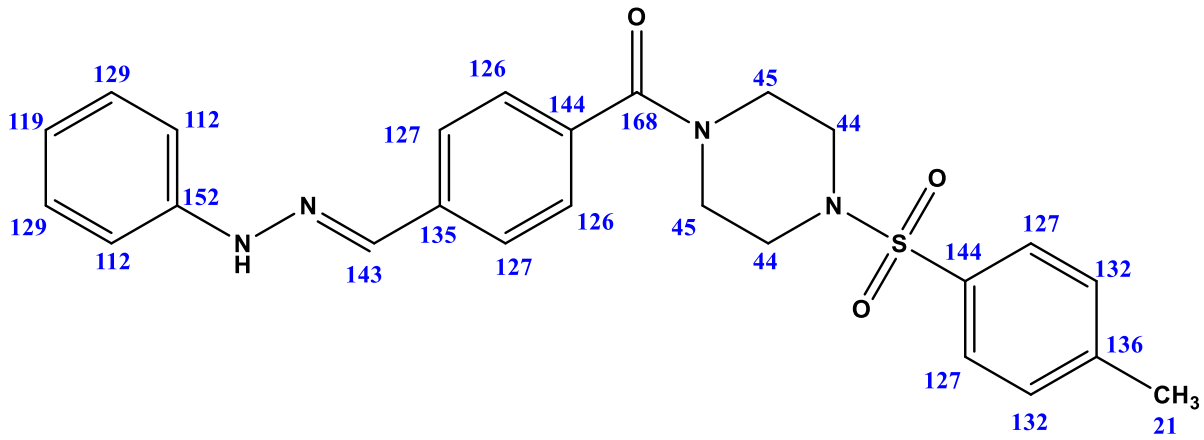

In C^{13} NMR, carbonyl carbons generally exhibit delta values between 180 and 220 ppm. However, the delta value of the amide carbonyl carbon in this structure has moved to165 ppm because of the conjugation between nitrogen's lone pair electrons and the carbonyl carbon. The carbon atoms adjacent to the hydrazine group are deshielded, and appeared at 152 and 143 ppm respectively. Similarly, the carbon next to the sulfonyl group showed a delta valueat144 ppm. The other carbons of the phenyl rings have showed delta values ranging from 115 to 134 ppm. The delta values of the piperazine ring's carbons were 46 and 47 ppm. The methyl carbon of the tolyl group displayed delta value at 21 ppm.

2b. Biological evaluation

1. Mycobacterium activity

The biological evaluation was begun by conducting an *in vitro* investigation. **Table 1** presents the activity results of each synthetic derivative (**E1–E6** and **F7–F19)** evaluated against the *$H_{37}Rv$* strain and given a MIC value in µM. Only compound **F13** from the category of hydrazine derivatives (**F7–F19)** exhibited considerable moderate activity, whereas the other hybrids were inactive. This implies that the combination of fluoro and nitro substituents on the aromatic ring at the left-hand side (L.H.S.). and right-hand side (R.H.S.) respectively inhibits the *$H_{37}Rv$* strain (**F13**, **Table 1**). Regarding hydrazide derivatives, the isoniazid hybrids displayed the best anti-TB potential with a MIC value of 3.125 µM (**E1** and **E2**). Other substituted and unsubstituted phenyl hydrazides did not show efficacy. This reveals that the phenyl Sulfonyl-piperazine and isoniazid hybrids boosted the anti-TB activity.

The concise description of the structural activity relationship (SAR) between all compounds and their anti-TB activity is presented in **Figure 2.**

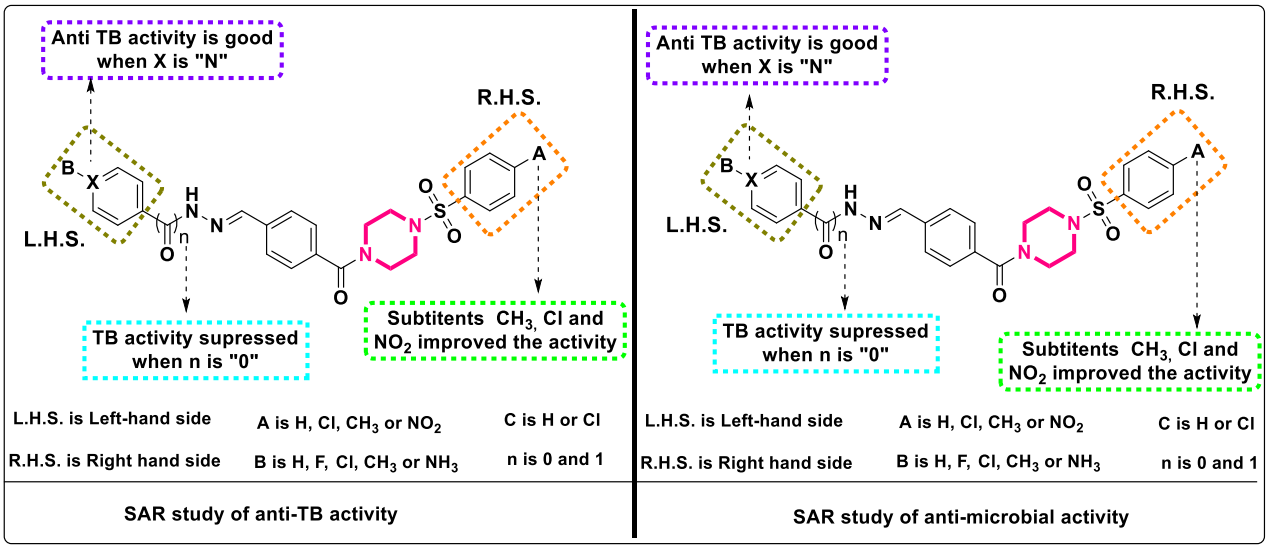

Figure 2: SAR studies of anti-TB activity and anti-microbial activity

2. Antimicrobial activity

Next, we conducted an *in vitro* antibacterial investigation in which all the compounds (**E1-E6** and **F7-F19** were tested against five gram-positive strains (*MRASA, Streptococcus pyrogens, Bacillus subtilis, Enterococcus faecium,* and *Staphylococcus aureus*) and three gram-negative strains (*Enterobacter hormaechei, Pseudomonas aerugenosa,* and *Escherichia coli*) illustrated in **Table 1**. None of the compounds has shown inhibition against *Streptococcus pyrogens* and *Staphylococcus aureus*. Among hydrazide hybrids (**E1-E6**), compounds with isoniazid and phenyl hydrazide displayed inhibition at 125 and 62.5 µg/mL against three gram-positive and three gram-negative strains (**E2** and **E6**, **Table 1**). Wherein methyl, chloro, and amino group substituted derivatives were inactive against all strains (**E3-E5**). In hydrazine derivatives, the halo group substituted phenyl on L.H.S. and with phenyl and nitro substituted phenyl on R.H.S. compounds showed inhibition up 250, 62.5 and 7.81 µg/mL (**E10-E14**). However, the inhibition was not observed when the halo and methyl group substituted at R.H.S (**F16-F19**). Of all the derivatives tested, **F10** found the most active one that showed inhibition at 7.81 µg/mL against *Enterococcus faecium* of gram-positive strain. The SAR

parameter is illustrated in **Figure2**, which demonstrates the relationship between the chemical structure and the biological activity of the compounds.

Table 1: Activity of synthesized derivatives (**E1–E6** and **F7–F19**) against growth of Gram positive, Gram negative and $H_{37}R_v$ bacterial strains.

Comp no.	**Gram positive bacteria (µg/ml)**					**Gram negative bacteria (µg/ml)**			**[i]$H_{37}R_V$ MIC(µM)**
	[a]10069	**[b]49247**	**[c]12344**	**[d]19434**	**[e]25923**	**[f]700232**	**[g]27853**	**[h]35218**	
E1	-	-	-	-	-	-	-	-	**3.125 µM**
E2	125	-	62.5	62.5		62.5	62.5	62.5	**3.125 µM**
E3	-	-	-	-	-	-	-	-	>50 µM
E4	-	-	-	-	-	-	-	-	>50 µM
E5	-	-	-	-	-	-	-	-	>50 µM
E6	62.5	-	62.5	62.5	-	62.5	62.5	62.5	>50 µM
F7	250	-	125	62.5	-	62.5	62.5	62.5	>50 µM
F8	-	-	-	-	-	-	-	-	>50 µM
F9	-	-	-	-	-	-	-	-	>50 µM
F10	250	-	62.5	7.81	-	62.5	62.5	62.5	>50 µM
F11	250	-	62.5	62.5	-	62.5	62.5	62.5	>50 µM
F12	250	-	62.5	62.5	-	62.5	62.5	62.5	>50 µM
F13	250	-	62.5	62.5	-	62.5	62.5	62.5	**25-50 µM**
F14	250	-	62.5	62.5	-	62.5	62.5	62.5	>50 µM

F15	-	-	-	-	-	-	-	-	>50 µM
F16	-	-	-	-	-	-	-	-	>50 µM
F17	-	-	-	-	-	-	-	-	>50 µM
F18	-	-	-	-	-	-	-	-	>50 µM
F19	-	-	-	-	-	-	-	-	>50 µM
NIH	-NA-	-NA-	-NA-	-NA-	-NA-	-NA-	-NA-	-NA-	**0.053**
Ciprofloxacin	≥ 0.49	≥ 0.49	≥ 0.49	≥ 0.49	≥ 0.49	≥ 0.49	≥ 0.49	≥ 0.49	-NA-
Vancomycin	0.00375	0.00375	-	-	-	-	-	-	-NA-

[a] methicillin resistant staphylococcus aureus (mrsa) 10069; [b] Streptococcus pyrogens 49247; [c]Bacillus subtilis 12344; [d] Enterococcus faecium 19434; [e] Staphylococcus aureus 25923; [f] Enterobacter hormaechei 700232; [g] Pseudomonas aerugenosa27853; [h] Escherichia coli 35218

The zone of inhibition was measured at concentration of 1000 µg/mL; Ciprofloxacin and Vancomycin were used as a standard. (-) indicates no activity.

[i]Minimal inhibitory concentration (MIC µM). (-NA-) indicates not applicable.*

3. Experimental

3a. Bioassays

Material and method

1. M. tuberculosis (MIC determination assays**)**

At 37°C with shaking (200 rpm), Middlebrook 7H9 broth (MB broth) supplemented with 0.05% Tween-80, 0.2% glycerol and 1x albumin dextrose-saline (ADS) was used to culture *mycobacterium*

tuberculosis $H_{37}Rv$ (M. TB). The compounds were prepared as 1000 µg/ml stocks in DMSO and evaluated MIC value for antimycobacterial activity at concentrations ranging from 50 to 3.125 µg/ml[21]

2. Antimicrobial

Method used: i) Agar diffusion assay[22] , ii) Broth Microdilution assay[23]

Concentration of compounds: Stock solution [1000 µg/ml] of each compound was prepared in DMSO. Agar diffusion is carried out by taking 5 micro liters from stock solution. Broth micro dilution Assay carried out by 2-fold serial dilution of 100 microliters from stock solution.

Media used:i) Microbiological media used for bacteria is Mueller Hinton Agar (M-H Agar) Composition (gL-1): Beef infusion solids 2.0; starch 1.5; Casein hydrolysate 17.5; Agar 17.0; Final pH (at 25°C) 7.3 ± 0.2. ii) Microbiological media used for bacteria is Mueller Hinton Broth (M-H Broth) Composition (gL-1): Beef infusion solids 2.0; starch 1.5; Casein hydrolysate 17.5; Final pH (at 25°C) 7.4 ± 0.2

3b. Chemistry

1. Material and method

All reactions were conducted under standard operating conditions without the use of any stringent conditions. All chemicals were obtained from Aldrich Chemical Co., Alfa Aesar, used as received without additional purification. Lab reagent (LR) grade solvents were used for extraction. The reaction progress was monitored on Merck TLC Silica gel 60 F254 plates, and the spots were visualized under ultraviolet (UV) light, followed by iodine or ninhydrin staining solution followed by heating.

^{1}H, and ^{13}C NMR spectra were recorded on 500, 400, 100, and 125 MHz NMR spectrometer using $CDCl_3$ as solvent unless otherwise stated. MS were made by means of ESI (Electron spray ionization). The ATR technique was used to record the Fourier transform infrared (FTIR) spectra in

the range of 400–4000 cm-1 on a Bruker Alpha FT-IR spectrometer. Unless otherwise specified, all reagents were weighed and handled in air.

2. Synthetic procedure

1. Preparation of benzohydrazide **(compound A1)**

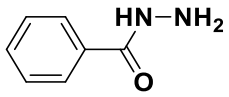

Two mmol of hydrazine was added to the stirring mixture of 1 mmol ethyl benzoate in 10 volumes of ethanol; the reaction mixture was refluxed for 5 hrs at 80° C[24]. After the reaction completion, the consumption of starting materials was confirmed by thin-layer chromatography (TLC). The solution was poured into ice-cold water on completion of the reaction to give a brown crystalline solid. The solid was filtered, washed with water, and recrystallised from ethanol to give compound **A1** (Yield 73%).

Compounds **A2** to **A5** were produced using the method described for compound **A** in **Scheme1**.

Preparation of1-(phenylsulfonyl)piperazine (compound C)

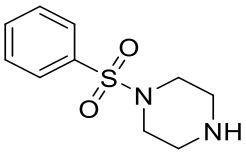

To the solution of 10.0 mmol of piperazine in Dichloromethane (DCM), 1.0 mmol of benzene sulfonyl chloride was added at 0°C, stirring the reaction mixture for 30 min[25]. After completion of the reaction, the consumption of starting materials was confirmed by TLC. The reaction mixture was quenched with water and extracted in DCM (3×40 mL), dried over anhydrous Na_2SO_4, and DCM evaporated in a vacuum to get compound **C** (Yield 89%).

Preparation of 4-(4-(phenylsulfonyl)piperazine-1-carbonyl)benzaldehyde (compound D)

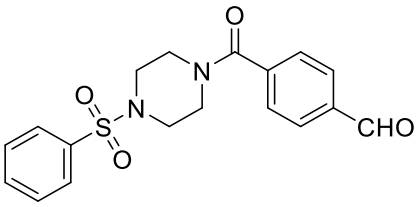

At room temperature, 1.0 mmol of EDC and 1.0 mmol of HOBT were added to a stirred solution of 1.0 mmol of 1-(phenylsulfonyl)piperazine and 1.2 mmol of 4-formylbenzoic acid in DCM. At 0°C, 3.0 mmol of trimethylamine (TEA) was added after 15 min. The mixture was stirred for 16 hrs at rt[26]. After the reaction completion, the consumption of both the starting materials was confirmed by TLC. The reaction mixture was quenched with water and extracted in DCM (3×40 mL), dried over anhydrous Na_2SO_4, and DCM evaporated in a vacuum to get compound **D** (Yield 69%).

Preparation of4-((2-phenylhydrazono)methyl)phenyl)(4-(phenylsulfonyl)piperazin-1-yl)methanone (compound F9)

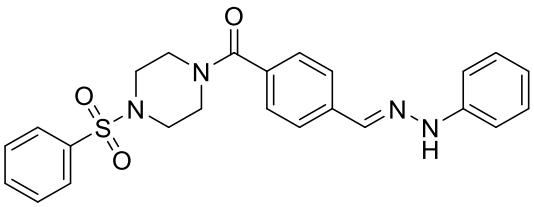

A catalytic amount of acetic acid was added to the stirred solution of 1.1 mmol of 1-(phenylsulfonyl)piperazine and 1.0 mmol of phenylhydrazine in ethanol. The resultant reaction mixture was stirred at 80°C for 16 hrs[27]. After the reaction completion, the consumption of both the starting material was confirmed by TLC. The reaction mixture was cooled to rt and poured into ice-cold water. The solid separated out was filtered, washed with water, and dried to get compound **F13** (Yield 72%).

Similarly, other derivatives (**E1–E6** and **F7–F19**) were prepare as per the procedure given for synthesis of **F13** (in **scheme 2**)

3. Experimental data

N'-(4-(4-((4-chlorophenyl)sulfonyl)piperazine-1-carbonyl)benzylidene)isonicotinohydrazide (E1)

White Solid, yield: 67%, mp: 212-219°C; FTIR (ATR, Vmax, cm-1):3233, 3070, 1653, 1544, 1344, 1154, 762; ^{1}H NMR (400 MHz, $CDCl_3$) δ 2.97 (s, 2H), 3.09 (s, 2H), 3.52(s, 2H), 3.84 (s, 2H), 7.22-7.34 (m, 2H), 7.5(d, J=8.4Hz, 2H), 7.59 (d, J=3.9Hz, 2H), 7.68(d, J=8.4Hz, 2H), 7.74(d, J=2.9Hz, 2H), 8.19(s, 1H), 8.73 (d, J=2.6Hz, 1H), 8.7 (d, J=2.3Hz, 1H), 10.58(s, 1H) ppm. ^{13}C NMR (125 MHz, $CDCl_3$) δ 150.57, 149.83, 148.61, 140.07, 136.41, 135.22, 133.74, 129.76, 129.09, 127.98, 127.72, 127.53, 127.41, 121.30. Mass (m/z): $[M+H]^+$ Calculated for $C_{24}H_{22}ClN_5O_4S$ is 512.11; Observed. = 512.72.

(N'-(4-(4-tosylpiperazine-1-carbonyl)benzylidene)isonicotinohydrazide) (E2)

White Solid yield: 73%, mp: 205-209°C; FTIR (ATR, Vmax, cm-1): 3612, 3009, 1666, 1552, 1346, 1162, 729; ^{1}H NMR (400 MHz, $CDCl_3$) δ 2.47(s, 3H), 2.96(s, 2H), 3.08(s, 2H), 3.52(s, 2H), 3.84(s, 2H), 7.29-7.38(m, 4H), 7.55-7.67(m, 4H), 7.74(d, J=4.5Hz, 2H), 8.22(s, 1H), 8.76-8.80(m, 2H), 10.21(s, 1H). ^{13}C NMR (125 MHz, $CDCl_3$) δ 150.6, 148.5, 148.5, 144.3, 132.0, 130.0, 129.9, 128.0, 128.0, 127.7, 127.6, 127.5, 127.4, 121.2, 45.4, 21.6. Mass (m/z): $[M+H]^+$ Calculated for C25H25N5O4S is 492.16; Observed. = 491.90.

4-methyl-N'-(4-(4-tosylpiperazine-1-carbonyl)benzylidene)benzohydrazide (E3)

White Solid, yield: 64%, mp: 155-160°C; FTIR (ATR, Vmax, cm-1): 3224, 3036, 1648, 1552, 1326, 1166, 725; ^{1}H NMR (400 MHz, $CDCl_3$) δ 2.43(s, 3H), 2.47(s, 3H), 2.95(s, 2H), 3.08(s, 2H), 3.51(s, 2H), 3.83(s, 2H), 7.26(t, J=8.9Hz, 3H), 7.26-7.38(m, 5H), 7.59-7.69(m, 4H), 7.79(d, J=3.1Hz, 2H), 8.25(s, 1H), 9.85(s, 1H). ^{13}C NMR (125 MHz, $CDCl_3$) LCMS (m/z): 168.8, 163.1, 160.4, 146.7, 143.9, 142.0, 136.7, 135.7, 132.1, 130.4, 130.0, 129.1, 127.8, 127.6, 127.0, 45.8, 45.0, 21.1. Mass (m/z): $[M+H]^+$ Calculated for C27H28N4O4S is 504.61; Observed. = 505.05.

4-chloro-N'-(4-(4-tosylpiperazine-1-carbonyl)benzylidene)benzohydrazide (E4)

White Solid, yield: 77%, mp: 158-163°C; FTIR (ATR, Vmax, cm-1): 3455, 3034, 1646, 1551, 1326, 1166, 725; ^{1}H NMR (400 MHz, $CDCl_3$) δ 2.45(s, 3H), 2.93(s, 2H), 3.06(s, 2H), 3.47(s, 2H), 3.80(s, 2H), 7.20(d, J=3.7Hz, 1H), 7.33-7.37(m, 4H), 7.54-7.63(m, 5H), 7.84(d, J=3.9Hz, 3H), 8.17(s, 1H), 10.67(s, 1H) ppm. ^{13}C NMR (125 MHz, $CDCl_3$) δ 21.62, 45.42, 127.36, 127.66, 127.73, 128.86,

129.10, 129.93, 130.02, 131.17, 132.06, 135.45, 136.15, 144.37, 169.76. Mass (m/z): $[M+H]^+$ Calculated for C26H25ClN4O4S is 525.13; Observed. = 524.85.

4-amino-N'-(4-(4-tosylpiperazine-1-carbonyl)benzylidene)benzohydrazide (E5)

Yellow Solid, mp: 157-163°C; FTIR (ATR, Vmax, cm-1): 3224, 3036, 1648, 1552, 1326, 1166, 725; ^{1}H NMR (400 MHz, $CDCl_3$) δ 11.52 (s, 1H), 8.40 (s, 1H), 7.80 – 7.60 (m, 6H), 7.44 (dd, J = 21.2Hz, 8.2 Hz, 4H), 6.60 (d, J = 8.6 Hz, 2H), 5.80 (s, 2H), 3.55 (d, J = 77.4 Hz, 4H), 2.95 (s, 5H), 2.42 (s, 3H). ^{13}C NMR (125 MHz, $CDCl_3$) 169.2, 157.8, 145.2, 144.3, 136.5, 136.4, 132.59, 130.4, 128.1, 128.0, 127.1, 119.8, 113.0, 46.2, 45.4, 21.54.

N'-(4-(4-(phenylsulfonyl)piperazine-1-carbonyl)benzylidene)benzohydrazide (E6)

White Solid, yield: 58%, mp: 221-223°C; FTIR (ATR, Vmax, cm-1): 3474, 3074, 1667, 1349, 1167, 741;^{1}H NMR (400 MHz, $CDCl_3$) δ 10.25 (s, 1H), 8.22 (s, 1H), 7.91 (t, J=8.5Hz, 2H), 7.74 (d, J=7.5Hz, 2H), 7.68-7.53 (m, 7H), 7.44 (t, J=7.05Hz, 1H), 7.26 (d, J=7.5Hz, 3H), 3.81 (s, 2H), 3.49 (s, 2H), 3.07 (s, 4H) ppm. ^{13}CNMR (125 MHz, $CDCl_3$) δ 169.8, 147.3, 147.2, 147.2, 136.0, 135.5, 135.1, 133.3, 132.8, 132.2, 129.4, 129.3, 128.6, 127.7, 127.6, 127.6, 127.5, 127.4, 45.42. Mass (m/z): $[M+H]^+$ Calculated for C25H24N4O4S is 477.15; Observed. = 476.85.

(4-((2-phenylhydrazono)methyl)phenyl)(4-tosylpiperazin-1-yl)methanone) (F7)

Yellow Solid, yield: 71%, mp: 152-158°C; FTIR (ATR, Vmax, cm-1): 3239, 3035, 1925, 1614, 1466, 1324, 1166, 758; ^{1}H NMR (400 MHz, $CDCl_3$) δ 2.46(s, 3H), 2.99(s, 2H), 3.08(s, 2H), 3.59(s, 2H), 3.85(s, 2H), 6.89-6.93(m, 1H), 7.11(dd, J=8.5Hz&J=1.0Hz, 2H), 7.29-7.38(m, 5H), 7.60(d, J=8.2Hz, 1H), 7.63-7.66(m, 5H, 7.87(s, 1H). ^{13}C NMR (125 MHz, $CDCl_3$) LCMS (m/z): 168.7, 152.36, 144.77, 143.81, 136.01, 135.94, 132.09, 129.98, 127.6, 126.6, 119.3, 112.57, 45.7, 44.9, 21.05. Mass $[M+H]^+$: Calculated for C25H26N4O3S is 463.17; Observed. = 462.85.

(4-((4-nitrophenyl)sulfonyl)piperazin-1-yl)(4-((2-phenylhydrazono)methyl)phenyl)methanone (F8)

Yellow solid, yield: 72%, mp: 184-190°C; FTIR (ATR, Vmax, cm-1): 3259, 2861, 1626, 1531, 1355, 1167, 703; ^{1}H NMR (400 MHz, $CDCl_3$) δ 8.37 (d, J = 8.6 Hz, 2H), 7.90 (d, J = 8.6 Hz, 2H), 7.70 –

7.52 (m, 3H), 7.27 – 7.24 (m, 3H), 7.21 (t, J = 7.7 Hz, 2H), 7.06 (d, J = 8.1 Hz, 2H), 6.81 (t, J = 7.3 Hz, 1H), 3.32 – 2.82 (m, 8H). ^{13}C NMR (100 MHz, $CDCl_3$) δ 170.55, 150.34, 144.26, 141.26, 137.98, 135.03, 133.07, 129.16, 128.78, 127.45, 125.88, 124.52, 120.10, 112.53, 49.63, 49.46, 49.29, 49.12, 48.94, 48.77. Mass (m/z): $[M+H]^+$ Calculated for C24H23N5O5S is 494.14; Observed. = 494.00

(4-((2-phenylhydrazono)methyl)phenyl)(4-(phenylsulfonyl)piperazin-1-yl)methanone (F9)

Yellow solid yield: 65%, mp: 205-210°C; FTIR (ATR, Vmax, cm-1): 3455, 3034, 1719, 1434, 1214, 1111, 725. ^{1}H NMR (400 MHz, $CDCl_3$) δ 7.77 – 7.73 (m, 2H), 7.67 – 7.61 (m, 4H), 7.57 (t, J = 7.7 Hz, 3H), 7.33 – 7.27 (m, 4H), 7.10 (d, J = 7.8 Hz, 2H), 6.89 (t, J = 7.2 Hz, 1H), 3.95 – 3.41 (m, 4H), 3.23 – 2.78 (m, 4H) ppm. ^{13}C NMR (125 MHz, $CDCl_3$) δ.16, 144.15, 137.36, 137.03, 135.43, 135.24, 133.93, 133.26, 129.31, 127.67, 127.62, 126.04, 120.49, 112.78, 77.25, 77.00, 76.75, 46.05.

(4-((2-(4-fluorophenyl)hydrazono)methyl)phenyl)(4-(phenylsulfonyl)piperazin-1-yl)methanone (F10)

Yellow solid yield: 72%, mp: 180-185°C; FTIR (ATR, Vmax, cm-1): 3259, 2859, 1628, 1420, 1166, 763; ^{1}H NMR (400 MHz, $CDCl_3$) δ 7.78 – 7.72 (m, 3H), 7.63 (dd, J = 11.0Hz, 8.1 Hz, 4H), 7.60 – 7.53 (m, 2H), 7.32 (d, J = 8.2 Hz, 2H), 7.07 – 7.02 (m, 2H), 7.01 – 6.94 (m, 2H), 3.93 – 3.44 (m, 4H), 3.19 – 2.79 (m, 4H). ^{13}C NMR (125 MHz, $CDCl_3$) δ 170.2, 140.50, 137.21, 135.61, 135.22, 134.06, 133.28, 129.31, 127.68, 126.05, 115.98, 115.80, 113.74, 46.94 ppm. Mass (m/z): $[M+H]^+$ Calculated for C24H23FN4O3S is 467.15; Observed. = 466.95.

(4-((2-(4-chlorophenyl)hydrazono)methyl)phenyl)(4-(phenylsulfonyl)piperazin-1-yl)methanone (F11)

Yellow solid yield: 70%, mp: 200-203°C; FTIR (ATR, Vmax, cm-1): 3452, 2869, 1597, 1356, 1173, 743; ^{1}H NMR (400 MHz, $CDCl_3$) δ 7.84 (s, 1H), 7.78 (t, J=1.3Hz, 1H), 7.76 (d, J=1.4Hz, 1H), 7.66 (s, 1H), 7.64 (d, J=1.7Hz, 2H), 7.59 (t, J=7Hz, 2H), 7.35 (d, J=8Hz, 2H), 7.26 (t, J=2.5Hz, 1H), 7.23 (t, J=2.5Hz, 1H).7.06 (t, J=2.5Hz, 1H), 7.04 (t, J=2.5Hz, 1H), 3.87 (s, 2H), 3.6 (s,2H), 3.1 (s, 4H) ppm. ^{13}C NMR (125 MHz, $CDCl_3$) δ.170.19, 142.89, 137.14, 136.23, 135.35, 134.34, 133.39, 129.42, 129.33, 127.79, 127.76, 126.26, 114.02 ppm. Mass (m/z): $[M+H]^+$ Calculated for C24H23ClN4O3S is 483.12; Observed. = 482.85.

(4-((2-(2,4-dichlorophenyl)hydrazono)methyl)phenyl)(4-(phenylsulfonyl)piperazin-1-yl)methanone (F12)

White Solid yield: 69%, mp: 194-198°C; FTIR (ATR, Vmax, cm-1): 3283, 2849, 1626, 1346, 1174, 740; ^{1}H NMR (400 MHz, $CDCl_3$) δ 8.12 (s, 1H), 7.81 (s, 1H), 7.77 – 7.72 (m, 2H), 7.69 – 7.62 (m, 3H), 7.60 – 7.54 (m, 2H), 7.53 (d, J = 8.8 Hz, 1H), 7.34 (d, J = 8.2 Hz, 2H), 7.29 (d, J = 2.6 Hz, 1H), 7.20 (dd, J = 8.8, 2.2 Hz, 1H), 3.98 – 3.34 (m, 4H), 3.22 – 2.53 (m, 4H). ^{13}C NMR (125 MHz, $CDCl_3$) δ 170.0, 139.0, 138.5, 136.7, 135.3, 134.8, 133.4, 129.4, 128.8, 128.2, 127.8, 126.5, 124.6, 117.3, 115.0, 46.3, 41.6 ppm. Mass (m/z): $[M+H]^+$ Calculated for $C_{24}H_{22}Cl_2N_4O_3S$ is 517.08; Observed. = 516.80.

(4-((2-(4-fluorophenyl)hydrazono)methyl)phenyl)(4-((4-nitrophenyl)sulfonyl)piperazin-1-yl)methanone (F13)

Yellow solid yield: 72%, mp: 168-174°C; FTIR (ATR, Vmax, cm-1): 3261, 2862, 1623, 1356, 1169, 749; ^{1}H NMR (400 MHz, $CDCl_3$) δ 8.42 (d, J = 8.8 Hz, 2H), 7.94 (d, J = 8.8 Hz, 2H), 7.73 (s, 1H), 7.67 – 7.59 (m, 3H), 7.33 (d, J = 8.1 Hz,2H), 7.08 – 7.02 (m, 2H), 6.99 (t, J = 8.7 Hz, 2H), 4.07 – 3.43 (m, 4H), 3.10 (s, 4H).^{13}C NMR (125 MHz, $CDCl_3$) δ 170.2, 150.5, 141.7, 140.6, 137.5, 135.6, 133.9, 128.9, 127.7, 116.0, 115.8, 114.0, 113.9, 51.1, 46.0 ppm. Mass (m/z): $[M+H]^+$ Calculated for $C_{24}H_{22}FN_5O_5S$ is 512.13; Observed. = 511.85.

(4-((2-(4-chlorophenyl)hydrazono)methyl)phenyl)(4-((4-nitrophenyl)sulfonyl)piperazin-1-yl)methanone (F14)

Yellow solid, yield: 67%, mp: 172-175°C; FTIR (ATR, Vmax, cm-1): 3254, 2863, 1622, 1350, 1164, 749; ^{1}H NMR (400 MHz, $CDCl_3$) δ 8.44 – 8.40 (m, 2H), 8.14 (s, 1H), 7.96 – 7.91 (m, 2H), 7.81 (s, 1H), 7.68 (d, J = 8.2 Hz, 2H), 7.53 (d, J = 8.8 Hz, 1H), 7.35 (d, J = 8.2 Hz, 2H), 7.30 (d, J = 2.1 Hz, 1H), 7.21 (dd, J = 8.8, 2.2 Hz, 1H), 4.05 – 3.46 (m, 4H), 3.10 (s, 4H). ^{13}C NMR (125 MHz, $CDCl_3$) δ 169.9, 150.4, 136.8, 134.5, 128.9, 128.2, 127.8, 126.5, 124.7, 117.4, 115.0, 51.8, 46.1 ppm. Mass (m/z): $[M+H]^+$ Calculated for $C_{24}H_{22}ClN_5O_5S$ is 528.10; Observed. = 527.80.

(4-((2-(2,4-dichlorophenyl)hydrazono)methyl)phenyl)(4-((4-nitrophenyl)sulfonyl)piperazin-1-yl)methanone (F15)

Yellow solid, yield: 70%, mp: 180-184; FTIR (ATR, Vmax, cm-1): 3281, 2866, 1639, 1355, 1174, 753; ^{1}H NMR (400 MHz, $CDCl_3$) δ 8.42 (d, J = 8.6 Hz, 2H), 7.95 (d, J = 8.6 Hz, 2H), 7.77 (s, 1H), 7.65 (d, J = 6.0 Hz, 3H), 7.33 (d, J = 8.1 Hz, 2H), 7.23 (d, J = 8.8 Hz, 2H), 7.04 (d, J = 8.7 Hz, 2H), 4.01 – 3.29 (m, 4H), 3.10 (s, 4H). ^{13}C NMR (125 MHz, $CDCl_3$) δ 169.9, 150.4, 136.8, 134.5, 128.9, 128.2, 127.8, 126.5, 124.7, 117.4, 115.0, 51.8, 46.1 ppm. Mass (m/z): $[M+H]^+$ Calculated for C24H21Cl2N5O5S is 562.06; Observed. = 561.75.

(4-((4-chlorophenyl)sulfonyl)piperazin-1-yl)(4-((2-(4-fluorophenyl)hydrazono)methyl)phenyl)methanone (F16)

Whit brown solid, yield: 78%, mp: 148-152°C; FTIR (ATR, Vmax, cm-1): 3422, 2866, 1603, 1160, 762; ^{1}H NMR (400 MHz, $CDCl_3$) δ 7.68 (d, J = 8.6 Hz, 2H), 7.63 (d, J = 7.5 Hz, 3H), 7.54 (d, J = 8.4 Hz, 2H), 7.33 (d, J = 8.1 Hz, 2H), 7.05 (dd, J = 8.9, 4.5 Hz, 2H), 6.98 (t, J = 8.6 Hz, 2H), 3.99 – 3.39 (m, 4H), 3.05 (s, 4H). ^{13}C NMR (125 MHz, $CDCl_3$) δ 169.5, 158.1, 156.4, 140.6, 140.0, 137.4, 135.6, 134.0, 133.8, 129.7, 129.1, 127.7, 126.1, 115.9, 113.9, 113.8, 46.1 ppm. Mass (m/z): $[M+H]^+$ Calculated for C24H22ClFN4O3S is 501.11; Observed. = 501.05.

(4-((2-(4-fluorophenyl)hydrazono)methyl)phenyl)(4-tosylpiperazin-1-yl)methanone (F17)

Yellow solid, yield: 74%, mp: 143-147°C; FTIR (ATR, Vmax, cm-1): 3421, 3040, 1612, 1347, 1167, 725; ^{1}H NMR (400 MHz, $CDCl_3$) δ 7.64 – 7.57 (m, 6H), 7.35 (d, J = 8.3 Hz, 2H), 7.31 (d, J = 8.2 Hz, 2H), 7.07 – 7.01 (m, 2H), 7.00 – 6.94 (m, 2H), 3.92 – 3.44 (m, 4H), 3.21 – 2.79 (m, J = 53.2 Hz, 4H), 2.45 (s, 3H). ^{13}C NMR (125 MHz, $CDCl_3$) δ 170.1, 158.5, 156.6, 144.2, 140.7, 137.3, 135.8, 134.3, 132.5, 129.9, 127.8, 127.7, 126.1, 116.0, 115.8, 113.9, 46.14, 45.54, 21.59 ppm. Mass (m/z): $[M+H]^+$ Calculated for C25H25FN4O3S is 481.16; Observed. = 480.90.

(4-((2-(2,4-dichlorophenyl)hydrazono)methyl)phenyl)(4-tosylpiperazin-1-yl)methanone (F18)

White Solid, yield: 59%, mp: 158-162°C; FTIR (ATR, Vmax, cm-1): 3421, 3040, 2339, 1612, 1347, 1110, 907, 725; ^{1}H NMR (400 MHz, $CDCl_3$) δ 2.4 (s, 3H), 2.98 (d, J=4.4Hz, 4H), 3.58 (s, 2H), 3.87 (s, 2H), 7.21 (dd, J=6.52Hz, J=2.2Hz, 1H), 7.3 (d, J=2.2Hz, 1H), 7.35-7.38 (m, 4H), 7.53 (d, J=8.8Hz,

1H), 7.63-7.69 (m, 4H), 7.82 (s, 1H), 8.1 (s, 1H) ppm. ^{13}C NMR (125 MHz, $CDCl_3$) δ 169.9, 144.2, 138.9, 138.5, 136.5, 134.8, 132.1, 129.9, 128.7, 128.1, 127.7, 127.7, 126.4, 124.5, 117.2, 114.9, 21.9. Mass (m/z): $[M+H]^+$ Calculated for C24H21Cl3N4O3S is 531.09; Observed. = 530.90.

(4-((4-chlorophenyl)sulfonyl)piperazin-1-yl)(4-((2-(2,4-dichlorophenyl)hydrazono)methyl)phenyl)methanone (F19)

White Solid, yield: 61%, mp: 180-183°C; FTIR (ATR, Vmax, cm-1): 3422, 3038, 2338, 1630, 1263, 1006, 944, 716; ^{1}H NMR (400 MHz, $CDCl_3$) δ 3.05 (s, 4H), 3.61 (s, 2H), 3.87 (s, 2H), 7.21 (dd, J=8.8Hz (long), J=2.2Hz(short), 1H), 7.30 (d, J=2.2Hz, 1H), 7.36 (d, J=8.1Hz, 2H) 7.53-7.57 (m, 3H), 7.38-3.71 (m, 4H), 7.82 (s, 1H), 8.16 (s, 1H) ppm. ^{13}C NMR (125 MHz, $CDCl_3$) δ 170.0, 140.0, 138.5, 138.4, 136.6, 134.6, 133.7, 129.7, 129.1, 128.7, 128.1, 127.7, 126.4, 124.6, 117.2, 114.9, 45.9, 45.3. Mass (m/z): $[M+H]^+$ Calculated for $C_{22}H_{21}Br_2N_5O$ is 552.87; Observed. = 552.80.

4. Conclusion

In this work, we have reported the synthesis and the antibacterial evaluation of series of phenylpiperazine sulphonamide and phenyl hydrazide (**E1-E6**) and hydrazine (**F7-F19**) hybrids. SAR study concluded the theisoniazid moiety containing analogues **E1** and **E2** exhibited potency against H_{37}Rv strain. In case of antimicrobial studies, we identified **F10** aspotent derivative against*Enterococcus faecium* micro-organism.

5. Acknowledgement

The authors are thankful to the Discipline of Pharmaceutical Sciences, College of Health Sciences, University of Kwa-Zulu Natal (UKZN), Durban, South Africa, and The M.S. University of Baroda, Vadodara, India and Institute of Translational Health Science and Technology,Faridabad, India for providing all the necessary facilities. R.K. gratefully acknowledges National Research Foundation-South Africa for funding this project (Grant Nos.103728 and 112079). The biological activities (anti mycobacterial and anti microbial activities) are not performed by student

6. Conflict of interest

Authors hereby declare that there are no financial/commercial conflicts of interest.

References

[1] Singh, S., Kaur, G., Mangla, V. and Gupta, M.K., 2015. Quinoline and quinolones: promising scaffolds for future antimycobacterial agents. Journal of enzyme inhibition and medicinal chemistry, 30(3), pp.492-504.

[2] Ahmed, M.H., Ibrahim, M.A., Zhang, J., Melek, F.R., El-Hawary, S.S., Jacob, M.R. and Muhammad, I., 2014. Methicillin-resistant Staphylococcus aureus, Vancomycin-resistant Enterococcus faecalis and Enterococcus faecium active Dimeric Isobutyrylphloroglucinol from Ivesiagordonii. Natural product communications, 9(2), p.1934578X1400900223.

[3] Antibiotic resistance, 2016, World Health Organization. https://www.betterhealth.vic.gov.au/health/conditionsandtreatments/antibiotic-resistant-bacteria

[4] The Hampstead Scientific Society. https://www.hampsteadscience.ac.uk/TheMedicinalChemistryofAntibiotics.pdf.

[5] Ananda Kumar, C.S., Vinaya, K., Narendra Sharath Chandra, J., Thimmegowda, N.R., Benaka Prasad, S.B., Sadashiva, C.T. and Rangappa, K.S., 2008. Synthesis and antimicrobial studies of novel 1-benzhydryl-piperazine sulfonamide and carboxamide derivatives. Journal of enzyme inhibition and medicinal chemistry, 23(4), pp.462-469.

[6] Shinde, R.R., Gaikwad, D. and Farooqui, M., 2020. Synthesis and antimicrobial activity of 2-(4-(benzo [d] thiazol-5-ylsulfonyl) piperazine-1-yl)-N-substituted acetamide derivatives. Journal of Heterocyclic Chemistry, 57(11), pp.3907-3917.

[7] Ceramella, J., Iacopetta, D., Catalano, A., Cirillo, F., Lappano, R. and Sinicropi, M.S., 2022. A review on the antimicrobial activity of Schiff bases: Data collection and recent studies. Antibiotics, 11(2), p.191.

[8] Aboul-Fadl, T., Abdel-Aziz, H.A., Abdel-Hamid, M.K., Elsaman, T., Thanassi, J. and Pucci, M.J., 2011. Schiff bases of indoline-2, 3-dione: potential novel inhibitors of mycobacterium tuberculosis (MTB) DNA gyrase. Molecules, 16(9), pp.7864-7879.

[9] Girase, P.S., Dhawan, S., Kumar, V., Shinde, S.R., Palkar, M.B. and Karpoormath, R., 2021. An appraisal of anti-mycobacterial activity with structure-activity relationship of piperazine and its analogues: A review. European Journal of Medicinal Chemistry, 210, p.112967.

[10] Burka, J.M., Bower, K.S., Vanroekel, R.C., Stutzman, R.D., Kuzmowych, C.P. and Howard, R.S., 2005. The effect of fourth-generation fluoroquinolones gatifloxacin and moxifloxacin on epithelial healing following photorefractive keratectomy. American journal of ophthalmology, 140(1), pp.83-87.

[11] Cervantes, L.J. and Mah, F.S., 2011. Clinical use of gatifloxacin ophthalmic solution for treatment of bacterial conjunctivitis. Clinical Ophthalmology, pp.495-502.

[12] Schultz, C., 2012. Gatifloxacin ophthalmic solution for treatment of bacterial conjunctivitis: safety, efficacy and patient perspective. Ophthalmology and eye Diseases, 4, pp.OED-S7383.

[13] Holmes, B., Brogden, R.N. and Richards, D.M., 1985. Norfloxacin: a review of its antibacterial activity, pharmacokinetic properties and therapeutic use. Drugs, 30, pp.482-513.

[14] Monk, J.P. and Campoli-Richards, D.M., 1987. Ofloxacin: a review of its antibacterial activity, pharmacokinetic properties and therapeutic use. Drugs, 33, pp.346-391.

[15] Ball, P., 2003. Efficacy and safety of levofloxacin in the context of other contemporary fluoroquinolones: a review. Current therapeutic research, 64(9), pp.646-661.

[16] Shimada, J., Nogita, T. and Ishibashi, Y., 1993. Clinical pharmacokinetics of sparfloxacin. Clinical pharmacokinetics, 25, pp.358-369.

[17] Rubinstein, E., 2001. History of quinolones and their side effects. Chemotherapy, 47(Suppl. 3), pp.3-8.

[18] Wise, R., Andrews, J.M. and Edwards, L.J., 1983. In vitro activity of Bay 09867, a new quinoline derivative, compared with those of other antimicrobial agents. Antimicrobial Agents and Chemotherapy, 23(4), pp.559-564.

[19] Shimizu, M., Takase, Y., Nakamura, S., Katae, H., Minami, A., Nakata, K. and Kurobe, N., 1976. Pipemidic acid: its activities against various experimental infections. Antimicrobial Agents and Chemotherapy, 9(4), pp.569-574.

[20] Child, J., Andrews, J.M. and Wise, R., 1995. Pharmacokinetics and tissue penetration of the new fluoroquinolone grepafloxacin. Antimicrobial agents and chemotherapy, 39(2), pp.513-515.

[21] Meena, C.L., Singh, P., Shaliwal, R.P., Kumar, V., Kumar, A., Tiwari, A.K., Asthana, S., Singh, R. and Mahajan, D., 2020. Synthesis and evaluation of thiophene based small molecules as potent inhibitors of Mycobacterium tuberculosis. European Journal of Medicinal Chemistry, 208, p.112772.

[22] Govender, H., Mocktar, C. and Koorbanally, N.A., 2018. Synthesis and Bioactivity of Quinoline-3-carboxamide Derivatives. Journal of Heterocyclic Chemistry, 55(4), pp.1002-1009.

[23] S Aremu, O., Gopaul, K., Kadam, P., Singh, M., Mocktar, C., Singh, P. and A Koorbanally, N., 2017. Synthesis, characterization, anticancer and antibacterial activity of some novel pyrano [2, 3-d] pyrimidinone carbonitrile derivatives. Anti-Cancer Agents in Medicinal Chemistry (Formerly Current Medicinal Chemistry-Anti-Cancer Agents), 17(5), pp.719-725.

[24] Okawa, T., Aramaki, Y., Yamamoto, M., Kobayashi, T., Fukumoto, S., Toyoda, Y., Henta, T., Hata, A., Ikeda, S., Kaneko, M. and Hoffman, I.D., 2017. Design, synthesis, and evaluation of the highly selective and potent G-protein-coupled receptor kinase 2 (GRK2) inhibitor for the potential treatment of heart failure. Journal of medicinal chemistry, 60(16), pp.6942-6990.

[25] Akbar, A., McNeil, N.M., Albert, M.R., Ta, V., Adhikary, G., Bourgeois, K., Eckert, R.L. and Keillor, J.W., 2017. Structure–activity relationships of potent, targeted covalent inhibitors that abolish both the transamidation and GTP binding activities of human tissue transglutaminase. Journal of medicinal chemistry, 60(18), pp.7910-7927.

[26] WO2014149164A1

[27] Mishra, C.B., Kumari, S., Angeli, A., Bua, S., Buonanno, M., Monti, S.M., Tiwari, M. and Supuran, C.T., 2018. Discovery of potent anti-convulsant carbonic anhydrase inhibitors: design, synthesis, in vitro and in vivo appraisal. European Journal of Medicinal Chemistry, 156, pp.430-443.

Chapter 5

Novel Piperazine-Coumarin hybrids as antibacterial agents

(Ready to communicate)

Abstract

Novel analogues of 4-methyl coumarin-(phenylsulfonyl) piperazinesand coumarin-(phenylsulfonyl)piperazine were designed using a molecular hybridization approach. All the synthesised compounds were evaluated for their *in vitro* anti-mycobacterium and anti-microbial activity against $H_{37}Rv$ and the broad range of antimicrobial gram-positive and gram-negative strains. Compounds **6g**, **6h**, **10d** and **10e** displayed moderate inhibition against gram-positive and gram-negative strains with MIC values in the range of 62.5-250 µg/mL (**table 1**) against *MRSA, Bacillus subtilis,* and *Enterococcus faecium,* and gram-negative strains *Enterobacter hormaechei, Pseudomonas aeruginosa,* and *Escherichia coli*. Further, the structure-activity relationship (SAR) demonstrated that substituents on phenyl ring improve the antimicrobial activity. Moreover, further modifications are required to discover active hybrids with enhanced potency.

1. Introduction

Antimicrobial resistance (AMR) is a worldwide life-threatening condition caused by the escalating conflict between humans and the micro biome[1]. The issue of microbial drug resistance poses a rising risk to human health. With the introduction of each new microorganism treatment over the past several decades, antibiotic resistance has arisen progressively globally [2]. Similarly, Tuberculosis has been fought for hundreds of years. It has killed almost a billion people and still affects a third of the world's population[3]. Research efforts worldwide have been boosted by the emergence of MDR and, more recently, XDR tuberculosis[4]. As no new anti-TB agents have been introduced into TB therapy in recent years, there is an immediate need to design and develop new treatments and techniques for a successful TB treatment[5].We have generated novel piperazine-

coumarin hybrids and tested them against antimicrobial and antitubercular strains to better grasp the issue surrounding resistance to such agents.

As shown in Fig-1, several natural coumarin compounds have been described with various biological activities such as antitubercular, antibacterial, antimicrobial, antifungal, anticancer, anticoagulant, antihypertensive, and anti-inflammatory[6]. Influenced by their biological potential, we conducted more research on their hybrid derivatives against other heterocyclic moieties. According to the study's findings, the combination of coumarin and piperazine displayed significant antibacterial action[7-8].Considering this, it must have been decided that combining coumarin and piperazine moieties would be beneficial since it could potentially increase the antibacterial activity of compounds.From this perspective, this research aims to invent novel coumarin-piperazine analogues.

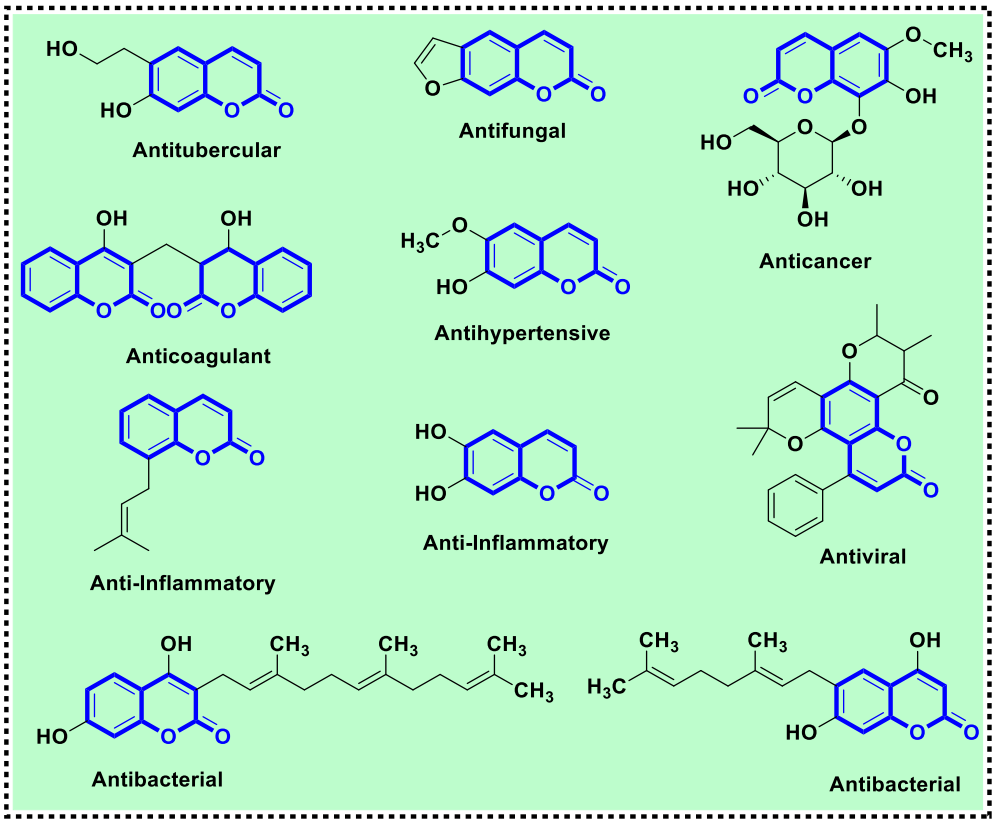

Figure 1 Natural coumarin biological active derivatives

In **Fig. 2**, the 4-methyl coumarin (A, B, and C) is more likely to be connected to a different heterocyclic moiety at the 7th position than the coumarin (D and E), which is connected at the 3rd position[9-10]. Based on this analysis, we synthesised 7 and 3-amino coumarins (scheme **2** and **3**), combined them with piperazine sulphonamides and phenylsulfonyl piperazine through acid amine

coupling, and examined their*in vitro* activity against gram-positive gram-negative and anti-TB bacterial strains.

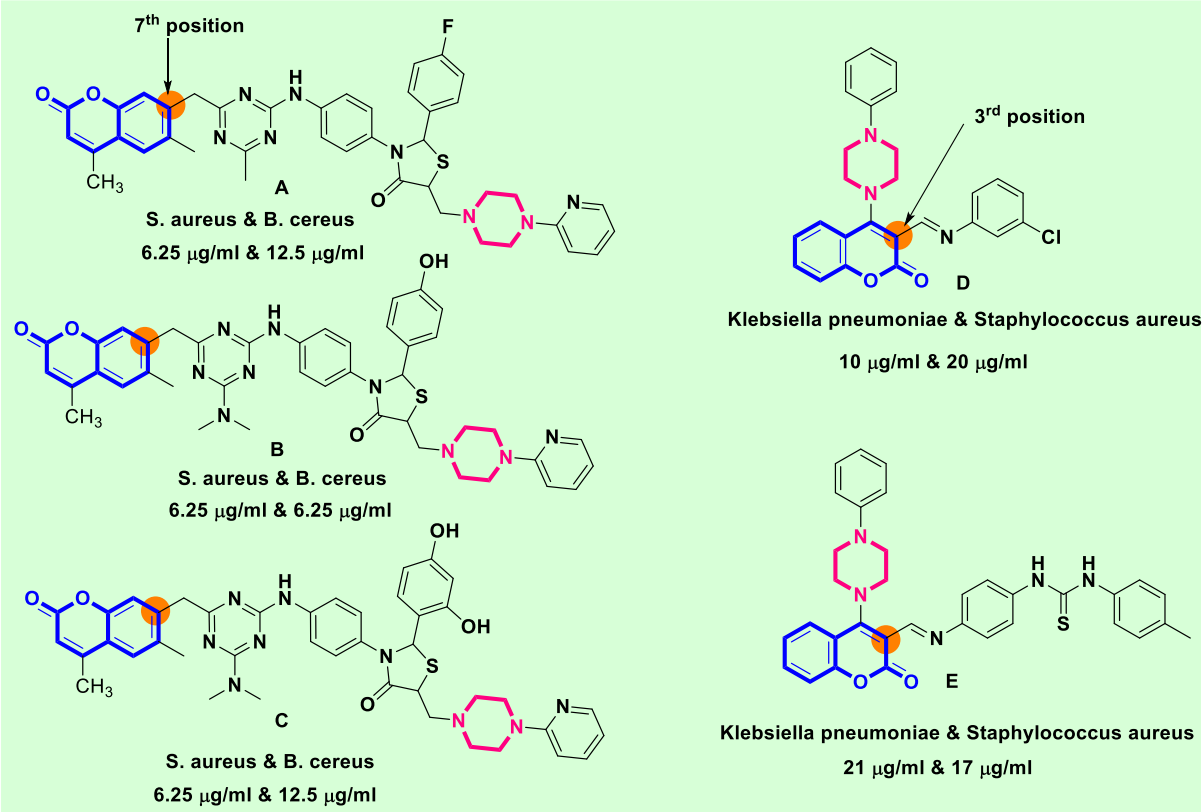

Figure 2 Coumarin piperazine hybrids with their antimicrobial activity

2. Result and discussion

2a. Chemistry

As shown in Scheme **I** and **II**, effective and easy synthetic routes were used to make the novel 7-amino coumarin-piperazine hybrid derivatives (**6a** to **6j**). **A** was prepared by nucleophilic attack of piperazine on benzene sulphonyl chloride[11]; to avoid piperazine di-substitution, ten equivalent of piperazine was used in DCM under cooling conditions. To avoid amine interference in coumarin synthesis, the amino group was protected, and ethyl (3-hydroxyphenyl)carbamate (**2)** was produced by reacting 3-aminophenol with ethyl carbonochloridate. Next, we synthesised ethyl (4-methyl-2-oxo-2H-chromen-7-yl)carbamate (**3**) using Pechmann-type condensation reaction between (**2)** and EAA in ethanolic H_2SO_4. The amine group of **3** was deprotected by hydrolysis in a solution of H_2SO_4 and

acetic acid, yielding compound7-amino-4-methyl-2H-chromen-2-one **4**[12]. Further **4** was N-acylated with 2-bromoacetyl bromide in DCM at 0°C to obtain 2-bromo-N-(4-methyl-2-oxo-2H-chromen-7-yl)acetamide**5**[13]. The final piperazine-coumarin hybrid **6a-j** was achieved by nucleophilicsubstitution reaction of **1** and **5** inDMFat rt[14].

To produce 3-amino coumarin-piperazine hybrid compounds, efficient and straightforward synthesis methods were adopted, as illustrated in Scheme III (**10a** to **10h**). The Knoevenagal type condensation reaction was used to prepare N-(2-oxo-2H-chromen-3-yl)acetamide**7** on reaction of 2-hydroxybenzaldehyde with acetyl glycine. The N-acetyl group of **7** was converted to 3-amino-2H-chromen-2-one (**8**), using the de-protection reaction of **7** by reflux in conc HCl and ethanol[15]. Next,**8** was acylated with Bromo acetyl bromide using the same method as used for the preparation of **5** to yield 2-Bromo-N-(2-oxo-2H-chromen-3-yl)acetamide (**9)**[13]. The final piperazine-coumarin hybrid **10** was achieved by reaction of **1** and **9,**as discussed in scheme (**II**) for synthesising**6a-j** by reaction of **9** and **1**[14].

1. Synthesis of phenylsulfonylpiperazine (**1a-1n**)

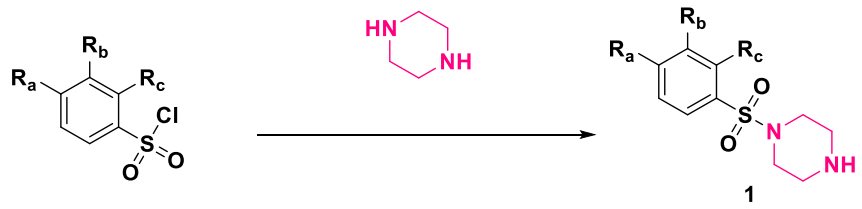

1

comp	R_a	R_b	R_c	comp	R_a	R_b	R_c
1a	H	H	H	1h	H	Cl	H
1b	H	H	H	1i	H	H	OCH_3
1c	Br	H	H	1j	H	H	F
1d	F	H	H	1k	H	H	CN
1e	NO_2	H	H	1l	H	F	H
1f	Cl	H	H	1m	H	OCH_3	H
1g	CH_3	H	H	1n	H	CN	H

Reaction conditions: i) DCM, 0-rt, 30 min

Scheme 1

2. Synthesis of compound (**6a-6j**)

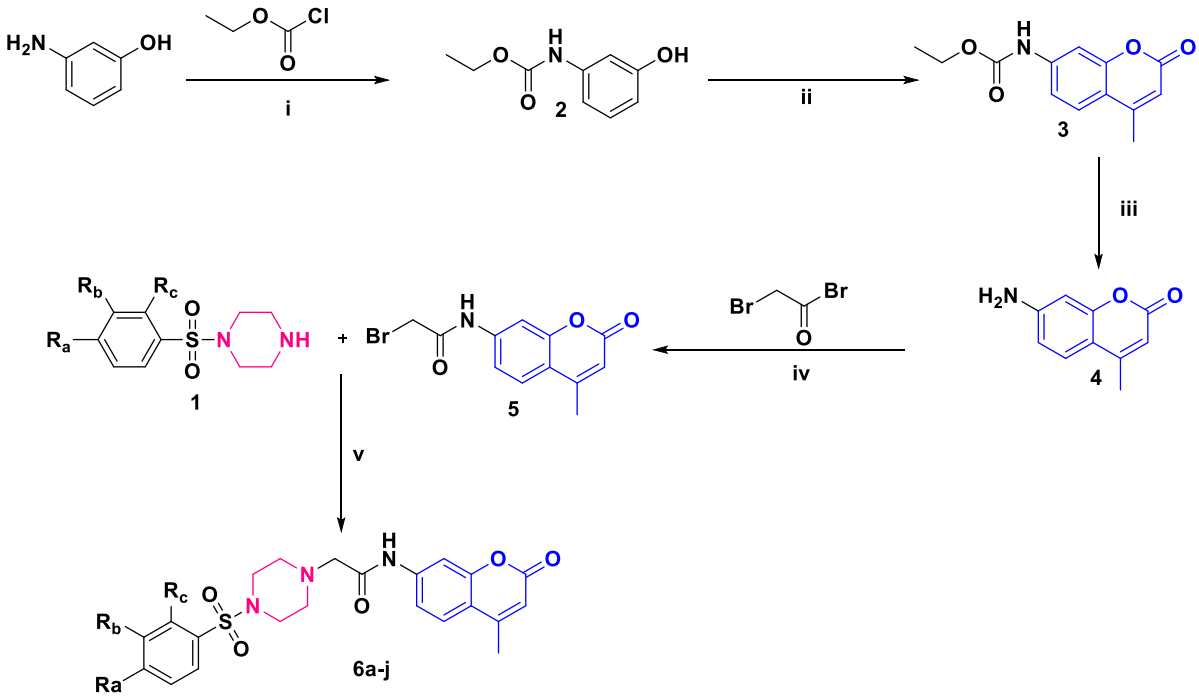

Comp	R_a	R_b	R_c	Comp	R_a	R_b	R_c
6a	H	H	H	6f	CH_3	H	H
6b	Br	H	H	6g	H	Cl	H
6c	F	H	H	6h	H	H	OCH_3
6d	NO_2	H	H	6i	H	H	F
6e	Cl	H	H	6j	H	H	CN

Reaction conditions:i) Ethyl acetate, rt, 3 hrs, ii) Ethyl acetoacetate, ethanolic H_2SO_4 4 hrs, iii) acetic acid, H_2SO_4, reflux, 4 hrs, iv) tri-ethyl amin (TEA), DCM, 0-rt, 2h, iv) TEA, DMF, rt, 16 hrs

Scheme 2

3. Synthesis of compound **(10a-10h)**

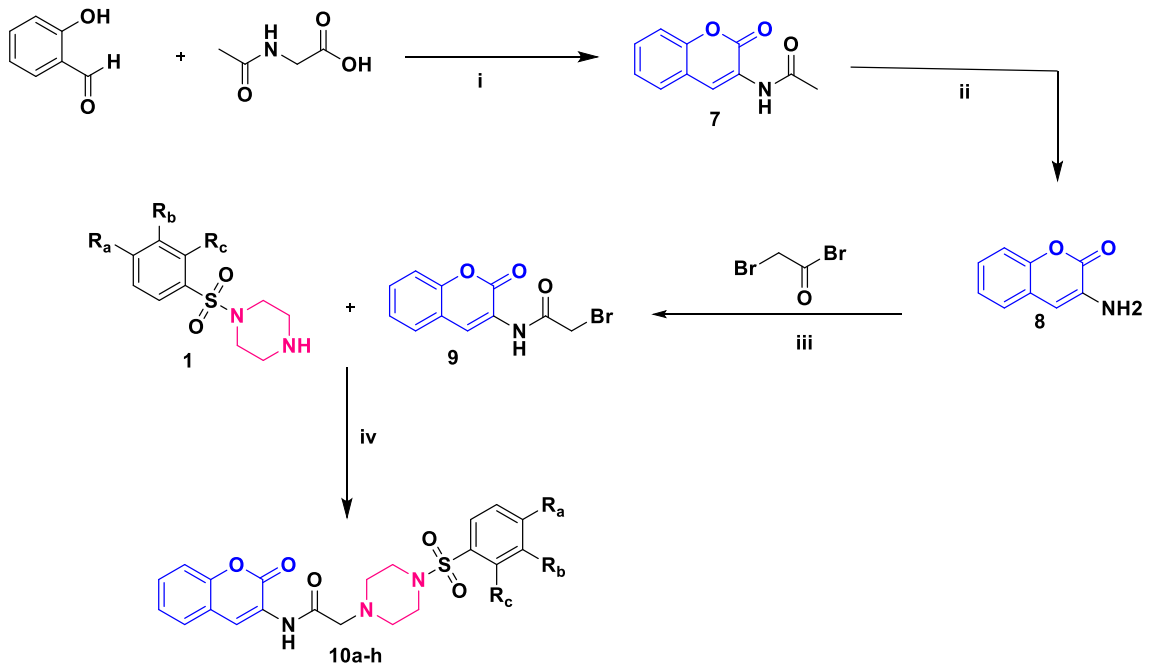

Comp	R_a	R_b	R_c	Comp	R_a	R_b	R_c
10a	Br	H	H	10e	H	H	F
10b	F	H	H	10f	H	H	OCH_3
10c	Cl	H	H	10g	H	H	CN
10d	H	Cl	H	10h	H	H	H

Reaction conditions: i) Sodium acetate, acetic anhydride, 100-110^{o}C, 4 hrs, ii) conc.HCl, ethanol, reflux, 4 hrs, iii) TEA, DCM, rt, 2hrs, iv)TEA, DMF, rt, 16 hrs

Scheme 3

NMR data discussion

2-(4-((4-fluorophenyl)sulfonyl)piperazin-1-yl)-N-(4-methyl-2-oxo-2H-chromen-7-yl)acetamide (6c)

^{1}H NMR

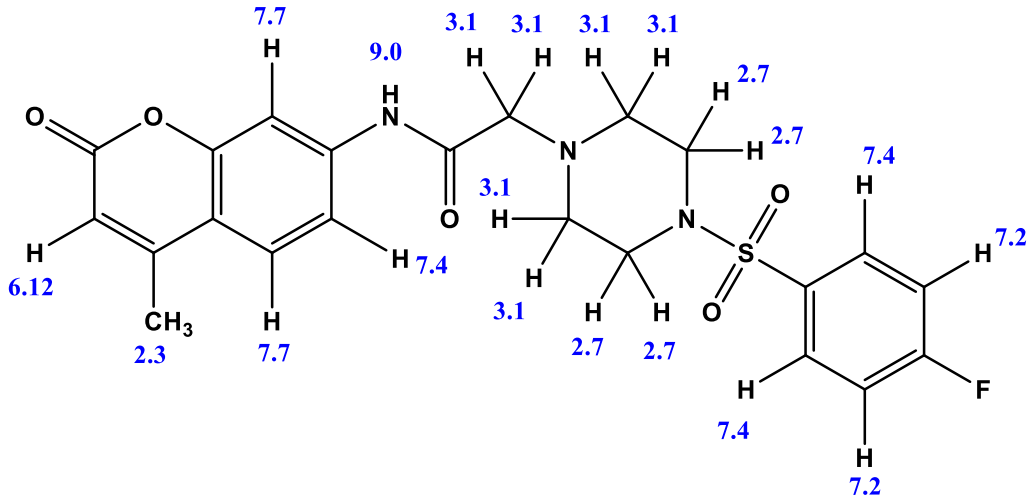

The amide proton is highly deshielded and it displayed a delta value at 9.0 ppm because of the resonance with the adjacent carbonyl carbon. The protons on the phenyl ring and the lactone ring displayed the delta value ranging from 7.7 to 7.2 ppm. Due to the difference in the t chemical environment, the piperazine ring showed two sets of protons appearing at 3.1 and 2.7 ppm respectively. The methyl protons of the lactone ring showed a delta value of 2.3 ppm.

^{13}C NMR

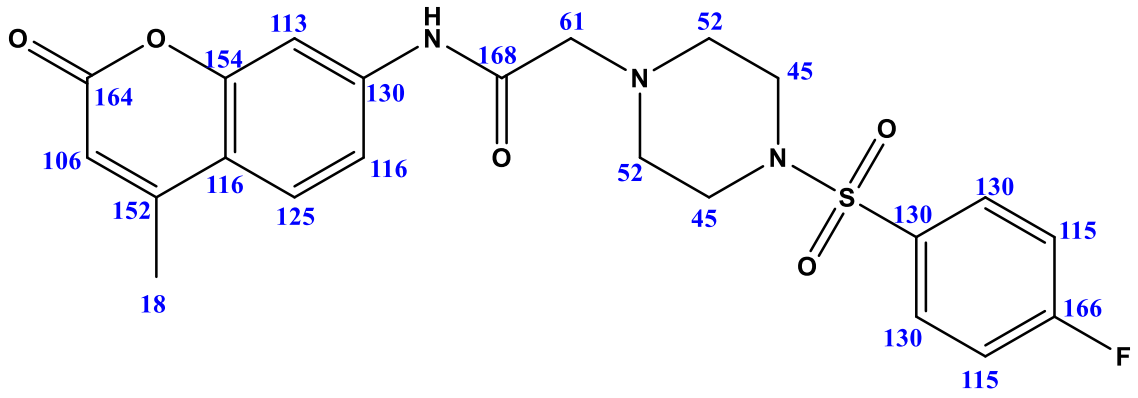

In C^{13} NMR, carbonyl carbons generally exhibit delta values between 180 and 220 ppm. However, the delta value of the carbonyl carbons in the lactoneringand of the amide group has moved to164 and 168 ppm respectively, because of the conjugation in the carbonyl carbon. The carbon atom adjacent to the fluorine substituent is deshielded, and it showed a delta value at166 ppm. Similarly, the quaternary carbons in the lactone ring are deshielded and showed delta value at 152 and 154 ppm respectively due to the conjugation with the carbonyl group. The other carbons of the phenyl and the

lactone rings showed delta values ranging from 106 to 130 ppm. The delta values of the piperazine ring's carbonsare25 and 45 ppm. The methyl protons on the phenyl ring displayed a delta value at 18 ppm.

2-(4-((4-fluorophenyl)sulfonyl)piperazin-1-yl)-N-(2-oxo-2H-chromen-3-yl)acetamide (10b)

^{1}H NMR

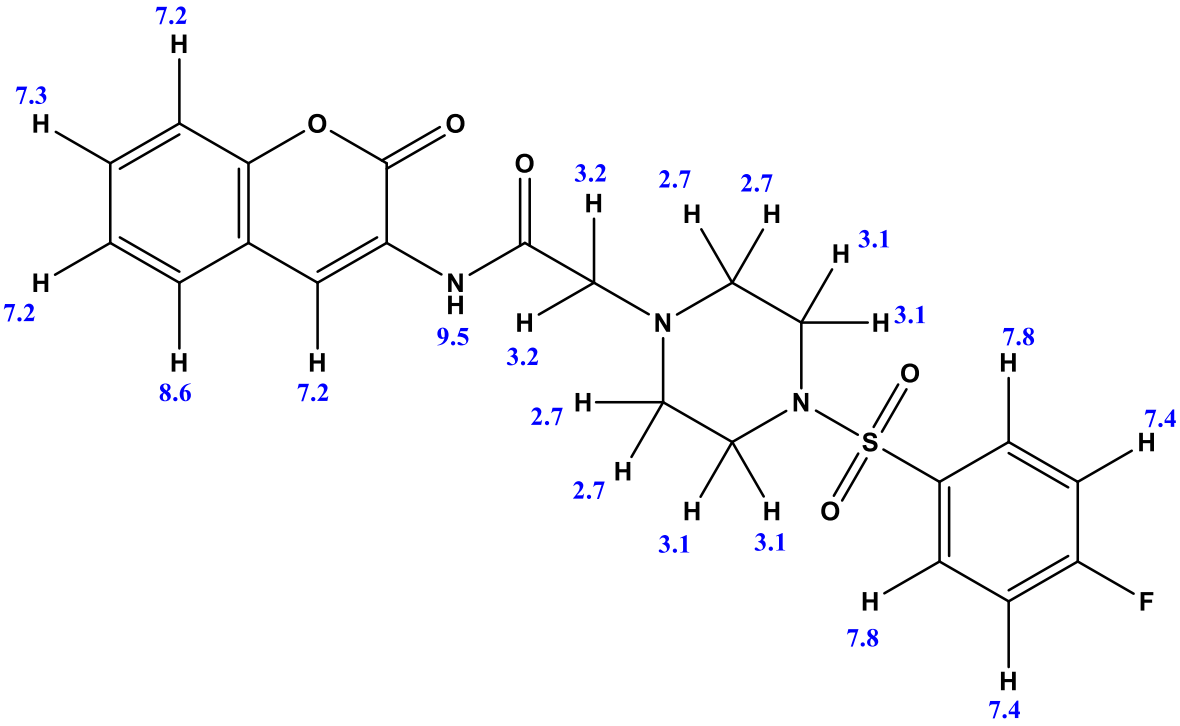

The amide proton is highly deshielded and it displayed a delta value at 9.5 ppm because of the resonance with the adjacent carbonyl group. The protons of the phenyl ring and the lactone ring displayed the delta value ranging from 7.8 to 7.2 ppm. Due to the difference in the chemical environment, the piperazine ring showed two sets of protons with the delta value of 3.1 and 2.7 ppm respectively. The methylene protons adjacent to the amide carbonyl group are deshielded and showed a delta value at3.2 ppm.

^{13}C NMR

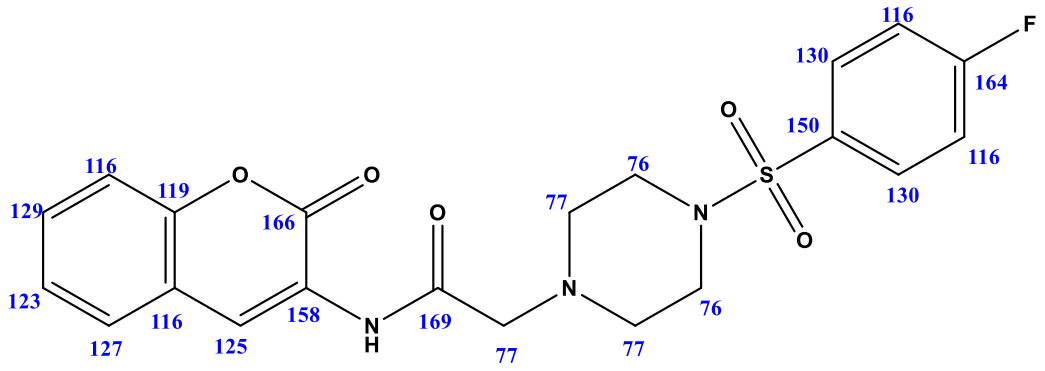

In C^{13} NMR, carbonyl carbons generally exhibit delta values between 180 and 220 ppm. However, the delta value of the carbonyl carbons in the lactoneringand of the amide group has moved to 166 and 169 ppm respectively because of the conjugation effect. The carbon atom adjacent to the fluorinesubstituent and the carbon atom adjacent to the sulfonyl group are deshielded and showed peaks at164 and 150 ppm respectively. The carbon adjacent to amide group showed delta value at 158 ppm and the carbon which is present between the amide carbonyl carbon and the piperazine nitrogen showed a peat at 77 ppm. The other carbons of the phenyl ring and the lactone ring have appeared ranging from 116 to 130 ppm. The delta value of the piperazine ring's carbons was 77 and 76 ppm.

2b. Biological evaluation

1. Mycobacterium activity

As indicated in the introduction, Novel hybrids of 3-methyl-7-amino coumarin with different phenylsulfonyl piperazine (**6a-j**) were initially synthesised and assessed for their anti-tuberculous efficacy in whole cells. The minimum inhibitory concentration (MIC) values against Mycobacterium tuberculosis (TB) *$H_{37}Rv$* were analysed and listed in **Table 1.** Phenylsulfonyl piperazines with hydrogen, bromo, chloro, fluoro, nitro, and methyl substitutions at the para position (**6a-f**) and compared their activity against *$H_{37}Rv$* at 50μM, but none of them showed positive results. Similarly, chloro-substituted phenylsulfonyl piperazineat the meta position did not show improved results. Further, we observed the behaviour of chloro, fluoro, methoxy and cyano at the ortho position (**6g-j**), but none produced any significant results. Next, we screened the activity of a series of 3-aminocoumarins with hybrids of meta and para-substituted phenylsulfonyl piperazine (**10a-10h**).

Activity data described below in table 1 indicts the need for the development of more piperazine coumarin derivatives to get better results.

2. Antimicrobial activity

After checking mycobacterium potential, all the compounds were tested against Gram-positive strains such as *methicillin-resistant staphylococcus aureus (MRSA), Streptococcus pyrogens, Bacillus subtilis, Enterococcus faecium,* and *Staphylococcus aureus*, andGram-negative strains such as *Enterobacter hormaechei, Pseudomonas aerugenosa*, and *Escherichia coli* (**Table 1**). Among the hybrids of 3-methyl-7-amino coumarin- phenylsulfonyl piperazine analogue (**6a-6j**), **6c**, **6g** and **6h** showed moderate activity against *MRSA, Bacillus subtilis, Enterococcus faecium*, *Enterobacter hormaechei, Pseudomonas aeruginosa, and Escherichia coli* strains. Fluoro substituted **6c** shown displayed inhibition of 250, 62.5, 62.5, 125, 125, 125 µg/mL against *MRSA, Bacillus subtilis, Enterococcus faecium*, *Enterobacter hormaechei, Pseudomonas aeruginosa, and Escherichia coli* strains respectively. Chloro and methoxy meta substituted analogues **6g** and **6h** displayed 250, 62.5, 62.5, 125, 62.5, 62.5 µg/mL and 250, 62.5, 62.5, 62.5, 62.5, 62.5µg/mL respectively against same strains. Chloro and fluoro substituted analogue **10d** and **10e** from 3-aminocoumarins-phenylsulfonyl piperazine derivatives also displayed moderate activity against *MRSA, Bacillus subtilis, Enterococcus faecium, Enterobacter hormaechei, Pseudomonas aeruginosa, and Escherichia coli* strains. This Structural activity relationship (SAR) study showed that further development of different meta-substituted derivatives might improve the antimicrobial activity.

Table 1: Activity of synthesized derivatives (**6a to 6j** and **10a-10h**) against growth of Gram positive, Gram negative and $H_{37}Rv$ bacterial strains.

Comp	**Gram positive bacteria**					**Gram negative bacteria**			**[i]$H_{37}R_V$ MIC(µM)**
	[a]10069	**[b]49247**	**[c]12344**	**[d]19434**	**[e] 25923**	**[f]700232**	**[g]27853**	**[h]35218**	
6a	-	-	-	-	-	-	-	-	>50
6b	-	-	-	-	-	-	-	-	>50

6c	250		62.5	62.5		125	125	125	>50
6d	-	-	-	-	-	-	-	-	>50
6e	-	-	-	-	-	-	-	-	<50
6f	-	-	-	-	-	-	-	-	>50
6g	250		62.5	62.5		62.5	62.5	62.5	>50
6h	125		62.5	62.5		62.5	62.5	62.5	>50
6i	-	-	-	-	-	-	-	-	>50
6j	-	-	-	-	-	-	-	-	>50
10a	-	-	-	-	-	-	-	-	>50
10b	-	-	-	-	-	-	-	-	>50
10c	-	-	-	-	-	-	-	-	>50
10d	may		62.5	62.5		125	62.5	62.5	<50
10e	250		62.5	62.5		62.5	62.5	62.5	>50
10f	-	-	-	-	-	-	-	-	>50
10g	-	-	-	-	-	-	-	-	>50
10h	-	-	-	-	-	-	-	-	>50
NIH	-NA-	-NA-	-NA-	-NA-	-NA-	-NA-	-NA-	-NA-	0.053
Ciprofloxacin	≥ 0.49	≥ 0.49	≥ 0.49	≥ 0.49	≥ 0.49	≥ 0.49	≥ 0.49	≥ 0.49	-NA-
Vancomycin	0.00375	0.00375	-	-	-	-	-	-	-NA-

[a] methicillin resistant staphylococcus aureus (mrsa) 10069; [b] Streptococcus pyrogens 49247; [c]Bacillus subtilis 12344; [d] Enterococcus faecium 19434; [e] Staphylococcus aureus 25923; [f] Enterobacter hormaechei 700232; [g] Pseudomonas aerugenosa 27853; [h] Escherichia coli35218

The zone of inhibition was measured at concentration of 1000 µg/mL; Ciprofloxacin and Vancomycin were used as a standard. (-) indicates no activity; -NA-indicates not applicable.

*[i] Minimal inhibitory concentration (MIC µM).**

3. Experimental

3a. Biology

1. Material and method

a. Mycobacterium tuberculosis

MIC determination assays

At 37°C with shaking (200 rpm), Middlebrook 7H9 broth (MB broth) supplemented with 0.05% Tween-80, 0.2% glycerol and 1x albumin dextrose-saline (ADS) was used to culture mycobacterium tuberculosis *$H_{37}Rv$* (M. TB). The compounds were prepared as 1000 µg/ml stocks in DMSO and evaluated MIC value for antimycobacterial activity at concentrations ranging from 50 µM[16]

b. Antimicrobial

Method used: i) Agar diffusion assay[17] , ii) Broth Microdilution assay[18]

Concentration of compounds: Stock solution [1000 µg/ml] of each compound was prepared in DMSO. Agar diffusion is carried out by taking 5 micro liters from stock solution. Broth micro dilution Assay carried out by 2-fold serial dilution of 100 microliters from stock solution.

Media used:i) Microbiological media used for bacteria is Mueller Hinton Agar (M-H Agar) Composition (gL-1): Beef infusion solids 2.0; starch 1.5; Casein hydrolysate 17.5; Agar 17.0; Final pH (at 25°C) 7.3 ± 0.2. ii) Microbiological media used for bacteria is Mueller Hinton Broth (M-H Broth) Composition (gL-1): Beef infusion solids 2.0; starch 1.5; Casein hydrolysate 17.5; Final pH (at 25°C) 7.4 ± 0.

3b. Chemistry

1. Material and method

All reactions were conducted under standard operating conditions without the use of any stringent conditions. All chemicals were obtained from Aldrich Chemical Co., Alfa Aesar, used as received without additional purification. Lab reagent (LR) grade solvents were used for extraction. The reaction progress was monitored on Merck TLC Silica gel 60 F254 plates, and the spots were visualized under ultraviolet (UV) light, followed by iodine or ninhydrin staining solution followed by heating.

NMR spectra were recorded on 400 and 100 MHz NMR spectrometer using $CDCl_3$ and DMSO as solvent unless otherwise stated. MS were made by means of ESI (Electron spray ionization). Unless otherwise specified, all reagents were weighed and handled in air.

2. Synthetic procedure

1. Synthesis of compound **1a-1n**

Preparation of 1-(phenylsulfonyl)piperazine (**Compound 1**)

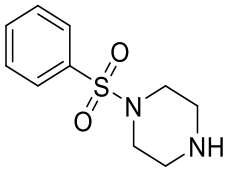

To the solution of 10.0 mmol of piperazine in DCM, the 1.0 mmol of benzenesulfonyl chloride was added at 0 °C, and the reaction mixture stirred for 30 min at rt. After the reaction completion, consumption of starting materials was confirmed by TLC. Reaction mixture was washed with water (3×40 mL), dried over anhydrous Na_2SO_4 and DCM layer was evaporated in vacuum to yield white solid.

Compound number **1b** to **1f** mentioned in scheme 1, were prepared using same procedure as illustrated in **scheme 1**

2. Synthesis of compound **6a-6j**

Preparation of ethyl (3-hydroxyphenyl)carbamate (**compound 2**)

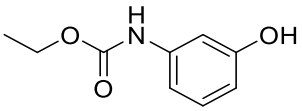

Ethyl chloroformate 1.0 mmol was added in one portion to a stirred suspension of m-aminophenol 1.0 mmolin ethyl acetate 20ml. A white precipitate formed immediately. The reaction mixture was stirred for 3 hrsat room temperature. The amine hydrochloride precipitate was removed by filtration, washed with ethyl acetate (5 mL) and filtrate was concentrated under reduced pressure to give colourless crystals of ethyl (3-hydroxyphenyl)carbamate.

Preparation of ethyl (4-methyl-2-oxo-2H-chromen-7-yl)carbamate(**compound 3**)

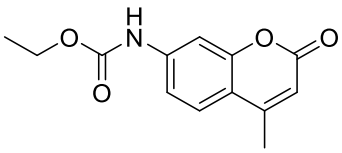

A solution of ethyl (3-hydroxyphenyl)carbamate 1 mmol and ethyl acetoacetate 1.2 mmol suspended in 20 mL of 70 % ethanolic H_2SO_4 and stirred at room temperature for 4 hrs. The product formation was monitored by TLC. On completion of reaction, the solution was poured into ice cold water (100 mL) to give brown crystalline solid. The solid was filtered, washed with water, and recrystallised from ethanol to give ethyl (4-methyl-2-oxo-2H-chromen-7-yl)carbamate.

Preparation of 7-amino-4-methyl-2H-chromen-2-one **(compound 4)**

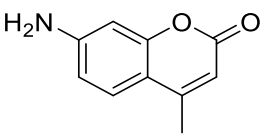

Ethyl (4-methyl-2-oxo-2H-chromen-7-yl)carbamatewas refluxed in a mixture of conc. H_2SO_4 and glacial acetic acid (1:1) for 4 hrs. The completion of reaction was checked by using TLC. After completion of reaction, the mixture was cooled to room temperature to give yellow precipitate.

Resulting mixture was poured into ice cold water (100 mL) and neutralized with 50% NaOH solution to give white solid. The solid obtained was filtered, washed with water, dried and recrystallized from ethanol to give 7-amino-4-methyl-2H-chromen-2-one.

Preparation of2-bromo-N-(4-methyl-2-oxo-2H-chromen-7-yl)acetamide **(compound 5)**

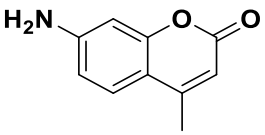

To the stirred solution of 1 mmol of 7-amino-4-methyl-2H-chromen-2-one and 3 volume of TEA in 10 volume DCM, 1 mmol of 2-bromoacetyl bromide was added at 0^{o}C.The resultant reaction mixture was stirred at rt for 2 hrs. After completion of the reaction, the solid reaction mass formed was filtered, washed with water and diethyl ether to get 2-bromo-N-(4-methyl-2-oxo-2H-chromen-7-yl)acetamide.

Preparation of N-(4-methyl-2-oxo-2H-chromen-7-yl)-2-(4-(phenylsulfonyl)piperazin-1-yl)acetamide **(compound 6a)**

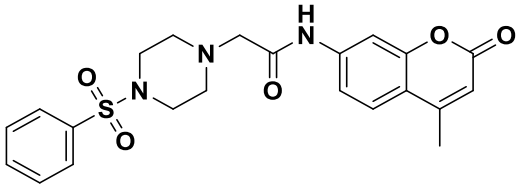

Mixture of 7-amino-4-methyl-2H-chromen-2-one 1 mmol and 1-(phenylsulfonyl)piperazine 1 mmol stirred in 10 volume of DMF in presence of 3 mmol of TEA at rt. The resultant reaction mixture was stirred for 16 hrs at rt. After the reaction completion, consumption of starting materials was confirmed by TLC. On completion of reaction, the rection mixture was poured into ice cold water to get white solid. The solid was filtered, washed with water and diethyl ether to give N-(4-methyl-2-oxo-2H-chromen-7-yl)-2-(4-(phenylsulfonyl)piperazin-1-yl)acetamide.

Similarly compound number **6b-j** were prepared using this procedure as illustrated in **scheme 2**

2. Synthesis of compound **6a-6j**

Preparation of N-(2-oxo-2H-chromen-3-yl)acetamide**(compound 7)**

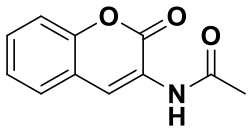

At 0 ^{o}C N-acetylglycine 1.0 mmol and sodium acetate 4.0 mmol were added to the stirred solution of salicylaldehyde 1.0 mmol in acetic anhydride 5.0 mmol and the mixture was refluxed at 100-110 ^{o}C for 4 hrs. Following the completion of the reaction on TLC, the reaction mass was poured into ice cold water to yield a solid. The solid was filtered, washed with 10 mL of ethyl acetate, dried, and then re-crystallized with ethanol to make the light yellow solid N-(2-oxo-2H-chromen-3-yl)acetamide. (Yield = 64 %).

Preparation of N-(2-oxo-2H-chromen-3-yl)acetamide**(compound 8)**

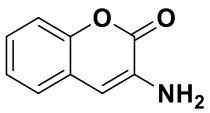

For 3-4 hrs, 10 mmol of N-(2-oxo-2H-chromen-3-yl)acetamidewas refluxed with 100 mL of ethanolic:HCl (7:3). TLC was used to monitor the completion of the reaction.After the reaction was done, the mixture was poured into ice-cold water to form a solid, which was then neutralised with a saturated solution of $NaHCO_3$. The solid was filtered, washed with 10 mL of ethyl acetate, dried, and then re-crystallized with ethanol to make the light brown crystals.

Preparation of 2-bromo-N-(2-oxo-2H-chromen-3-yl)acetamide **(compound 9)**

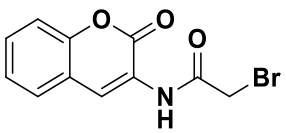

To the stirred solution of 1 mmol of N-(2-oxo-2H-chromen-3-yl)acetamide and 3 volume of TEA in 10 volume of DCM, 1 mmol of 2-bromoacetyl bromide was added at 0^{o}C. resultant reaction mixture was stirred at rt for 2 hrs. Following the completion of the reaction on TLC, The solid

reaction mass formed was filtered, washed with water and diethyl ether to get 2-bromo-N-(2-oxo-2H-chromen-3-yl)acetamide.

Preparation of N-(2-oxo-2H-chromen-3-yl)-2-(4-(phenylsulfonyl)piperazin-1-yl)acetamide **(compound 10h)**

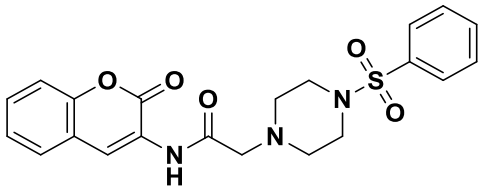

Mixture of 2-bromo-N-(2-oxo-2H-chromen-3-yl)acetamide 1mmol and 1-(phenylsulfonyl)piperazine 1mmol stirred in 10 volume of DMF in presence of 3mmol of TEA at rt. The resultant reaction mixture was stirred at rt for 16 hrs. After the reaction completion, consumption of starting materials was confirmed by TLC. After reaction completion, the reaction mixture was poured into ice cold water which formed white solid mass. The solid was filtered, washed with water and diethyl ether to give N-(2-oxo-2H-chromen-3-yl)-2-(4-(phenylsulfonyl)piperazin-1-yl)acetamide.

Similarly compound (**10a-g**) were prepared using this procedure as illustrated in **scheme 3**

3. Experimental data

N-(4-methyl-2-oxo-2H-chromen-7-yl)-2-(4-(phenylsulfonyl)piperazin-1-yl)acetamide (6a)

White brown solid, yield: 74%, mp: 150-158°C; FTIR (ATR, Vmax, cm-1): 3613, 2860, 1702, 1563, 1169, 740; ^{1}H NMR (400 MHz, $CDCl_3$) δ 10.083 (s, 1H), 7.74 (m, 4H), 7.69 (t, J = 6.5Hz, 3H), 7.54 (d, J=8.4Hz, 1H), 6.25 (s, 1H), 3.19 (s, 2H), 2.978 (s, 4H), 2.59 (s, 4H), 2.37 (s, 3H) ppm. ^{13}C NMR (125 MHz, $CDCl_3$) δ 169.29, 160.47, 153.95, 153.55, 142.34, 135.27, 133.78, 129.92, 128.06, 126.21, 116.05, 115.57, 112.7, 106.48, 61.54, 52.05, 46.15, 18.44 ppm. LCMS (m/z): $[M+H]^+$ Calculated for C22H23N3O5S is 442,14; Observed. = 441.85.

2-(4-((4-bromophenyl)sulfonyl)piperazin-1-yl)-N-(4-methyl-2-oxo-2H-chromen-7-yl)acetamide (6b)

White solid, yield: 68%, mp: 160-166°C; FTIR (ATR, Vmax, cm-1): 3430, 2836, 1723, 1572, 1173, 753; ^{1}H NMR (400 MHz, $CDCl_3$) δ 2.42(s, 3H), 2.75(t, J=4.71Hz, 4H), 3.16(s, 4H), 3.20(s, 2H), 5.32(s, 1H), 6.21(d, J=1.0Hz, 1H), 7.47(d, J=1.26Hz, 1H), 7.54-7.55(m, 1H), 7.6(d, J=8.7Hz, 2H), 7.76(d, J=8.5Hz, 2H), 8.92(s, 1H) ppm. ^{13}C NMR (125 MHz, $CDCl_3$) δ 177.72, 167.86, 156.88, 152.18, 139.4, 132.6, 129.2, 125.3, 113.8, 106.9, 106.9, 99.5, 52.6, 45.87, 18.62. LCMS (m/z): $[M+H]^+$ Calculated for C22H22BrN3O5S is 520,05; Observed. = 521.70.

2-(4-((4-fluorophenyl)sulfonyl)piperazin-1-yl)-N-(4-methyl-2-oxo-2H-chromen-7-yl)acetamide (6c)

White solid, yield: 58%, mp: 153-158; FTIR (ATR, Vmax, cm-1): 3390, 2852, 1695, 1512, 1174, 146; ^{1}H NMR (400 MHz, $CDCl_3$) δ 9.01 (s, 1H), 7.79 (s, 2H), 7.49 (s, 3H), 7.24 (t, J=8.0Hz, 2H), 6.12 (s, 1H), 3.19 (s, 2H), 3.13 (s, 4H), 2.72 (s, 4H), 2.37 (s, 3H) ppm. ^{13}C NMR (125 MHz, $CDCl_3$) δ 168.0, 166.02, 164.0, 160.8, 154.0, 152.3, 130.5, 130.4, 125.3, 116.7, 116.4, 115.5, 113.4, 106.9, 61.6, 52.5, 45.8, 18.6 ppm. LCMS (m/z): $[M+H]^+$ Calculated for C22H22FN3O5S is 460.13; Observed. = 446.00.

N-(4-methyl-2-oxo-2H-chromen-7-yl)-2-(4-((4-nitrophenyl)sulfonyl)piperazin-1-yl)acetamide (6d)

White solid, yield: 52%, mp: 152-158C; FTIR (ATR, Vmax, cm-1): 3259, 2835, 1723, 1572, 1348, 1173, 715; ^{1}H NMR (400 MHz, $CDCl_3$) δ 8.40 (d, J = 8.7 Hz, 2H), 7.95 (d, J = 8.8 Hz, 2H), 7.48 (m, 2H), 7.44 (d, J = 1.3 Hz, 1H), 6.16 (s, 1H), 3.17 (s, 5H), 2.74 (s, 5H), 2.37 (s, 3H) ppm. ^{13}C NMR (125 MHz, $CDCl_3$) δ 168.0, 161.3, 155.1, 154.1, 152.6, 151.5, 150.4, 141.82, 140.4 ,128.9, 125.4, 124.6, 116.4, 115.5, 113.5, 107.0, 61.57, 52.6, 45.8, 18.6 ppm. LCMS (m/z): $[M+H]^+$ Calculated for C22H22FN3O5S is 487.12; Observed. = 487.05.

2-(4-((4-chlorophenyl)sulfonyl)piperazin-1-yl)-N-(4-methyl-2-oxo-2H-chromen-7-yl)acetamide (6e)

White Solid yield: 82%, mp: 182-184°C; FTIR (ATR, Vmax, cm-1): 3275, 2854, 1719, 1511, 1346, 1163, 724;^{1}H NMR (400 MHz, DMSO) δ 2.36 (d, J=0.7, 3H), 2.6 (s, 4H), 2.98 (s, 4H), 3.20 (s, 2H),

6.23 (d, J=1.1Hz, 1H), 7.5 (dd, J=8.7Hz(long), J=2.0Hz (short), 1H), 7.66 (d, J=8.6Hz, 1H), 7.73-7.78 (m, 5H), 10.05 (s, 1H) ppm. ^{13}C NMR (125 MHz, $CDCl_3$) δ 169.2, 160.4, 153.8, 153.4, 142.2, 138.7, 134.1, 129.9, 126.1, 116.0, 115.0, 112.7, 106.4, 61.4, 52.0, 46.0, 18.4 ppm. LCMS (m/z): $[M+H]^+$ Calculated for C22H22ClN3O5S is 476,10; Observed. = 475.85

N-(4-methyl-2-oxo-2H-chromen-7-yl)-2-(4-tosylpiperazin-1-yl)acetamide (6f)

White solid yield: 80%, mp: 181-183°C; FTIR (ATR, Vmax, cm-1): 3308, 2855, 1702, 1522, 1345, 1168, 731; ^{1}H NMR (400 MHz, $CDCl_3$) δ 2.41 (s, 3H), 2.5 (s, 3H), 2.73 (t, J=4.6Hz, 4H), 3.1 (s, 4H), 3.19 (s, 2H), 7.34-7.41 (m, 3H), 7.52 (d, J=8.6Hz, 1H), 7.59-7.63 (m, 2H), 7.67 (d, J=8.1Hz, 2H), 8.97 (s, 1H) ppm. ^{13}C NMR (125 MHz, $CDCl_3$) δ 167.9, 160.9, 154.1, 152.1, 144.1, 140.4, 132.3, 129.9, 129.9, 127.8, 127.6, 125.4, 116.3, 115.4, 113.5, 106.8, 61.63, 52.6, 45.9, 21.6, 18.6 ppm. LCMS (m/z): $[M+H]^+$ Calculated for C22H23N3O5S is 456.15; Observed. = 455.85.

2-(4-(3-chlorophenyl)piperazin-1-yl)-N-(4-methyl-2-oxo-2H-chromen-7-yl)acetamide (6g)

White solid yield: 84%, mp: 173-180°C; FTIR (ATR, Vmax, cm-1): 3294, 2825, 1695, 1528, 1346, 1177, 758; ^{1}H NMR (400 MHz, $CDCl_3$) δ 2.42 (d, J=1.0, 3H), 2.81 (t, J=4.8Hz, 4H), 3.26 (s, 2H), 3.30 (t, J=4.8Hz, 4H), 6.21 (d, J=1.0Hz, 1H), 6.81-6.87 (m, 2H), 6.91 (t, J=2.0Hz, 1H), 7.20 (t, J=8.2Hz, 1H), 7.51-7.52 (m, 2H), 7.68 (d, J=1.6Hz, 1H), 9.36 (s, 1H) ppm. ^{13}C NMR (125 MHz, $CDCl_3$) δ 168.5, 160.9, 154.3, 152.1, 151.9, 140.6, 135.0, 130.1, 125.3, 119.8, 116.2, 116.0, 115.3, 114.2, 113.5, 106.9, 61.9, 53.3, 84.9, 18.6 ppm. LCMS (m/z): $[M+H]^+$ Calculated for C22H22ClN3O3 is 412.13; Observed. = 411.90.

2-(4-(2-methoxyphenyl)piperazin-1-yl)-N-(4-methyl-2-oxo-2H-chromen-7-yl)acetamide (6h)

White solid yield: 77%, mp: 175-179°C; FTIR (ATR, Vmax, cm-1): 3262, 2814, 1702, 1566, 1328, 1170, 743; ^{1}H NMR (400 MHz, $CDCl_3$) δ 2.40 (s, 3H), 2.85 (t, J=4.2Hz, 4H), 3.17 (s, 4H), 3.25 (s, 2H), 8.87 (s, 2H), 6.18 (s, 1H), 6.88-7.06 (m, 4H), 7.53(s, 2H), 7.69 (s, 2H), 9.48 (s, 1H) ppm. ^{13}C NMR (125 MHz, $CDCl_3$) δ 168.9, 160.9, 154.3, 152.2, 152.1, 140.8, 140.7, 125.2, 123.3, 121.0, 118.2, 116.1, 115.3, 113.4, 111.2, 106.9, 62.0, 55.4, 53.7, 50.8, 18.6 ppm. LCMS (m/z): $[M+H]^+$ Calculated for C23H25N3O4 is 408,18; Observed. = 407.90.

2-(4-(2-fluorophenyl)piperazin-1-yl)-N-(4-methyl-2-oxo-2H-chromen-7-yl)acetamide (6i)

White Solid yield: 81%, mp: 172-175°C; FTIR (ATR, Vmax, cm-1): 3532, 2842, 1723, 1521, 1343, 1152, 726; ^{1}H NMR (400 MHz, $CDCl_3$) δ 2.41 (s, 3H), 2.83 (s, 4H), 3.20 (s, 4H), 3.26 (s, 2H), 6.19 (s, 1H), 6.96-7.11 (m, 4H), 7.55 (s, 2H), 7.66 (s, 1H), 9.43 (s, 1H) ppm. ^{13}C NMR (125 MHz, $CDCl_3$) δ 168.7, 161.0, 156.9, 154.4, 154.2, 152.2, 140.7, 139.6, 139.5, 125.33, 124.5, 124.5, 122.9, 122.9, 119.0, 119.0, 116.3, 116.2, 116.1, 115.3, 113.4, 106.9, 62.0, 53.6, 50.6, 50.6, 18.63 ppm. LCMS (m/z): $[M+H]^+$ Calculated for C22H22FN3O3 is 396,16; Observed. = 396.50.

2-(4-(2-cyanophenyl)piperazin-1-yl)-N-(4-methyl-2-oxo-2H-chromen-7-yl)acetamide (6j)

White solid yield: 84%, mp: 160-165°C; FTIR (ATR, Vmax, cm-1): 3236, 2825, 1715, 1519, 1329, 1148, 762; ^{1}H NMR (400 MHz, $CDCl_3$) δ 2.4(d, J=1.1Hz, 3H), 2.88 (t, J=4.6Hz, 4H), 3.28 (s, 1H), 3.33 (t, J=4.4Hz, 4H), 6.2 (d, J=1.1Hz, 1H), 7.05-7.08 (m, 2H), 7.52-7.62 (m, 5H), 9.38 (s, 1H) ppm. ^{13}C NMR (125 MHz, $CDCl_3$) δ 168.5, 160.9, 155.2, 154.2, 152.2, 140.7, 134.4, 133.9, 125.3, 122.3, 118.8, 118.2, 116.2, 115.3, 113.4, 106.8, 106.3, 61.8, 53.5, 51.6, 18.6 ppm. LCMS (m/z): $[M+H]^+$ Calculated for C23H22N4O3 is 403,17; Observed. = 402.90.

2-(4-((4-bromophenyl)sulfonyl)piperazin-1-yl)-N-(2-oxo-2H-chromen-3-yl)acetamide (10a)

White solid yield: 62%, mp: 184-189°C; FTIR (ATR, Vmax, cm-1): 3420, 2822, 1722, 1511, 1355, 1145, 713;^{1}H NMR (400 MHz, $CDCl_3$) δ 2.73(t, J=4.7Hz, 4H), 3.20(s, 4H), 3.23(s, 2H), 7.32-7.34(m, 2H), 7.45-7.49(m, 1H), 7.51(dd, J=7.5Hz&J=1.3Hz, 1H), 7.64-7.67(m, 2H), 7.73(t, J=2.1Hz, 1H), 7.75(t, J=2.1Hz, 1H), 8.6(s, 1H), 9.5(s, 1H) ppm. ^{13}C NMR (125 MHz, $CDCl_3$) δ 45.91, 52.67, 61.70, 116.41, 119.64, 123.40, 123.75, 125.23, 127.82, 129.11, 129.89, 132.66, 134.90, 158.60, 168.99 ppm. LCMS (m/z): $[M-H]^+$ Calculated for C21H20BrN3O5S is 504,03; Observed. = 504.00. White Solid

2-(4-((4-fluorophenyl)sulfonyl)piperazin-1-yl)-N-(2-oxo-2H-chromen-3-yl)acetamide (10b)

White solid yield: 65%, mp: 178-182°C; FTIR (ATR, Vmax, cm-1): 3318, 2831, 1706, 1495, 1326, 1166, 727; ^{1}H NMR (400 MHz, $CDCl_3$) δ 2.73(t, J=4.71Hz, 4H), 3.18(s, 4H), 3.22(s, 2H), 7.24-7.32(m, 4H), 7.43-7.51(m, 2H), 7.79-7.83(m, 2H), 8.64(s, 1H), 9.56(s, 1H) ppm. ^{13}C NMR (125 MHz,

$CDCl_3$) δ 45.9, 52.6, 61.6, 116.3, 116.5, 116.7, 119.63, 123.40, 123.65, 125.22, 127.80, 129.86, 130.30, 130.39, 150.09, 158.57, 164.13, 166.67, 169.02 ppm. LCMS (m/z): $[M+H]^+$ Calculated for C21H20FN3O5S is 446,11; Observed. = 446.00.

2-(4-((4-chlorophenyl)sulfonyl)piperazin-1-yl)-N-(2-oxo-2H-chromen-3-yl)acetamide (10c)

White Solid yield: 75%, mp: 194-196°C; FTIR (ATR, Vmax, cm-1):3310, 2855, 1721, 1511, 1170, 760; ^{1}H NMR (400 MHz, $CDCl_3$) δ 2.73 (t, J=4.5Hz, 4H), 3.19 (s, 2H), 3.22 (s, 2H), 7.28-7.33 (m, 2H), 7.44-7.75 (m, 2H), 7.55-7.58 (m, 2H), 7.72 (d, J=8.5Hz, 2H), 8.64 (s, 1H), 9.55 (s, 1H) ppm. ^{13}C NMR (125 MHz, $CDCl_3$) δ 150.1, 139.8, 134.3, 129.8, 129.6, 129.0, 127.8, 125.2, 123.7, 123.4, 119.6, 116.3, 61.6, 52.6, 45.9 ppm. LCMS (m/z): $[M+H]^+$ Calculated for C21H20ClN3O5S is 442.14; Observed. = 441.90.

2-(4-(3-chlorophenyl)piperazin-1-yl)-N-(2-oxo-2H-chromen-3-yl)acetamide (10d)

White solid yield: 69%, mp: 175-181°C; FTIR (ATR, Vmax, cm-1): 3305, 2828, 1716, 1506, 1176, 765; ^{1}H NMR (400 MHz, $CDCl_3$) δ 2.79 (t, J=4.7Hz, 4H), 3.27 (s, 2H), 3.33 (t, J=4.8Hz, 4H), 6.80-6.85 (m, 2H), 6.91 (t, J=4.0Hz, 1H), 7.1 (t, J=8.1Hz, 1H), 7.28-7.37(m, 2H), 7.44-7.49 (m, 1H), 7.51-7.54 (m ,1H), 8.69 (s, 1H), 9.95 (s, 1H) ppm. ^{13}C NMR (125 MHz, $CDCl_3$) δ 169.7, 158.5, 152.0, 150.1, 134.9, 130.2, 130.0, 129.7, 128.0, 127.7, 125.3, 125.1, 124.1, 123.6, 123.3, 119.7, 119.6, 119.4, 116.12, 114.1, 61.88, 53.3, 48.9 ppm. LCMS (m/z): $[M+H]^+$ Calculated for C21H20ClN3O3 is 398,12; Observed. = 397.90.

2-(4-(2-fluorophenyl)piperazin-1-yl)-N-(2-oxo-2H-chromen-3-yl)acetamide (10e)

White solid yield: 79%, mp: 177-183°C; FTIR (ATR, Vmax, cm-1): 3306, 2821, 1720, 1517, 1177, 776; ^{1}H NMR (400 MHz, $CDCl_3$) δ 2.83 (t, J=4.6Hz, 4H), 3.24 (t, J=4.4Hz, 4H), 3.28 (s, 2H), 6.94-6.11 (m, 4H), 7.28-7.35 (m, 2H(, 7.43-7.47 (m, 1H), 7.51 (dd, J=3.7Hz (long), J=1.1Hz(short), 1H), 8.7 (s, 1H), 10.0 (s, 1H) ppm. ^{13}C NMR (125 MHz, $CDCl_3$) δ 179.9, 158.5, 156.9, 154.4, 150.1, 139.8, 139.7, 129.6, 127.7, 125.1, 124.5, 124.5, 123.7, 123.2, 122.7, 122.7, 119.8, 119.1, 119.1, 116.3, 116.2, 116.0, 61.9, 53.6, 50.6, 50.6 ppm. LCMS (m/z): $[M+H]^+$ Calculated for C21H20FN3O3 is 382,15; Observed. = 382.25.

2-(4-(2-cyanophenyl)piperazin-1-yl)-N-(2-oxo-2H-chromen-3-yl)acetamide (10f)

White solid yield: 74%, mp: 175-182°C; FTIR (ATR, Vmax, cm-1):3435, 2848, 1702, 1495, 1141, 759. ^{1}H NMR (400 MHz, $CDCl_3$) δ 2.87 (t, J=4.6Hz, 4H), 3.30 (s, 2H), 3.35(t, J=4.3Hz, 4H), 7.03-7.09 (m, 2H), 7.28-7.35 (m, 2H), 7.44-7.48 (m, 2H), 7.52 (t, J=7.1Hz, 2H), 7.57 (dd, J=3.75Hz(long), J=1.1Hz (short), 1H), 8.70 (s, 1H), 9.99(s, 1H) ppm. ^{13}C NMR (125 MHz, $CDCl_3$) δ 169.8, 158.6, 145.4, 150.1, 134.3, 133.9, 129.6, 127.7, 125.1, 123.7, 123.3, 122.2, 119.8, 119.0, 118.3, 116.3, 106.3, 61.7, 53.4, 51.7 ppm. LCMS (m/z): $[M+H]^+$ Calculated for C22H20N4O3 is 389.15; Observed. = 389.05.

2-(4-(2-methoxyphenyl)piperazin-1-yl)-N-(2-oxo-2H-chromen-3-yl)acetamide (10g)

White solid yield: 75%, mp: 163-170°C; FTIR (ATR, Vmax, cm-1):3433, 2846, 1716, 1506, 1240, 750; ^{1}H NMR (400 MHz, $CDCl_3$) δ 2.84(s, 4H), 3.21(s, 4H), 3.27(s, 2H), 3.87 (s, 3H), 6.87 (d, J=3.9Hz, 1H), 6.95(t, J=7.2Hz, 1H), 7.00-7.04 (m, 2H), 7.28-7.24 (m, 2H), 7.42-7.46 (m, 1H), 7.50 (d, J=2.4Hz, 1H), 8.69 (s, 1H), 10.02 (s, 1H) ppm. ^{13}C NMR (125 MHz, $CDCl_3$) δ 170.2, 158.5, 152.1, 150.1, 129.6, 127.7, 125.0, 123.8, 129.2, 123.2, 121.0, 119.8, 118.4, 116.3, 111.15, 62.0, 55.39, 53.7, 50.74 ppm. LCMS (m/z): $[M+H]^+$ Calculated for C22H23N3O4 is 394,17; Observed. = 394.50.

N-(2-oxo-2H-chromen-3-yl)-2-(4-(phenylsulfonyl)piperazin-1-yl)acetamide (10h)

White Solid yield: 78%, mp: 142-146°C; FTIR (ATR, Vmax, cm-1):3231, 2894, 1718, 1514, 1168, 876, 740; ^{1}H NMR (400 MHz, $CDCl_3$) δ = 9.57 (s, 1H), 7.79 (d, J=7.4 Hz, 3H), 7.71 (t, J = 7.6Hz, 3H), 7.50 (t, J=7.7Hz, 1H), 7.40-7.32 (m, 2H), 3.24 (s, 2H), 2.97 (s, 4H), 2.65 (s, 4H) ppm. ^{13}C NMR (125 MHz, $CDCl_3$) δ 169.99, 158.18, 150.04, 135.11, 133.91, 130.18, 129.96, 128.36, 128.02, 125.54, 124.12, 122.80, 119.89, 116.41 ppm. LCMS (m/z): $[M+H]^+$ Calculated for C21H21N3O5S is 428,12; Observed. = 428.35.

4. Conclusion

In conclusion, we have successfully synthesised and characterised a small library of novel hybrid molecules using various spectroscopic techniques. (FT-IR, mass and NMR). In addition, the anti-mycobacterial activity of all newly synthesised compounds against the M. tuberculosis H37 Rv strain

was evaluated *in vitro*. Based on a comprehensive examination of the experimental data, it was possible to conclude that the hybrid molecules possessed less anti-tubercular activity. Moreover, additional modifications are required to increase the activity to develop efficient anti-tubercular agents against the parental and drug-resistant strains of tuberculosis.

5. Acknowledgement

The authors are thankful to the Discipline of Pharmaceutical Sciences, College of Health Sciences, University of Kwa-Zulu Natal (UKZN), Durban, South Africa, and The M.S. University of Baroda, Vadodara, India and Institute of Translational Health Science and Technology,Faridabad, India for providing all the necessary facilities. R.K. gratefully acknowledges National Research Foundation-South Africa for funding this project (Grant Nos.103728 and 112079). The biological activities (anti mycobacterial and anti microbial activities) are not performed by student.

6. Conflict of interest

Authors hereby declare that there are no financial/commercial conflicts of interest.

References

[1] Bitla, S., Gayatri, A.A., Puchakayala, M.R., Bhukya, V.K., Vannada, J., Dhanavath, R., Kuthati, B., Kothula, D., Sagurthi, S.R. and Atcha, K.R., 2021. Design and synthesis, biological evaluation of bis-(1, 2, 3-and 1, 2, 4)-triazole derivatives as potential antimicrobial and antifungal agents. Bioorganic & Medicinal Chemistry Letters, 41, p.128004.

[2] Prestinaci, F., Pezzotti, P. and Pantosti, A., 2015. Antimicrobial resistance: a global multifaceted phenomenon. Pathogens and global health, 109(7), pp.309-318.

[3] Moraski, G.C., Markley, L.D., Chang, M., Cho, S., Franzblau, S.G., Hwang, C.H., Boshoff, H. and Miller, M.J., 2012. Generation and exploration of new classes of antitubercular agents: The optimization of oxazolines, oxazoles, thiazolines, thiazoles to imidazo [1, 2-a] pyridines and isomeric 5, 6-fused scaffolds. Bioorganic & medicinal chemistry, 20(7), pp.2214-2220.

[4] Moraski, G.C., Chang, M., Villegas-Estrada, A., Franzblau, S.G., Möllmann, U. and Miller, M.J., 2010. Structure–activity relationship of new anti-tuberculosis agents derived from oxazoline and oxazole benzyl esters. European journal of medicinal chemistry, 45(5), pp.1703-1716.

[5] Shah, S.R. and Katariya, K.D., 2020. 1, 3-Oxazole-isoniazid hybrids: Synthesis, antitubercular activity, and their docking studies. Journal of Heterocyclic Chemistry, 57(4), pp.1682-1691.

[6] Venugopala, K.N., Rashmi, V. and Odhav, B., 2013. Review on natural coumarin lead compounds for their pharmacological activity. BioMed research international, 2013.

[7] Patel, D., Kumari, P. and Patel, N., 2012. Synthesis of 3-{4-[4-dimethylamino-6-(4-methyl-2-oxo-2 H-chromen-7-yloxy)-[1, 3, 5] triazin-2-ylamino]-phenyl}-2-phenyl-5- (4-pyridin-2-yl-piperazin-1-ylmethyl)-thiazolidin-4-one and their biological evaluation. Medicinal Chemistry Research, 21, pp.2926-2944.

[8] Ostrowska, K., 2020. Coumarin-piperazine derivatives as biologically active compounds. Saudi Pharmaceutical Journal, 28(2), pp.220-232.

[9] Patel, D., Kumari, P. and Patel, N., 2012. Synthesis of 3-{4-[4-dimethylamino-6-(4-methyl-2-oxo-2 H-chromen-7-yloxy)-[1, 3, 5] triazin-2-ylamino]-phenyl}-2-phenyl-5- (4-pyridin-2-yl-piperazin-1-ylmethyl)-thiazolidin-4-one and their biological evaluation. Medicinal Chemistry Research, 21, pp.2926-2944.

[10] P Lakum, H., R Shah, D. and H Chikhalia, K., 2015. The novel derivatives of 3-(iminomethyl)-2H-chromen-2-one with thiourea and piperazine structural motive: Rationale, synthesis, antimicrobial and anti-TB evaluation. Letters in Drug Design & Discovery, 12(4), pp.324-341.

[11] Akbar, A., McNeil, N.M., Albert, M.R., Ta, V., Adhikary, G., Bourgeois, K., Eckert, R.L. and Keillor, J.W., 2017. Structure–activity relationships of potent, targeted covalent

inhibitors that abolish both the transamidation and GTP binding activities of human tissue transglutaminase. Journal of medicinal chemistry, 60(18), pp.7910-7927.

[12] Pozdnev, V.F., 1990. Improved method for synthesis of 7-amino-4-methylcoumarin. Chemistry of Heterocyclic Compounds, 26(3), pp.264-265.

[13] Durgapal, S.D., Soni, R., Umar, S., Suresh, B. and Soman, S.S., 2017. Anticancer Activity and DNA Binding Studies of Novel 3, 7-Disubstituted Benzopyrones. ChemistrySelect, 2(1), pp.147-153.

[14] Thamban Chandrika, N., Shrestha, S.K., Ngo, H.X., Tsodikov, O.V., Howard, K.C. and Garneau-Tsodikova, S., 2018. Alkylated piperazines and piperazine-azole hybrids as antifungal agents. Journal of Medicinal Chemistry, 61(1), pp.158-173.

[15] Durgapal, S.D., Soni, R., Soman, S.S. and Prajapati, A.K., 2020. Synthesis and mesomorphic properties of coumarin derivatives with chalcone and imine linkages. Journal of Molecular Liquids, 297, p.111920.

[16] Meena, C.L., Singh, P., Shaliwal, R.P., Kumar, V., Kumar, A., Tiwari, A.K., Asthana, S., Singh, R. and Mahajan, D., 2020. Synthesis and evaluation of thiophene based small molecules as potent inhibitors of Mycobacterium tuberculosis. European Journal of Medicinal Chemistry, 208, p.112772.

[17] Govender, H., Mocktar, C. and Koorbanally, N.A., 2018. Synthesis and Bioactivity of Quinoline-3-carboxamide Derivatives. Journal of Heterocyclic Chemistry, 55(4), pp.1002-1009.

[18] S Aremu, O., Gopaul, K., Kadam, P., Singh, M., Mocktar, C., Singh, P. and A Koorbanally, N., 2017. Synthesis, characterization, anticancer and antibacterial activity of some novel pyrano [2, 3-d] pyrimidinone carbonitrile derivatives. Anti-Cancer Agents in Medicinal Chemistry (Formerly Current Medicinal Chemistry-Anti-Cancer Agents), 17(5), pp.719-725.

Chapter 6

Facile Synthesis of Amides Through TransamidationWith Iodine Under Neat Conditions

Published: Published in chemistry select (DOI: 10.1002/slct.202103237)

Graphical Abstract

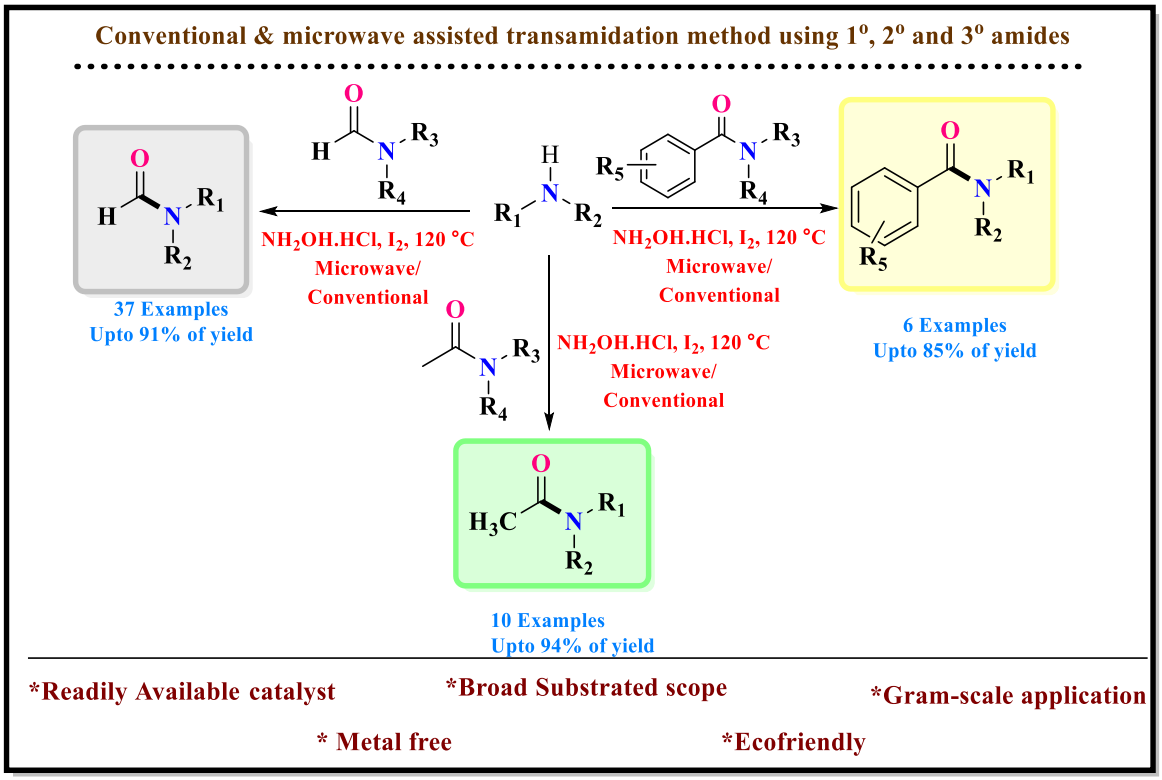

Abstract

Iodine and $NH_2OH.HCl$ mediated transamidation of unactivated amides with a variety of amines under thermal/microwave irradiations have been presented in this chapter. The current strategy is effective for a wide variety of primary, secondary, and tertiary amides and allows formylation, acylation, and benzoylation of various amines. The primary advantages of the current protocol are simple, rapid, absence of metal catalyst, low-cost starting material as a solvent, and low environmental impact during the synthesis process.

Introduction

The amide bonds are a significant functional group in both industrial and medicinal chemistry[1,2]. Due to the inert nature of the amide bond, the development of an easy and effective transamidation technique has garnered considerable attention[3]. Transamidation is a versatile and important strategy for the preparation of several natural products[4], proteins[5], peptides[6], alkaloids[7,8], pharmaceutical agents[9], polymers[10,11], pesticides[12], etc. As a result, tremendous effort has been expended on developing synthetic procedures to synthesize diversified amides. Numerous groups, including our own, have since conducted an extensive study to improve their strategies' efficiency[13–21].

The utilization of metal catalysts to generate amides from various starting materials has a particular area of interest for the various research groups. Ni(II) metal complex[22], $Ni(quin)_2$[23], has recognized as a highly efficient catalyst for the *N*-formylation and *N*-acylation of aromatic, aliphatic, and heterocyclic amines. Gong and co-workers have also reported the transamidation reaction, using 15 mol% Cobalt (II) at 150^{o}C temperature[24]. Along with metal catalysts, the non-metal catalysts have also been successfully catalyzedamidation transformations, with ammonium carbonate[25] and related compounds acting as the most prominent example. Krishnamurthy and co-workers have reported a new amide bond formation between hydroxamic acids and amines[26].

We have modified a new transamidation method under conventional heating and microwave radiation that utilizes the $NH_2OH.HCl$ and catalytic iodine with a shorter reaction time and a broad scope. In the current study, primary (1^o), secondary (2^o), and tertiary (3^o) unactivated formamides, acetamide and benzamide derivatives were well tolerated and provided the desired products in good to excellent yields. Additionally, we conducted a comparison of conventional and microwave-assisted reactions.

Results and Discussion

The optimization of the reaction was explored through the conventional method using ideal substrates *o*-anisidine (**1e**) 1.0 mmol, DMF (**2c)** (5.0 V)and 0.5 equivalent (equiv.) of I_2 during optimization study **Figure 1**. Initially, the transamidation potential was investigated using different solvents, and

the results indicated that solvent selection had a stronger effect on the yield of the desired product. The reaction performed in water and DMF afforded the desired product in 85% and 93% yield (**Graph 1**), respectively. The reactions were conducted in DMSO to determine the solvent impact; **3e** was produced in trace amounts. We finalized amide (**2c)** as reactant and solvent from these results, so all the optimization studies were performed under neat conditions. When **2c** amount was reduced from 5.0 to 3.0 equiv., the product was obtained in 92% yield. Whereas reducing **2c** by 2.0 to 1.0 vol. significantly decreased the yield of **3e**, this could be possible if this volume was insufficient for proper stirring (**Graph 2**). As a result, we fixed 3.0 vol. of **2c** for the following optimization of reaction. Further, reducing equivs. of $NH_2OH.HCl$ from 1.0 equiv. to 0.5 equiv. resulted in a significant reduction in yield (57% **Graph 3**). Whereas, the increase in its use up to 2.0 equiv. did not provide the further improvement in yield (89%). Thus, the use of 1.0 equiv. of reagent results in the best reaction outcome (92% **Graph 3**). When the reaction temperature was reduced to 100^{o} C, a reduced yield (27%) of **3e** was observed (**Graph-4**). Additionally, time played a crucial role in reaction completion; reducing reaction time to 1.0 h resulted in a decline in yield of **3e** to 61% (**Graph-5**).

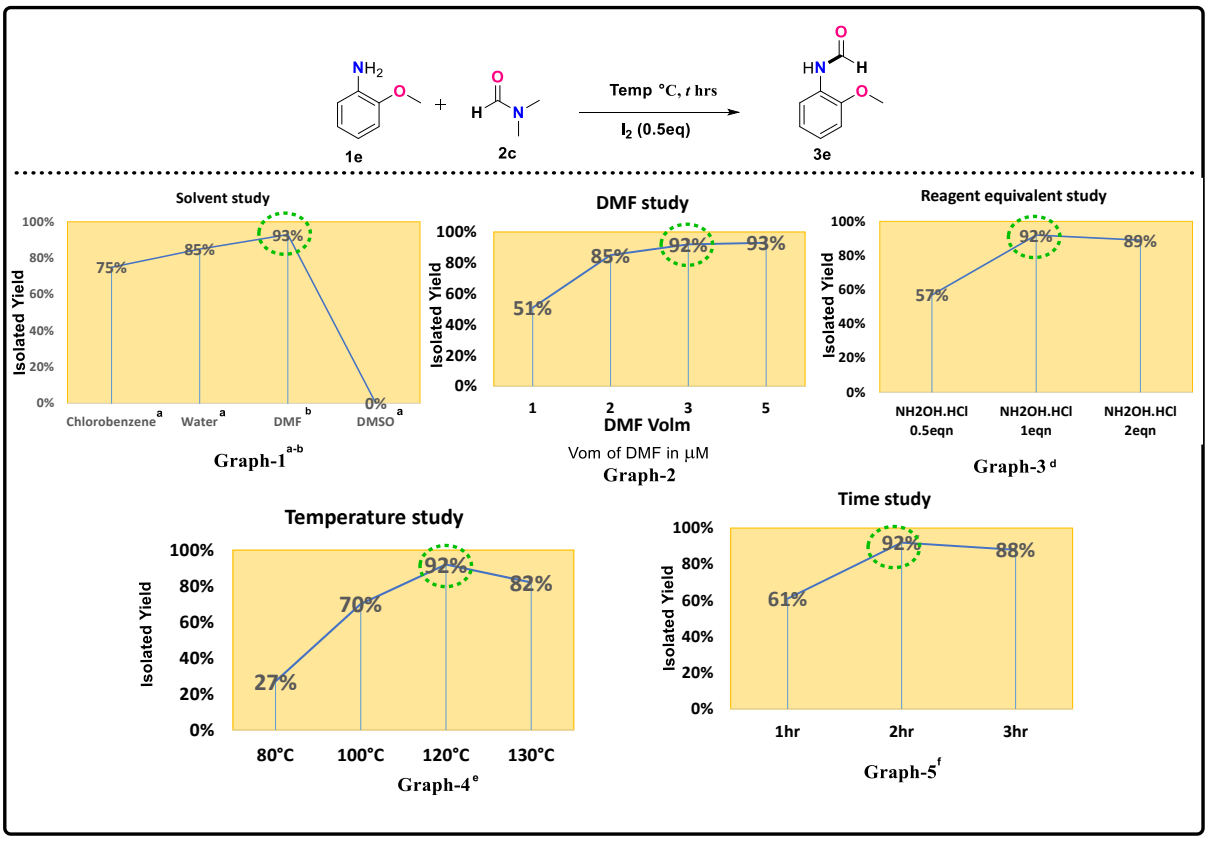

Figure 1 Graphical representation of reaction optimizations.

[a]Conditions: *o*-anisidine **1e** 1.0 mmol, formamide **2c** (3.0 vol.), $NH_2OH.HCl$ = 1.0 equiv, Temp = 120 ^oC, Time = 2.0 hr, Solvent = 5.0 vol (Supporting information; Table 1; Entry = 1-2 & 4); [b]Conditions: *o*-anisidine **1e** 1.0 mmol, formamide **2c** (5.0 vol.) (Supporting information; Table 1; Entry = 3), $NH_2OH.HCl$ = 1.0 equiv, Temp = 120 ^oC, Time = 2.0 hrs, [c]Conditions: *o*-anisidine **1e** 1.0 mmol, formamide **2c** (1.0-5.0 vol.) (Supporting information; Table 1; Entry = 5-8), $NH_2OH.HCl$ = 1.0 equiv, Temp = 120 ^oC, Time = 2.0 hrs; [d]Conditions: *o*-anisidine **1e** 1.0 mmol, formamide **2c** 3.0 vol., $NH_2OH.HCl$ = 1.0 equiv(Supporting information; Table 1; Entry = 9-11), Temp = 120 ^oC, Time = 2.0 hrs; [e]Conditions: *o*-anisidine **1e** 1.0 mmol, formamide **2c** 3.0 vol., $NH_2OH.HCl$ = 1.0 equiv, Temp = 80-130 ^oC (Supporting information; Table 1; Entry = 12-15), Time = 2.0 hrs; [f]Conditions: *o*-anisidine **1e** 1.0 mmol, formamide **2c** 3.0 vol., $NH_2OH.HCl$ = 1.0 equiv, Temp = 120 ^oC, Time = 1-3 hrs (Supporting information; Table 1; Entry = 16-18).

Based on the above-optimized reaction condition, we studied the *N*-formylation of diversified amines. In order to explore the flexibility and the scope of protocol, we allowed reacting a variety of substituted aromatic (**1a-1ae**), hetero aromatic (**1ah-ai**), aliphatic amines (**1aj-ak**), and 2^o amines (**3af-3ag**) with **2c** under optimal conditions (**Scheme 1**). It's worth noting that the anilines with electron-donating groups such as hydroxyl (-OH), and methoxy ($-OCH_3$) provided an excellent yield **(**88-91%, **3b-f)** of desired compounds. However, similar products (**3d** and **3f)** were also generated in high yields (88-91%) after microwave irradiation (150W) at 120°C for 40 minutes. Remarkably, the *ortho*-substitutedhydroxyl and methoxy groups have shown comparatively more yield than *meta* and *para* derivatives (91% and 90%, **3b** and **3e**). Additionally, we compared the reactivity of anisidine and thio-anisidine (**3g**, 69%) and resulted demonstrated that *p*-thio anisidine (**3g**, 69%) yielded a lower *N*-formylated product than *p*-anisidine (**3f**, 88%). However, in the presence of a strong electron-withdrawing group, *viz*: *o*-nitro aniline, we obtained poor yield for **3i** (38%), and on the other hand, p-nitro anilines were failed to show corresponding *N*-formylation (**3h** and **3j**). Interestingly, substrates containing a keto group also reacted efficiently and provided good yield for **3u** and **3v** (64% and 73%). However, Moderate yields were obtained when acid and ester substituted anilines were used as a substrate. (61% and 49%, **3w** and **3x**). The halogen-substituted anilines (I, Cl, Br, F) have shown good compatibility and provided moderate to an excellent yield of corresponding *N*-formylated products (44-85%, **3k-r**), respectively.

Further, we attempted poly-substituted anilines, the 2,6 dibromo-4-methyl aniline **3z** shown traces of product obviously due to electronic impact at the *ortho* position of aniline. The compounds with *ortho* and *para* di-substituted anilines (**3y, 3aa,3ab** and **3ac**) shown the reaction compatibility toward the *N*-formylation with 60%, 78%, 75% and 81% of respective yield. The *meta* and *para* di-substituted anilines have shown good to a moderate yield of the desired product (84% and 53%, **3ad** and **3ae**). The 2^o anilines *viz*:*N*,*N*-diphenyl amine (**3ag)** yielded 28% of the desired product, whereas *N*-methyl aniline (**3af)** produced 52% of the product which demonstrated the steric hindrance caused by the bulky group. Following aromatic amines, we explored hetero aromatic amines, and isolated yield demonstrated the flexibility of this method (38% and 55%, **3ah** and **3ai**). Finally, we

investigated aliphatic and heterocyclic amines, and the experimental results demonstrated their compatibility with this method.

Scheme 1[c]: $NH_2OH.HCl$-promoted transamidation of N,N-dimethylforamide (**2c**) with amines: scope of amines.

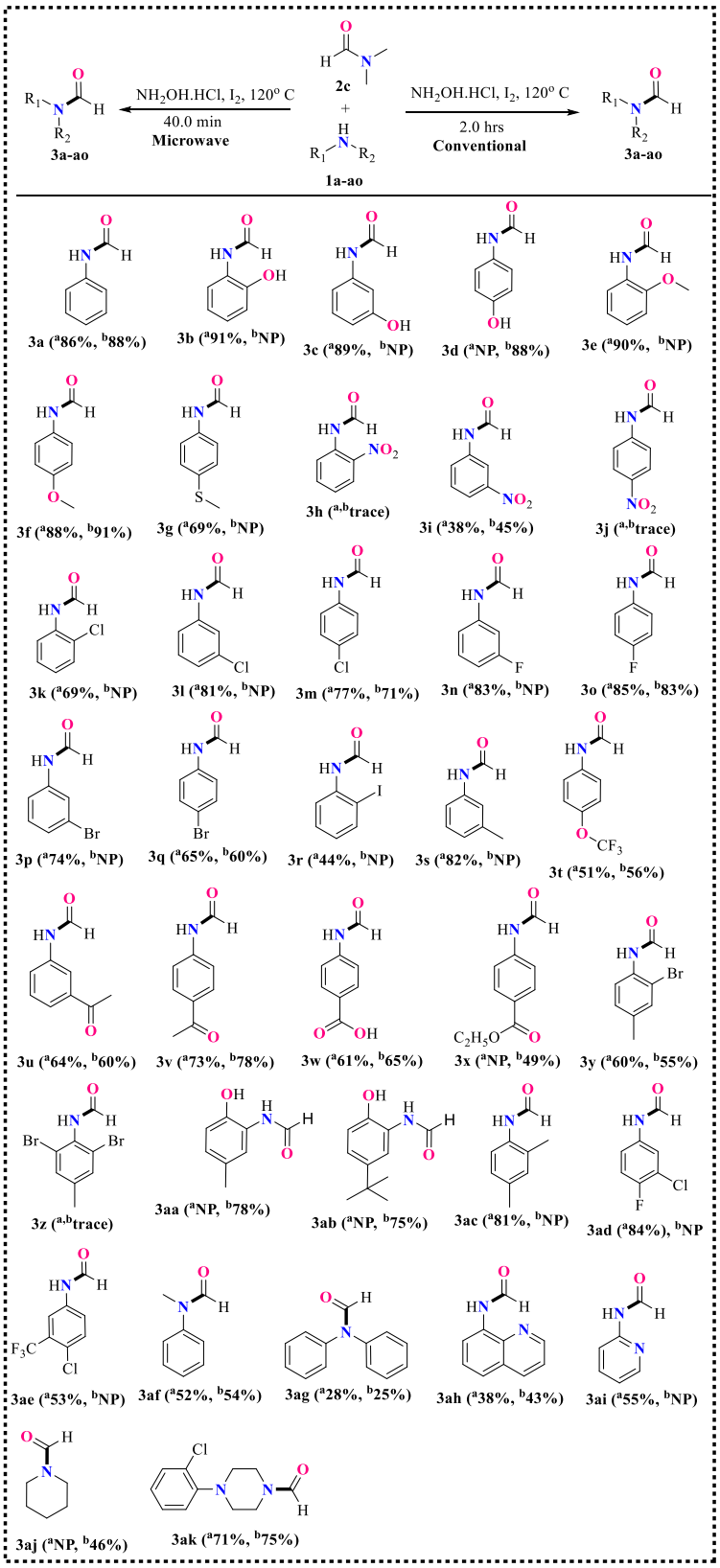

[a]Conventional method isolated yield, [b]Microwave method isolated yield, [c]All the reactions were conducted on a 1.0 mmol scale of amine, 3.0 mmol of amide, 1.0 mmol of $NH_2OH.HCl$, 0.5 mmol of I_2 under air for 2.0 hrs., using neat conditions, **NP**: Not performed.

After determining the formylation scope further, we evaluated the acylation and benzoylation of amines as illustrated in **scheme 2**. We successfully performed *N*-acylation of various substituted anilines (**1A-J, Scheme 2**) on treating them with simple *N*-*N*-dimethyl acetamide (**2f**)in **Scheme 2**. The acylation of *o*-methoxy aniline (**3C**) produced 94% of the required product, whereas the *o*-amino phenol produced 89% of the desired product (**3B**). The *m*-nitro aniline transformed to corresponding product (**3D**) in poor 32% yield under both thermal/microwave conditions. Among the *ortho* and *para*chloro anilines, the reactivity of *ortho* substituent is lower than *para* derivatives (58% and 73%, **3E** and **3F**). The electron-withdrawing halo alkyl and halo alkoxy group substituted aniline derivatives also tolerated acylation under our method (62%and 45%, **3G** and **3H**). The compatibility of *N*-methyl aromatic 2^o amine (**3I**) and *N*-benzyl piperazine (**3J**) has also been proven. Consequently, we presented some of the benzoylated derivatives; we treated different amines (**1K-P**) with *N*,*N*-dimethyl benzamide (**2j**) and isolated corresponding benzoylated compounds with moderate to good yield (**Scheme-2**). The *para* anisidine derivatives showed a better conversion its *ortho* derivative (85% and 90%, **3K** and **3L**). The chloro substituted aniline produced good yield of the final product (73%, **3M**). The electron-deficient tri-fluoro methyl ($-CF_3$) substituted aniline comfortably allowed benzoylation using this method (45%, **3N**). Interestingly, we also established its compatibility with 2^o aniline and aliphatic amine (58% and 60%, **3O** and **3P**).

Scheme 2[c]: $NH_2OH.HCl$-promoted transamidation of N,N-dimethyl acetamide (2f) and N,N-dimethyl benzamide (2j) with diversified amines (1A-S):

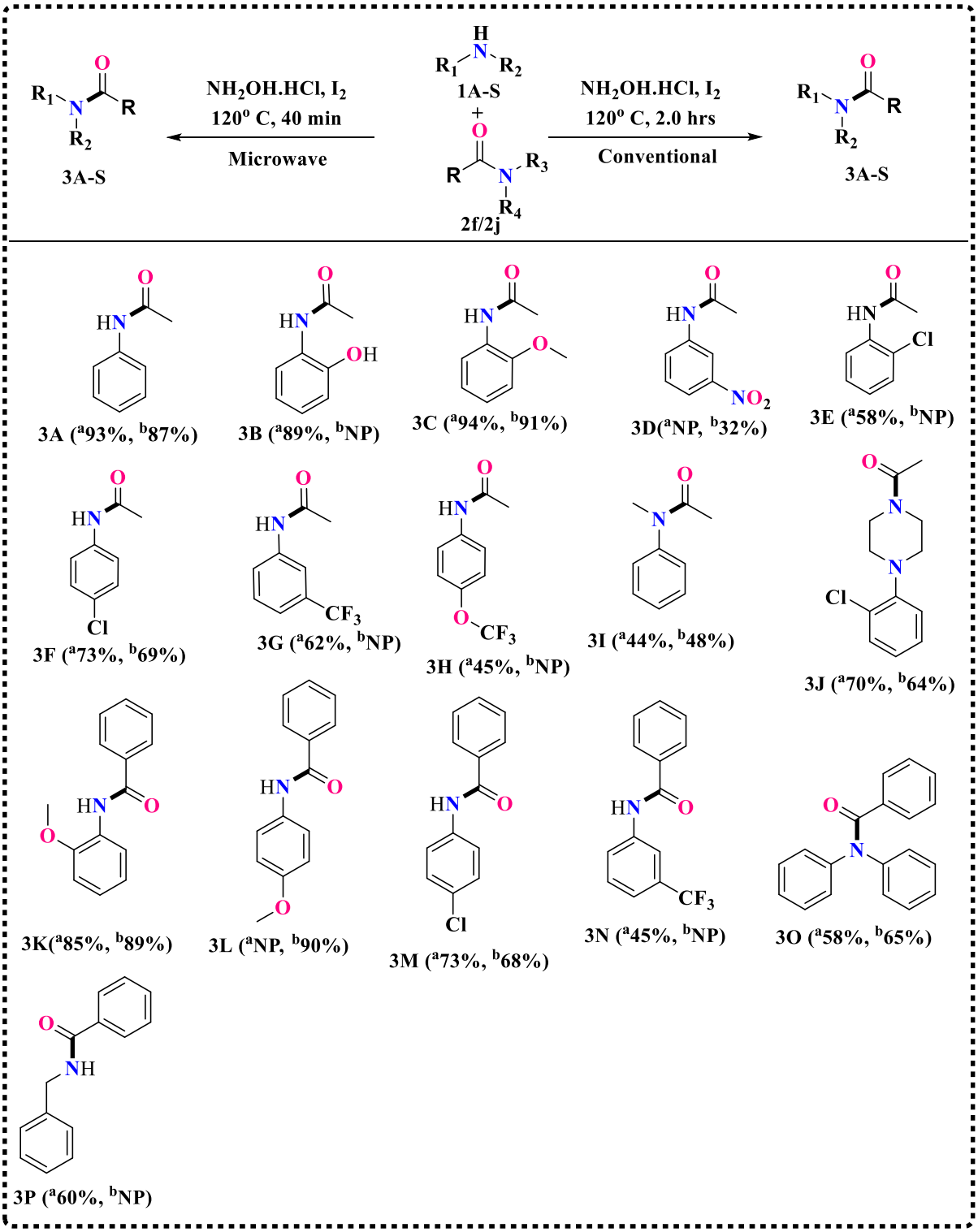

[a]Conventional method isolated yield, [b]Microwave method isolated yield, [c]All the reactions were conducted on a 1.0 mmol scale of amine, 3.0 mmol of amide, 1.0 mmol of $NH_2OH.HCl$, 0.5 mmol of I_2 under air for 2.0 hrs., using neat conditions, **NP**: Not performed.

Table 1 describes the scope of different substituted amides. Overall study concluded that reactivity of furamide (entry **1**, **4** and **9**) is better than acetamides and benzamide derivatives. In case of amides the, increase in substituents on amine group reduces the product yield (entry **4-8**)

Table 1: The substrate scope of **1a** with diversified amides (**2a-j**).

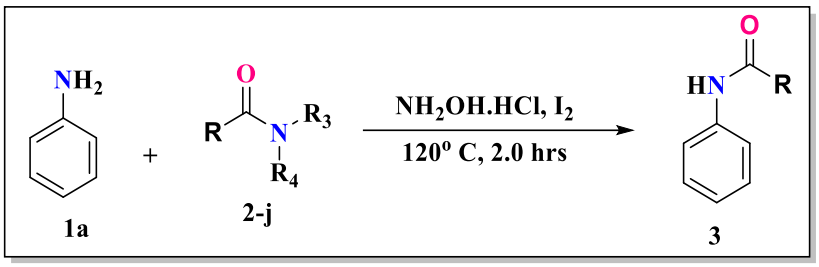

S.No.[a]	Amide	Product	Isolated yield (%)
1	 **2a**	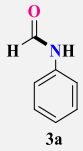 **3a**	94%
2	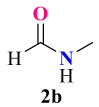 **2b**	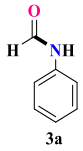 **3a**	91%
3	 **2c**	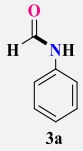 **3a**	90%
4	 **2d**	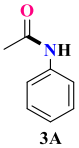 **3A**	89%

5	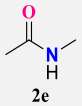 **2e**	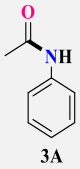 **3A**	74%
6	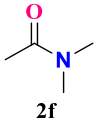 **2f**	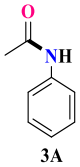 **3A**	71%
7	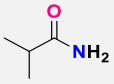 2g	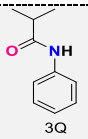 3Q	62%
8	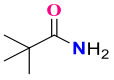 **2h**	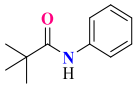 **3R**	54%
9	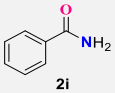 **2i**	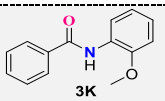 **3K**	80%
10	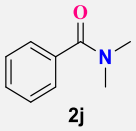 **2j**	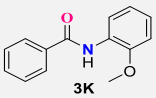 **3K**	85%

[a] All reactions were performed on a 1.0 mmol scale of **1a**, 3.0 equiv. of different amides (**2a-j**), under air for 2.0 hrs., using neat conditions

The gram-scale reaction of *o*-anisidine (**1e**) and **2c** were carried out utilizing the 1.0 equiv. of $NH_2OH.HCl$ as a catalyst on conventional heating **Scheme 3[A]**, provided an excellent yield of 93%, respectively. A competition experiment was also conducted to determine the reaction's selectivity, and the results reveal that the reactivity of an amine is greater than that of the hydroxyl group, resulting in the formation of the selective transamidation product **Scheme 3[B]**. After this success, to demonstrate the role of hydroxyl amine hydrochloride salt, further investigations were conducted using triethyl amine hydrochloride salt using similar reaction conditions and the results are reported in **Scheme 3[C].**

Scheme 3: **(A):** Conversion of **o**-anisidine **1e** on a gram scale; (**B**): Chemoselectivityof N-formylation reaction; (**C**):Reaction with TEA.HCl salt.

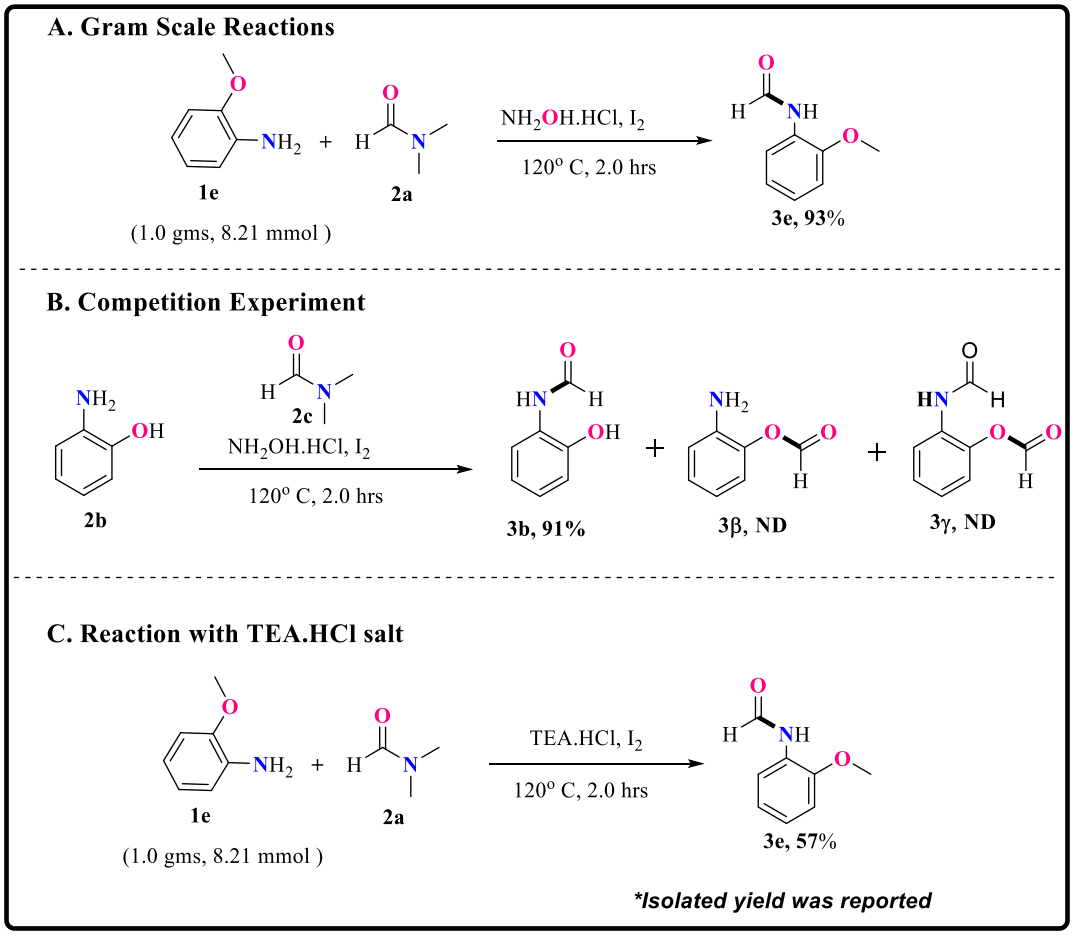

Scheme 3: Control experiment

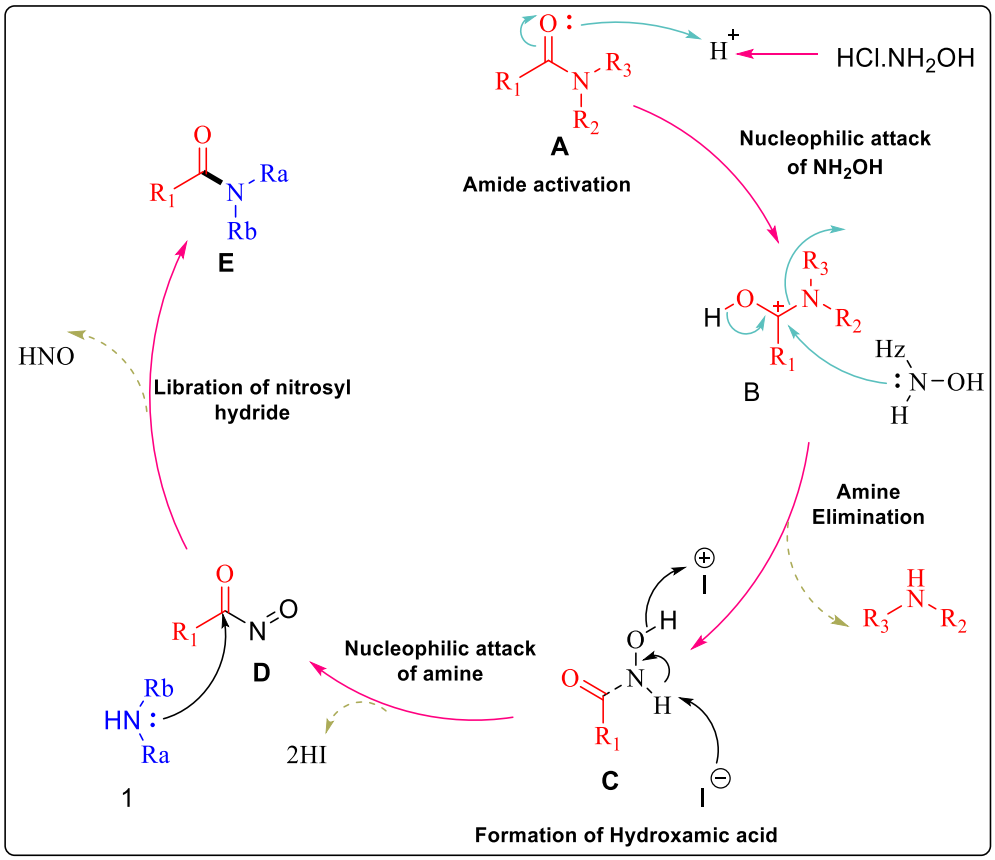

Scheme 4: The plausible mechanism for transamidation reaction.

Based upon the previously reported protocols the plausible mechanism for transamidation is depicted in **Scheme 4**. Firstly, amide **A** was activated[27] by hydroxylamine hydrochloride salt afforded intermediate **B,** which then converted in to intermediate **C** on nucleophilic attack of hydroxyl amine[26]. Iodine helps removal of 2H from intermediate **C** to produces acyl nitroso intermediate **D.** The nucleophilic attack of amine on intermediate **D**, leads the final amide product **E.**

Experimental Section

All the chemicals were purchased from Sigma Aldrich Chemical Co., and Alfa Aesar suppliers, which were used without further purification. The majority of reactions were performed out under regular operating conditions. Lab reagent (LR) grade solvents were used for extraction and chromatographic columns purchased from Roma-chem. The reaction progress was monitored on Merck TLC Silica gel 60 F254 plates, TLC plates visualized under ultraviolet (UV) light, followed by iodine or ninhydrin staining solution.

^{1}H, ^{13}C, and ^{19}F Nuclear magnetic resonance (NMR) spectra were recorded on 400, 100, 377 MHz NMR instruments using $CDCl_3$ and DMSO-d6 as solvents unless otherwise stated. Chemical shifts were expressed in parts per million (ppm) with respect to TMS used as an internal standard. Unless otherwise specified, all reagents were weighed and handled in air.

Synthesis of *N*-formylation of amines

As shown in scheme **1**, **2** and **3**, a mixture of amine 1 (1.0 equiv), amide 2 (3.0 vol.), I_2 (0.5 equiv), and $NH_2OH.HCl$ (1.0 equiv) was stirred in a 20.0 mL sealed vial under atmospheric air at 120 °C for 2.0 hrs. After bringing the mixture to room temperature, the reaction mixture and 10 mL of 5% bicarbonate solution was added into a separating funnel, the resultant mixture was extracted with ethyl acetate (3 X 20 mL). The combined organic layers were dried with anhydrous Na_2SO_4. Under vacuum, the solvent was evaporated, and the crude product was purified using column chromatography (silica gel, EtOAc/Hexane) in order to obtain a pure product.

General Experimental Procedure (**GEP-1**)

***N*-formylation of amines:**

A mixture of amine **1** (1.0 equiv), amide **2** (3.0 Vol), I_2 (0.5 equiv), and $NH_2OH.HCl$ (1.0 equiv) was stirred in a 20.0 ml sealed vial under atmospheric air at 120 °C for 2.0 hrs. After bringing the mixture to room temperature, the reaction mixture and 10 mL of 5% bicarbonate solution was added into a separating funnel, the resultant mixture was extracted with ethyl acetate (3 X 20 mL). The combined organic layers were dried with anhydrous Na_2SO_4. Under vacuum, the solvent was evaporated, and the crude product was purified using column chromatography (silica gel, EtOAc/Hexane) in order to obtain a pure product.

The same stoichiometry has been followed under microwave reactor at 120 °C for 40 min. Similar procedure was followed for acylation and benzoylation of amines.

Spectroscopic data of compounds

N-phenylformamide[28](**Scheme 2**, **entry 3a**) (**CAS No. 103-70-8)**

Using the experimental procedure **GEP-1**, the product was obtained as yellow solid in 86% yield; A mixture of rotamers is observed; **^{1}H NMR** (400 MHz, $CDCl_3$) δ 9.22 (Minor rotamer, s, 0.44H), 8.71 (Major rotamer, d, *J* = 11.3 Hz, 0.48H), 8.60 (Minor rotamer, s, 0.42H), 8.34 (Major rotamer, s, 0.50H), 7.58 (d, *J* = 8.2 Hz, 1.0H), δ 7.36 – 7.29 (m, 2.0H), 7.19 (t, *J* = 7.4 Hz, 0.47H), 7.13 (t, *J* = 7.1 Hz, 1.42H); **^{13}C NMR** (100 MHz, $CDCl_3$) δ major rotamer 163.23, 136.84, 129.41, 125.24, 118.78, minor rotamer 159.90, 137.09, 129.69, 124.74, 120.23.

N-(2-Hydroxy-4-methylphenyl)formamide[29]**(Scheme 2, entry3b) (CAS No. 2843-27-8)**

Using the experimental procedure **GEP-1**, the product was obtained as brown solid in 91% yield; **^{1}H NMR** (400 MHz, DMSO) δ 9.92 (s, 1H), 9.55 (s, 1H), 8.28 (s, 1H), 8.02 (d, *J* = 7.9 Hz, 1H), 6.94 – 6.82 (m, 2H), 6.75 (*t*, *J* = 7.4 Hz, 1H); **^{13}C NMR** (100 MHz, DMSO): δ 163.47, 160.03, 148.97, 146.73, 126.00, 125.48, 125.34, 124.19, 121.76, 120.83, 119.53, 119.00, 116.10, 115.10.

N-(3-hydroxyphenyl)formamide[30]**(Scheme 2, entry 3c) (CAS No. 24891-35-8)**

Using the experimental procedure **GEP-1**, the product was obtained as brown oil in 89% yield. A mixture of rotamers is observed; **^{1}H NMR** (400 MHz, DMSO) δ 10.02 (d, *J* = 12.3 Hz, 0.98H), 9.51 (minor rotamer, s, 0.27H), 9.41 (major rotamer, s, 0.73H), 8.72 (minor rotamer, d, *J* = 11.0 Hz, 0.28H), 8.22 (major rotamer, d, *J* = 1.1 Hz, 0.72H), 7.18 (s, 0.73H), 7.08 (t, *J* = 8.0 Hz, 1.0H), 6.94 (d, *J* = 8.0 Hz, 0.73H), 6.63 (d, *J* = 8.0 Hz, 0.27H), 6.57 (s, 0.27H), 6.51 – 6.46 (m, 0.99H); **^{13}C NMR** (100 MHz, DMSO) δ Major rotamer: 159.45, 157.70, 139.24, 129.56, 110.80, 106.40, minor rotamer: 162.38, 158.26, 139.47, 130.19, 110.85, 104.76.

N-(4-hydroxyphenyl)formamide[31]**(Scheme 2, entry 3d) (CAS No. 41656-75-1)**

Using the experimental procedure **GEP-1**, the product was obtained as brown solid in 88% yield. A mixture of rotamers is observed; **^{1}H NMR** (400 MHz, DMSO) δ 9.85 (t, *J* = 13.6 Hz, 1.01H), 9.23 (s, 1H), 8.51 (Minor rotamer, d, *J* = 11.2 Hz, 0.23H), 8.17 (Major rotamer, d, *J* = 1.8 Hz, 0.74H), 7.38 (d, *J* = 8.8 Hz, 1.52H), 6.98 (d, *J* = 8.7 Hz, 0.46H), 6.72 (t, *J* = 6.9 Hz, 2H); **^{13}C NMR** (100 MHz, DMSO) δ Major rotamer: 155.83, 150.55, 126.98, 117.82, 112.19, minor rotamer: 159.55, 151.22, 126.66, 117.22, 112.81.

N-(2-methoxyphenyl)formamide[32](**Scheme 2, entry3e**) (**CAS No. 23896-88-0**)

Using the experimental procedure **GEP-1**, the product was obtained as brown solid in 90% yield; A mixture of rotamers is observed; **^{1}H NMR** (400 MHz, $CDCl_3$) δ 8.89 (Minor rotamer, s, 0.26H), 8.47 (Major rotamer, s, 0.66H), 8.35 (Major rotamer, d, *J* = 7.9 Hz, 0.71H), 7.91 (s, 0.61H), 7.79 (s, 0.31H), 7.18 (d, *J* = 7.8 Hz, 0.33H), 7.06 (t, *J* = 7.8 Hz, 0.6H), 7.15 – 7.01 (m, 0.33H), 6.97-6.87 (m, 2H), 3.86 (d, *J* = 7.3 Hz, 3H); **^{13}C NMR** (100 MHz, $CDCl_3$) δ major rotamer: 158.91, 147.91, 124.35, 121.13, 110.15, 55.79, minor rotamers: 161.59, 148.88, 126.80, 125.33, 120.54, 111.38.

N-(4-methoxyphenyl) formamide[33](**Scheme 2**, **entry 3f**) (**CAS No. 5470-34-8**)

Using the experimental procedure **GEP-1**, the product was obtained as reddish brown solid in 88% yield. A mixture of rotamers is observed; **^{1}H NMR** (400 MHz, $CDCl_3$) δ 8.52 (t, *J* = 13.2 Hz, 0.84H), 8.28 (Major rotamer, s, 0.52H), 7.88 (Minor rotamer, s, 0.43H), 7.43 (d, *J* = 8.8 Hz, 1.03H), 7.03 (d, *J* = 8.7 Hz, 0.92H), 6.85 (dd, *J* = 14.3, 8.8 Hz, 1.98H), 3.77 (d, *J* = 7.5 Hz, 3H). **^{13}C NMR** (100 MHz, $CDCl_3$) δ Major rotamer: 159.33, 157.68, 129.74, 121.74, 114.97, 55.55, minor rotamer: 163.42, 156.77, 130.13, 121.61, 114.28, 55.63.

N-(4-(methylthio)phenyl)formamide[34](**Scheme 2**, **entry 3g**) (**CAS No. 170288-29-6**)

Using the experimental procedure **GEP-1**, the product was obtained as cream solid in 69% yield. A mixture of rotamers is observed; **^{1}H NMR** (400 MHz, $CDCl_3$) δ 8.65 (Minor rotamer, d, *J* = 11.2 Hz, 0.49H), 8.58 (Minor rotamer, s, 0.42H), 8.36 (Major rotamer, s, 0.55H), 7.69 (Major rotamer, br, s, 0.46H), 7.49 (d, *J* = 8.4 Hz, 1H), 7.25 (dd, *J* = 10.8, 8.6 Hz, 2.19H), 7.05 (d, *J* = 8.3 Hz, 1H), 2.48 (d, *J* = 5.1 Hz, 3H). **^{13}C NMR** (100 MHz, $CDCl_3$) δ Major rotamer: 159.25, 134.52, 127.95, 120.77, 16.61, minor rotamer: 162.82, 135.43, 128.52, 119.76, 16.58.

N-(3-nitrophenyl)formamide[35](**Scheme 2**, **entry 3i**) (**CAS No.102-38-5**)

Using the experimental procedure **GEP-1**, the product was obtained as yellow solid in 38% yield. A mixture of rotamers is observed; **^{1}H NMR** (400 MHz, DMSO) δ 10.67 (Major rotamer, s, 0.83H), 10.48 (Minor rotamer, d, *J* = 10.3 Hz, 0.17H), 8.95 (minor rotamer, d, *J* = 10.7 Hz, 0.17H), 8.61 (major rotamer, s, 0.83H), 8.38 (s, 0.85H), 8.02 (s, 0.17H), 7.91 (dd, *J* = 16.1, 8.1 Hz, 1.87H), 7.61 (t,

J = 8.1 Hz, 1.0H). **^{13}C NMR** (100 MHz, DMSO) δ Major rotamer: 160.35, 139.23, 130.31, 125.12, 118.16, 113.35, minor rotamer: 162.73, 139.92, 130.75, 123.12, 117.84, 111.57.

N-(2-chlorophenyl)formamide[30](**Scheme 2**, **entry3k**) (**CAS No. 2596-93-2**)

Using the experimental procedure **GEP-1**, the product was obtained as yellow oil in 69% yield; A mixture of rotamers is observed; **^{1}H NMR** (400 MHz, $CDCl_3$) δ 8.73 (Minor rotamer, d, *J* = 11.1 Hz, 0.32H), 8.52 (Major rotamer, s, 0.69H), 8.41 (d, *J* = 8.2 Hz, 0.67H), 7.81 (s, 0.89), 7.43 (d, *J* = 8.0 Hz, 0.33H), 7.37 (d, *J* = 8.0 Hz, 0.67H), 7.27 (dd, *J* = 8.9, 5.8 Hz, 1.38H), 7.15 – 7.11 (m, 0.31H), 7.06 (t, *J* = 7.7 Hz, 0.70H). **^{13}C NMR** (100 MHz, CDCl3) δ Major rotamer: 159.03,129.23, 127.92, 125.26, 122.70, 161.73, 130.43, 128.13, 126.09, 122.14.

N-(3-chlorophenyl) formamide[34](**Scheme 2**, **entry 3l**) (**CAS No. 139-71-9**)

Using the experimental procedure **GEP-1**, the product was obtained as off white solid in 81%; **^{1}H NMR** (400 MHz, $CDCl_3$) δ 8.72 – 8.58 (m, 1H), 8.30 (s, 1H), 7.59 (s, 1H), 7.32 (d, *J* = 8.1 Hz, 1H), 7.24 – 7.13 (m, 1H), 7.04 (d, *J* = 7.2 Hz, 1H).**^{13}C NMR** (100 MHz, $CDCl_3$) δ 162.60, 159.26, 138.08, 134.87, 130.95, 130.25, 125.49, 125.05, 120.25, 118.91, 118.05, 116.84.

N-(4-chlorophenyl) formamide[36] (**Scheme 2**, **entry 3m**) (**CAS No. 2617-79-0**)

Using the experimental procedure **GEP-1**, the product was obtained as off-white solid in 77% yield. A mixture of rotamers is observed; **^{1}H NMR** (400 MHz, $CDCl_3$) δ 8.78 (Minor rotamer, br, s, 0.31H), 8.66 (Minor rotamer, d, *J* = 11.3 Hz, 0.39H), 8.37 (Major rotamer, s, 0.51H), 7.82 (Major rotamer, br, s, 0.45H), 7.51 (d, *J* = 8.4 Hz, 1H), 7.31 (q, *J* = 7.2 Hz, 1.86H), 7.06 (d, *J* = 8.4 Hz, 0.77H); **^{13}C NMR** (100 MHz, $CDCl_3$) δ Major rotamer: 159.34, 135.53, 129.24, 121.40, minor rotamer: 162.83, 135.42, 130.91, 120.20.

N-(3-fluorophenyl)formamide[37](**Scheme 2**, **entry 3n**) (**CAS No. 1428-10-0**)

Using the experimental procedure **GEP-1**, the product was obtained as yellow solid in 83% yield. A mixture of rotamers is observed; **^{1}H NMR** (400 MHz, $CDCl_3$) δ 8.98 (Minor rotamer, s, 042H), 8.73 (Minor rotamer, d, *J* = 11.2 Hz, 0.47H), 8.39 (Major rotamer, s, 0.60H), 8.11 (Major rotamer, d, *J* = 4.0 Hz, 0.53H), 7.50 (d, *J* = 10.7 Hz, 0.57H), 7.39 – 6.81 (m, 1.71H), 6.95 – 6.82 (m, 2H); **^{13}C NMR**

(100 MHz, $CDCl_3$) δ Major rotamer: 164.41 (d, *J* = 48.22 Hz), 162.88, 138.56 (d, *J* = 5.10 Hz), 130.31 (d, *J* = 9.32 Hz), 115.43, 111.64 (d, *J* = 21.14 Hz), 107.75 (d, *J* = 26.07 Hz), Minor rotamer: 161.96 (d, *J* = 46.14 Hz), 159.69, 138.46 (d, *J* = 5.77 Hz), 131.22 (d, *J* = 9.3 Hz), 114.15 (d, *J* = 2.96 Hz), 112.11 (d, *J* = 21.00 Hz), 106.02 (d, *J* = 24.97 Hz) ; **^{19}F NMR** (377 MHz, $CDCl_3$) δ -110.46, -110.48, -110.50, -110.52, -111.18, -111.21, -111.22, -111.23, -111.24.

N-(4-fluorophenyl) formamide[38](**Scheme 2**, **entry 3o**) (**CAS No. 459-25-6**)

Using the experimental procedure **GEP-1**, the product was obtained as off-white solid in 85% yield. A mixture of rotamers is observed; **^{1}H NMR** (400 MHz, $CDCl_3$) δ 8.63 (Minor rotamer, s, 0.33H), 8.57 (Major rotamer, d, *J* = 11.0 Hz, 0.50H), 8.33 (Major rotamer, s, 0.60H), 7.76 (Minor rotamer, s, 0.47H), 7.50 (dd, *J* = 8.7, 4.8 Hz, 1.17H), 7.11 – 6.96 (m, 3H); **^{13}C NMR** (100 MHz, $CDCl_3$) δ Major rotamer: 161.37 (d, *J* = 85.32 Hz), 159.33, 132.98, 121.99 (d, *J* = 7.88 Hz), 115.87 (d, *J* = 22.45 Hz), minor rotamer: 163.22, 158.51, 132.85, 121.29 (d, *J* = 8.2 Hz), 116.66 (d, *J* = 22.74 Hz); **^{19}F NMR** (377 MHz, $CDCl_3$) δ -116.84, -116.85, -116.86, -116.87, -116.89, -116.89, -116.91, -117.06, -117.07, -117.08, -117.09, -117.10, -117.11, -117.12.

N-(3-chlorophenyl)formamide[28](**Scheme 2**, **entry 3p**) (**CAS No. 139-71-9**)

Using the experimental procedure **GEP-1**, the product was obtained as yellow solid in 74% yield. A mixture of rotamers is observed; **^{1}H NMR** (400 MHz, $CDCl_3$) δ 8.72 (t, *J* = 11.9 Hz, 0.83H), 8.38 (s, 0.55H), 7.82 (s, 1.0H), 7.47 (d, *J* = 8.0 Hz, 0.56H), 7.36 – 7.17 (m, 2.4H), 7.06 (d, *J* = 8.0 Hz, 0.44H), **^{13}C NMR** (100 MHz, $CDCl_3$) δ Major rotamer: 159.36, 130.52, 127.97, 123.08, 122.78, 118.58, minor rotamers: 162.68, 131.18, 128.41, 123.46, 121.78, 117.32.

N-(4-bromophenyl)formamide[39](**Scheme 2**, **entry 3q**) (**CAS No. 2617-78-9**)

Using the experimental procedure **GEP-1**, the product was obtained as yellow solid in 65% yield. A mixture of rotamers is observed; **^{1}H NMR** (400 MHz, $CDCl_3$) δ 8.66 (Major rotamer, d, *J* = 11.1 Hz, 0.51H), 8.61 (Minor rotamer, s, 0.35H), 8.37 (Major rotamer, s, 0.62H), 7.62 (minor rotamer, s, 0.47H), 7.48 (s, 0.99H), 7.44 (d, *J* = 8.2 Hz, 2.20H), 6.98 (d, *J* = 8.6 Hz, 0.92H); **^{13}CNMR** (100 MHz,

$CDCl_3$) δ Major rotamer: 159.20, 132.21, 121.21, 117.63, minor rotamer: 162.63, 132.92, 120.45, 118.42.

N-(2-iodophenyl)formamide[29] (**Scheme 2**, **entry 3r**) (**CAS NO. 10113-39-0**)

Using the experimental procedure **GEP-1**, the product was obtained as brown solid in 44% yield; A mixture of rotamers is observed;**^{1}H NMR** (400 MHz, $CDCl_3$) δ 8.73 (Minor rotamer, s, 0.33H), 8.69 (Major rotamer, d, *J* = 11.0 Hz, 0.62H), 8.36 (Major rotamer, s, 0.44H), 7.85 (Minor rotamer, s, 0.38H), 7.55 (d, *J* = 7.9 Hz, 0.86H), 7.37-7.30 (m, 1.92H), 7.21 – 7.07 (m, 1.44H). **^{13}C NMR** (100 MHz, $CDCl_3$) δ major rotamer: 163.03, 137.04, 129.99, 125.40, 118.93, minor rotamer: 159.44, 136.84, 129.84, 124.90, 120.17.

N-m-tolylformamide[40](**Scheme 2**, **entry 3s**) (**CAS No. 3085-53-8**)

Using the experimental procedure **GEP-1**, the product was obtained as brown oil in 82% yield; A mixture of rotamers is observed; **^{1}H NMR** (400 MHz, $CDCl_3$) δ 8.98 (Major rotamer, br s, 0.51H), 8.71 (Major rotamer, d, *J* = 11.4 Hz, 0.56H), 8.35 (Minor rotamer, s, 0.45H), 8.11 (Minor rotamer, br d, *J* = 5.0 Hz, 0.42H), 7.39 (s, 0.44H), 7.33 (d, *J* = 8.1 Hz, 0.44H), 7.20 (dt, *J* = 12.0, 7.9 Hz, 1.0H), 6.99 (d, *J* = 7.6 Hz, 0.55H), 6.93 (d, *J* = 10.8 Hz, 1.52H), 2.32 (d, *J* = 10.8 Hz, 3H). **^{13}C NMR** (100 MHz, $CDCl_3$) δ Major rotamer: 163.16, 139.87, 136.81, 129.56, 125.60, 119.54, 115.80, 21.41, minor rotamer: 159.57, 139.05, 137.01, 128.91, 126.09, 120.79, 117.24, 21.47.

N-(4-(trifluoromethoxy)phenyl)formamide[39](**Scheme 2**, **entry 3t)** (**CAS No. 85293-36-3**)

Using the experimental procedure **GEP-1**, the product was obtained as yellow oil in 51% yield. A mixture of rotamers is observed; **^{1}H NMR** (400 MHz, $CDCl_3$) δ 8.66 (Major rotamer, d, *J* = 11.2 Hz, 0.43H), 8.50 (Minor rotamer, br, s, 0.35H), 8.38 (s, 0.64H), 7.59 (t, *J* = 9.4 Hz, 1.74H), 7.25 – 7.11 (m, 3H); **^{13}C NMR** (100 MHz, $CDCl_3$) δ 122.74, 121.97, 121.31, 120.23, Major rotamer: 159.18, 135.59, minor rotamer: 162.69, 135.52; **^{19}F NMR** (377 MHz, $CDCl_3$) δ -58.16 (major rotamer, s), -58.22 (minor rotamer, s).

N-(3-acetylphenyl)formamide[41](**Scheme 2**, **entry 3u**) (**CAS No.72801-78-6**)

Using the experimental procedure **GEP-1**, the product was obtained as white solid in 64% yield. A mixture of rotamers is observed; **^{1}H NMR** (400 MHz, $CDCl_3$) δ 9.00 (d, *J* = 10.5 Hz, 0.36H), 8.86 (Minor rotamer, d, *J* = 11.1 Hz, 0.39H), 8.42 (Major rotamer, s, 0.65H), 8.38 (br, s, 0.73H), 7.93 (dd, *J*= 13.4, 8.5 Hz, 0.2.02H), 7.67 (d, *J* = 8.5 Hz, 1.24H), 7.18 (d, *J* = 8.4 Hz, 0.80H), 2.57 (d, *J* = 4.4 Hz, 3H); **^{13}C NMR** (100 MHz, $CDCl_3$) δ Major rotamer: 159.27, 133.30, 129.87, 119.40, minor rotamer: 162.27, 133.75, 130.52, 117.35.

N-(4-acetylphenyl)formamide[42](**Scheme 2, entry 3v**) (**CAS No. 41656-75-1**)

Using the experimental procedure **GEP-1**, the product was obtained as white solid in 73% yield. A mixture of rotamers is observed; **^{1}H NMR** (400 MHz, $CDCl_3$) δ 8.93 (Minor rotamer, d, *J* = 10.8 Hz, 0.36H), 8.75 (Minor rotamer, d, *J* = 11.2 Hz, 0.38H), 8.47 (Major rotamer, s, 0.53H), 8.42 (Major rotamer, s, 0.69H), 8.07 (s, 0.67H), 7.92 (d, *J* = 8.1 Hz, 0.68H), 7.73 (d, *J* = 7.5 Hz, 0.76H), 7.67 (d, *J* = 7.7 Hz, 0.65H), 7.46-7.38 (m, 1.05H), 7.32 (d, *J* = 8.3 Hz, 0.38H),2.58 (d, *J* = 9.2 Hz, 3H), **^{13}C NMR** (100 MHz, $CDCl_3$) δ Major rotamer: 198.34, 159.83, 137.83, 129.53, 124.85, 119.42, minor rotamer: 197.66, 162.74, 138.53, 130.18, 123.20, 117.84.

4-formamidobenzoic acid[43](**Scheme 2**, **entry 3w**) (**CAS No.28533-43-9**)

Using the experimental procedure **GEP-1**, the product was obtained as brown oil in 61% yield. A mixture of rotamers is observed; **^{1}H NMR** (400 MHz, $CDCl_3$) δ 8.85 (s, 0.48H), 8.69 (d, *J* = 11.3 Hz, 0.55H), 8.35 (s, 0.47H), 8.00 (s, 0.45H), 7.55 (d, *J* = 8.1 Hz, 0.93H), 7.39 – 7.27 (m, 2H), 7.18 (t, *J* = 7.4 Hz, 0.53H), 7.11 (dd, *J* = 10.9, 8.0 Hz, 1.47H); **^{13}C NMR** (100 MHz, $CDCl_3$) δ Major rotamer: 163.09, 136.87, 129.97, 125.37, 118.90, minor rotamer: 159.55, 137.06, 129.15, 124.87, 120.19.

Ethyl 4-formamidobenzoate[44](**Scheme 2**, **entry 3x**) (**CAS No.5422-63-9**)

Using the experimental procedure **GEP-1**, the product was obtained as white solid in 49% yield. A mixture of rotamers is observed; **^{1}H NMR** (400 MHz, DMSO) δ 10.53 (Major rotamer, s, 0.73H), 10.46 (Minor rotamer, d, *J* = 10.7 Hz, 0.25H), 8.96 (Minor rotamer, d, *J* = 10.7 Hz, 0.24H), 8.35 (Major rotamer, s, 0.75H), 7.91 (t, *J* = 10.5 Hz, 2.01H), 7.71 (d, *J* = 8.5 Hz, 1.53H), 7.31 (t, *J* = 7.6

Hz, 0.61H), 4.28 (q, *J* = 7.1 Hz, 2H), 1.30 (t, *J* = 7.1 Hz, 3H); **^{13}C NMR** (100 MHz, DMSO) δ Major rotamer: 160.11, 142.43, 130.32, 118.62, minor rotamer: 162.53, 142.90, 121.19, 116.43.

N-(2-bromo-4-methylphenyl)formamide[45](**Scheme 2**, **entry 3y**) (**CAS No.353284-16-9**)

Using the experimental procedure **GEP-1**, the product was obtained as off-white solid in 60% yield. A mixture of rotamers is observed; **^{1}H NMR** (400 MHz, $CDCl_3$) δ 8.62 (d, *J* = 11.2 Hz, 0.35H), 8.45 (s, 0.66H), 8.22 (d, *J* = 8.3 Hz, 0.66H), 7.62 (br, s, 0.82H), 7.42 (s, 0.48H), 7.36 (s, 0.49H), 7.12 (t, *J* = 8.8 Hz, 1.32H), 2.30 (d, *J* = 7.8 Hz, 3H). **^{13}C NMR** (100 MHz, CDCl3) δ Major rotamer: 158.88, 133.88, 132.72, 129.42, 122.24, 114.78, minor rotamers: 161.90, 135.93, 132.88, 129.17, 119.17, 119.46, 113.04.

N-(2-hydroxy-5-methylphenyl)formamide[46](**Scheme 2**, **entry 3aa**) (**CAS No.74642-14-1**)

Using the experimental procedure **GEP-1**, the product was obtained as brown solid in 78% yield. A mixture of rotamers is observed; **^{1}H NMR** (400 MHz, DMSO) δ 9.65 (s, 0.87H), 9.50 (s, 0.99H), 9.18 (d, *J* = 10.9 Hz, 0.16H), 8.51 (Minor rotamer, d, *J* = 11.2 Hz, 0.16H), 8.26 (Major rotamer, s, 0.84H), 7.85 (s, 0.83H), 6.93 (s, 0.15H), 6.74 (dt, *J* = 14.8, 7.3 Hz, 2H), 2.18 (s, 3H); **^{13}C NMR** (100 MHz, DMSO) δ Major rotamer: 160.11, 142.43, 130.32, 118.62, minor rotamer: 162.53, 142.90, 131.19, 124.56.

N-(5-(tert-butyl)-2-hydroxyphenyl)formamide[47](**Scheme 2**, **entry 3ab**) (**CAS No.2305056-85-1**)

Using the experimental procedure **GEP-1**, the product was obtained as brown solid in 75% yield. A mixture of rotamers is observed; **^{1}H NMR** (400 MHz, DMSO) δ 9.67 (s, 0.81H), 9.53 (s, 0.99H), 9.18 (Minor rotamer, d, *J* = 11.0 Hz, 0.17H), 8.52 (Minor rotamer, d, *J* = 11.2 Hz, 0.17H), 8.27 (Major rotamer, s, 0.82H), 8.07 (Major rotamer, d, *J* = 1.4 Hz, 0.82H), 7.10 (s, 0.16H), 6.99 (d, *J* = 8.4 Hz, 0.18H), 6.93 (dd, *J* = 8.4, 1.8 Hz, 0.80H), 6.79 (t, *J* = 10.1 Hz, 0.98H), 1.22 (s, 9H). **^{13}C NMR** (100 MHz, DMSO) δ Major: 159.98, 144.41, 141.25, 125.41, 120.81, 117.92, 115.62, minor rotamer; 163.63, 146.67, 141.89, 124.54, 122.03, 122.03, 119.06, 114.64.

N-(2,4-dimethylphenyl)formamide[48](**Scheme 2**, **entry 3ac**) (**CAS No.60397-77-5**)

Using the experimental procedure **GEP-1**, the product was obtained as off-white solid in 81% yield. A mixture of rotamers is observed; **^{1}H NMR** (400 MHz, $CDCl_3$) δ 8.45 (d, *J* = 11.2 Hz, 0.62H), 8.39 (s, 0.37H), 8.17 (br, s, 0.58H), 7.66 (d, *J* = 8.6 Hz, 0.36H), 7.35 (br, s, 0.28H), 7.00 (t, *J* = 7.2 Hz, 2.69H), 2.29 (d, *J* = 10.3 Hz, 3H), 2.24 (d, *J* = 15.6 Hz, 3H). **^{13}C NMR** (100 MHz, $CDCl_3$) δ Major rotamer: 159.50, 136.08, 132.53, 130.23, 127.63, 121.46, minor rotamer: 163.82, 135.45, 131.96, 129.26, 127.26, 127.36, 123.52.

N-(3-chloro-4-fluorophenyl)formamide[49](**Scheme 2**, **entry 3ad**) (**CAS No.770-22-9**)

Using the experimental procedure **GEP-1**, the product was obtained as off-white solid in 84% yield. A mixture of rotamers is observed; **^{1}H NMR** (400 MHz, $CDCl_3$) δ 8.64 (d, *J* = 19.6 Hz, 0.34H), 8.58 (d, *J* = 11.0 Hz, 0.45H), 8.35 (s, 0.77H), 7.72 (dd, *J* = 6.4, 2.1 Hz, 0.48H), 7.39 – 7.32 (m, 0.87H), 7.20 – 7.04 (m, 0.76H), 7.02 – 6.95 (m, 2H). **^{13}C NMR** (100 MHz, $CDCl_3$) δ Major rotamer: 159.30, 156.71 (d, *J* = 84.35 Hz), 133.53, 122.46, 121.45, 119.87 (d, *J* = 67.2 Hz), 116.86 (d, *J* = 22.18 Hz), minor rotamer: 162.88, 154.26 (d, *J* = 83.92 Hz), 133.56, 121.58, 121.27, 119.07 (d, *J* = 84.35 Hz),117.67 (d, *J* = 22.38 Hz); **^{19}F NMR** (377 MHz, $CDCl_3$) δ -119.23, -119.25, -119.27, -119.48, -119.50, -119.51, -119.51, -119.52, -119.53.

N-(4-chloro-3-(trifluoromethyl)phenyl)formamide (**Scheme 2**, **entry 3ae**) (**CAS No.656-96-2**)

Using the experimental procedure **GEP-1**, the product was obtained as yellow solid in 53% yield. A mixture of rotamers is observed; **^{1}H NMR** (400 MHz, $CDCl_3$) δ 8.70 (s, 0.77H), 8.41 (s, 1H), 7.85 (d, *J* = 15.4 Hz, 1.18H), 7.75 (d, *J* = 8.6 Hz, 0.61H), 7.50 (d, *J* = 8.5 Hz, 1.11H), 7.47 – 7.40 (m, 0.42H), 7.24 (d, *J* = 8.5 Hz, 0.41H); **^{13}C NMR** (100 MHz, $CDCl_3$) δ 135.76 Major rotamer: 159.36, 132.29, 129.06 (d, *J* = 31.39 Hz), 124.11, 123.91, 121.19, 119.08 (q), minor rotamer: 162.35, 133.03, 127.71, 123.71, 122.69, 120.99, 117.91 (q); **^{19}F NMR** (377 MHz, $CDCl_3$) δ -62.91 (minor, s), -63.05 (minor, s).

N-methyl-N-phenylformamide[36](**Scheme 2**, **entry 3af**) (**CAS No.93-61-8**)

Using the experimental procedure **GEP-1**, the product was obtained as yellow oil in 52% yield. **^{1}H NMR** (400 MHz, $CDCl_3$) δ 8.44 (s, 1H), 7.38 (t, *J* = 7.8 Hz, 2H), 7.25 (t, *J* = 7.4 Hz, 1H), 7.14 (d, *J* =

8.1 Hz, 2H), 3.29 (s, 3H); **^{13}C NMR** (100 MHz, $CDCl_3$) δ 162.42, 142.21, 129.66, 129.09, 126.46, 126.32, 123.69, 122.42, 32.09.

N,N-diphenylformamide[50](**Scheme 2**, **entry 3ag**) (**CAS No. 607-00-1**)

Using the experimental procedure **GEP-1**, the product was obtained as yellow solid in 28% yield. **^{1}H NMR** (400 MHz, $CDCl_3$) δ 8.59 (s, 1H), 7.32 (dd, *J* = 12.8, 7.3 Hz, 4H), 7.21 (td, *J* = 11.6, 6.4 Hz, 4H), 7.09 (d, *J* = 7.8 Hz, 2H); **^{13}C NMR** (100 MHz, $CDCl_3$) δ 161.85, 141.90, 139.75, 129.80, 129.29, 127.15, 126.97, 126.22, 125.20.

N-(quinolin-8-yl)formamide[51](**Scheme 2**, **entry 3ah**) (**CAS No. 62937-22-8**)

Using the experimental procedure **GEP-1**, the product was obtained as brown solid in 38% yield.A mixture of rotamers is observed; **^{1}H NMR** (400 MHz, $CDCl_3$) δ 9.61 (br, s, 0.80H), 9.20 (br, s, 0.11H), 8.84 (t, *J* = 18.7 Hz, 0.12H), 8.56 (d, *J* = 4.1 Hz, 0.98H), 8.49 (dd, *J* = 11.5, 7.0 Hz, 0.89H), 8.44 (s, 0.88H), 7.93 (d, *J* = 8.3 Hz, 1.0H), 7.29-7.01 (m, 3.19H); **^{13}C NMR** (100 MHz, $CDCl_3$) δ Major rotamer: 159.98, 144.41, 141.25, 125.41, 120.81, 117.92, 114.64, minor rotamer: 163.63, 146.67, 141.89, 124.54, 122.03, 119.06, 115.62.

N-(pyridin-2-yl)formamide[52](**Scheme 2**, **entry 3ai**) (**CAS No. 34813-97-3**)

Using the experimental procedure **GEP-1**, the product was obtained as brown solid in 55%; **^{1}H NMR** (400 MHz, $CDCl_3$) δ 10.58 (s, 1H), 9.28 (d, *J* = 10.0 Hz, 0.57H), 8.33 (s, 1H), 8.24 (s, 0.60H), 8.06 (d, *J* = 7.9 Hz, 0.45H), 7.78 – 7.771 (m, 1H), 7.08 (d, *J* = 5.6 Hz, 1H), 6.92 (d, *J* = 7.9 Hz, 0.59H).**^{13}C NMR** (100 MHz, $CDCl_3$) δ 162.13, 160.31, 151.65, 148.06, 138.70, 138.31, 119.76, 119.22, 113.78, 111.12.

piperidine-1-carbaldehyde[53] **(Scheme 2, entry 3aj) (CAS No.2591-86-8)**

Using the experimental procedure **GEP-1**, the product was obtained as yellow oil in 46%; **^{1}H NMR** (400 MHz, $CDCl_3$) δ 7.78 (s, 1H), 3.26 (t, *J* = 4.8 Hz, 2H), 3.10 (t, *J* = 4.8 Hz, 2H), 1.47 (d, *J* = 4.2 Hz, 2H), 1.37 – 1.31 (m, 4H).**^{13}C NMR** (100 MHz, $CDCl_3$) δ 160.34, 46.34, 40.11, 26.31, 26.14, 24.66, 24.23.

4-(2-chlorophenyl)piperazine-1-carbaldehyde (**Scheme 2**, **entry 3ak**) (**CAS No.1497871-12-1**)

Using the experimental procedure **GEP-1**, the product was obtained as light brown solid in 71% yield;**^{1}H NMR** (400 MHz, CDCl3) δ 8.07 (s, 1H), 7.43 (d, J = 7.9 Hz, 1H), 7.30 (t, J = 7.7 Hz, 1H), 7.15 (d, J = 8.0 Hz, 1H), 7.07 (t, J = 7.6 Hz, 1H), 3.63 – 3.44 (m, 4H), 3.00 – 2.94 (m, 2H), 2.93 – 2.87 (m, 2H). **^{13}C NMR** (100 MHz, CDCl3) δ 168.97, 148.63, 130.32, 128.11, 127.79, 124.36, 121.28, 51.64, 50.59, 45.08.

N-phenylacetamide[54]**(Scheme 3. entry 3A) (CAS No.103-84-4)**

Using the experimental procedure **GEP-1**, the product was obtained as colourless oil in 93%; **^{1}H NMR** (400 MHz, $CDCl_3$) δ 7.91 (s, 1H), 7.43 (d, *J* = 8.0 Hz, 2H), 7.21 (t, *J* = 7.7 Hz, 2H), 7.02 (t, *J* = 7.4 Hz, 1H), 2.08 (s, 3H). **^{13}C NMR** (100 MHz, $CDCl_3$) δ 169.05, 138.03, 129.03, 124.47, 120.25, 24.47.

N-(2-hydroxyphenyl)acetamide[55]**(Scheme 3. entry 3B)**(**CAS No.614-80-2**)

Using the experimental procedure **GEP-1**, the product was obtained as white solid in 89%; **^{1}H NMR** (400 MHz, DMSO) δ 9.73 (s, 1H), 9.30 (s, 1H), 7.67 (d, *J* = 7.9 Hz, 1H), 6.93 (t, *J* = 7.5 Hz, 1H), 6.85 (d, *J* = 7.7 Hz, 1H), 6.75 (t, *J* = 7.6 Hz, 1H), 2.09 (s, 3H). **^{13}C NMR** (100 MHz, DMSO) δ 169.02, 147.89, 126.42, 124.65, 122.37, 118.98, 115.95, 23.59.

N-(2-methoxyphenyl)acetamide[56]**(Scheme 3. Entry 3C) z(CAS No.93-26-5)**

Using the experimental procedure **GEP-1**, the product was obtained as white solid in 94%; **^{1}H NMR** (400 MHz, $CDCl_3$) δ 8.34 (d, *J* = 7.9 Hz, 1H), 7.78 (s, 1H), 7.03 (t, *J* = 7.7 Hz, 1H), 6.94 (t, *J* = 7.7 Hz, 1H), 6.86 (d, *J* = 8.1 Hz, 1H), 3.87 (s, 3H), 2.19 (s, 3H). **^{13}C NMR** (100 MHz, $CDCl_3$) δ 168.32, 147.79, 127.78, 123.72, 121.17, 119.92, 109.98, 55.73, 29.78, 24.96.

N-(3-nitrophenyl)acetamide[37]**(Scheme 3. entry 3D) (CAS No.121-89-1)**

Using the experimental procedure **GEP-1**, the product was obtained as yellow solid in 32%; **^{1}H NMR** (400 MHz, $CDCl_3$) δ 10.44 (s, 1H), 8.60 (t, *J* = 2.0 Hz, 1H), 7.87 (dd, *J* = 8.2, 2.1 Hz, 2H), 7.57 (t, *J* = 8.2 Hz, 1H), 2.09 (s, 3H). **^{13}C NMR** (100 MHz, $CDCl_3$) δ 166.08, 144.94, 137.39, 127.07, 121.86, 114.49, 110.03, 109.93, 21.01.

N-(2-chlorophenyl)acetamide[57]**(Scheme 3. entry 3E) (CAS No.533-17-5)**

Using the experimental procedure **GEP-1**, the product was obtained as colourless oil in 58%; **^{1}H NMR** (400 MHz, DMSO) δ 8.55 (d, *J* = 8.0 Hz, 1H), 7.86 (s, 1H), 7.56 (d, *J* = 8.0 Hz, 1H), 7.47 (t, *J* = 7.1 Hz, 1H), 7.24 (t, *J* = 7.6 Hz, 1H), 2.44 (s, 3H). **^{13}C NMR** (100 MHz, DMSO) δ 168.40, 134.72, 130.68, 129.08, 127.81, 124.74, 121.84, 77.48, 77.16, 76.84, 24.91.

N-(4-chlorophenyl)acetamide[58]**(Scheme 3. entry 3F) (CAS No.99-91-2)**

Using the experimental procedure **GEP-1**, the product was obtained as light yellow solid in 73%; **^{1}H NMR** (400 MHz, DMSO) δ 10.05 (s, 1H), 7.60 (d, *J* = 8.8 Hz, 2H), 7.33 (d, *J* = 8.8 Hz, 2H), 2.04 (s, 3H). **^{13}C NMR** (100 MHz, DMSO) δ 168.42, 138.24, 128.52, 126.49, 120.47, 120.38, 23.94.

N-(3-(trifluoromethyl)phenyl)acetamide[59]**(Scheme 3. entry 3G) (CAS No.349-76-8)**

Using the experimental procedure **GEP-1**, the product was obtained as white solid in 62%; **^{1}H NMR** (400 MHz, DMSO) δ 10.27 (s, 1H), 8.08 (s, 1H), 7.75 (d, *J* = 8.2 Hz, 1H), 7.53 (t, *J* = 8.0 Hz, 1H), 7.36 (t, *J* = 11.5 Hz, 1H), 2.08 (s, 3H). **^{13}C NMR** (100 MHz, DMSO) δ 168.91, 151.00, 140.03, 130.32, 129.90, 122.44, 119.31, 119.27, 117.78, 114.98, 114.94, 111.27, 110.71, 24.00, 20.55.

N-(4-(trifluoromethoxy)phenyl)acetamide[60]**(Scheme 3. entry 3H) (CAS No.85013-98-5)**

Using the experimental procedure **GEP-1**, the product was obtained as Colourless Solid in 45%; **^{1}H NMR** (400 MHz, $CDCl_3$) δ 7.95 (s, 1H), 7.53 (d, *J* = 8.8 Hz, 2H), 7.14 (d, *J* = 8.5 Hz, 2H), 2.16 (s, 3H). **^{13}C NMR** (100 MHz, $CDCl_3$) δ 169.00, 145.43, 136.71, 128.95, 127.92, 127.80, 121.87, 121.77, 121.32, 119.32, 24.46.

N-methyl-N-phenylacetamide[52]**(Scheme 3. entry 3I) (CAS No.579-10-2)**

Using the experimental procedure **GEP-1**, the product was obtained as light brown solid in 44%; **^{1}H NMR** (400 MHz, DMSO) δ 7.44 (t, *J* = 7.0 Hz, 2H), 7.32 (d, *J* = 7.5 Hz, 3H), 3.14 (s, 3H), 1.75 (s, 3H). **^{13}C NMR** (100 MHz, DMSO) δ 144.39, 129.56, 127.38, 127.06, 36.52, 22.17.

1-(4-(2-chlorophenyl)piperazin-1-yl)ethan-1-one **(Scheme 3. entry 3J) (CAS No.150557-82-7)**

Using the experimental procedure **GEP-1**, the product was obtained as light yellow solid in 70%; **^{1}H NMR** (400 MHz, DMSO) δ 7.43 (d, *J* = 7.9 Hz, 1H), 7.31 (t, *J* = 7.7 Hz, 1H), 7.15 (d, *J* = 8.0 Hz, 1H), 7.07 (t, *J* = 7.6 Hz, 1H), 3.58 (t, *J* = 4.4 Hz, 4H), 2.97 (t, *J* = 4.4 Hz, 2H), 2.90 (t, *J* = 4.4 Hz,

2H), 2.05 (s, 3H). **^{13}C NMR** (100 MHz, $CDCl_3$) δ 168.32, 148.64, 130.30, 128.08, 127.72, 124.22, 121.09, 51.15, 50.73, 45.90, 45.47, 41.02, 21.18, 8.45.

N-(2-methoxyphenyl)benzamide[61] **(Scheme 4. entry 3K) (CAS No.5395-00-6)**

Using the experimental procedure **GEP-1**, the product was obtained as white solid in 85%; **^{1}H NMR** (400 MHz, DMSO) δ 9.39 (s, 1H), 7.98 (d, *J* = 7.4 Hz, 2H), 7.84 (d, *J* = 7.9 Hz, 1H), 7.59 (t, *J* = 7.3 Hz, 3H), 7.18 (t, *J* = 7.8 Hz, 1H), 7.09 (d, *J* = 7.5 Hz, 1H), 6.98 (t, *J* = 7.6 Hz, 1H), 3.84 (s, 3H). **^{13}C NMR** (100 MHz, DMSO) δ 164.90, 151.30, 134.51, 131.53, 128.44, 127.38, 126.87, 125.55, 123.99, 120.17, 111.34, 55.69.

N-(4-methoxyphenyl)benzamide[62]**(Scheme 4. entry 3L) (CAS No.7472-54-0)**

Using the experimental procedure **GEP-1**, the product was obtained as white solid in 90%; **^{1}H NMR** (400 MHz, DMSO) δ 10.12 (s, 1H), 7.96 (d, *J* = 7.8 Hz, 2H), 7.69 (d, *J* = 8.8 Hz, 2H), 7.61 – 7.47 (m, 3H), 6.94 (d, *J* = 8.8 Hz, 2H), 3.75 (s, 3H). **^{13}C NMR** (100 MHz, DMSO) δ 165.06, 155.53, 135.02, 132.20, 131.29, 128.27, 127.48, 121.96, 113.69.

N-(4-chlorophenyl)benzamide[63] **(Scheme:4. Entry 3M) (CAS No.2866-82-2)**

Using the experimental procedure **GEP-1**, the product was obtained as white solid in 73%; **^{1}H NMR** (400 MHz, DMSO) δ 10.41 (s, 1H), 7.98 (d, *J* = 7.5 Hz, 2H), 7.85 (d, *J* = 8.8 Hz, 2H), 7.61 – 7.50 (m, 3H), 7.40 (d, *J* = 8.8 Hz, 2H).**^{13}C NMR** (100 MHz, DMSO) δ 165.60, 138.14, 134.64, 131.61, 128.42, 128.33, 127.65, 127.22, 121.85, 121.76.

N-(3-(trifluoromethyl)phenyl)benzamide[63]**(Scheme 4. entry 3N) (CAS No.1939-24-8)**

Using the experimental procedure **GEP-1**, the product was obtained as white solid in 45%; **^{1}H NMR** (400 MHz, DMSO) δ 10.68 (s, 1H), 8.30 (s, 1H), 8.10 (d, *J* = 8.0 Hz, 1H), 8.02 (d, *J* = 7.9 Hz, 1H), 7.65 – 7.51 (m, 2H), 7.45 (d, *J* = 7.8 Hz, 1H). **^{13}C NMR** (101 MHz, DMSO) δ 140.00, 131.87, 129.79, 128.41, 127.77, 123.82.

N,N-diphenylbenzamide[64] **(Scheme 4. entry 3O) (CAS No.4051-56-3)**

Using the experimental procedure **GEP-1**, the product was obtained as yellow solid in 58%; **^{1}H NMR** (400 MHz, DMSO) δ 7.73-7.64 (m, 7H), 7.32 – 7.14 (m, 4H), 7.00 (t, *J* = 8.4 Hz, 4H). **^{13}C NMR** (100

MHz, DMSO) δ 188.20, 169.86, 159.63, 149.42, 149.08, 142.53, 142.05, 141.96, 130.18, 128.24, 127.86, 124.21, 123.83, 123.71, 122.71, 114.98, 112.94, 111.25.

N-benzylbenzamide[65] **(Scheme 4. entry 3P) (CAS No.1485-70-7)**

Using the experimental procedure **GEP-1**, the product was obtained as white solid in 60%; **^{1}H NMR** (400 MHz, DMSO) δ 9.08 (s, 1H), 7.92 (d, *J* = 7.2 Hz, 2H), 7.55 – 7.50 (m, 1H), 7.47 (t, *J* = 7.5 Hz, 2H), 7.33 (d, *J* = 4.1 Hz, 4H), 7.26 – 7.21 (m, 1H). **^{13}C NMR** (100 MHz, DMSO) δ 166.17, 139.70, 134.32, 131.19, 128.28, 128.24, 127.23, 127.17, 126.68.

N-phenylisobutyramide[66]**(Scheme 5. entry 3Q) (CAS No.4406-41-1)**

Using the experimental procedure **GEP-1**, the product was obtained as white solid in 62%; **^{1}H NMR** (400 MHz, $CDCl_3$) δ 7.53 (d, *J* = 8.0 Hz, 2H), 7.43 (s, 1H), 7.30 (t, *J* = 7.7 Hz, 2H), 7.09 (t, *J* = 7.3 Hz, 1H), 2.57 – 2.47 (m, 1H), 1.24 (d, *J* = 6.8 Hz, 6H). **^{13}C NMR** (100 MHz, $CDCl_3$) δ 176.72, 138.24, 128.99, 124.23, 120.11, 77.47, 77.15, 76.84, 36.64, 19.69.

N-phenylpivalamide[62] **(Scheme 5. entry 3R) (CAS No.6625-74-7)**

Using the experimental procedure **GEP-1**, the product was obtained as white solid in 54%; **^{1}H NMR** (400 MHz, $CDCl_3$) δ 7.52 (d, *J* = 8.3 Hz, 2H), 7.31 (t, *J* = 7.7 Hz, 3H), 7.10 (t, *J* = 7.4 Hz, 1H), 1.32 (s, 9H). ^{13}C NMR (100 MHz, $CDCl_3$) δ 176.73, 138.16, 129.02, 124.29, 120.17, 39.68, 27.72.

Conclusion

In conclusion, we demonstrated that hydroxylamine hydrochloride and iodine are effective catalysts for the transamidation of amines and 1°, 2°, and 3°unactivated amides as carbonyl sources utilizing thermal/microwave irradiation. The approach displayed a broad substrate scope and produced desired product from moderate to good yield. Additionally, given the method's advantages, it requires a low-cost, readily available, and less toxic catalyst, and consumes less time and neat reaction conditions.

ACKNOWLEDGMENTS

The authors are thankful to the Discipline of Pharmaceutical Sciences, College of Health Sciences, University of Kwa-Zulu Natal (UKZN), Durban, South Africa, for providing all the necessary

facilities. R.K. gratefully acknowledges National Research Foundation-South Africa (NRF-SA) for funding this project (Grant Nos. 129247 and 112079).

References

[1] Mahesh, S., Tang, K.C. and Raj, M., 2018. Amide bond activation of biological molecules. Molecules, 23(10), p.2615..

[2] Zhao, F., Li, P., Liu, X., Jia, X., Wang, J. and Liu, H., 2019. Recent Advances in the Addition of Amide/Sulfonamide Bonds to Alkynes. Molecules, 24(1), p.164.

[3] Todorovic, M. and Perrin, D.M., 2020. Recent developments in catalytic amide bond formation. Peptide Science, 112(6), p.e24210..

[4] Song, H. and Naismith, J.H., 2020. Enzymatic methylation of the amide bond. Current Opinion in Structural Biology, 65, pp.79-88.

[5] Cierpicki, T. and Otlewski, J., 2001. Amide proton temperature coefficients as hydrogen bond indicators in proteins. Journal of biomolecular NMR, 21, pp.249-261.

[6] Badland, M., Crook, R., Delayre, B., Fussell, S.J., Gladwell, I., Hawksworth, M., Howard, R.M., Walton, R. and Weisenburger, G.A., 2017. A comparative study of amide-bond forming reagents in aqueous media–Substrate scope and reagent compatibility. Tetrahedron letters, 58(46), pp.4391-4394.

[7] S. Shi, R. Lalancette, R. Szostak, M. Szostak, *Chem. - A Eur. J.***2016**, *22*, 11949-53.

[8] Subramani, M. and Rajendran, S.K., 2019. Mild, Metal-Free and Protection-Free Transamidation of N-Acyl-2-piperidones to Amino Acids, Amino Alcohols and Aliphatic Amines and Esterification of N-Acyl-2-piperidones. European Journal of Organic Chemistry, 2019(22), pp.3677-3686..

[9] Handoko, Satishkumar, S., Panigrahi, N.R. and Arora, P.S., 2019. Rational design of an organocatalyst for peptide bond formation. Journal of the American Chemical Society,

141(40), pp.15977-15985.

[10] S. Nilawar, Q. Dasgupta, G. Madras, K. Chatterjee, *Emergent Mater.***2019**, *9*, 1213-1223.

[11] Chaudhari, M.B. and Gnanaprakasam, B., 2019. Recent Advances in the Metal-Catalyzed Activation of Amide Bonds. Chemistry–An Asian Journal, 14(1), pp.76-93.

[12] Wang, Z.J., Gao, Y., Hou, Y.L., Zhang, C., Yu, S.J., Bian, Q., Li, Z.M. and Zhao, W.G., 2014. Design, synthesis, and fungicidal evaluation of a series of novel 5-methyl-1H-1, 2, 3-trizole-4-carboxyl amide and ester analogues. European Journal of Medicinal Chemistry, 86, pp.87-94.

[13] Yin, J., Zhang, J., Cai, C., Deng, G.J. and Gong, H., 2018. Catalyst-free transamidation of aromatic amines with formamide derivatives and tertiary amides with aliphatic amines. Organic letters, 21(2), pp.387-392.

[14] Allen, C.L., Atkinson, B.N. and Williams, J.M., 2012. Transamidation of primary amides with amines using hydroxylamine hydrochloride as an inorganic catalyst. Angewandte Chemie International Edition, 51(6), pp.1383-1386.

[15] Dineen, T.A., Zajac, M.A. and Myers, A.G., 2006. Efficient transamidation of primary carboxamides by in situ activation with N, N-dialkylformamide dimethyl acetals. Journal of the American Chemical Society, 128(50), pp.16406-16409.

[16] Shimizu, Y., Morimoto, H., Zhang, M. and Ohshima, T., 2012. Microwave-Assisted Deacylation of Unactivated Amides Using Ammonium-Salt-Accelerated Transamidation. Angewandte Chemie, 124(34), pp.8692-8695.

[17] Fang, J., Peng, Z., Yang, Y., Wang, J., Guo, J. and Gong, H., 2018. Graphene-Oxide-Promoted Direct Dehydrogenative Coupling Reaction of Aromatics. Asian Journal of Organic Chemistry, 7(2), pp.355-358.

[18] Shi, S. and Szostak, M., 2017. Pd–PEPPSI: A general Pd–NHC precatalyst for Buchwald–Hartwig cross-coupling of esters and amides (transamidation) under the same reaction conditions. Chemical communications, 53(76), pp.10584-10587.

[19] Zhang, M., Imm, S., Bähn, S., Neubert, L., Neumann, H. and Beller, M., 2012. Efficient Copper (II)-Catalyzed Transamidation of Non-Activated Primary Carboxamides and Ureas with Amines. Angewandte Chemie International Edition, 16(51), pp.3905-3909.

[20] Singh, D.P., Allam, B.K., Singh, K.N. and Singh, V.P., 2014. A binuclear Mn (II) complex as an efficient catalyst for transamidation of carboxamides with amines. RSC Advances, 4(3), pp.1155-1158.

[21] Ma, J., Zhang, J. and Gong, H., 2019. Mn (II)-Catalyzed N-Acylation of Amines. Synthesis, 51(03), pp.693-703.

[22] Buchspies, J., Rahman, M.M. and Szostak, M., 2021. Transamidation of Amides and Amidation of Esters by Selective N–C (O)/O–C (O) Cleavage Mediated by Air-and Moisture-Stable Half-Sandwich Nickel (II)–NHC Complexes. Molecules, 26(1), p.188.

[23] Sonawane, R.B., Rasal, N.K. and Jagtap, S.V., 2017. Nickel-(II)-catalyzed N-formylation and N-acylation of amines. Organic letters, 19(8), pp.2078-2081.

[24] Ma, J., Zhang, F., Zhang, J. and Gong, H., 2018. Cobalt (II)-Catalyzed N-Acylation of Amines through a Transamidation Reaction. European Journal of Organic Chemistry, 2018(35), pp.4940-4948.

[25] Chen, J., Xia, Y. and Lee, S., 2020. Transamidation for the synthesis of primary amides at room temperature. Organic letters, 22(9), pp.3504-3508.

[26] Krishnamurthy, M., Vishwanatha, T.M., Panguluri, N.R., Panduranga, V. and Sureshbabu, V.V., 2015. Iodine-mediated oxidative coupling of hydroxamic acids with amines towards a new peptide-bond formation. Synlett, 26(18), pp.2565-1569.

[27] Tian, Q., Gan, Z., Wang, X., Li, D., Luo, W., Wang, H., Dai, Z. and Yuan, J., 2018. Imidazolium chloride: An efficient catalyst for transamidation of primary amines. Molecules, 23(9), p.2234.

[28] Li, W.D., Zhu, D.Y., Li, G., Chen, J. and Xia, J.B., 2019. Iron-catalyzed selective N-methylation and N-formylation of amines with CO2. Advanced Synthesis & Catalysis, 361(22), pp.5098-5104.

[29] Ghosh, T., Jana, S. and Dash, J., 2019. KO t Bu-promoted transition-metal-free transamidation of primary and tertiary amides with amines. Organic letters, 21(17), pp.6690-6694.

[30] Yadav, J.K., Yadav, P., Awasthi, S.K. and Agarwal, A., 2020. Efficient N-formylation of primary aromatic amines using novel solid acid magnetic nanocatalyst. RSC advances, 10(67), pp.41229-41236.

[31] Liu, H., Nie, Z., Shao, J., Chen, W. and Yu, Y., 2019. Mild and facile synthesis of formamide: reduction and functionalization of CO 2 using NaBH (OAc) 3 under atmospheric pressure. Green Chemistry, 21(13), pp.3552-3555.

[32] Leong, B.X., Teo, Y.C., Condamines, C., Yang, M.C., Su, M.D. and So, C.W., 2020. A NHC-silyliumylidene cation for catalytic N-formylation of amines using carbon dioxide. ACS Catalysis, 10(24), pp.14824-14833.

[33] Wu, S., Huang, Z., Jiang, X., Yan, F., Li, Y. and Du, C.X., 2021. Recyclable Oxofluorovanadate-Catalyzed Formylation of Amines by Reductive Functionalization of CO2 with Hydrosilanes. ChemSusChem, 14(7), pp.1763-1766.

[34] Yu, Y., Zhang, Y., Sun, C., Shi, L., Wang, W. and Li, H., 2020. Copper Promoted Aerobic Oxidative C (sp3)–C (sp3) Bond Cleavage of N-(2-(Pyridin-2-yl)-ethyl) anilines. The Journal of Organic Chemistry, 85(4), pp.2725-2732.

[35] Yin, J., Zhang, J., Cai, C., Deng, G.J. and Gong, H., 2018. Catalyst-free transamidation of aromatic amines with formamide derivatives and tertiary amides with aliphatic amines. Organic letters, 21(2), pp.387-392.

[36] Zhang, Q., Lin, X.T., Fukaya, N., Fujitani, T., Sato, K. and Choi, J.C., 2020. Selective N-formylation/N-methylation of amines and N-formylation of amides and carbamates with

carbon dioxide and hydrosilanes: promotion of the basic counter anions of the zinc catalyst. Green Chemistry, 22(23), pp.8414-8422.

[37] Sonawane, R.B., Rasal, N.K., Bhange, D.S. and Jagtap, S.V., 2018. Copper-(II) catalyzed N-formylation and N-acylation of aromatic, aliphatic, and heterocyclic amines and a preventive study in the C-N cross coupling of amines with aryl halides. ChemCatChem, 10(17), pp.3907-3913.

[38] Amirsoleimani, M., Khalilzadeh, M.A. and Zareyee, D., 2021. Preparation and catalytic evaluation of a palladium catalyst deposited over modified clinoptilolite (Pd@ MCP) for chemoselective N-formylation and N-acylation of amines. Journal of Molecular Structure, 1225, p.129076.

[39] Zhang, R., Zhang, J.C., Zhang, W.Y., He, Y.Q., Cheng, H., Chen, C. and Gu, Y.C., 2020. A practical approach for the transamidation of N, N-dimethyl amides with primary amines promoted by sodium tert-butoxide under solvent-free conditions. Synthesis, 52(21), pp.3286-3294.

[40] Yadav, L.S., Venkatesh, R., Raghavendra, M., Ramakrishnappa, T., Dhananjaya, N. and Nagaraju, G., 2020. Synthesis of Nano ZnO: A Catalyst for N-formylation of Aromatic Amines and Biodiesel Application. Current Nanomaterials, 5(1), pp.66-78.

[41] Karimi, B., Mansouri, F. and Vali, H., 2015. A Highly Water-Dispersible/Magnetically Separable Palladium Catalyst: Selective Transfer Hydrogenation or Direct Reductive N-Formylation of Nitroarenes in Water. ChemPlusChem, 80(12), pp.1750-1759.

[42] Li, J., Tu, D.H., Zhang, J., Li, J., Xue, Y., Xu, Q., Du, Y., Li, C. and Lu, J., 2020. High yield production of Co@ N-doped carbon catalyst and its application in carbonylation of amines to form formamides. Catalysis Communications, 147, p.106138.

[43] Tajbakhsh, M., Hosseinzadeh, R. and Tajbakhsh, M., 2013. TiO2 NPs as Catalyst for N-Formylation and N-Acetylation of Amines Under Solvent–Free Conditions. Letters in Organic

Chemistry, 10(9), pp.657-663.

[44] Škoch, K., Císařová, I. and Štěpnička, P., 2018. Selective gold-catalysed synthesis of cyanamides and 1-substituted 1H-tetrazol-5-amines from isocyanides. Chemistry–A European Journal, 24(52), pp.13788-13791.

[45] Mazumdar, W., Jana, N., Thurman, B.T., Wink, D.J. and Driver, T.G., 2017. Rh2 (II)-catalyzed ring expansion of cyclobutanol-substituted aryl azides to access medium-sized N-heterocycles. Journal of the American Chemical Society, 139(14), pp.5031-5034.

[46] Hosseini-Sarvari, M. and Sharghi, H., 2006. ZnO as a new catalyst for N-formylation of amines under solvent-free conditions. The Journal of Organic Chemistry, 71(17), pp.6652-6654.

[47] Yang, Y., Li, Y., Zhang, Z., Zhao, Y. and Feng, W., 2019. Metal-free N-formylation of 2-aminophenols using dimethylformamide and CSA. Synthetic Communications, 49(8), pp.1040-1046.

[48] Mutra, M.R., Dhandabani, G.K. and Wang, J.J., 2018. Mild Access to N-Formylation of Primary Amines using Ethers as C1 Synthons under Metal-Free Conditions. Advanced Synthesis & Catalysis, 360(20), pp.3960-3968.

[49] Kaboudin, B. and Khodamorady, M., 2010. Organic reactions in water: A practical and convenient method for the N-formylation of amines in water. Synlett, 2010(19), pp.2905-2907.

[50] Llopis, N., Gisbert, P. and Baeza, A., 2020. Direct synthesis of N, N-disubstituted formamides by oxidation of imines using an HFIP/UHP system. The Journal of Organic Chemistry, 85(17), pp.11072-11079.

[51] Pichardo, M.C., Tavakoli, G., Armstrong, J.E., Wilczek, T., Thomas, B.E. and Prechtl, M.H., 2020. Copper-Catalyzed Formylation of Amines by using Methanol as the C1 Source. ChemSusChem, 13(5), pp.882-887.

[52] Li, C., Wang, M., Lu, X., Zhang, L., Jiang, J. and Zhang, L., 2020. Reusable Brønsted acidic

ionic liquid efficiently catalyzed N-formylation and N-acylation of amines. ACS Sustainable Chemistry & Engineering, 8(11), pp.4353-4361.

[53] Zhang, K., Zong, L. and Jia, X., 2021. Bifunctional Ru-loaded Porous Organic Polymers with Pyridine Functionality: Recyclable Catalysts for N-Formylation of Amines with CO2 and H2. Advanced Synthesis & Catalysis, 363(5), pp.1335-1340.

[54] Ramachandran, P.V. and Hamann, H.J., 2021. Ammonia-borane as a Catalyst for the Direct Amidation of Carboxylic Acids. Organic Letters, 23(8), pp.2938-2942.

[55] Xiaoming, W., Tobias, G., Andreas, L. and Frank, G., 2017. Cp* Rh (III)/Bicyclic Olefin Cocatalyzed C–H Bond Amidation by Intramolecular Amide Transfer.

[56] Kathiravan, S. and Nicholls, I.A., 2017. Monoprotected l-Amino Acid (l-MPAA), Accelerated Bromination, Chlorination, and Iodination of C (sp2)− H Bonds by Iridium (III) Catalysis. Chemistry–A European Journal, 23(29), pp.7031-7036.

[57] Kashyap, B. and Phukan, P., 2013. A new ferrocene-based bulky pyridine as an efficient reusable homogeneous catalyst. RSC advances, 3(35), pp.15327-15336.

[58] Dev, D., Kalita, T., Mondal, T. and Mandal, B., 2021. Ethyl 2-Cyano-2-(2-nitrobenzenesulfonyloxyimino) Acetate (ortho-NosylOXY)-Mediated Double Beckmann Rearrangement of Ketoximes under Microwave Irradiation: A Mechanistic Perception. Advanced Synthesis & Catalysis, 363(5), pp.1427-1435.

[59] BHAISARE, R.D., GOPI, H.N. and MALI, S.M., 2013. Thioacids Mediated Selective and Mild N-Acylation of Amines.

[60] Lee, K.N., Lei, Z., Morales-Rivera, C.A., Liu, P. and Ngai, M.Y., 2016. Mechanistic studies on intramolecular C–H trifluoromethoxylation of (hetero) arenes via OCF 3-migration. Organic & biomolecular chemistry, 14(24), pp.5599-5605.

[61] Mair, B.A., Fouad, M.H., Ismailani, U.S., Munch, M. and Rotstein, B.H., 2020. Rhodium-catalyzed addition of organozinc iodides to carbon-11 isocyanates. Organic letters, 22(7),

pp.2746-2750.

[62] Rashed, M.N., Masuda, K., Ichitsuka, T., Koumura, N., Sato, K. and Kobayashi, S., 2021. Zirconium Oxide-Catalyzed Direct Amidation of Unactivated Esters under Continuous-Flow Conditions. Advanced Synthesis & Catalysis, 363(10), pp.2529-2535.

[63] Sen, A., Dhital, R.N., Sato, T., Ohno, A. and Yamada, Y.M., 2020. Switching from biaryl formation to amidation with convoluted polymeric nickel catalysis. ACS Catalysis, 10, pp.14410-14418.

[64] Fairley, M., Bole, L.J., Mulks, F.F., Main, L., Kennedy, A.R., O'Hara, C.T., García-Alvarez, J. and Hevia, E., 2020. Ultrafast amidation of esters using lithium amides under aerobic ambient temperature conditions in sustainable solvents. Chemical Science, 11(25), pp.6500-6509.

[65] Wang, Z., Matsumoto, A. and Maruoka, K., 2020. Efficient cleavage of tertiary amide bonds via radical–polar crossover using a copper (II) bromide/Selectfluor hybrid system. Chemical Science, 11(45), pp.12323-12328.

[66] Li, J.S., Xie, X.Y., Jiang, S., Yang, P.P., Li, Z.W., Lu, C.H. and Liu, W.D., 2021. Reagent-free aerobic oxidative synthesis of amides from aldehydes and isothiocyanates. Organic Chemistry Frontiers, 8(4), pp.697-701.

Chapter 7

Summary and conclusion

The bacterial infectious disease from mycobacterium and microbials are a major health concern worldwide. The treatment and management of bacterial infections have become more difficult since the appearance of drug-resistant strains of the disease.This has prompted scientists all around the world to work on creating new, fast-acting, and powerful antibiotics. Piperazine-isoniazid hybrids showed promising in *vitro* activity against antitubercular strains $H_{37}Rv$. Based on a survey of the literature, we have designed three series of phenyl piperazine hybrids with distinct biologically active chemical components and tested them against anti-TB strain $H_{37}Rv$ and broad range of antimicrobial gram positive and gram negative strains. Among all synthesised derivatives from first series (**chapter 3**), isoniazid and phenyl-piperazine together (compound **c8**) showed a synergistic effect of mycobacterial activity. The antimicrobial data concluded that, more modifications were required in order to achieve antibacterial activity.

In another series, hybrids of phenylpiperazine sulphonamide (**E1**-**E6**) and phenyl hydrazide (**F7**-**F19**) were synthesised and tested for antibacterial activity in this study.The SAR research found that the isoniazid moiety present in analogues **E1** and **E2** was effective against the $H_{37}Rv$ strain. Our antimicrobial experiments showed that **F10** was the most effective derivative against the bacterium *Enterococcus faecium*. In final series, using a variety of spectroscopy methods, we have effectively synthesised and described a small collection of new hybrid compounds. All freshly synthesised substances were also tested *in vitro* for their anti-mycobacterial action against the M. TB H37Rv strain. In-depth analysis of the trial data led to the conclusion that the combination molecules were less effective at fighting tuberculosis. Anti-tubercular drugs that are effective against both the ancestral and drug-resistant types of TB will require further changes to enhance activity.

Future Scope

Organic chemists will benefit from this study and the presented work because they will better understand the difficulties inherent in creating effective antimycobacterial and antimicrobial

compounds. The SAR study will help research to improve the activity against mycobacterium (*$H_{37}Rv$*) and microbial (*MRSA, Streptococcus pyrogens, Bacillus subtilis, Enterococcus faecium, Staphylococcus aureus, Enterobacter hormaechei, Pseudomonas aerugenosa*, and *Escherichia coli*) strains by bringing the different substitutions on presented active analogues. Additionally, the piperazine-isoniazid derivatives disclosed in this work showed potency against *$H_{37}Rv$* strain. This may help us for further development of similar derivatives against mycobacterium strain.

Furthermore, the approach described in this study on trans amidation could help researchers in the synthesis step of formylation, acetylation, and benzoylation without the use of any hazardous metal catalyst or hazardous reagent.

APPENDEX-I (Chapter-3 supplementary information)

IR, NMR and Mass Spectrum of compounds c1-c15

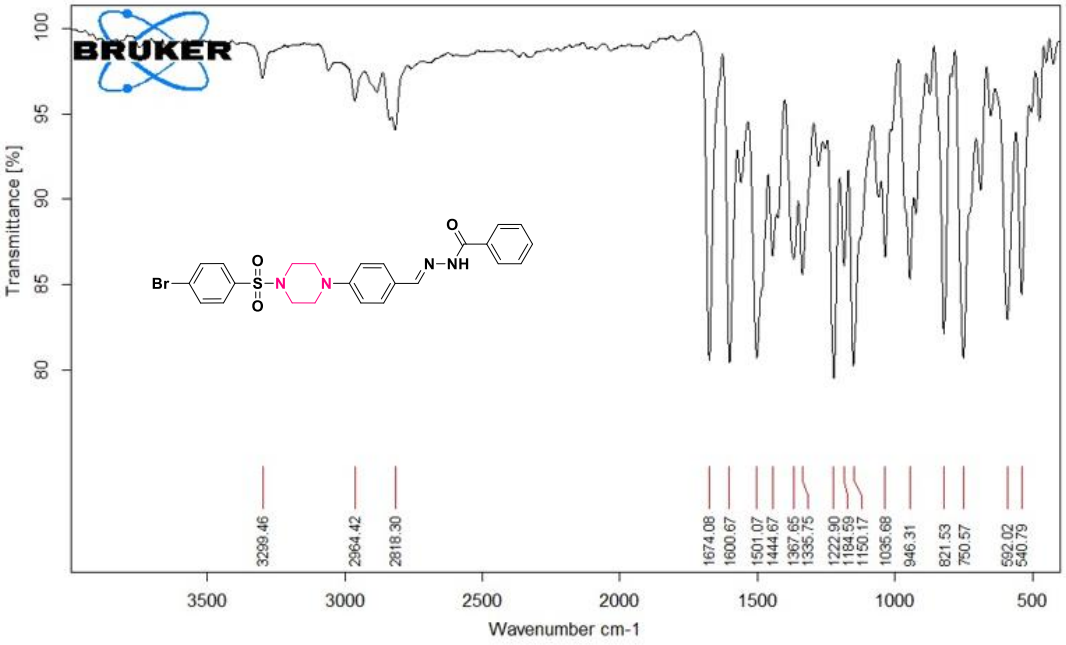

IR spectrum of compound c1(Chapter 3)

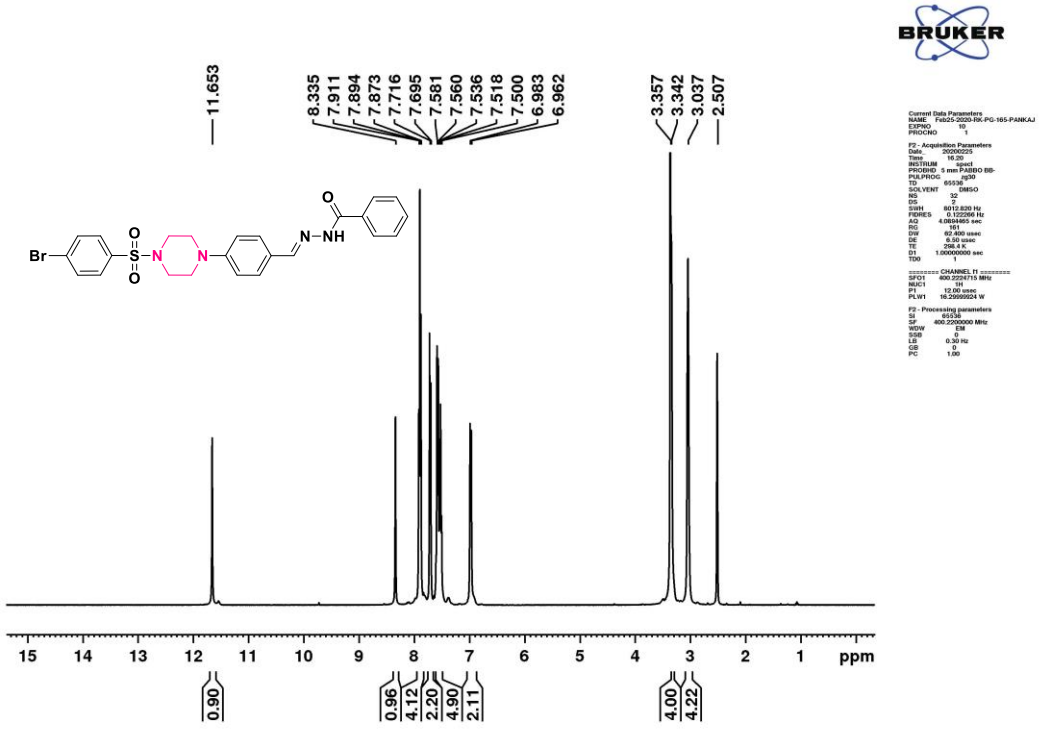

^{1}H NMR spectrum of compound c1(Chapter 3)

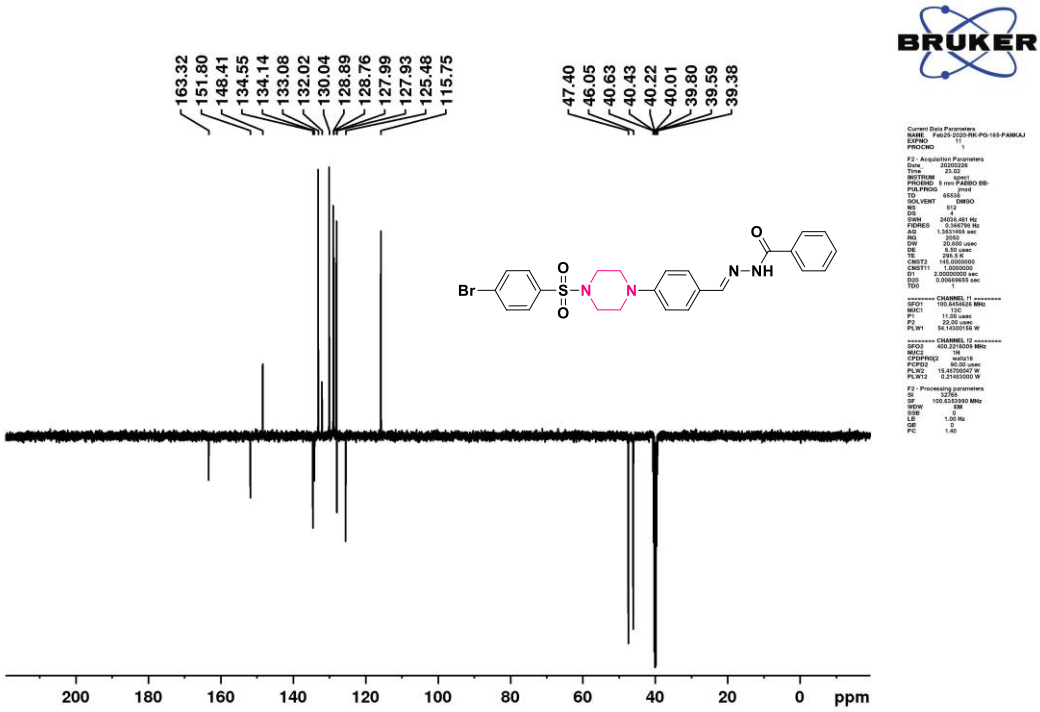

^{13}C NMR spectrum of compound c1(Chapter 3)

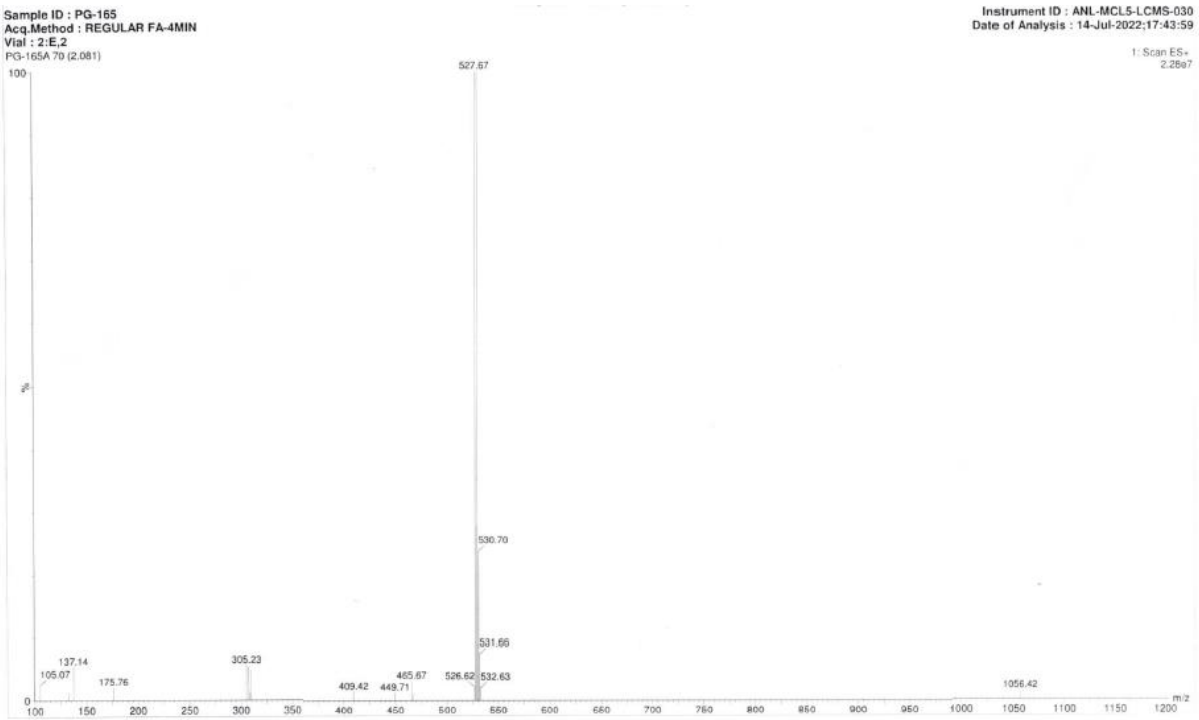

Mass spectrum of compound c1(Chapter 3)

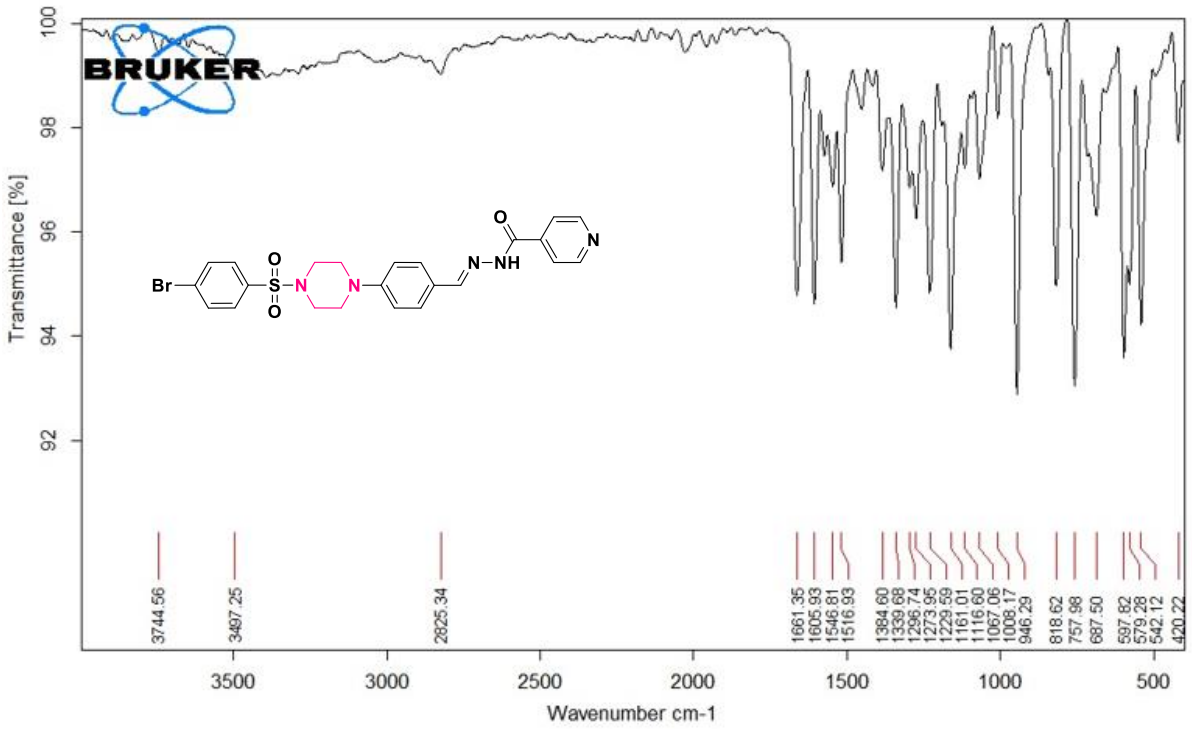

IR spectrum of compound c2(Chapter 3)

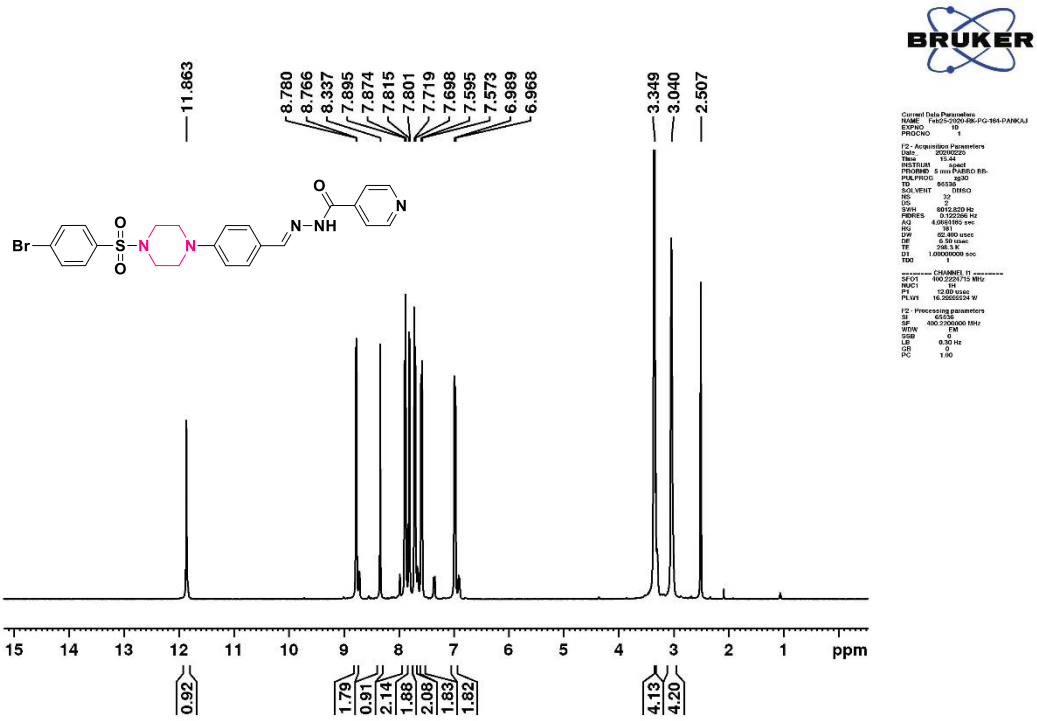

^{1}H NMR spectrum of compound c2(Chapter 3)

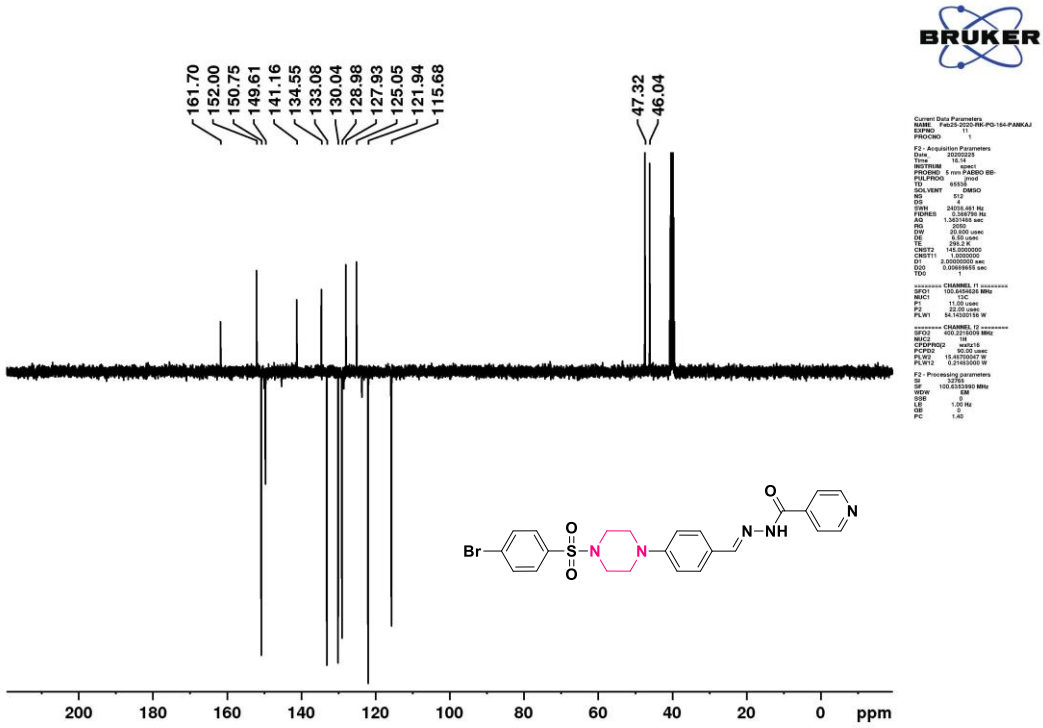

^{13}C NMR spectrum of compound c2(Chapter 3)

Peak#:3 R.Time:1.452(Scan#:441)
MassPeaks:319 Polarity:Positive
Spectrum Mode:Averaged 1.442-1.455(439-443)
BG Mode:Calc Segment 1 - Event 1

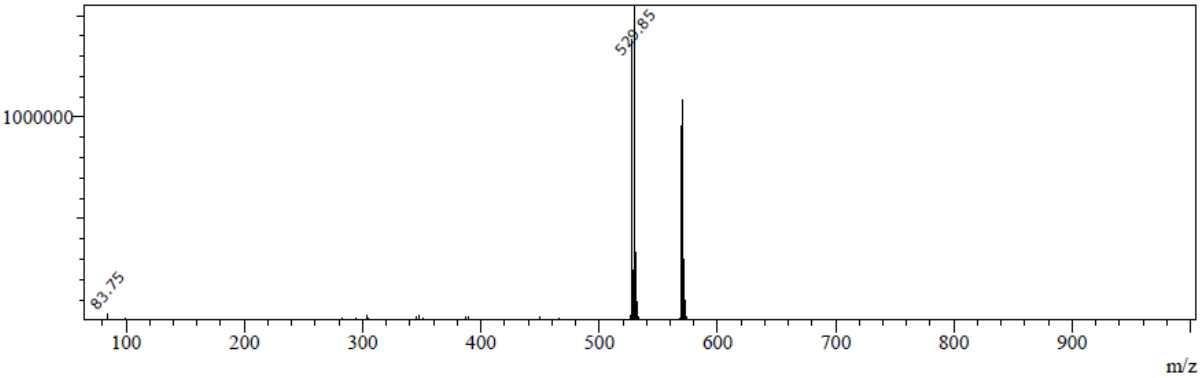

Mass spectrum of compound c2(Chapter 3)

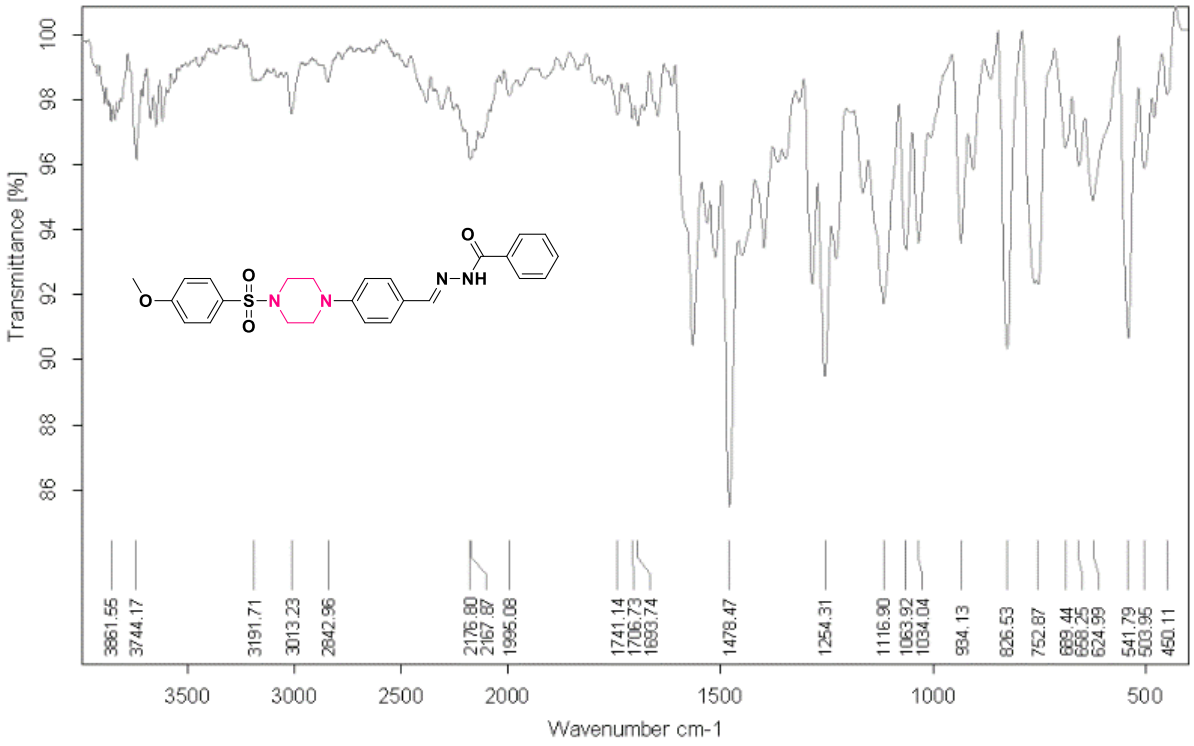

IR spectrum of compound c3(Chapter 3)

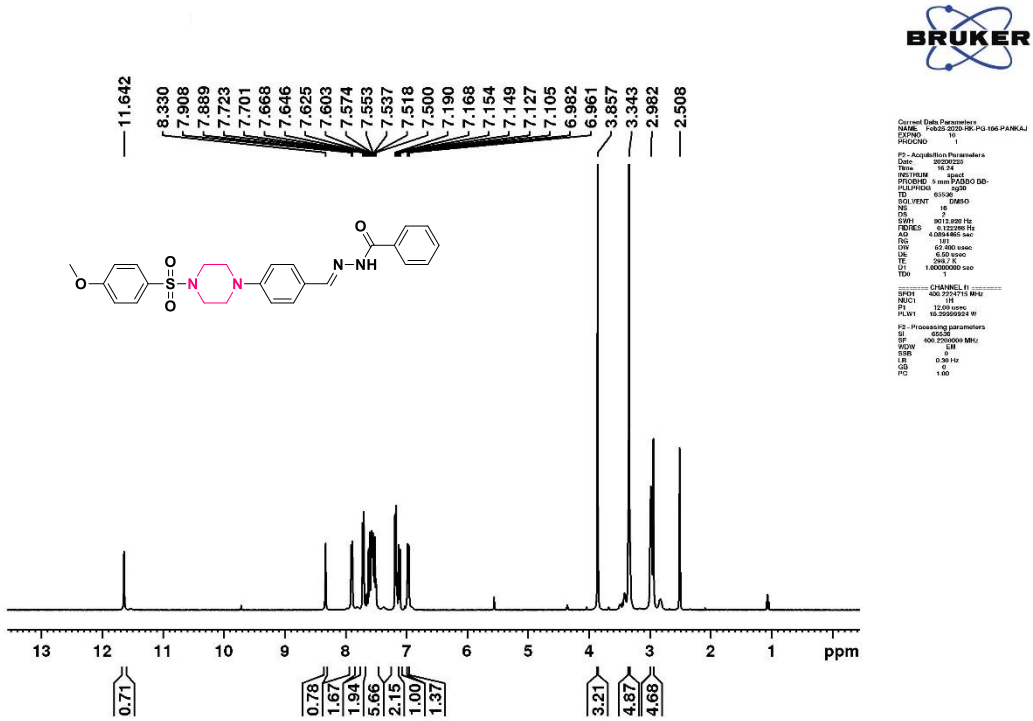

^{1}H NMR spectrum of compound c3(Chapter 3)

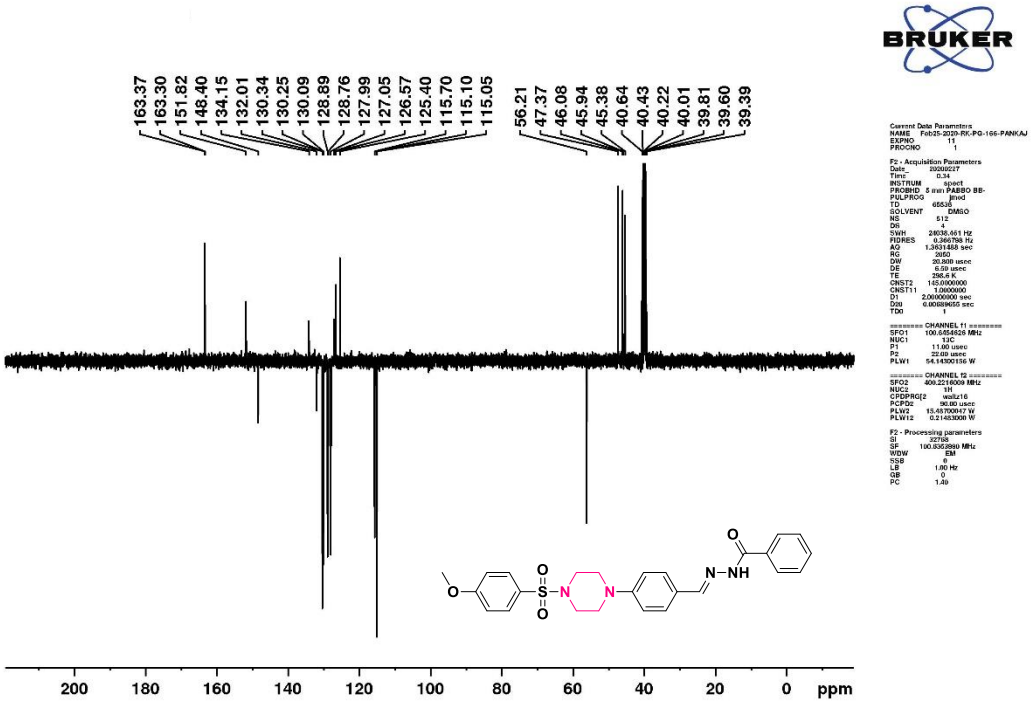

^{13}C NMR spectrum of compound c3(Chapter 3)

Peak#:1 R.Time:1.357(Scan#:413)
MassPeaks:356 Polarity:Positive
Spectrum Mode:Averaged 1.348-1.362(411-415)
BG Mode:Calc Segment 1 - Event 1

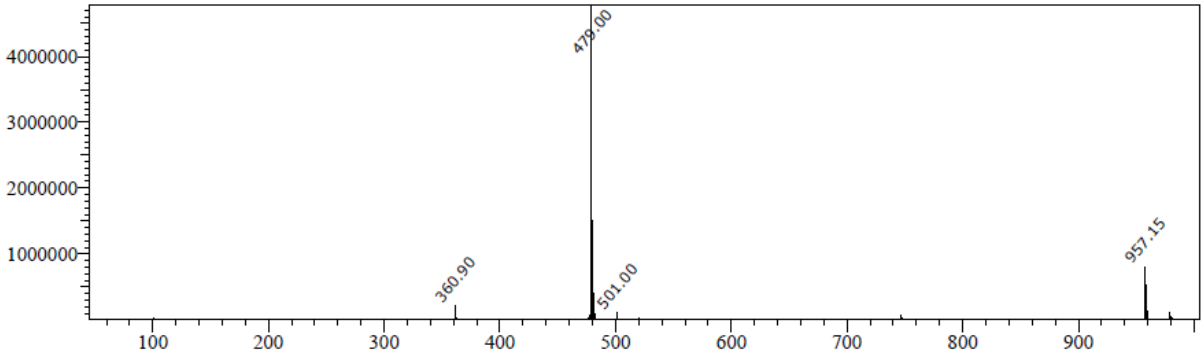

Mass spectrum of compound c3(Chapter 3)

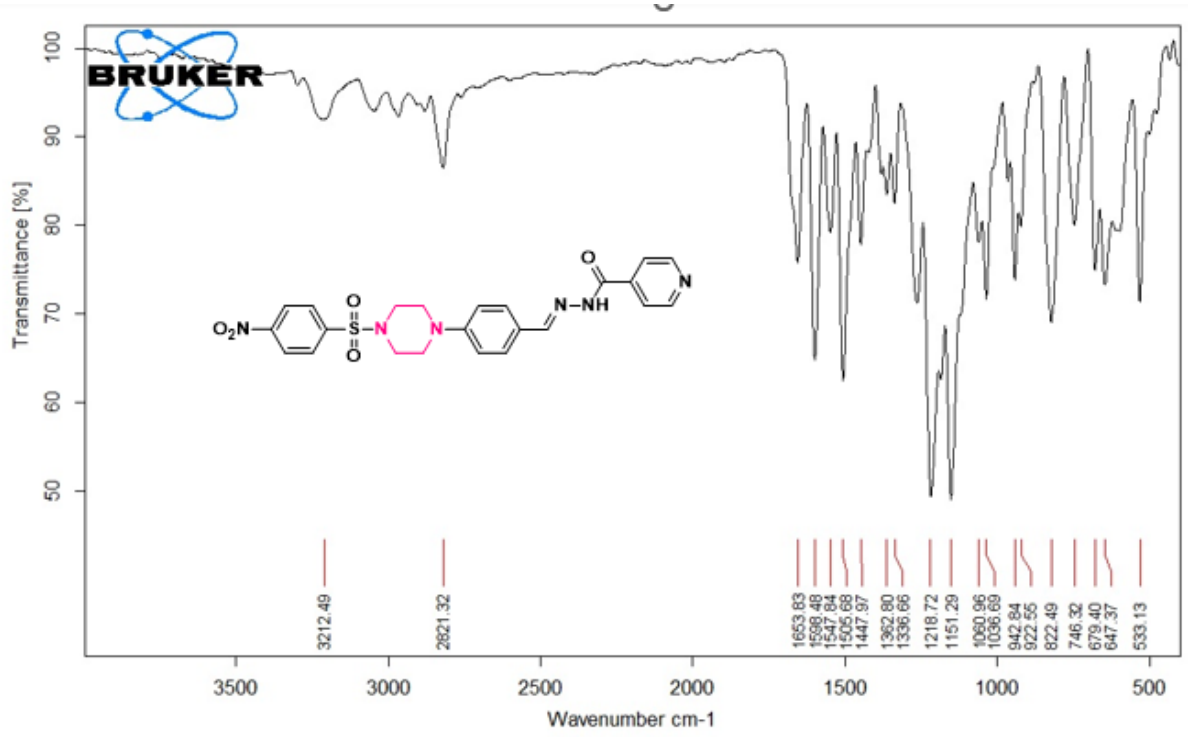

IR spectrum of compound c4(Chapter 3)

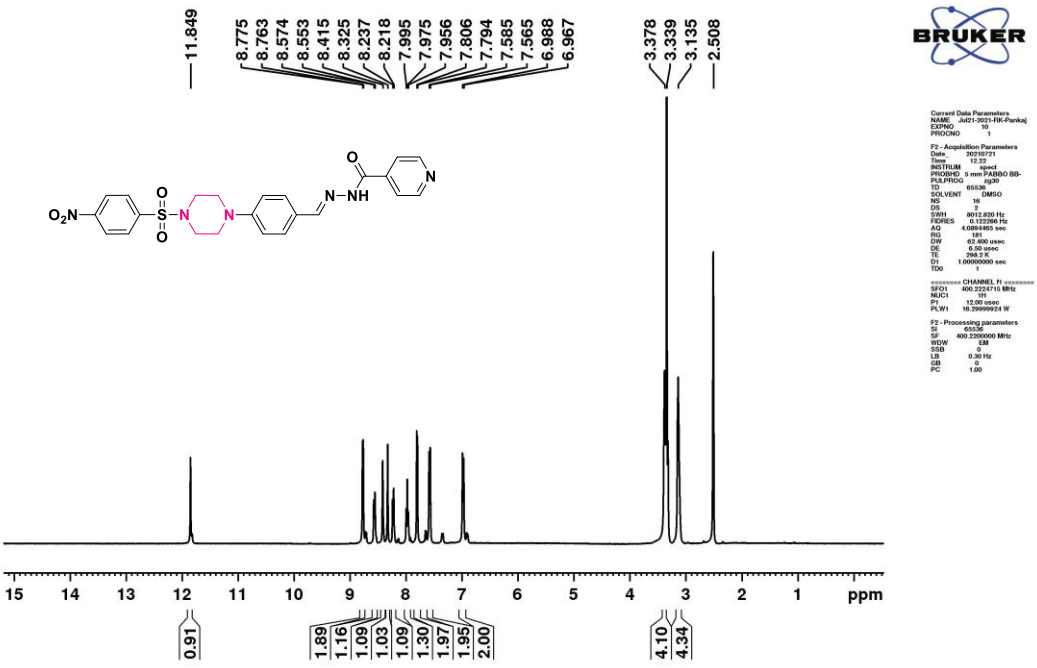

^{1}H NMR spectrum of compound c4(Chapter 3)

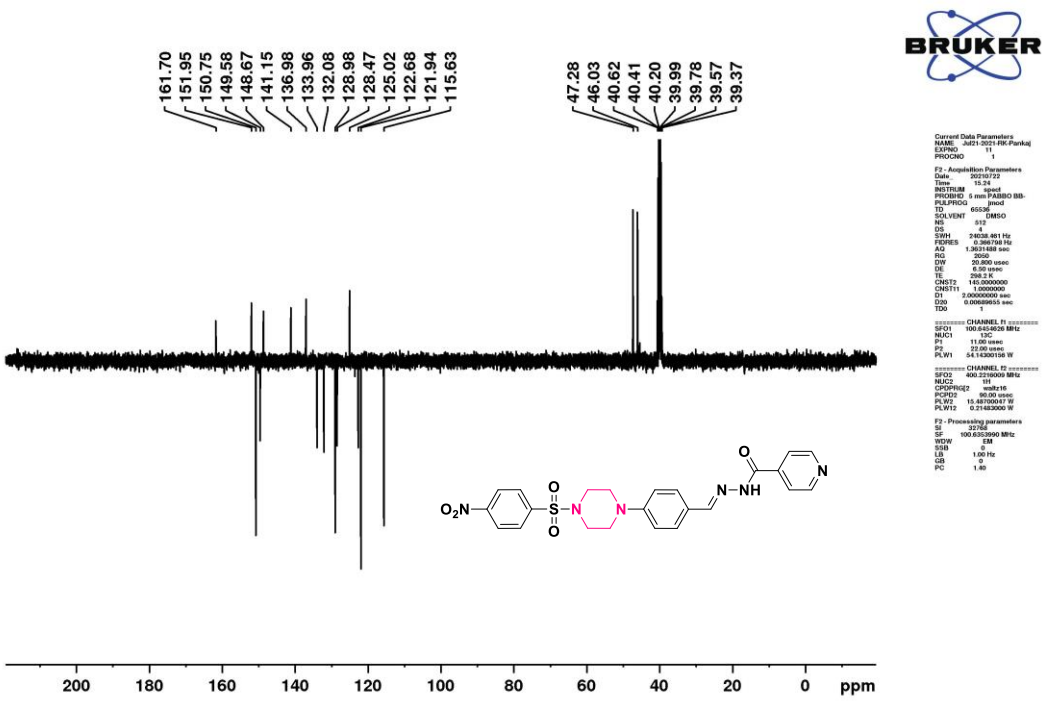

^{13}C NMR spectrum of compound c4(Chapter 3)

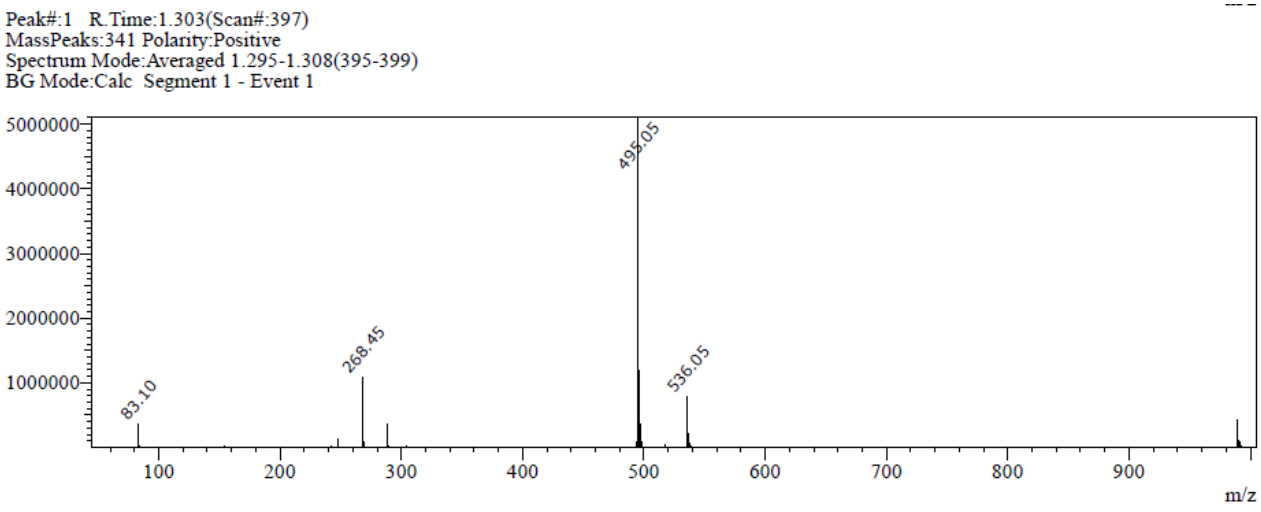

Mass spectrum of compound c4(Chapter 3)

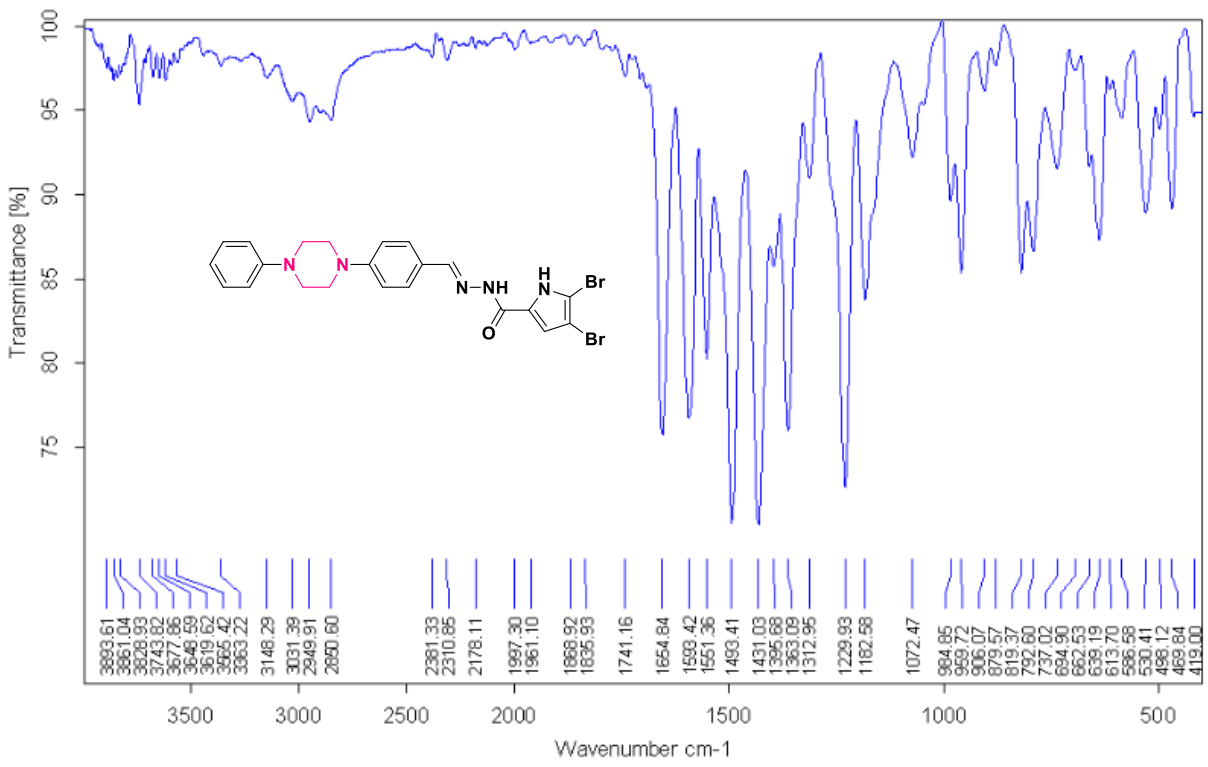

[1]H NMR spectrum of compound c5(Chapter 3)

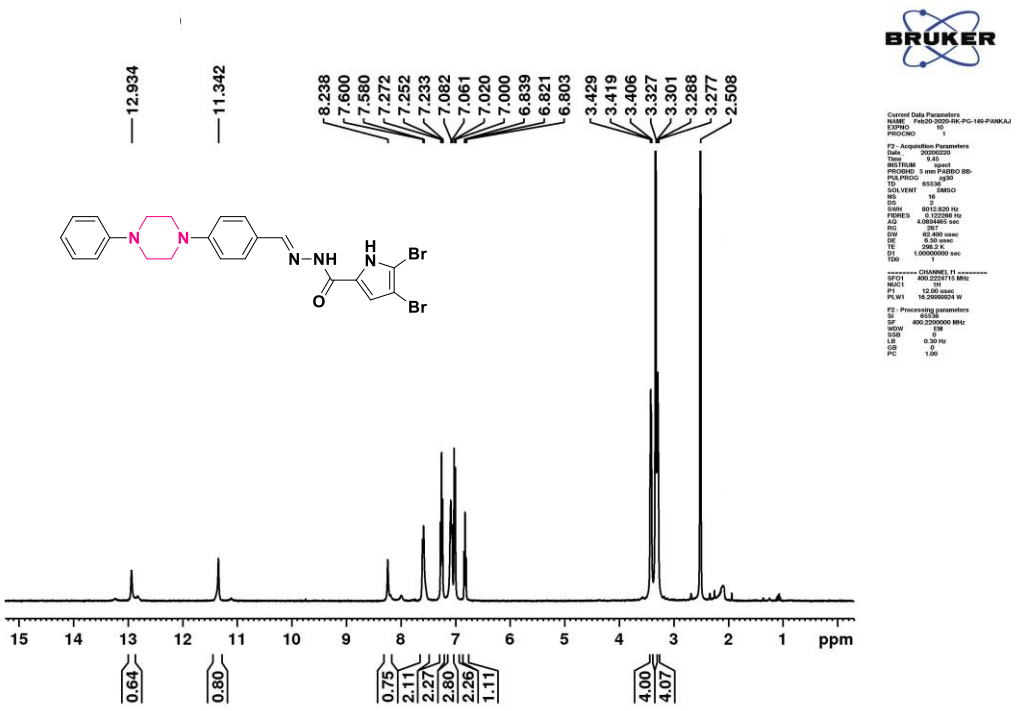

[1]H NMR spectrum of compound c5(Chapter 3)

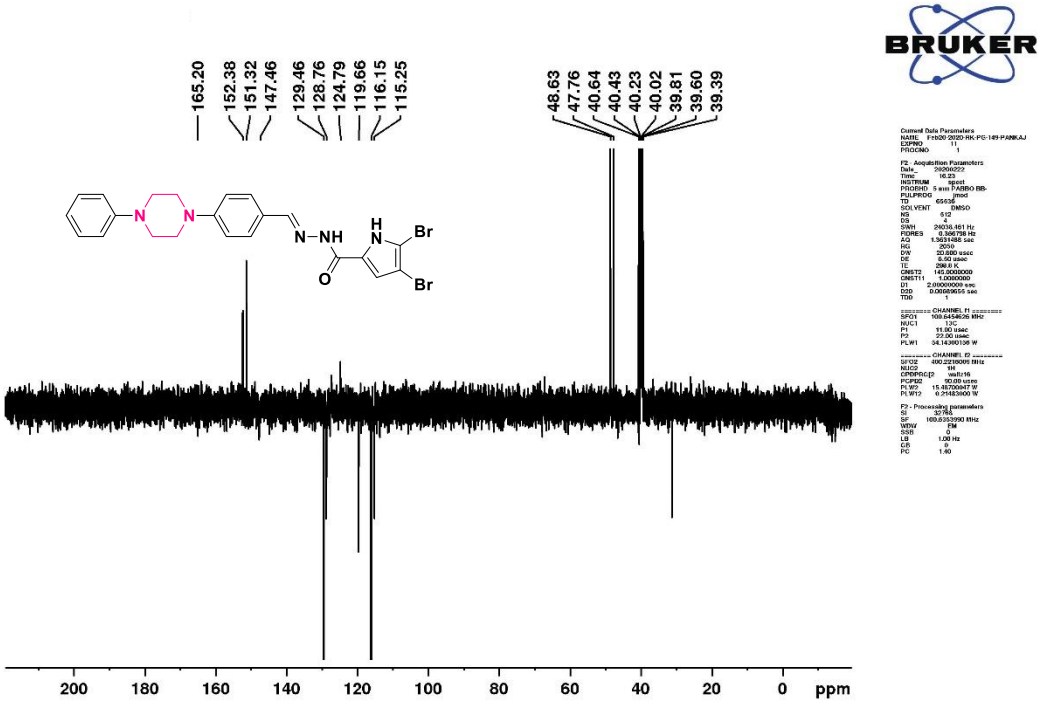

^{13}C NMR spectrum of compound c5(Chapter 3)

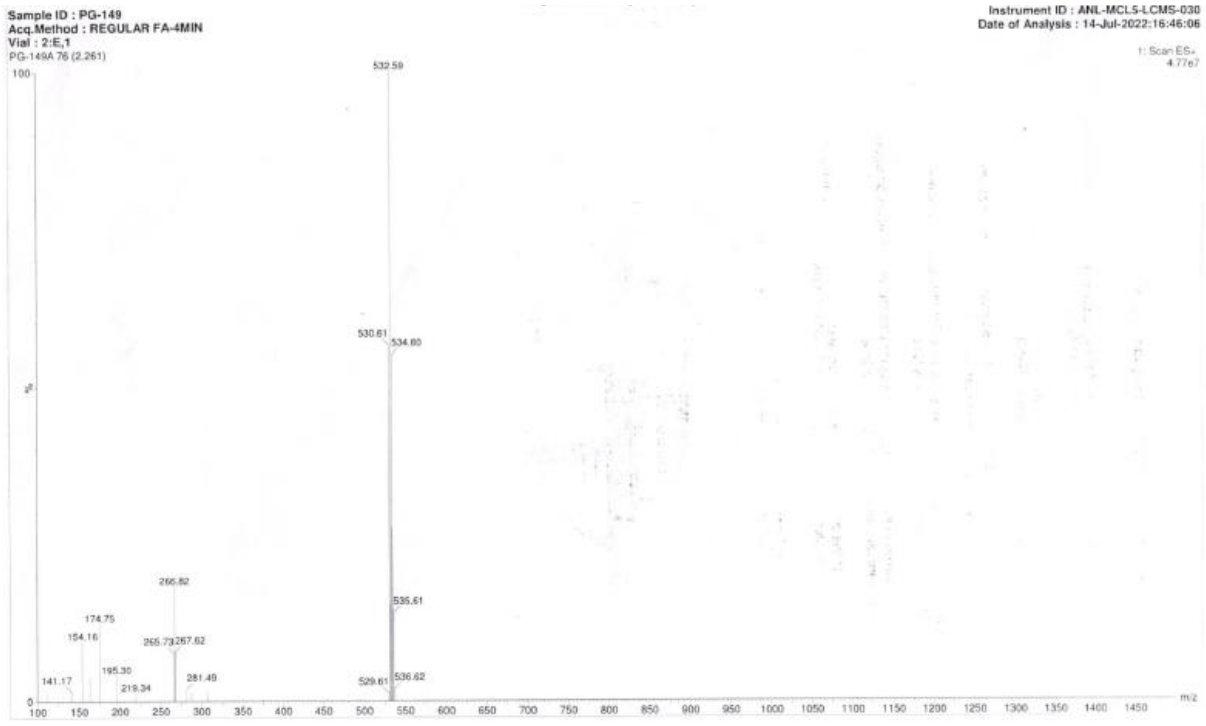

Mass spectrum of compound c5(Chapter 3)

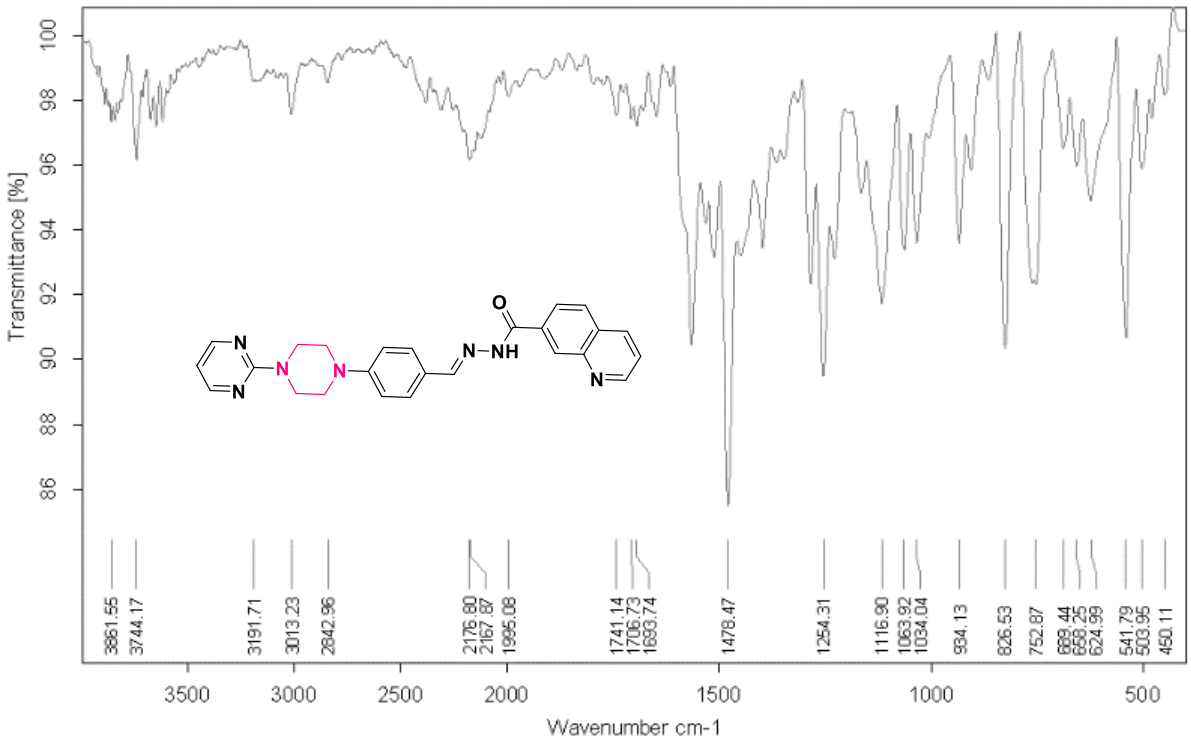

IR spectrum of compound c6(Chapter 3)

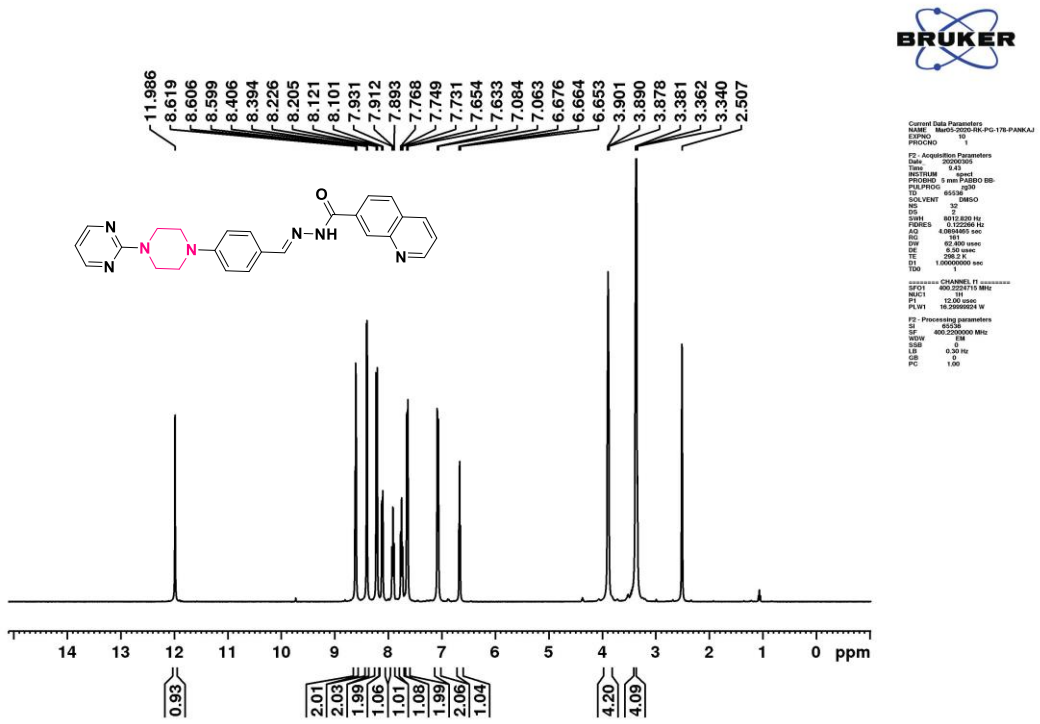

^{1}H NMR spectrum of compound c6(Chapter 3)

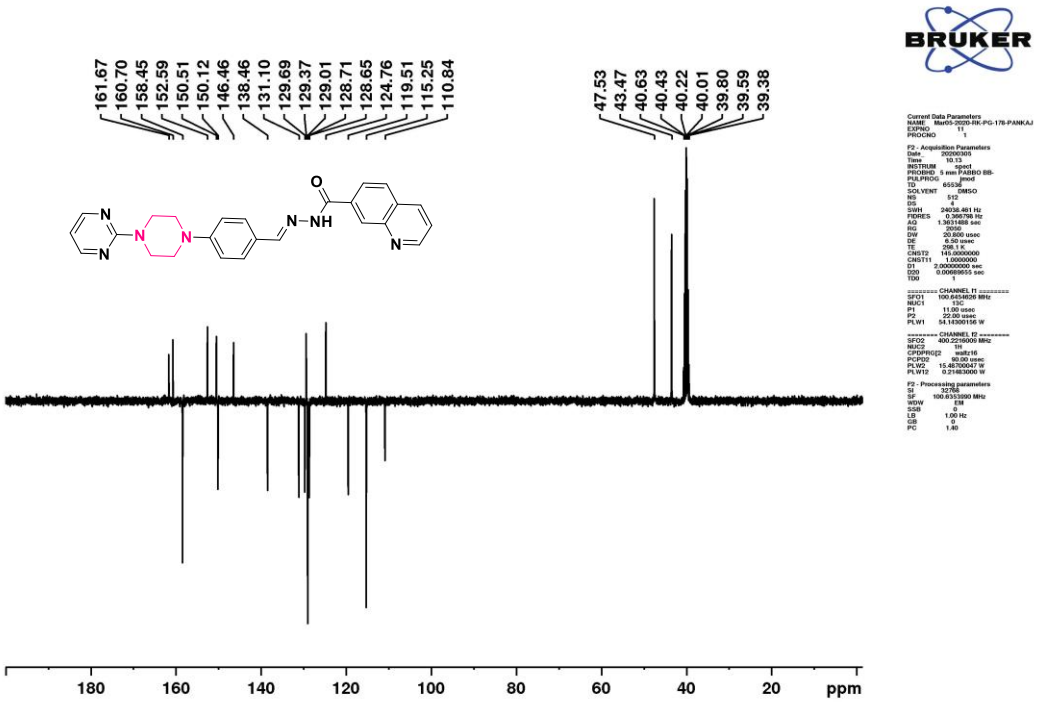

^{13}C NMR spectrum of compound c6(Chapter 3)

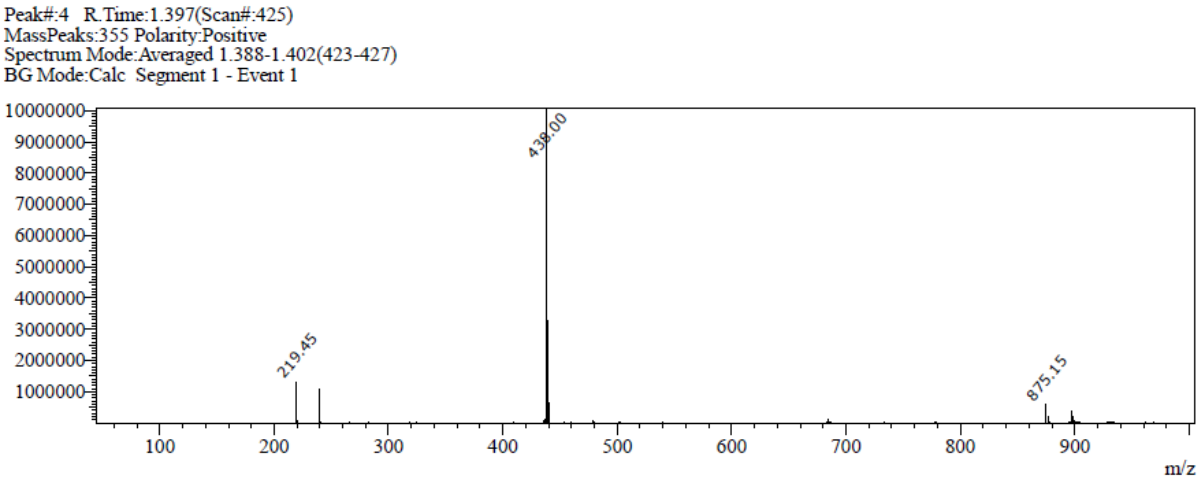

Mass spectrum of compound c6(Chapter 3)

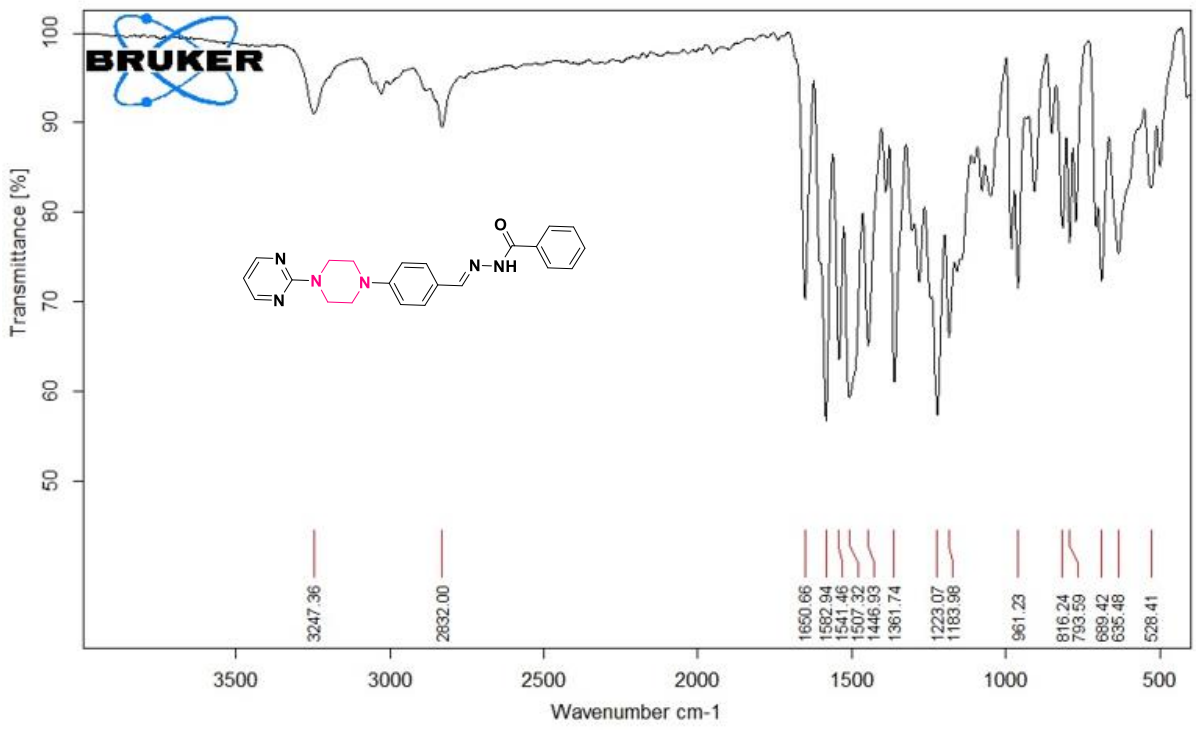

IR spectrum of compound c7(Chapter 3)

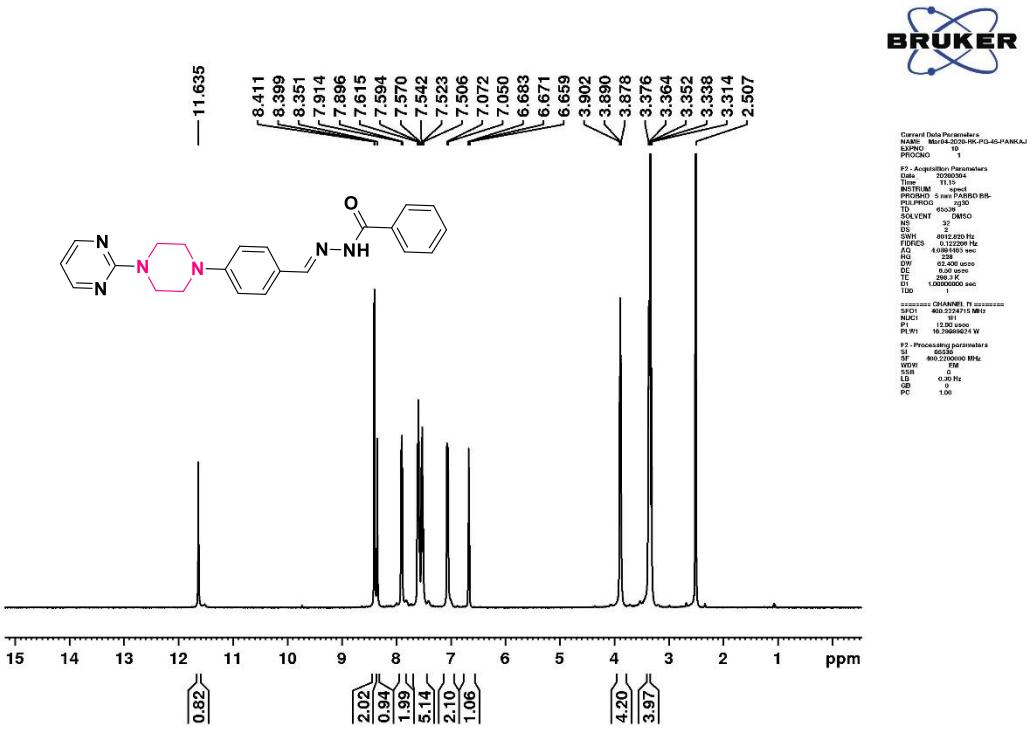

^{1}H NMR spectrum of compound c7(Chapter 3)

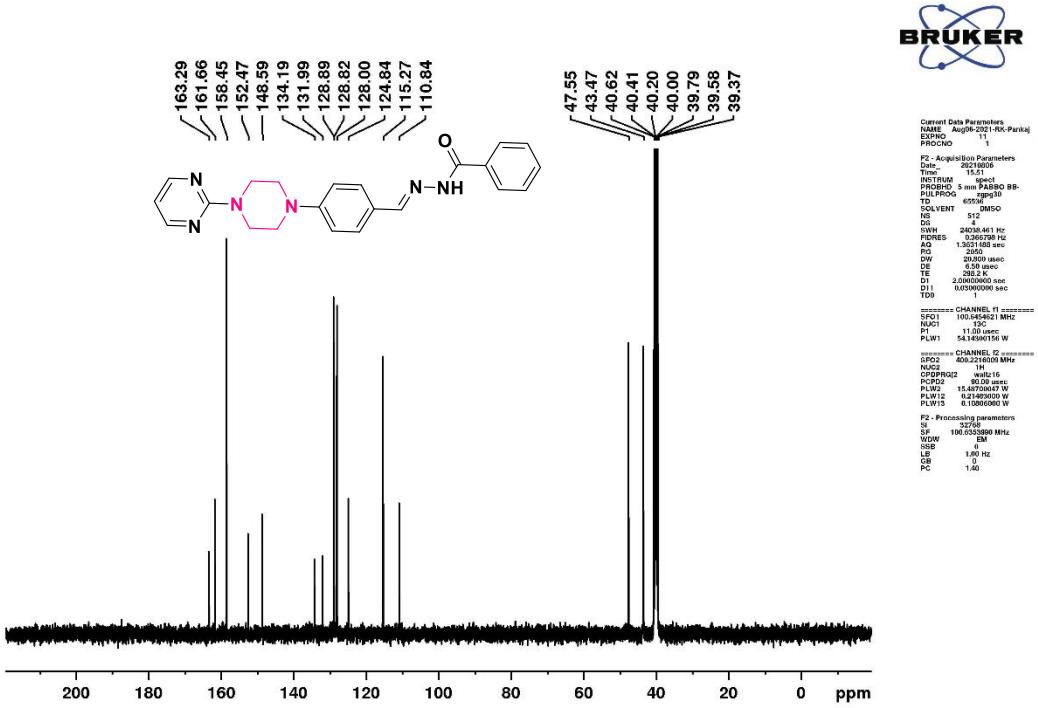

^{13}C NMR spectrum of compound c7(Chapter 3)

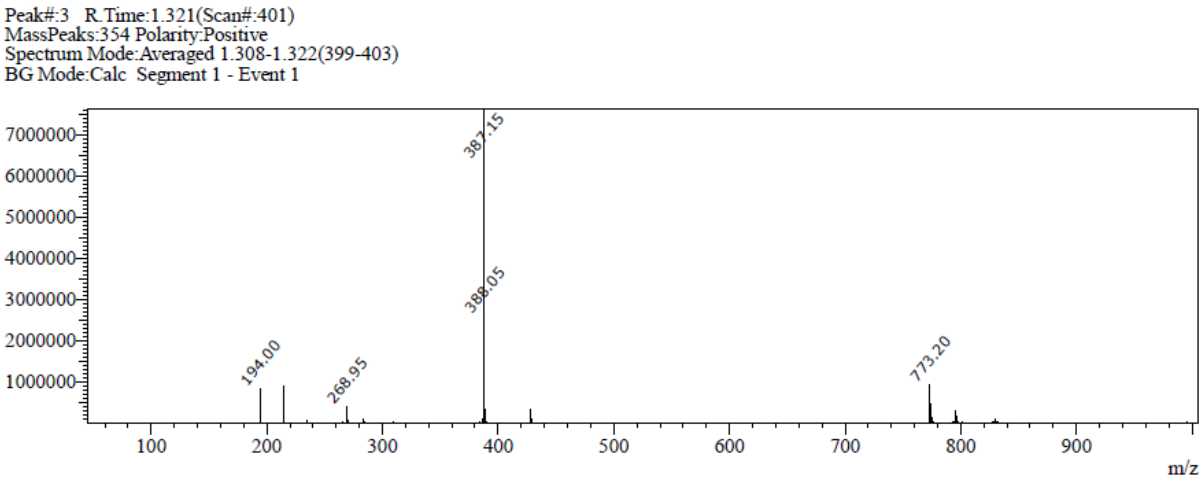

Mass spectrum of compound c7(Chapter 3)

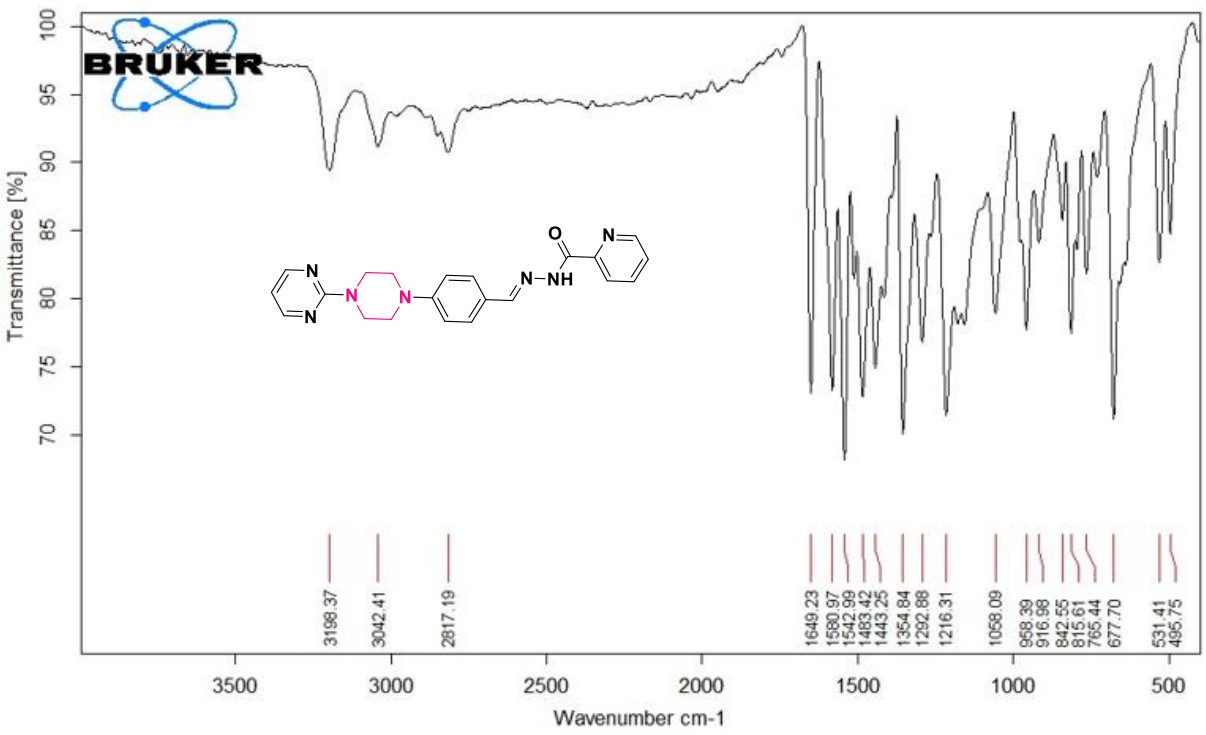

IR spectrum of compound c8(Chapter 3)

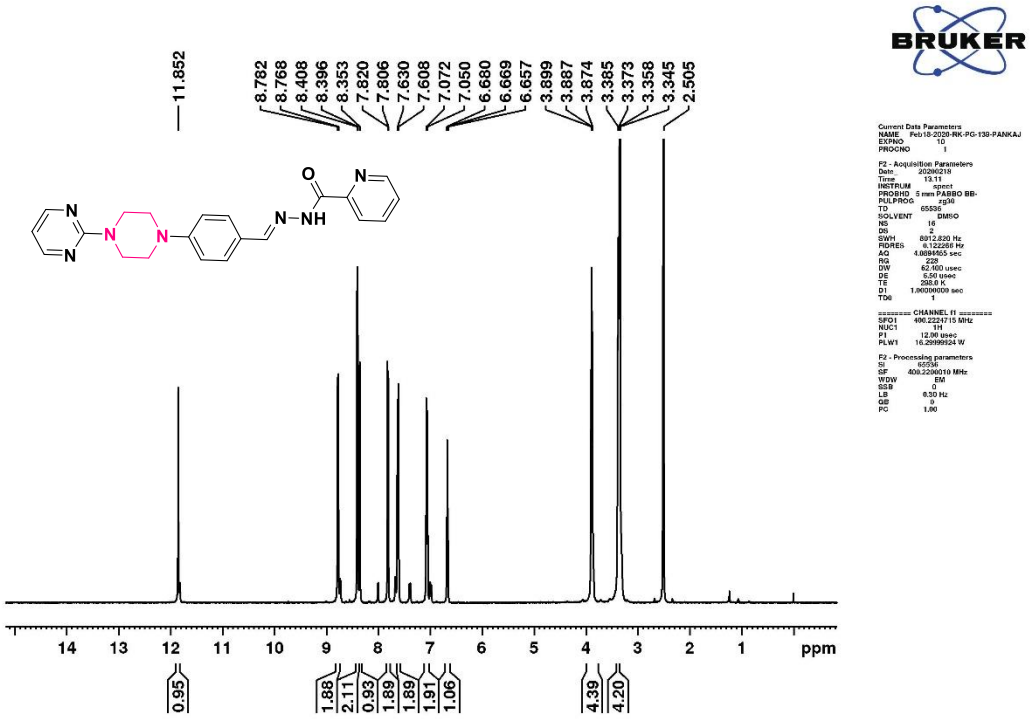

^{1}H NMR spectrum of compound c8(Chapter 3)

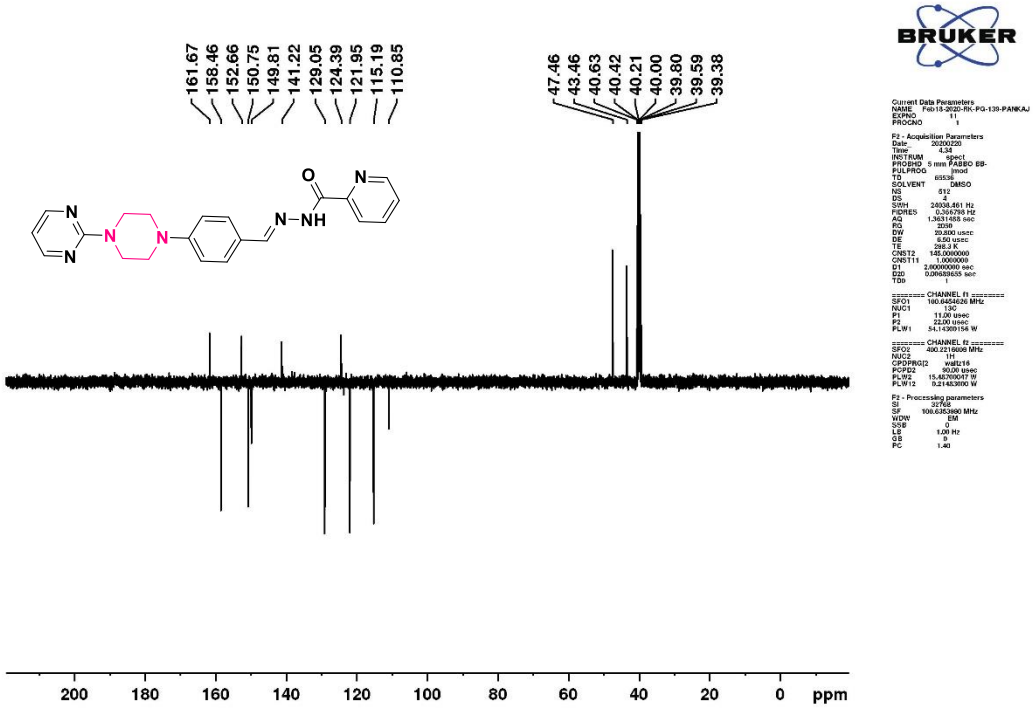

^{13}C NMR spectrum of compound c8(Chapter 3)

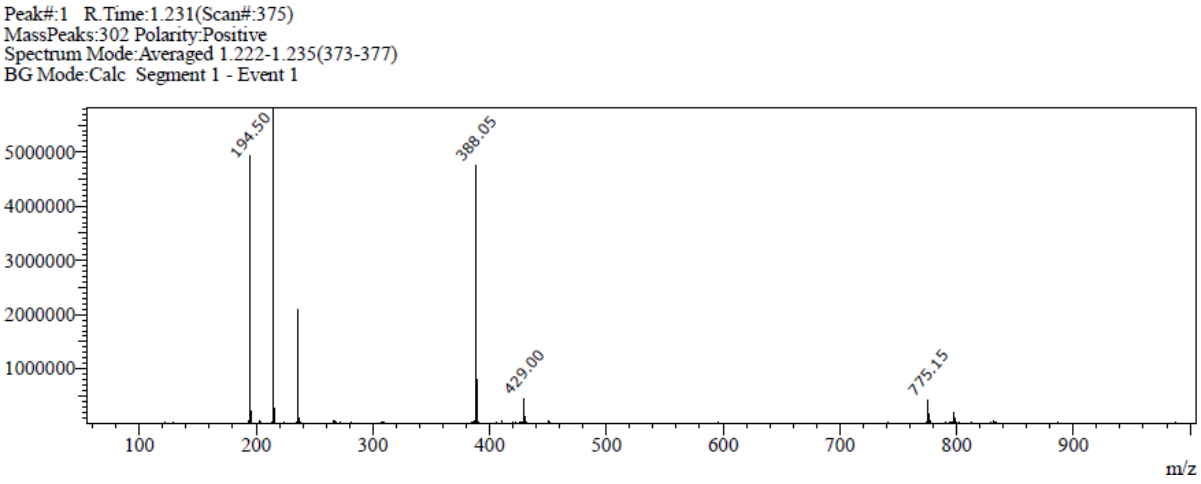

Mass spectrum of compound c8(Chapter 3)

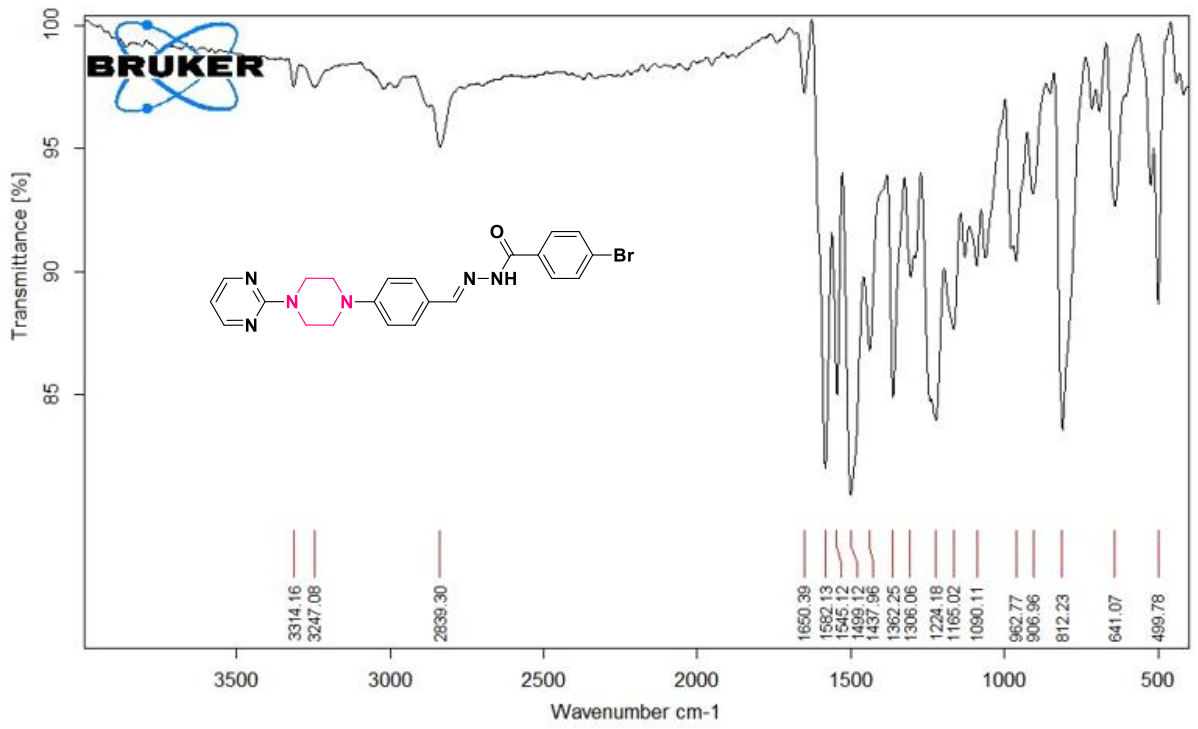

IR spectrum of compound c9(Chapter 3)

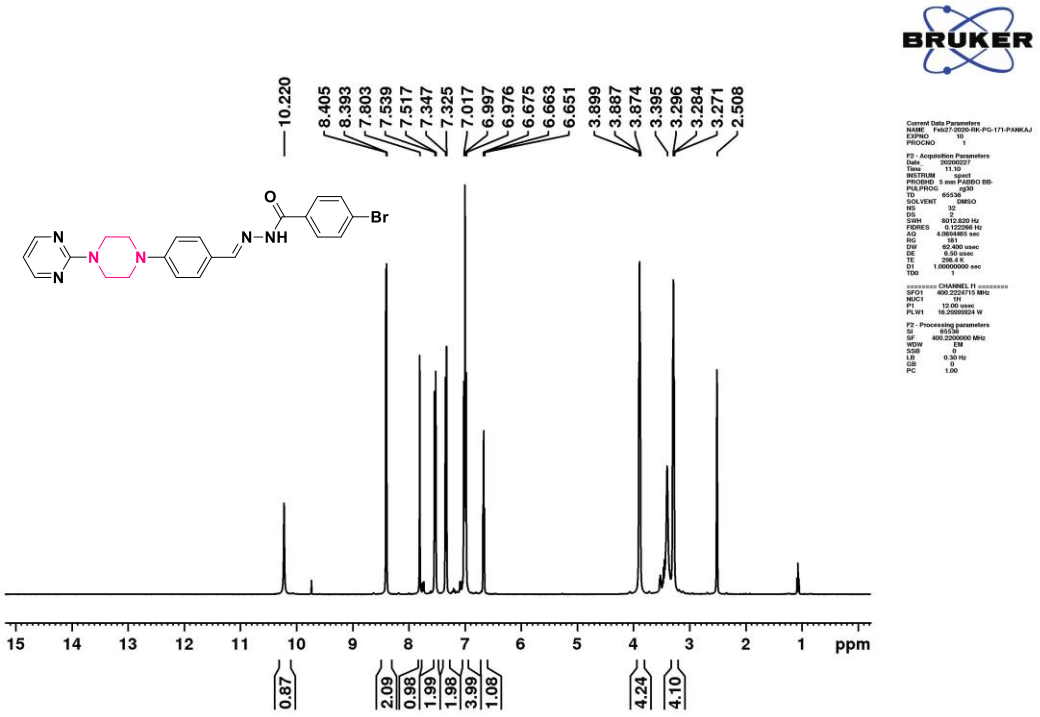

^{1}H NMR spectrum of compound c9(Chapter 3)

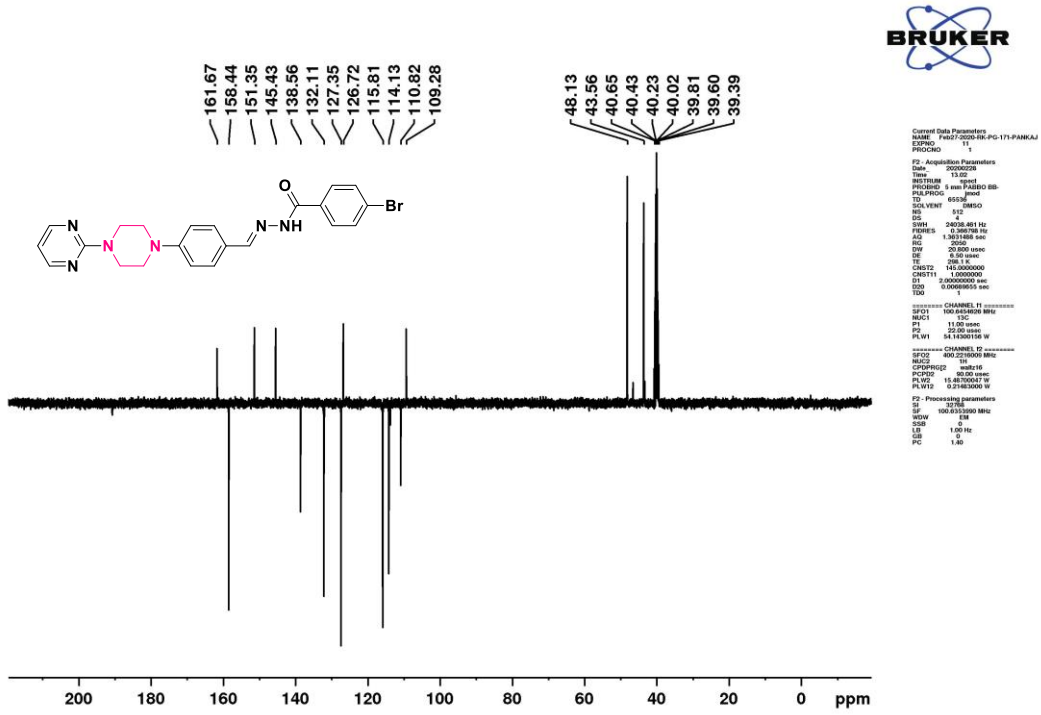

^{13}C NMR spectrum of compound c9(Chapter 3)

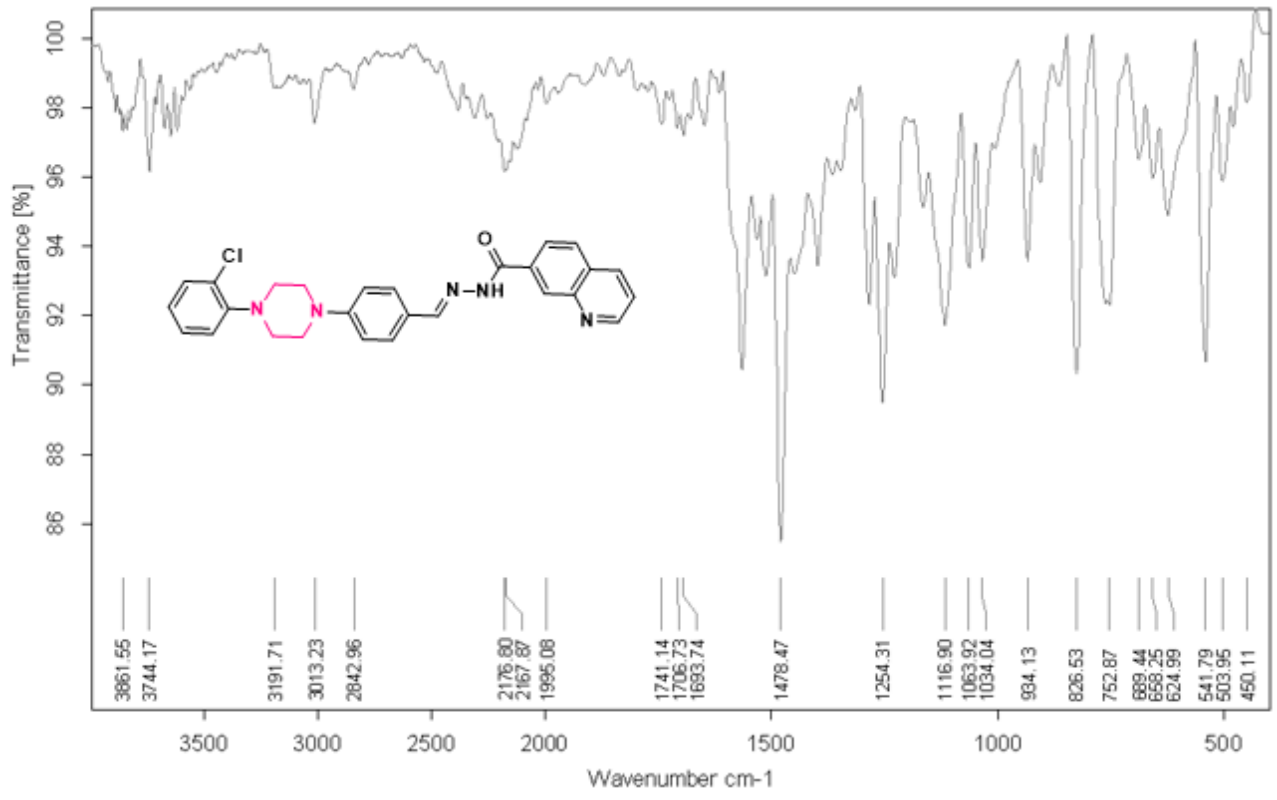

IR spectrum of compound c10(Chapter 3)

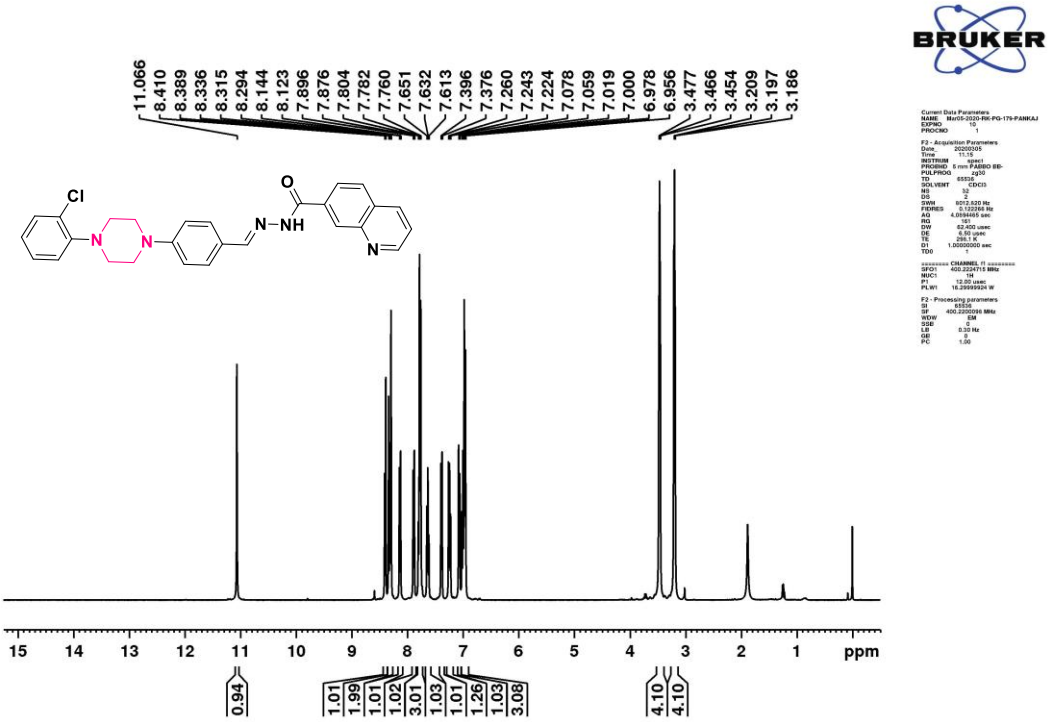

^{1}H NMR spectrum of compound c10(Chapter 3)

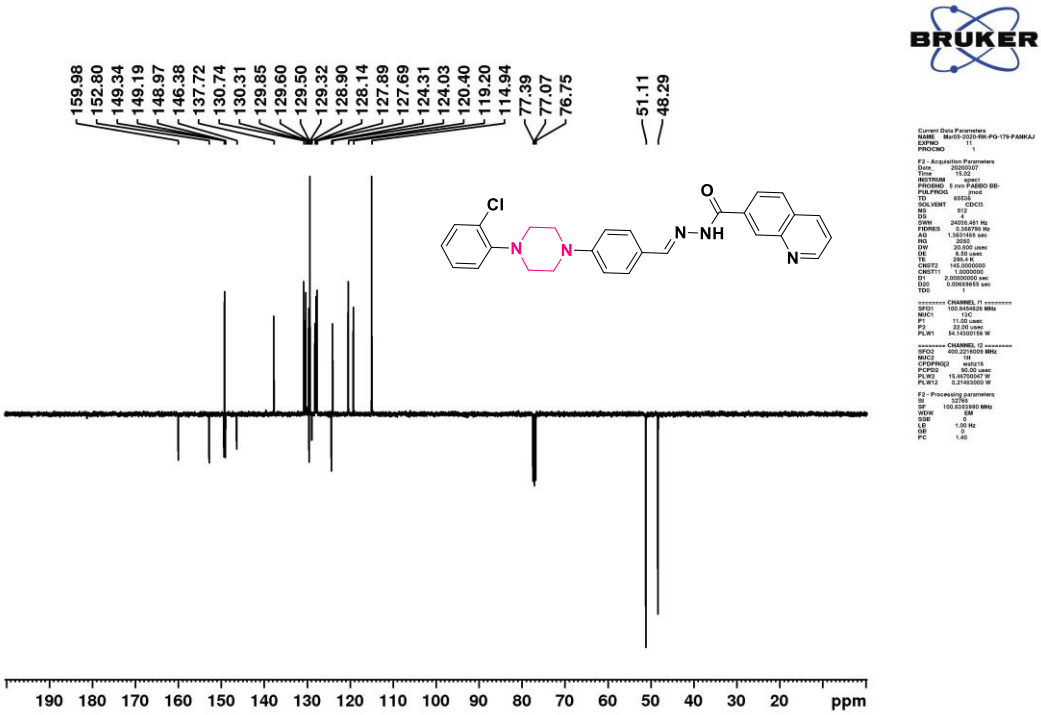

^{13}C NMR spectrum of compound c10(Chapter 3)

c11

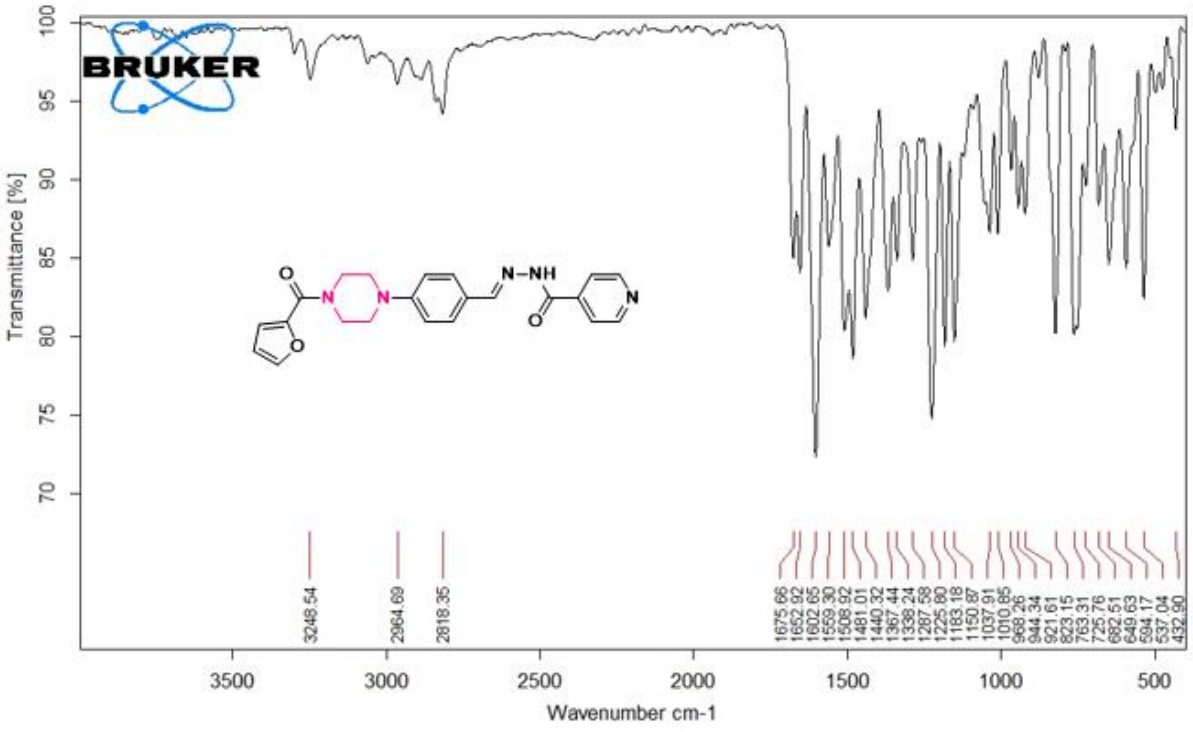

IR spectrum of compound c11.

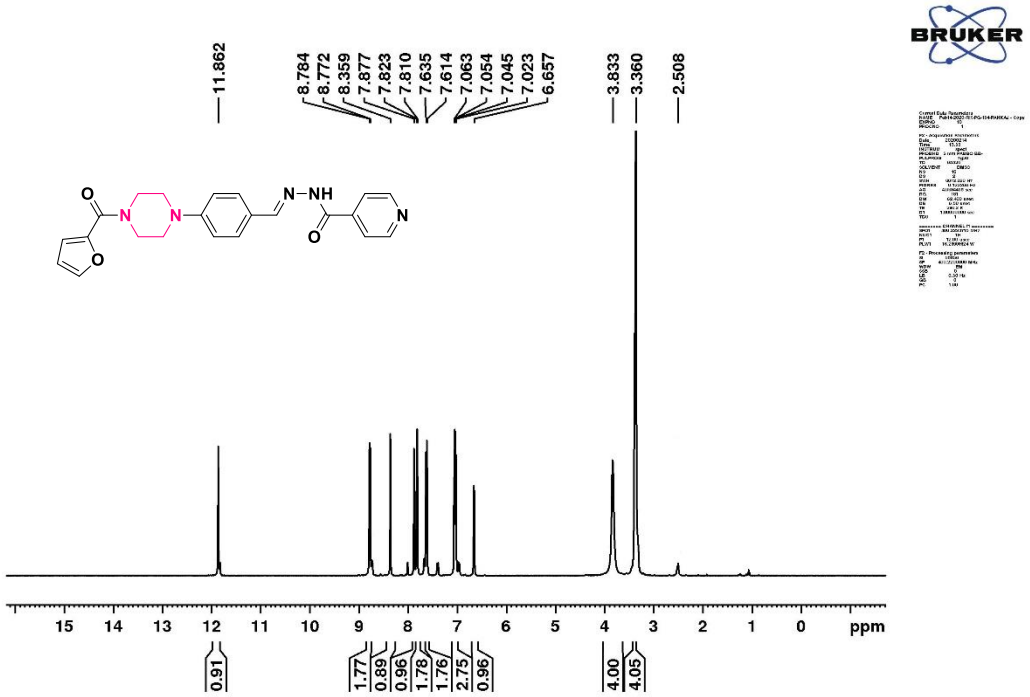

^{1}H NMR spectrum of compound c11(Chapter 3)

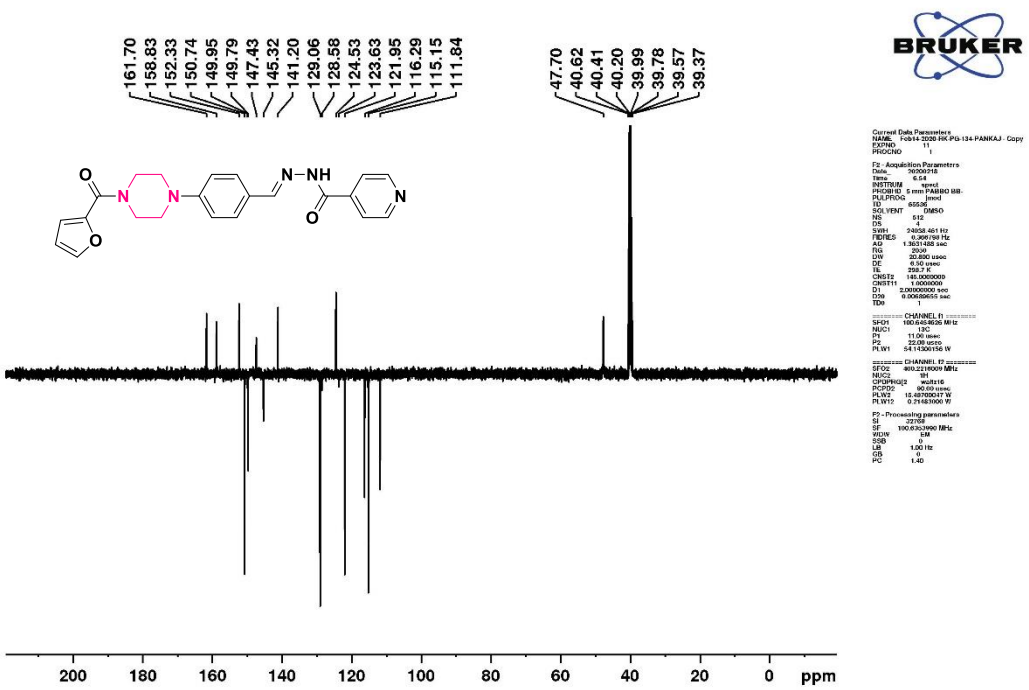

^{13}CNMR spectrum of compound c11(Chapter 3)

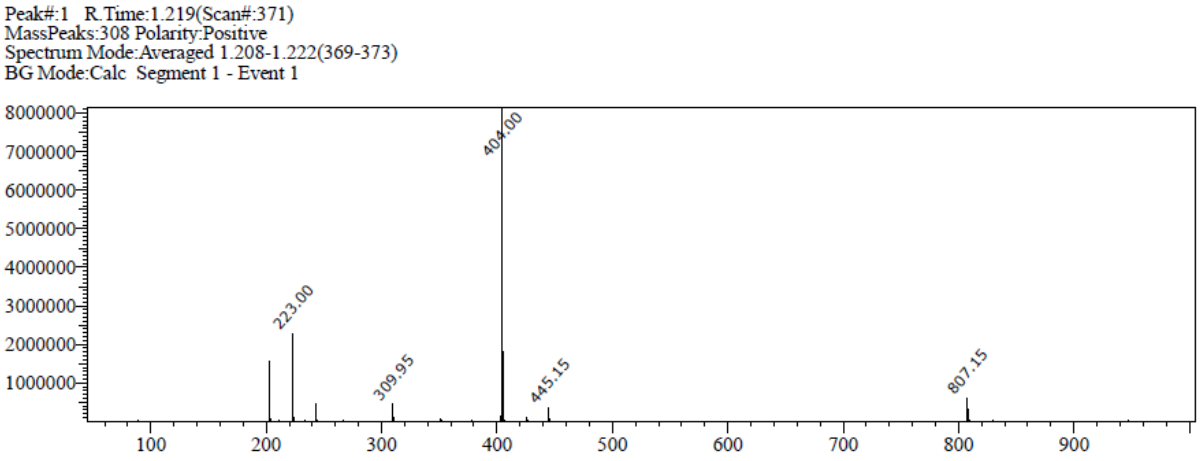

Mass spectrum of compound c11(Chapter 3)

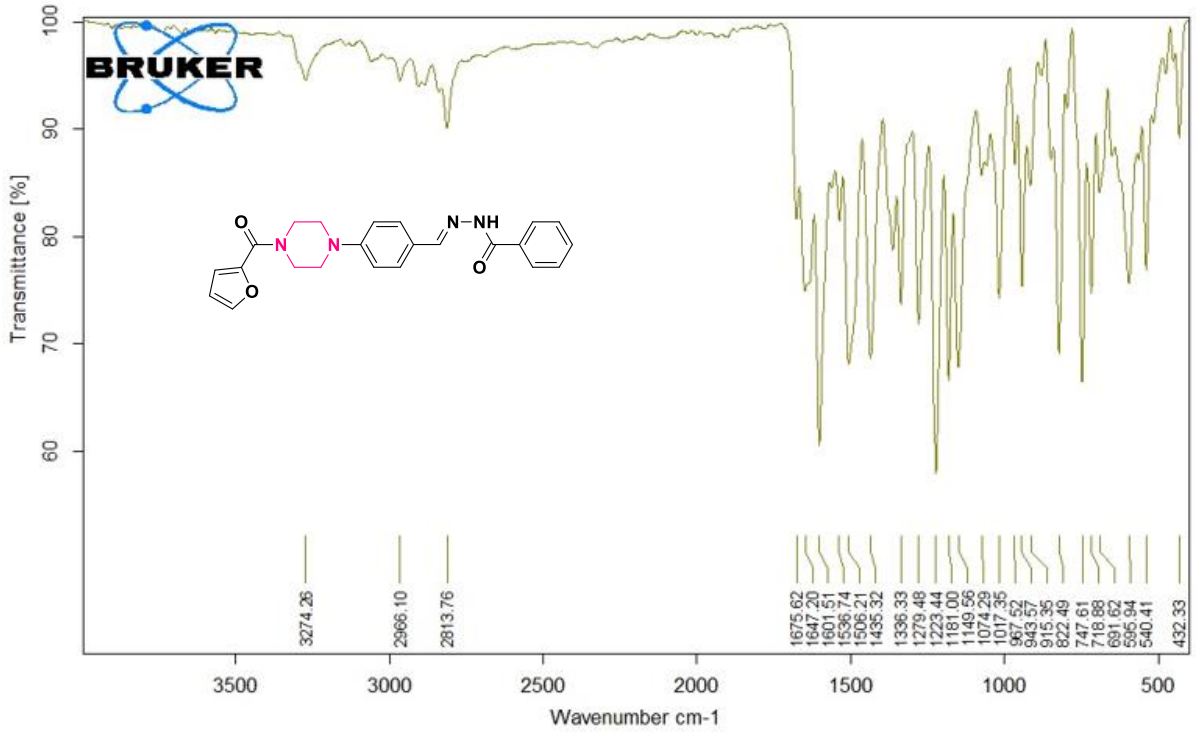

IR spectrum of compound c12(Chapter 3)

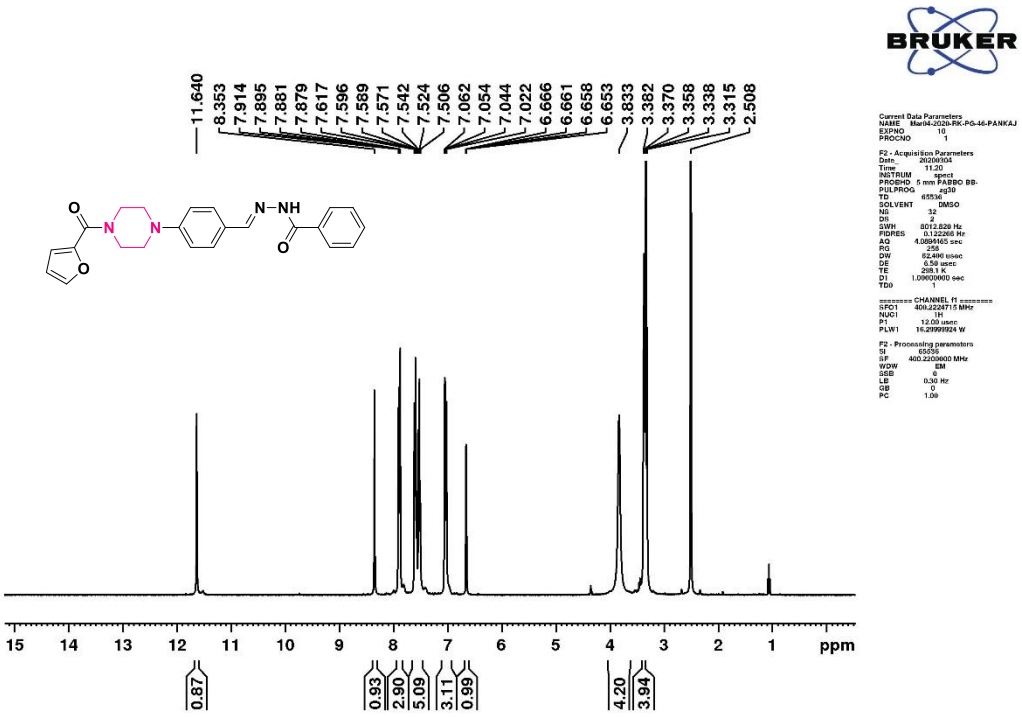

^{1}H NMR spectrum of compound c12(Chapter 3)

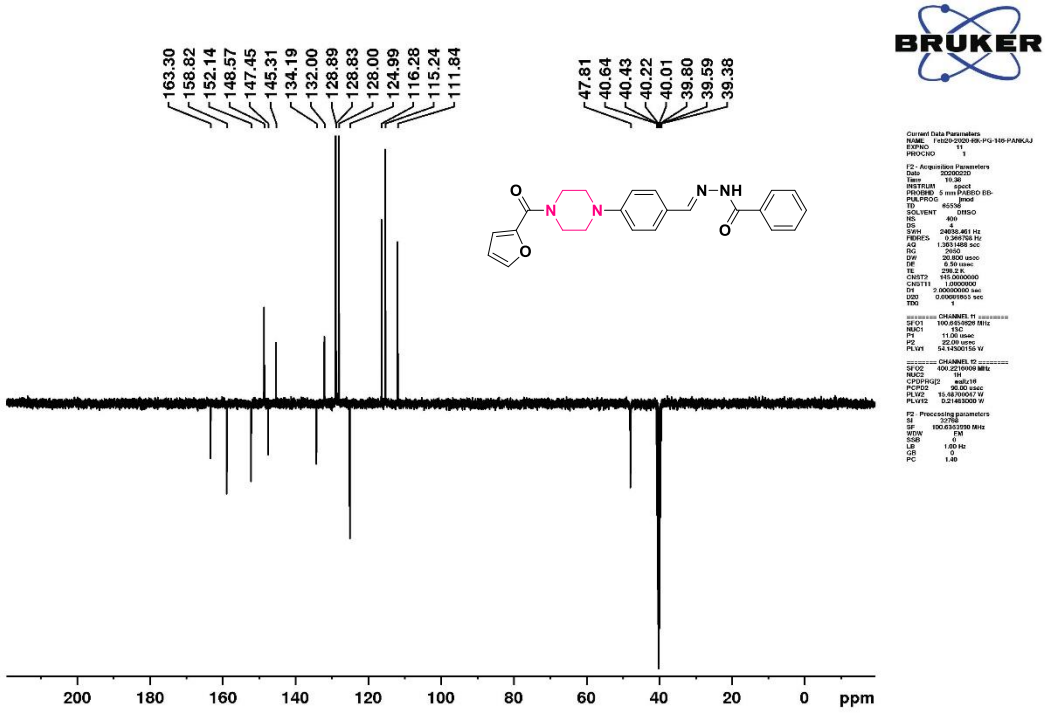

^{13}C NMR spectrum of compound c12(Chapter 3)

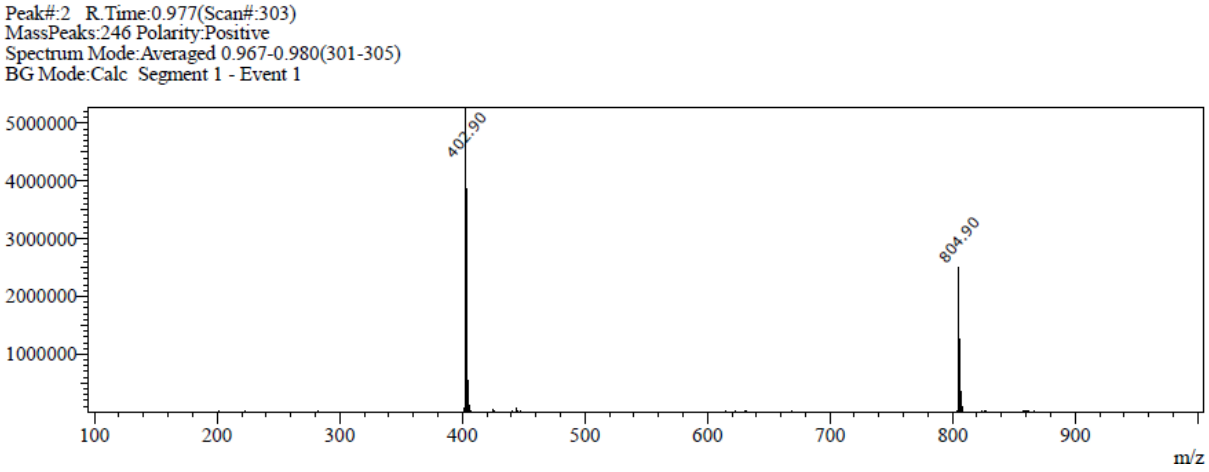

Mass spectrum of compound c12(Chapter 3)

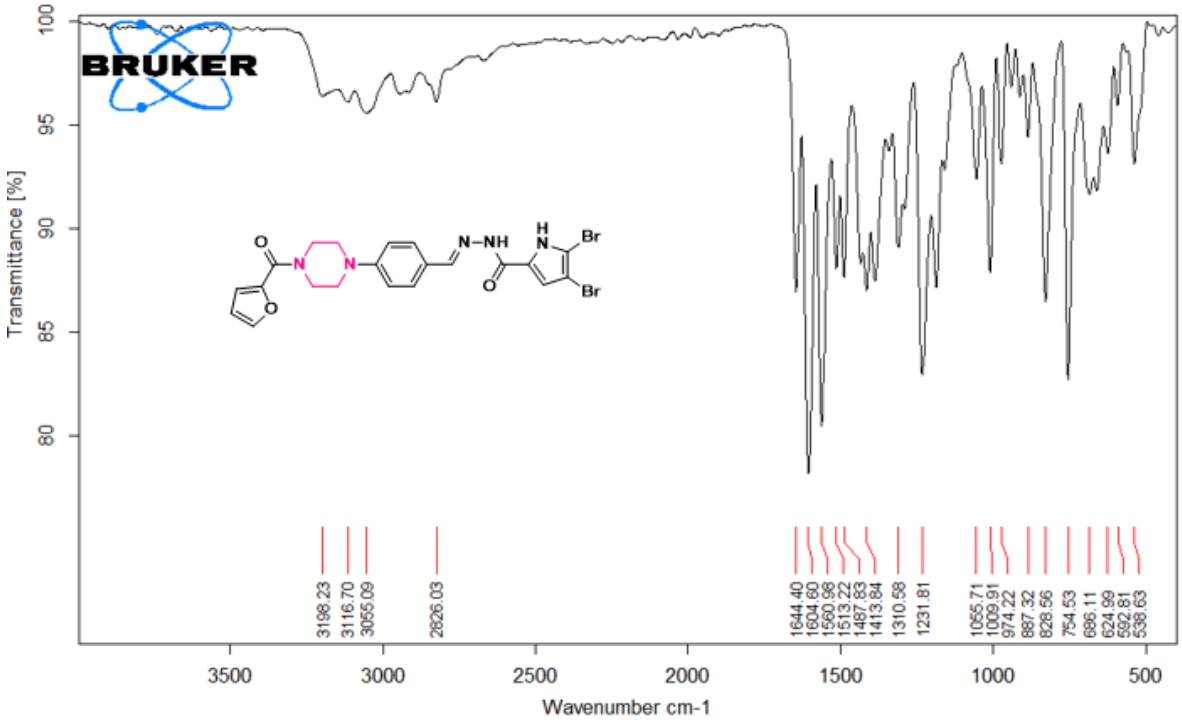

IR spectrum of compound c13(Chapter 3)

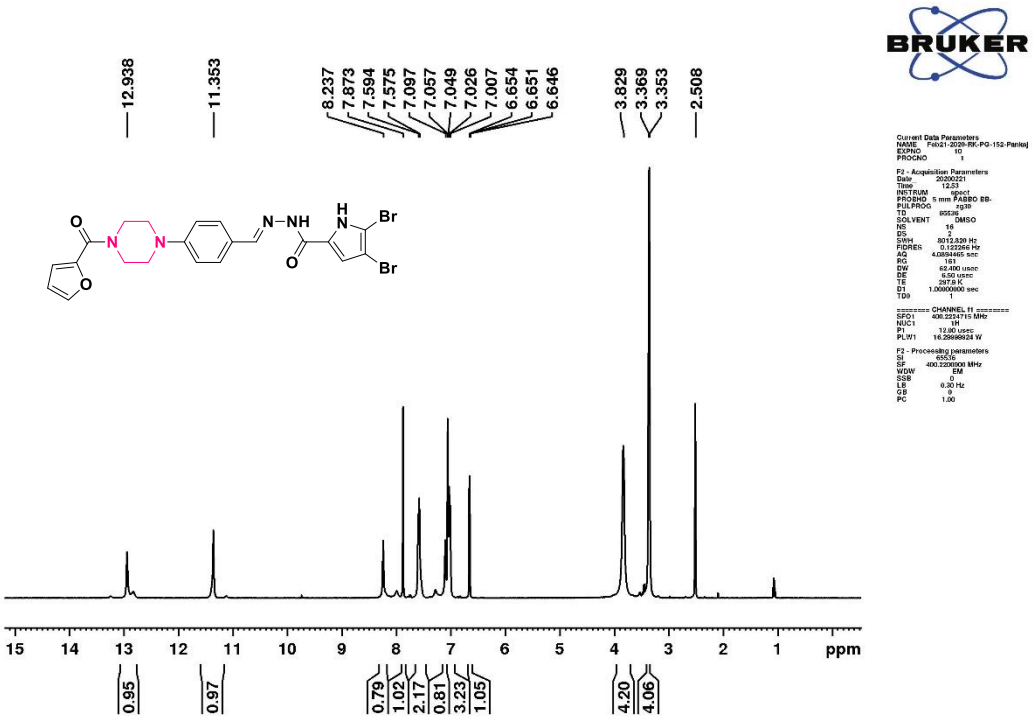

^{1}H NMR spectrum of compound c13(Chapter 3)

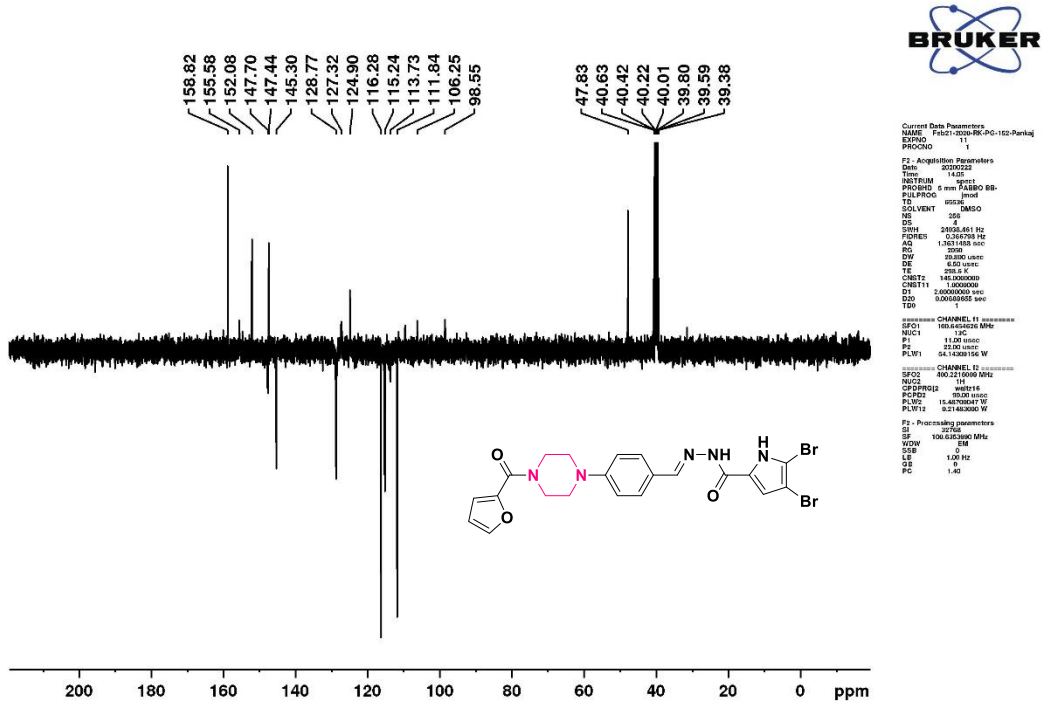

^{13}C NMR spectrum of compound c13(Chapter 3)

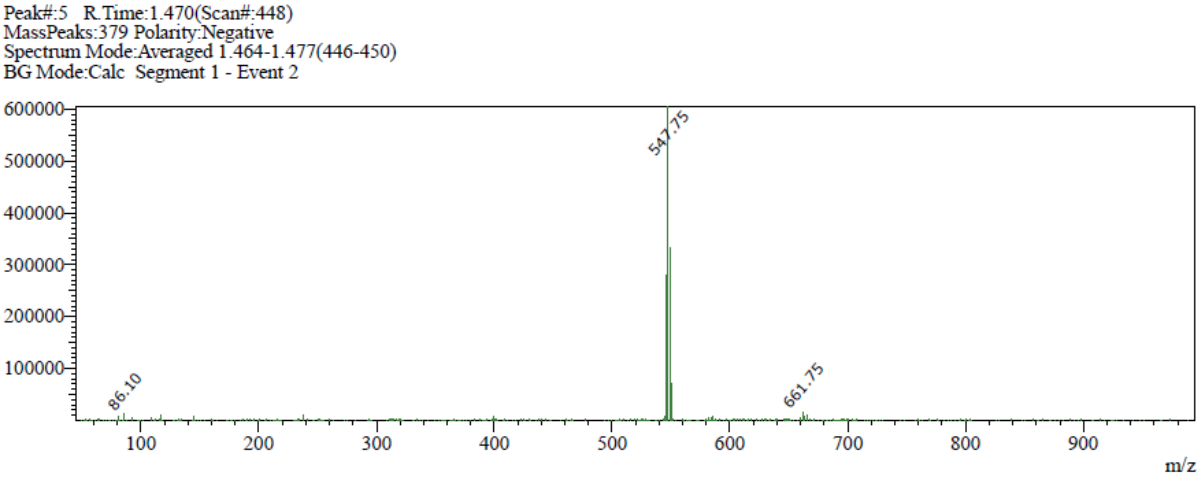

Mass spectrum of compound c13(Chapter 3)

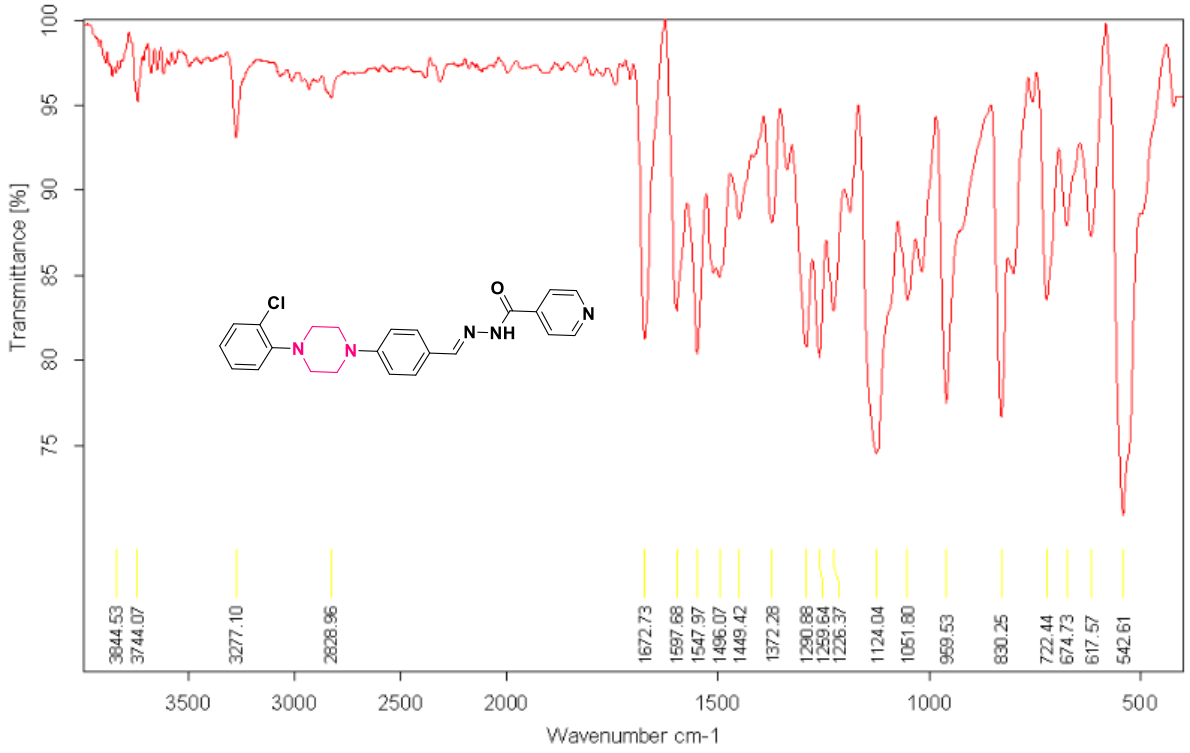

IR spectrum of compound c14(Chapter 3)

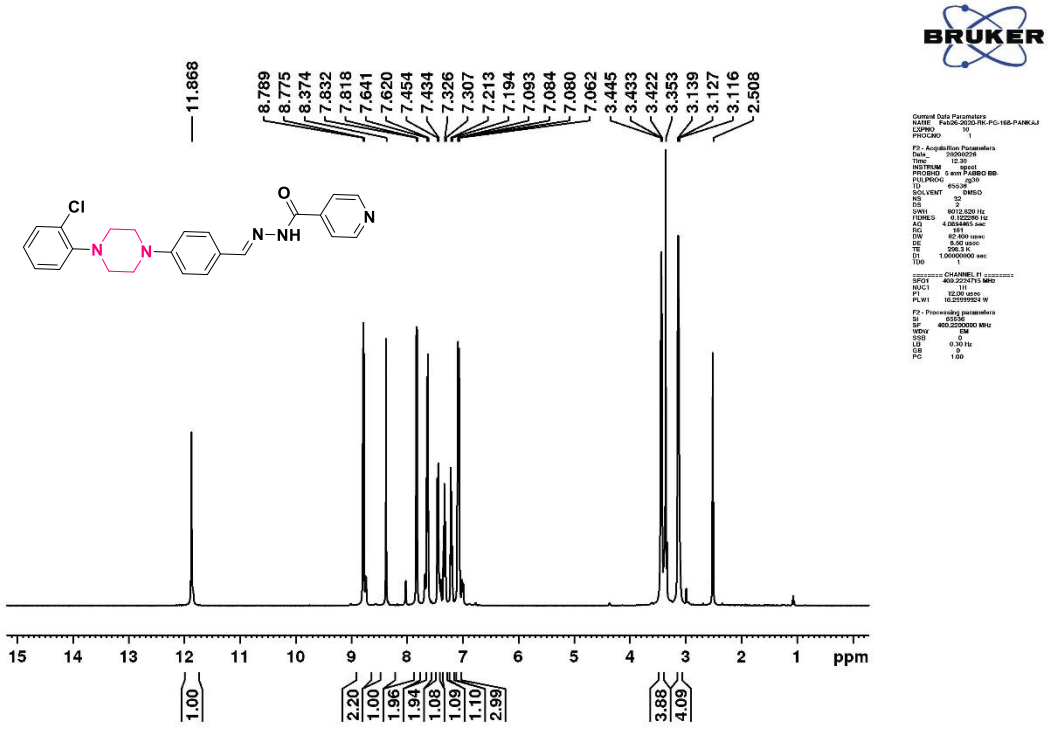

^{1}H NMR spectrum of compound c14(Chapter 3)

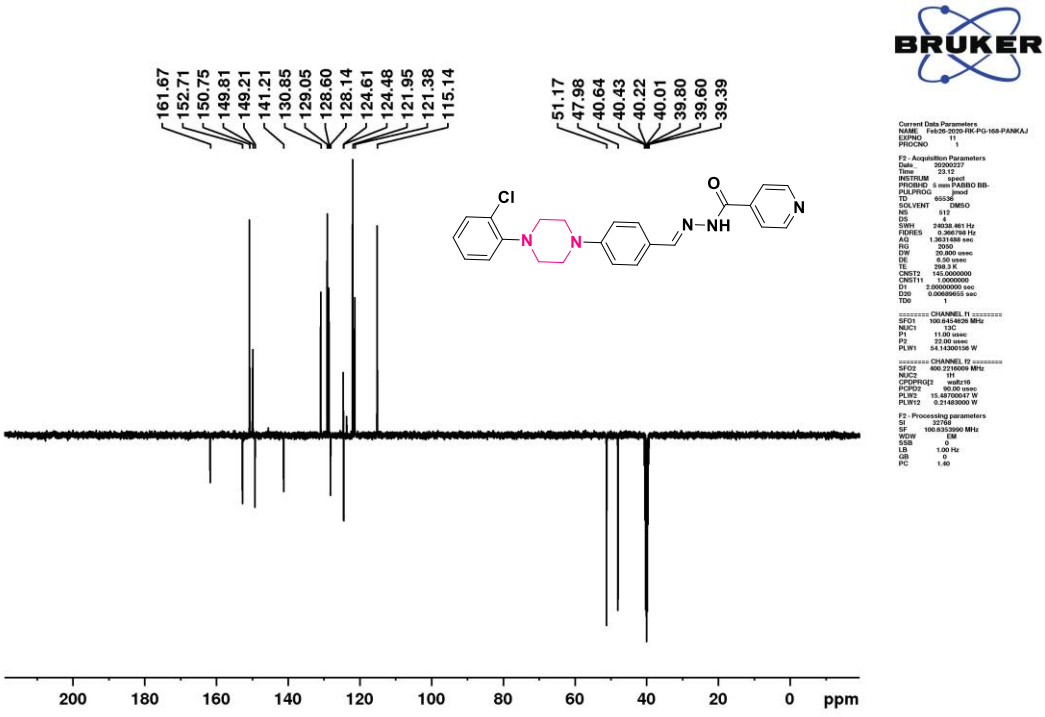

^{13}C NMR spectrum of compound c14(Chapter 3)

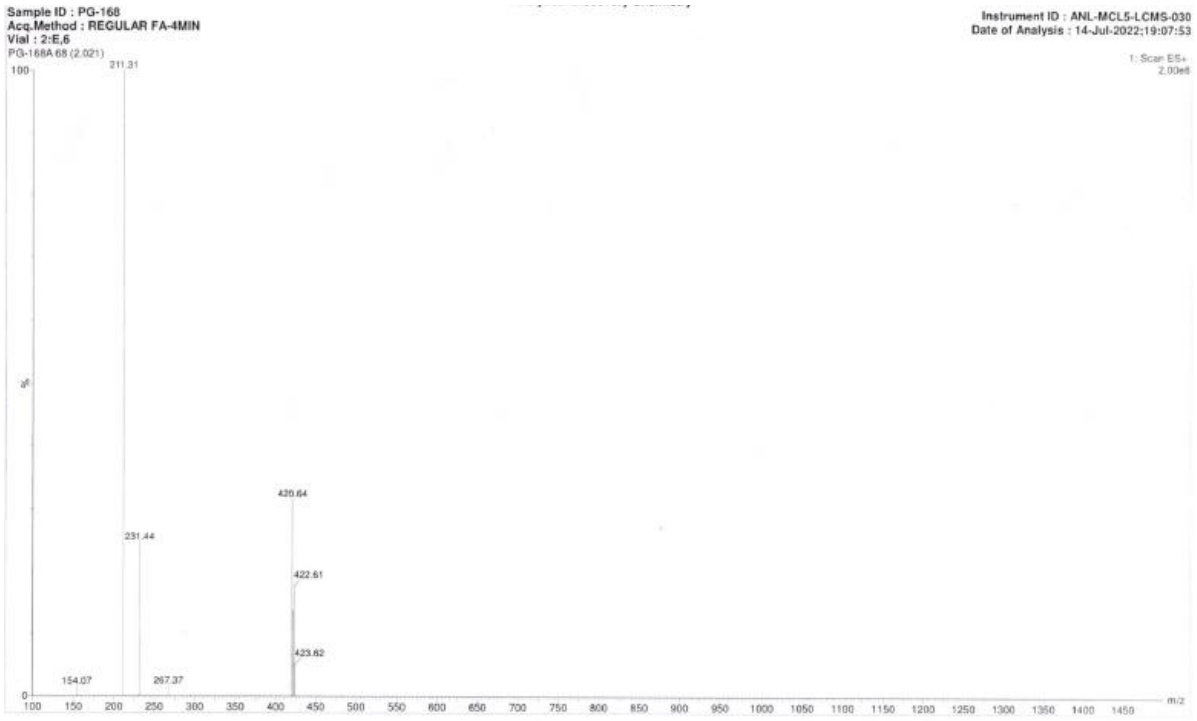

Mass spectrum of compound c14(Chapter 3)

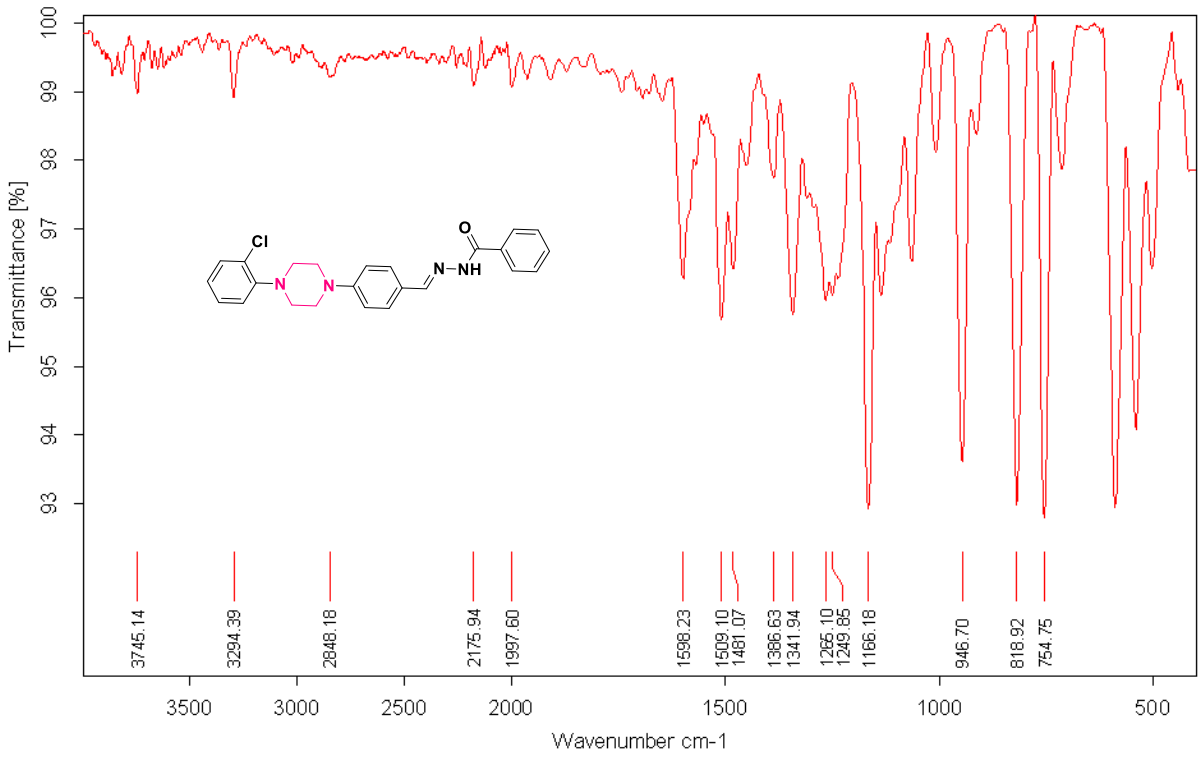

IR spectrum of compound c15(Chapter 3)

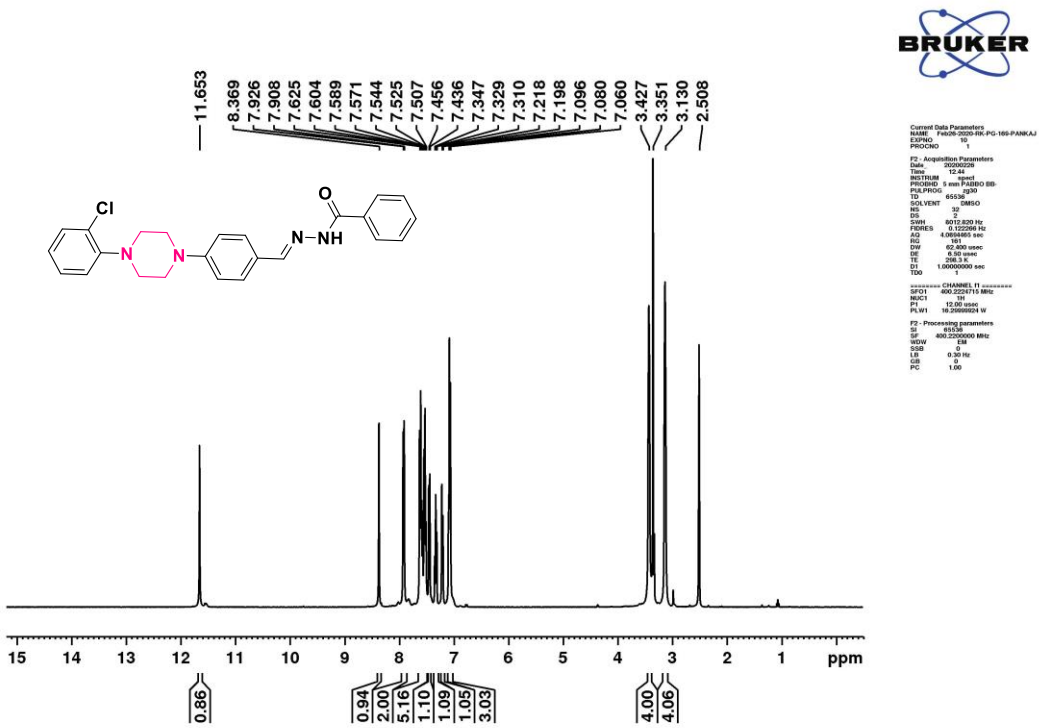

^{1}H NMR spectrum of compound c15(Chapter 3)

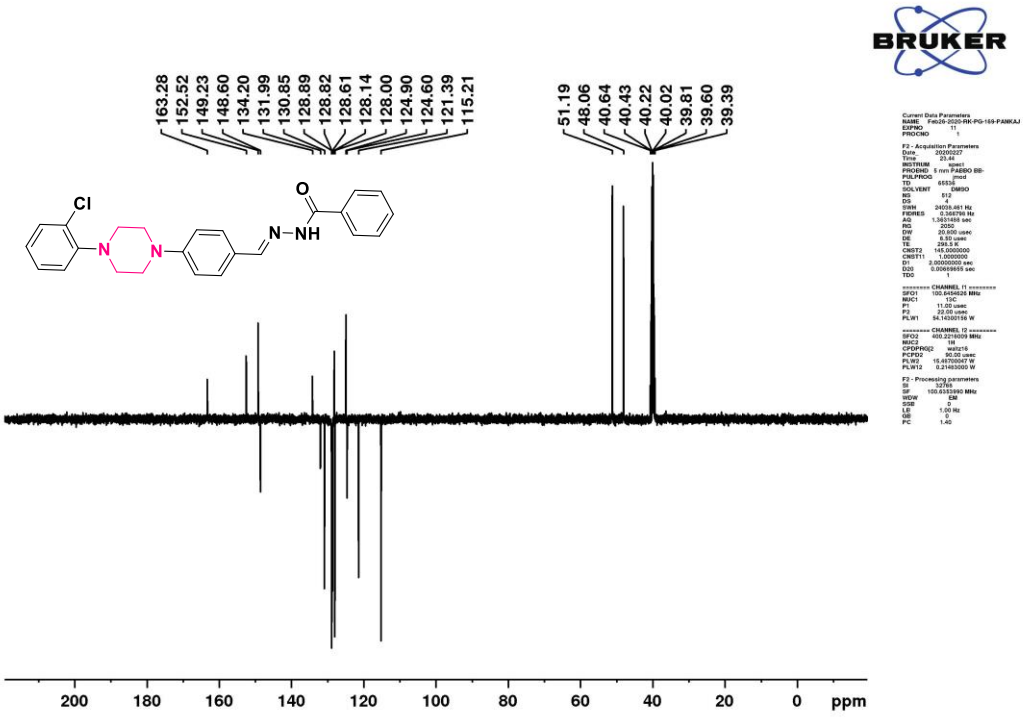

^{13}C NMR spectrum of compound c15(Chapter 3)

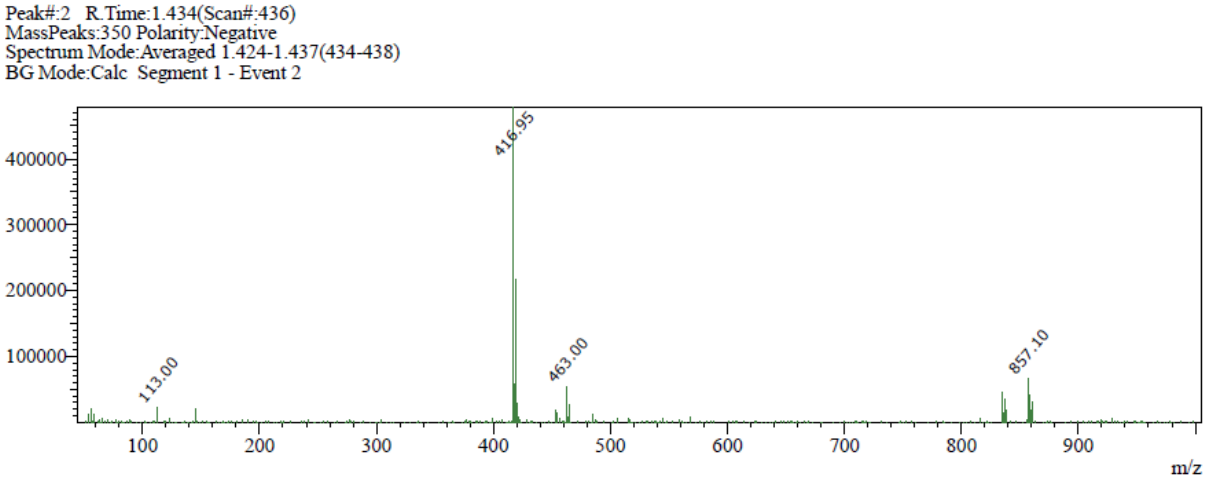

Mass spectrum of compound c15(Chapter 3)

APPENDEX-II (Chapter-4 supplementary information)

IR, NMR and Mass Spectrum of compoundsE1-E6 and F7-F19

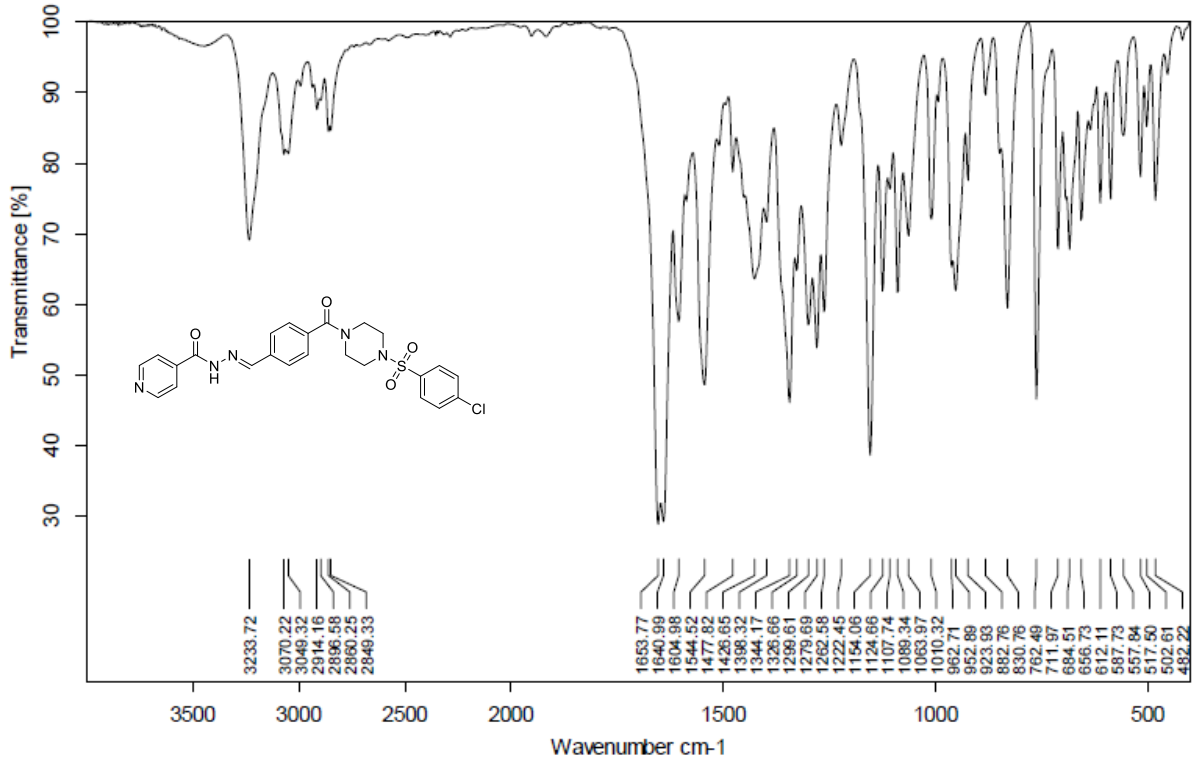

IR spectrum of compound E1 (Chapter 4)

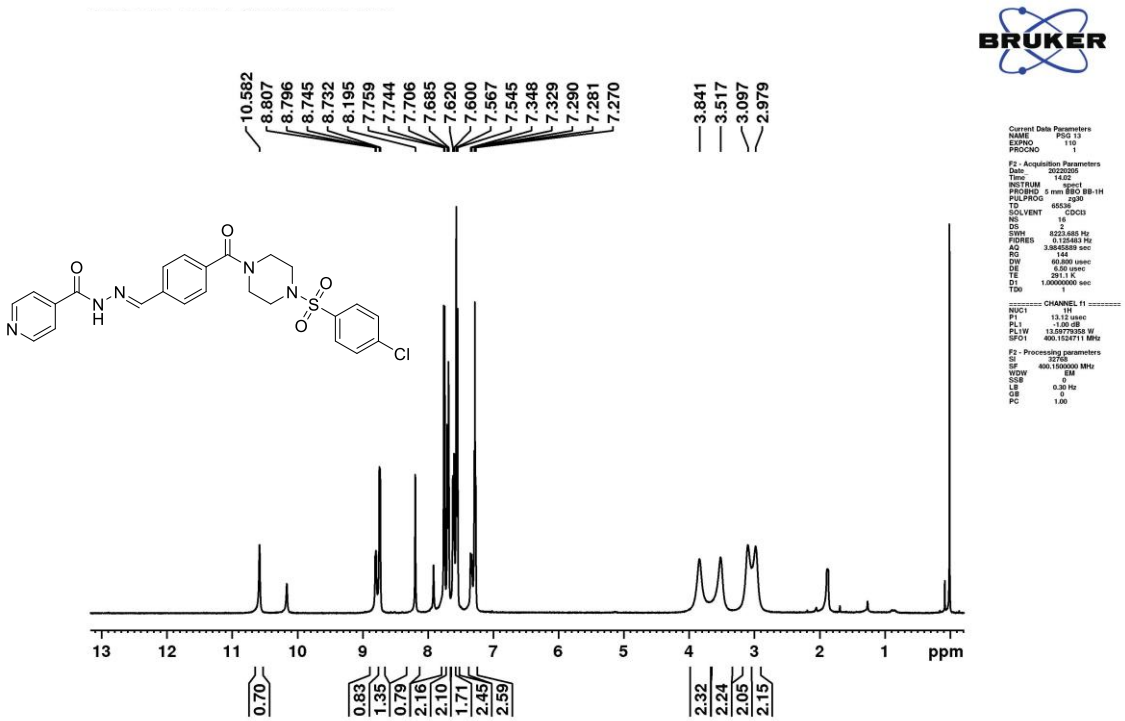

^{1}H NMR spectrum of compound E1 (Chapter 4)

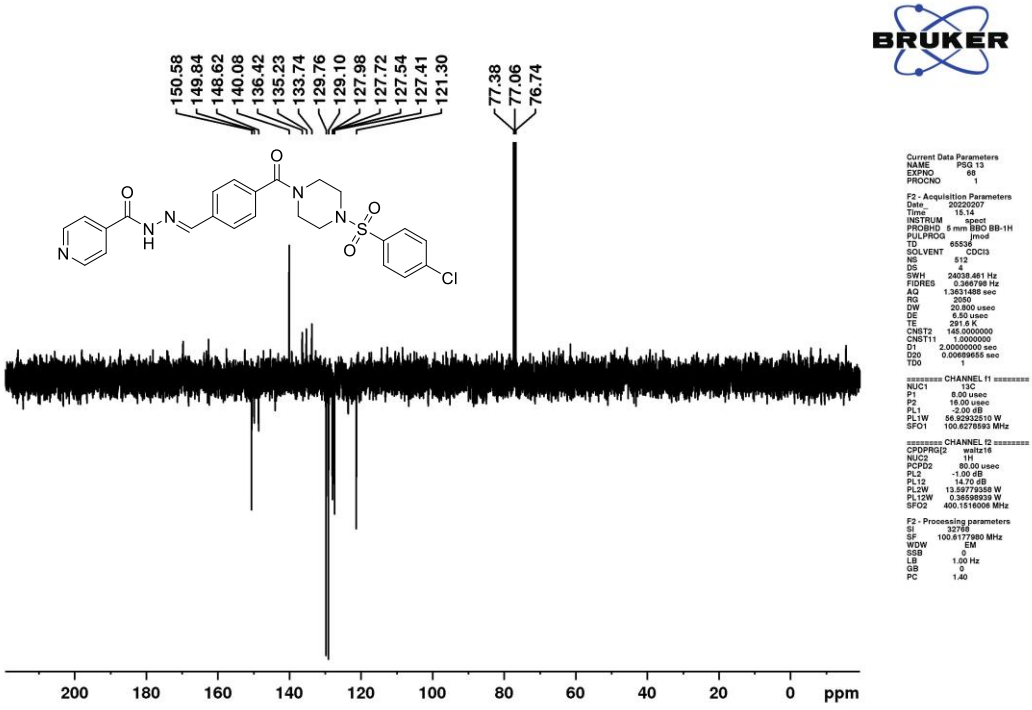

^{13}C NMR spectrum of compound E1 (Chapter 4)

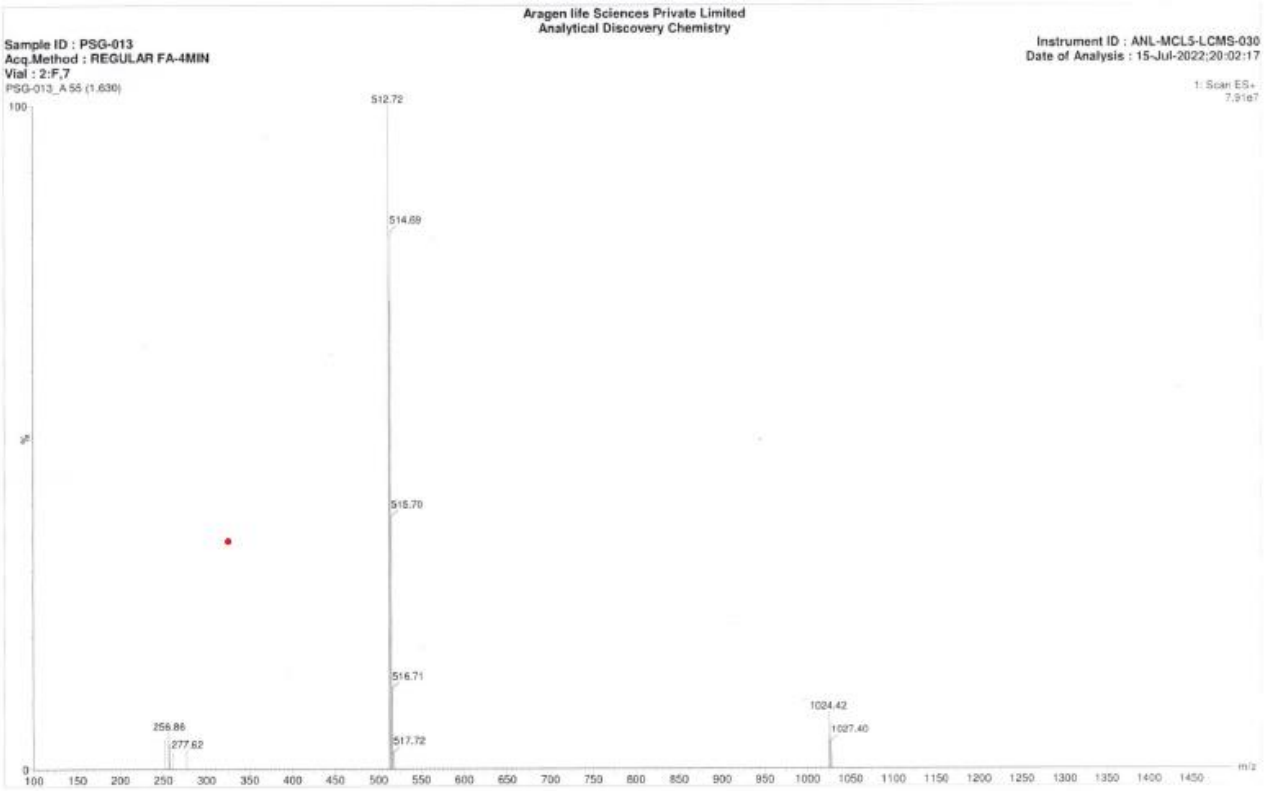

Mass spectrum of compound E1 (Chapter 4)

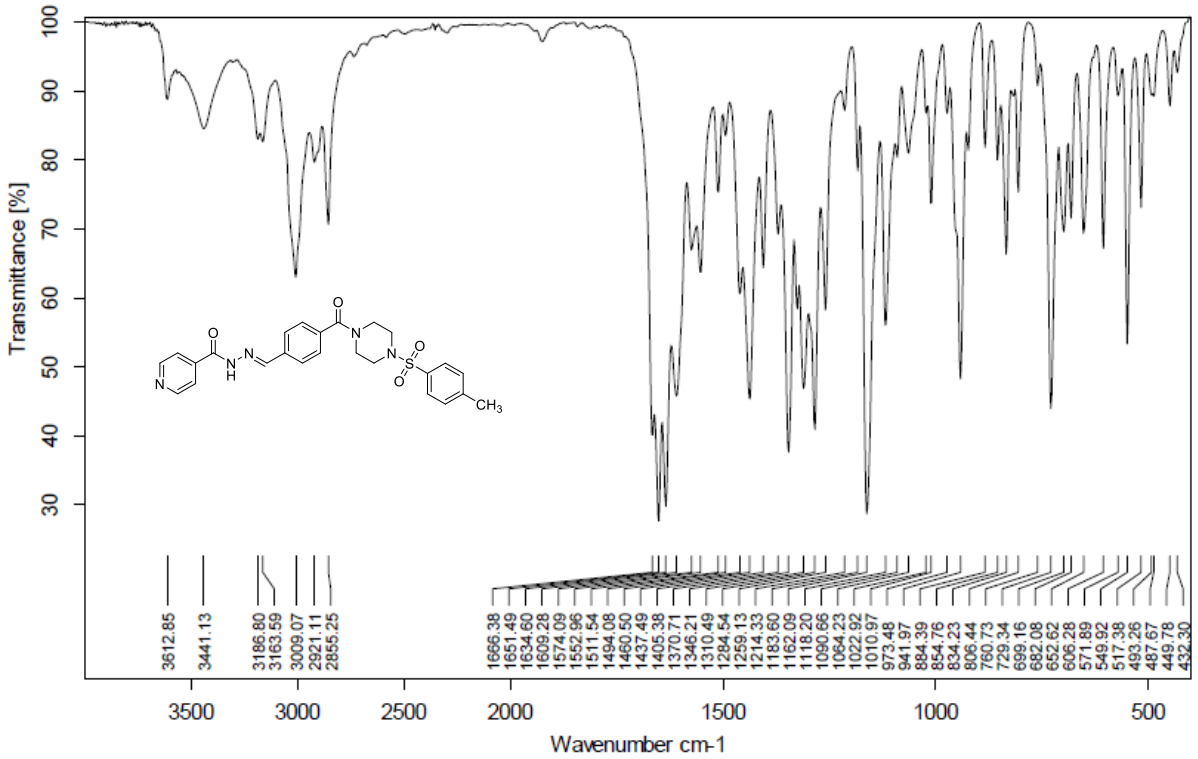

IR spectrum of compound E2 (Chapter 4)

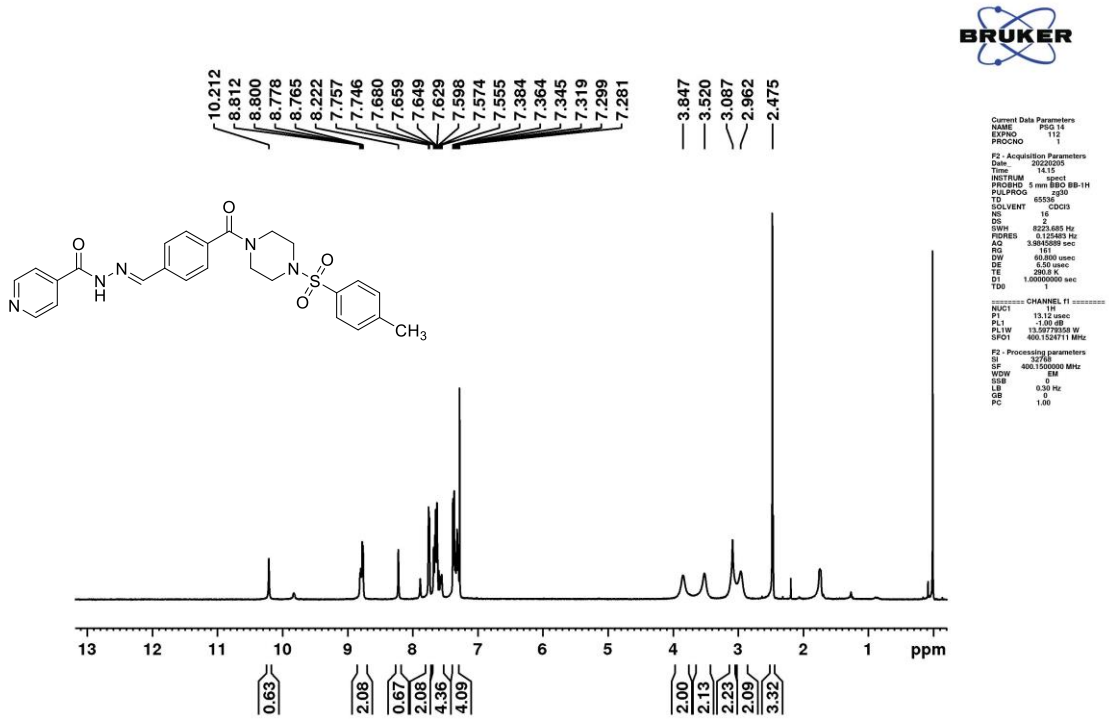

^{1}H NMR spectrum of compound E2 (Chapter 4)

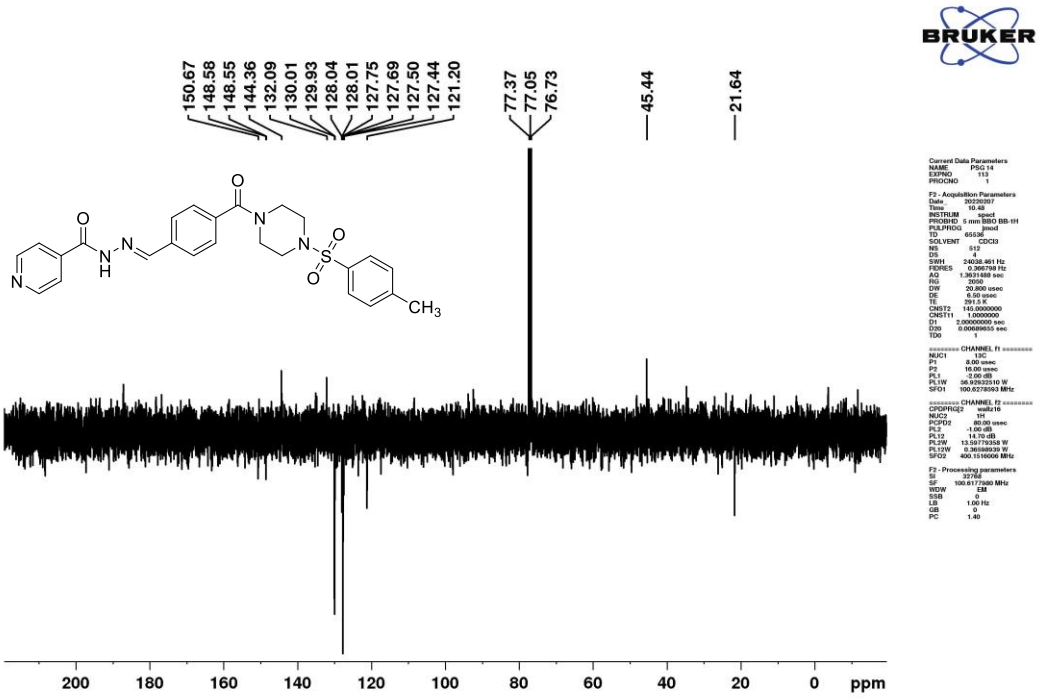

^{13}C NMR spectrum of compound E2 (Chapter 4)

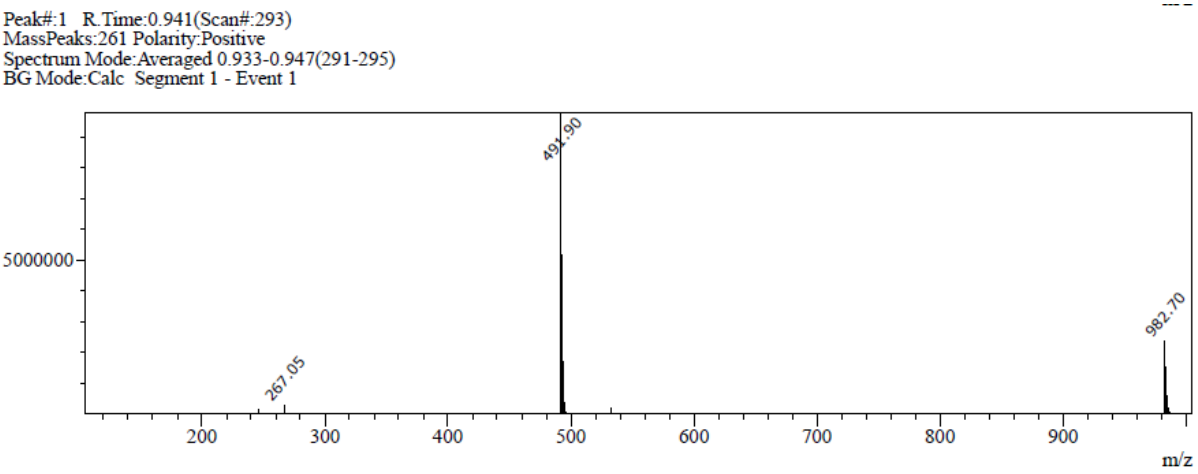

Mass spectrum of compound E2 (Chapter 4)

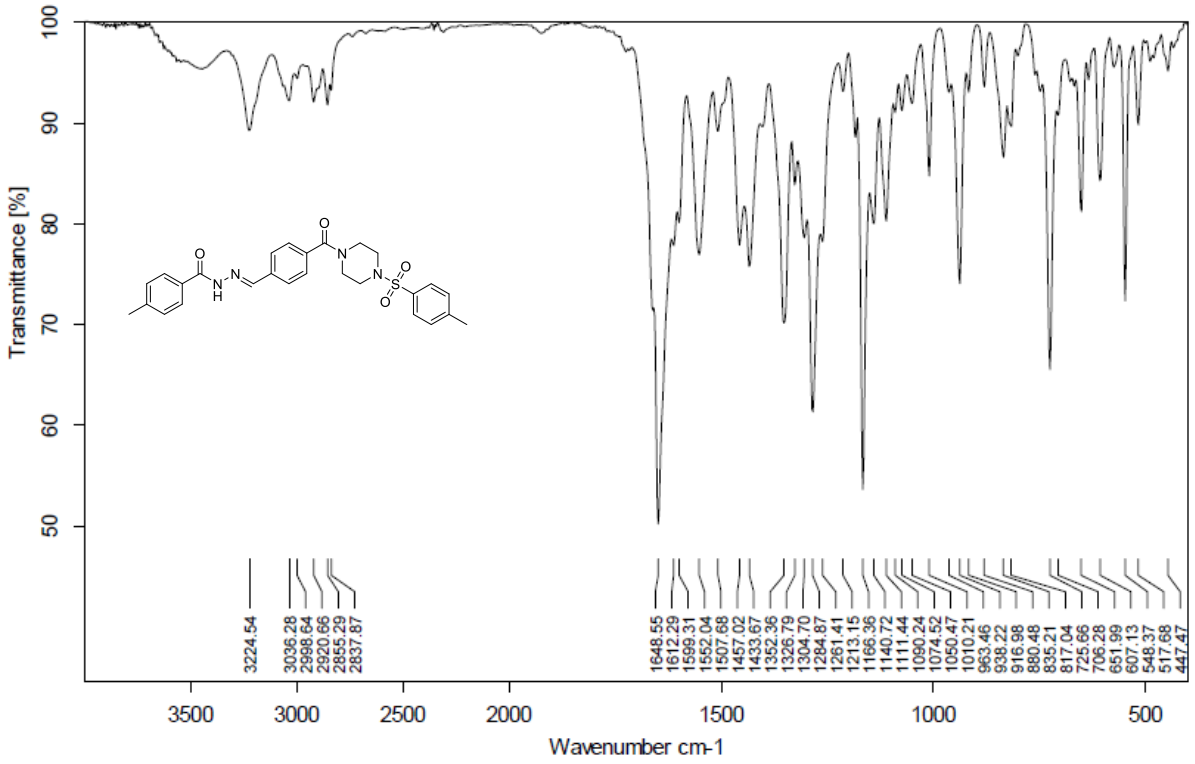

IR spectrum of compound E3 (Chapter 4)

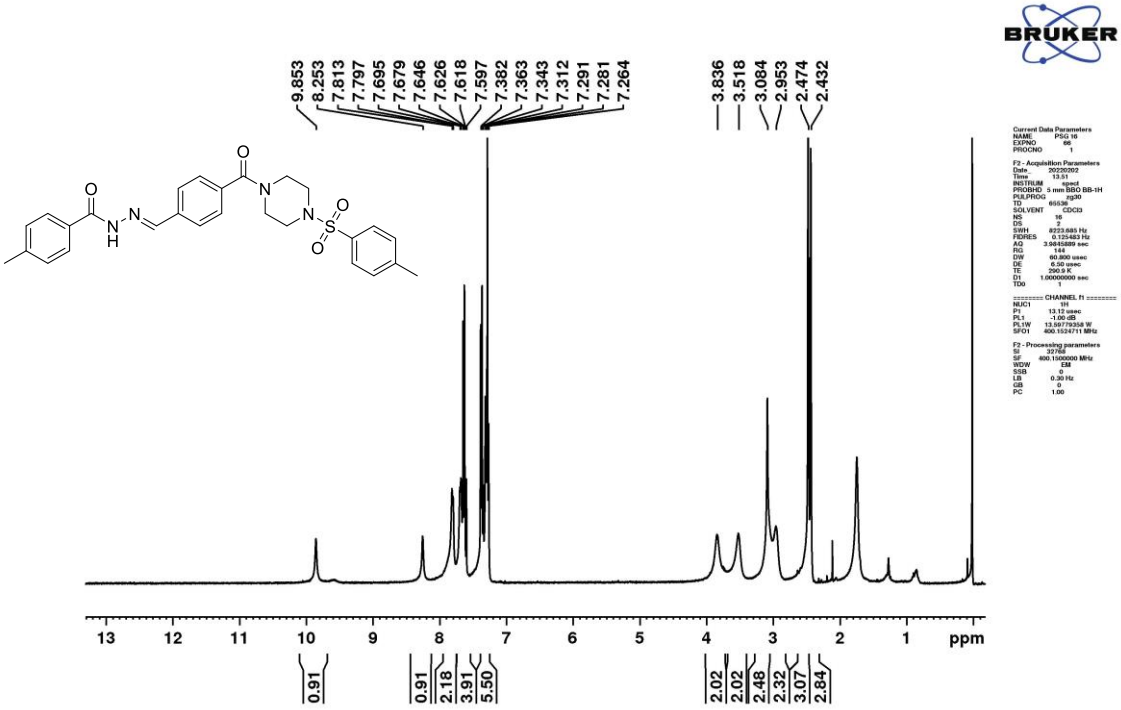

^{1}H NMR spectrum of compound E3 (Chapter 4)

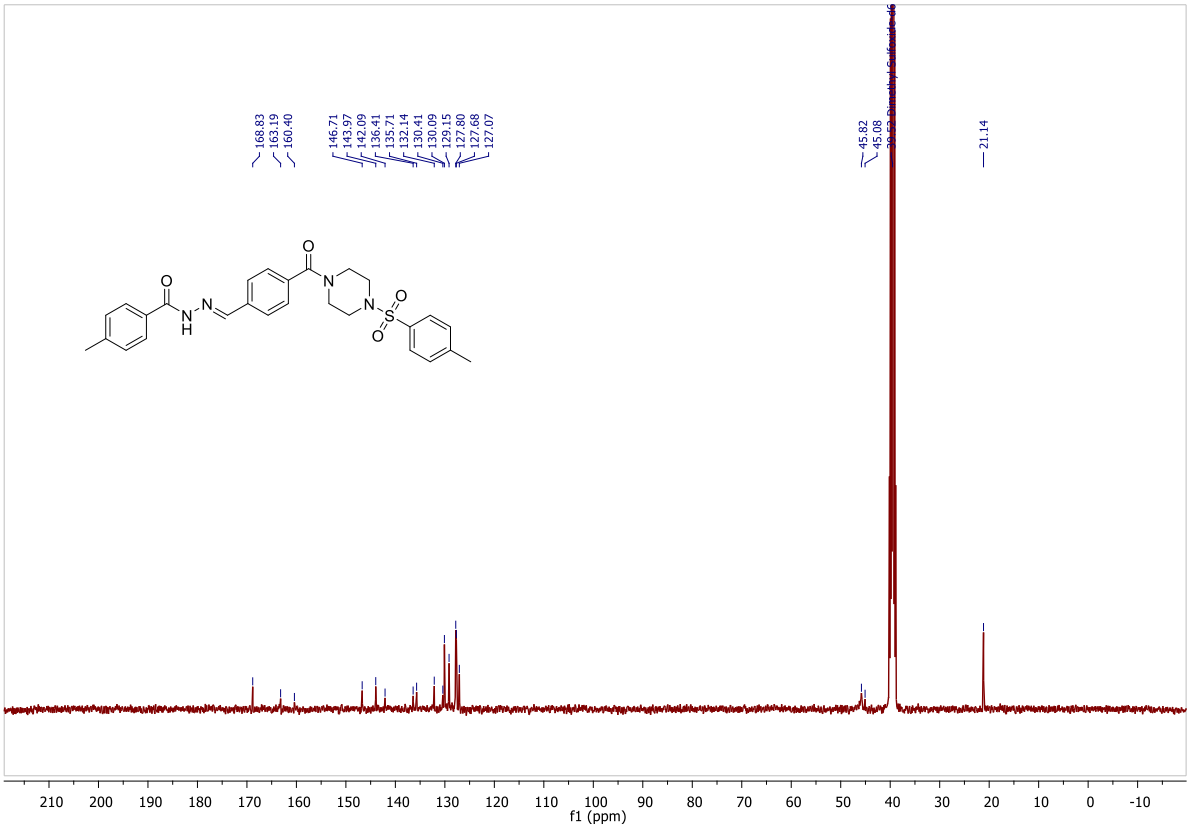

^{13}C NMR spectrum of compound E3 (Chapter 4)

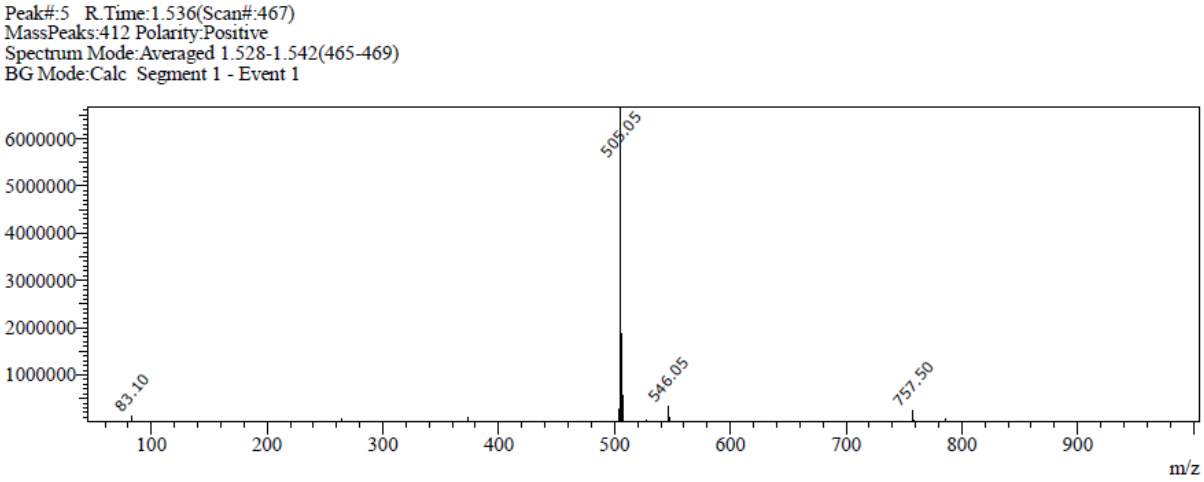

Mass spectrum of compound E3 (Chapter 4)

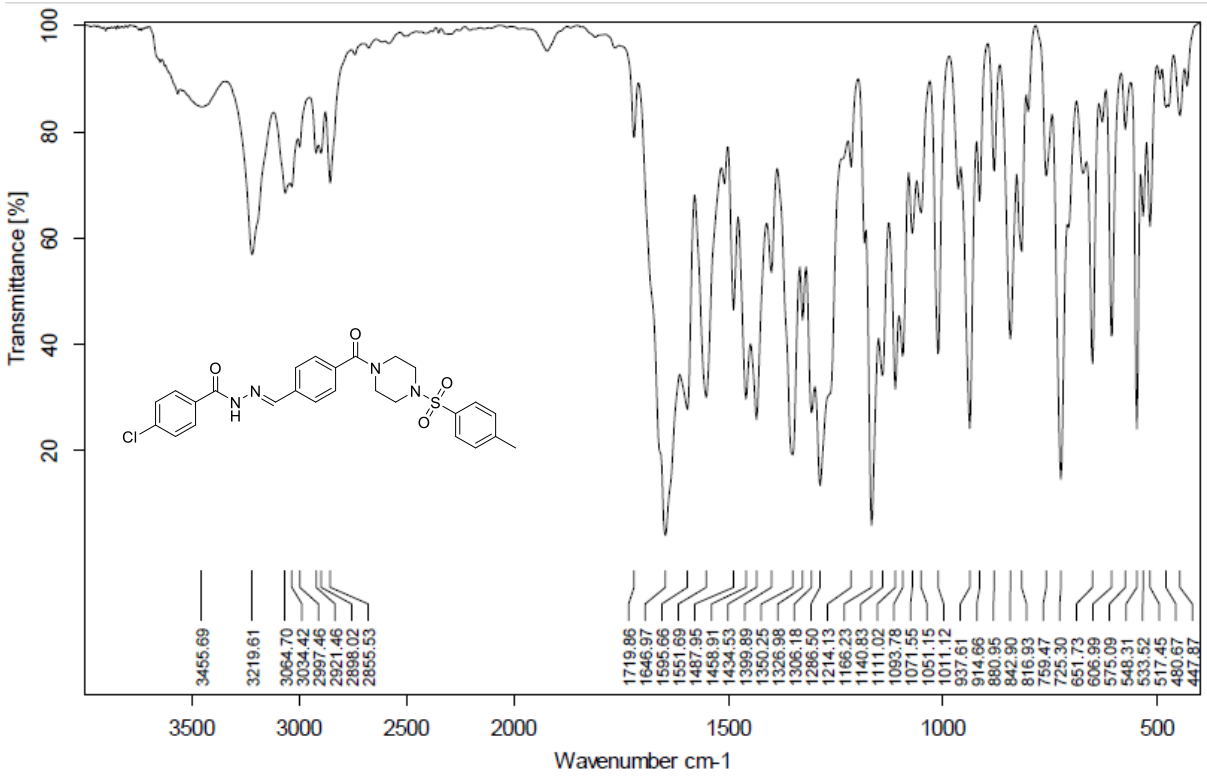

IR spectrum of compound E4 (Chapter 4)

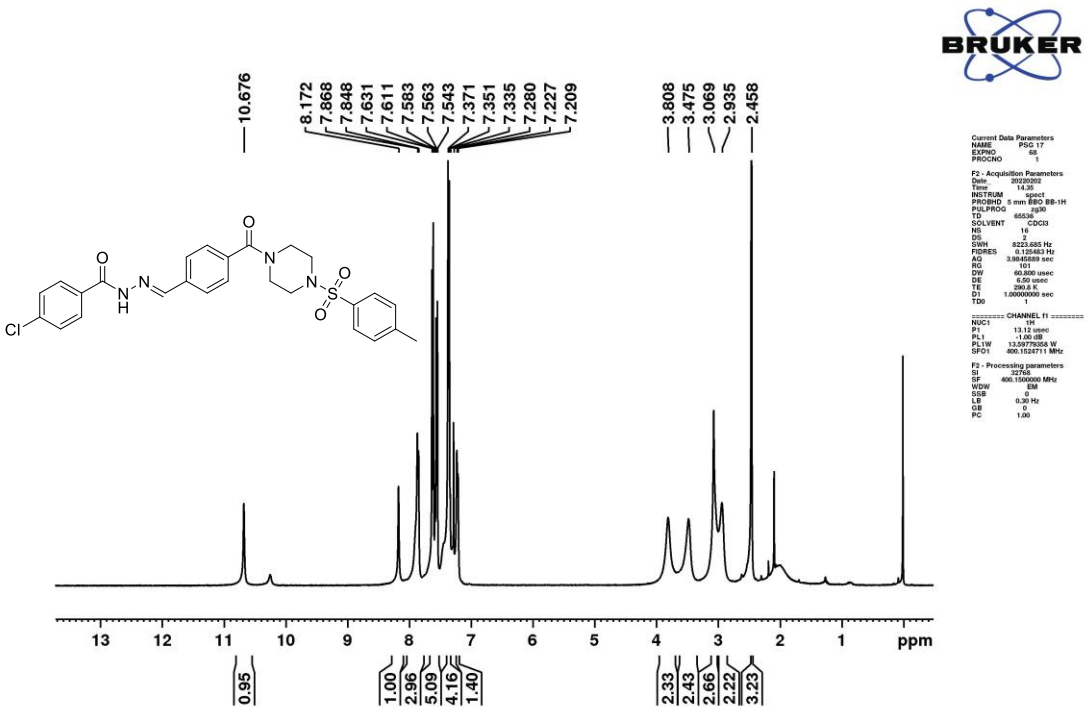

^{1}H NMR spectrum of compound E4 (Chapter 4)

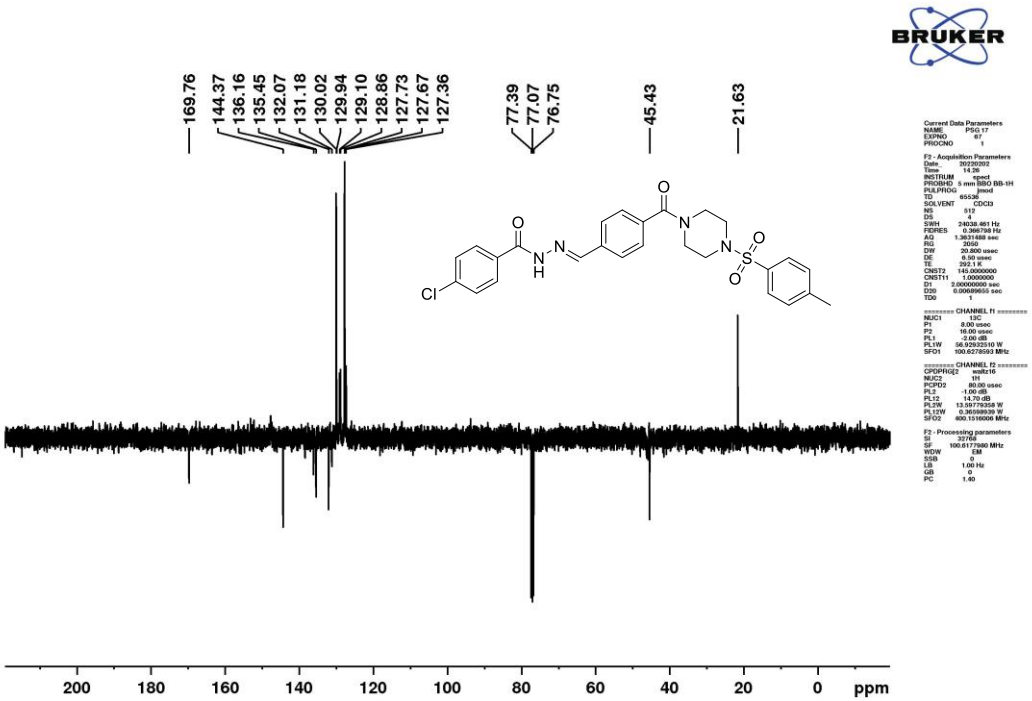

^{13}C NMR spectrum of compound E4 (Chapter 4)

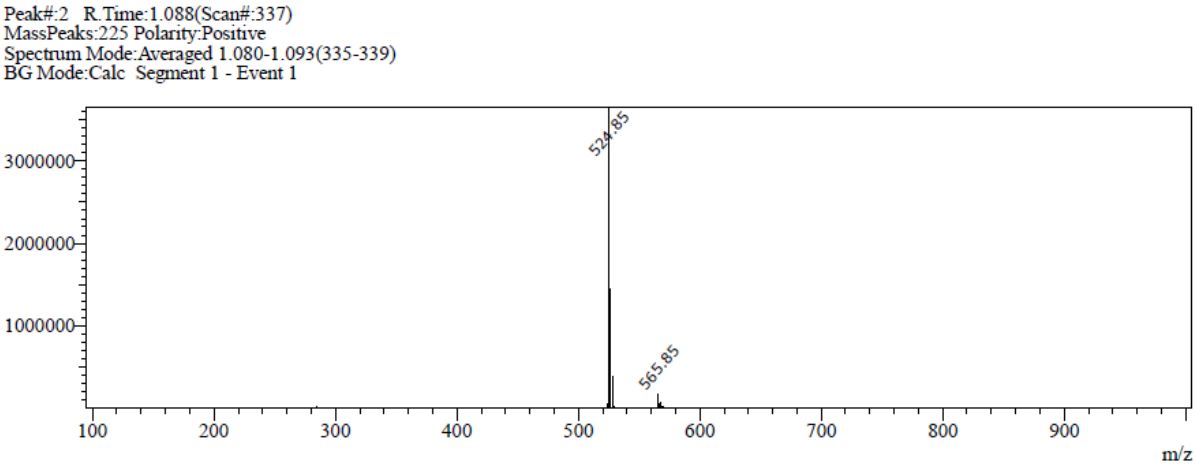

Mass spectrum of compound E4 (Chapter 4)

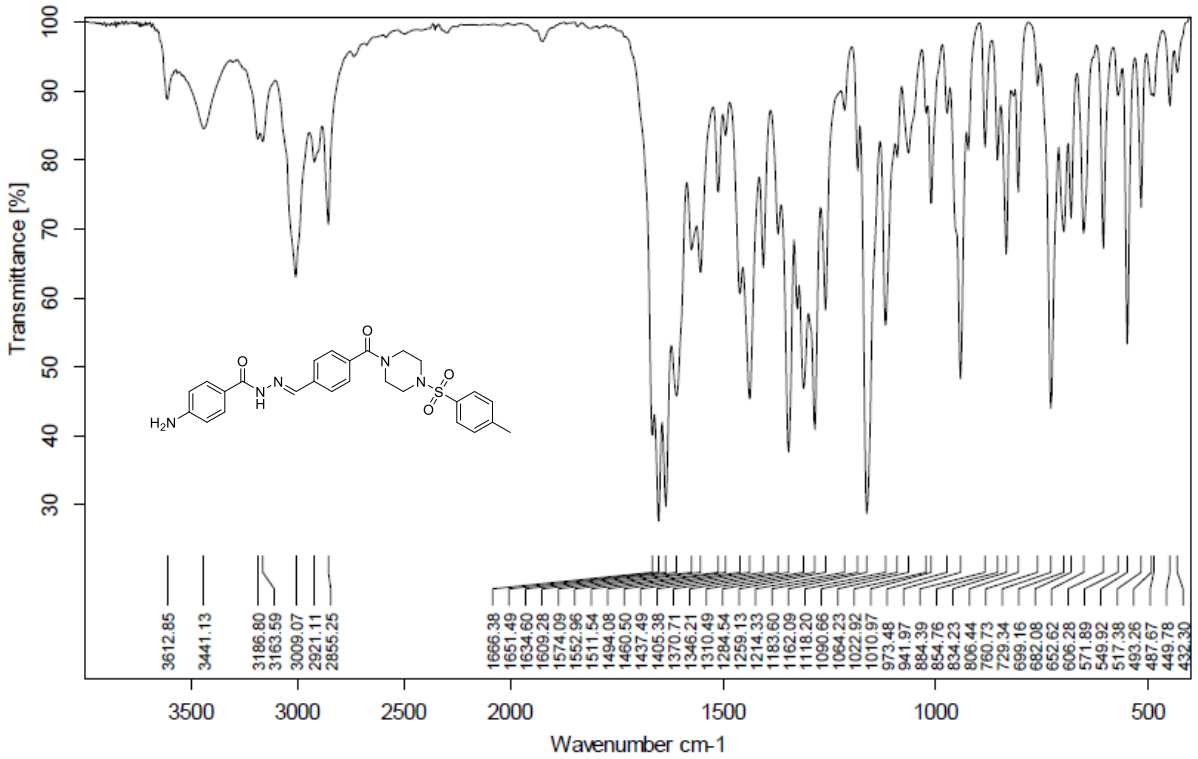

IR spectrum of compound E5 (Chapter 4)

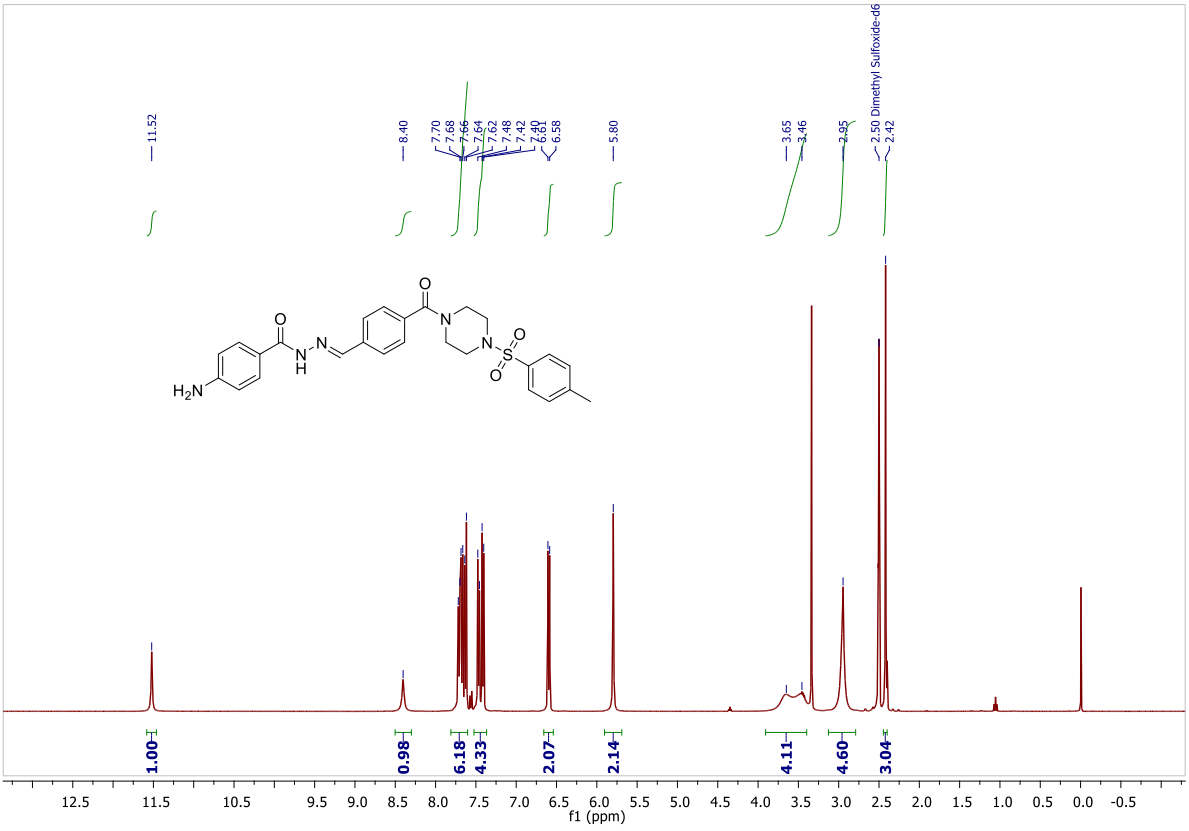

^{1}H NMR spectrum of compound E5 (Chapter 4)

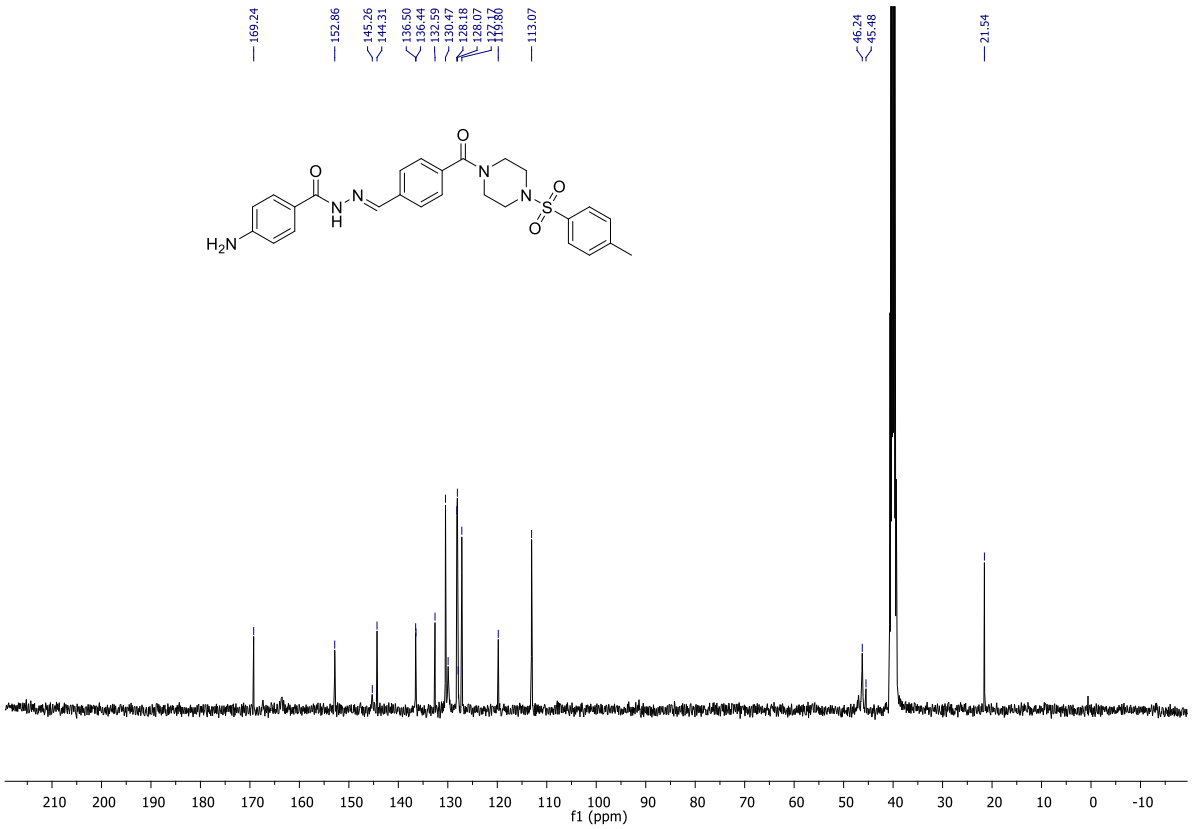

^{13}C NMR spectrum of compound E5 (Chapter 4)

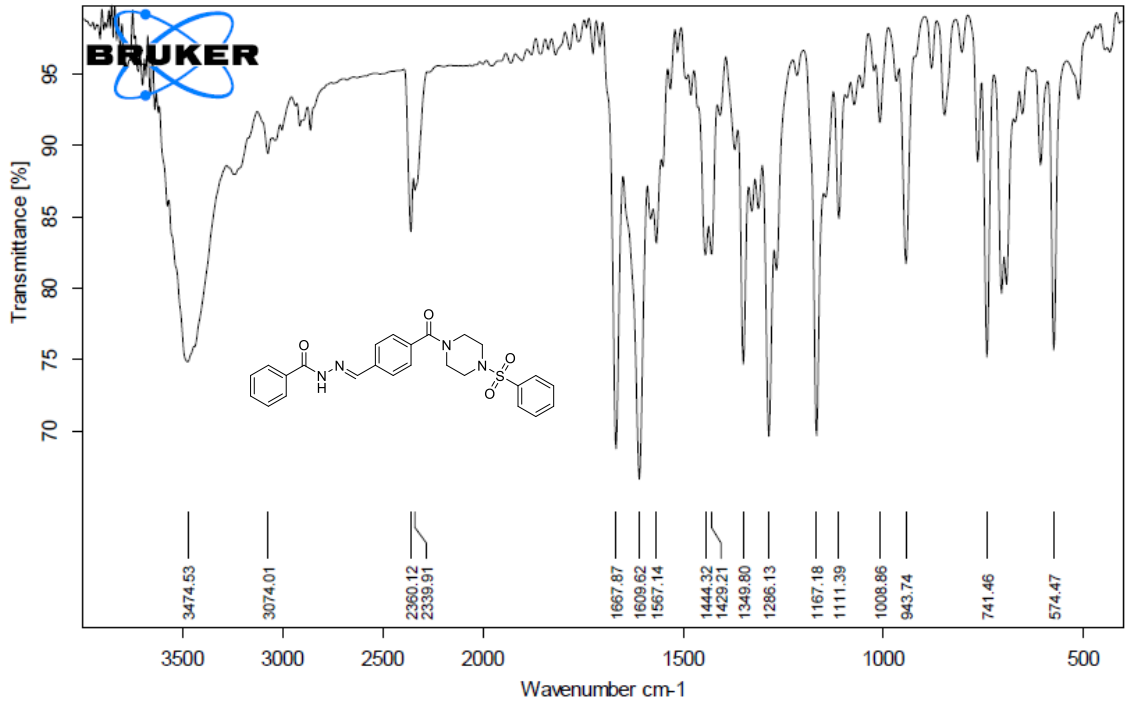

IR spectrum of compound F6 (Chapter 4)

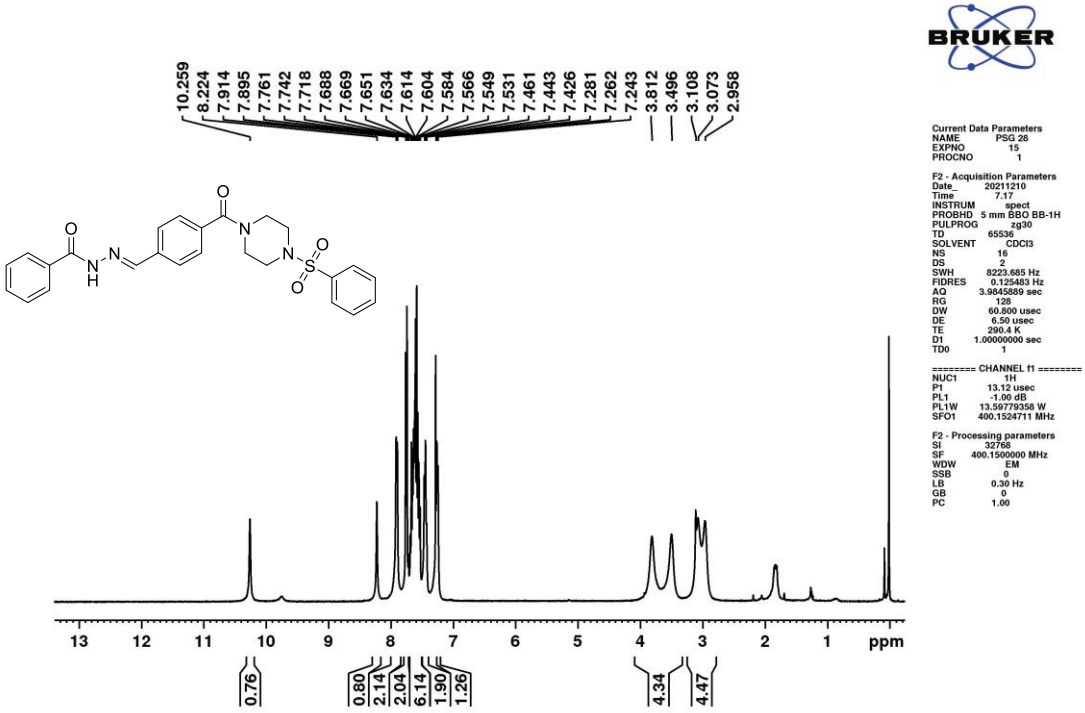

^{1}H NMR spectrum of compound F6 (Chapter 4)

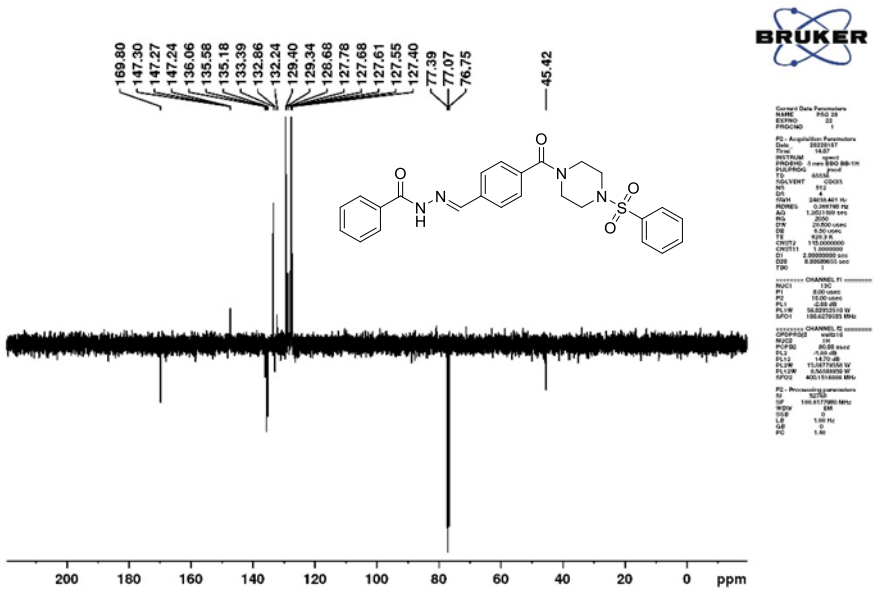

^{13}C NMR spectrum of compound F6 (Chapter 4)

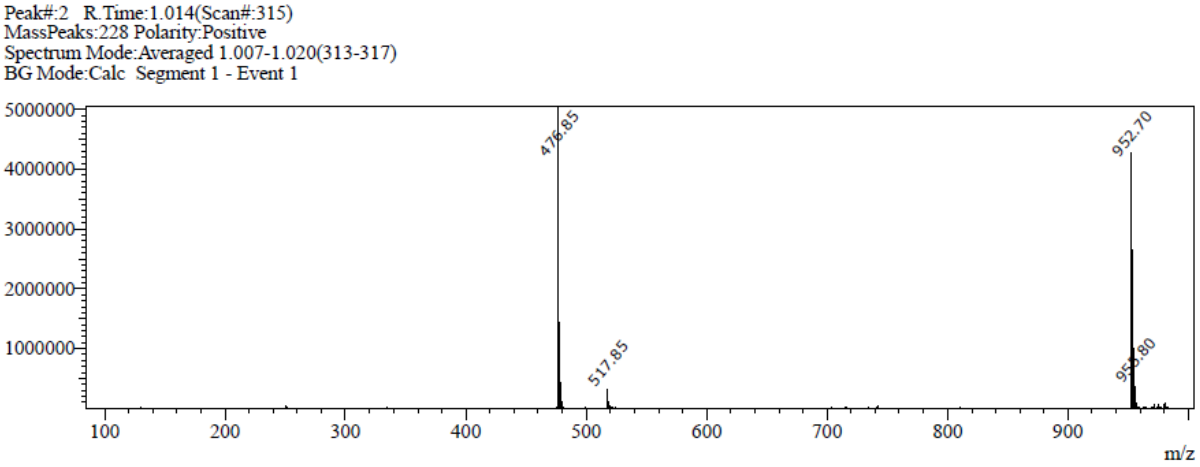

Mass spectrum of compound F6 (Chapter 4)

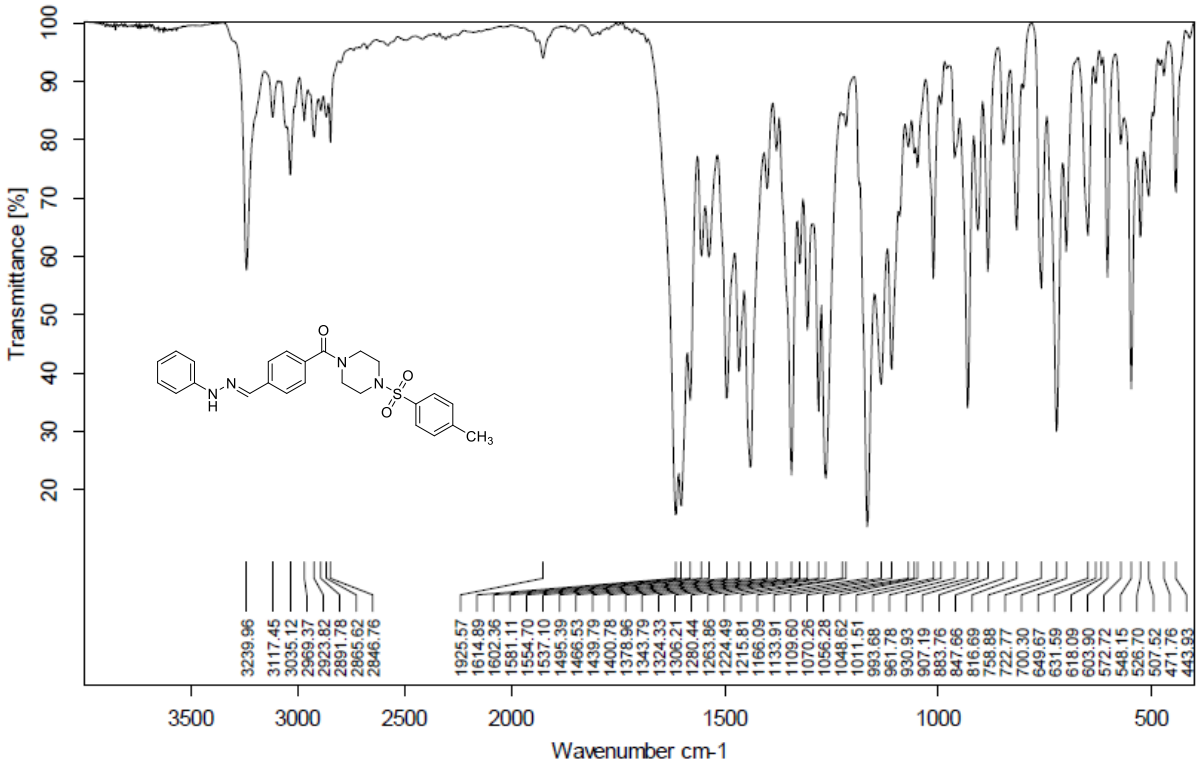

IR spectrum of compound F7 (Chapter 4)

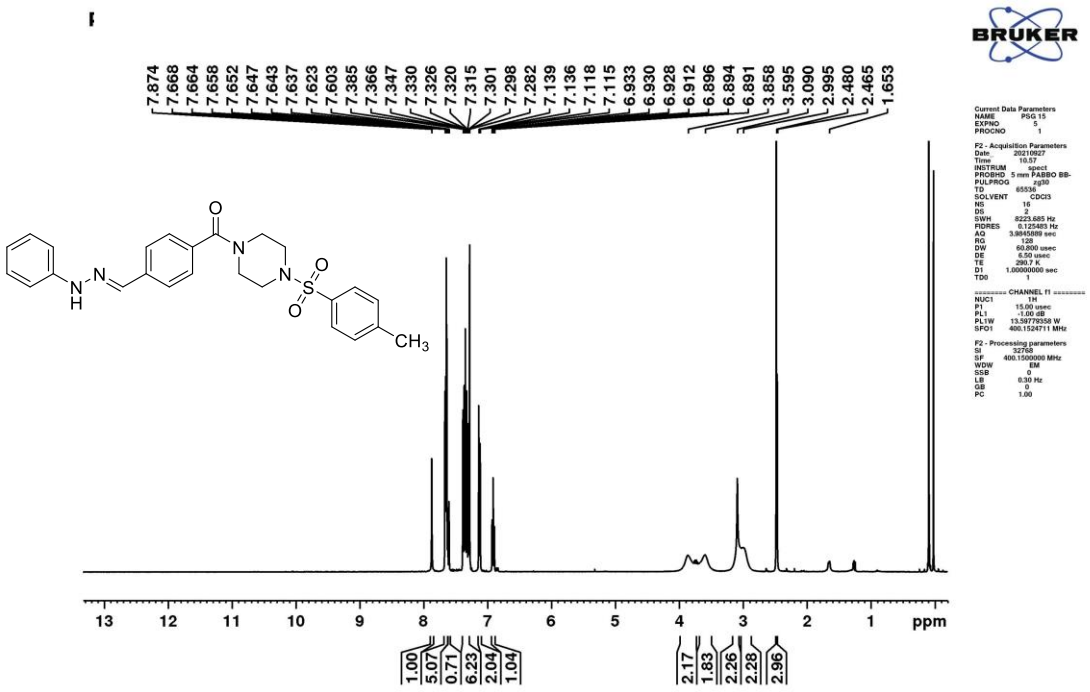

^{1}H NMR spectrum of compound F7 (Chapter 4)

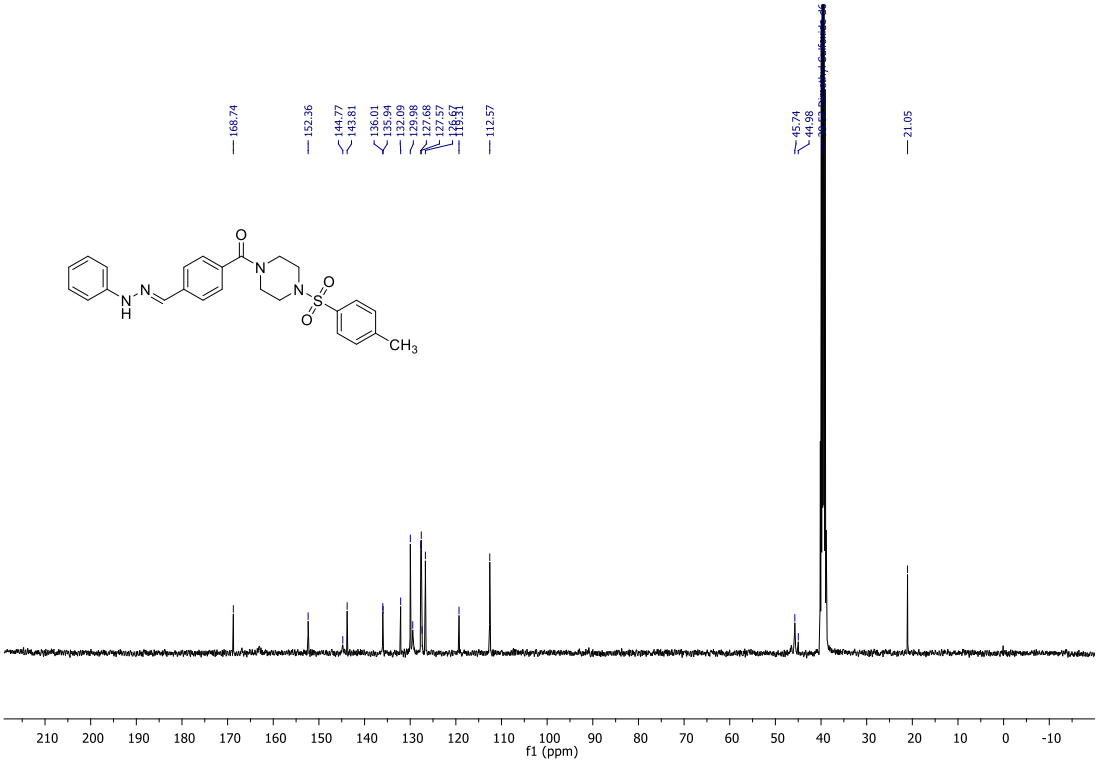

^{13}C NMR spectrum of compound F7 (Chapter 4)

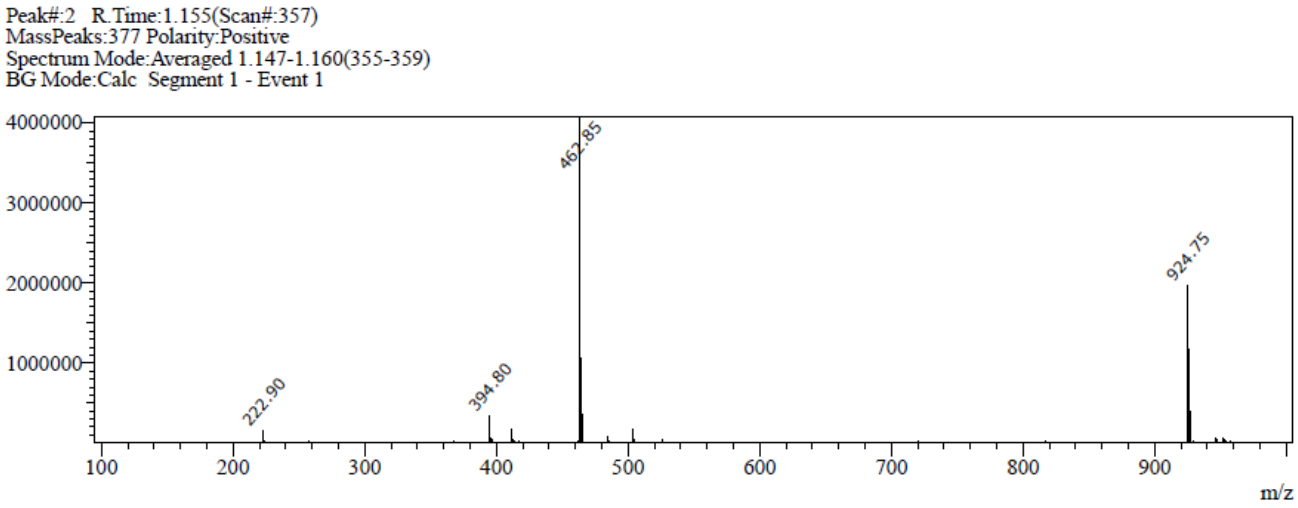

Mass spectrum of compound F7 (Chapter 4)

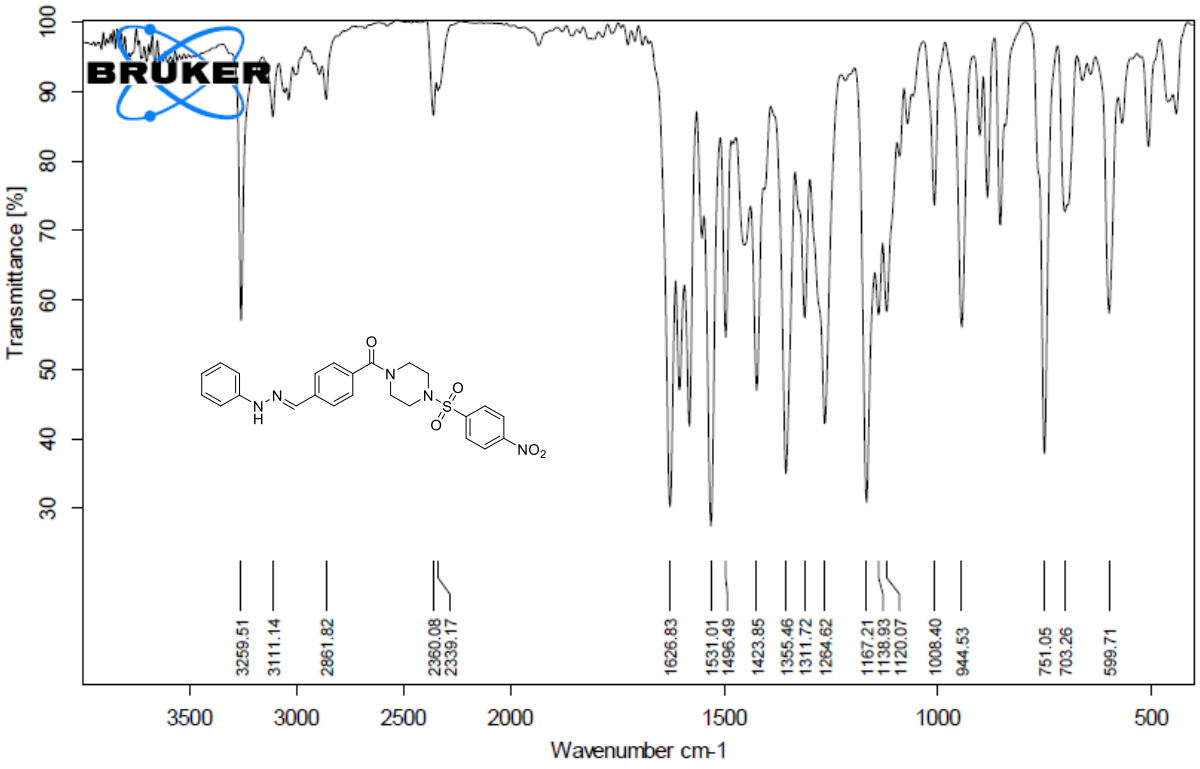

IR spectrum of compound F8 (Chapter 4)

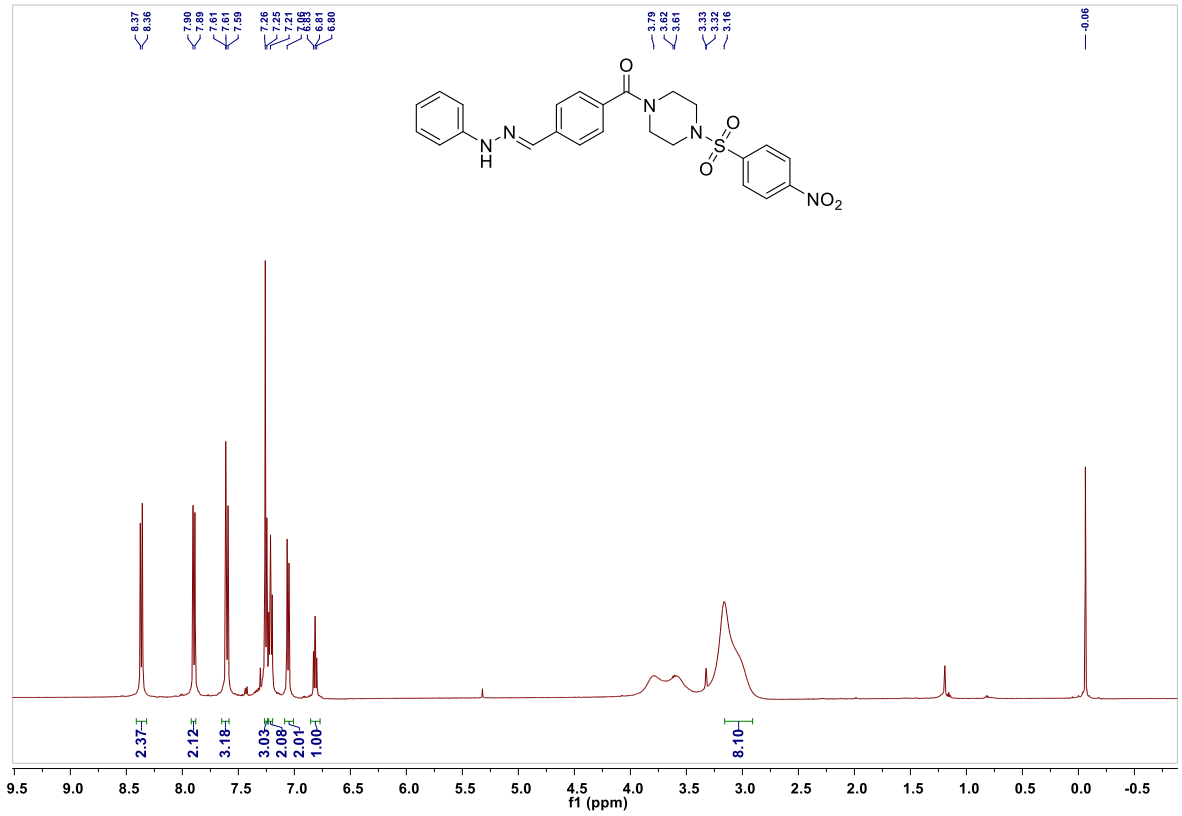

^{1}H NMR spectrum of compound F8 (Chapter 4)

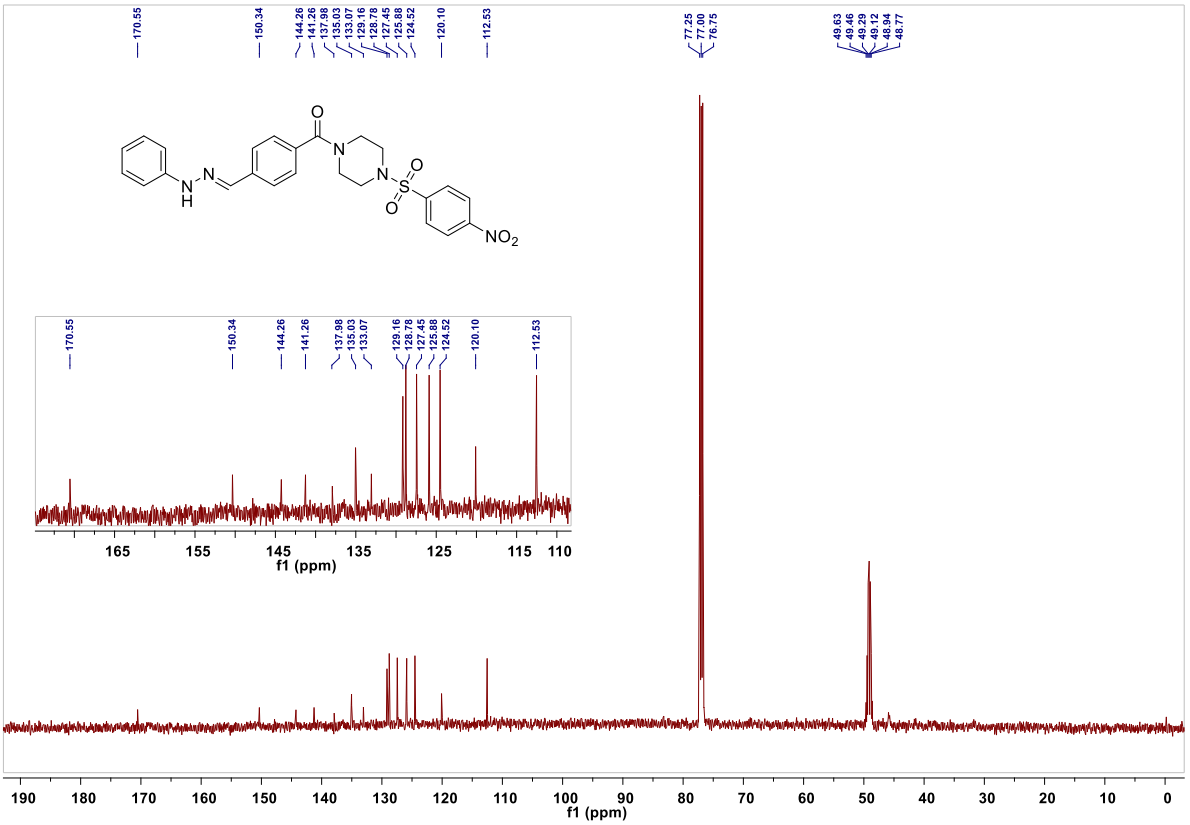

^{13}C NMR spectrum of compound F8 (Chapter 4)

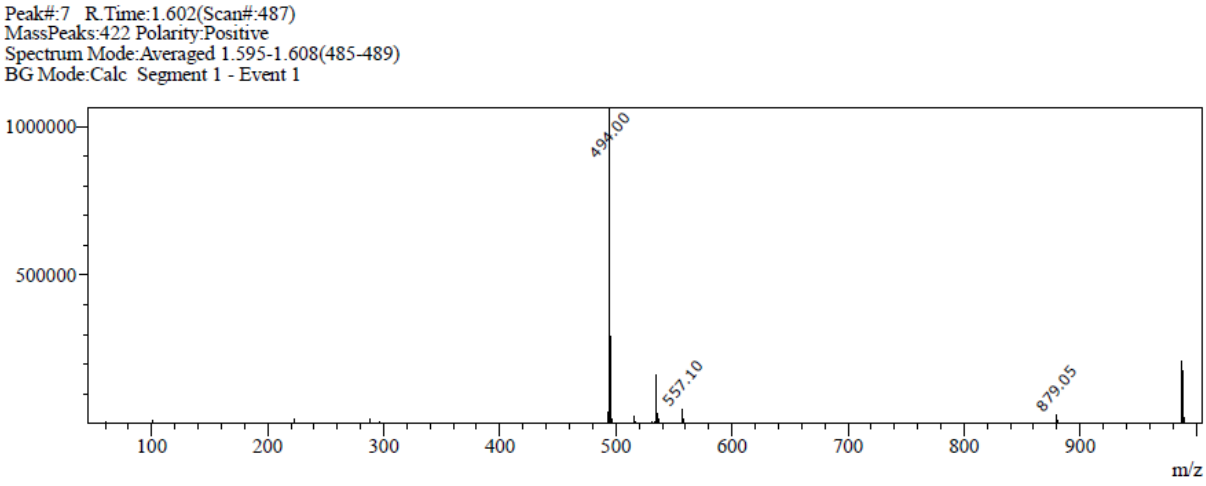

Mass spectrum of compound F9 (Chapter 4)

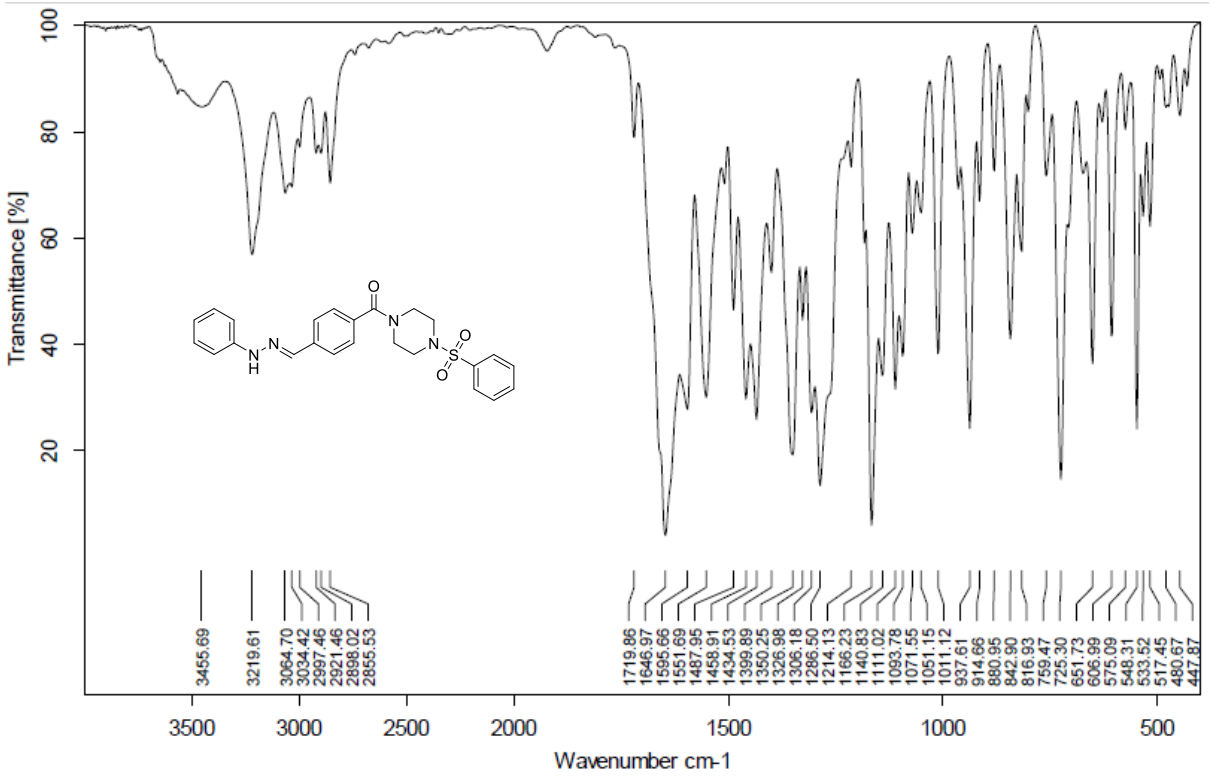

IR spectrum of compound F9 (Chapter 4)

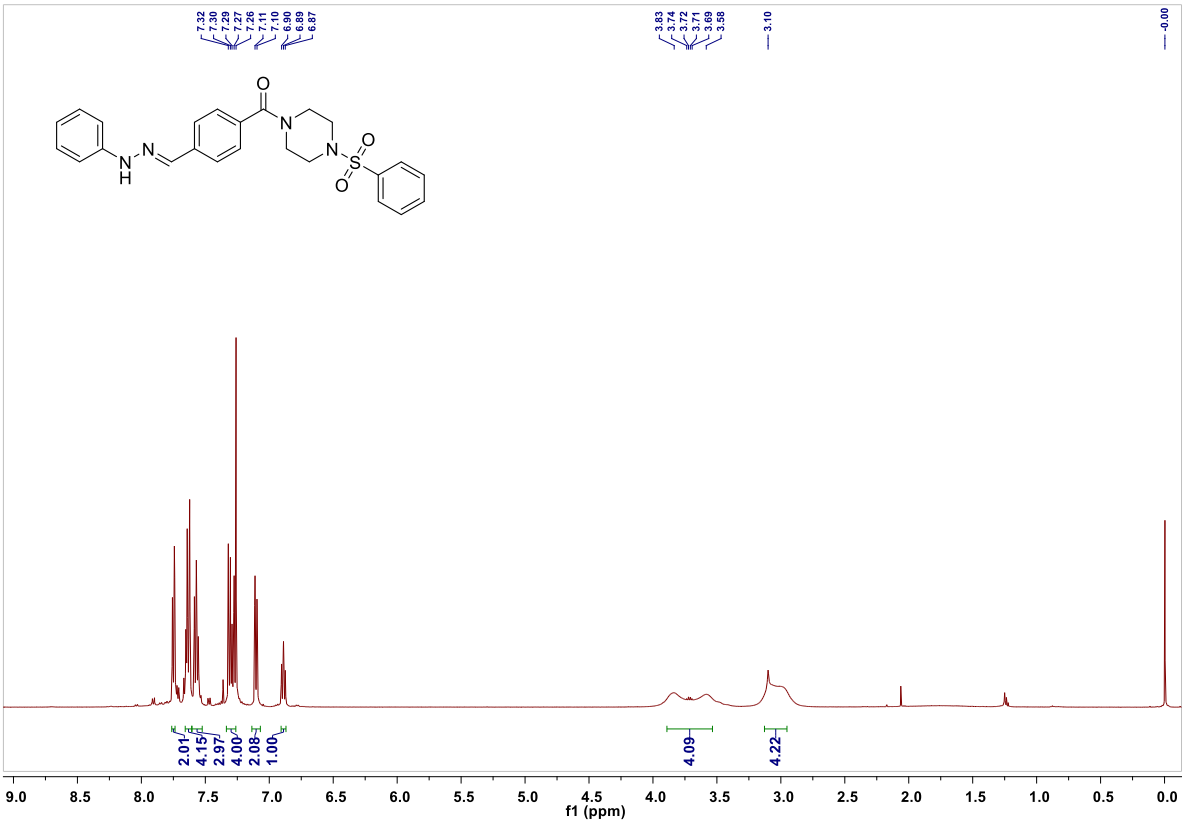

^{1}H NMR spectrum of compound F9 (Chapter 4)

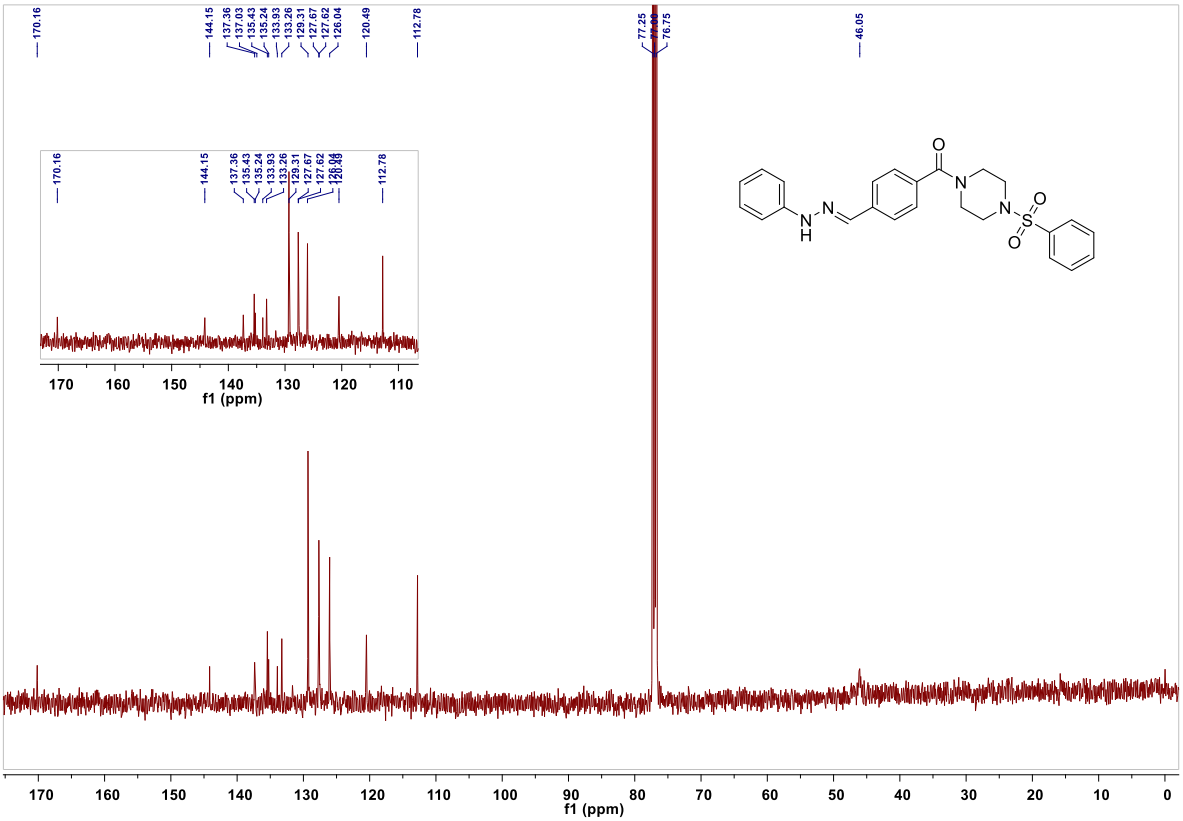

^{13}C NMR spectrum of compound F9 (Chapter 4)

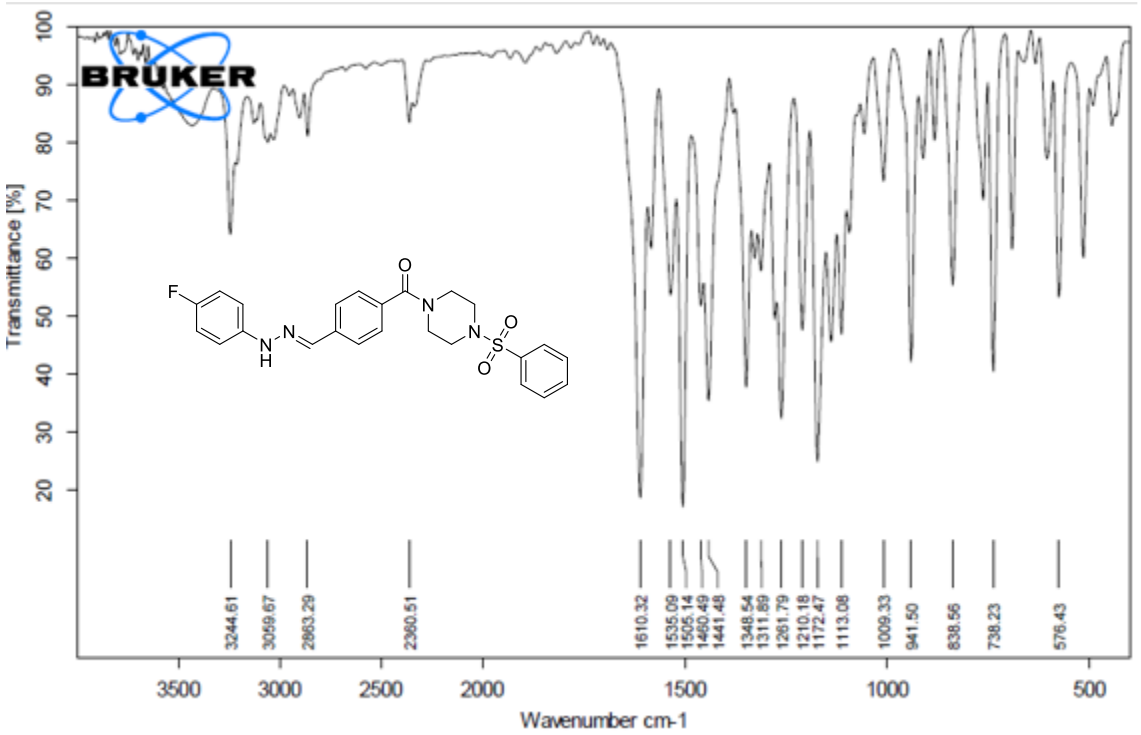

IR spectrum of compound F10 (Chapter 4)

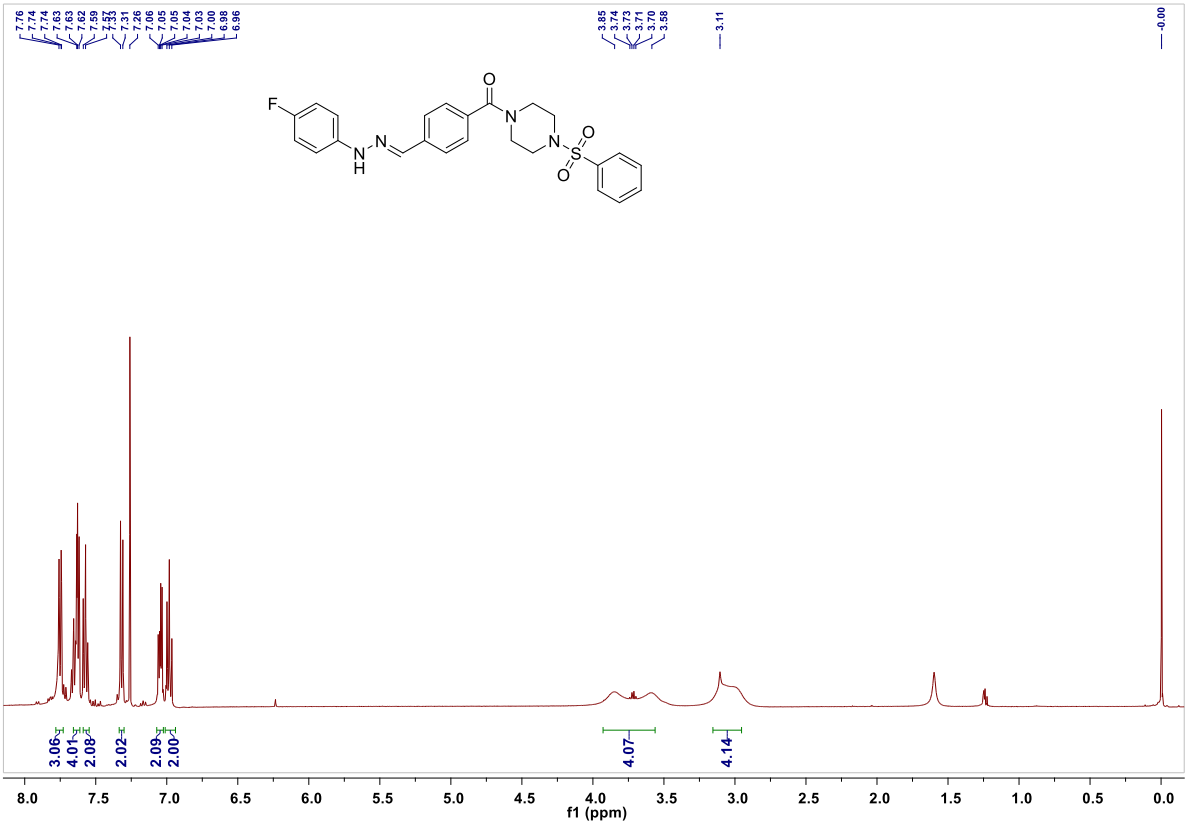

^{1}H NMR spectrum of compound F10 (Chapter 4)

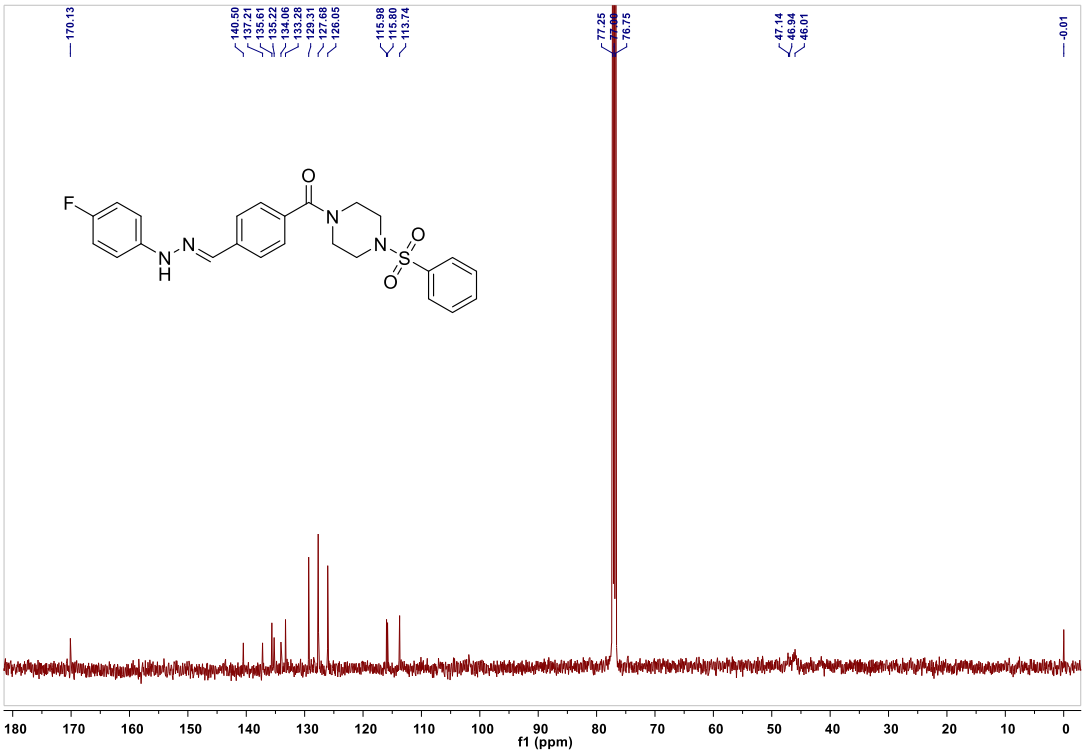

^{13}C NMR spectrum of compound F10 (Chapter 4)

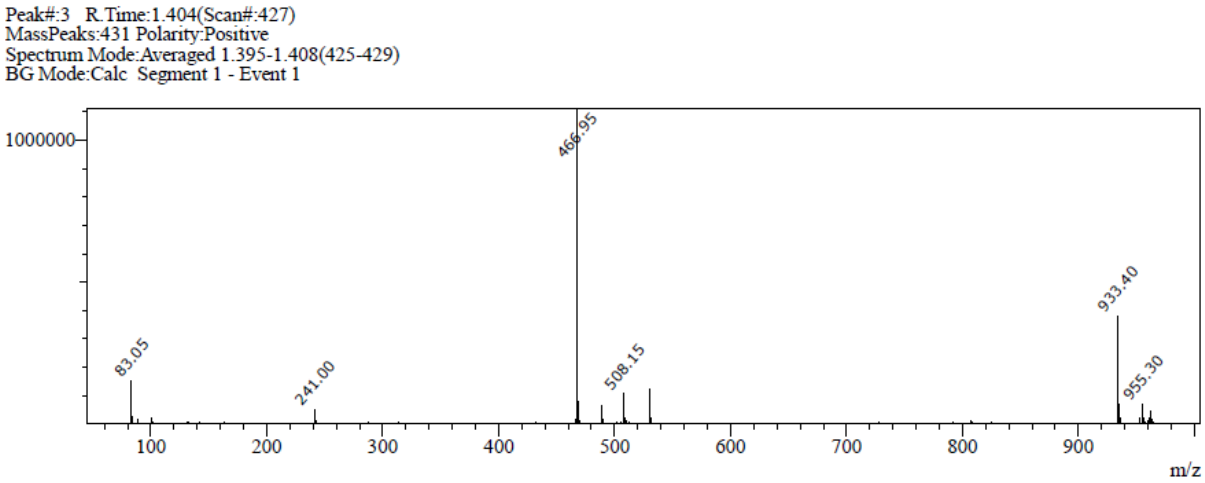

Mass spectrum of compound F10 (Chapter 4)

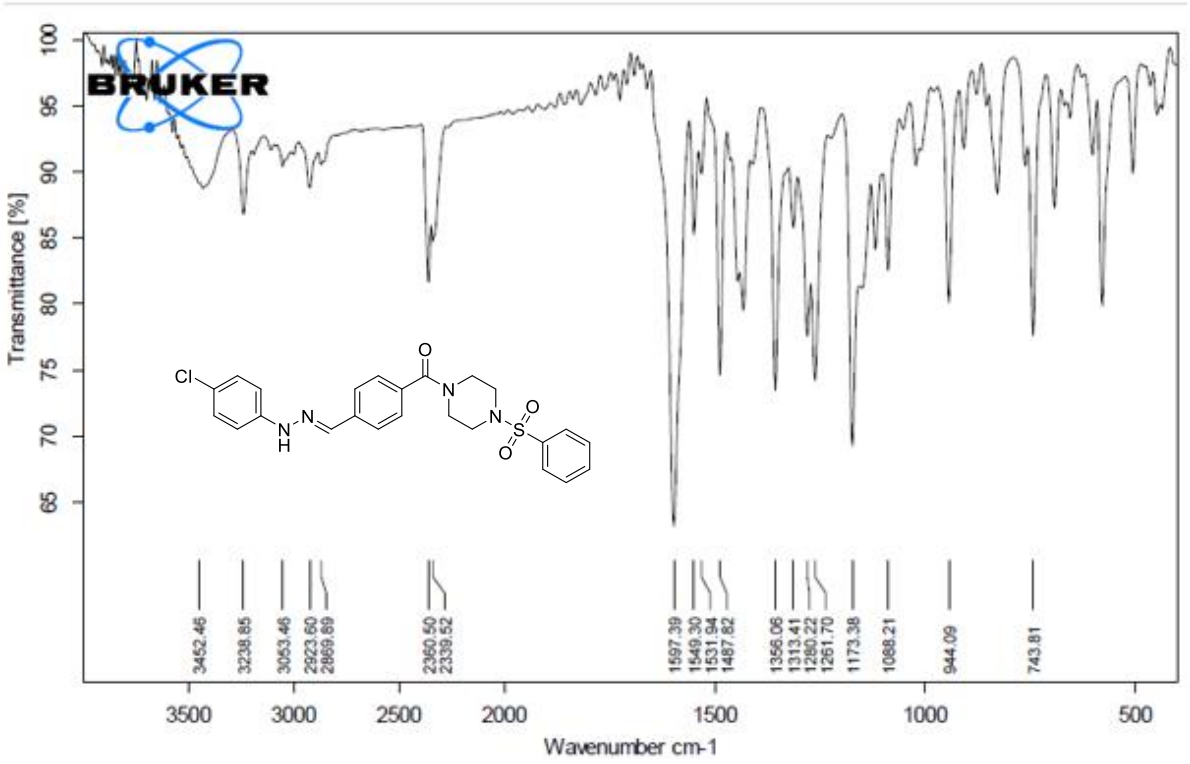

IR spectrum of compound F11 (Chapter 4)

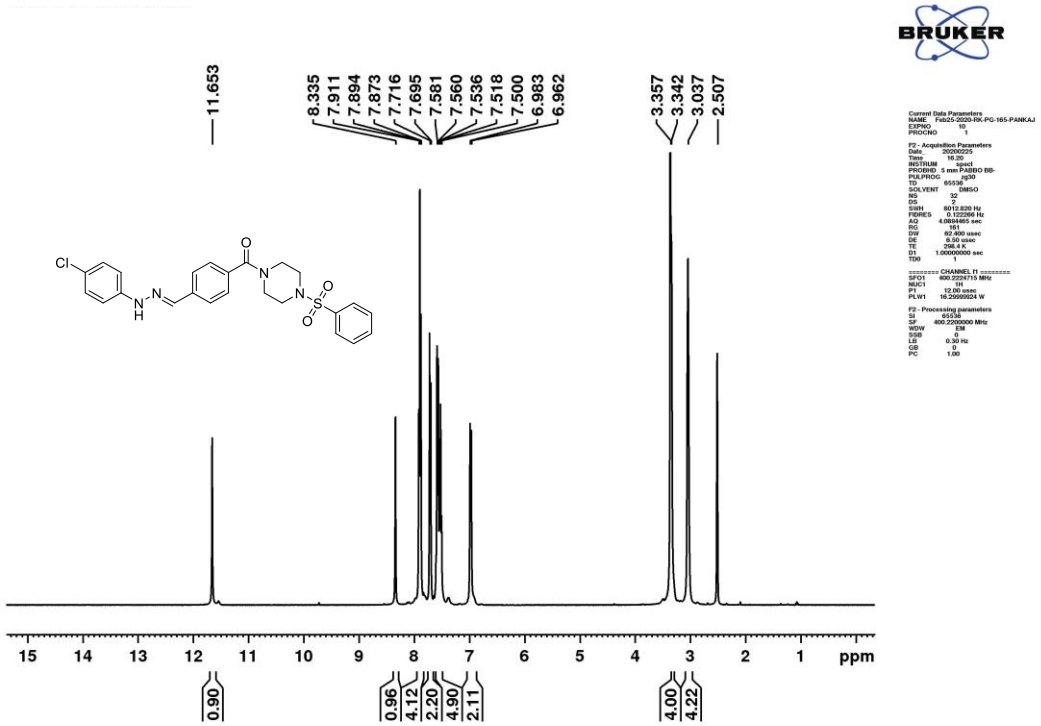

^{1}H NMR spectrum of compound F11 (Chapter 4)

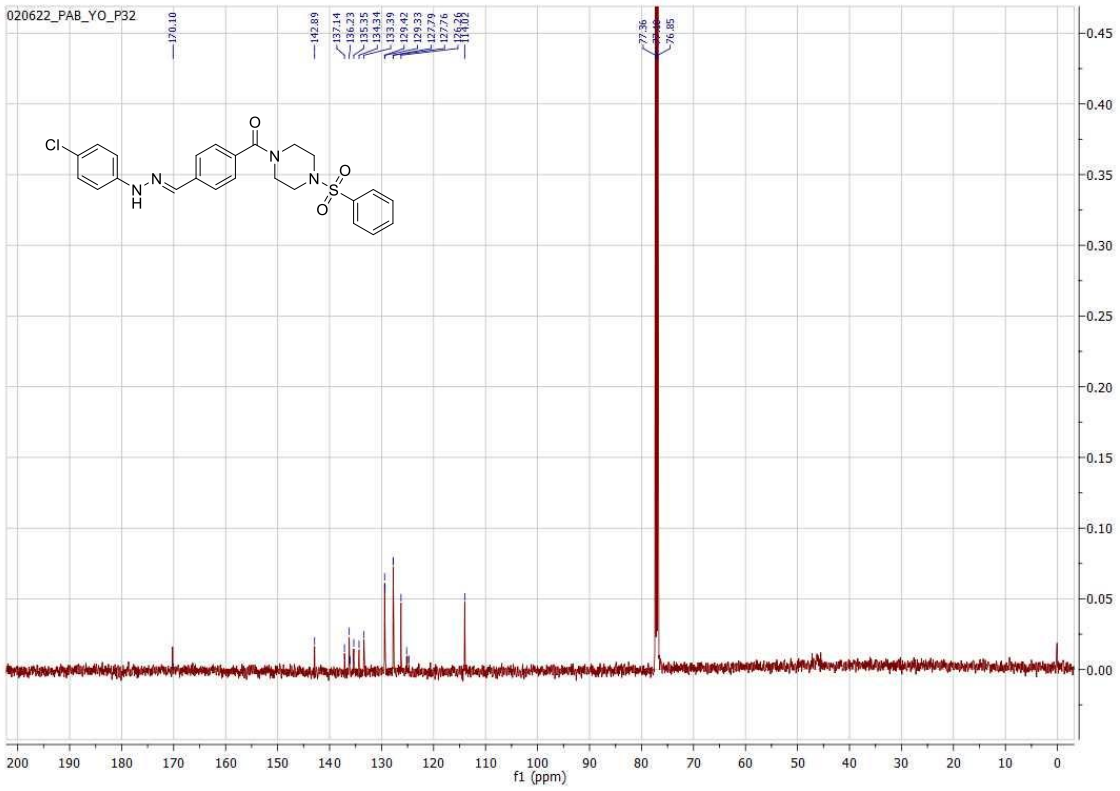

^{13}C NMR spectrum of compound F11 (Chapter 4)

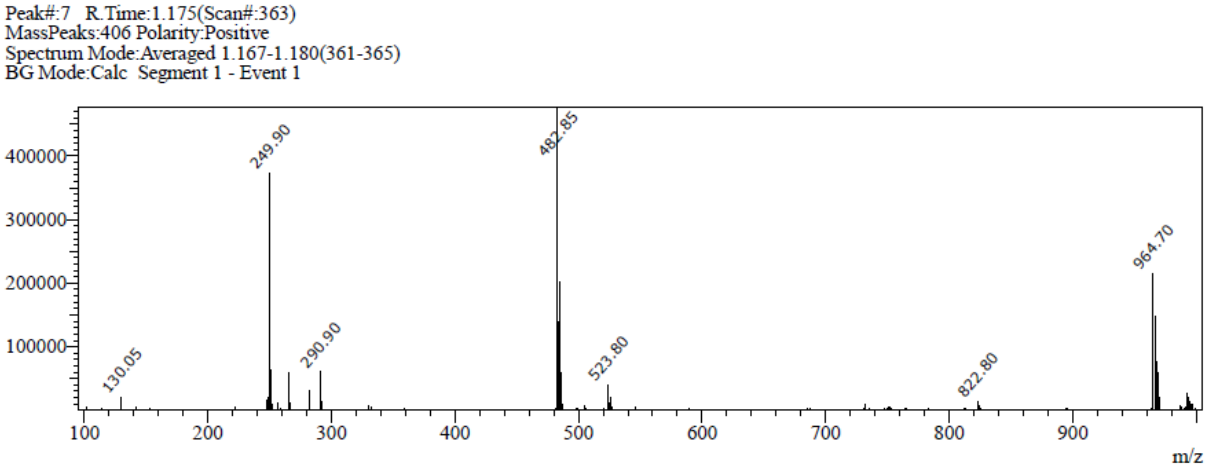

Mass spectrum of compound F11 (Chapter 4)

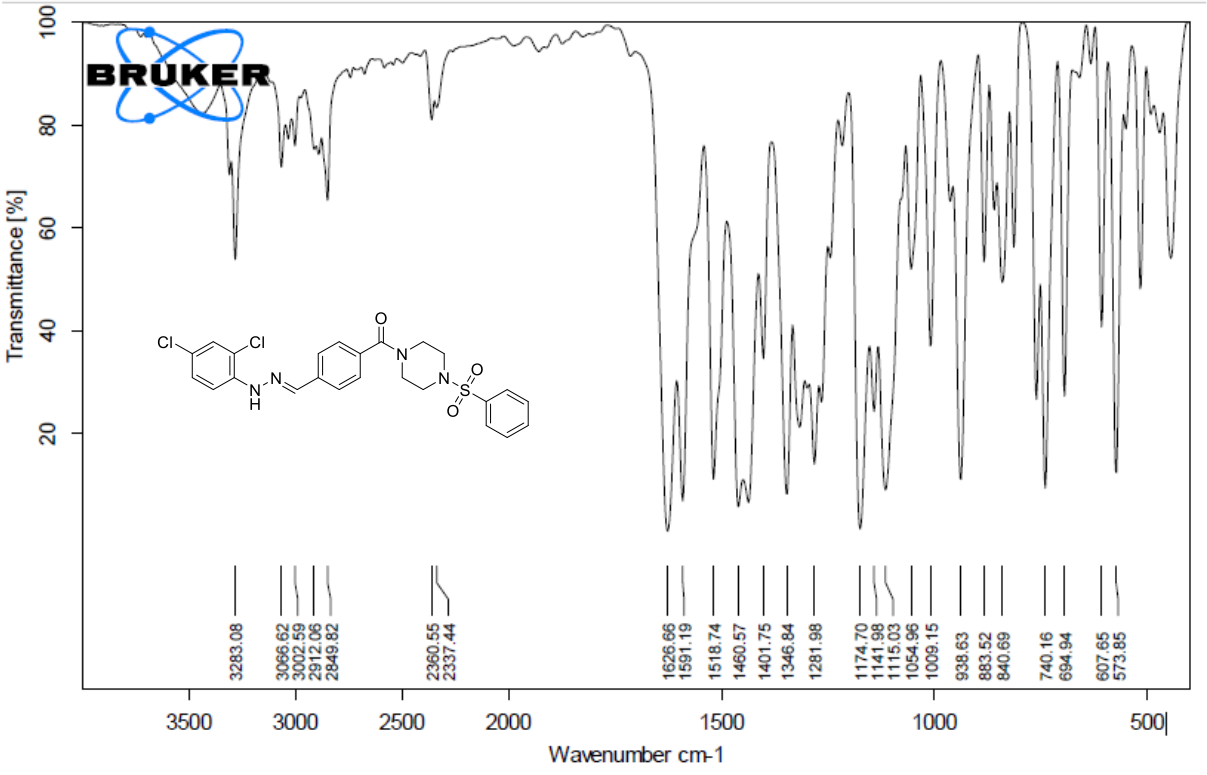

IR spectrum of compound F12 (Chapter 4)

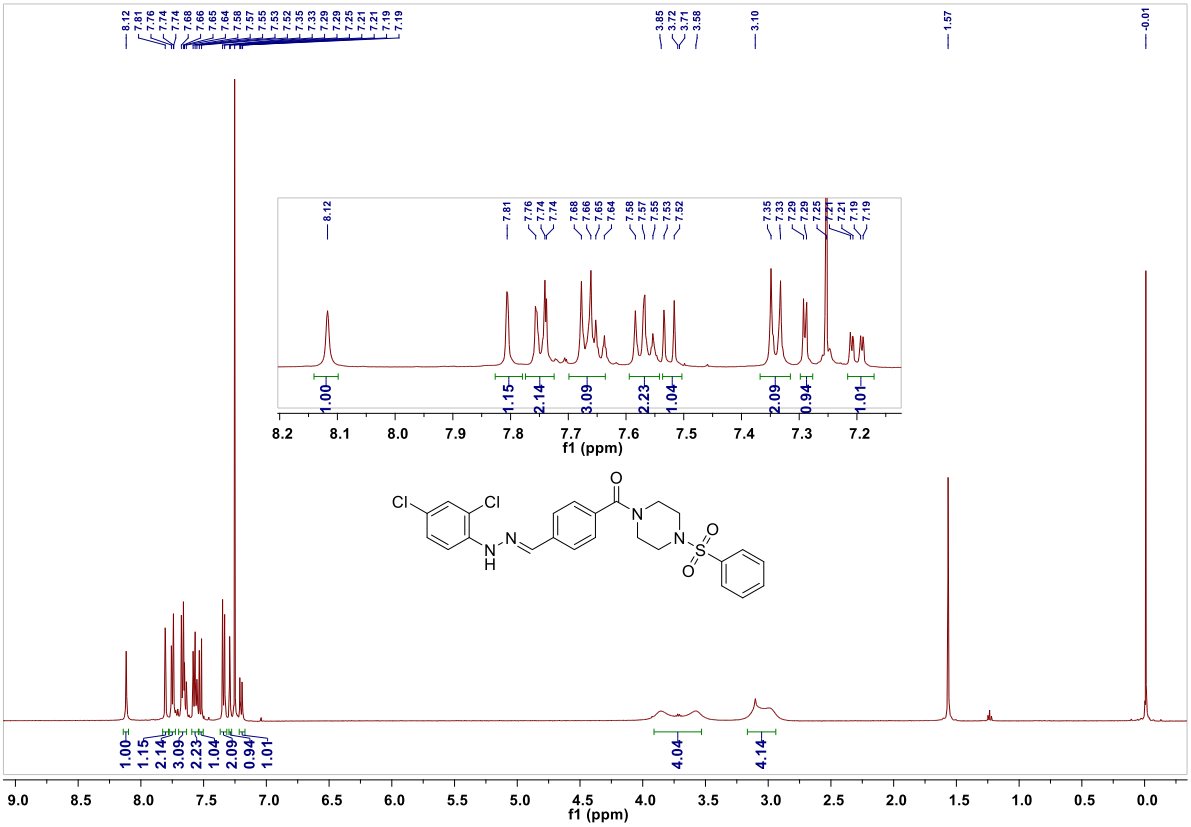

[1]H NMR spectrum of compound F12 (Chapter 4)

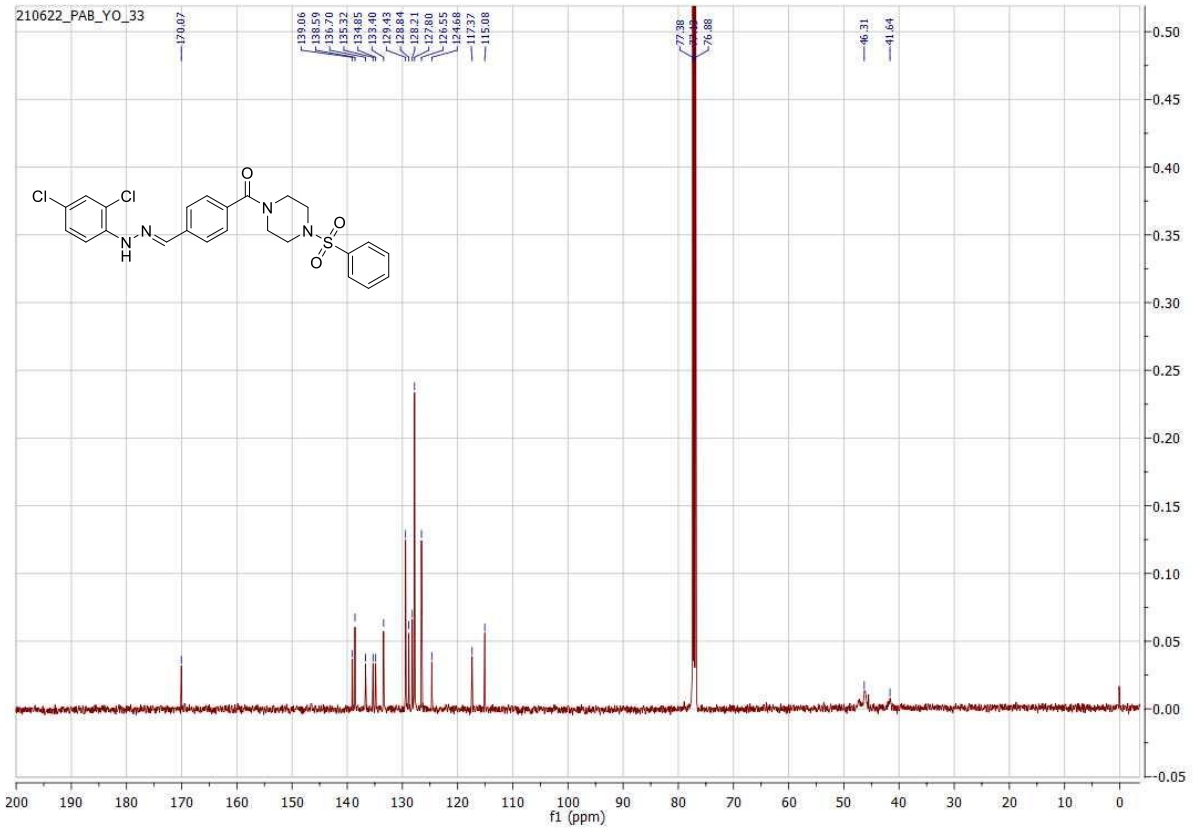

^{13}C NMR spectrum of compound F12 (Chapter 4)

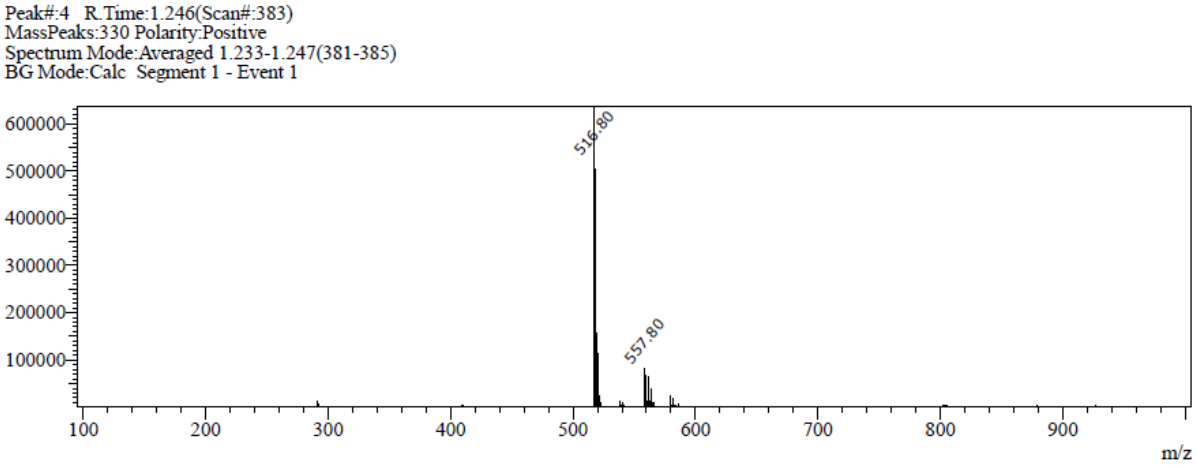

Mass spectrum of compound F12 (Chapter 4)

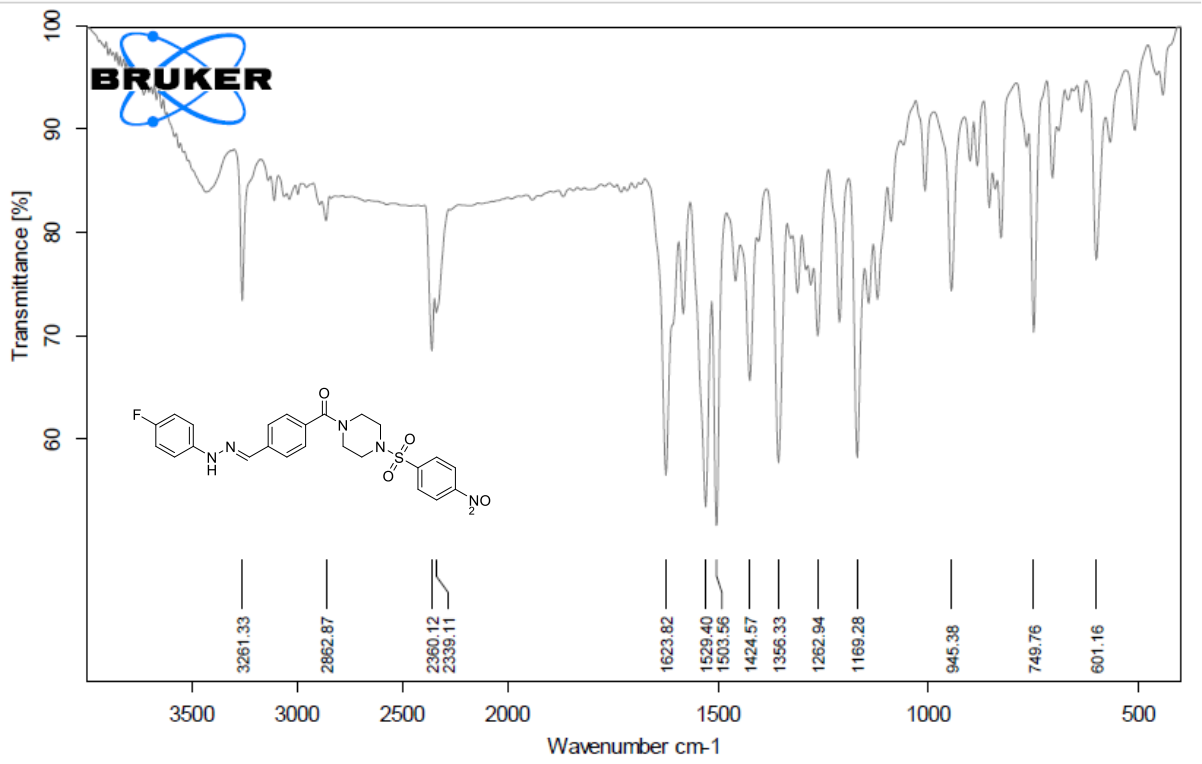

IR spectrum of compound F13 (Chapter 4)

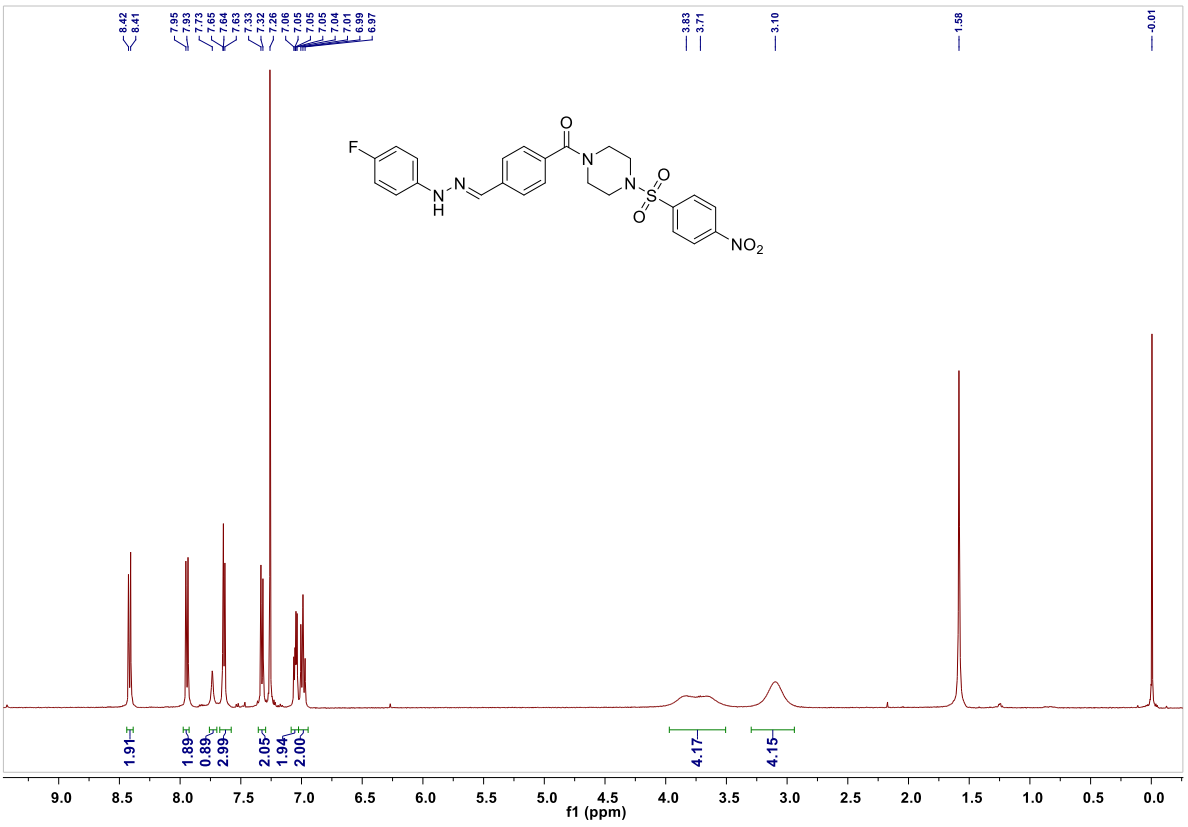

^{1}H NMR spectrum of compound F13 (Chapter 4)

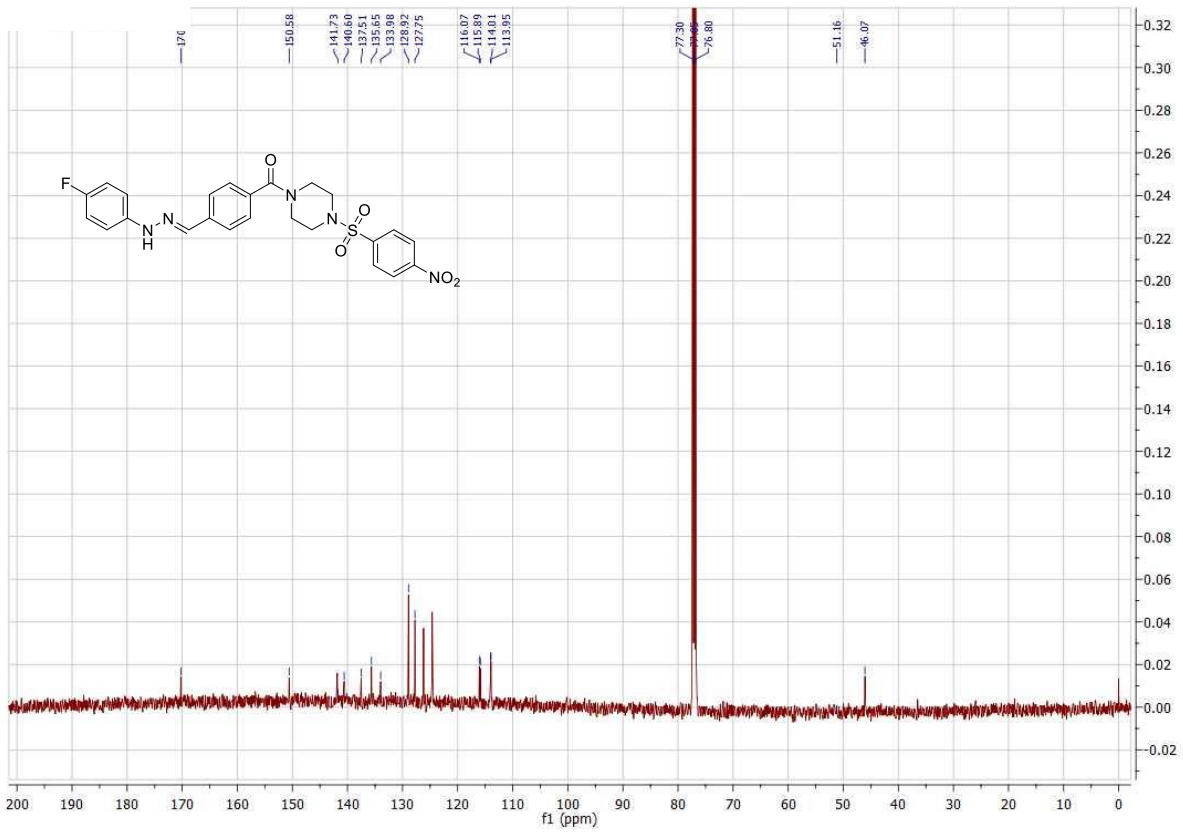

^{13}C NMR spectrum of compound F13 (Chapter 4)

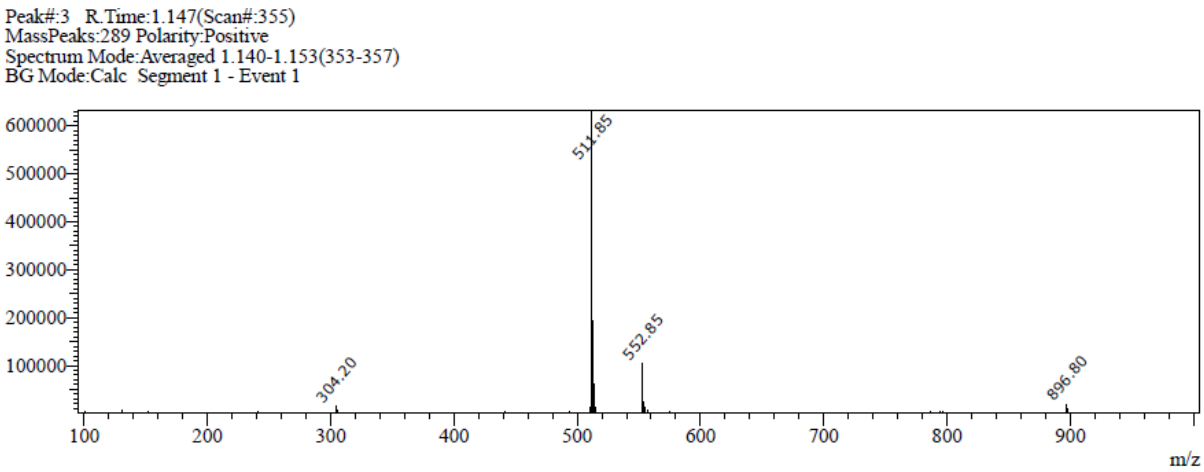

Mass spectrum of compound F13 (Chapter 4)

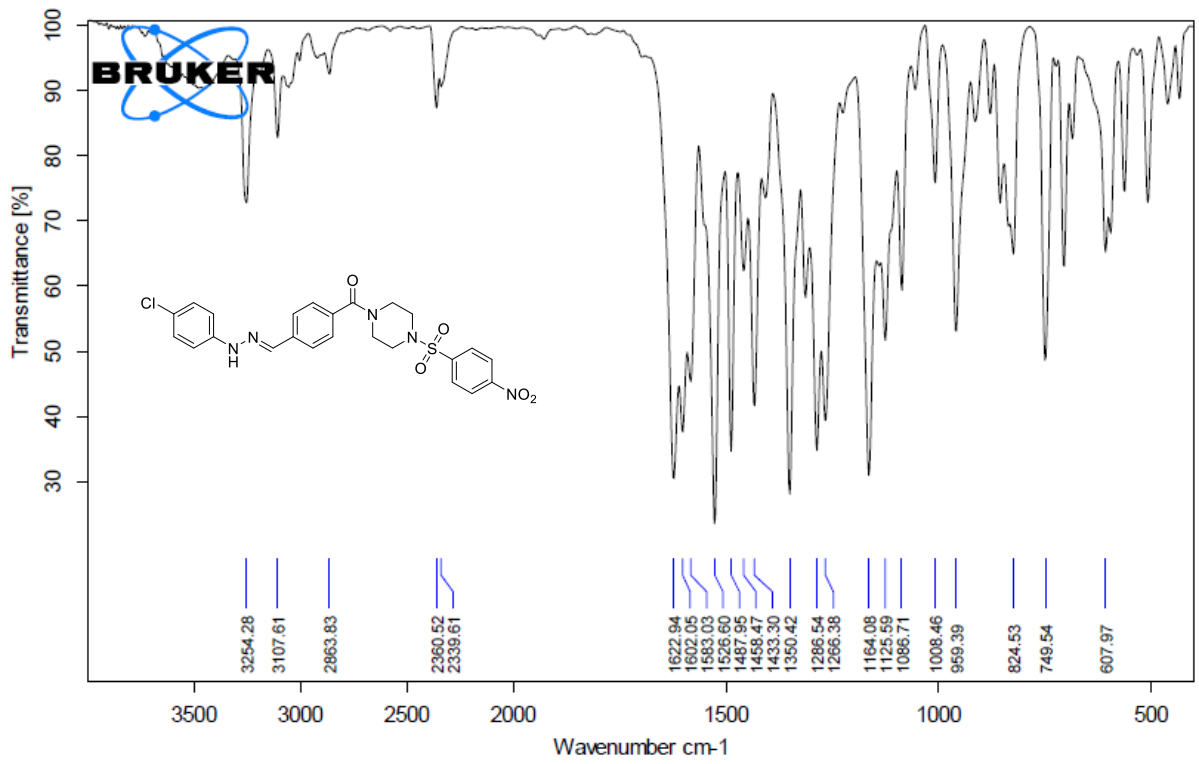

IR spectrum of compound F14 (Chapter 4)

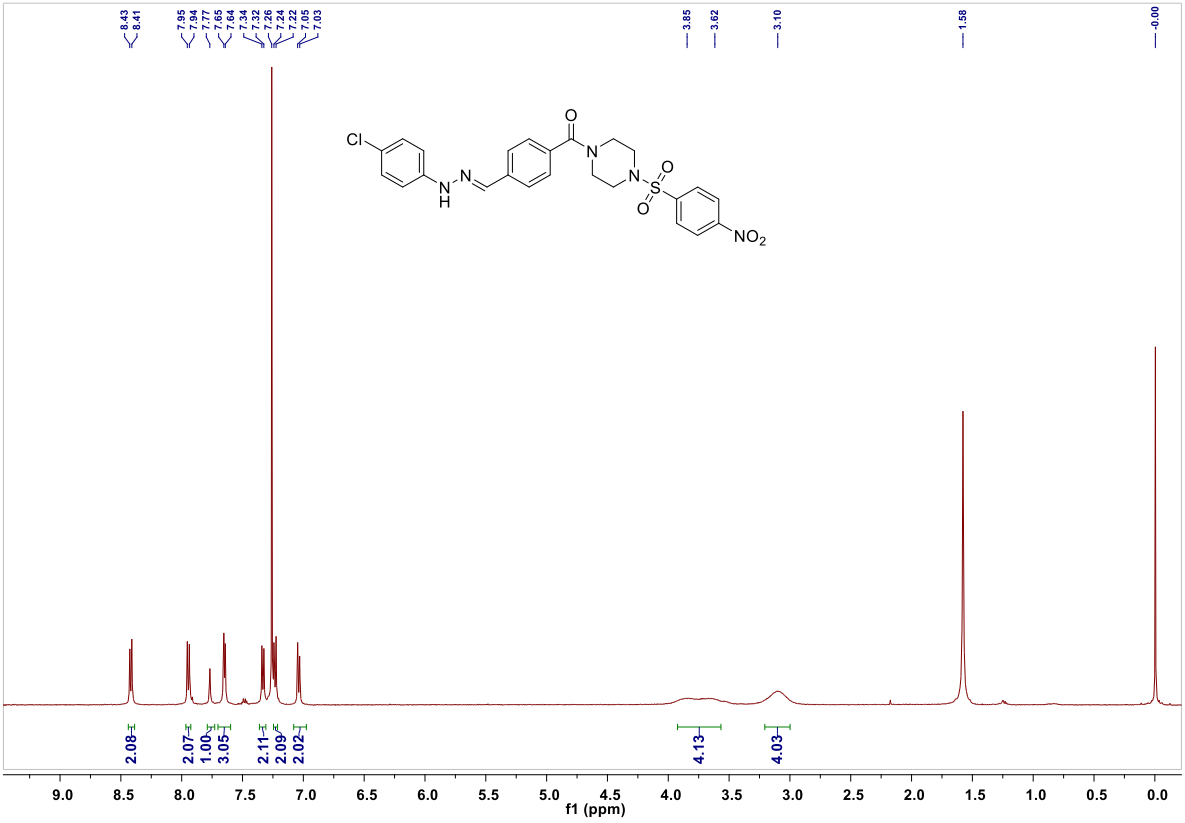

^{1}H NMR spectrum of compound F14 (Chapter 4)

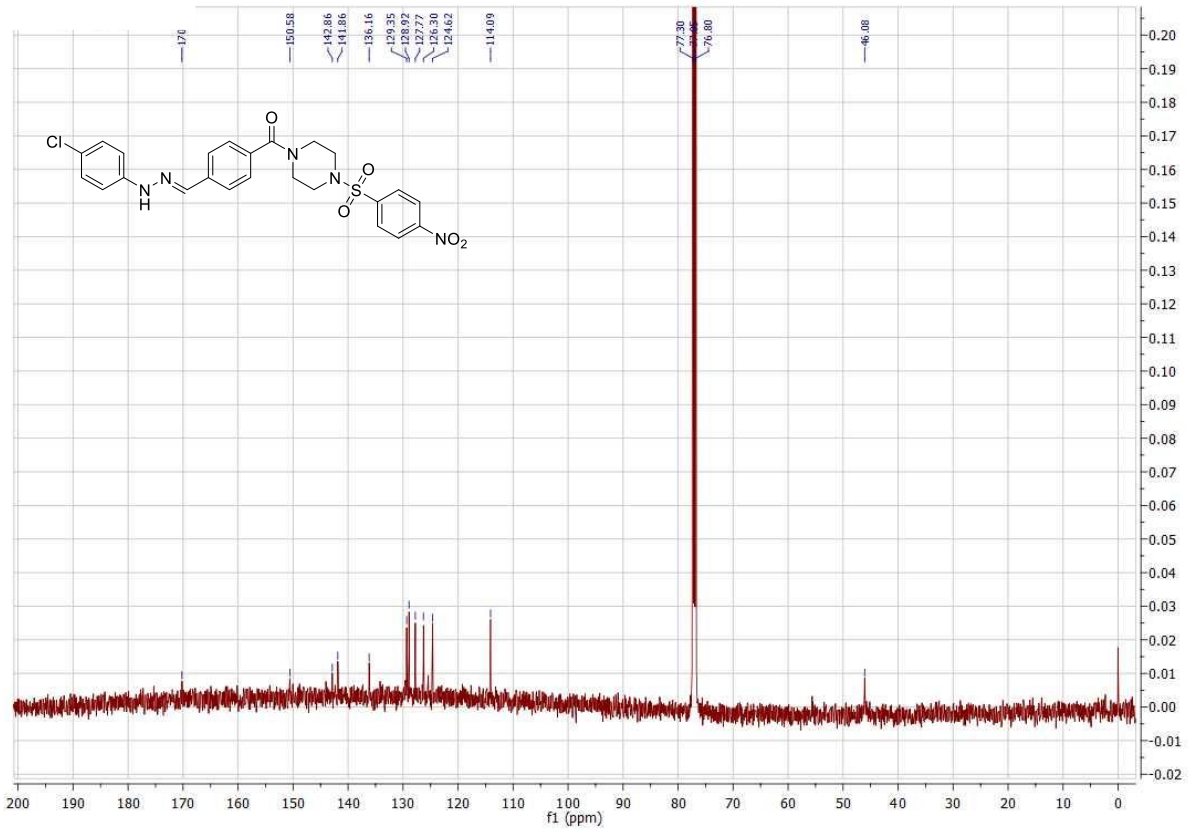

^{13}C NMR spectrum of compound F14 (Chapter 4)

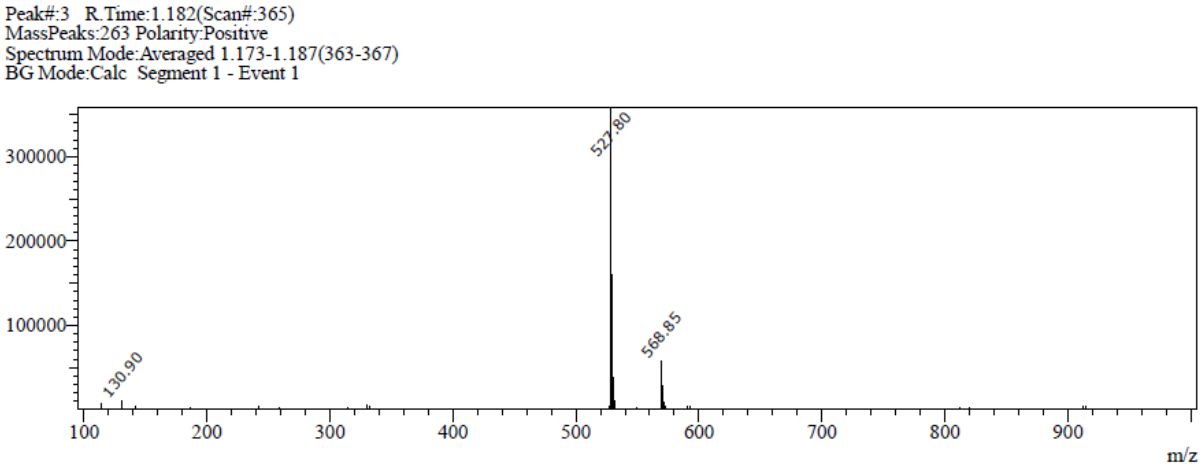

Mass spectrum of compound F14 (Chapter 4)

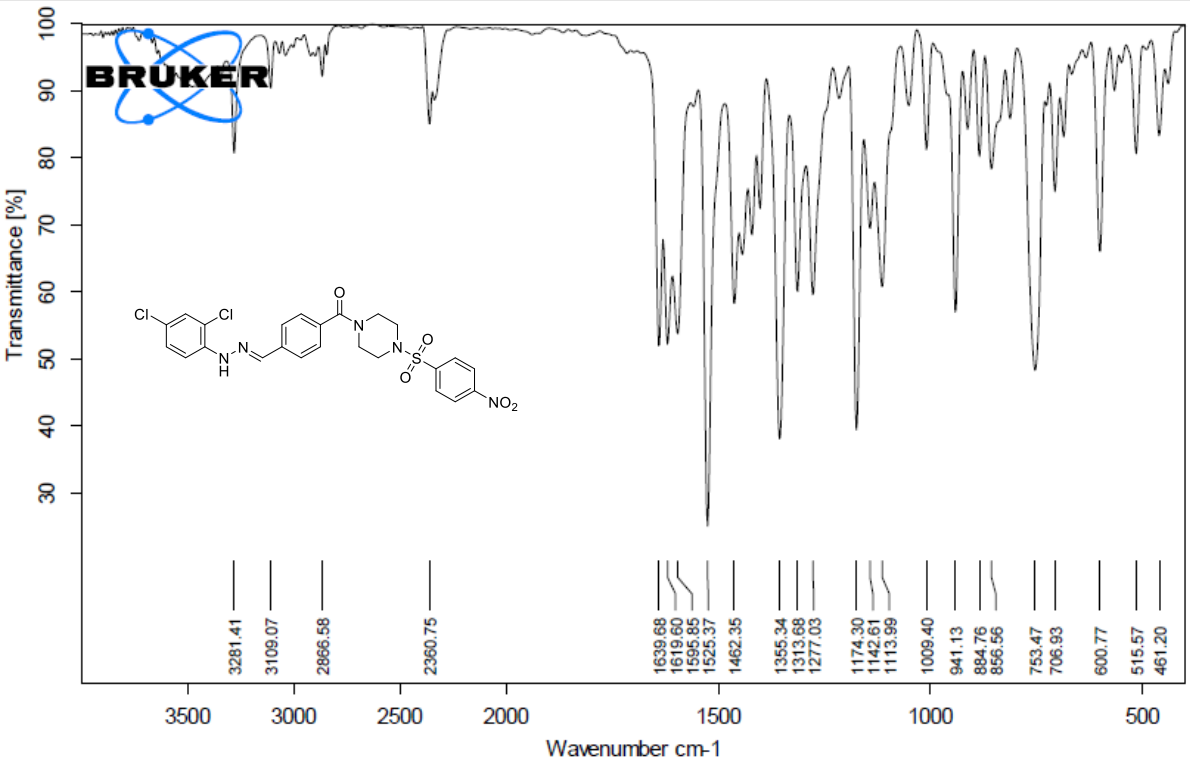

IR spectrum of compound F15 (Chapter 4)

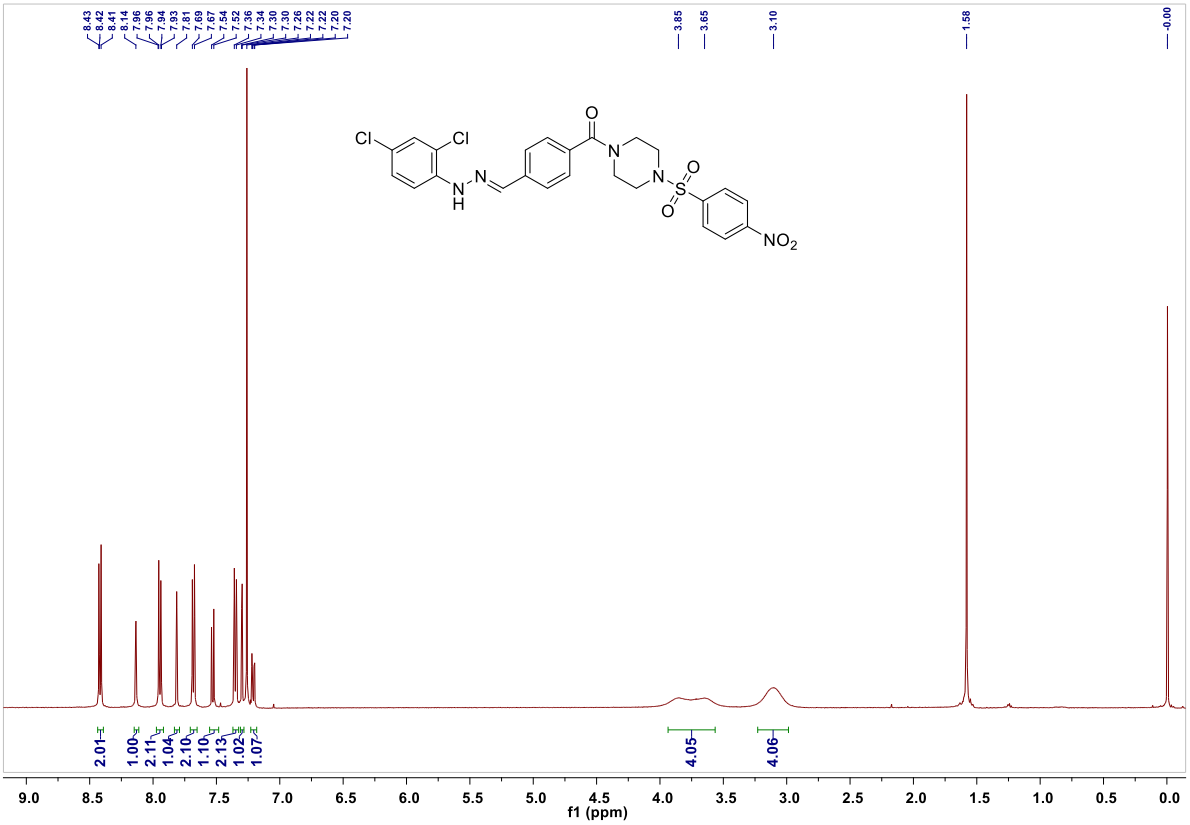

^{1}H NMR spectrum of compound F15 (Chapter 4)

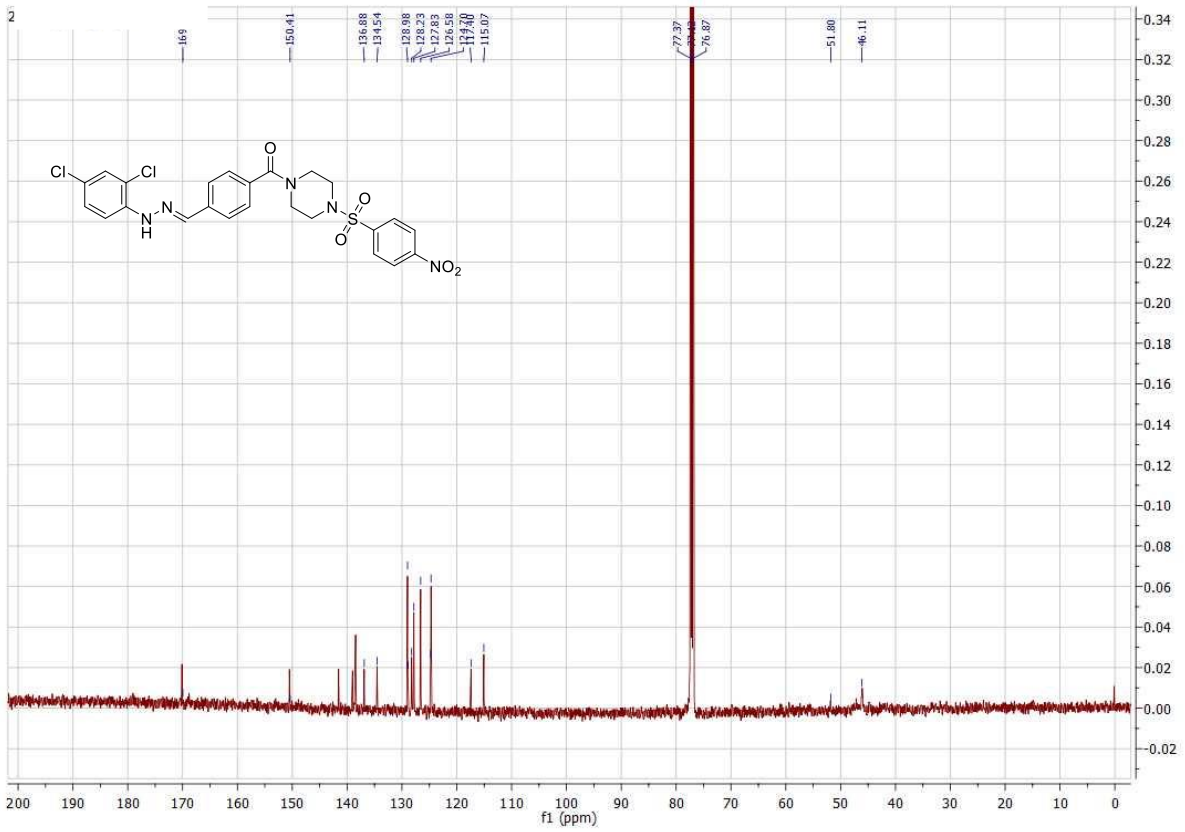

^{13}C NMR spectrum of compound F15 (Chapter 4)

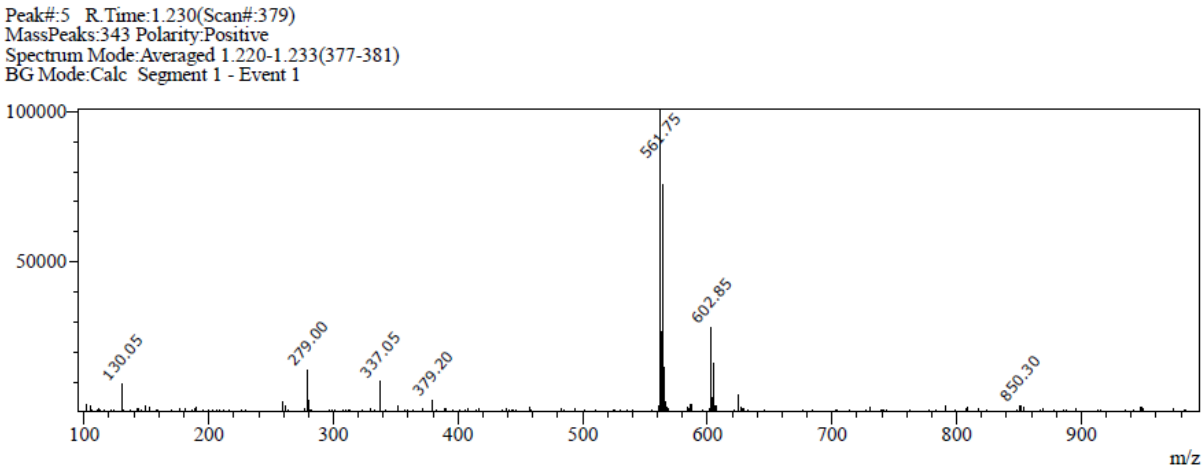

Mass spectrum of compound F15 (Chapter 4)

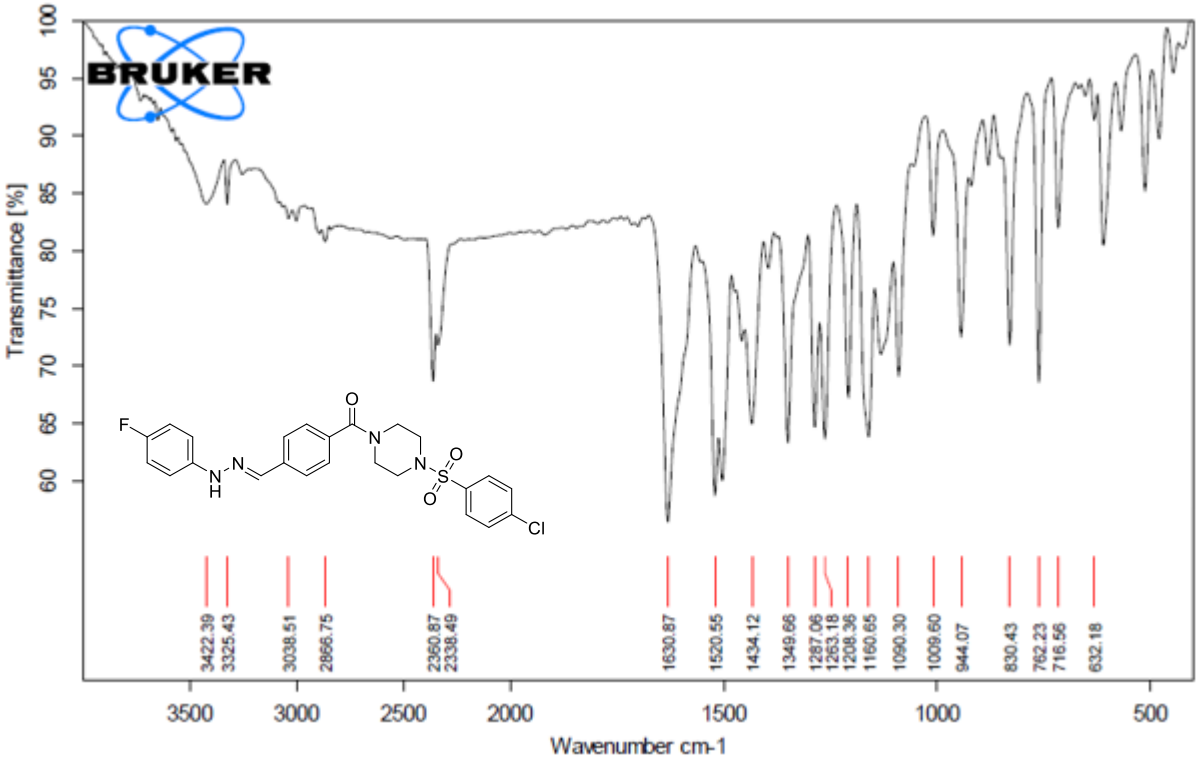

IR spectrum of compound F16 (Chapter 4)

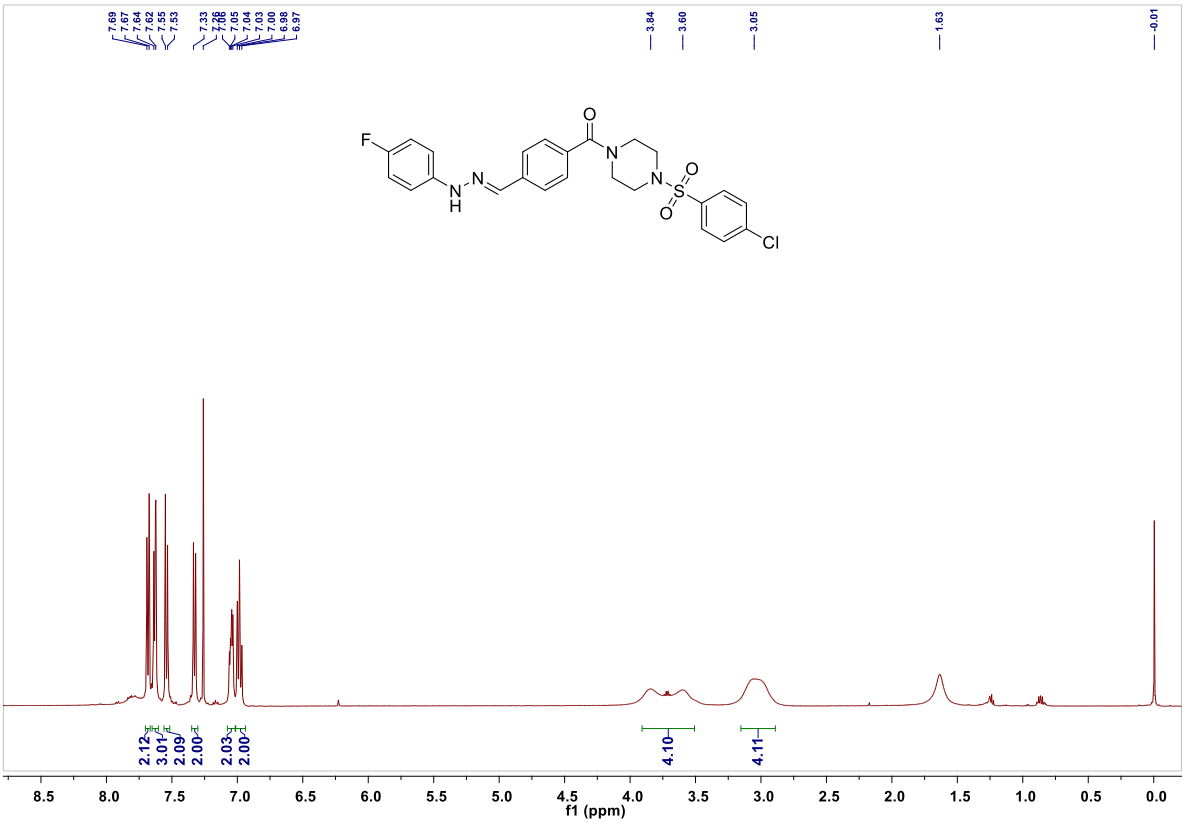

^{1}H NMR spectrum of compound F16 (Chapter 4)

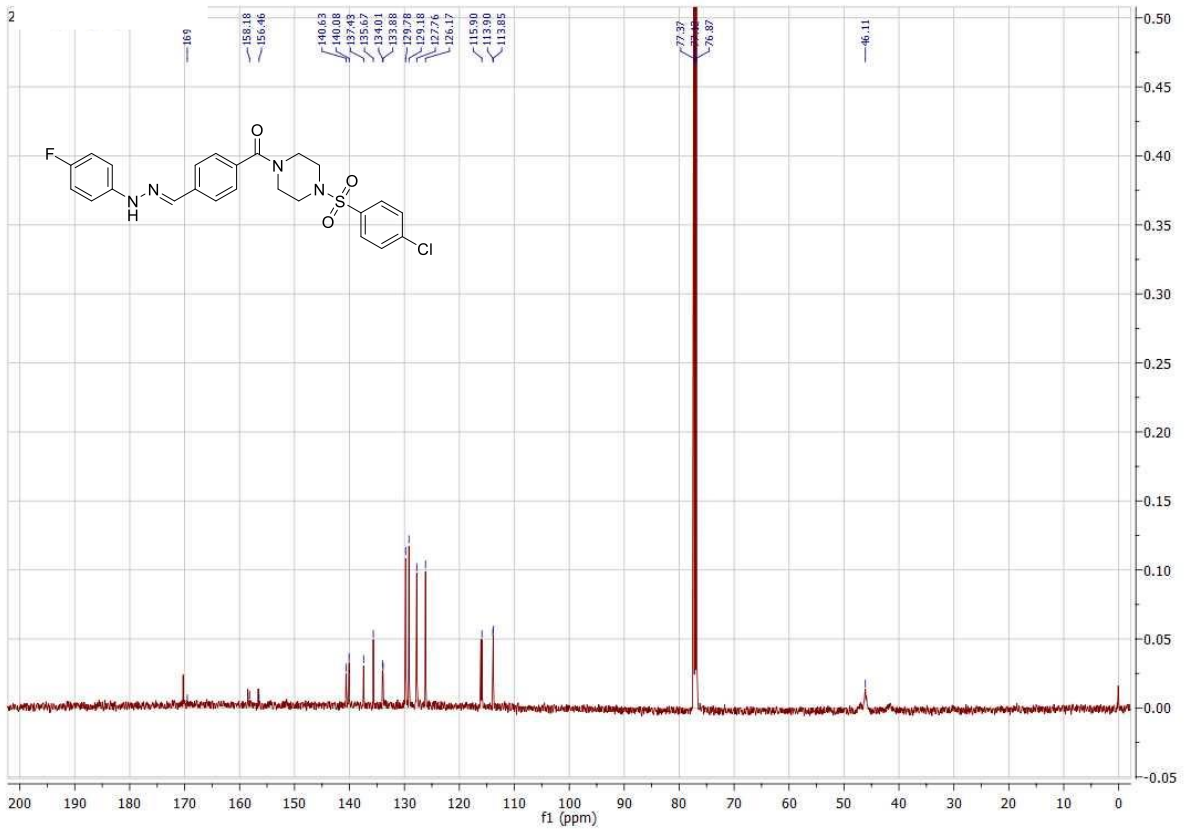

^{13}CNMR spectrum of compound F16 (Chapter 4)

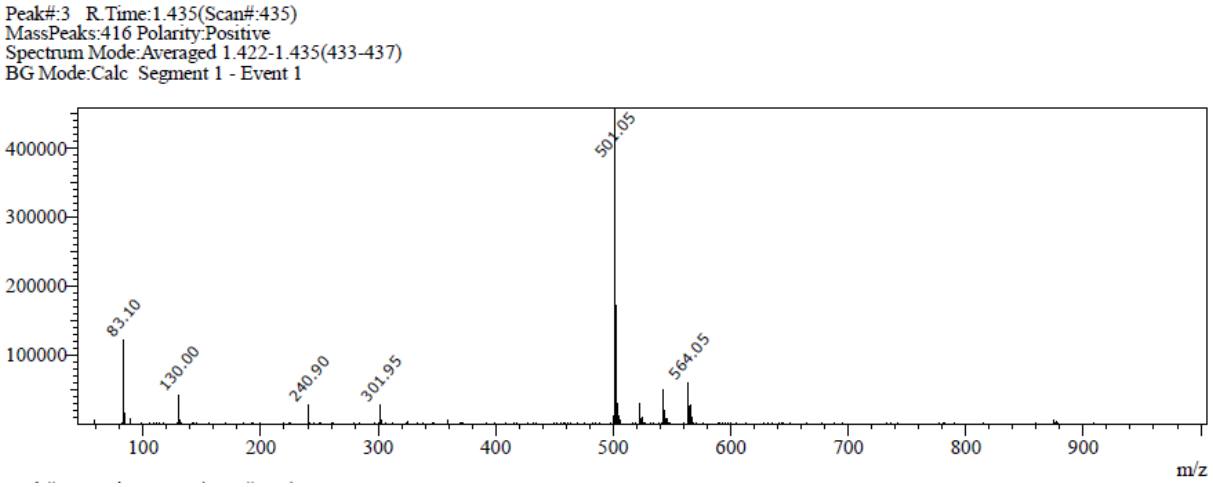

Mass spectrum of compound F16 (Chapter 4)

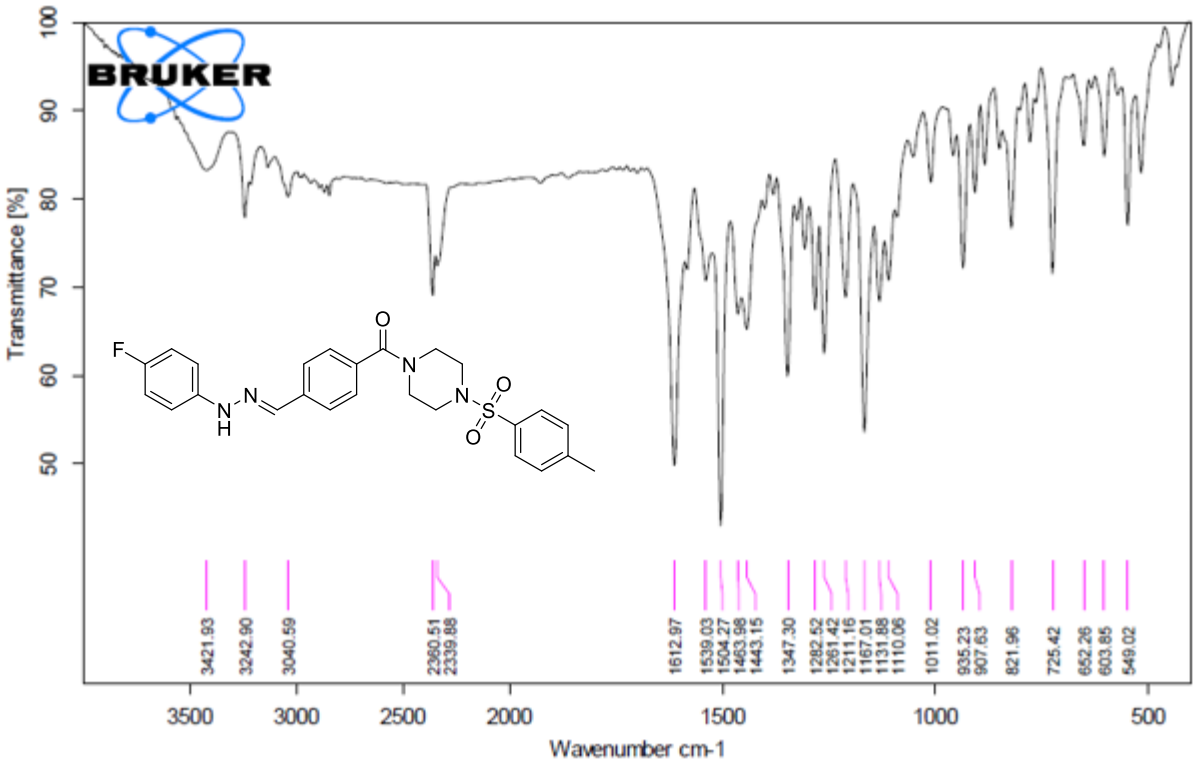

IR spectrum of compound F17 (Chapter 4)

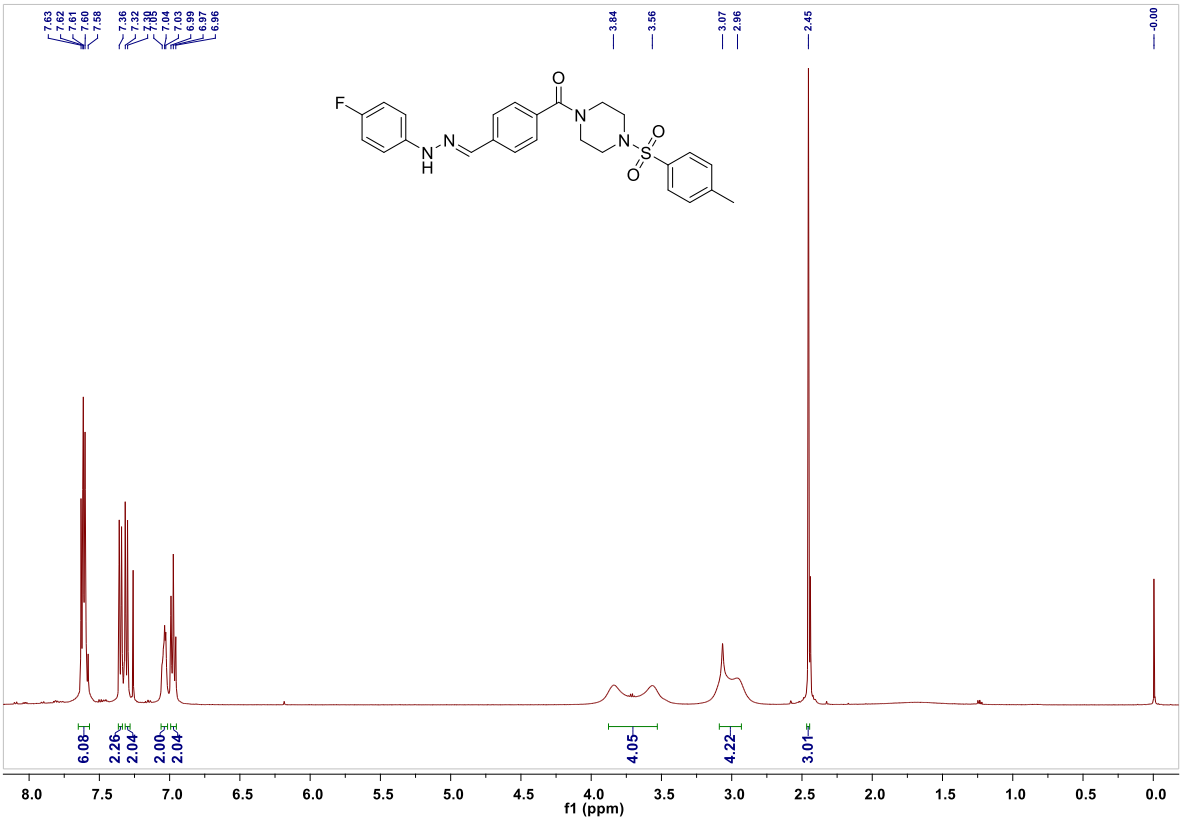

^{1}H NMR spectrum of compound F17 (Chapter 4)

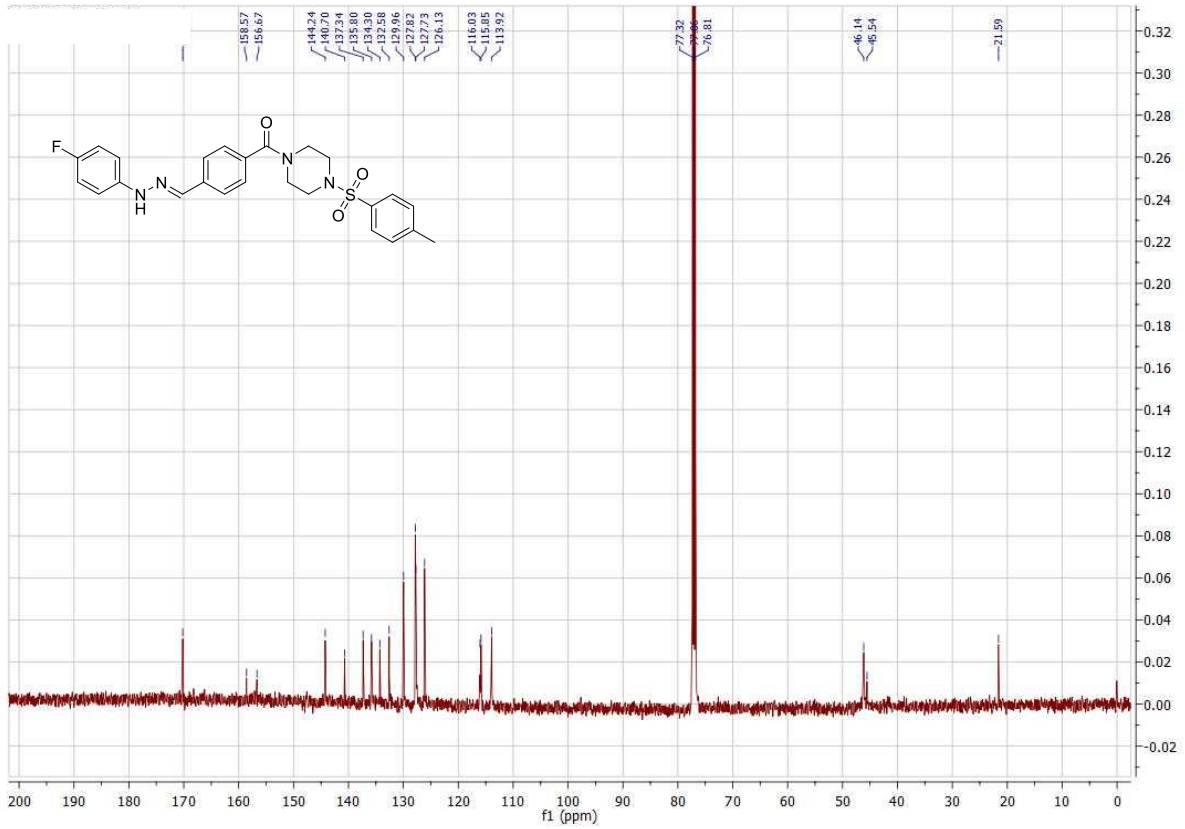

^{13}C NMR spectrum of compound F17 (Chapter 4)

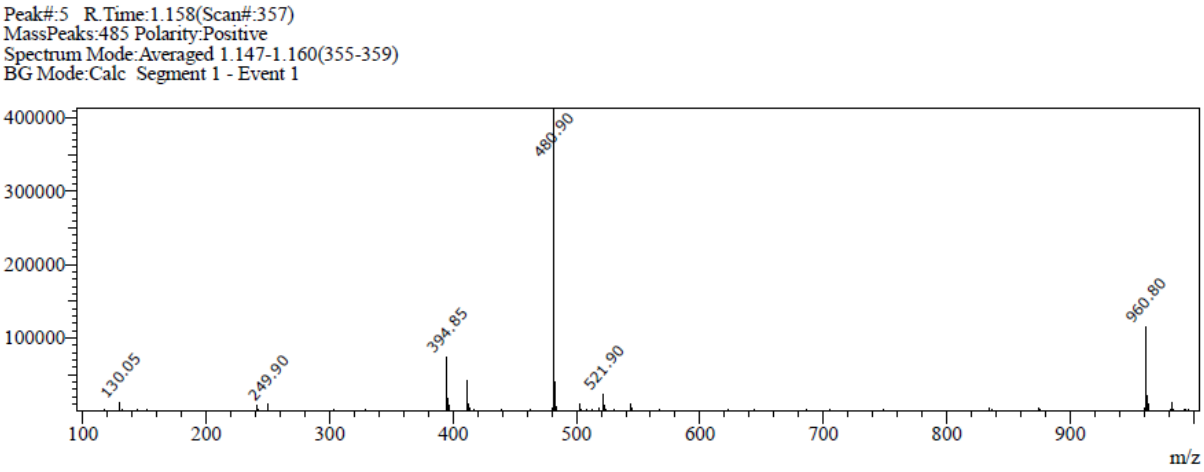

Mass spectrum of compound F17 (Chapter 4)

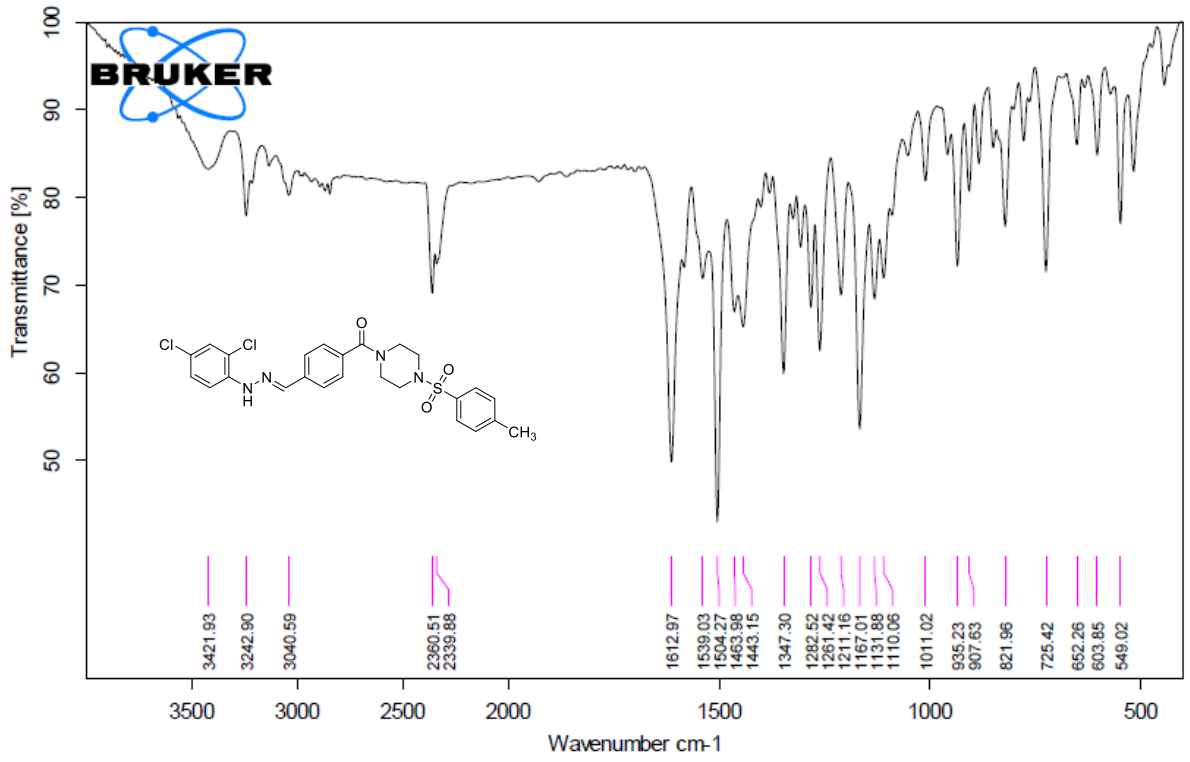

IR spectrum of compound F18 (Chapter 4)

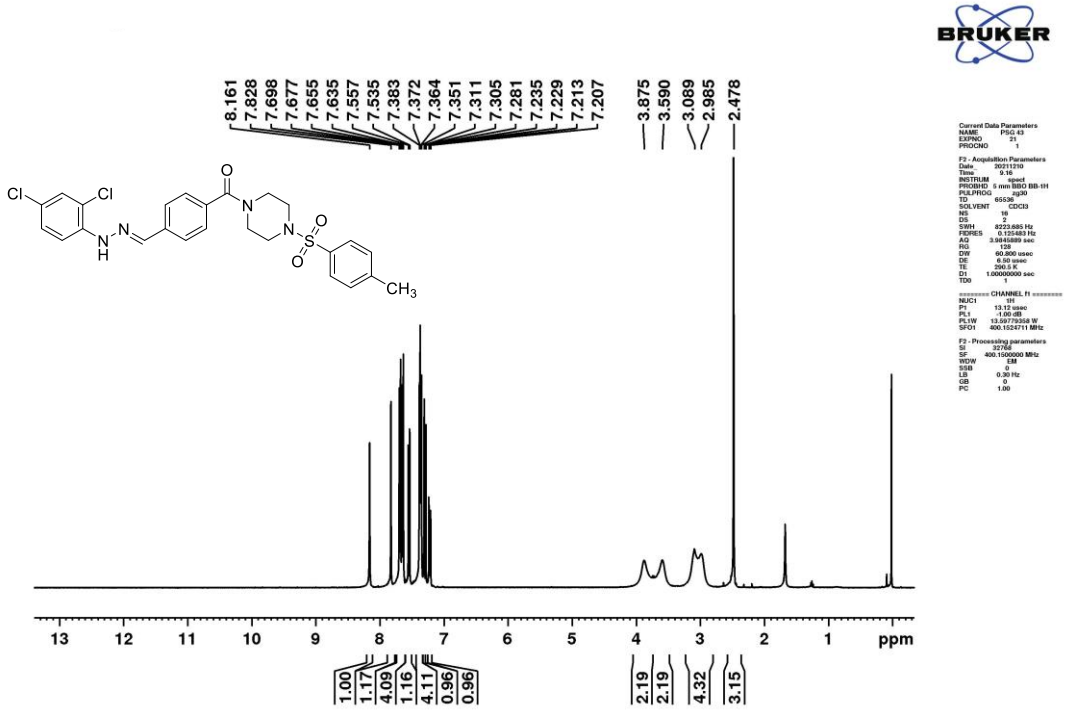

^{1}H NMR spectrum of compound F18 (Chapter 4)

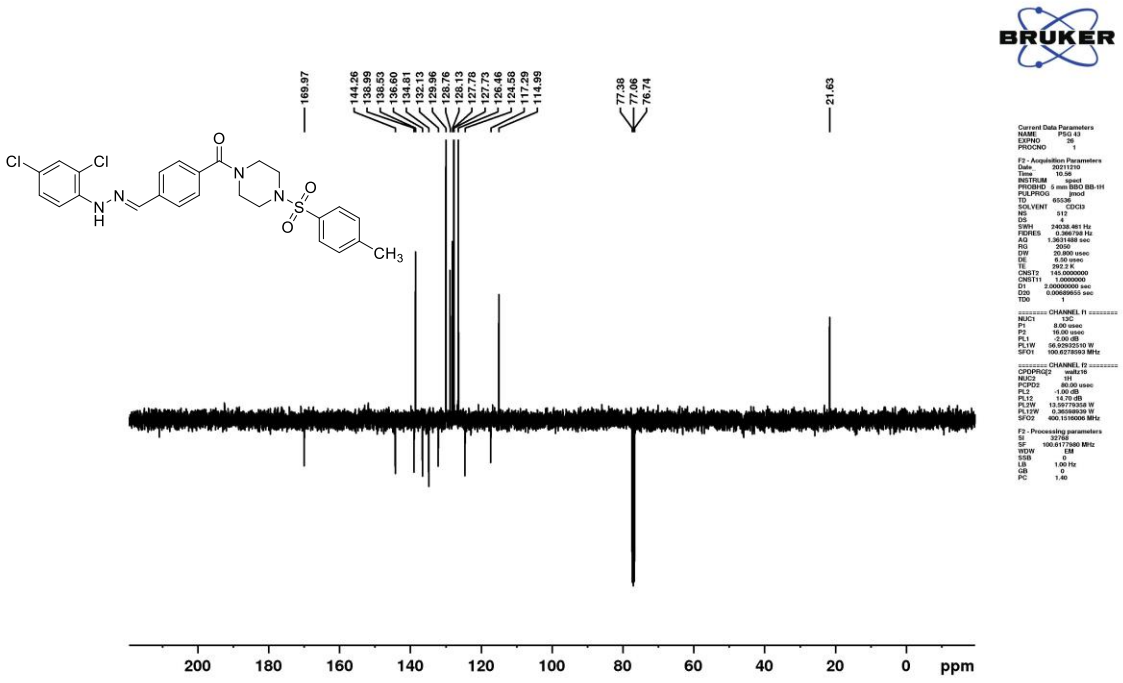

^{13}C NMR spectrum of compound F18 (Chapter 4)

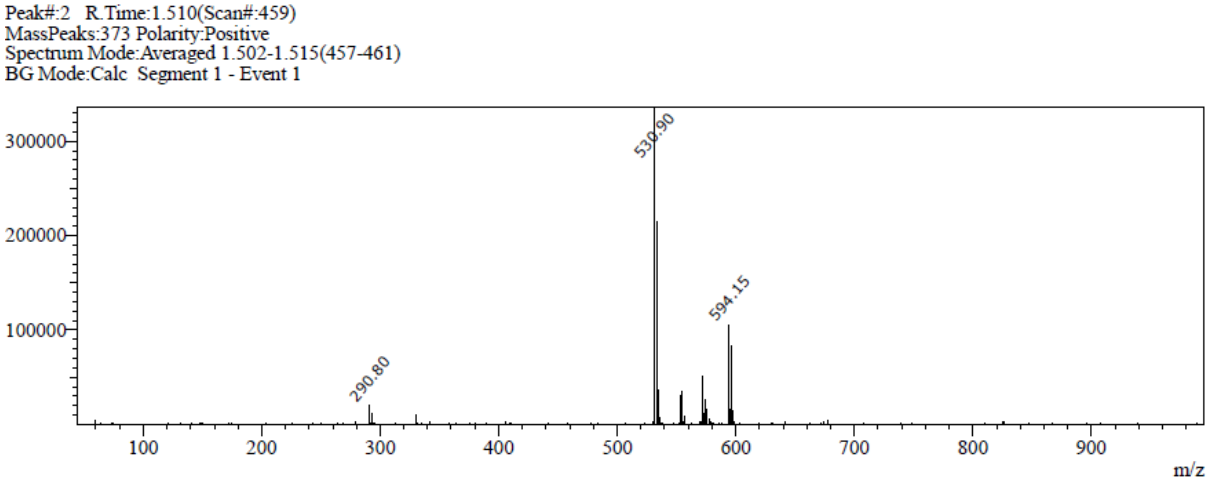

Mass spectrum of compound F18 (Chapter 4)

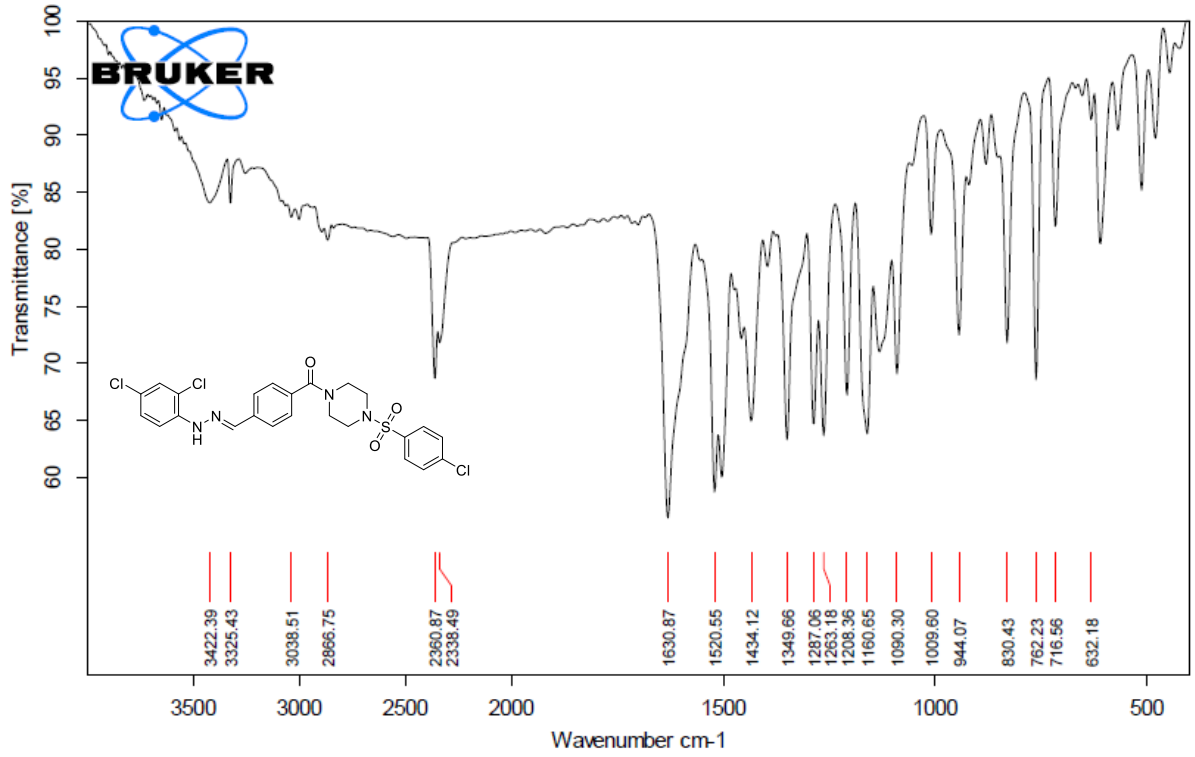

IR spectrum of compound F19 (Chapter 4)

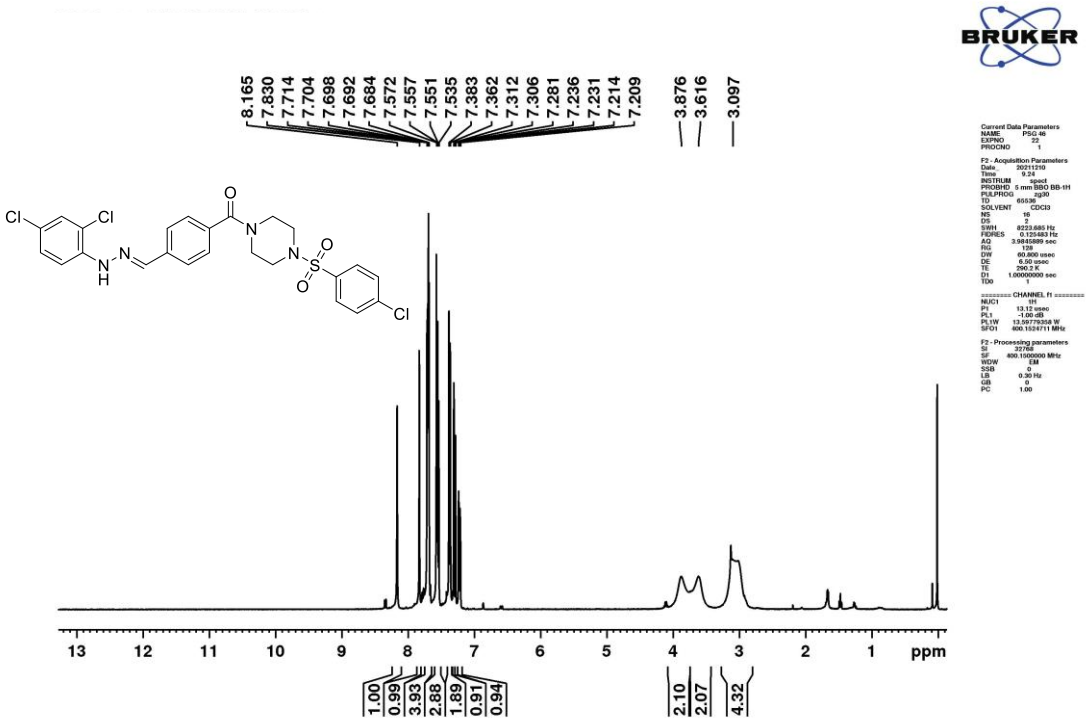

^{1}H NMR spectrum of compound F19 (Chapter 4)

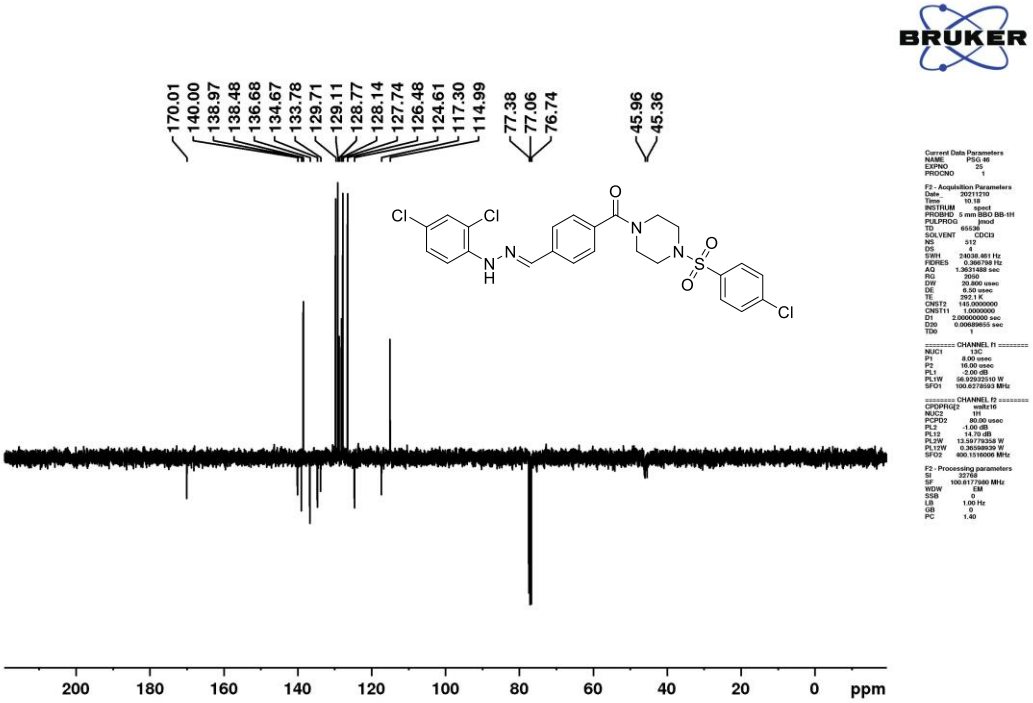

^{13}C NMR spectrum of compound F19 (Chapter 4)

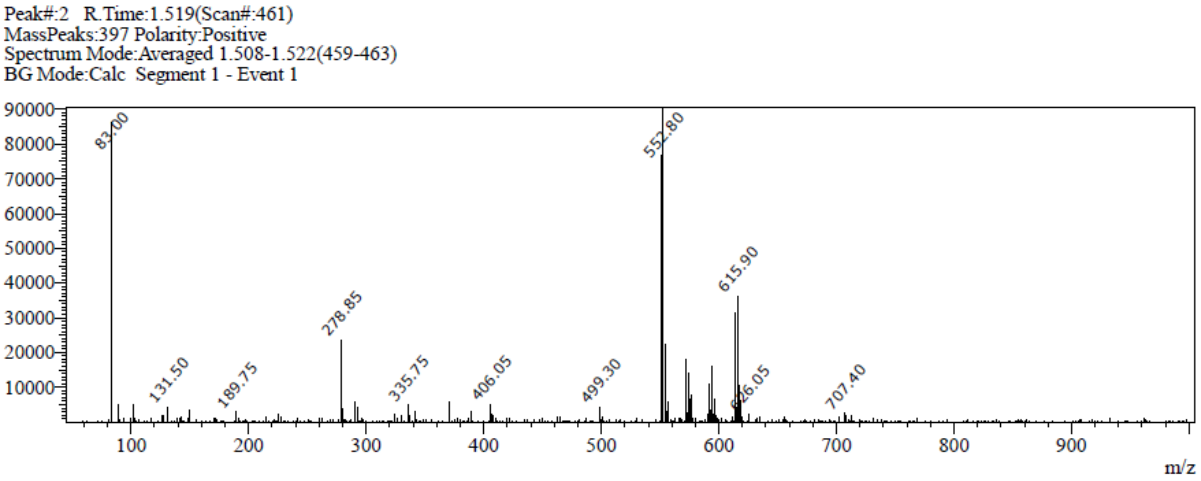

Mass spectrum of compound F19 (Chapter 4)

APPENDEX-III (Chapter-5 supplementary information)

IR, NMR and Mass Spectrum of compounds 6a to 6j and 10a-10h

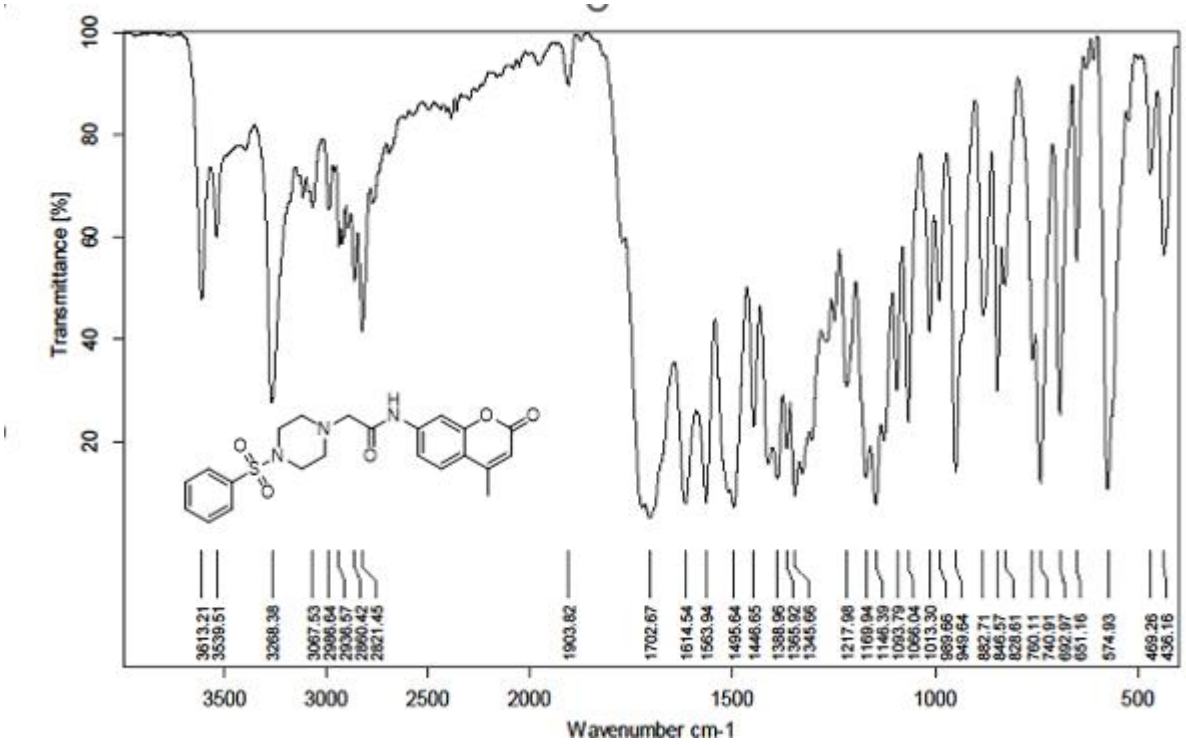

IR spectrum of compound 6a (Chapter 5)

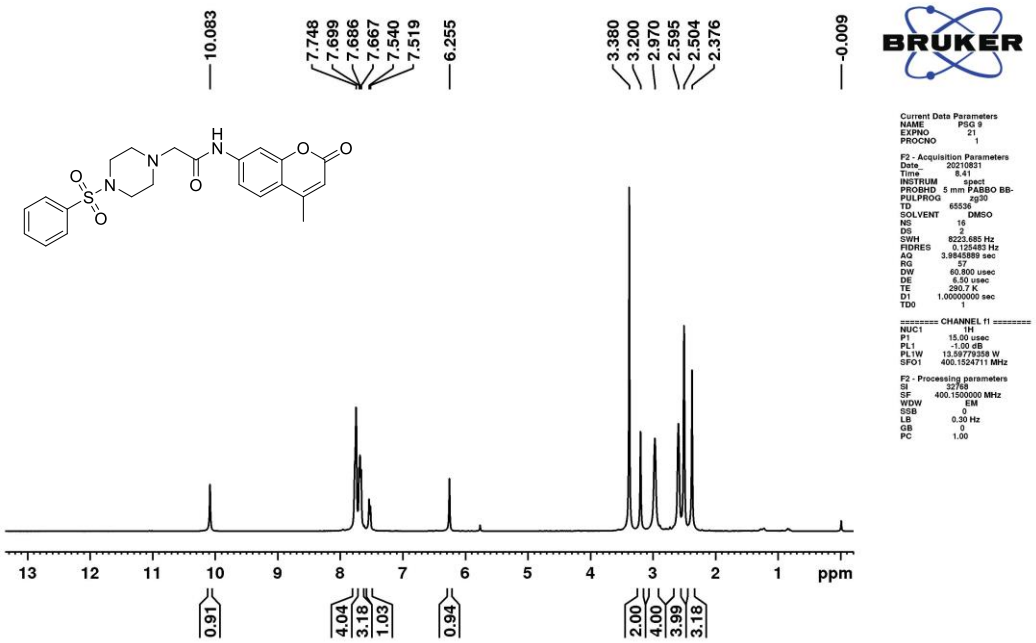

^{1}H NMR spectrum of compound 6a (Chapter 5)

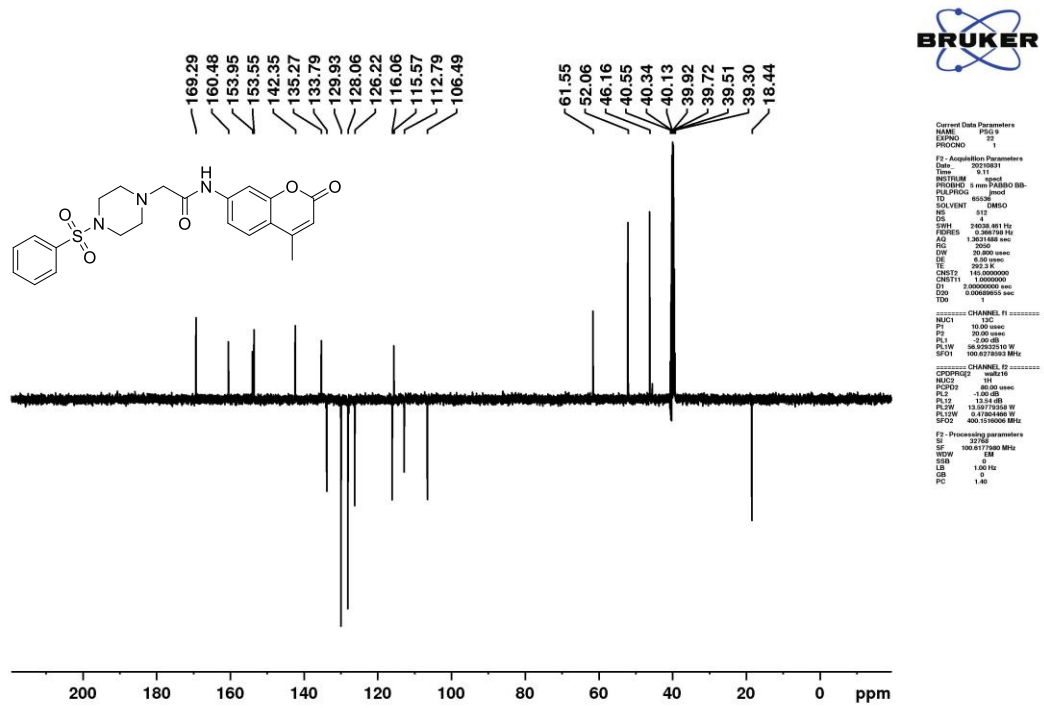

Fig. ^{13}C NMR spectrum of compound 6a (Chapter 5)

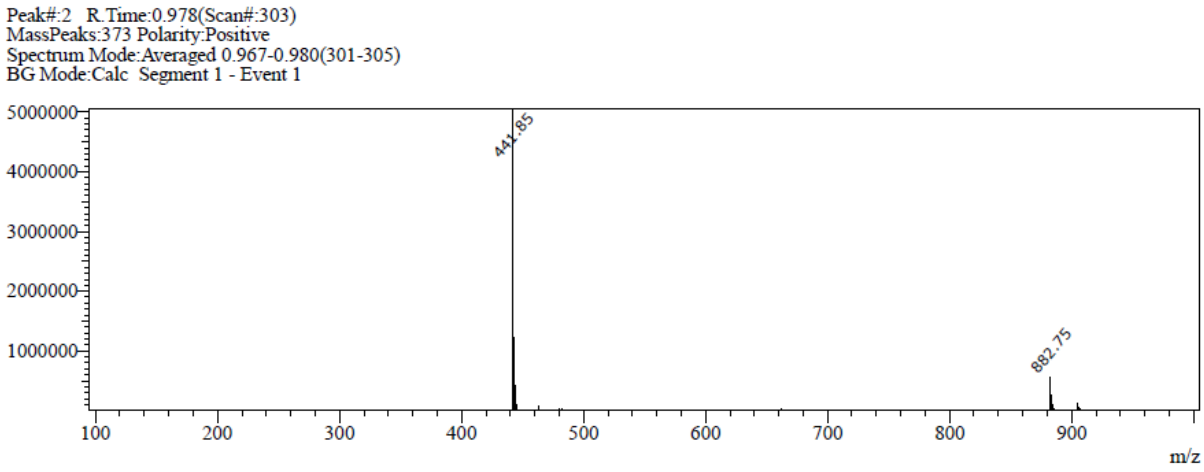

Mass spectrum of compound 6a (Chapter 5)

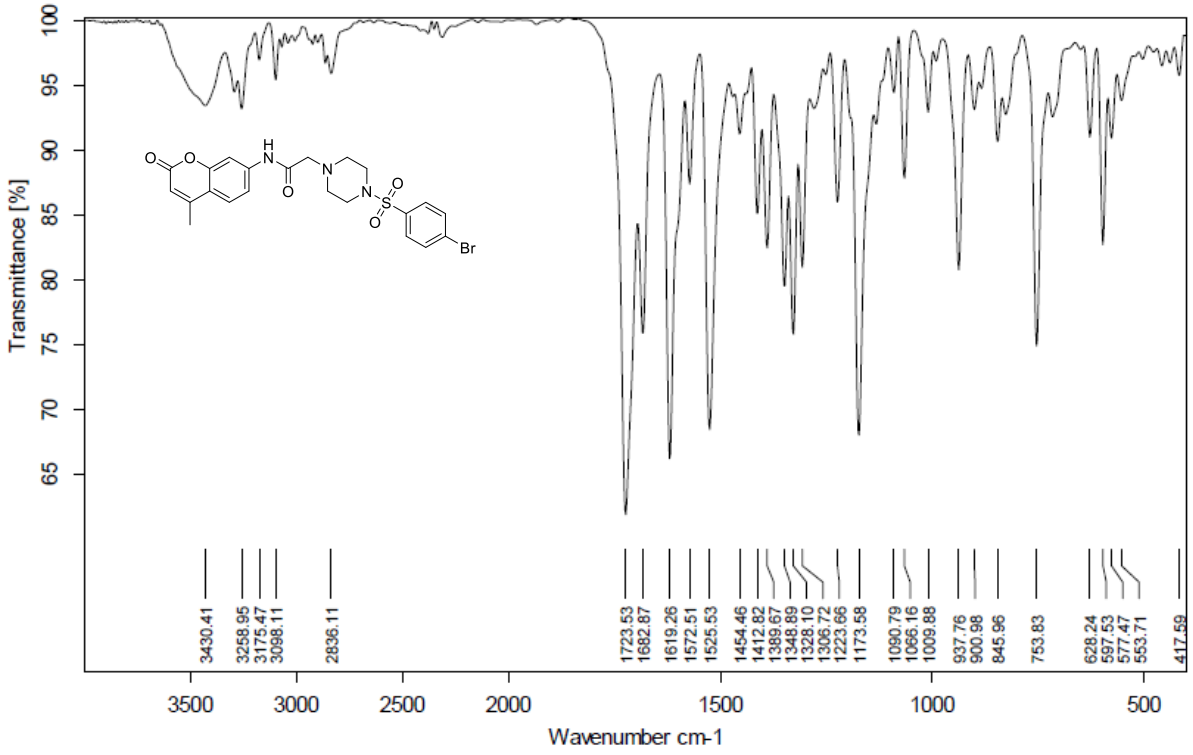

IR spectrum of compound 6b (Chapter 5)

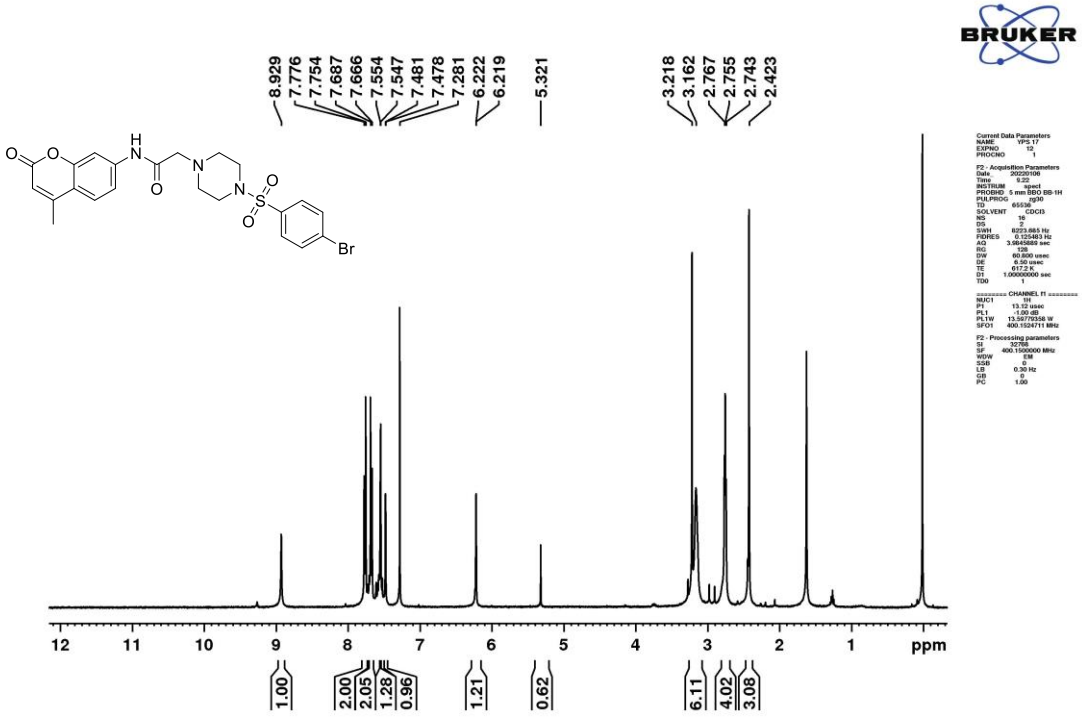

^{1}H NMR spectrum of compound 6b (Chapter 5)

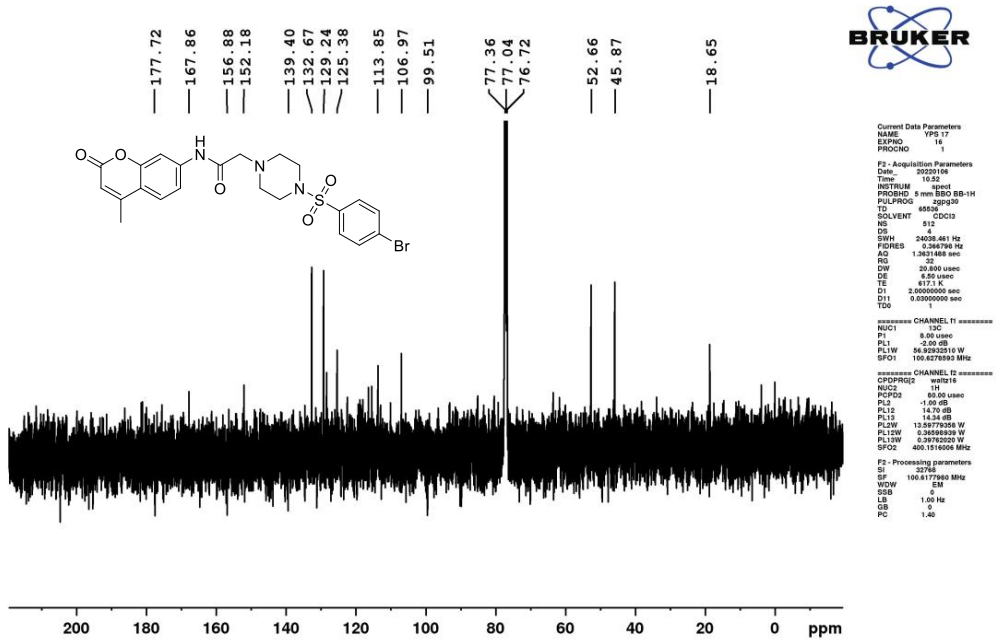

^{13}C NMR spectrum of compound 6b (Chapter 5)

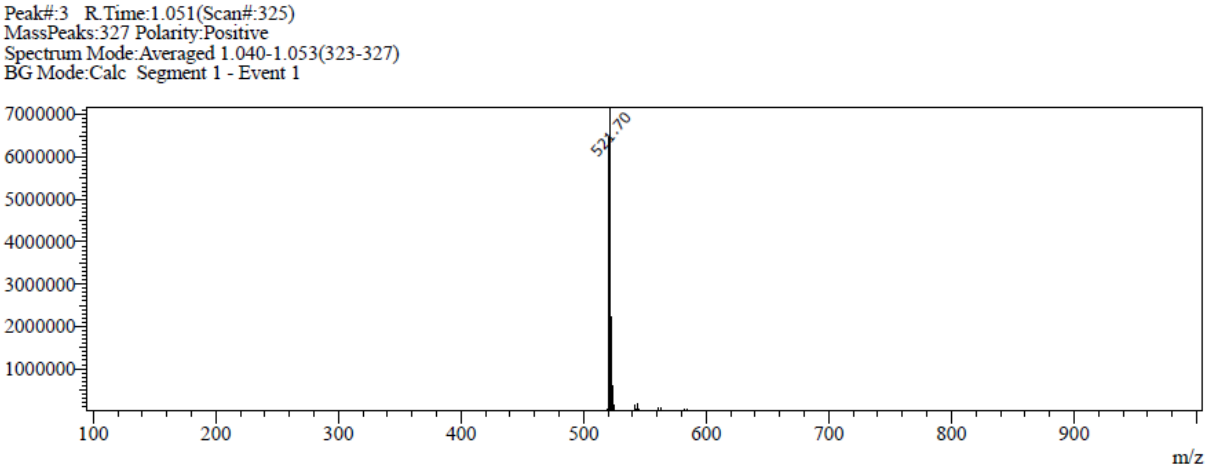

Mass spectrum of compound 6b (Chapter 5)

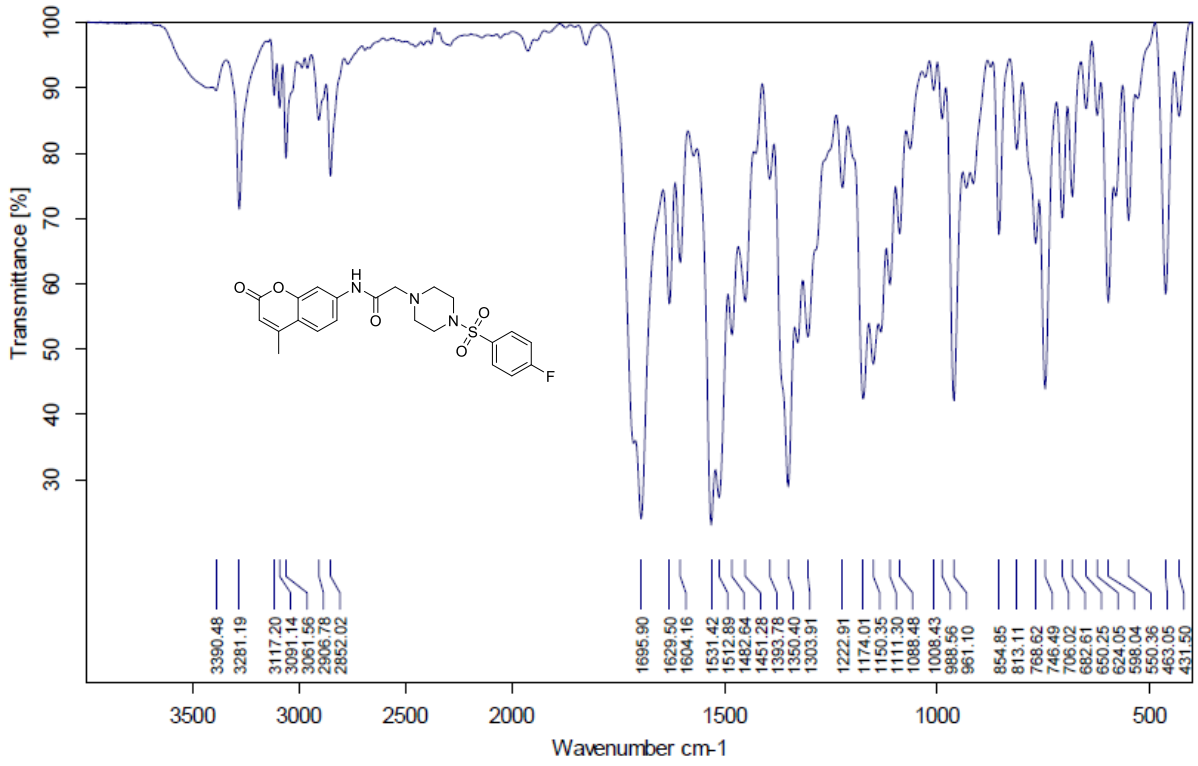

IRspectrum of compound 6c (Chapter 5)

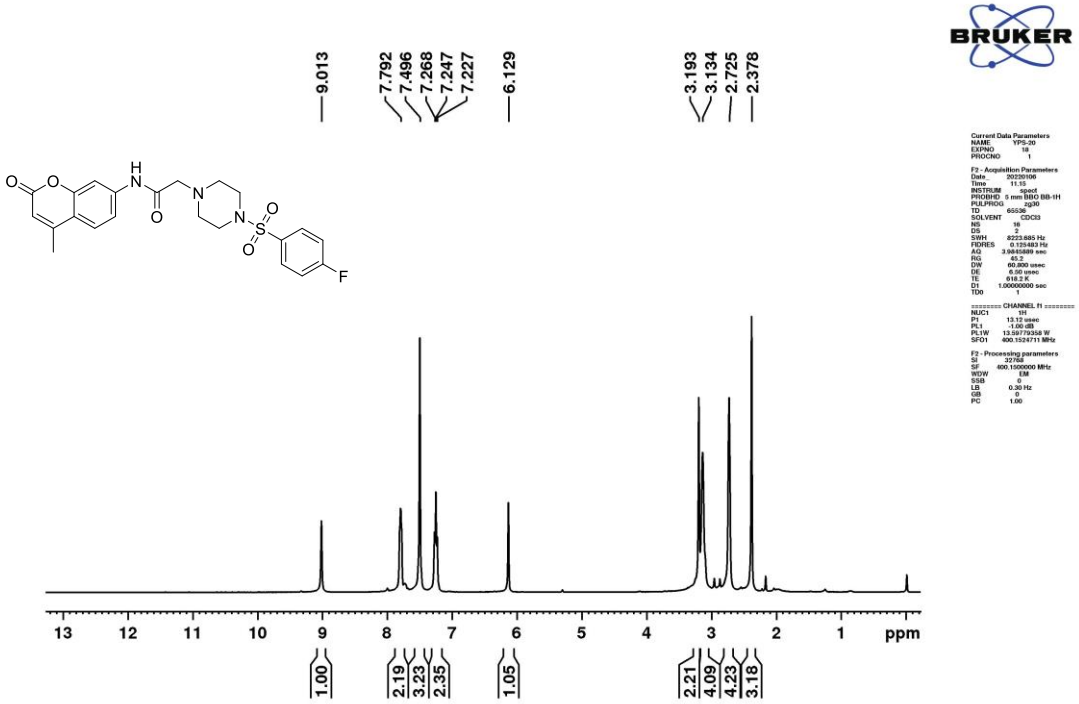

^{1}H NMR spectrum of compound 6c (Chapter 5)

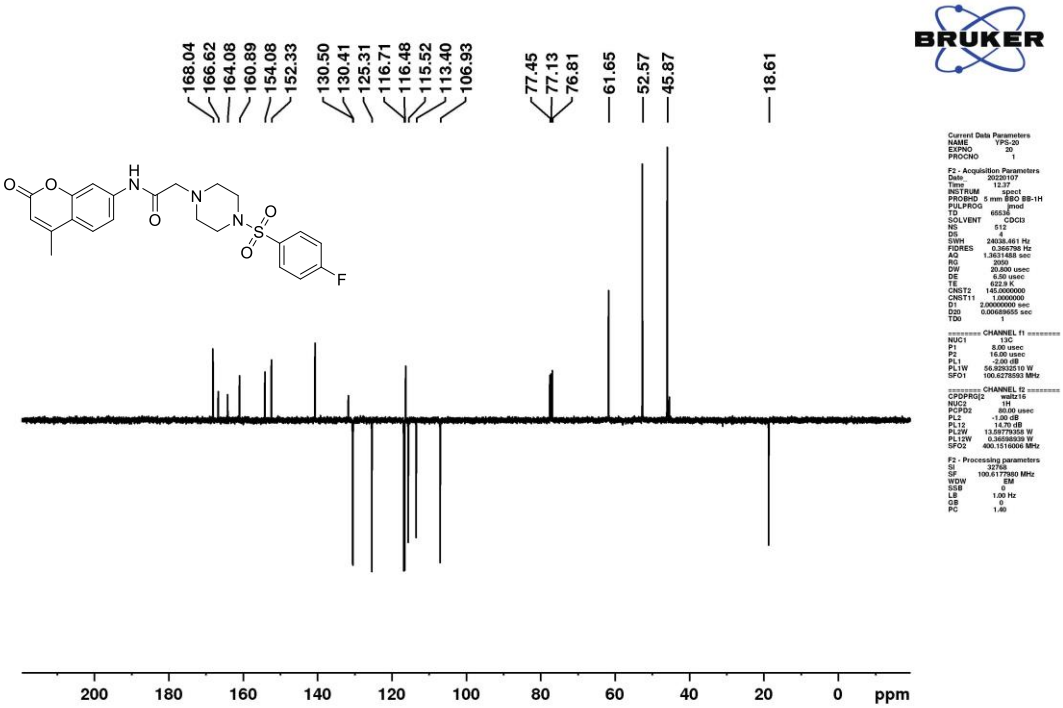

^{13}C NMR spectrum of compound 6c (Chapter 5)

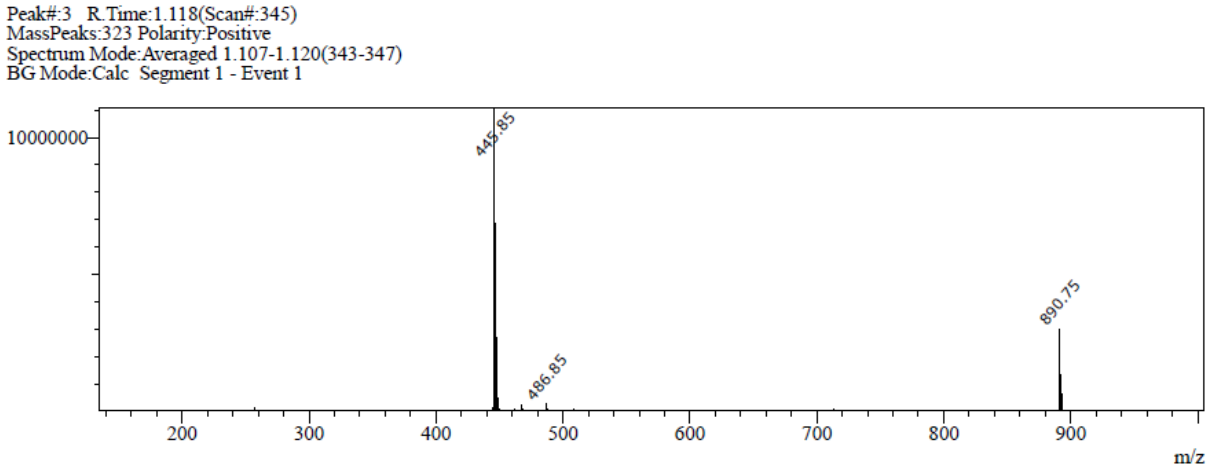

Mass spectrum of compound 6c (Chapter 5)

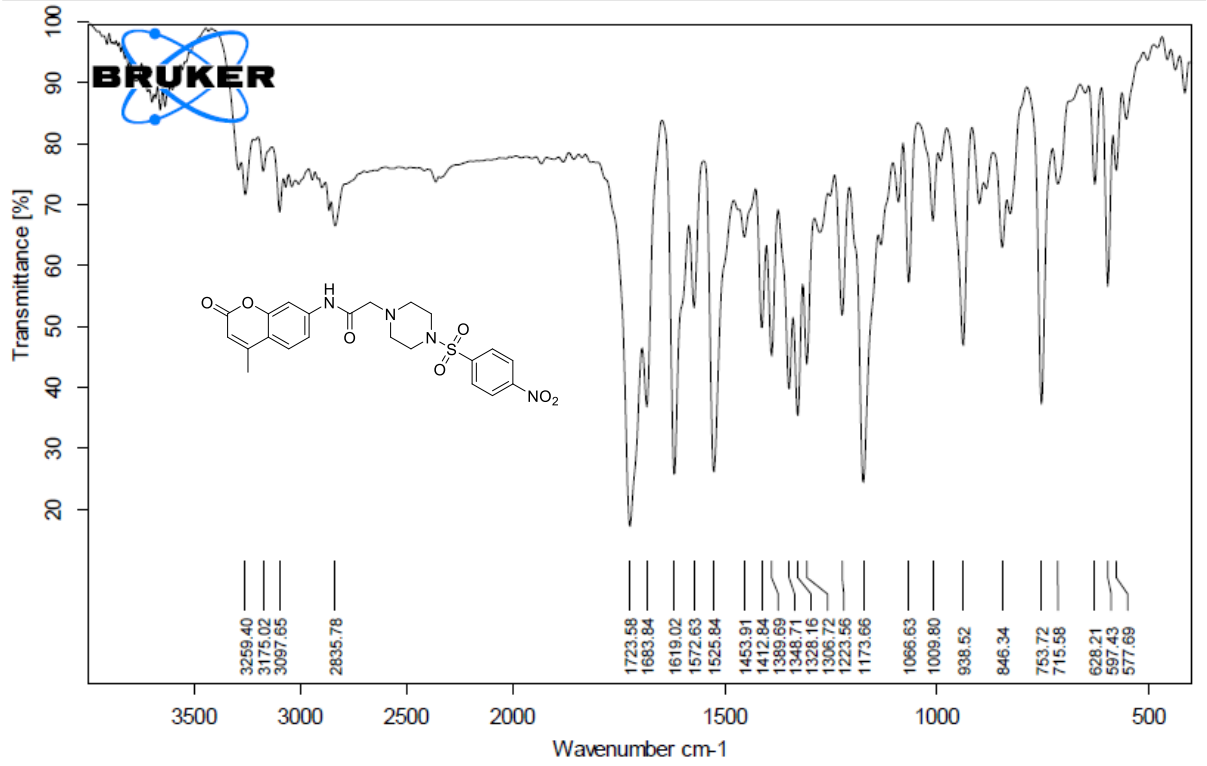

IRspectrum of compound 6d (Chapter 5)

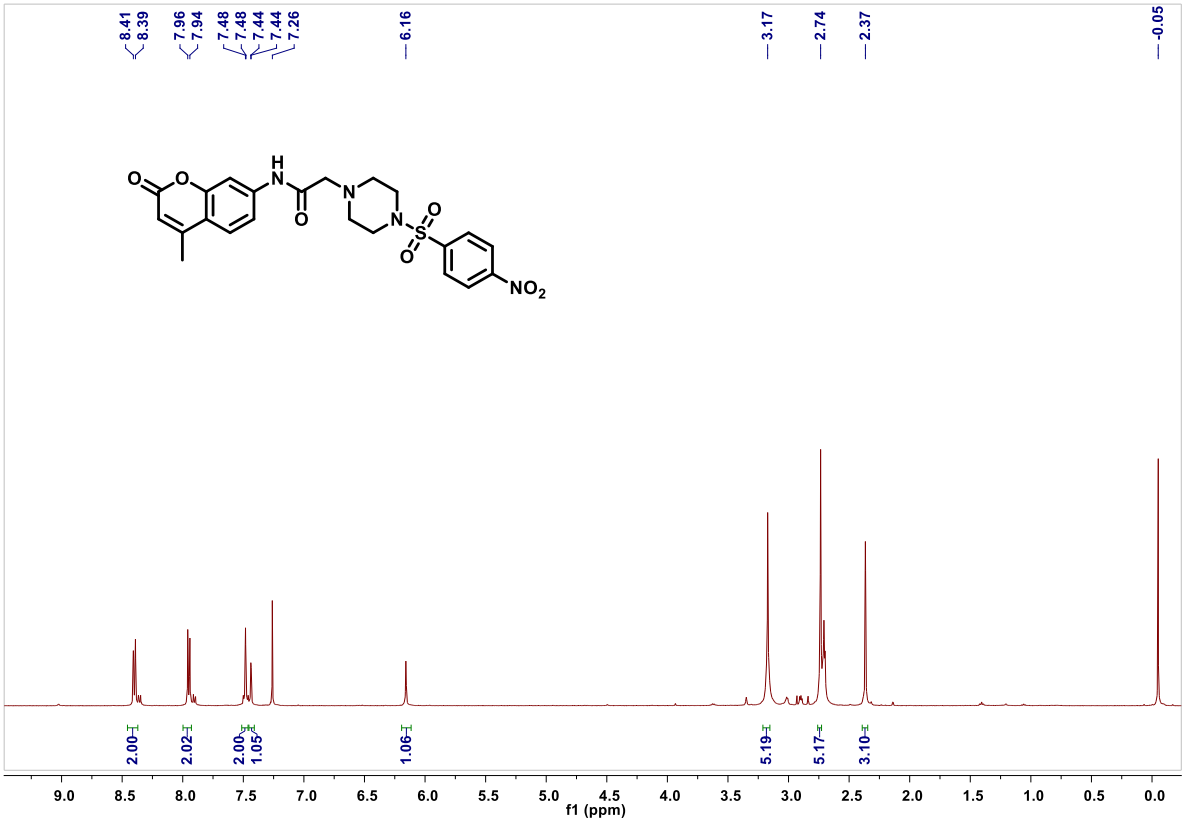

^{1}H NMR spectrum of compound 6d (Chapter 5)

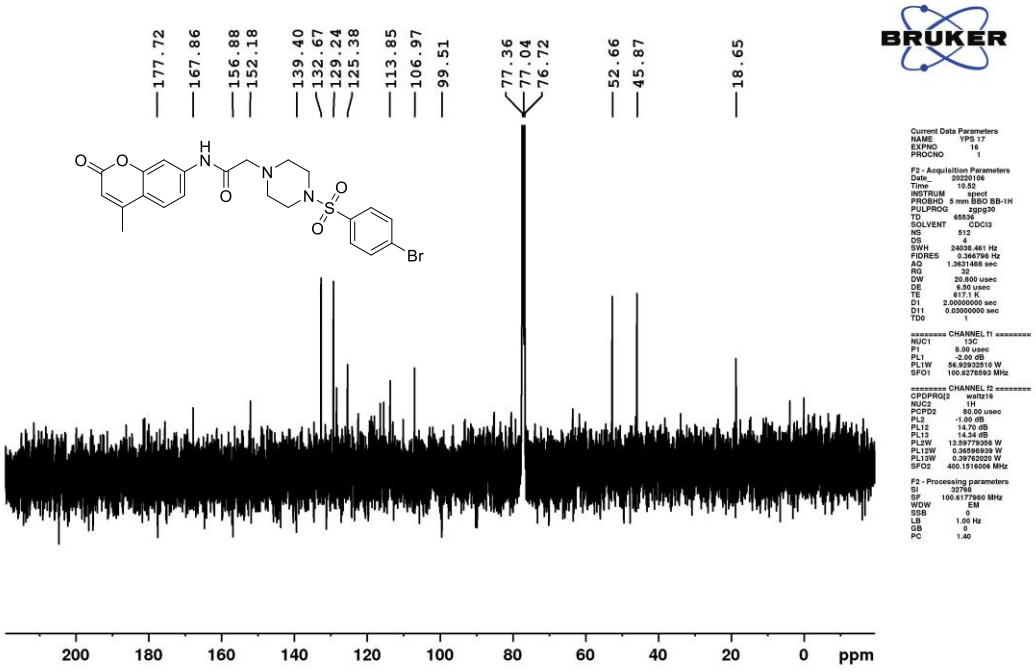

^{13}C NMR spectrum of compound 6d (Chapter 5)

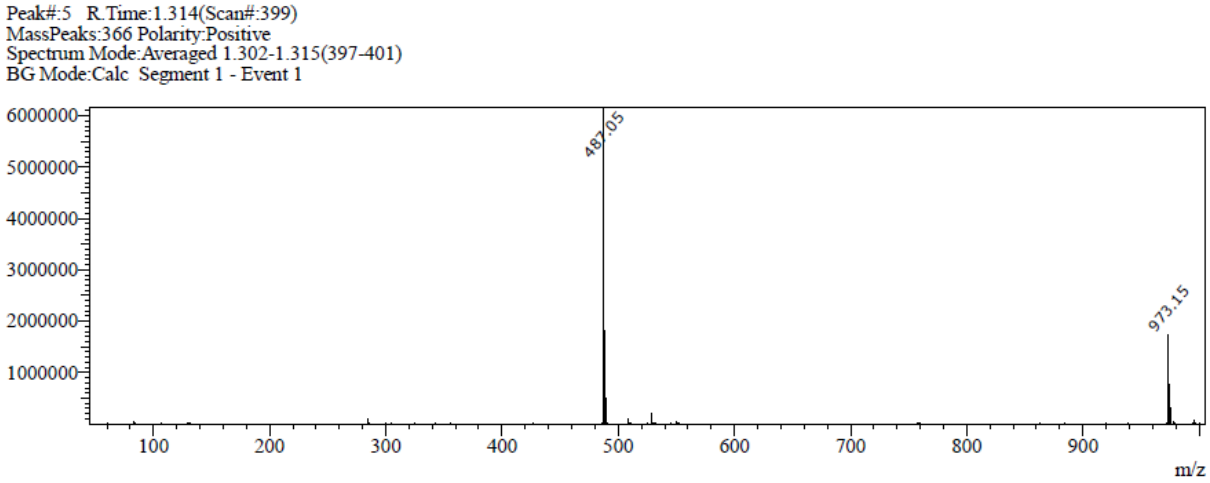

Mass spectrum of compound 6d (Chapter 5)

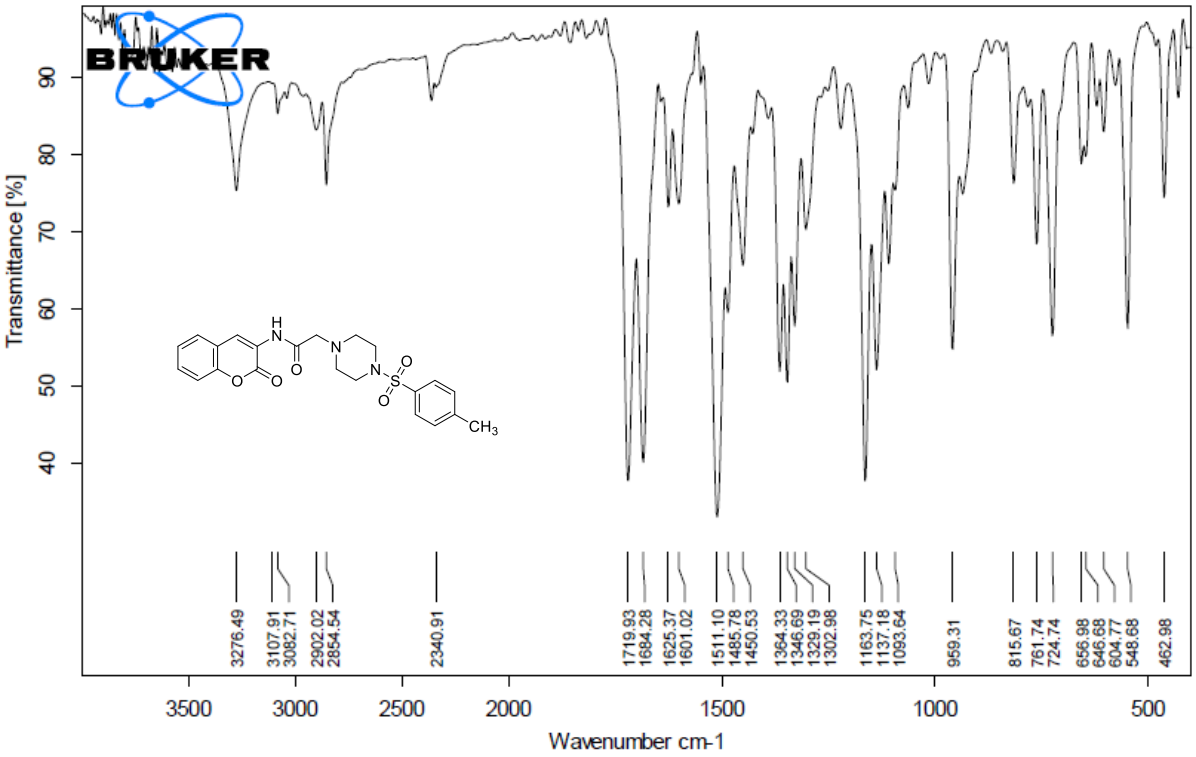

IRspectrum of compound 6e (Chapter 5)

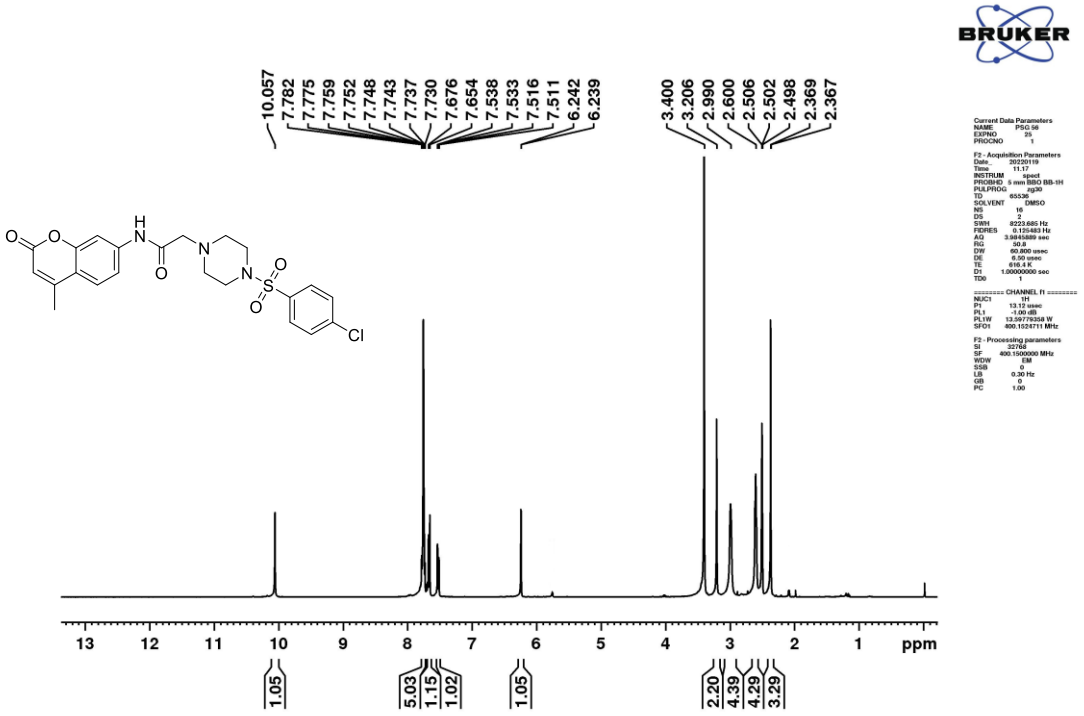

^{1}H NMR spectrum of compound 6e (Chapter 5)

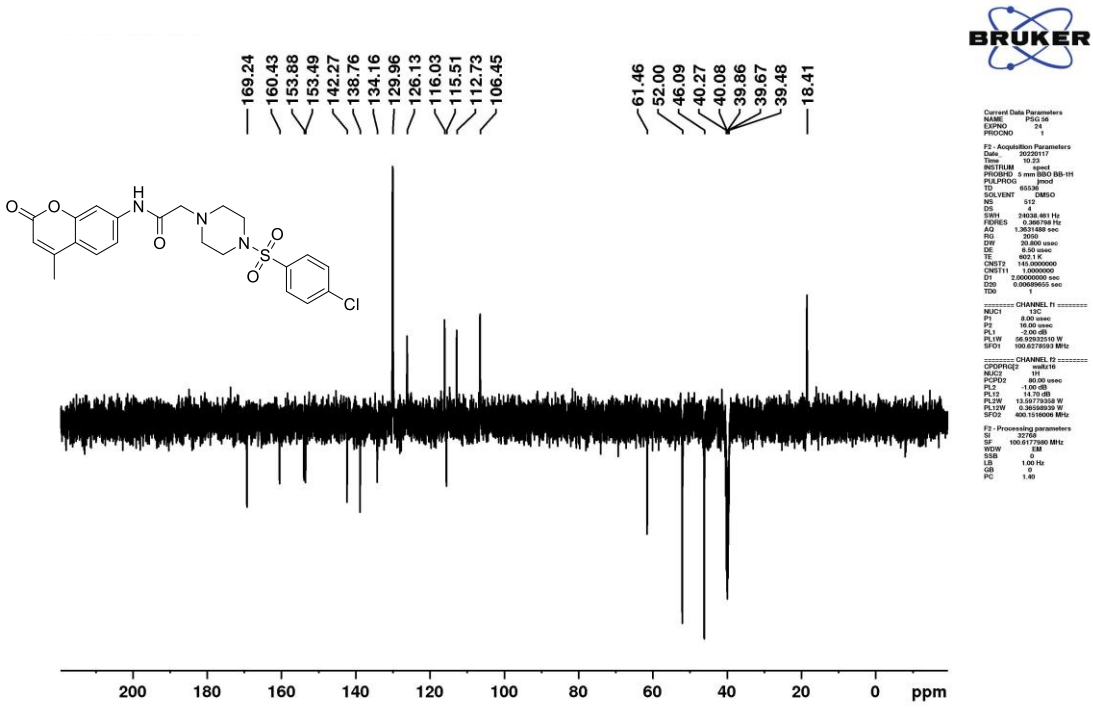

^{13}C NMR spectrum of compound 6e (Chapter 5)

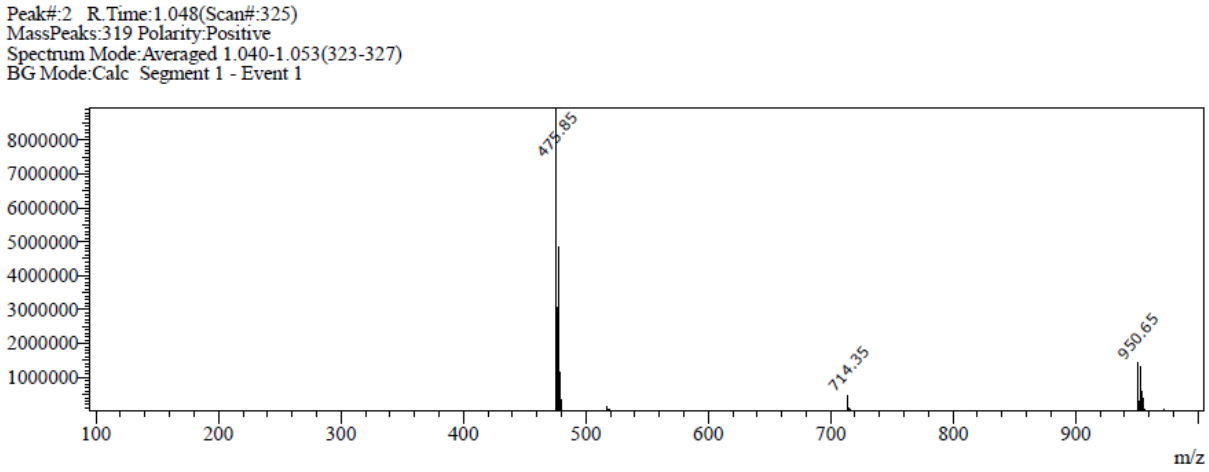

Mass spectrum of compound 6e (Chapter 5)

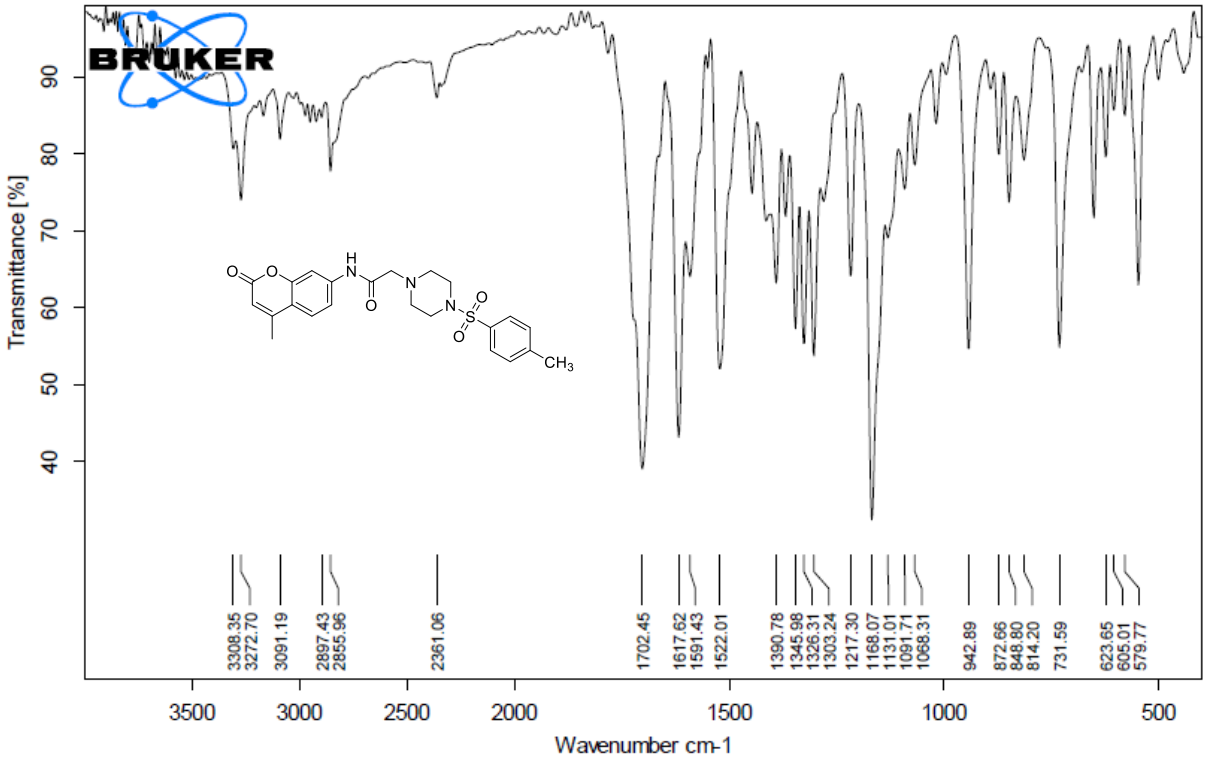

IR spectrum of compound 6f (Chapter 5)

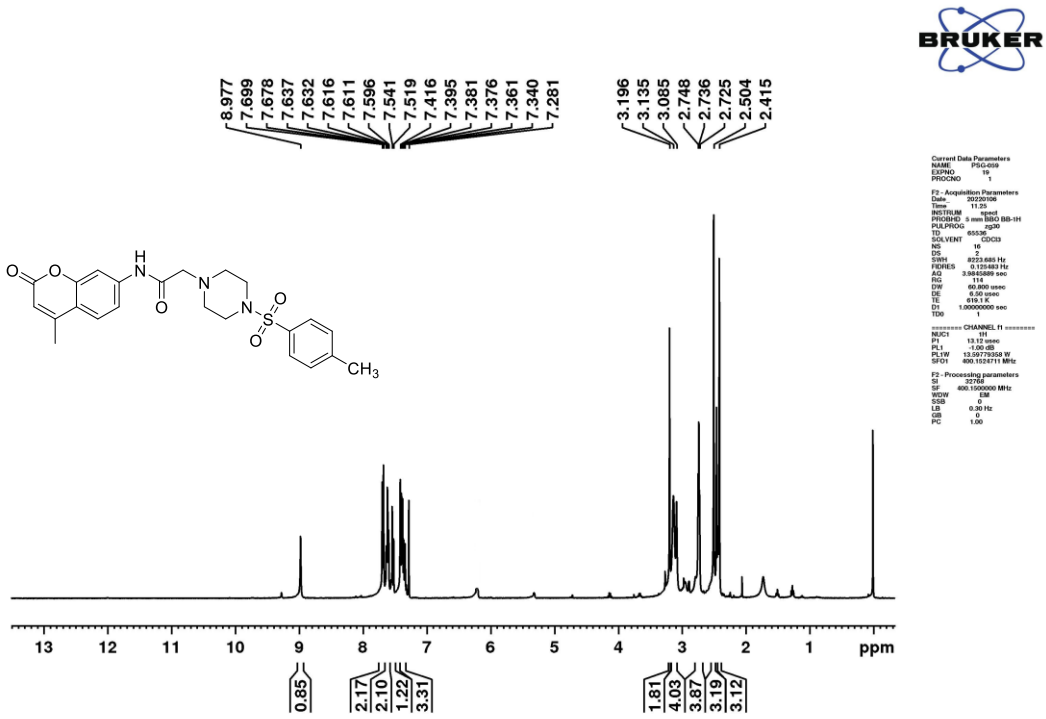

^{1}H NMR spectrum of compound 6f (Chapter 5)

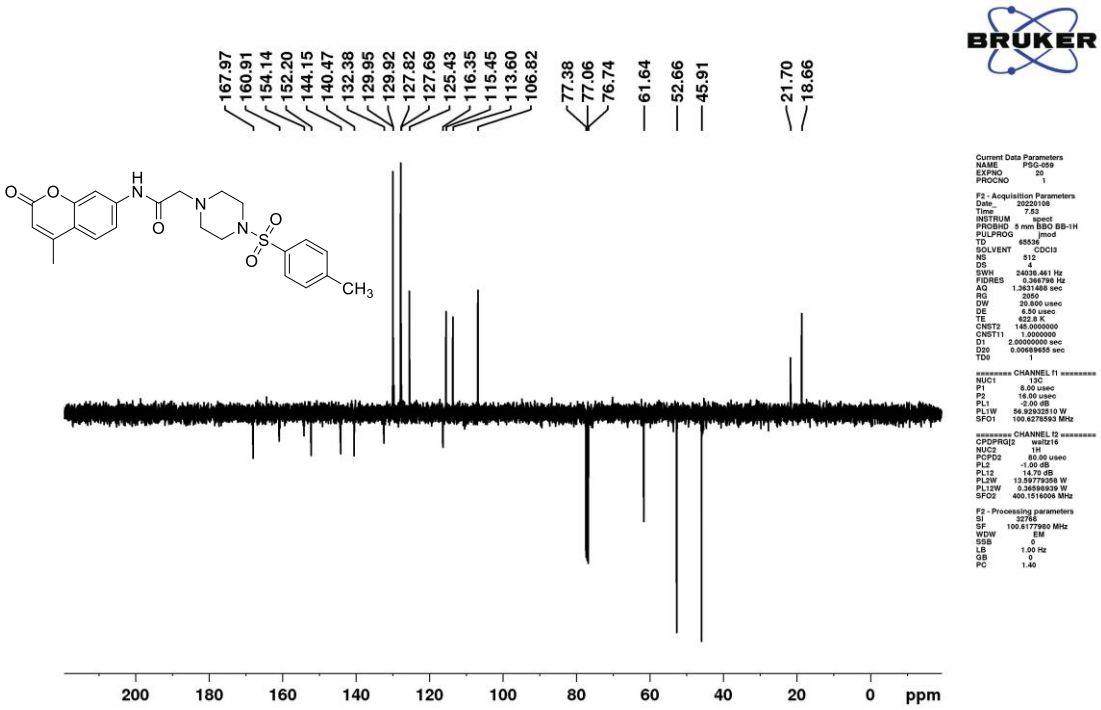

^{13}C NMR spectrum of compound 6f (Chapter 5)

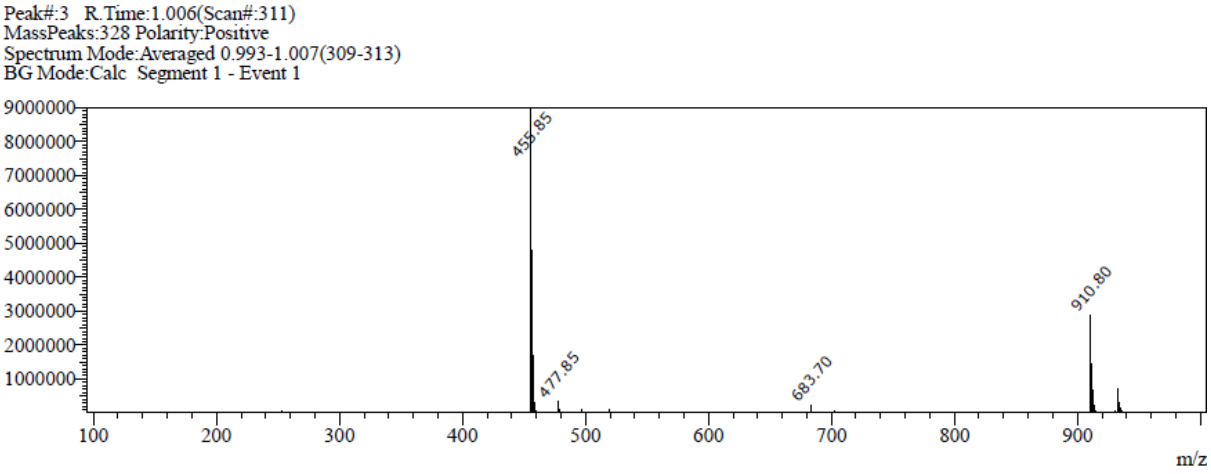

Mass spectrum of compound 6f (Chapter 5)

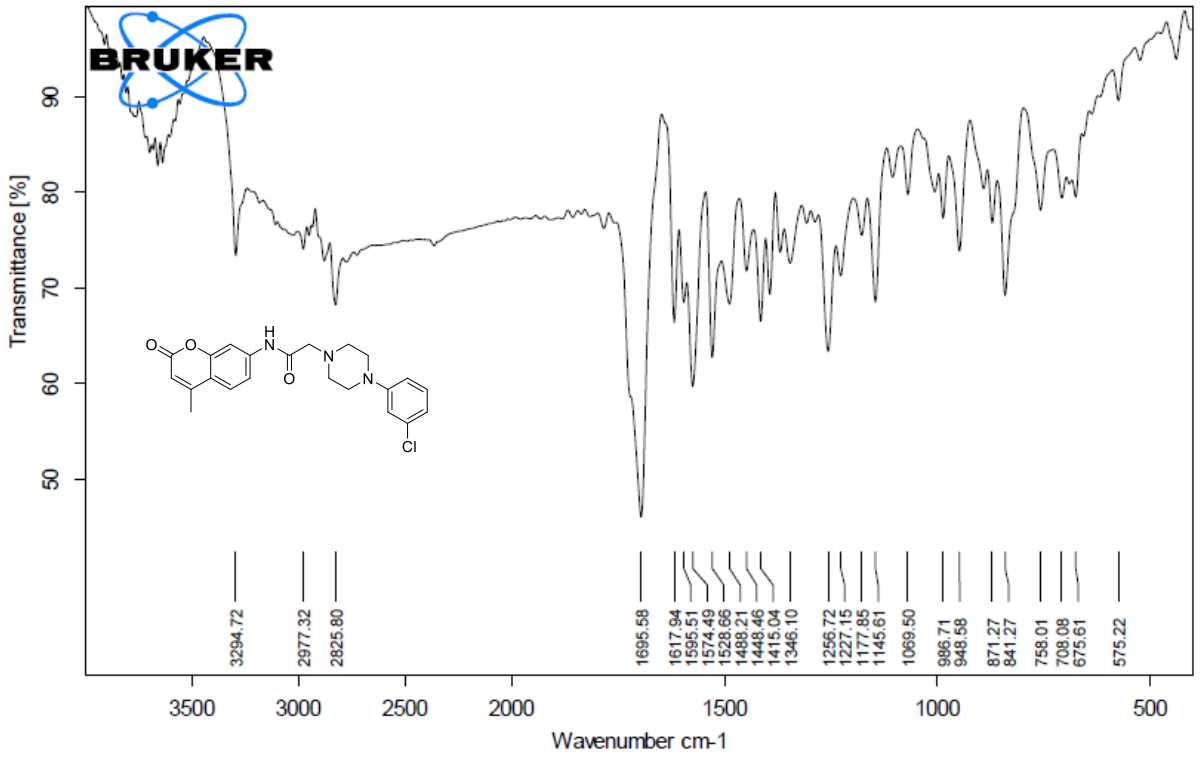

IRspectrum of compound 6g (Chapter 5)

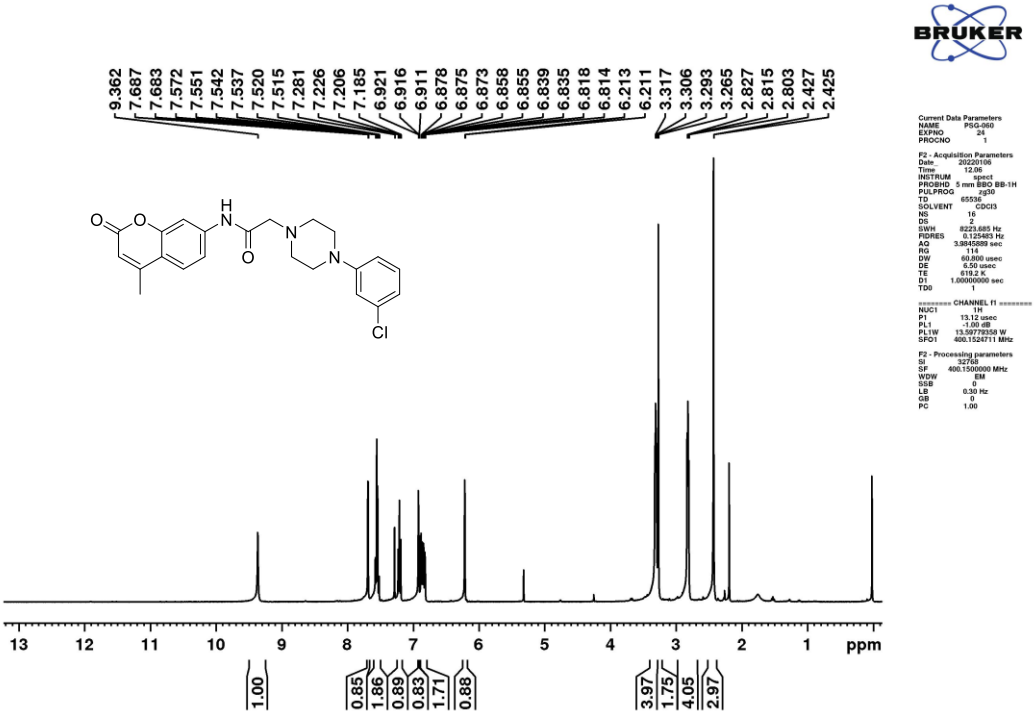

^{1}H NMR spectrum of compound 6g (Chapter 5)

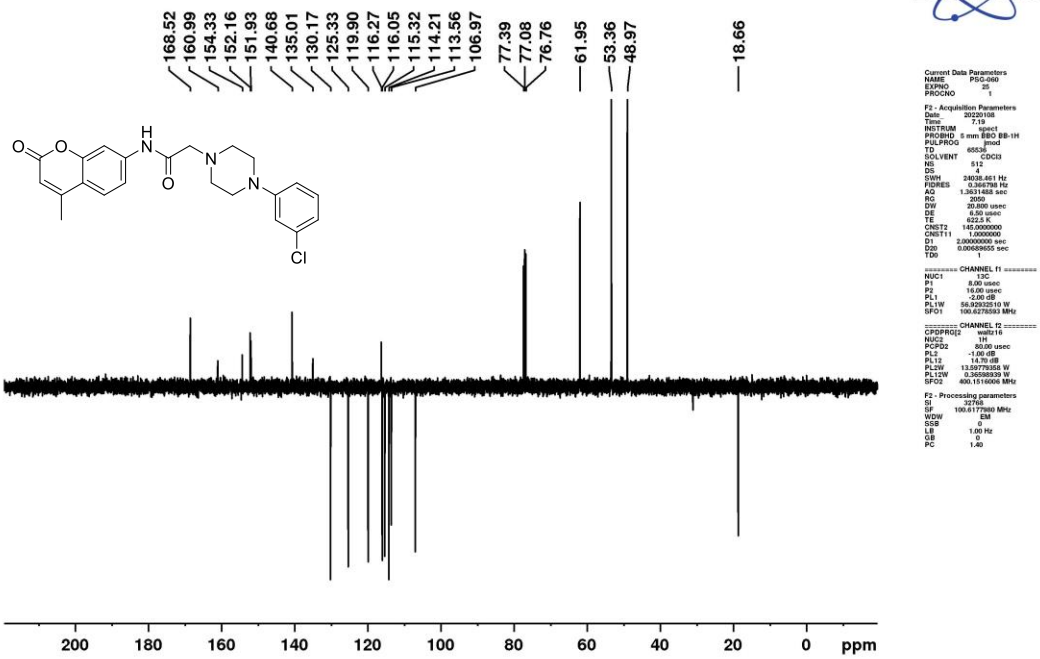

^{13}C NMR spectrum of compound 6g (Chapter 5)

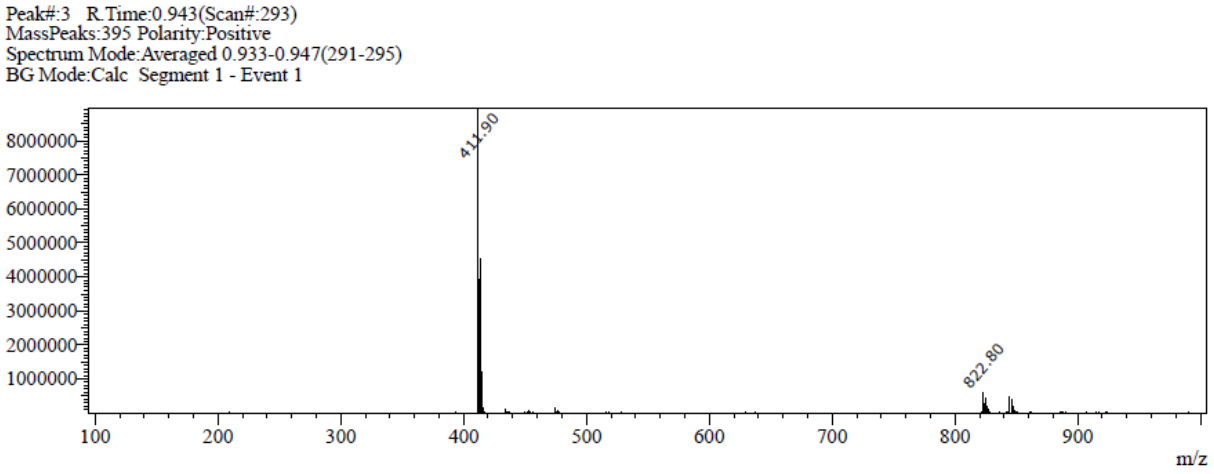

Mass spectra spectrum of compound 6g (Chapter 5)

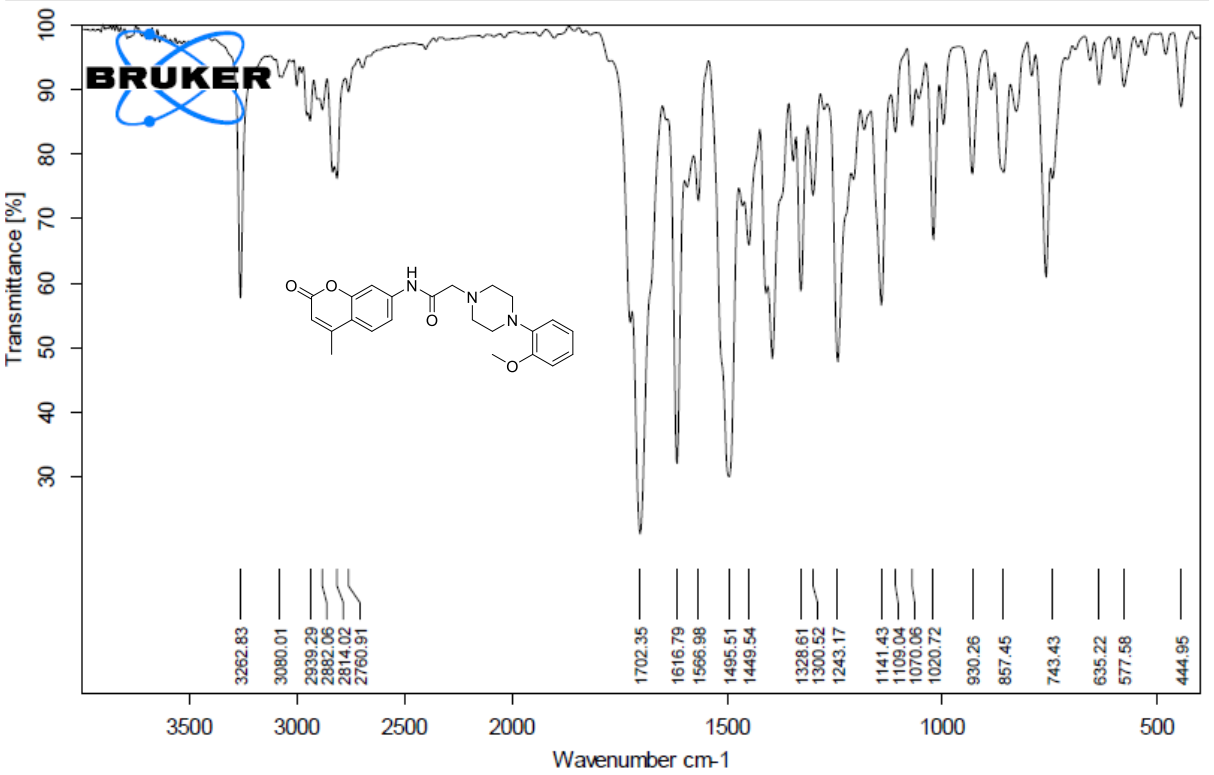

IRspectrum of compound 6h (Chapter 5)

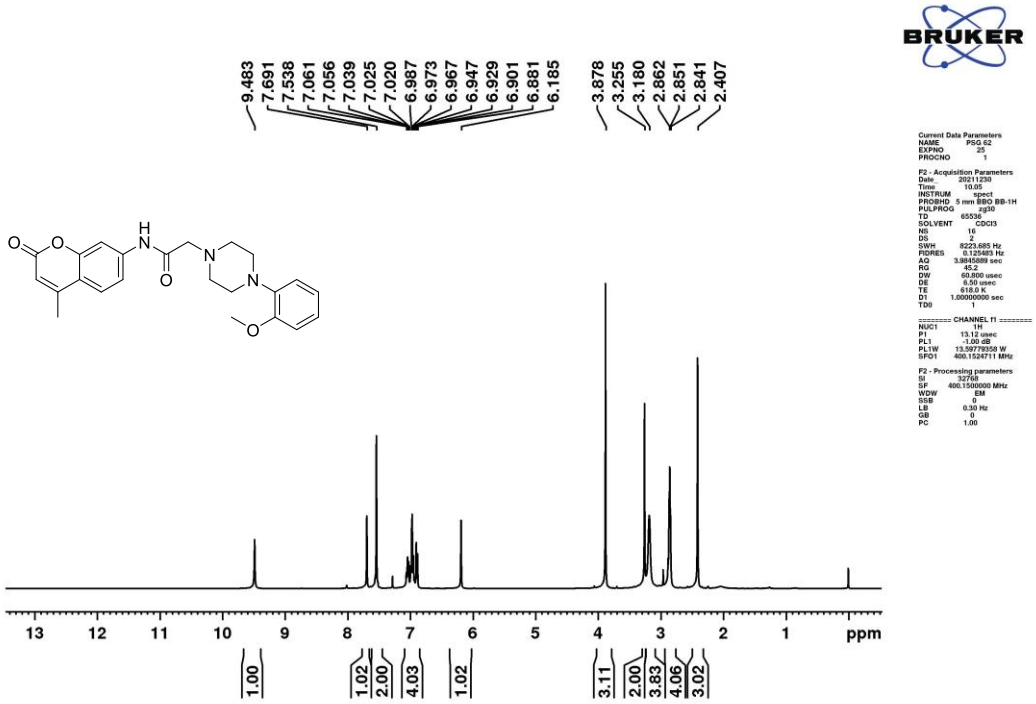

^{1}H NMR spectrum of compound 6h (Chapter 5)

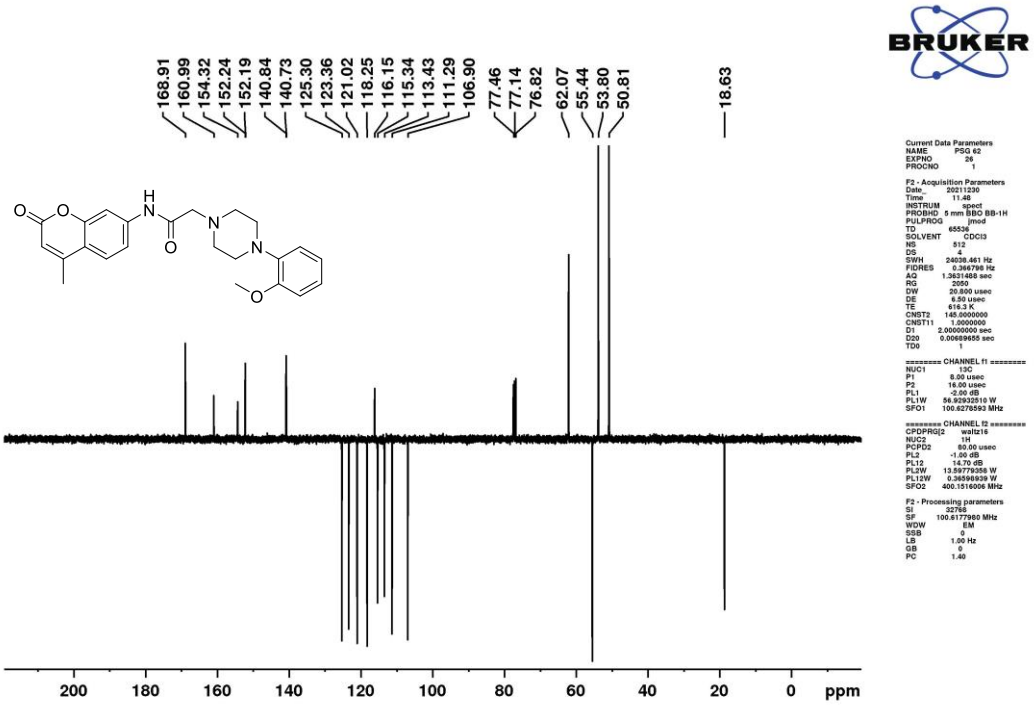

^{13}C NMR spectrum of compound 6h (Chapter 5)

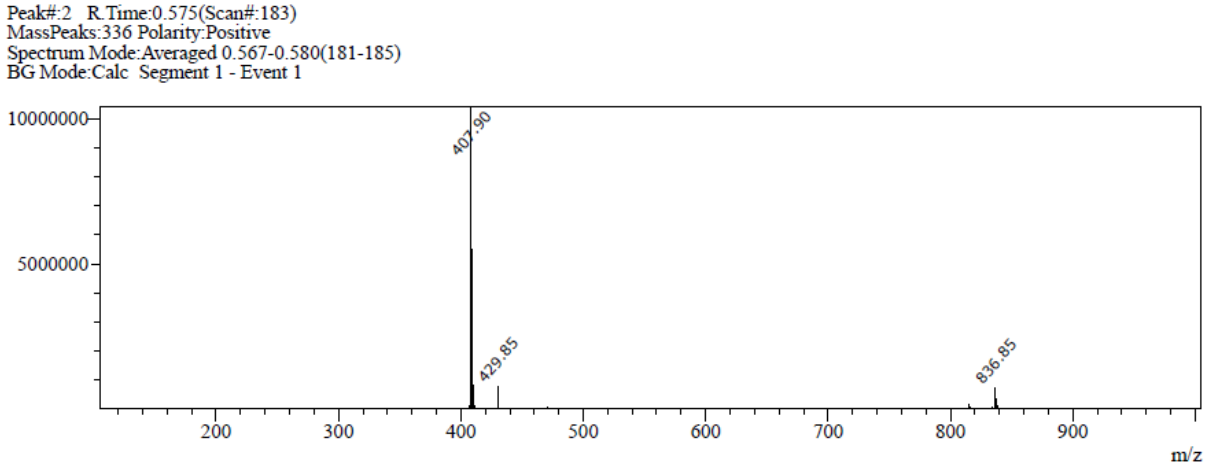

Mass spectrum of compound 6h (Chapter 5)

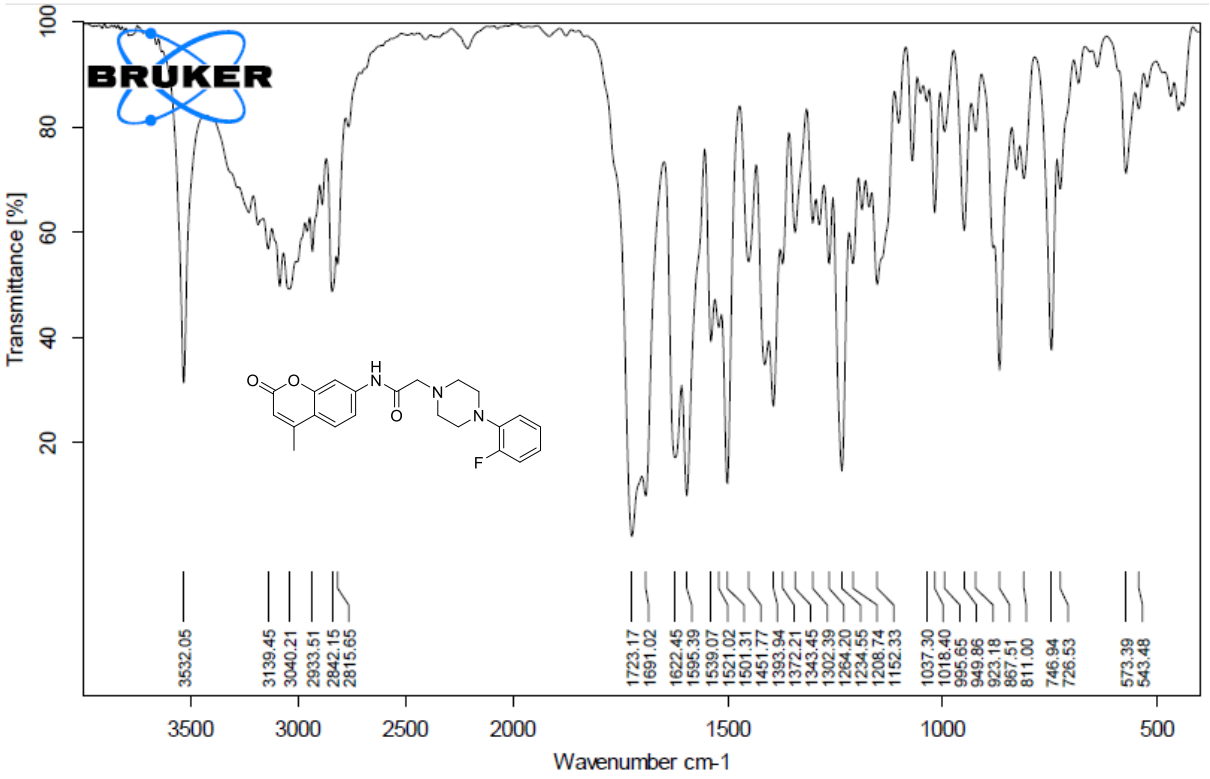

IRspectrum of compound 6i (Chapter 5)

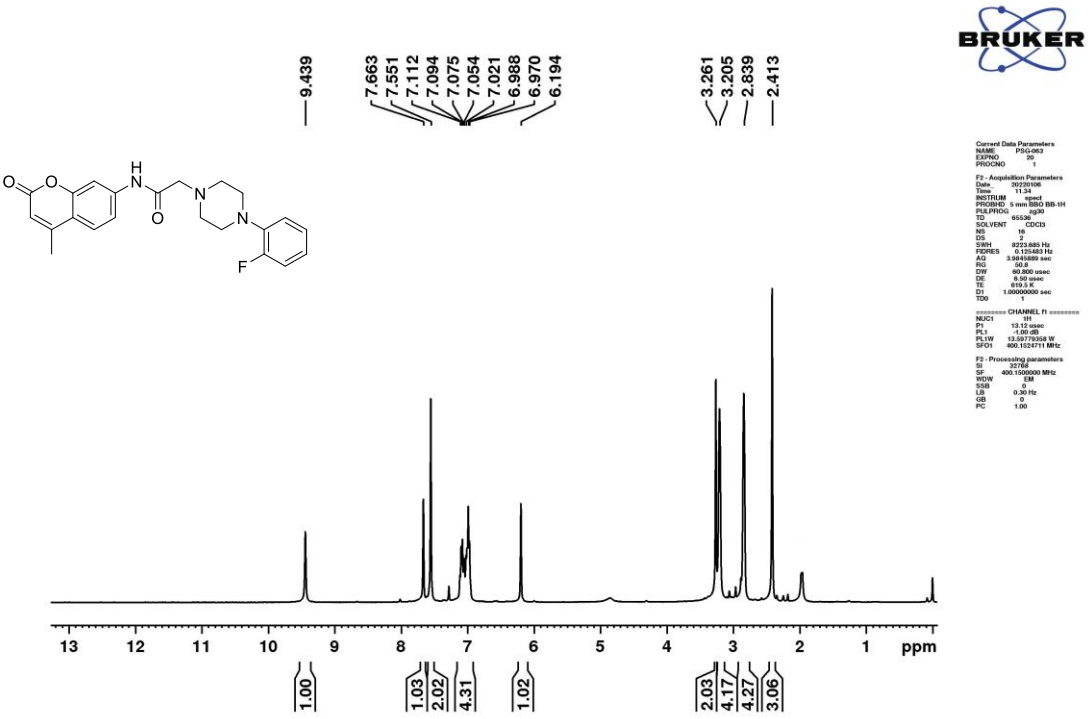

^{1}H NMR spectrum of compound 6i (Chapter 5)

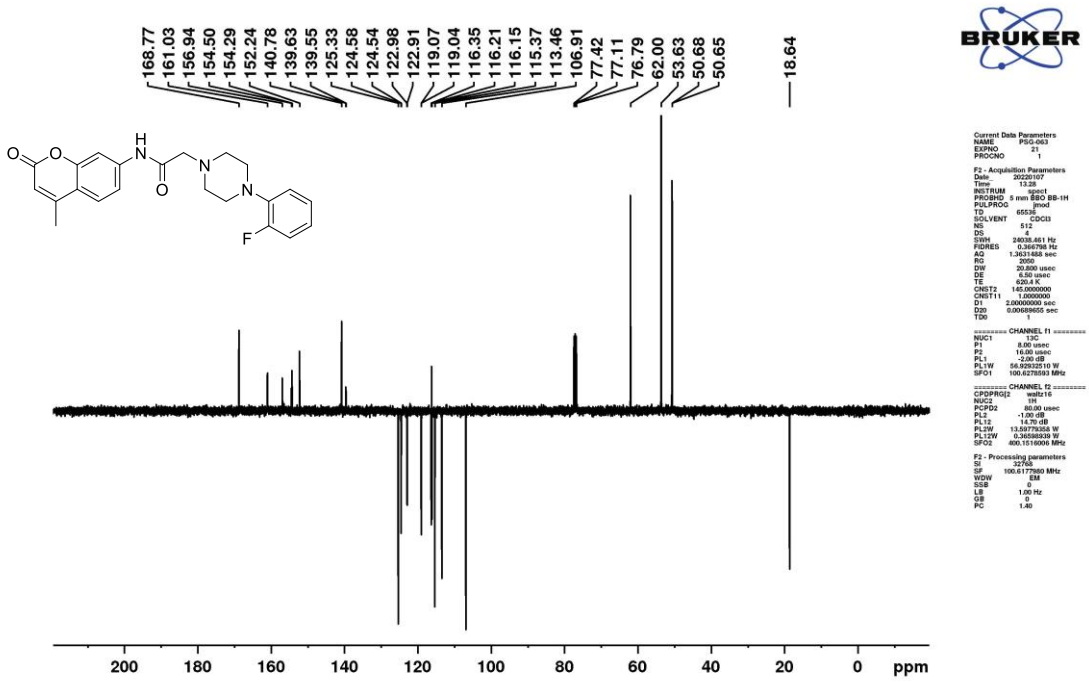

^{13}C NMRspectrum of compound 6i (Chapter 5)

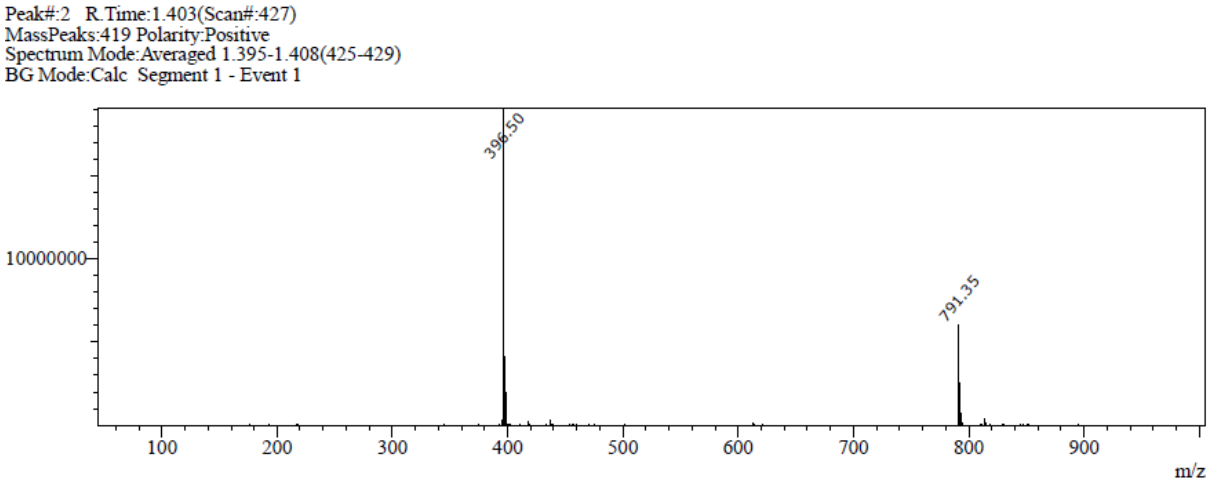

Mass spectrum of compound 6i (Chapter 5)

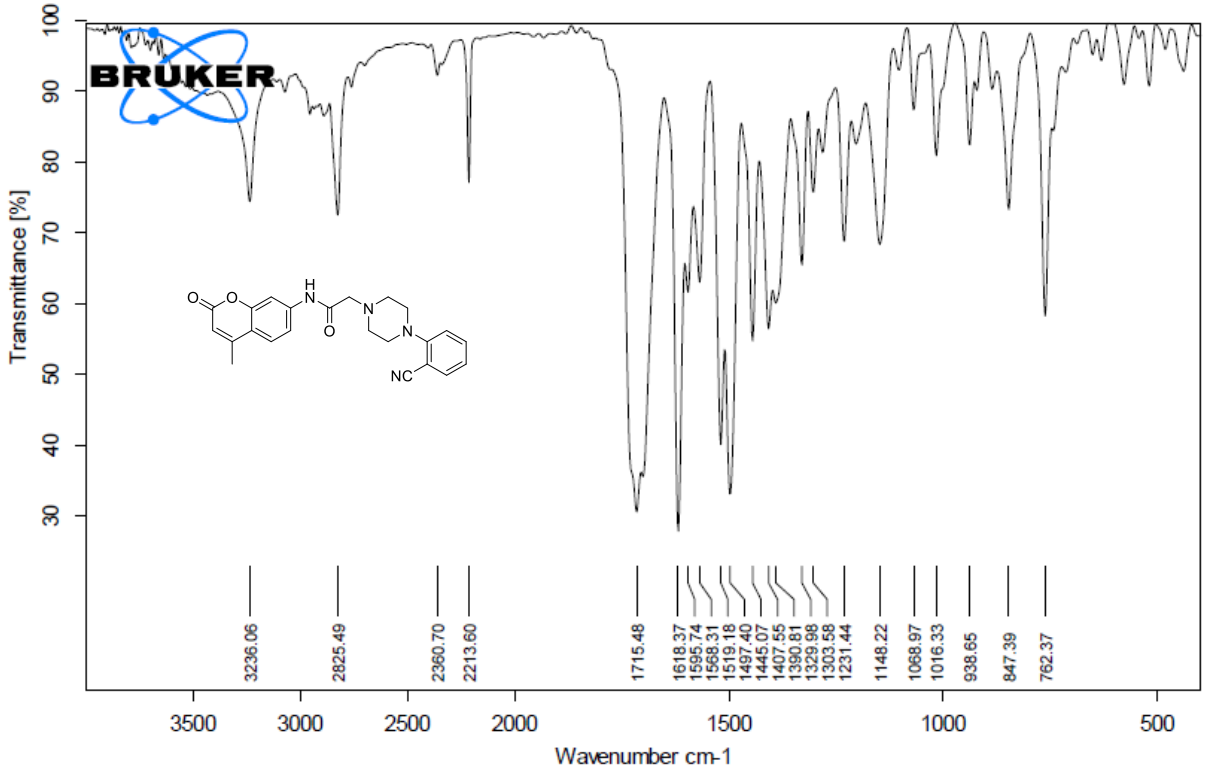

IRspectrum of compound 6j (Chapter 5)

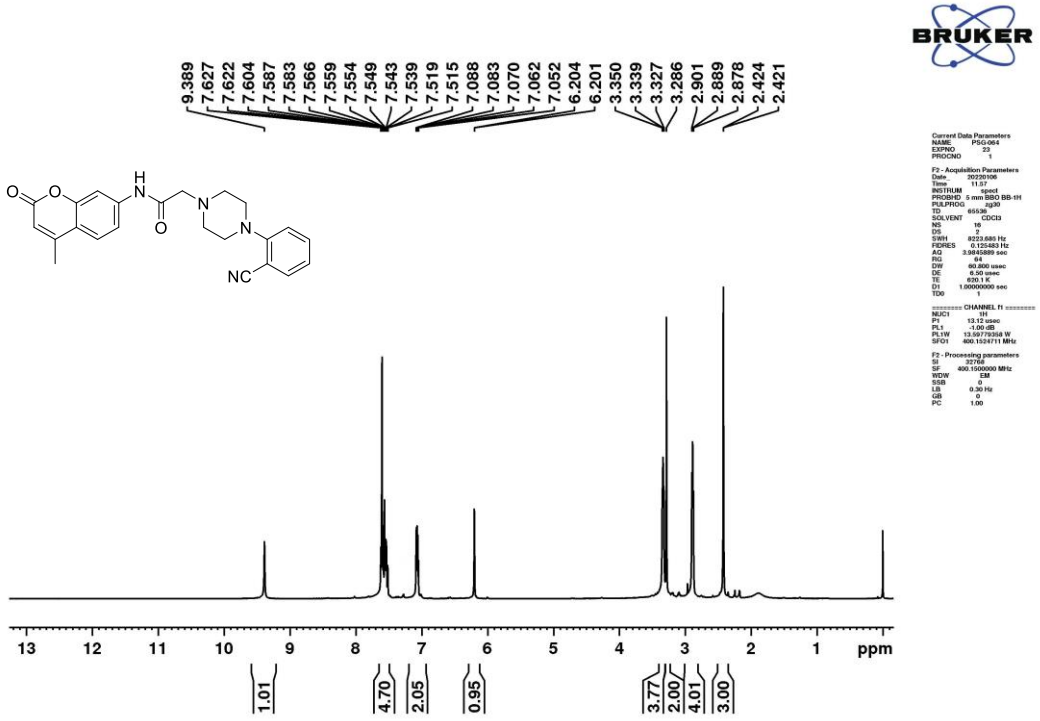

^{1}H spectrum of compound 6j (Chapter 5)

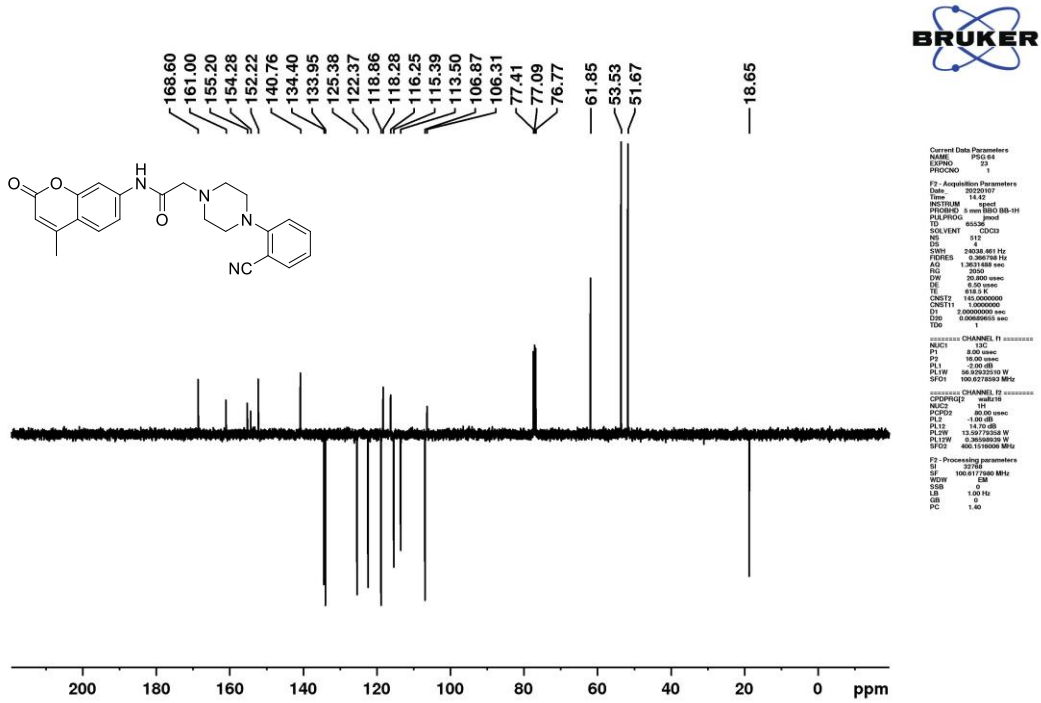

^{13}C NMR spectrum of compound 6j (Chapter 5)

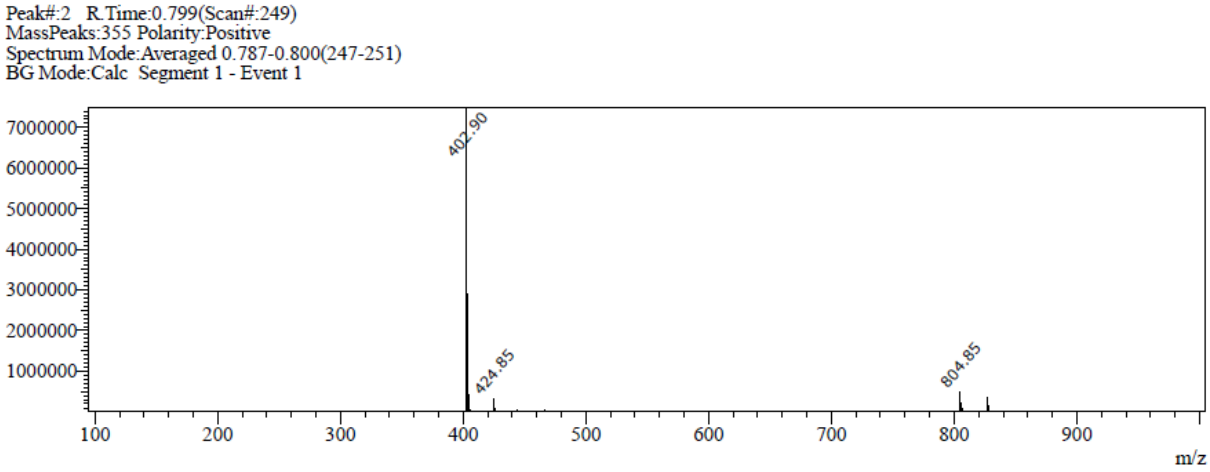

Mass spectrum of compound 6j (Chapter 5)

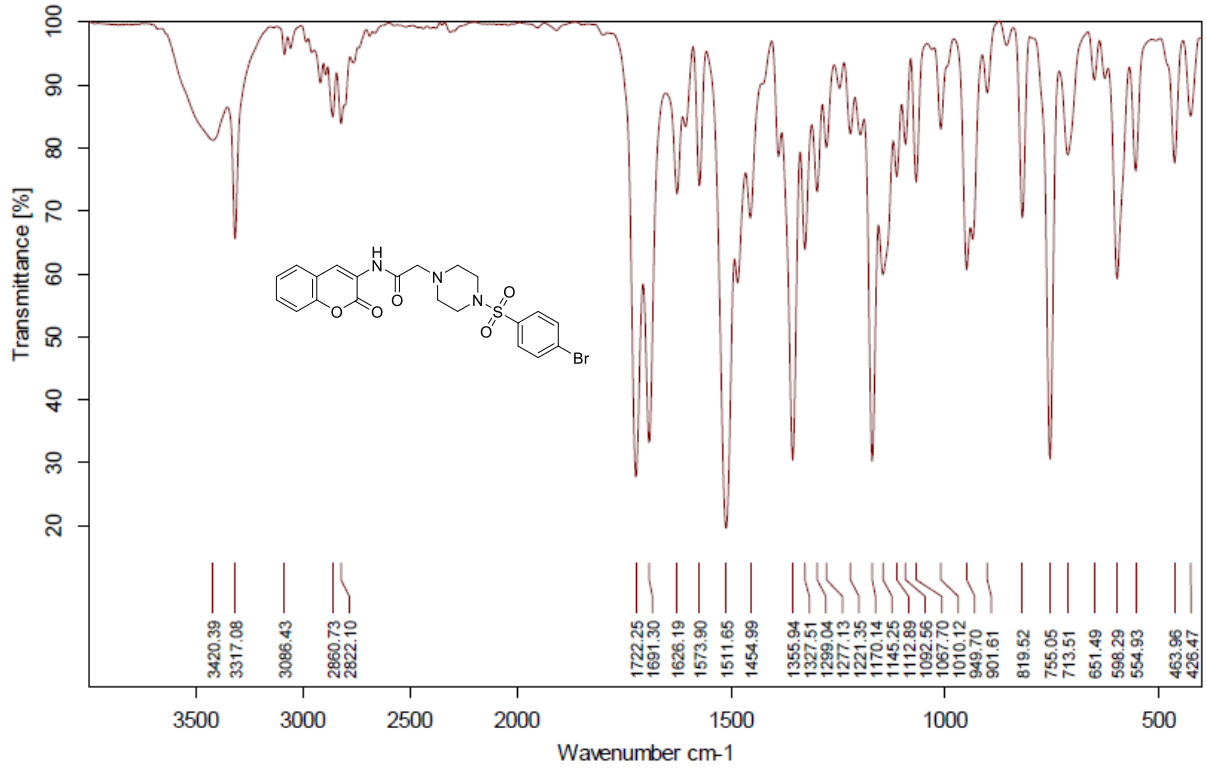

IRspectrum of compound 10a (Chapter 5)

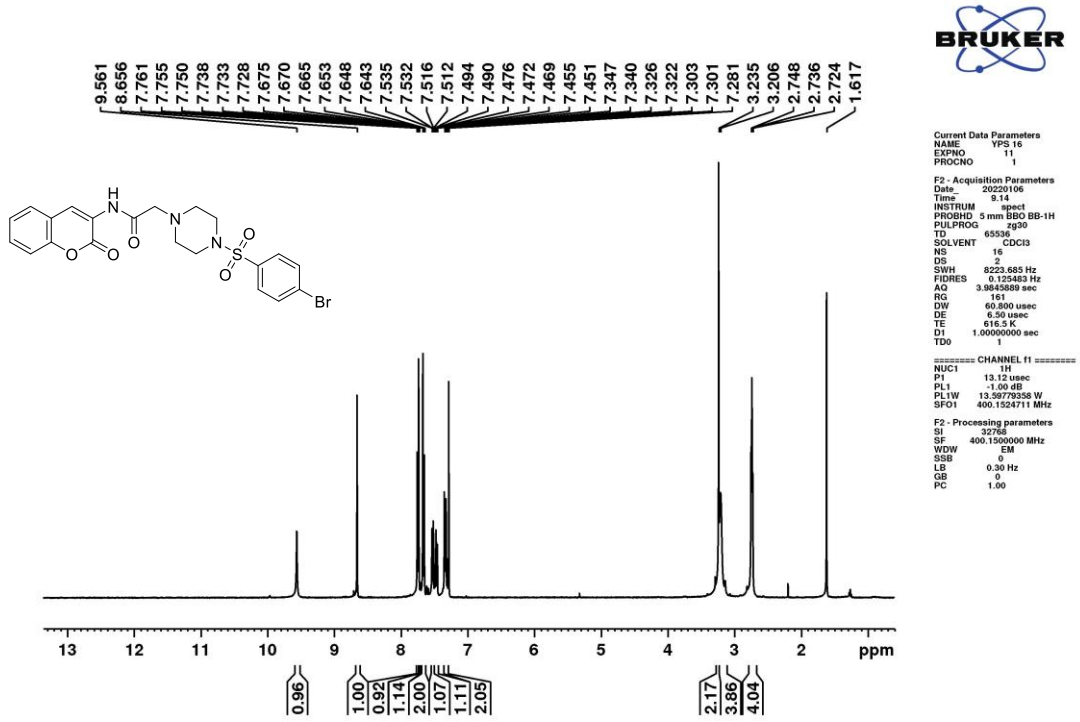

^{1}H NMR spectrum of compound 10a (Chapter 5)

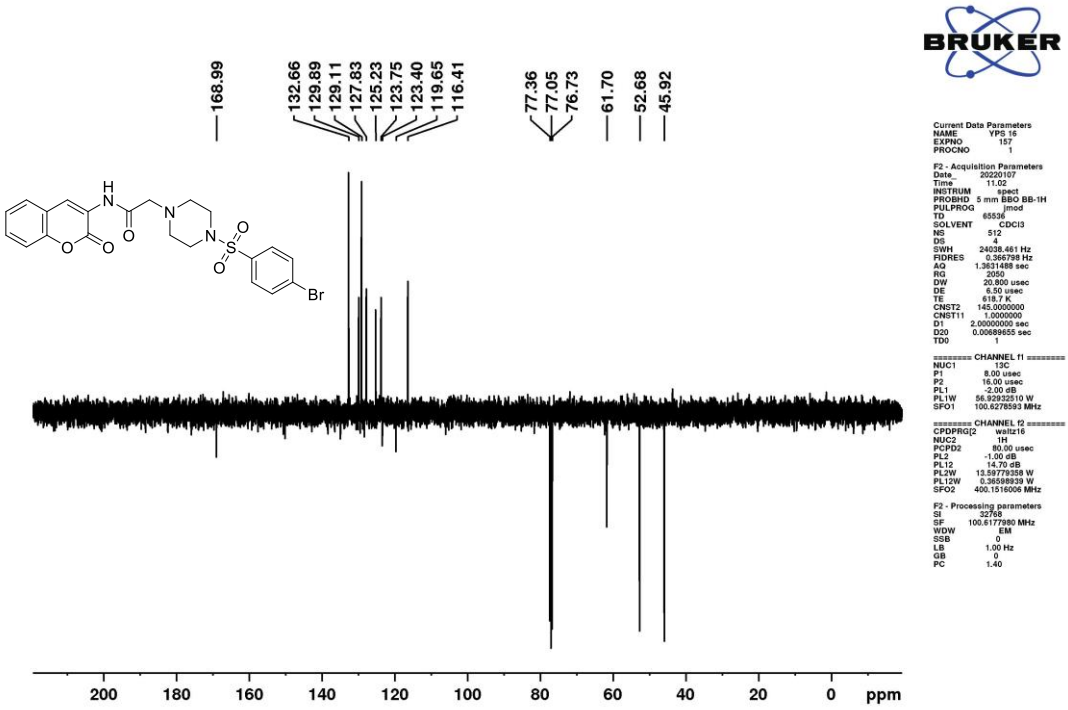

^{13}C NMR spectrum of compound 10a (Chapter 5)

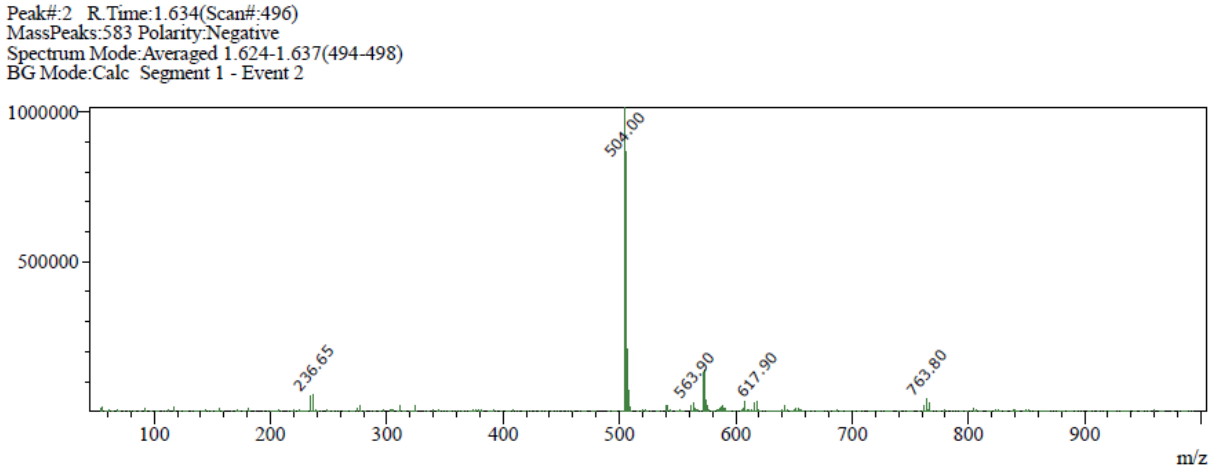

Mass spectrum of compound 10a (Chapter 5)

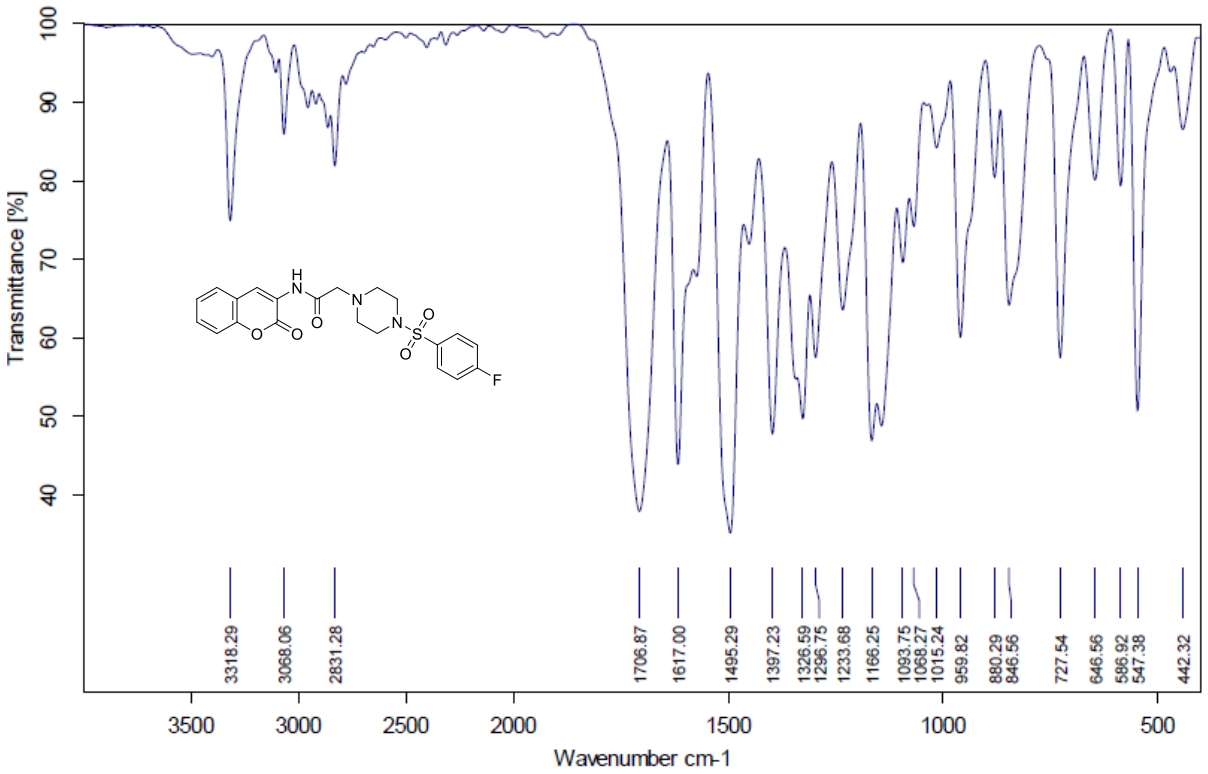

IRspectrum of compound 10b (Chapter 5)

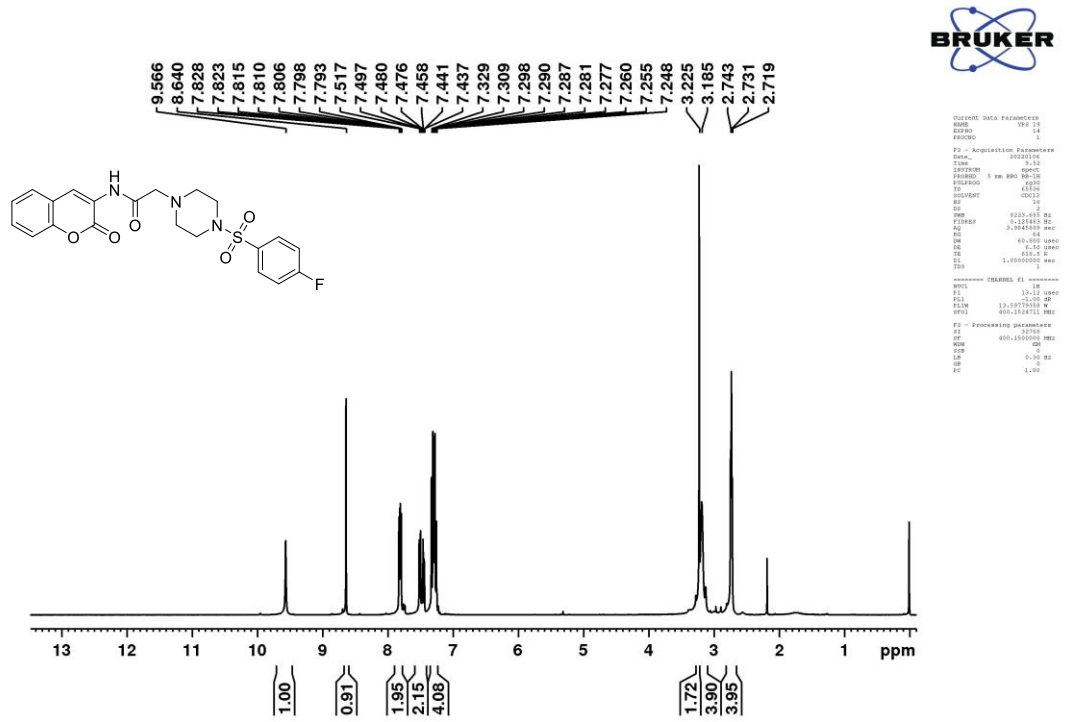

^{1}H NMR spectrum of compound 10b (Chapter 5)

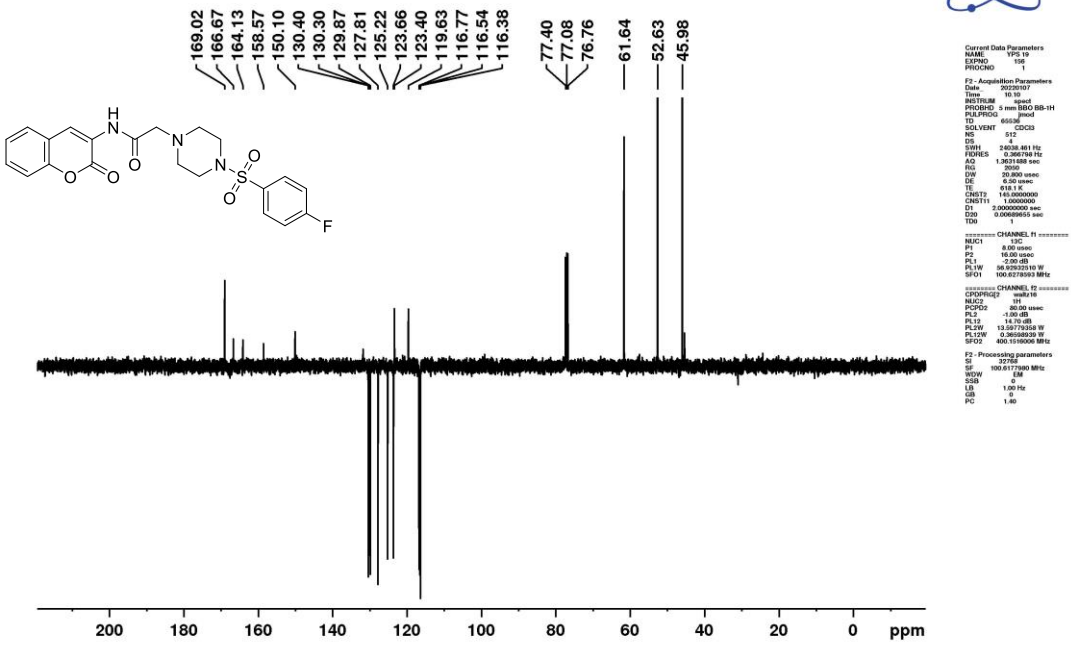

^{13}C NMR spectrum of compound 10b (Chapter 5)

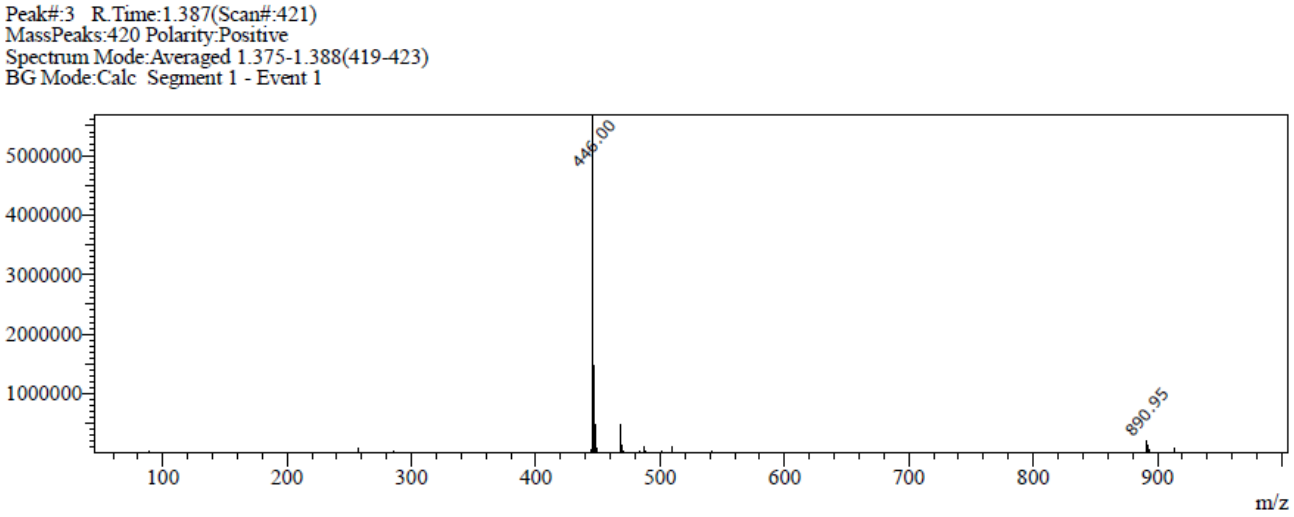

Mass spectrum of compound 10b (Chapter 5)

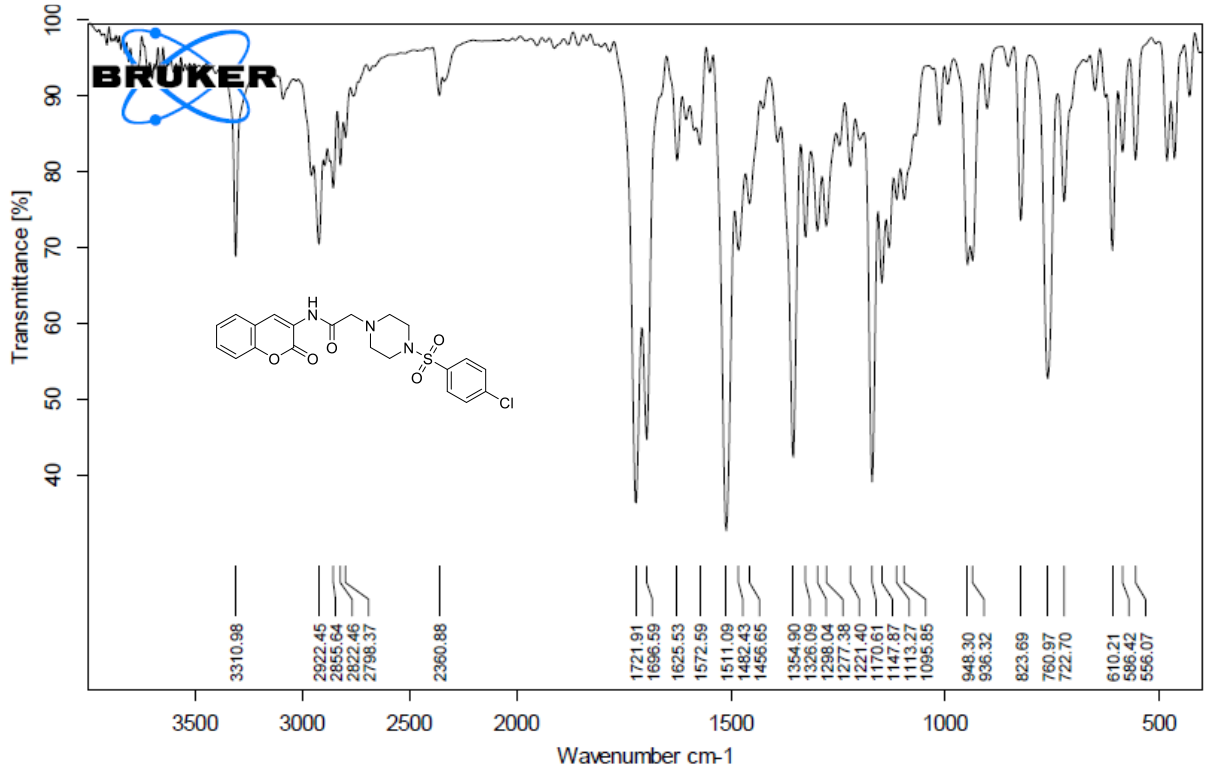

IRspectrum of compound 10c (Chapter 5)

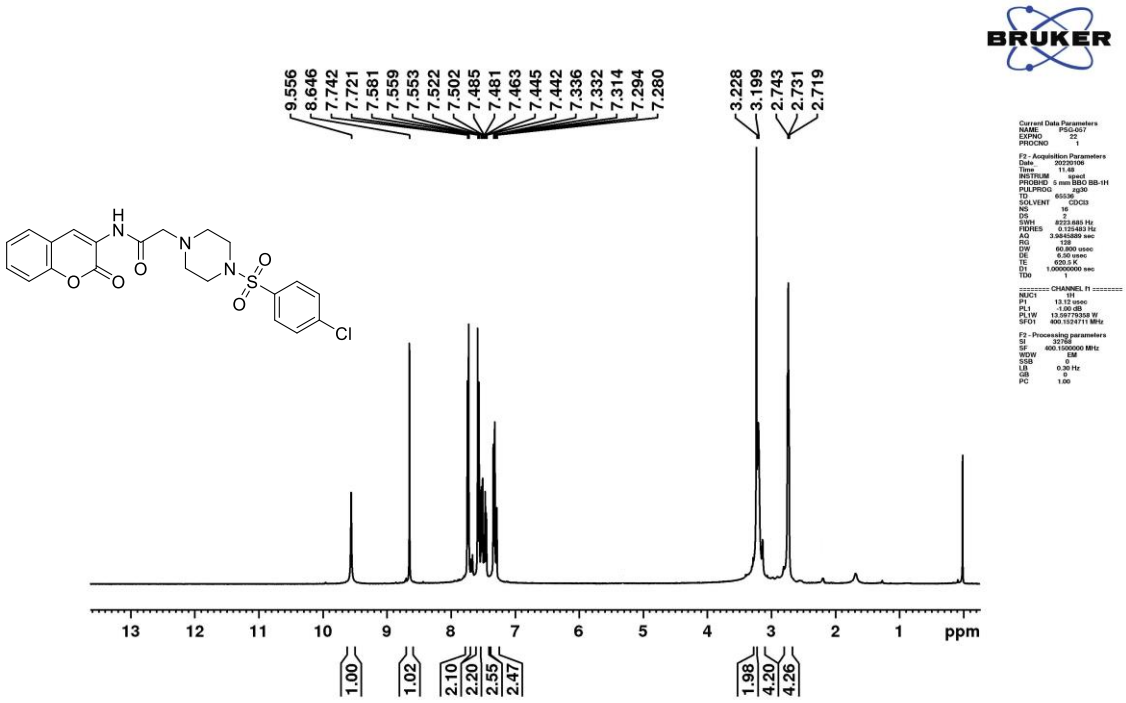

^{1}H NMR spectrum of compound 10c (Chapter 5)

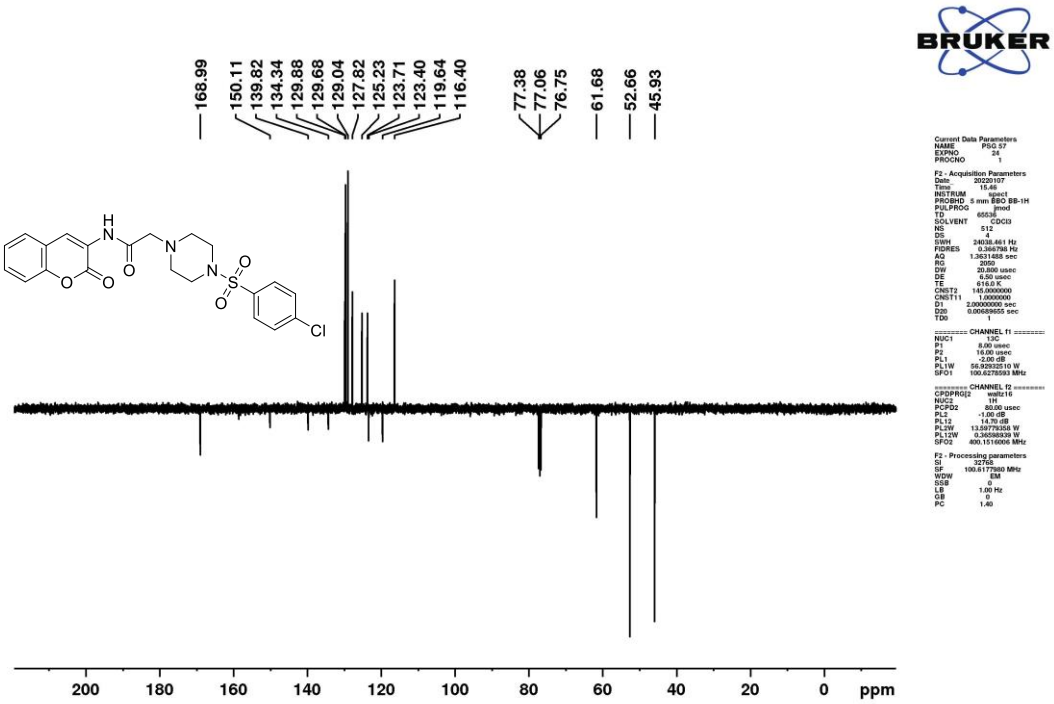

^{13}CNMR spectrum of compound 10c (Chapter 5)

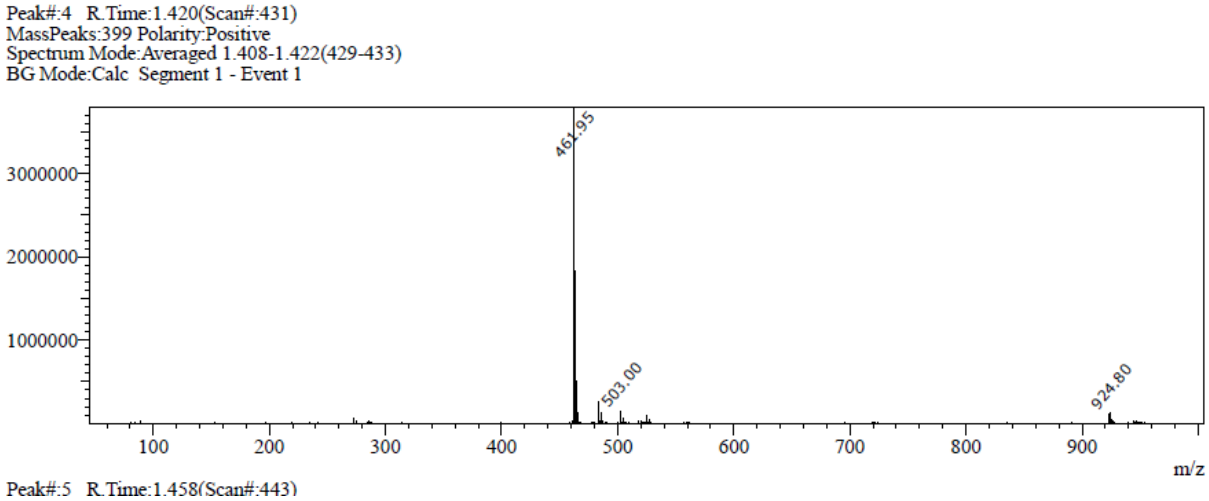

Mass spectra spectrum of compound 10c (Chapter 5)

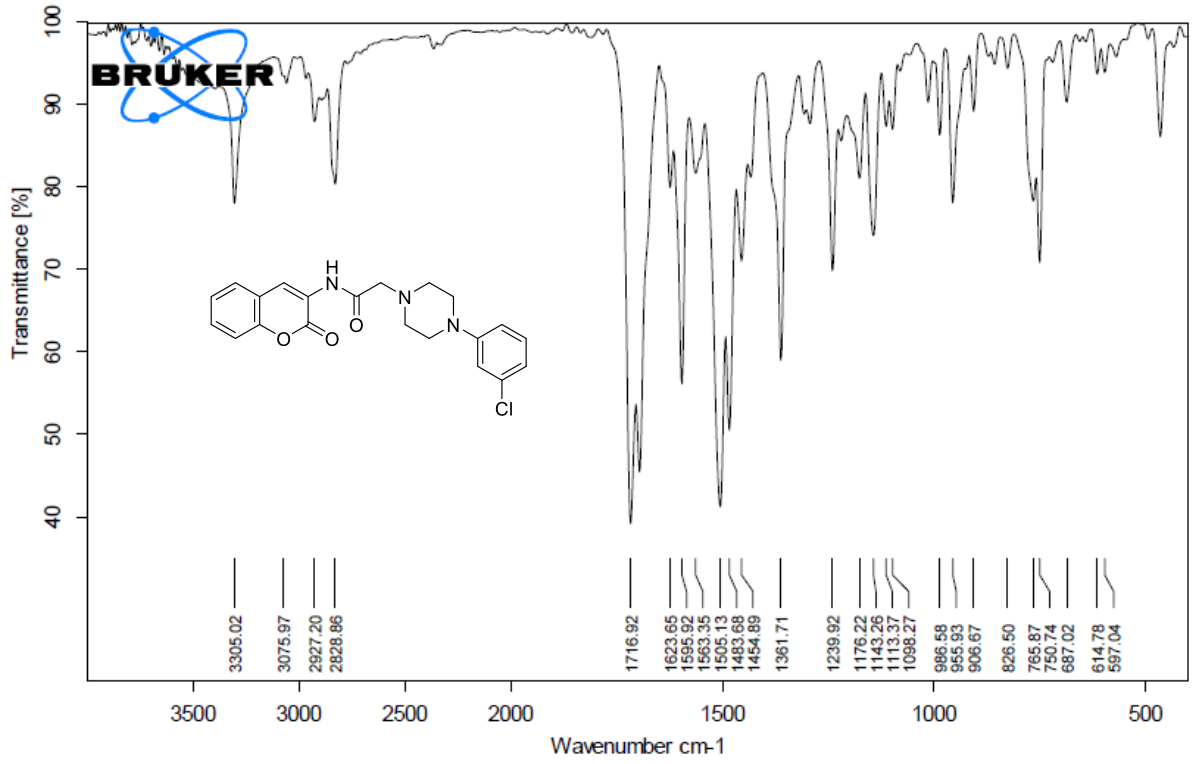

IRspectrum of compound 10d (Chapter 5)

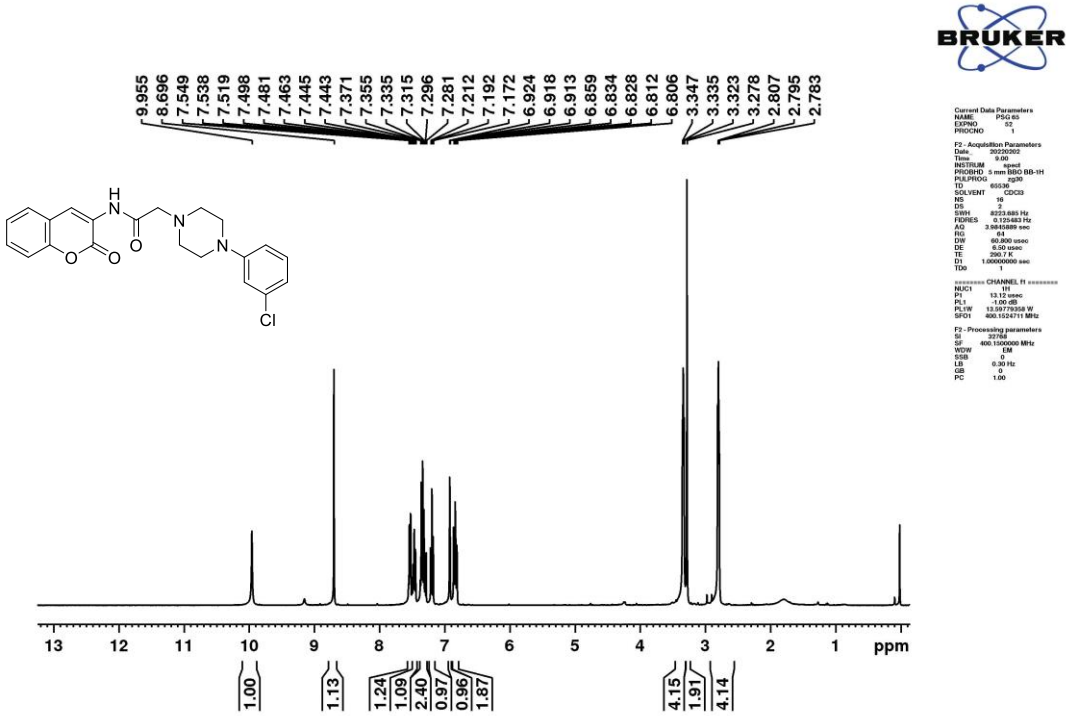

^{1}H NMR spectrum of compound 10d (Chapter 5)

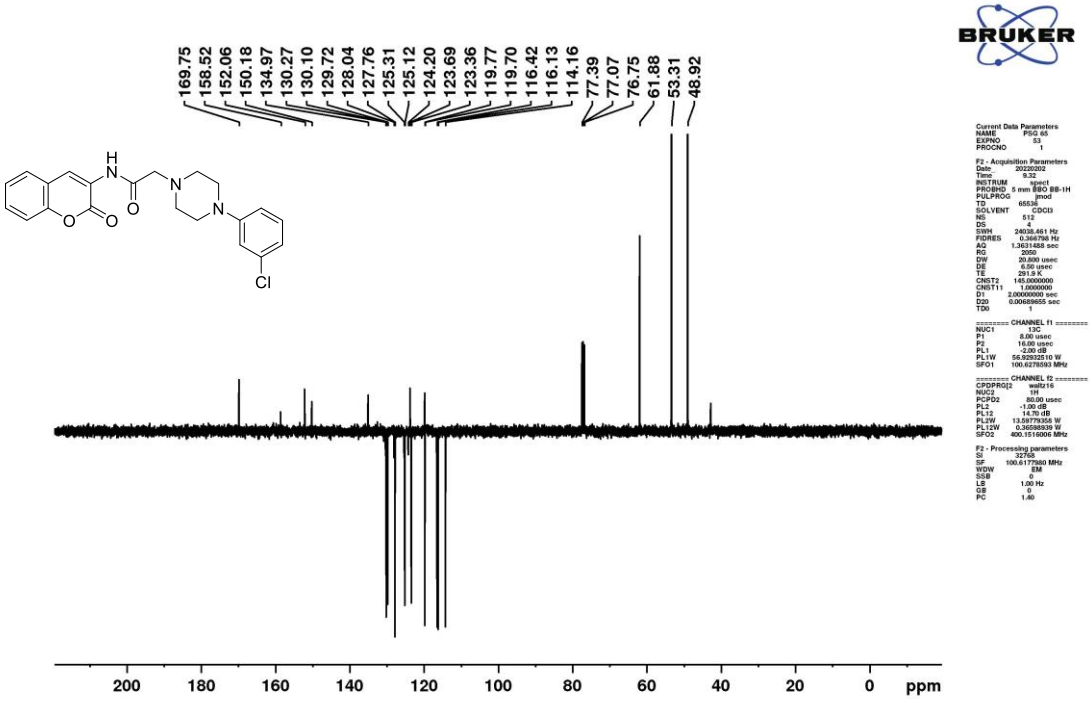

^{13}C NMR spectrum of compound 10d (Chapter 5)

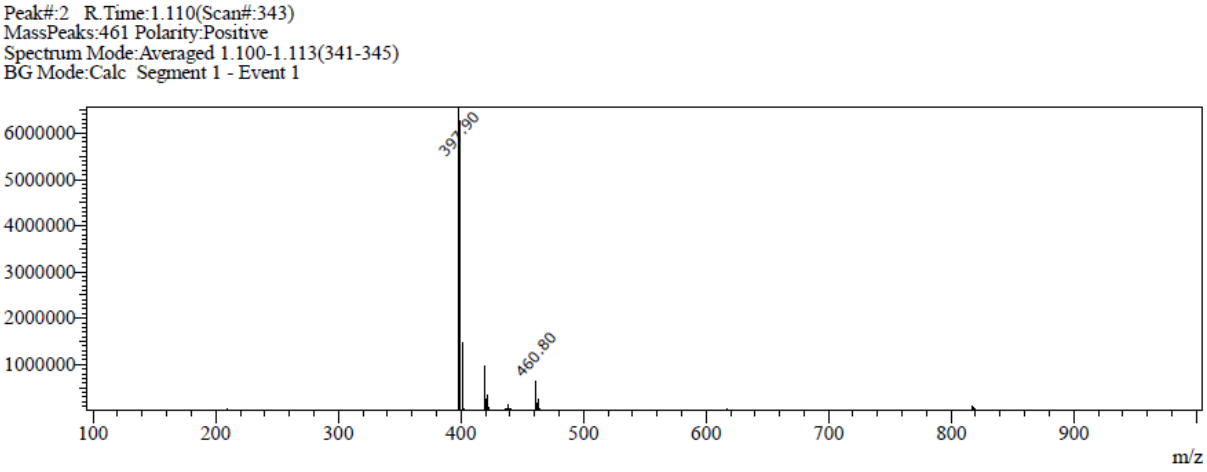

Mass spectra spectrum of compound 10d (Chapter 5)

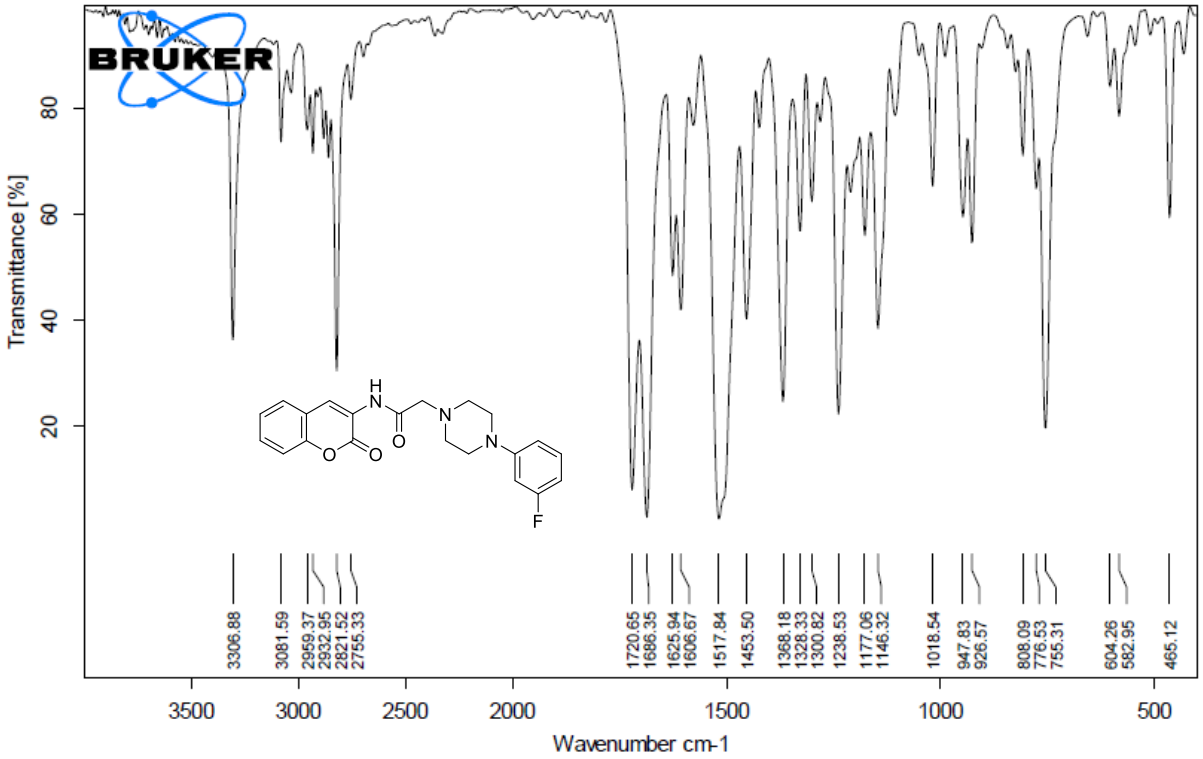

IRspectrum of compound 10e (Chapter 5)

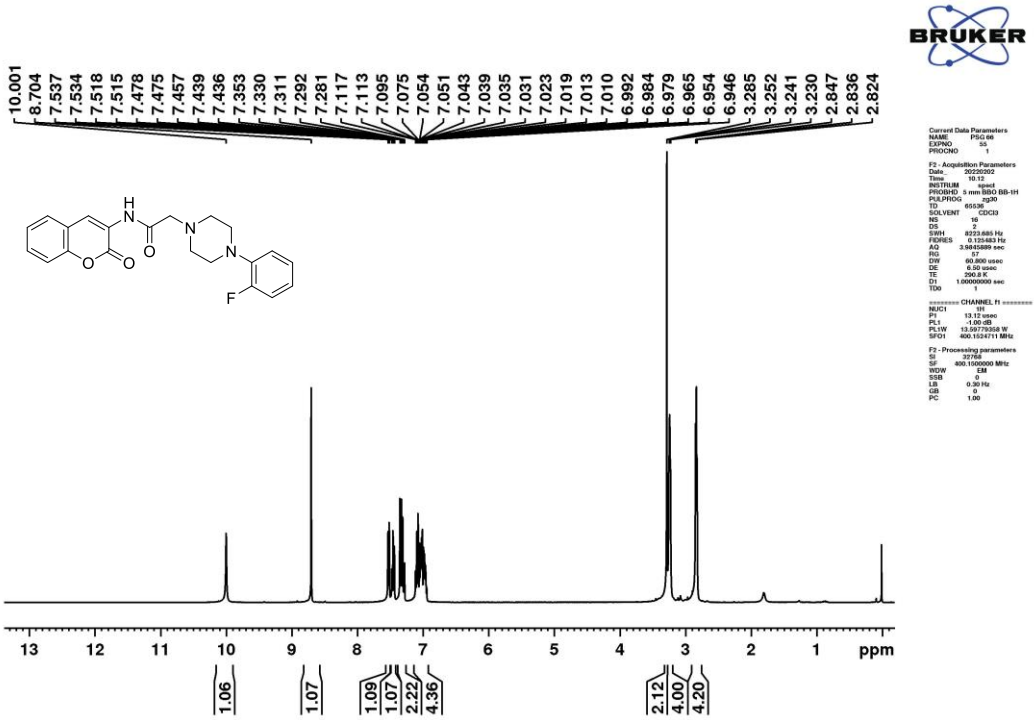

^{1}H NMR spectrum of compound 10e (Chapter 5)

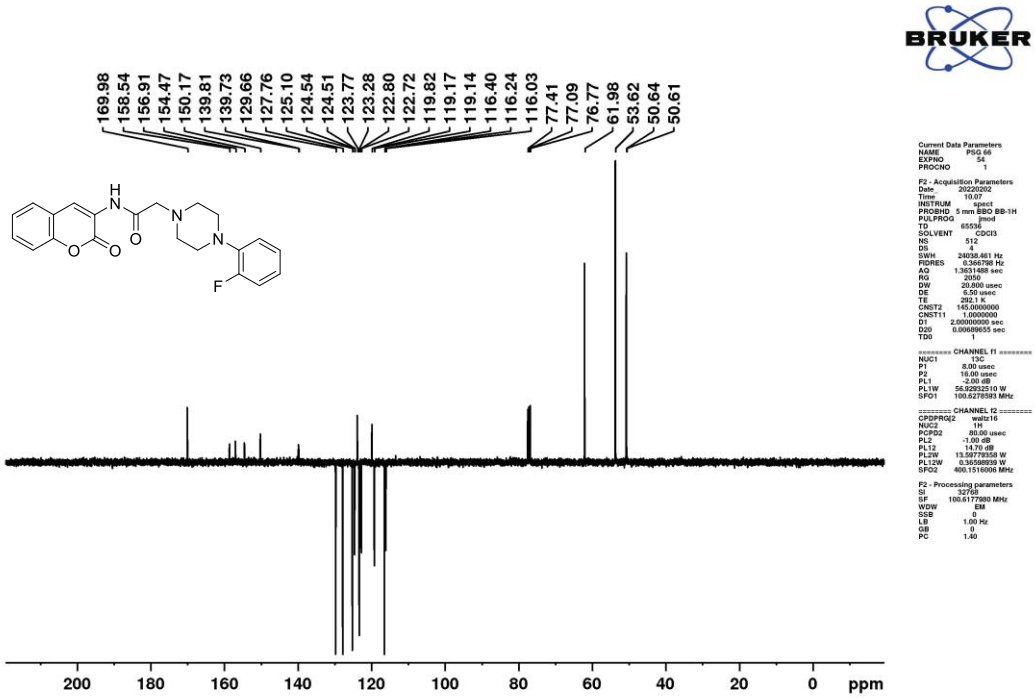

^{13}C NMR spectrum of compound 10e (Chapter 5)

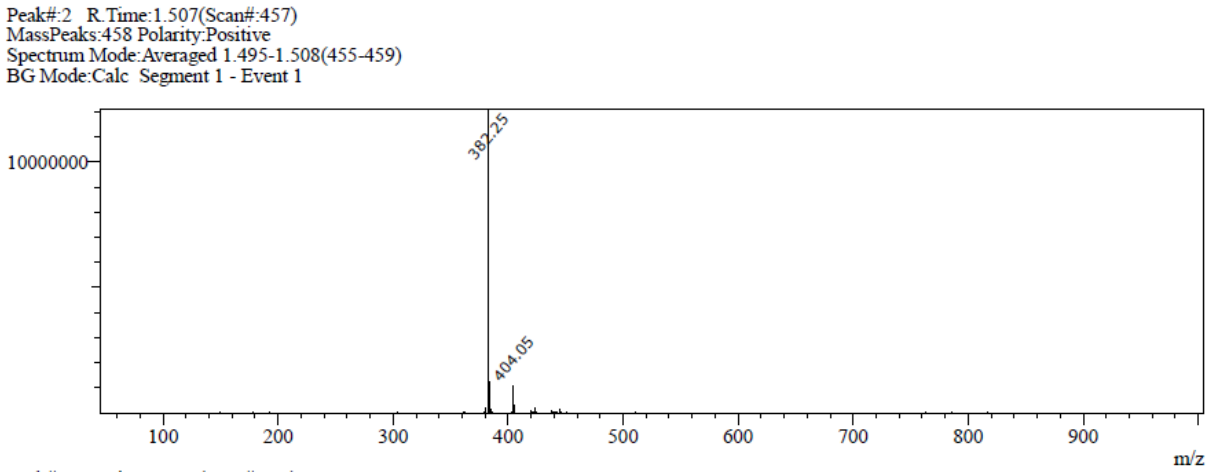

Mass spectrum of compound 10e (Chapter 5)

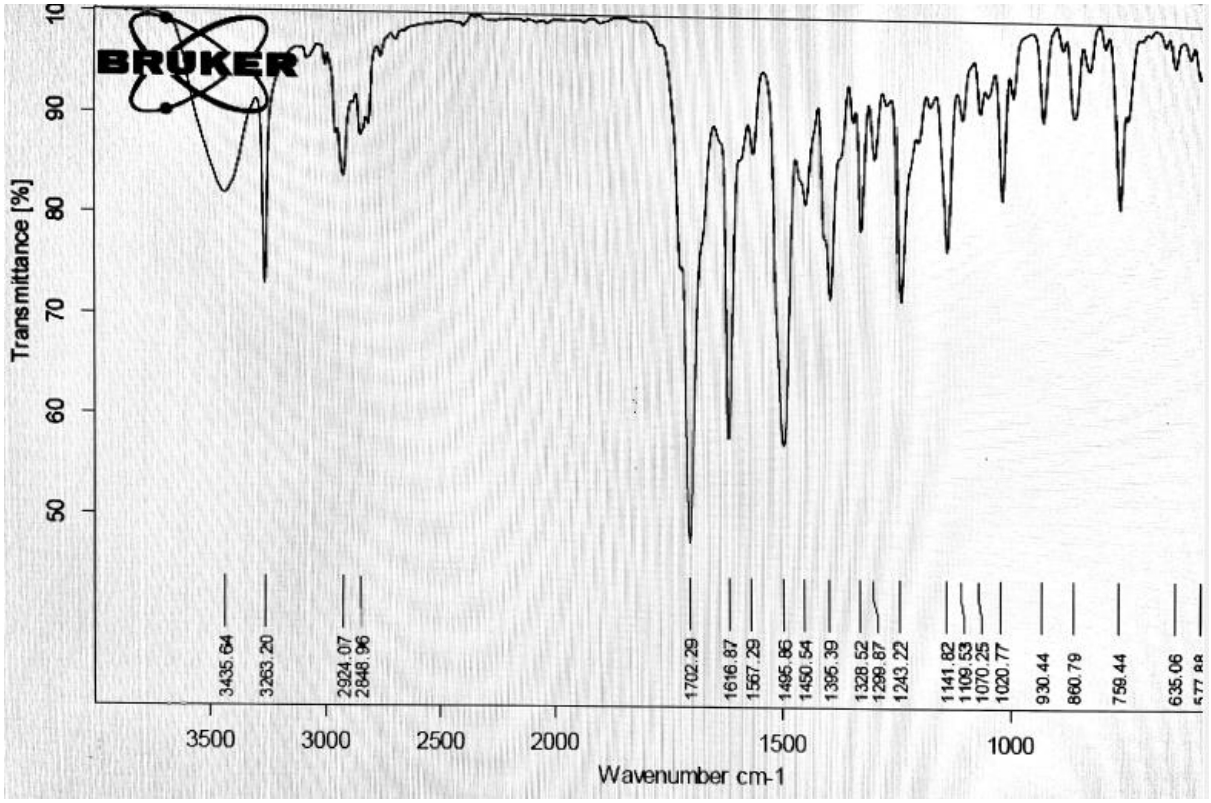

IRspectrum of compound 10f (Chapter 5)

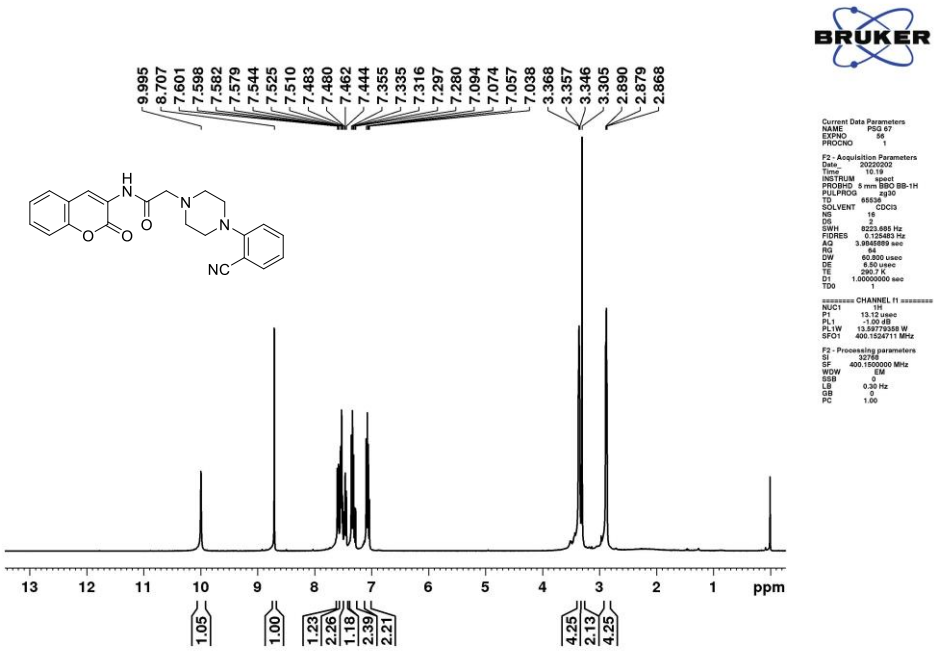

^{1}H NMR spectrum of compound 10f (Chapter 5)

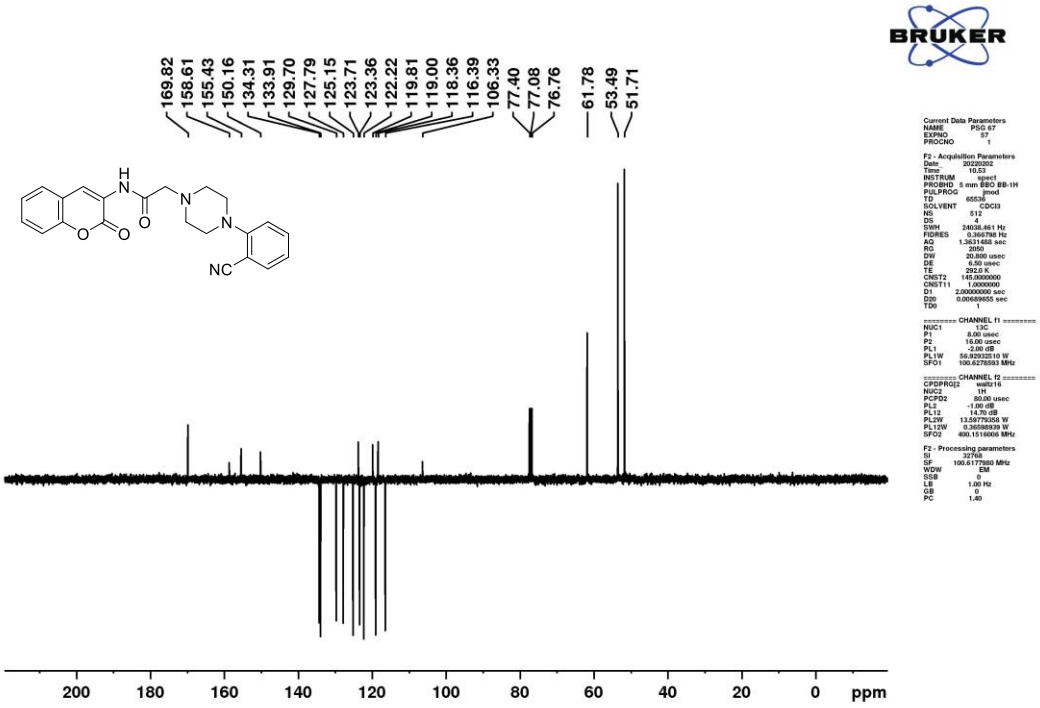

^{13}C NMR spectrum of compound 10f (Chapter 5)

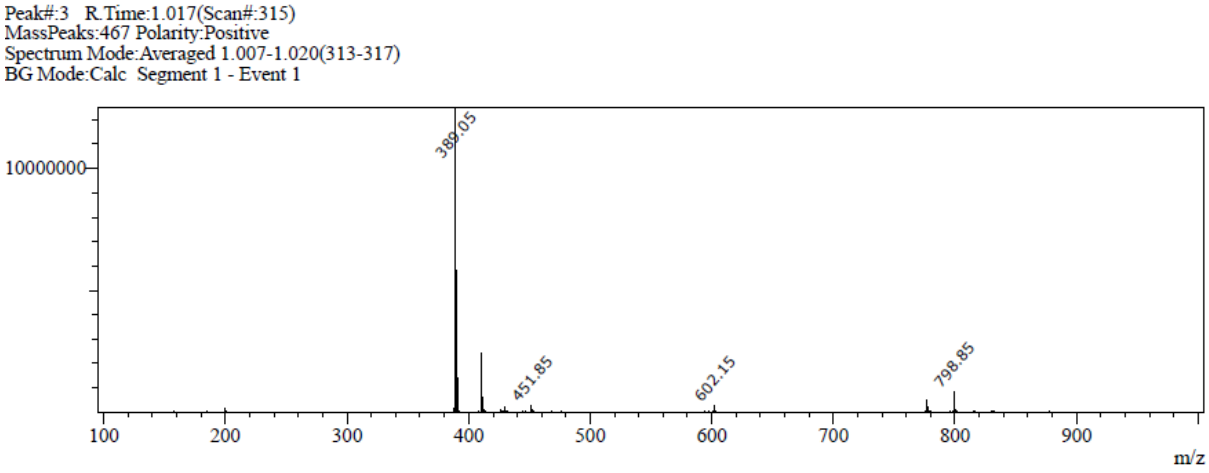

Mass spectrum of compound 10f (Chapter 5)

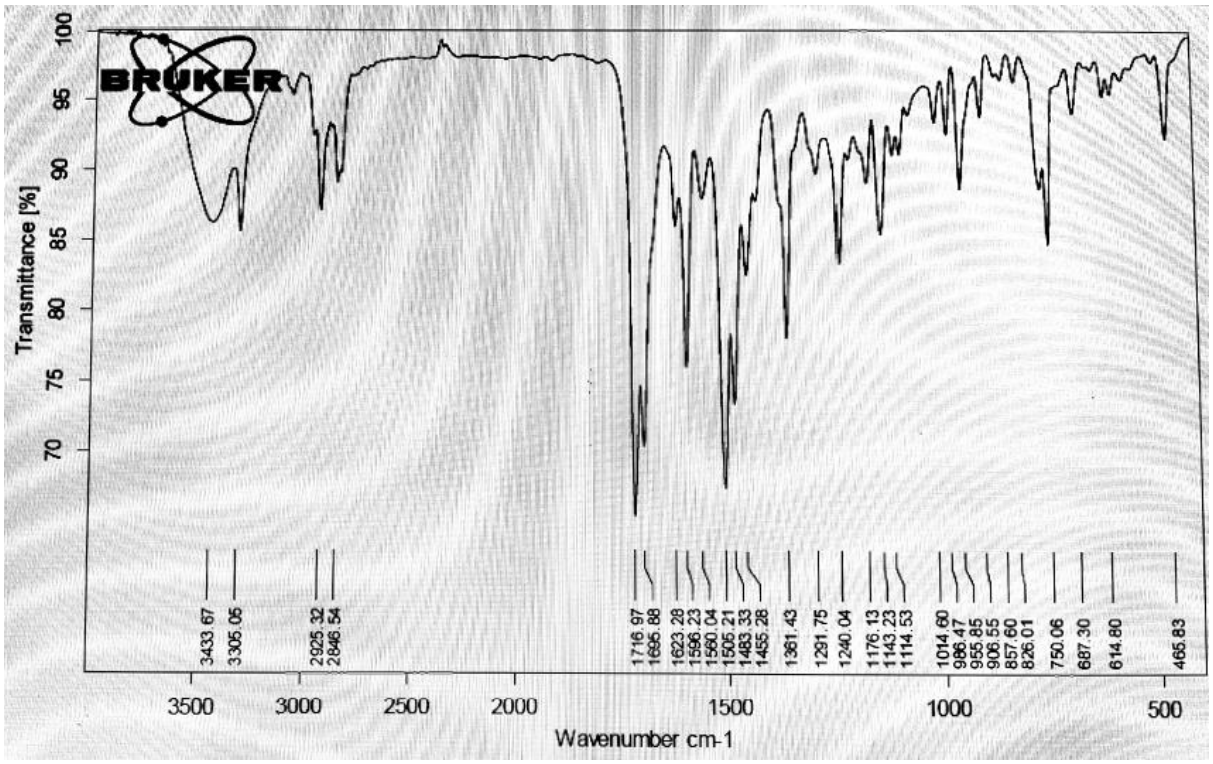

IRspectrum of compound 10g (Chapter 5)

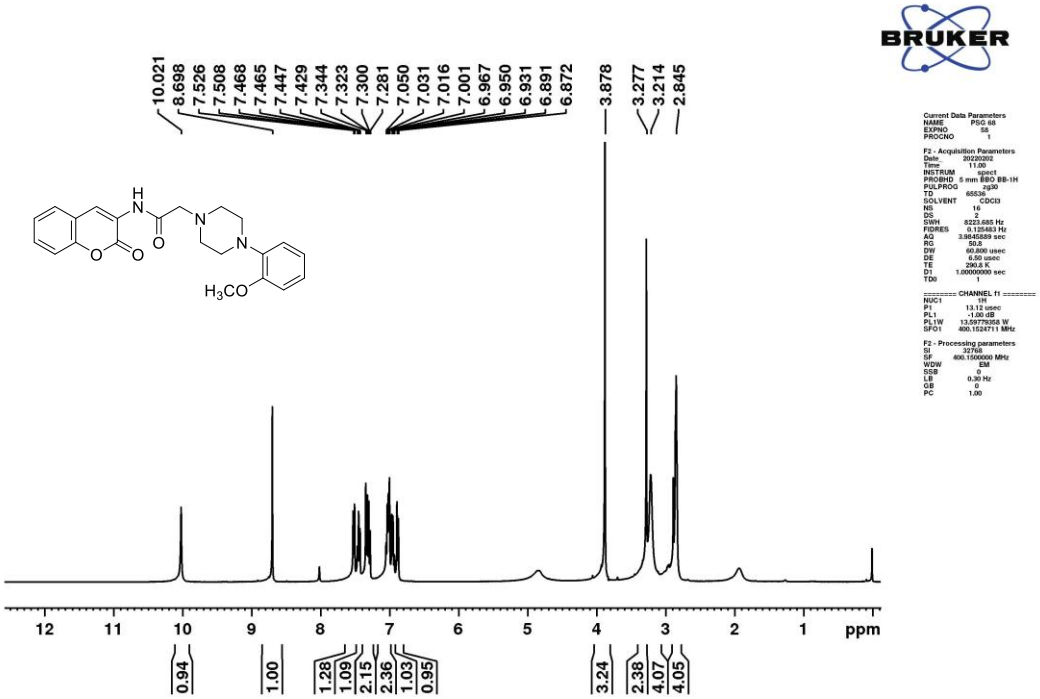

^{1}H NMR spectrum of compound 10g (Chapter 5)

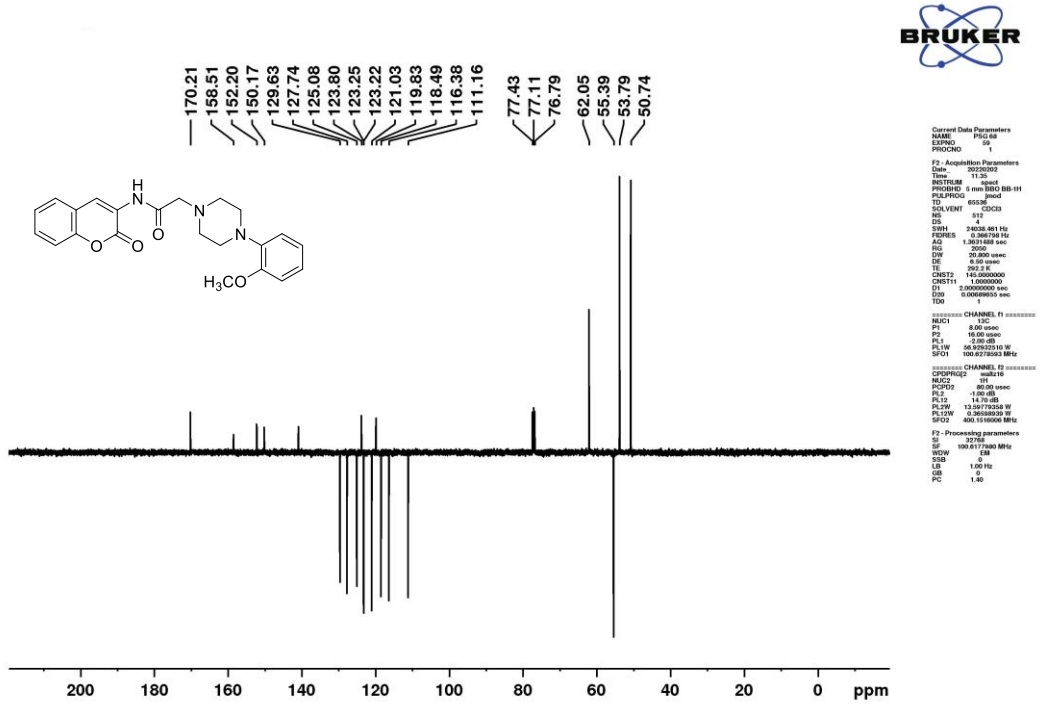

^{13}C NMR spectrum of compound 10g (Chapter 5)

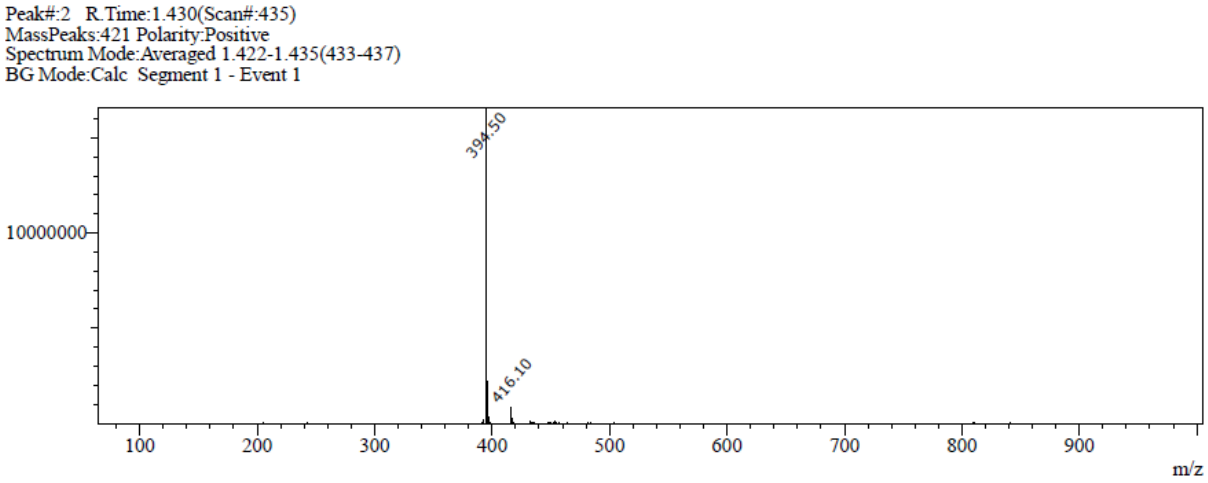

Mass spectrum of compound 10g (Chapter 5)

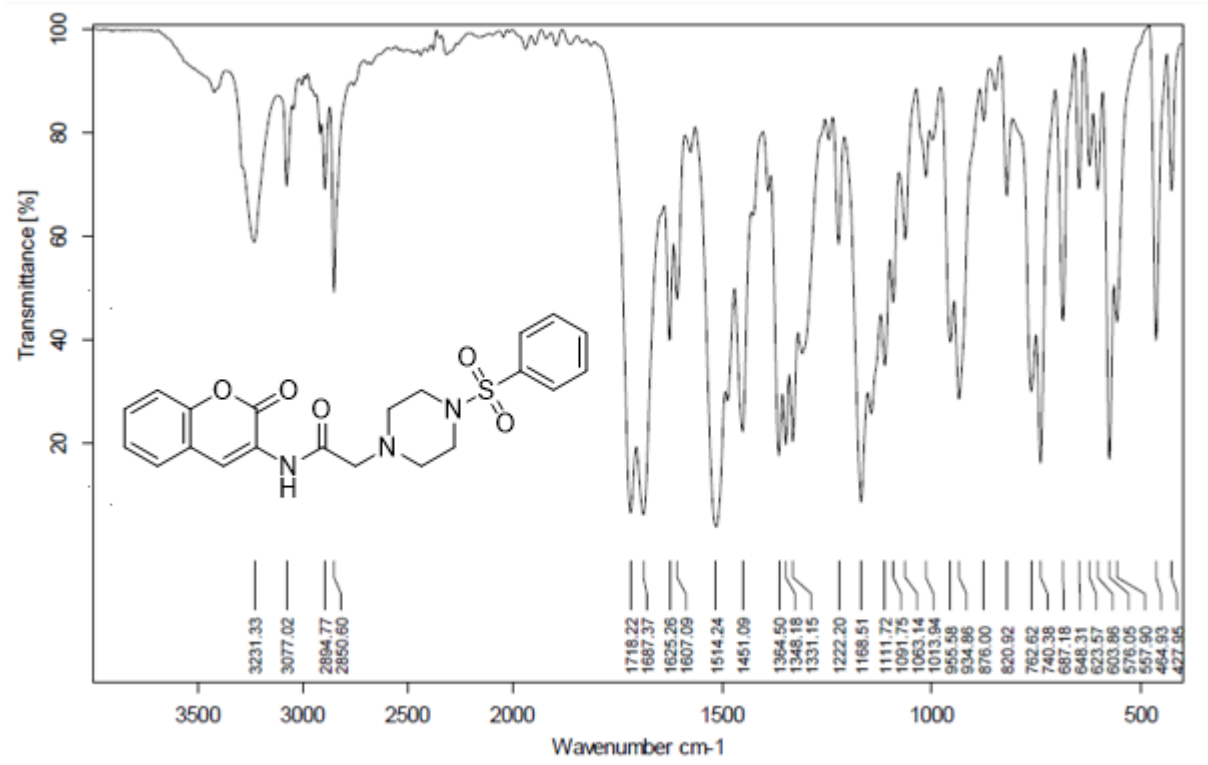

IRspectrum of compound 10h (Chapter 5)

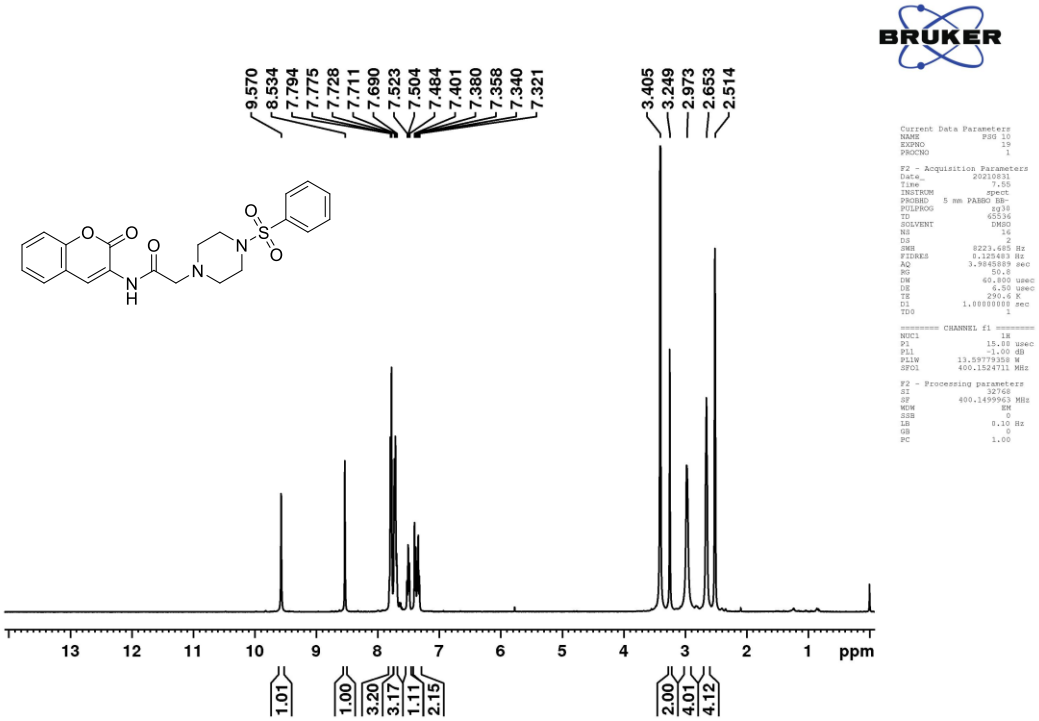

^{1}H NMR spectrum of compound 10h (Chapter 5)

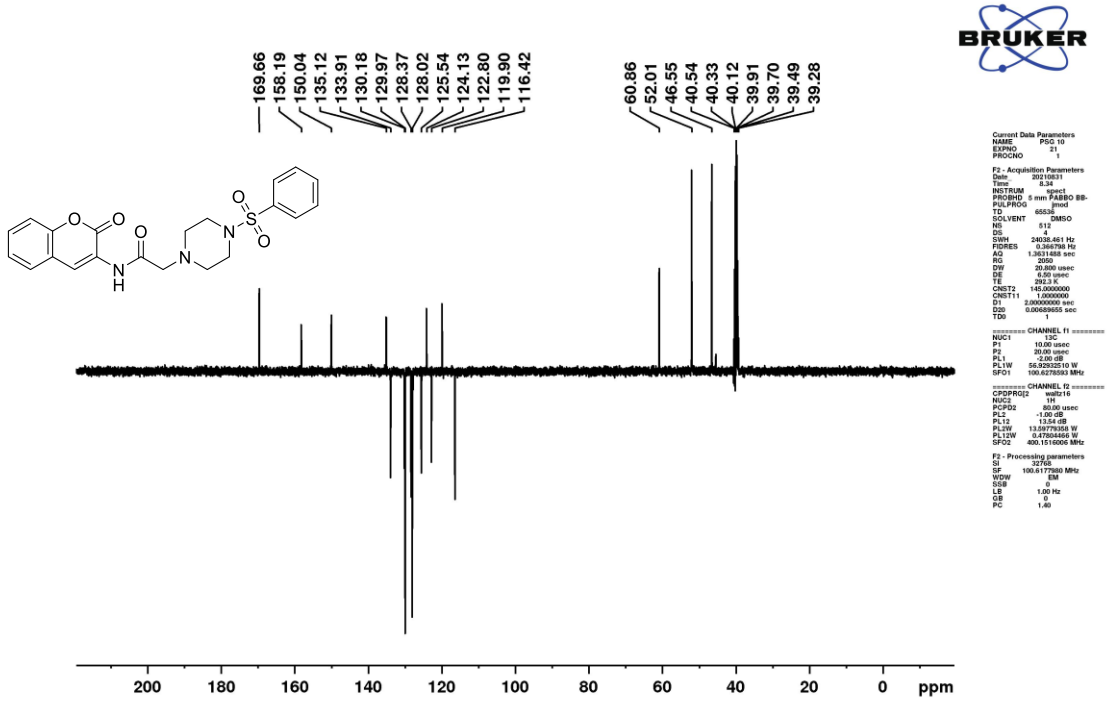

^{13}C NMR spectrum of compound 10h (Chapter 5)

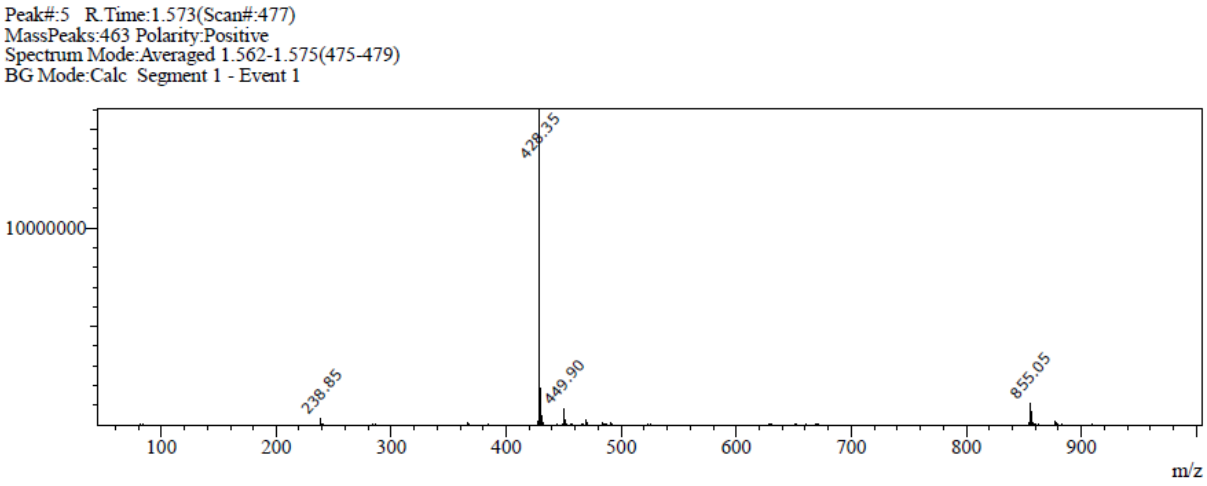

Mass spectrum of compound 10h (Chapter 5)

APPENDEX-I (Chapter-6 supplementary information)

NMR Spectrum of compound 3a-3ak and 3A-3R

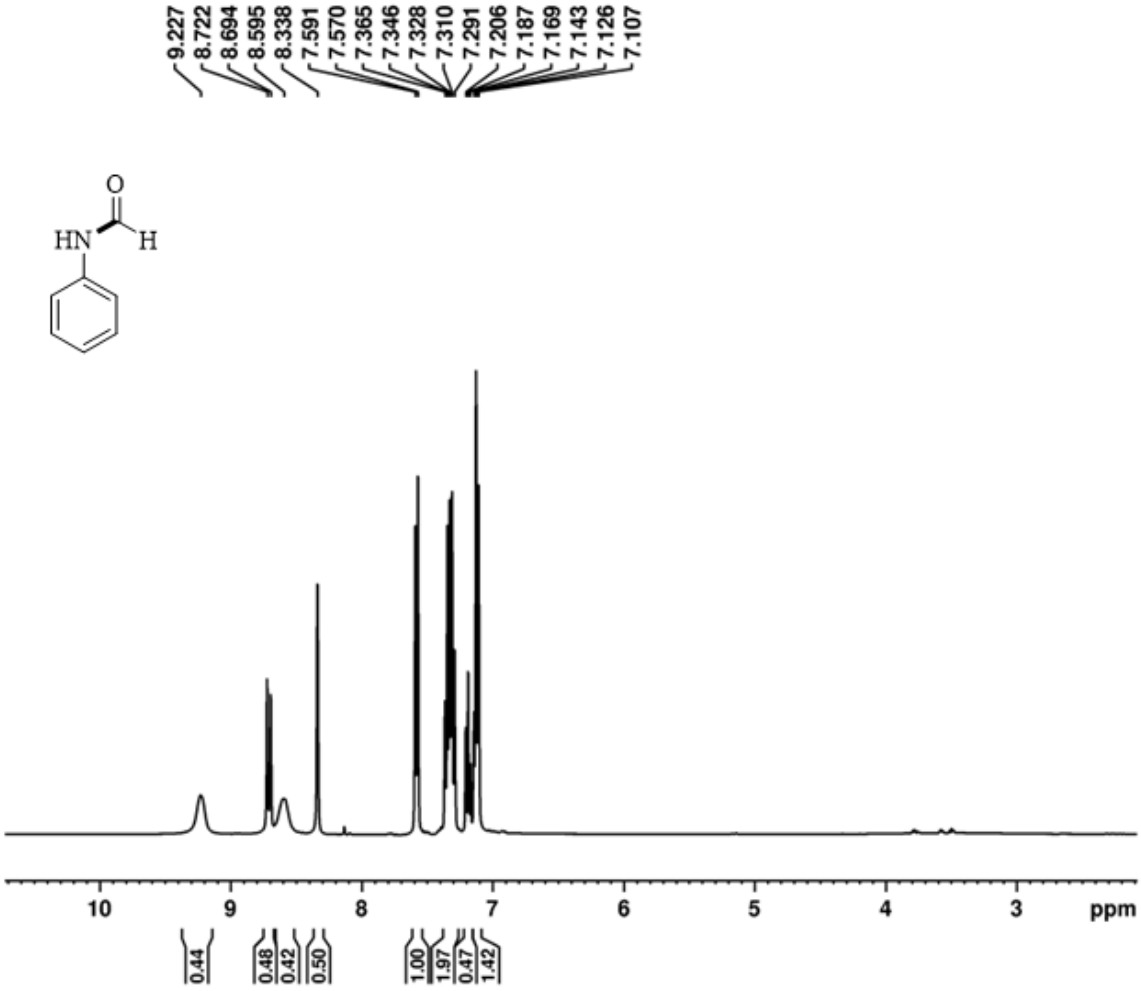

^{1}H NMR spectrum of **3a** (Chapter 6)

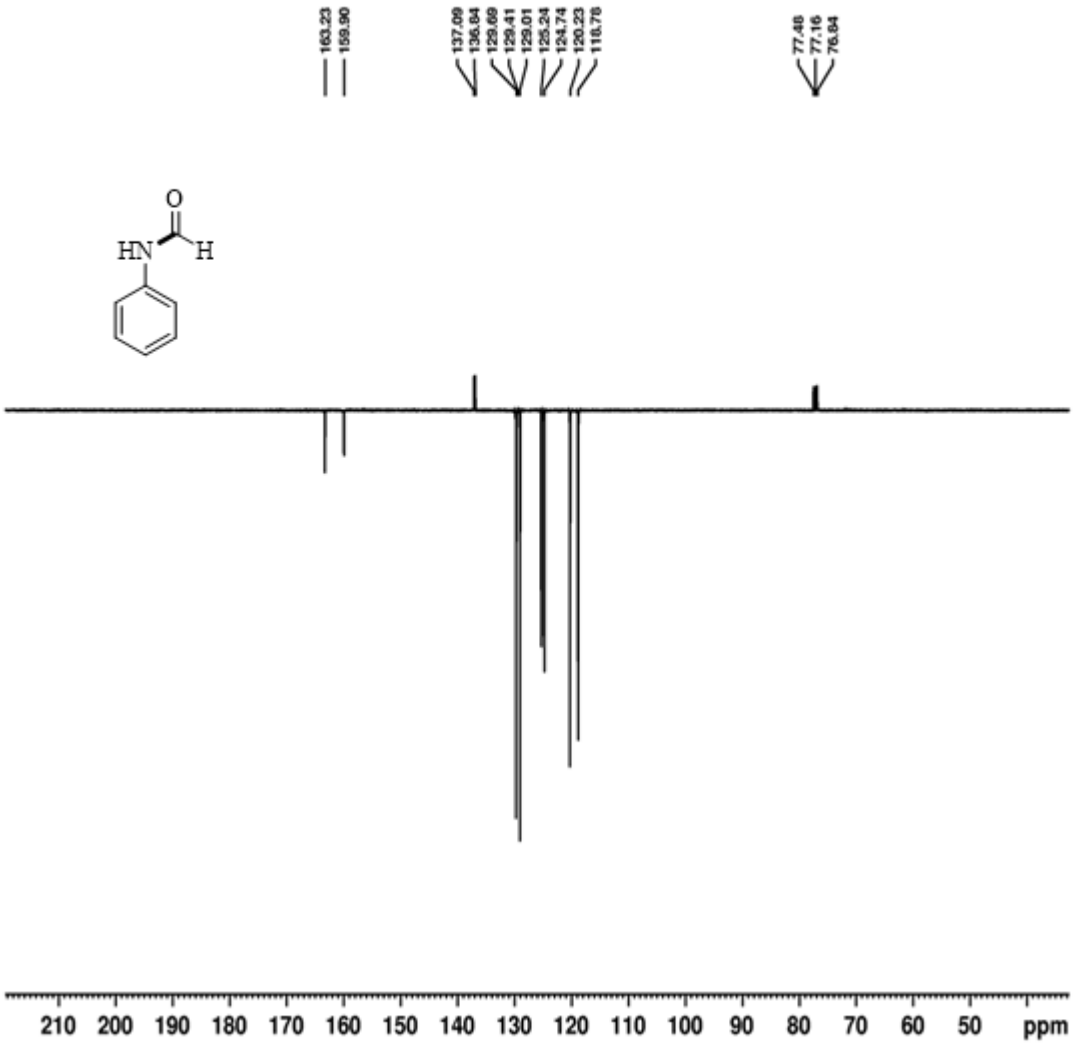

^{13}C spectrum of **3a (Chapter 6)**

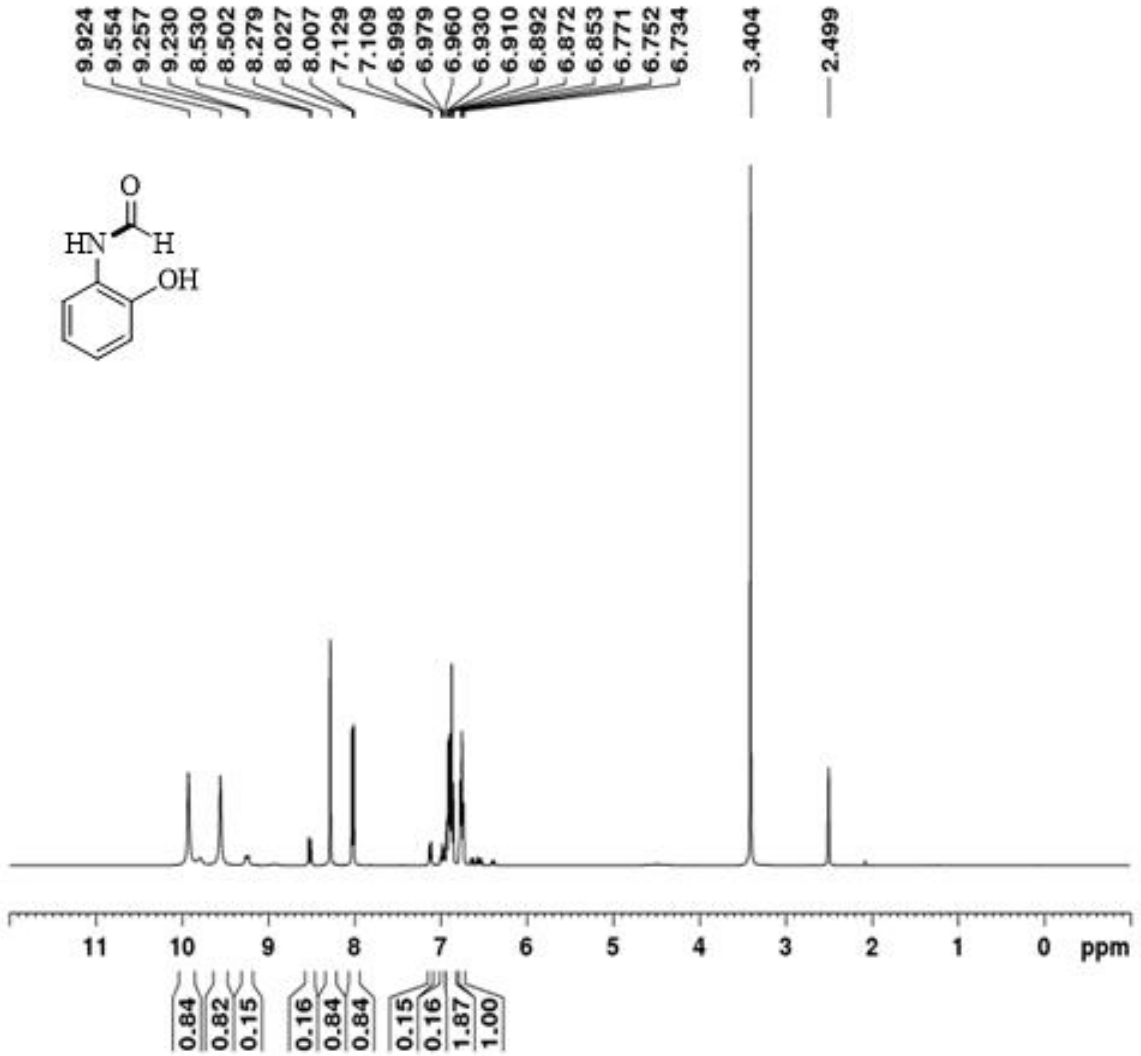

^{1}H NMR spectrum of **3b** (Chapter 6)

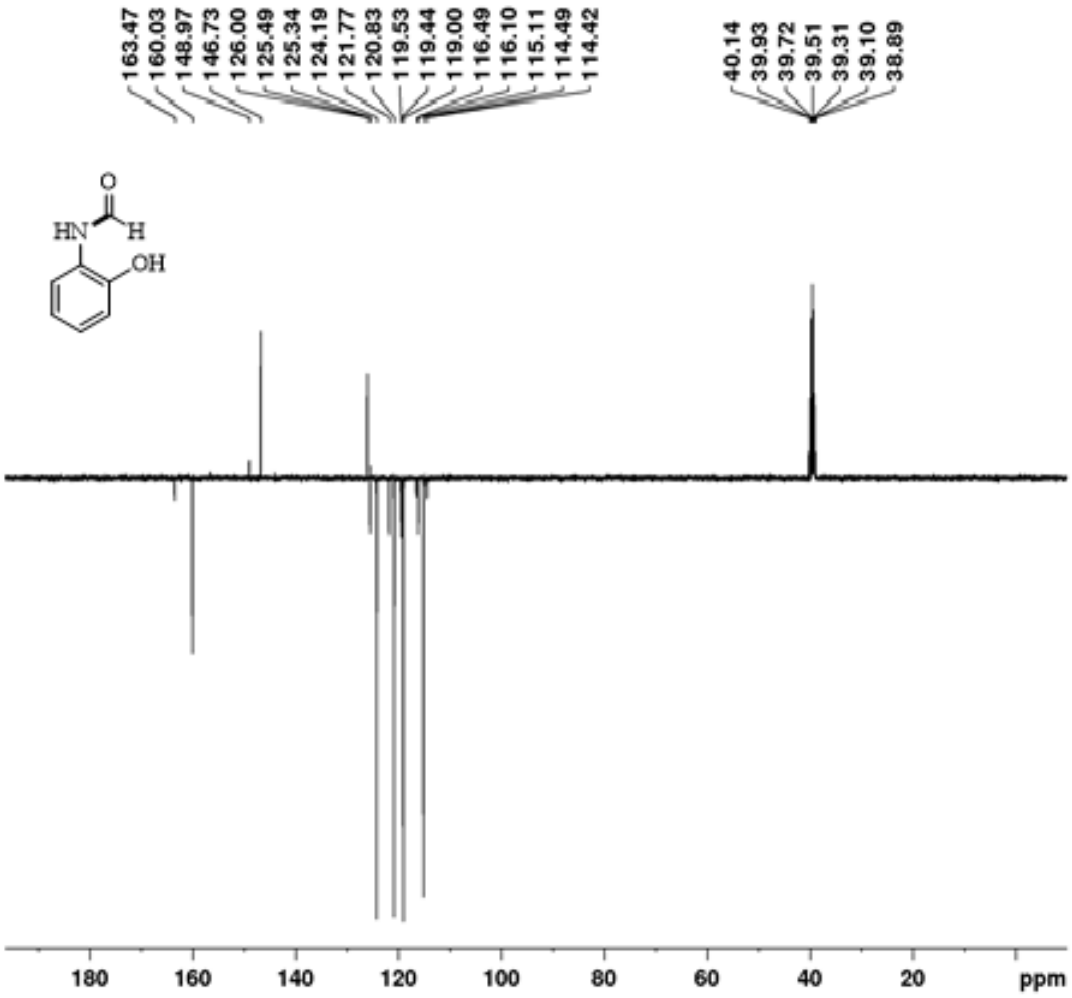

^{13}C spectrum of **3b (Chapter 6)**

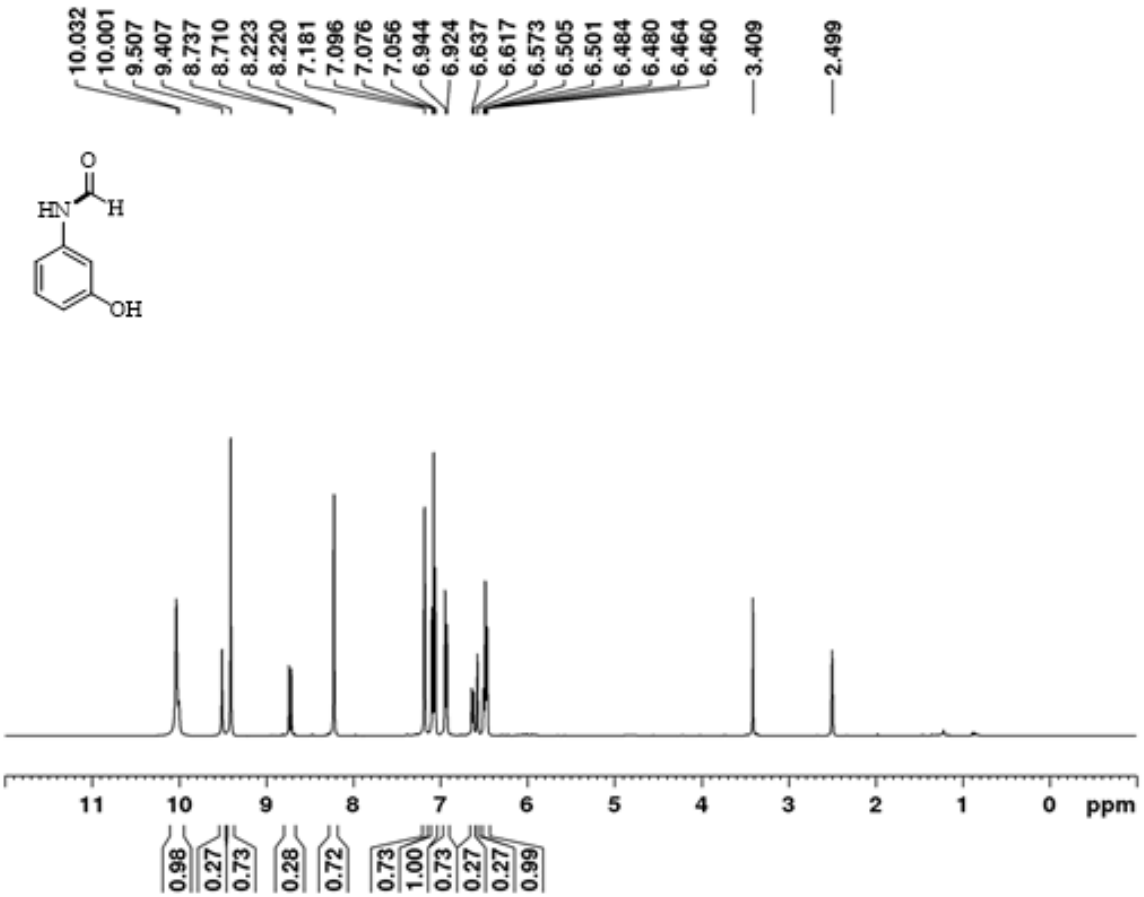

^{1}H NMR spectrum of **3c (Chapter 6)**

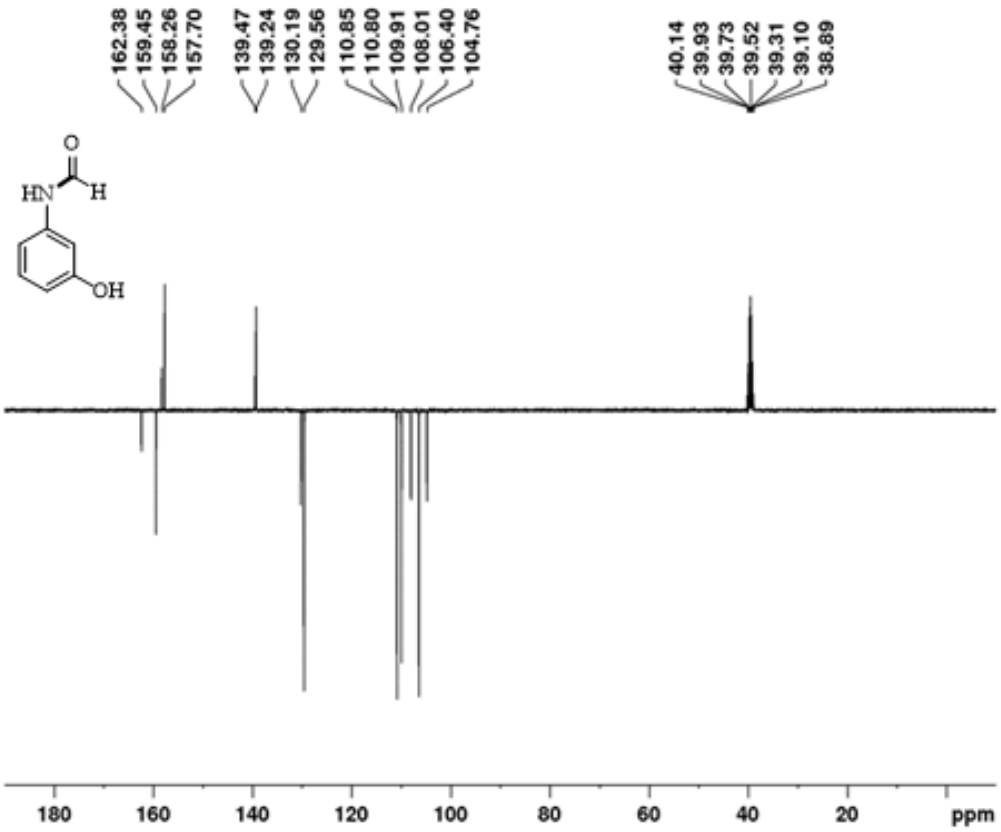

^{13}C spectrum of **3c (Chapter 6)**

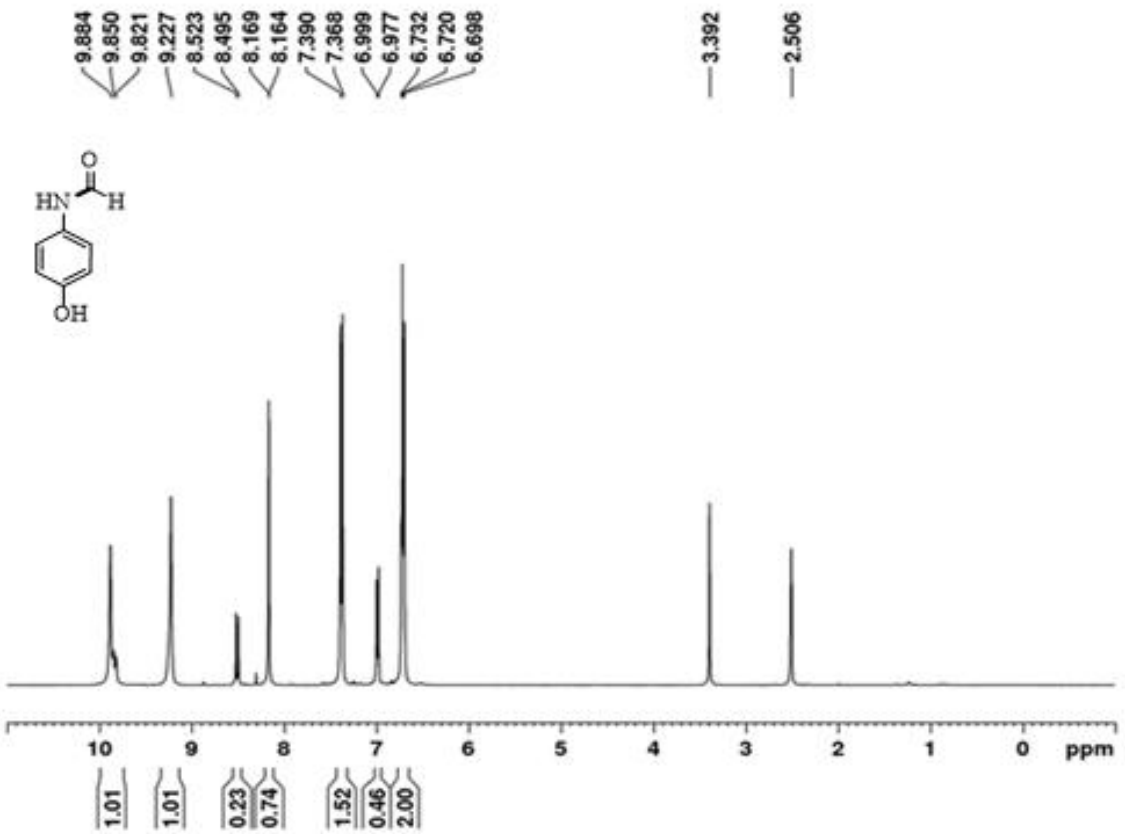

^{1}H NMR spectrum of **3d (Chapter 6)**

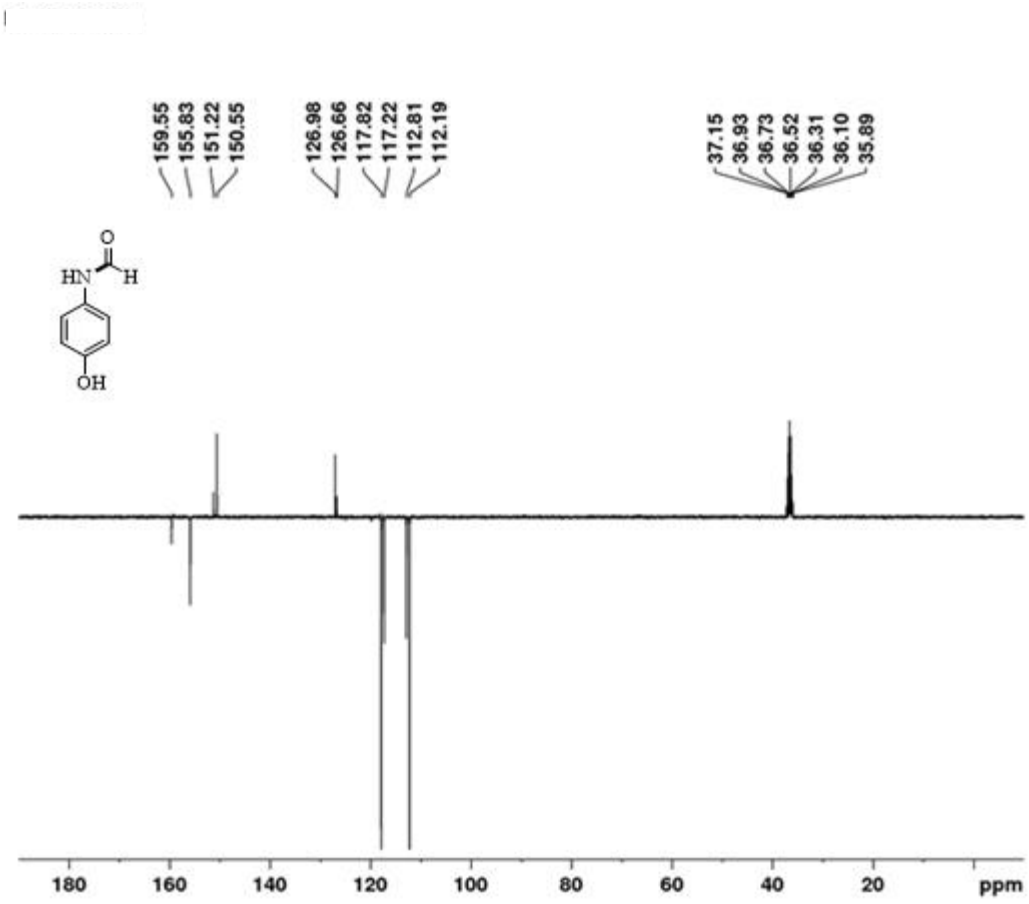

^{13}C spectrum of **3d (Chapter 6)**

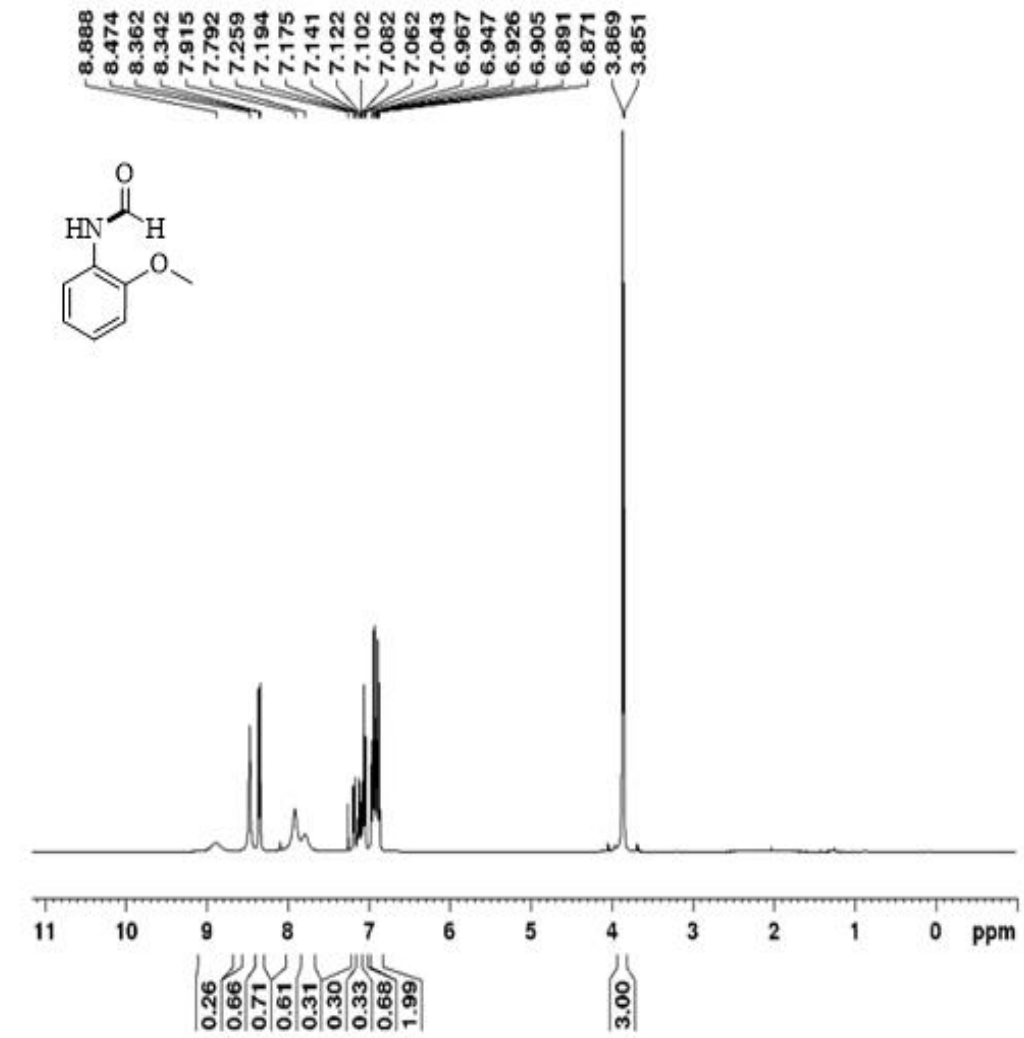

^{1}H NMR spectrum of **3e (Chapter 6)**

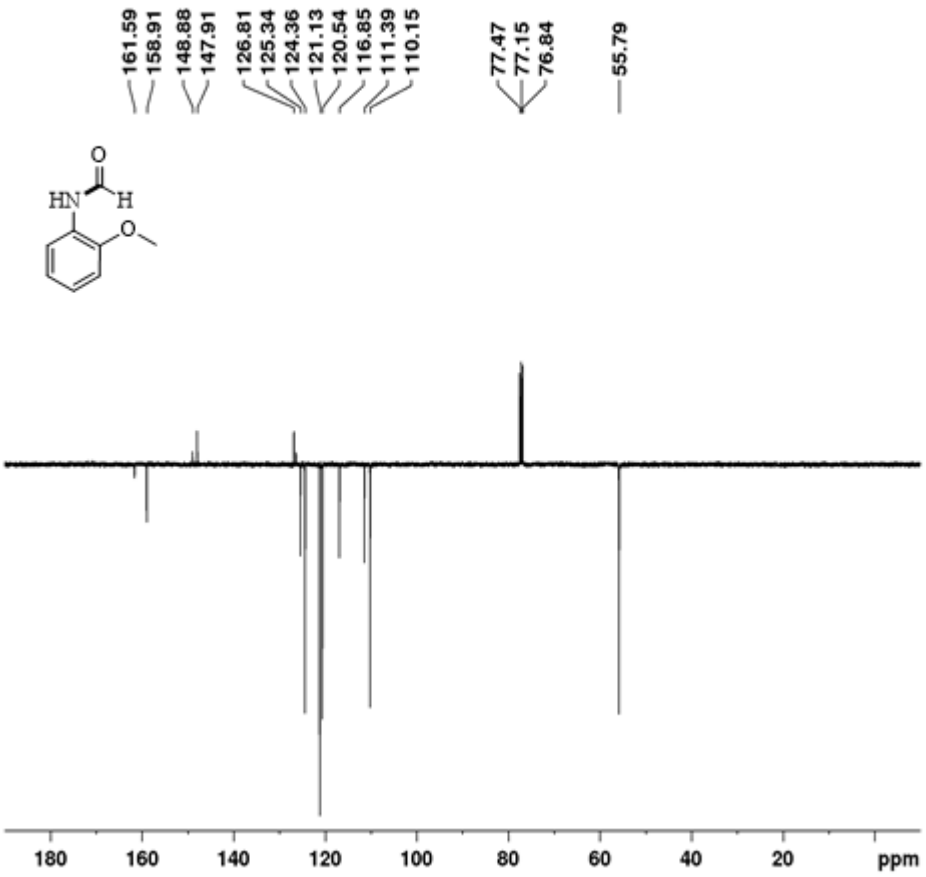

^{13}C spectrum of **3e (Chapter 6)**

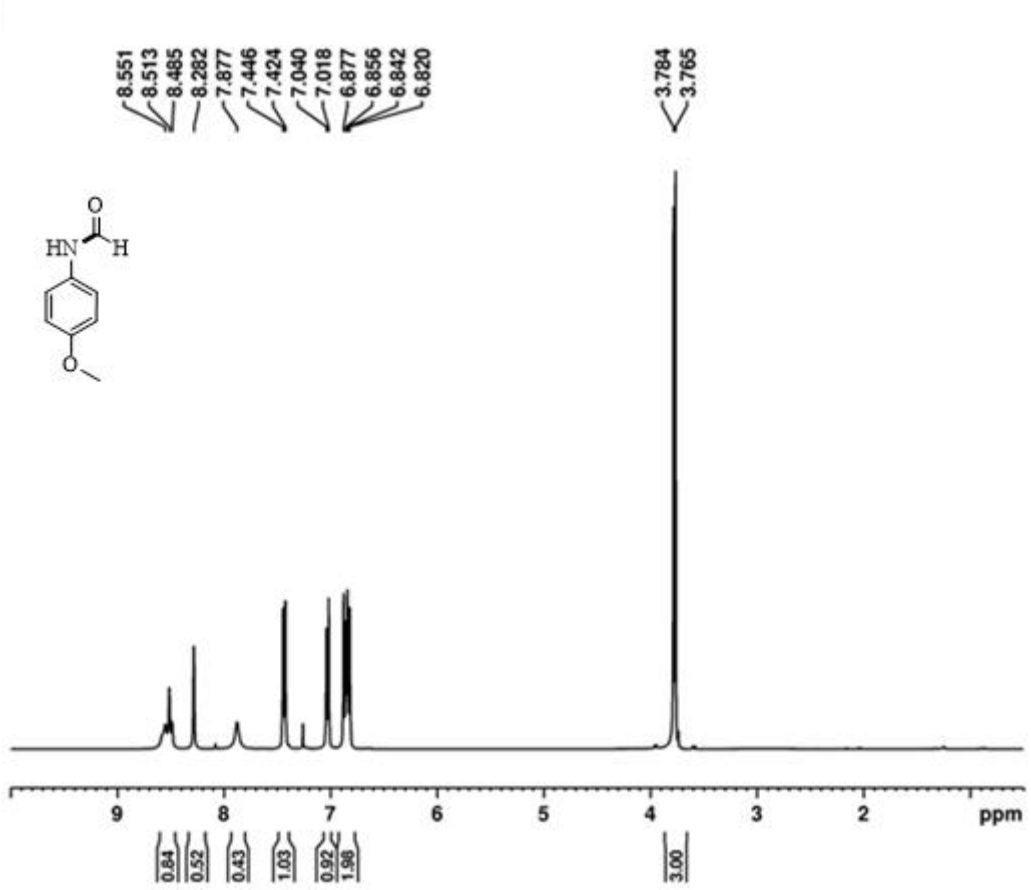

^{1}H NMR spectrum of **3f (Chapter 6)**

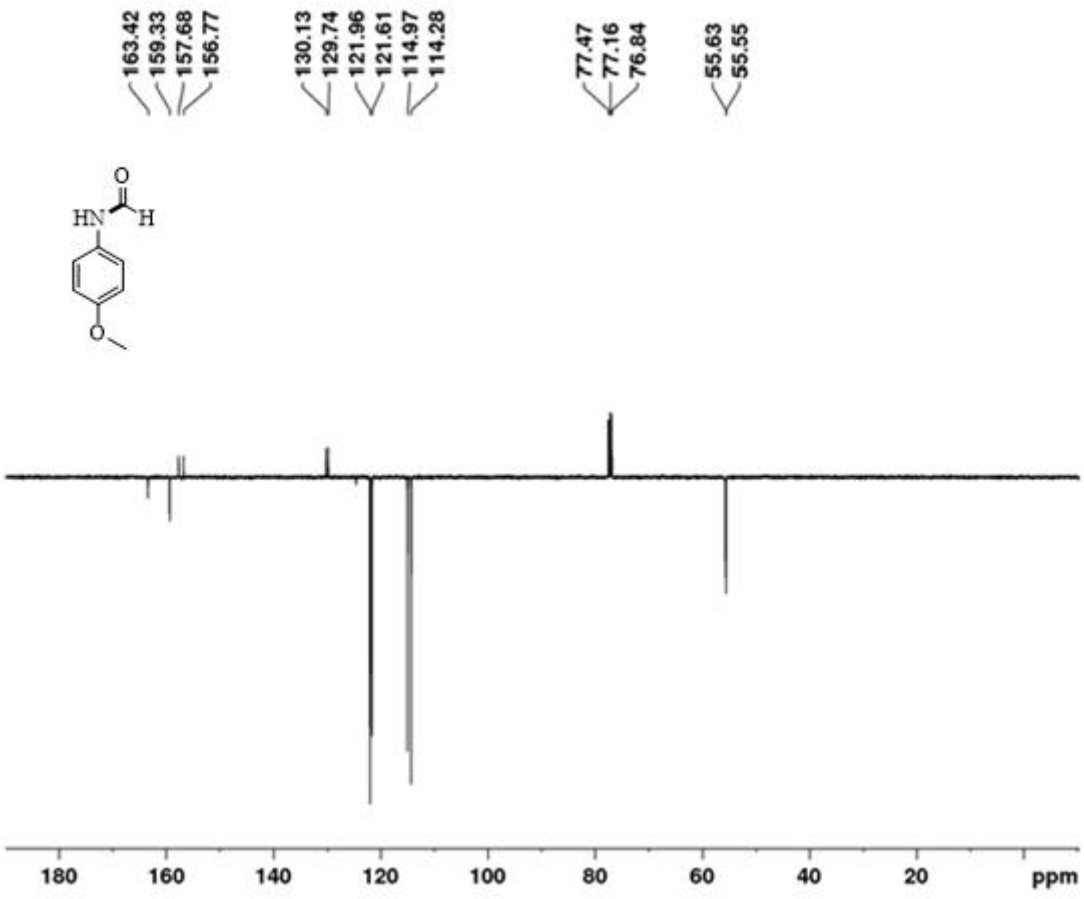

^{13}C spectrum of **3f (Chapter 6)**

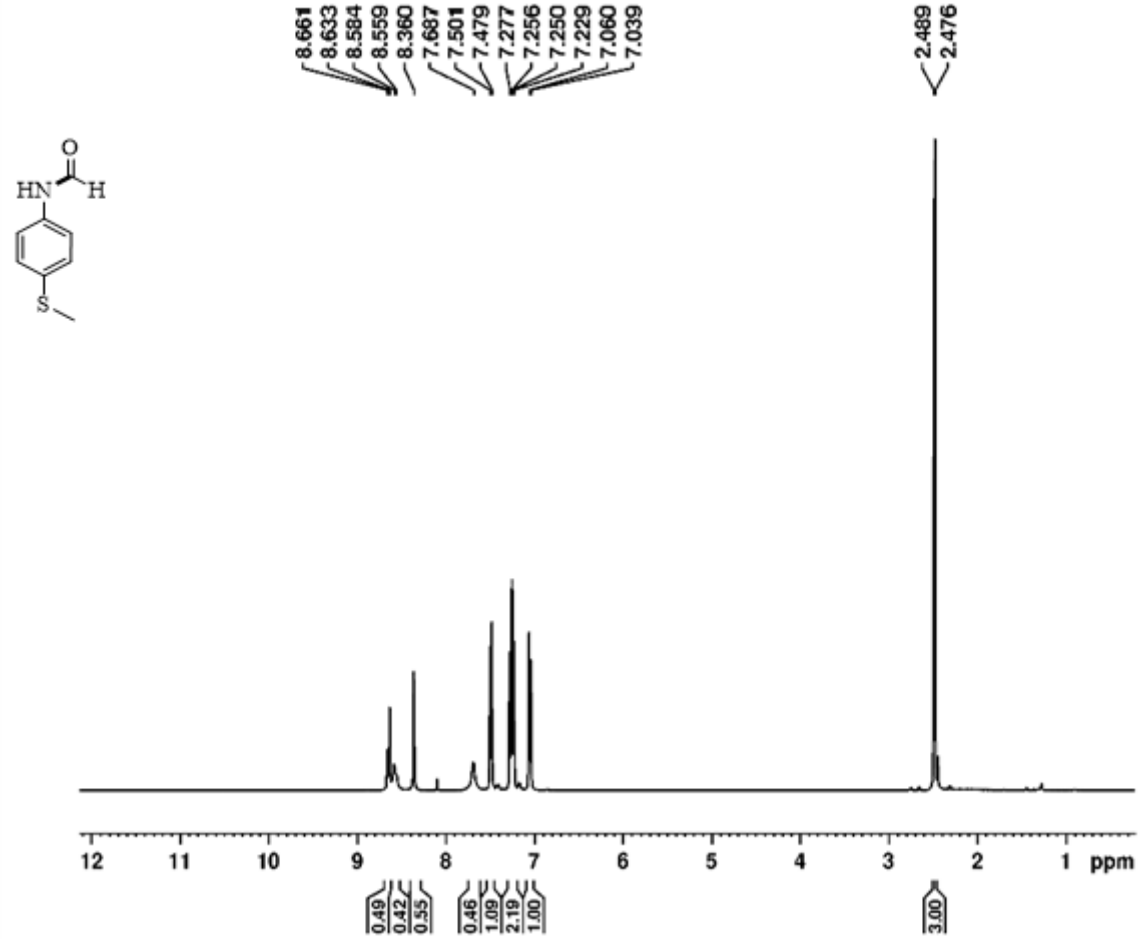

^{1}H NMR spectrum of **3g (Chapter 6)**

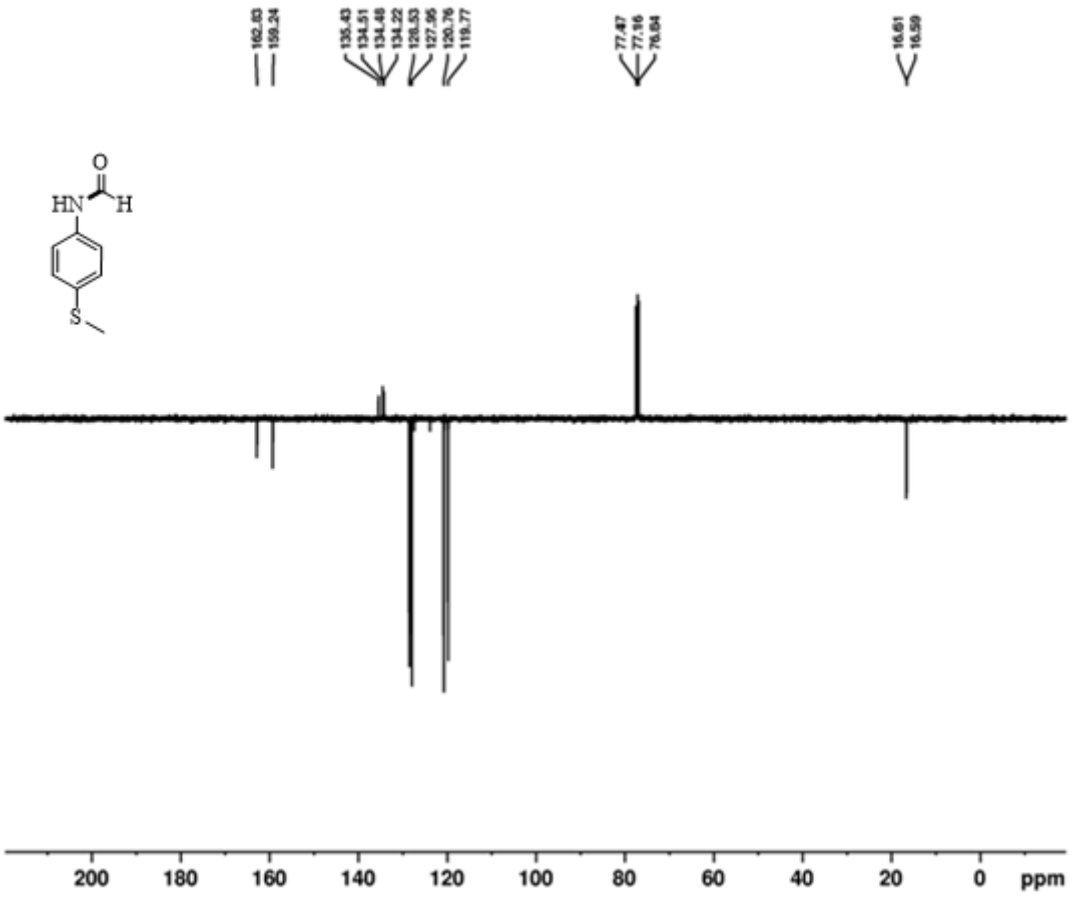

^{13}C spectrum of **3g (Chapter 6)**

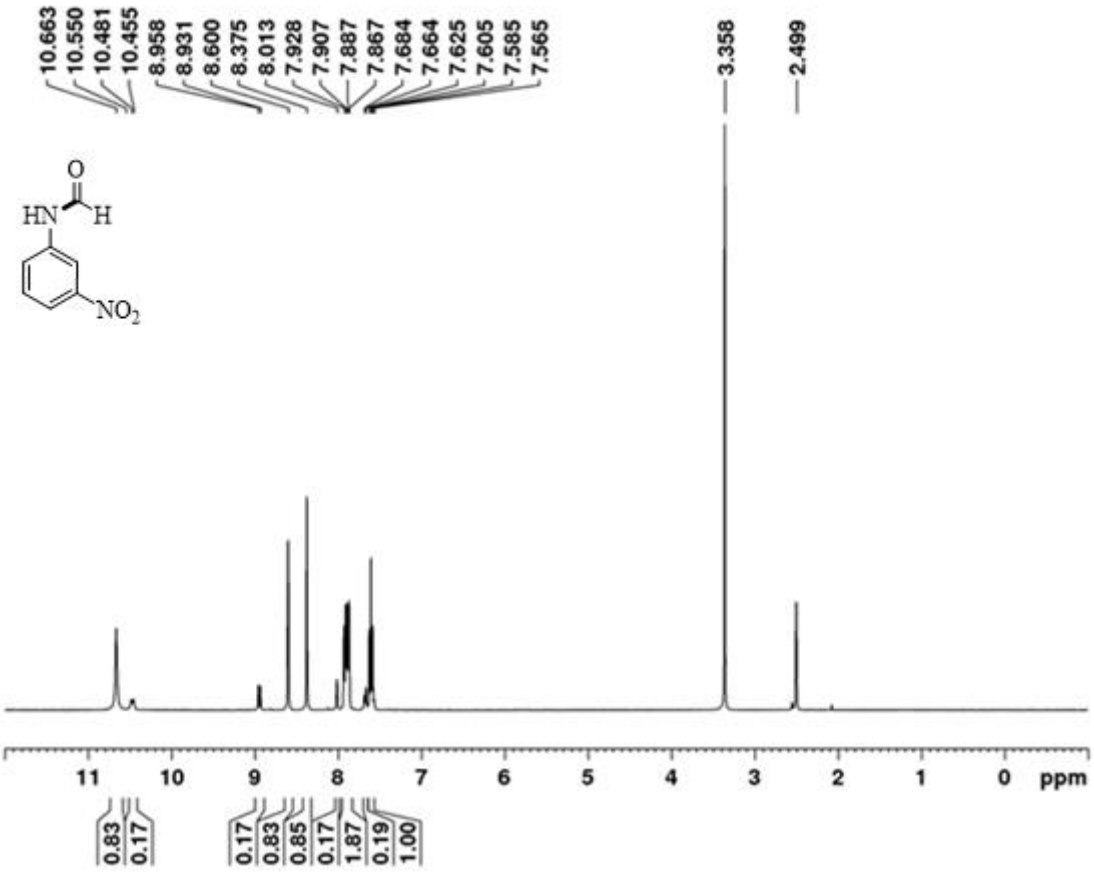

^{1}H NMR spectrum of **3i (Chapter 6)**

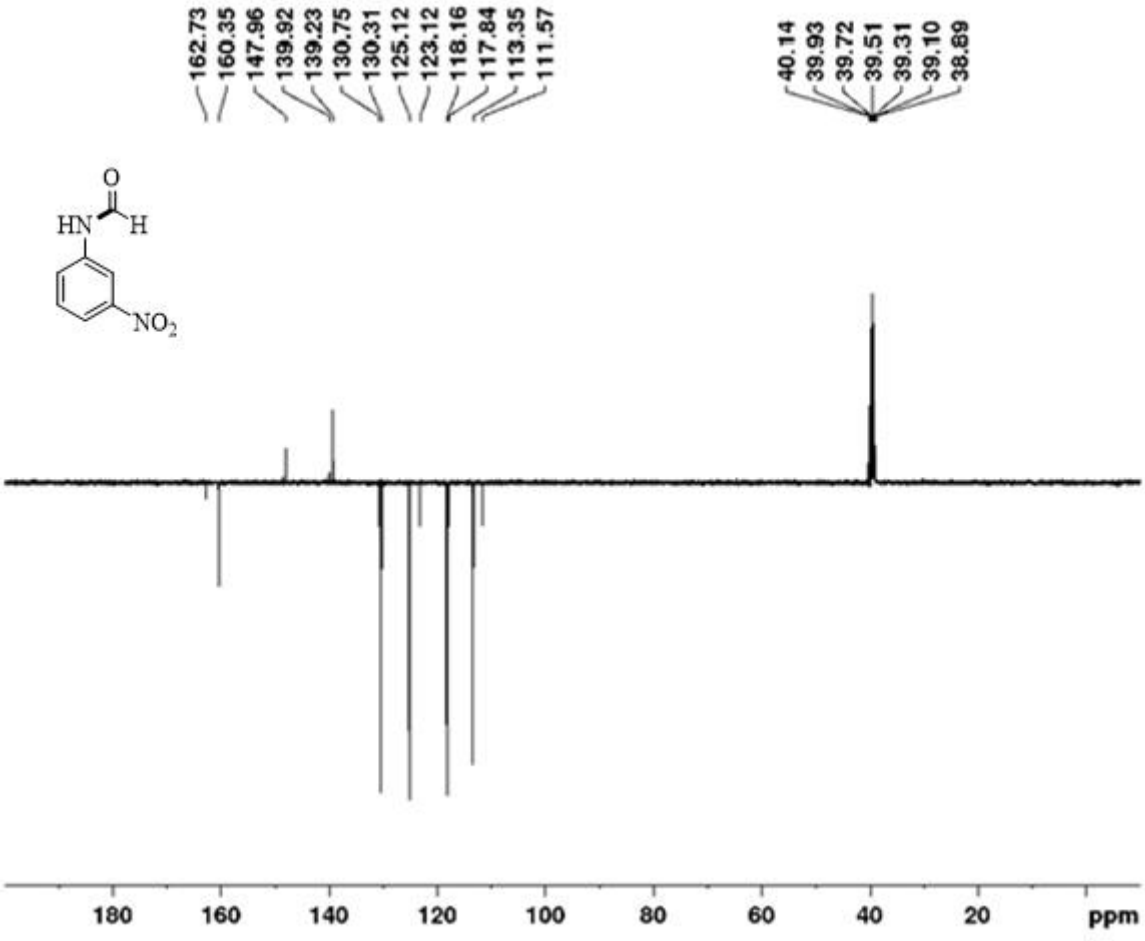

^{13}C spectrum of **3i (Chapter 6)**

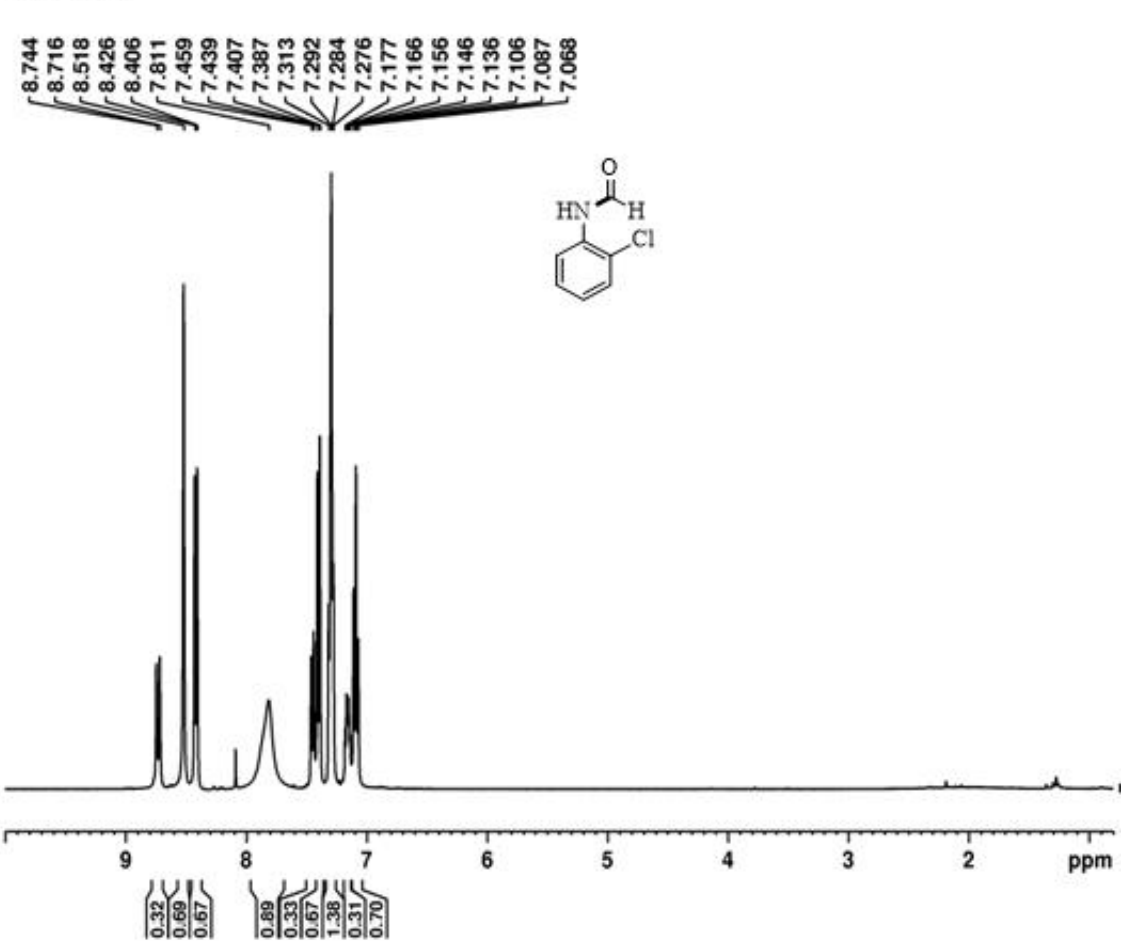

^{1}H NMR spectrum of **3k (Chapter 6)**

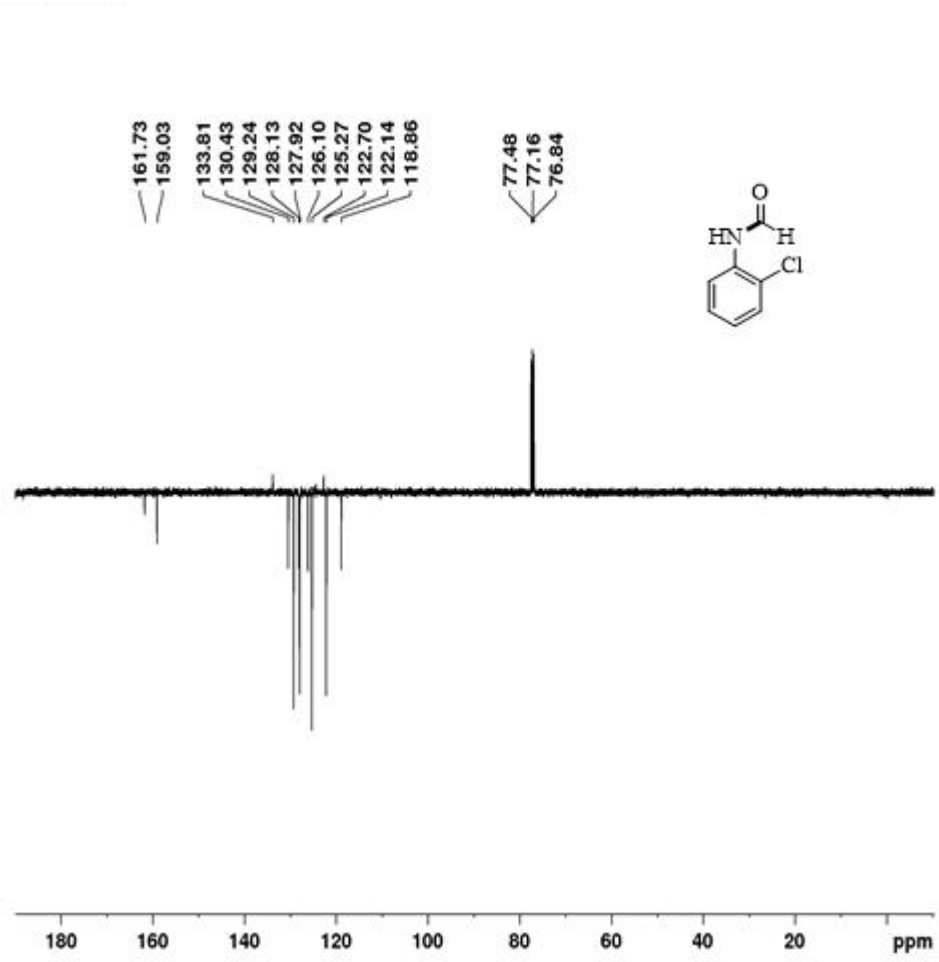

^{13}C spectrum of **3k (Chapter 6)**

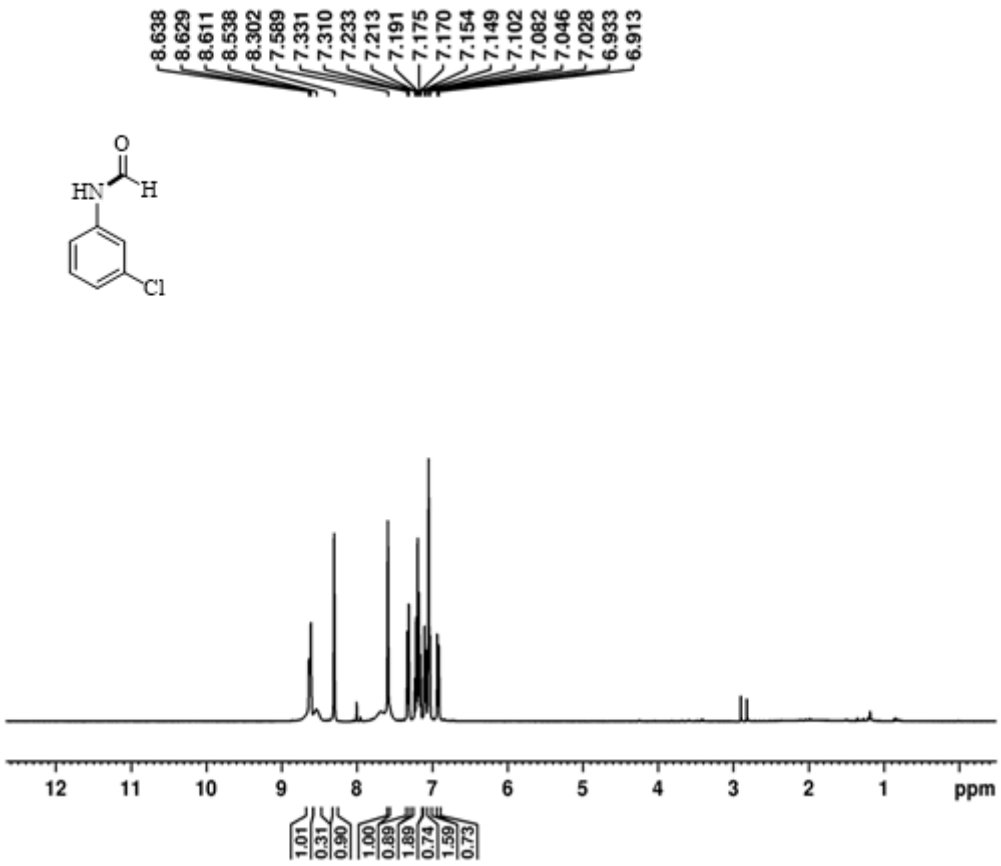

^{1}H NMR spectrum of **3l (Chapter 6)**

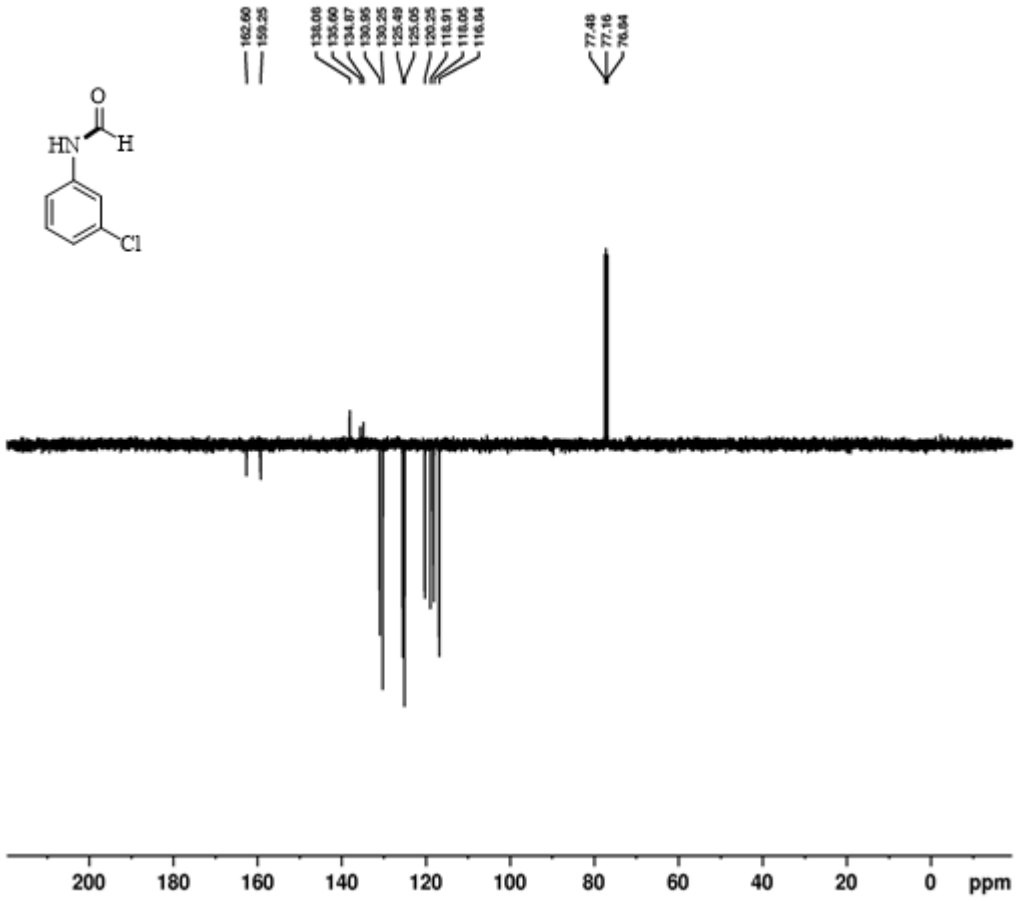

^{13}C spectrum of **3l (Chapter 6)**

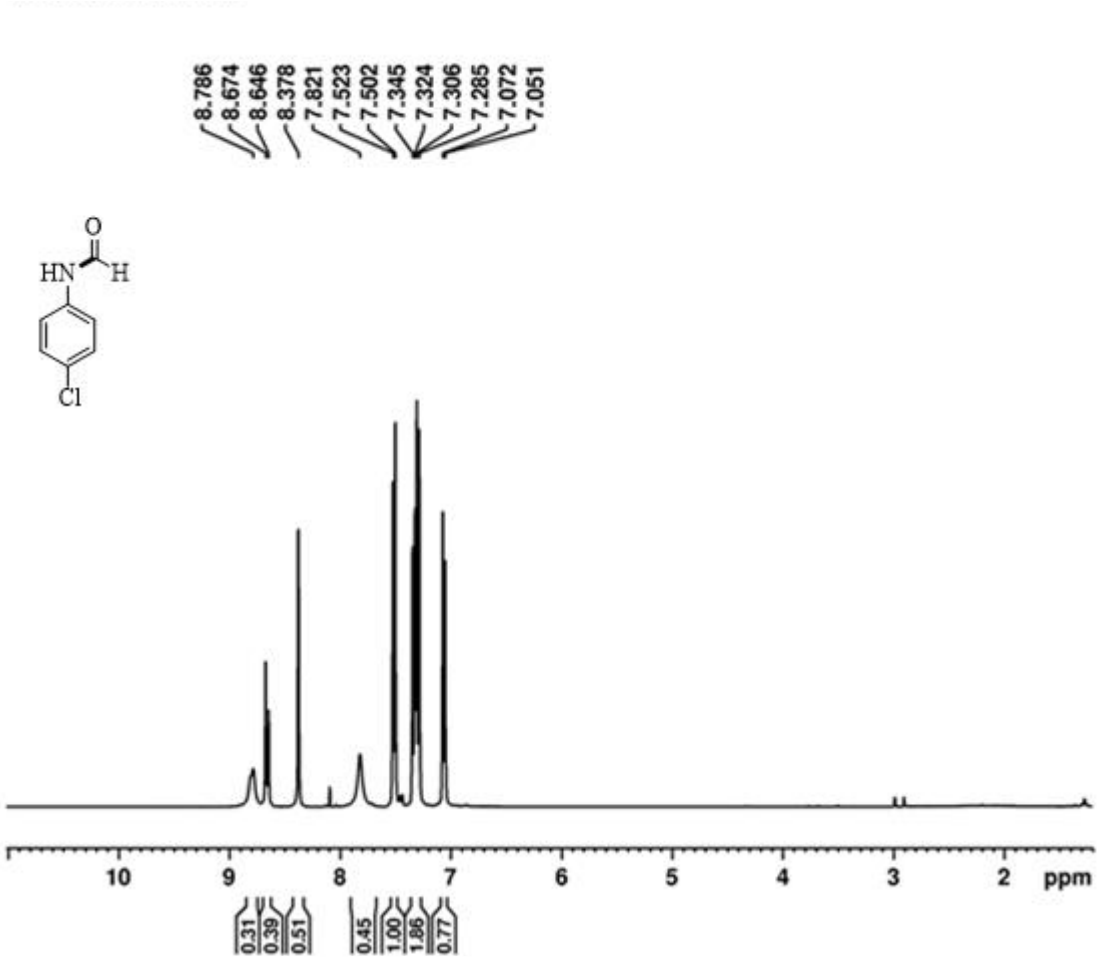

^{1}H NMR spectrum of **3m (Chapter 6)**

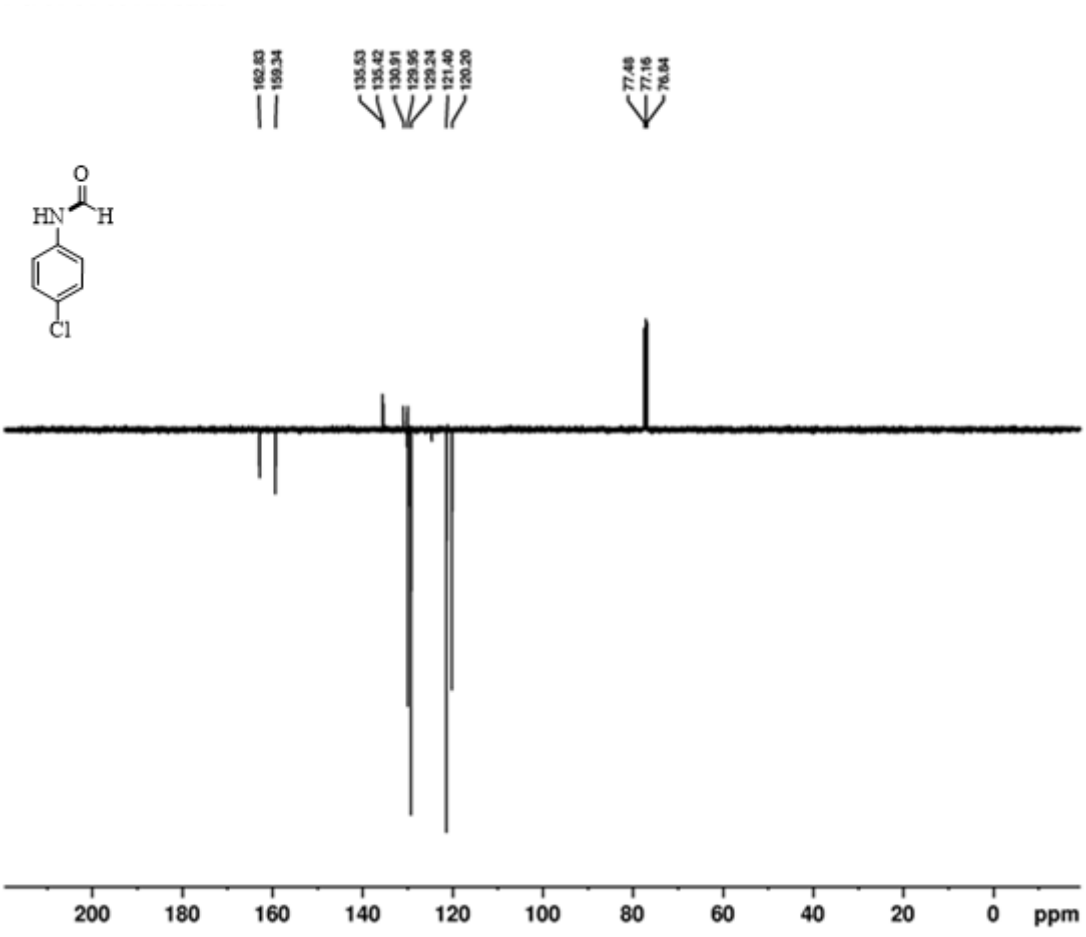

^{13}C spectrum of **3m (Chapter 6)**

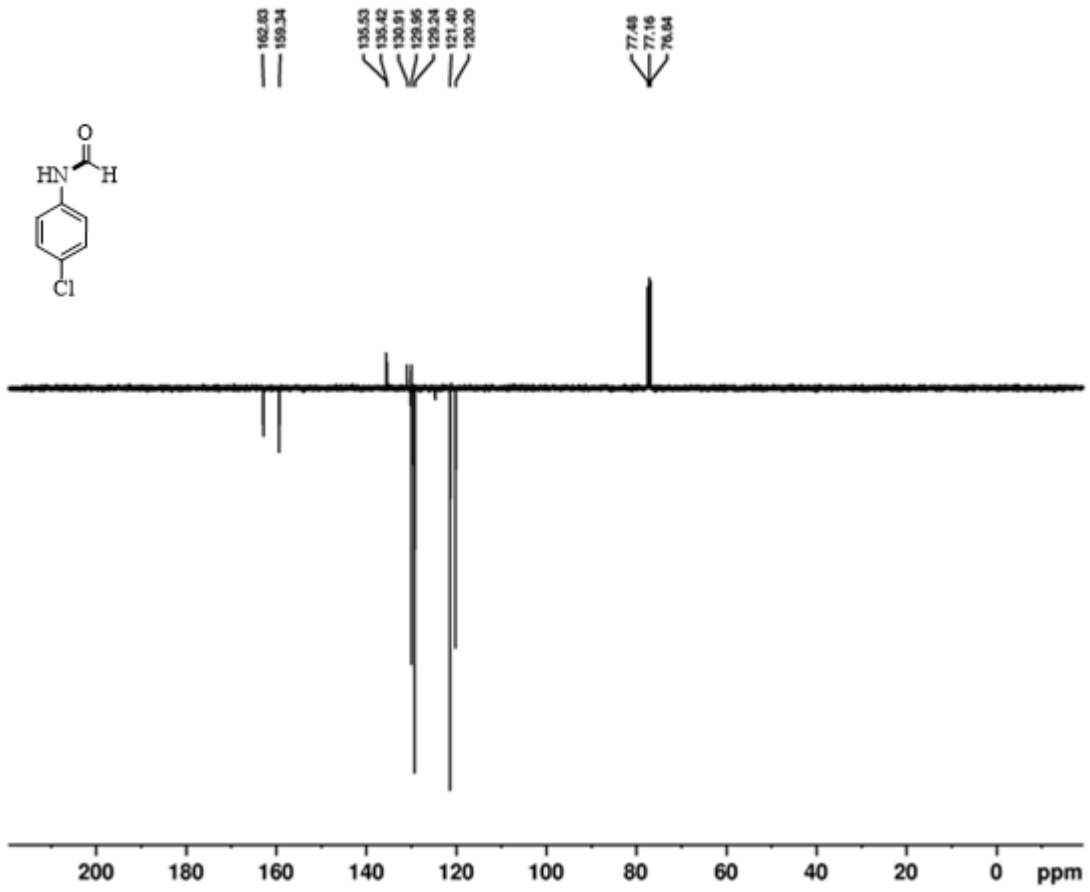

^{13}C spectrum of **3m (Chapter 6)**

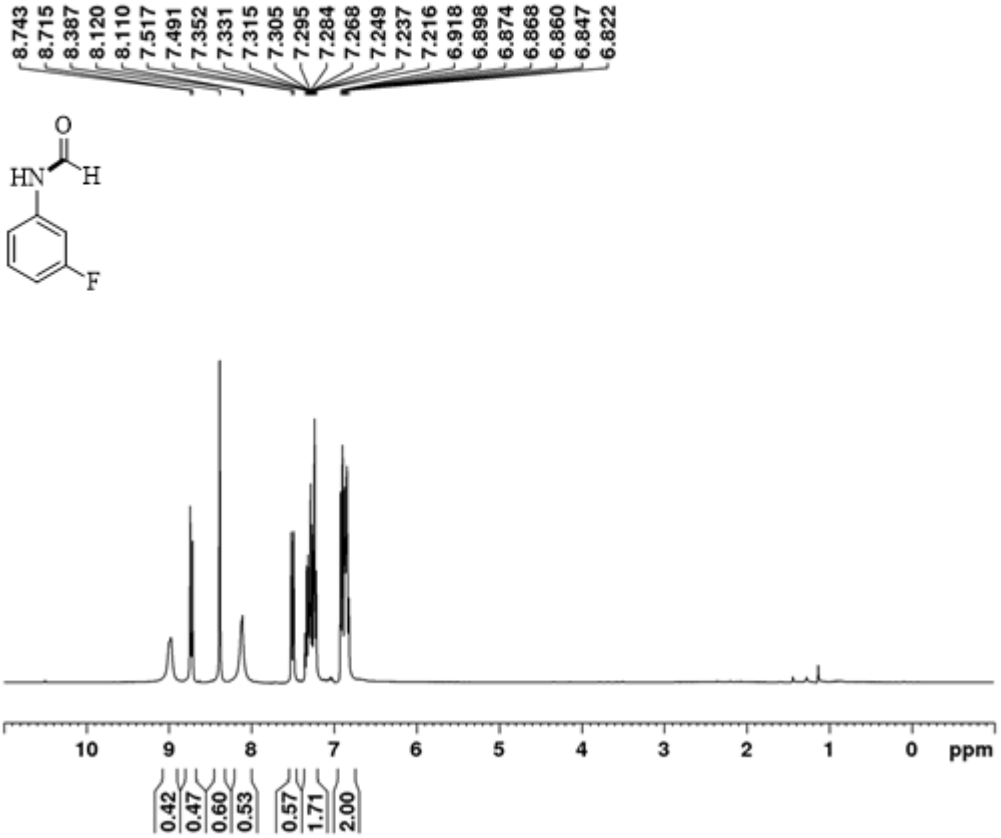

^{1}H NMR spectrum of **3n (Chapter 6)**

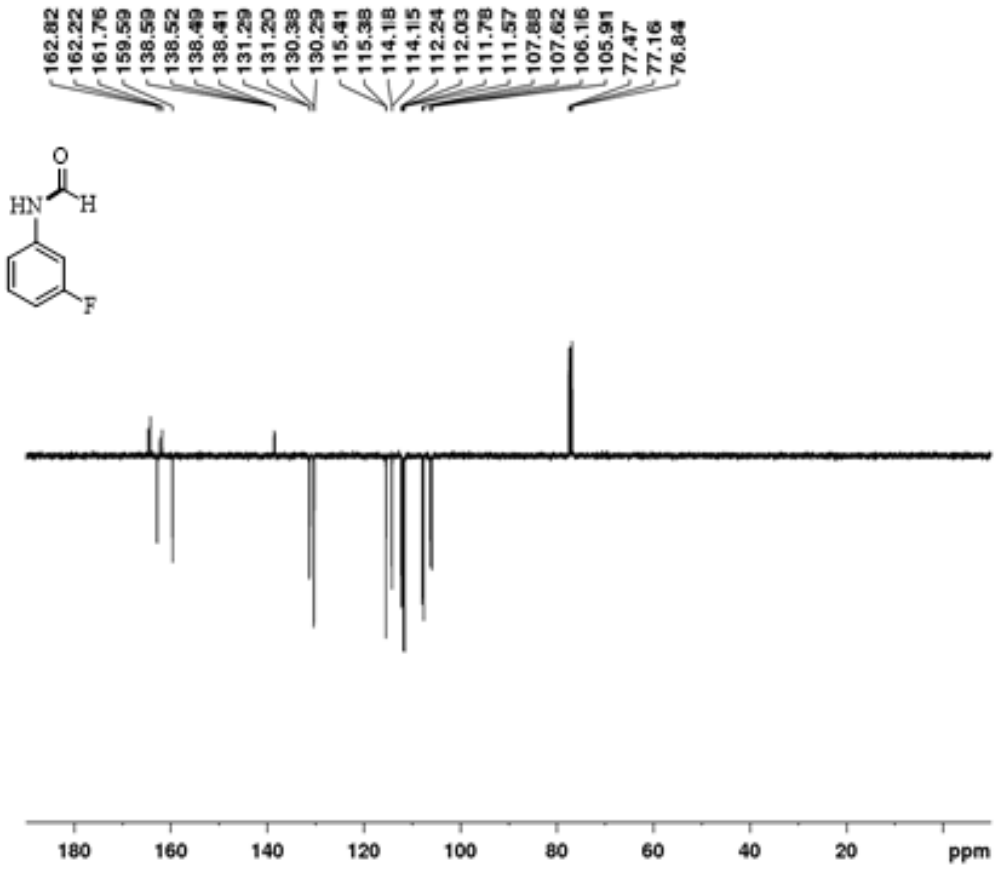

^{13}C spectrum of **3n (Chapter 6)**

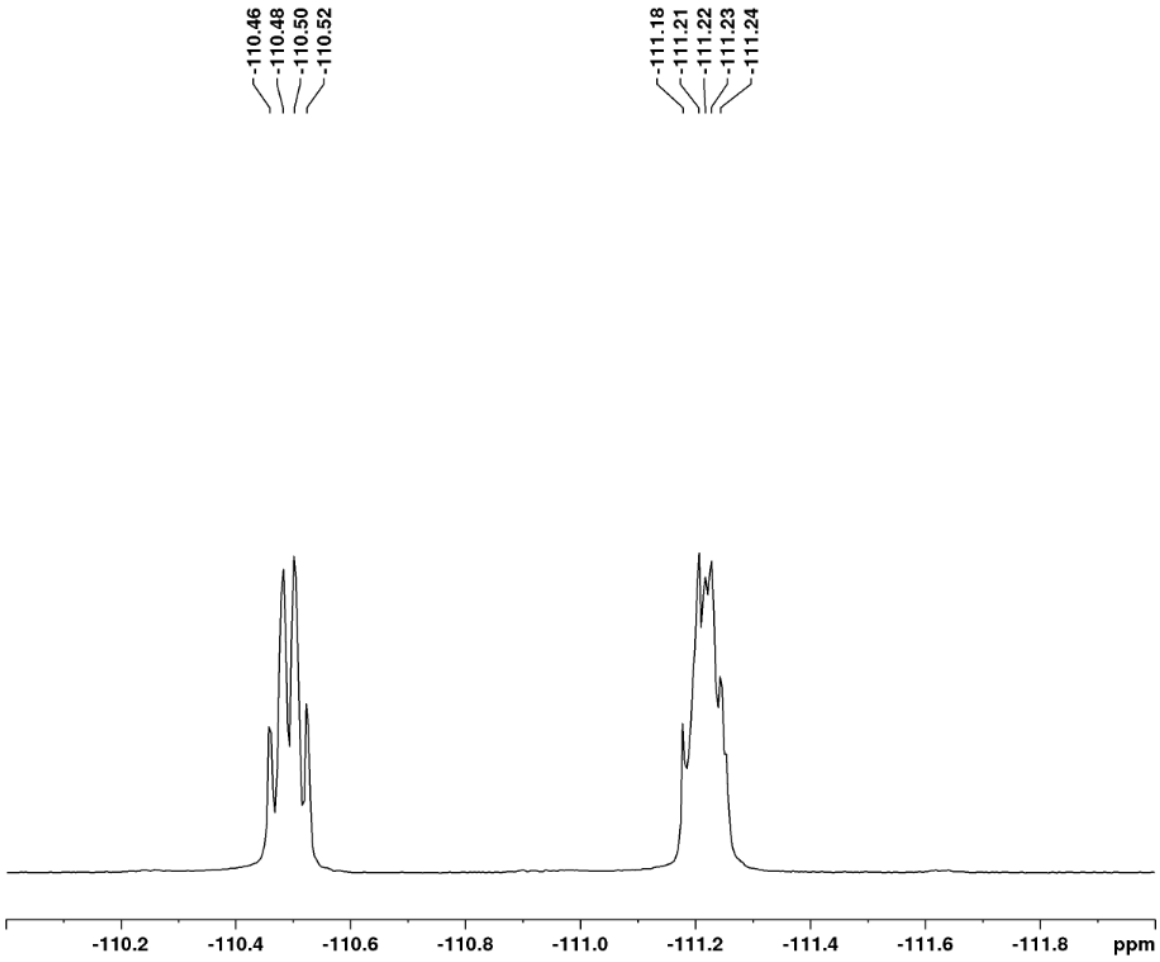

^{19}F spectrum of **3n (Chapter 6)**

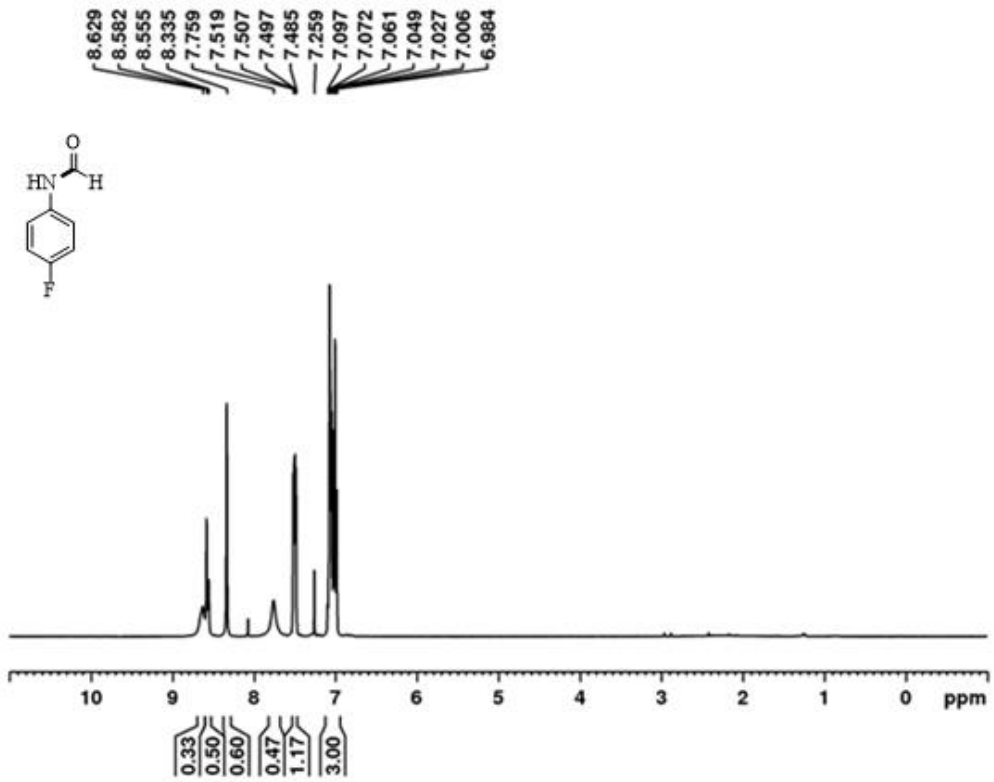

^{1}H NMR spectrum of **3o (Chapter 6)**

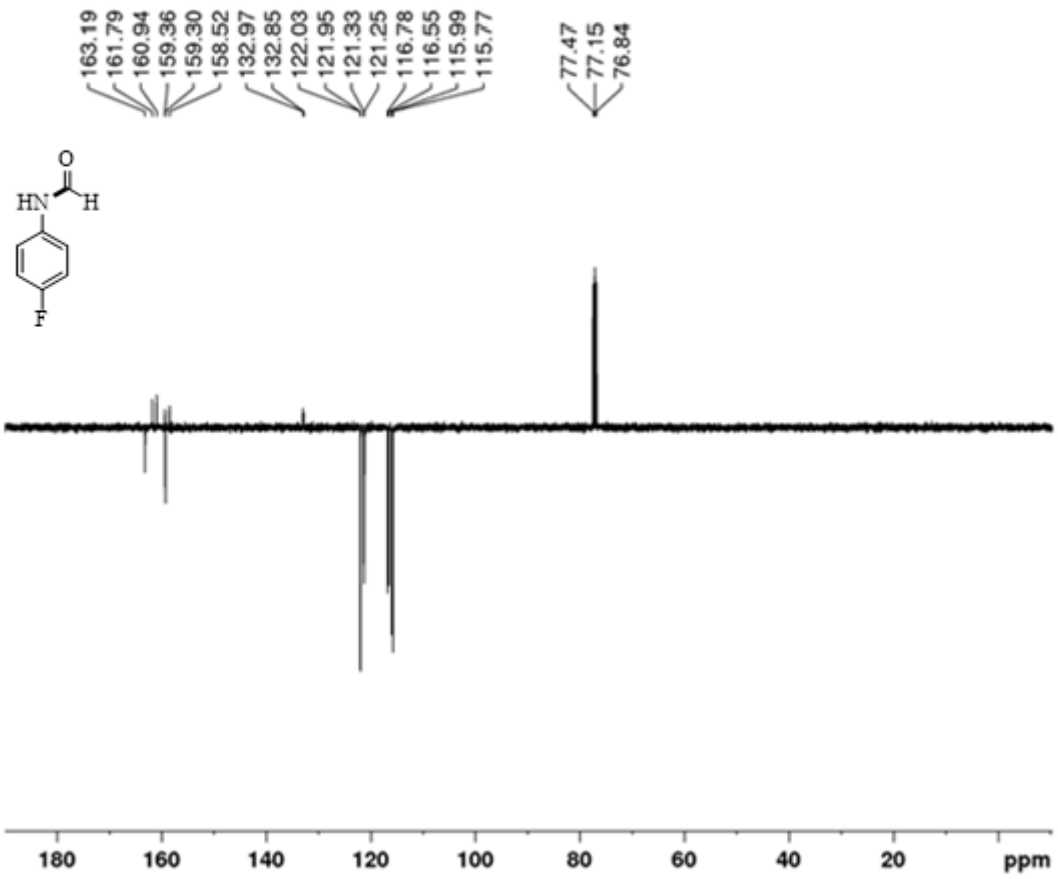

^{13}C spectrum of **3o (Chapter 6)**

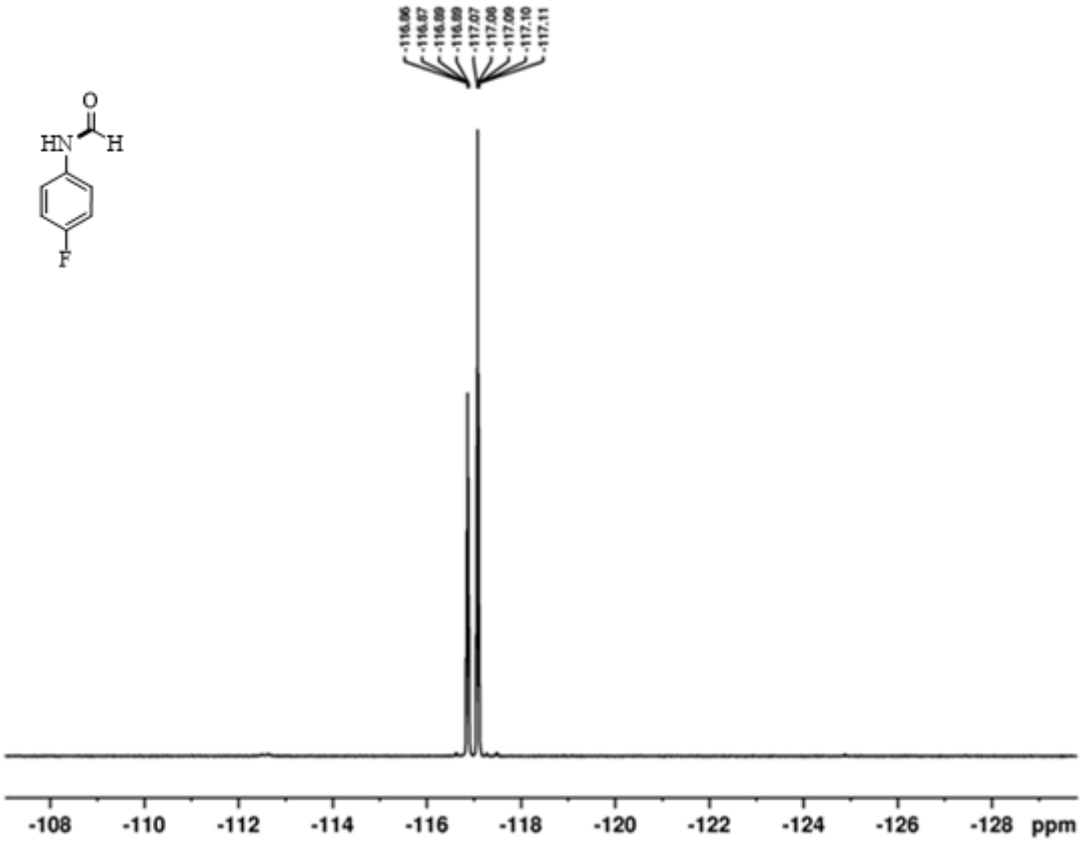

^{19}F spectrum of **3o (Chapter 6)**

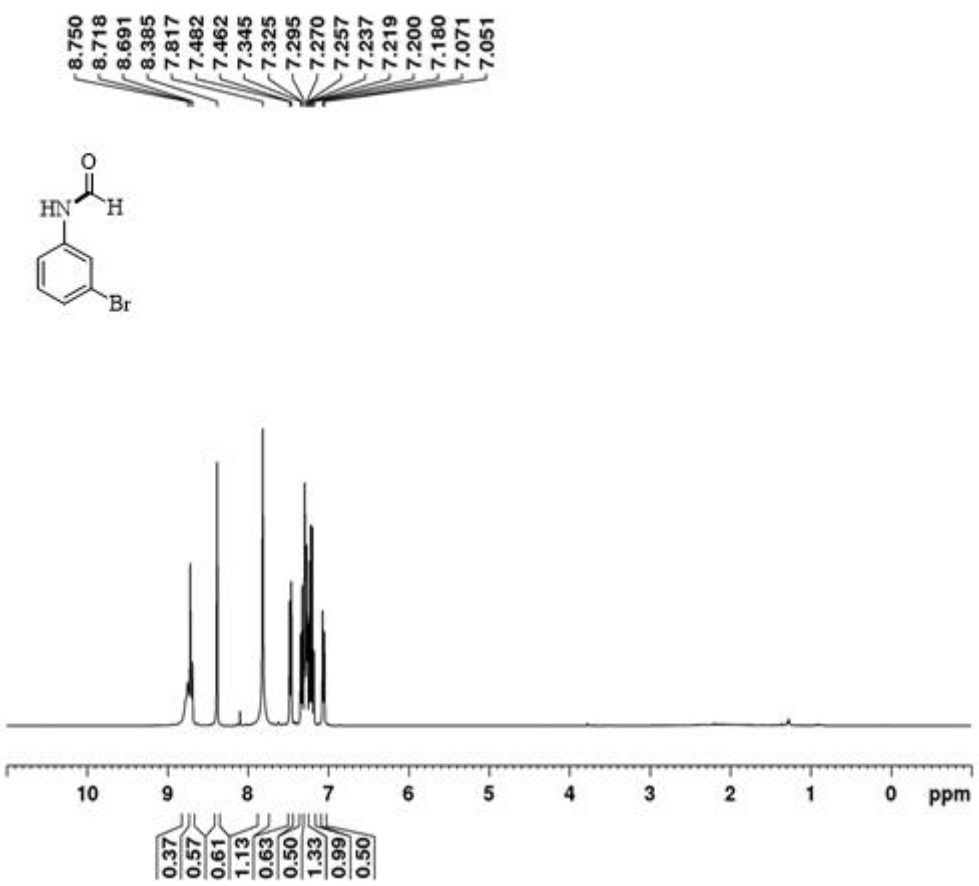

^{1}H NMR spectrum of **3p (Chapter 6)**

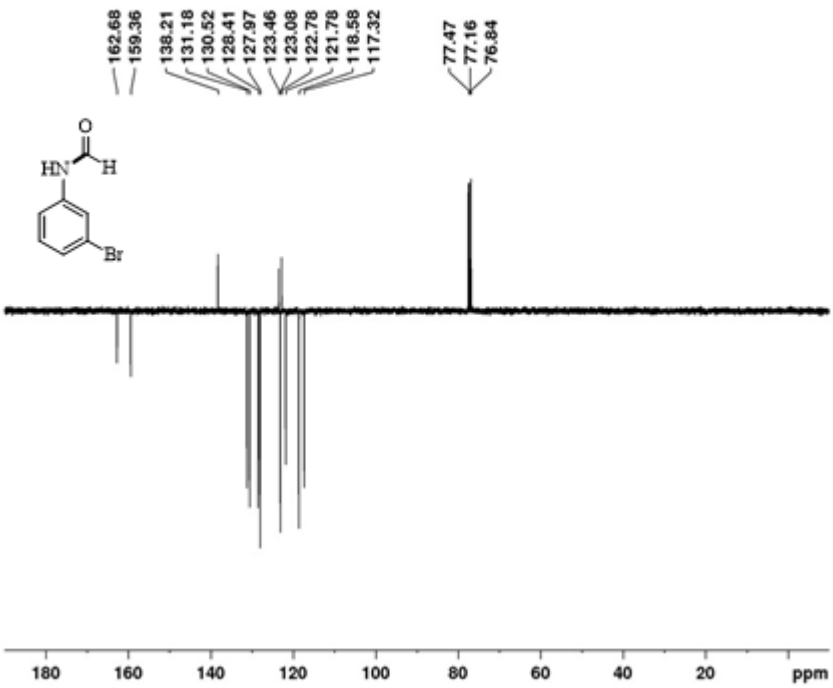

^{13}C spectrum of **3p (Chapter 6)**

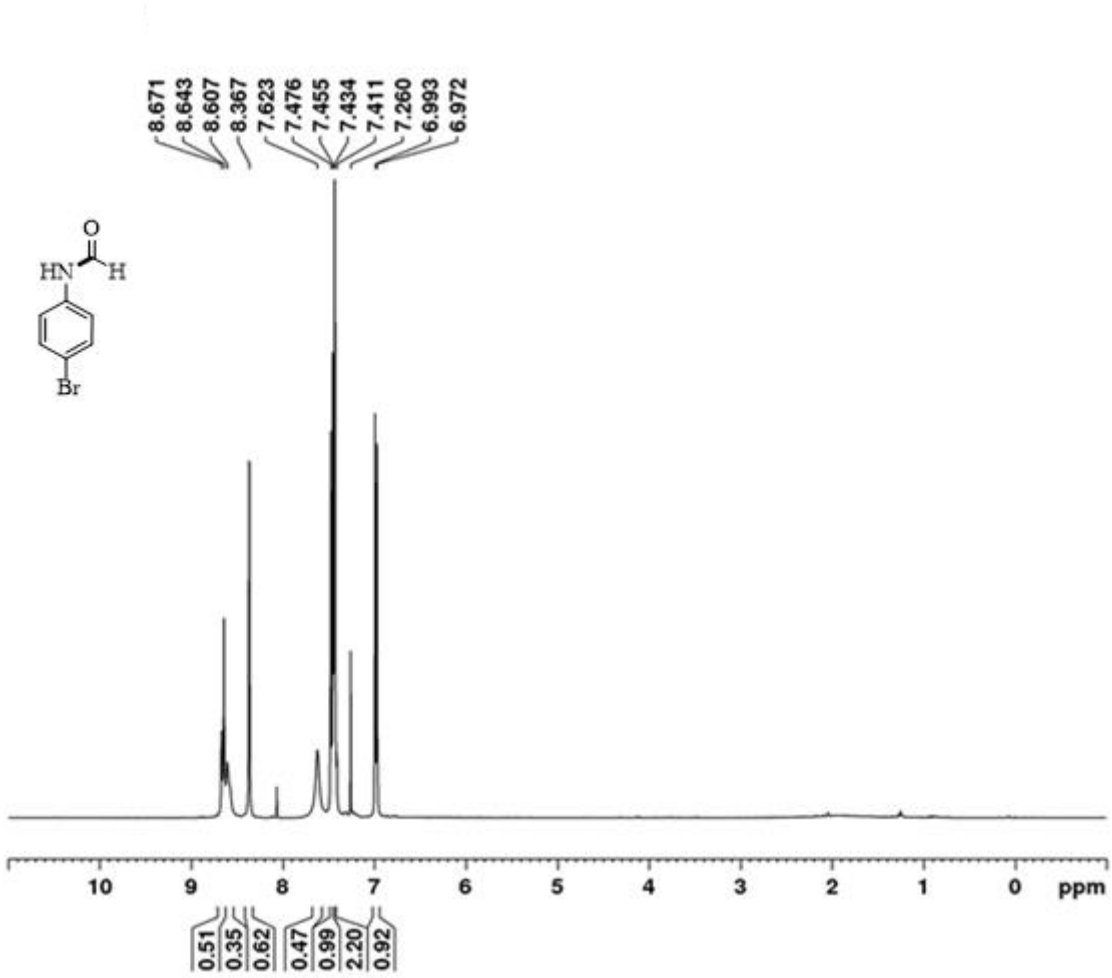

^{1}H NMR spectrum of **3q (Chapter 6)**

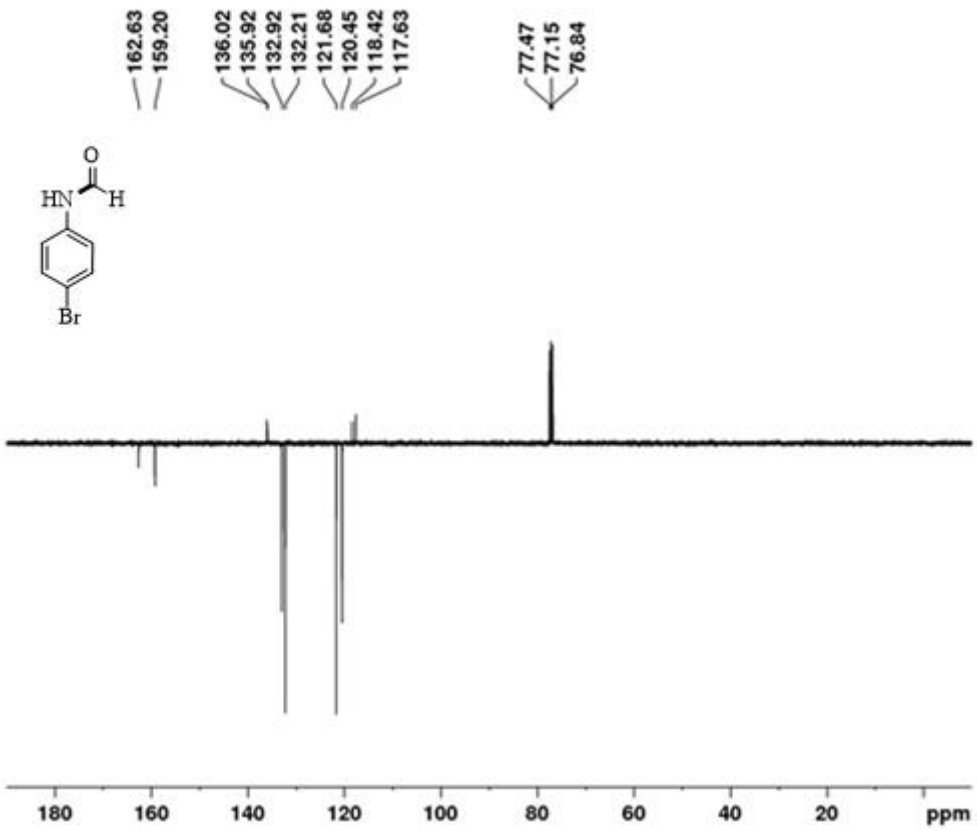

^{13}C spectrum of **3q (Chapter 6)**

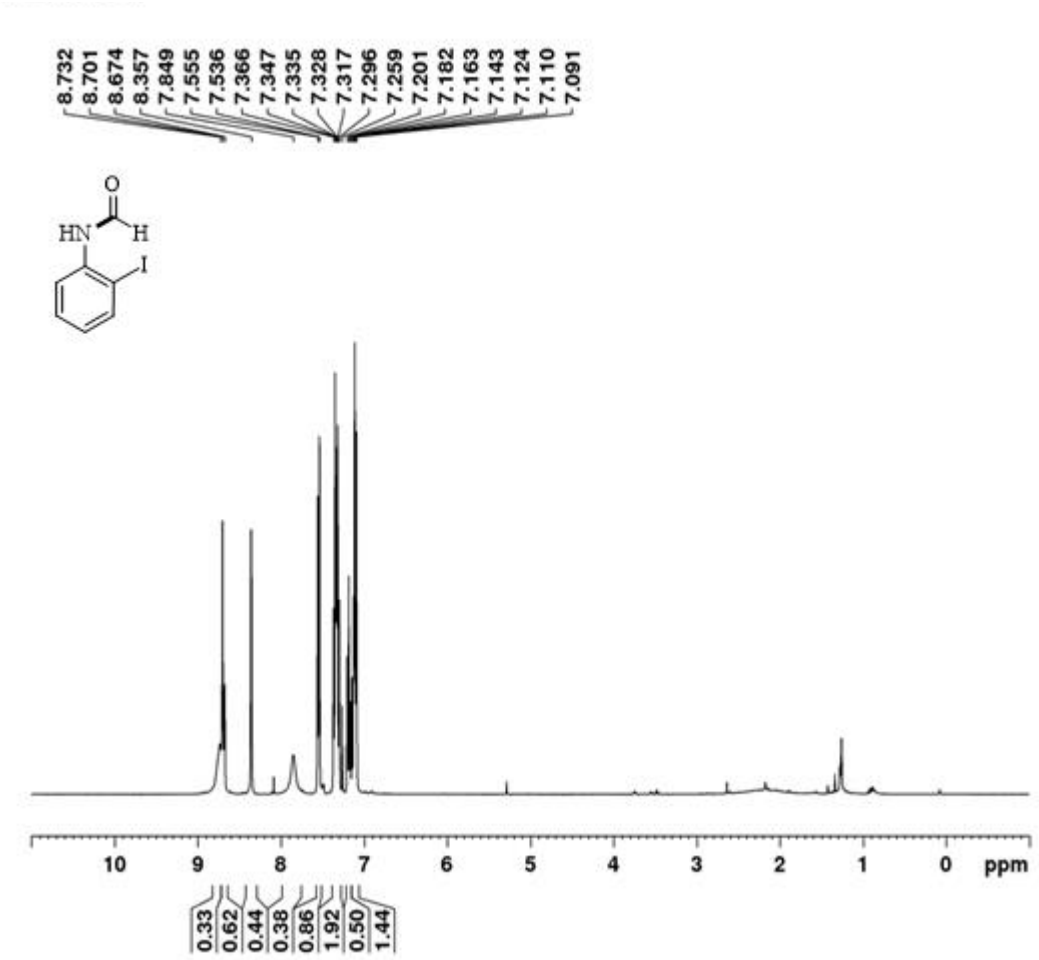

^{1}H NMR spectrum of **3r (Chapter 6)**

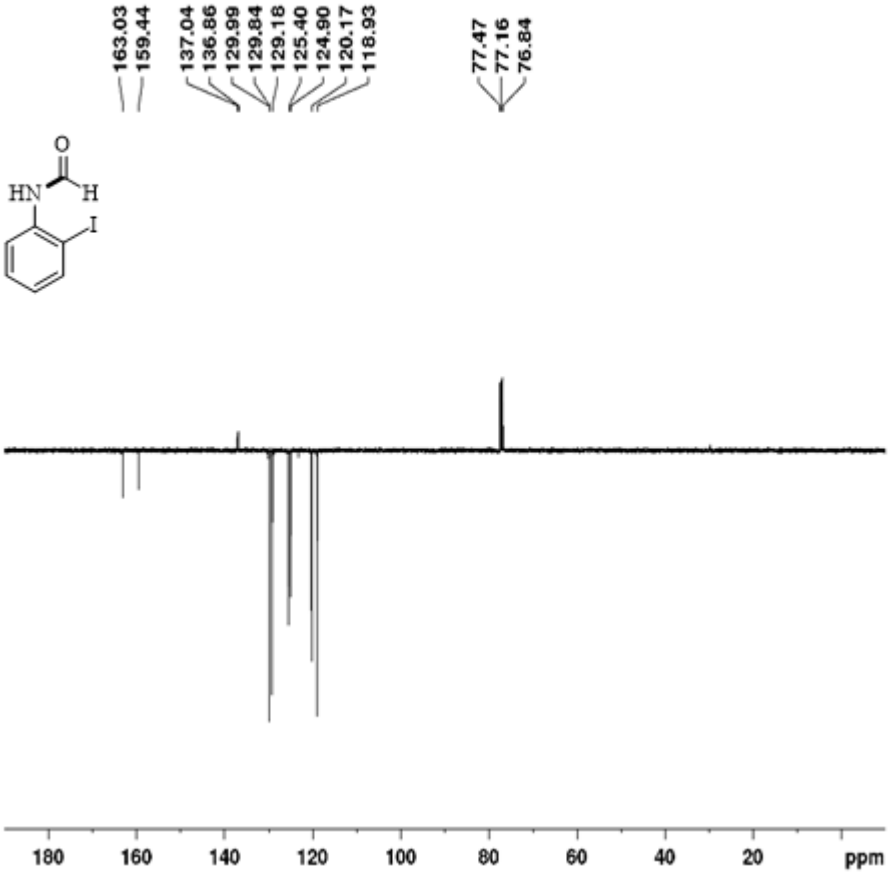

^{13}C spectrum of **3r (Chapter 6)**

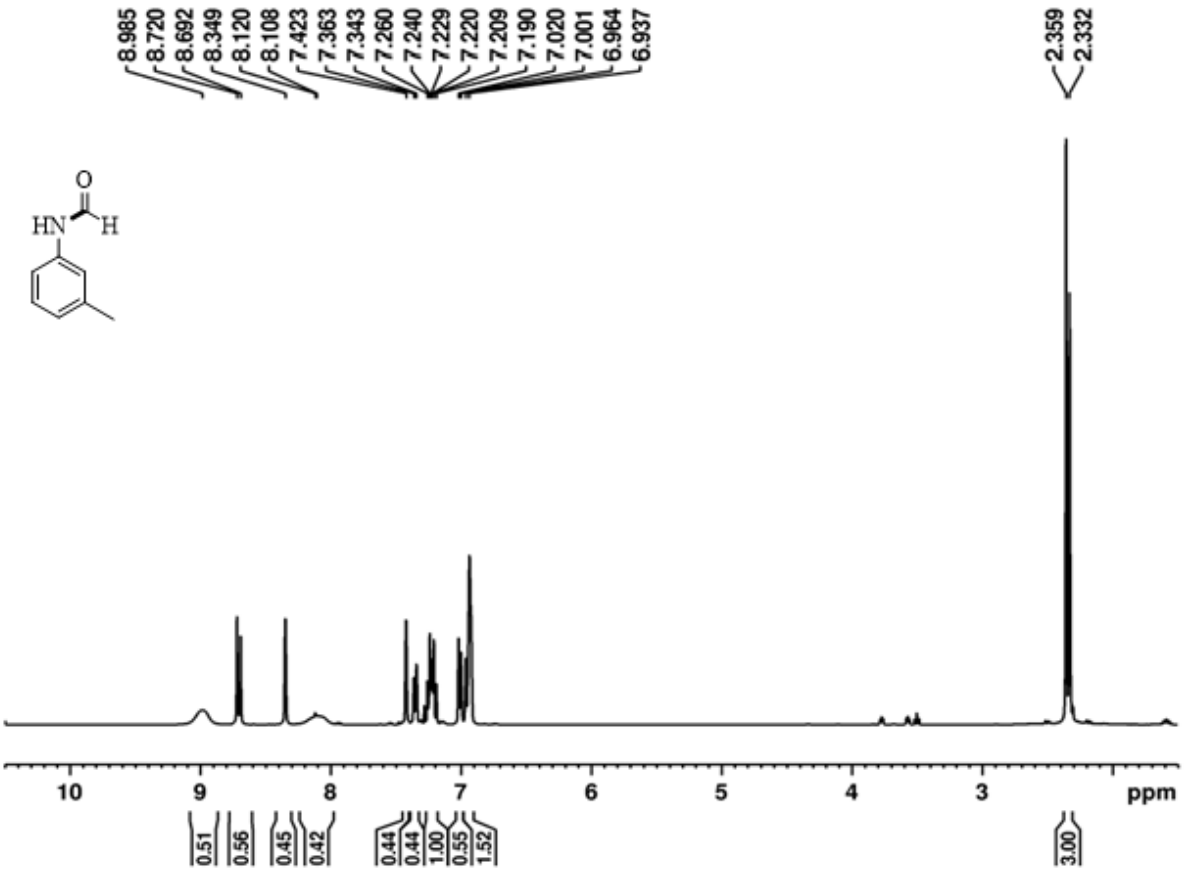

^{1}H NMR spectrum of **3s (Chapter 6)**

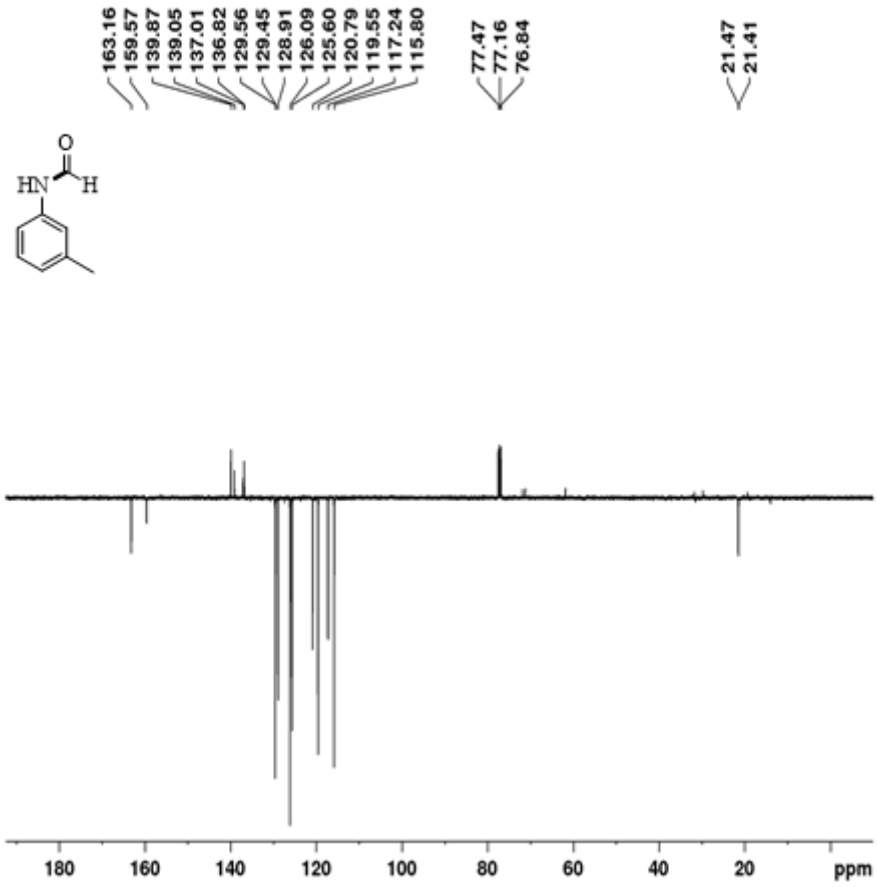

^{13}C spectrum of **3s (Chapter 6)**

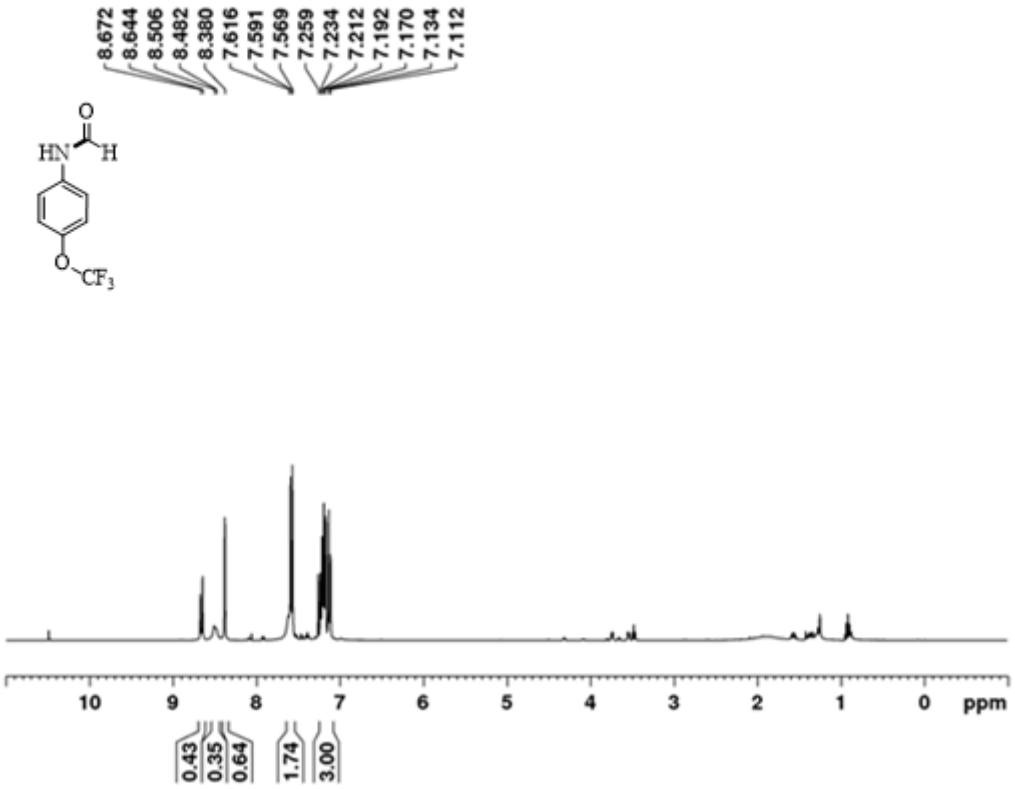

^{1}H NMR spectrum of **3t (Chapter 6)**

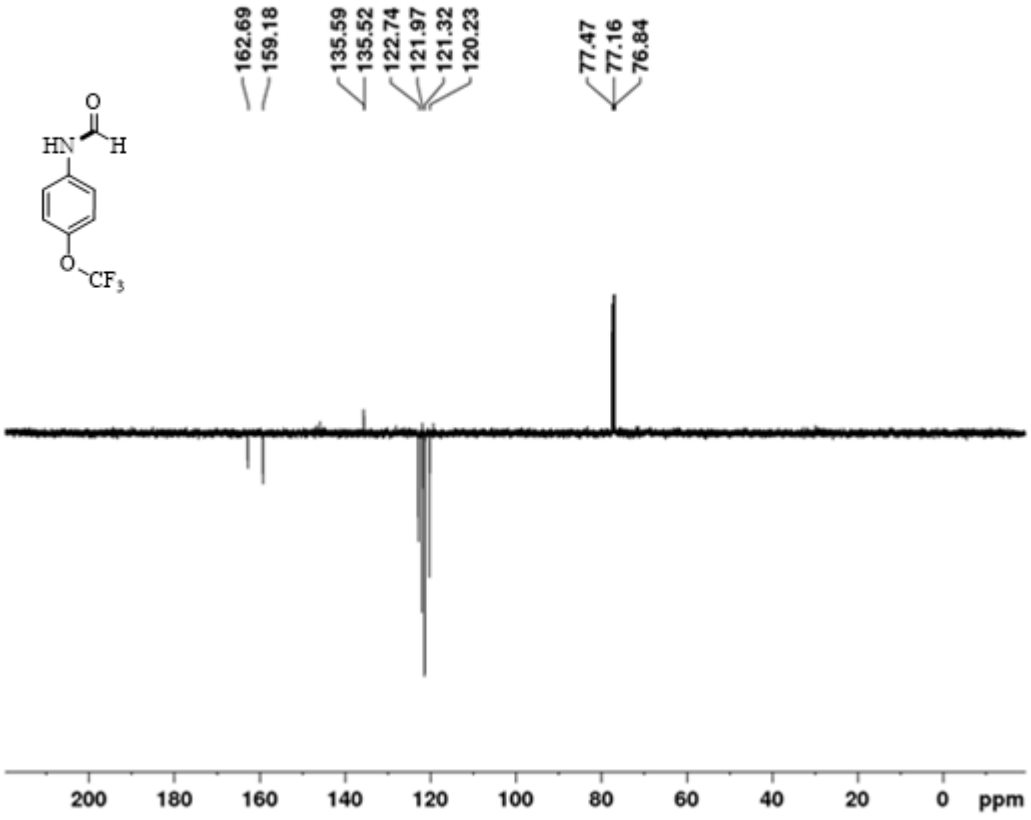

^{13}C spectrum of **3t (Chapter 6)**

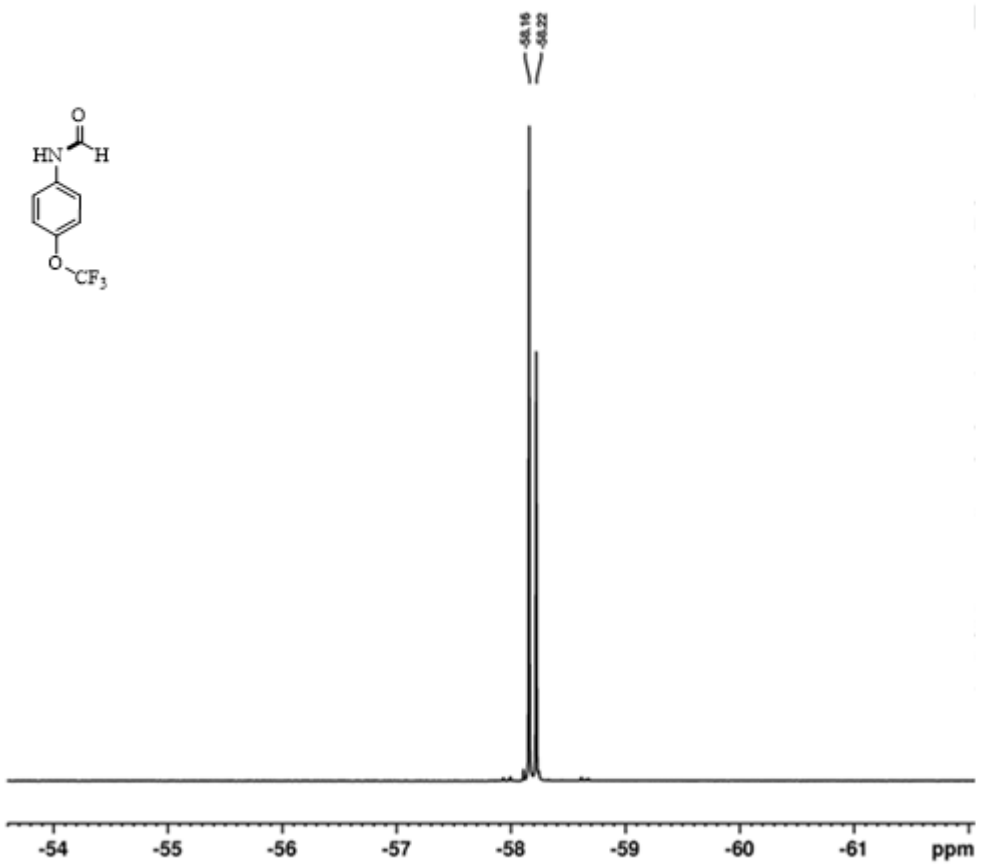

^{19}F spectrum of **3t (Chapter 6)**

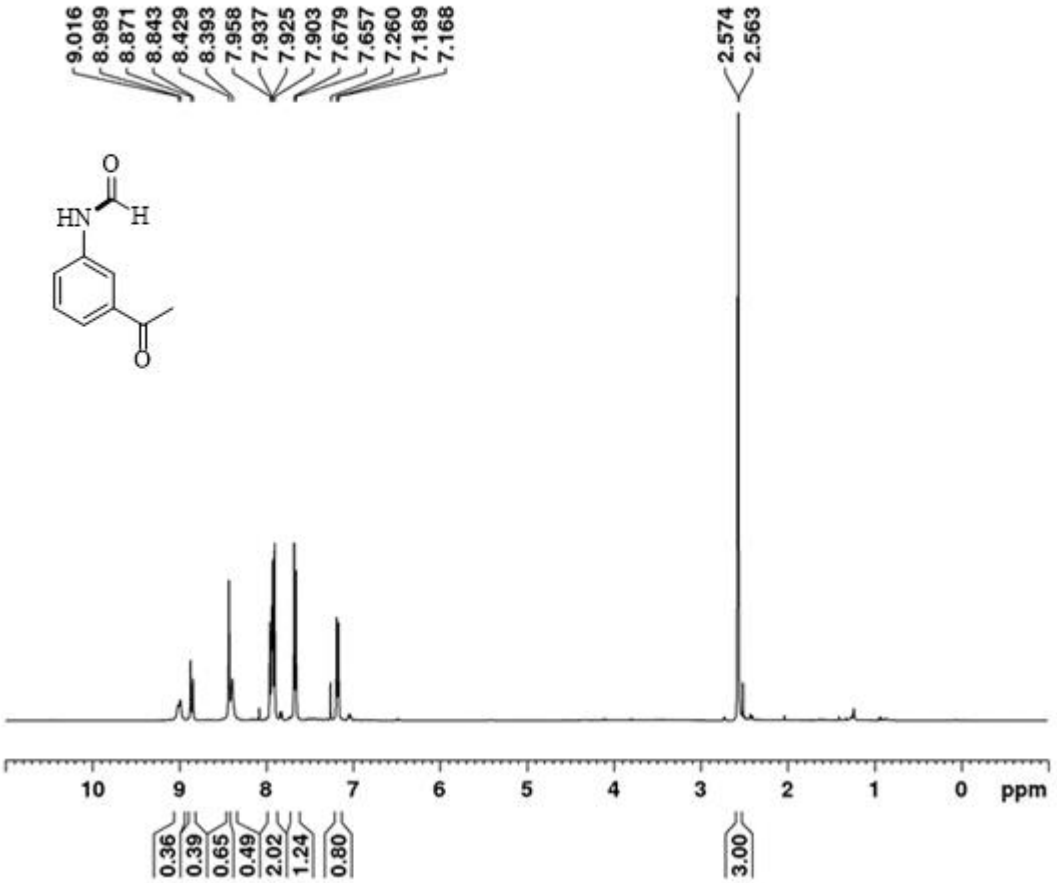

^{1}H NMR spectrum of **3u (Chapter 6)**

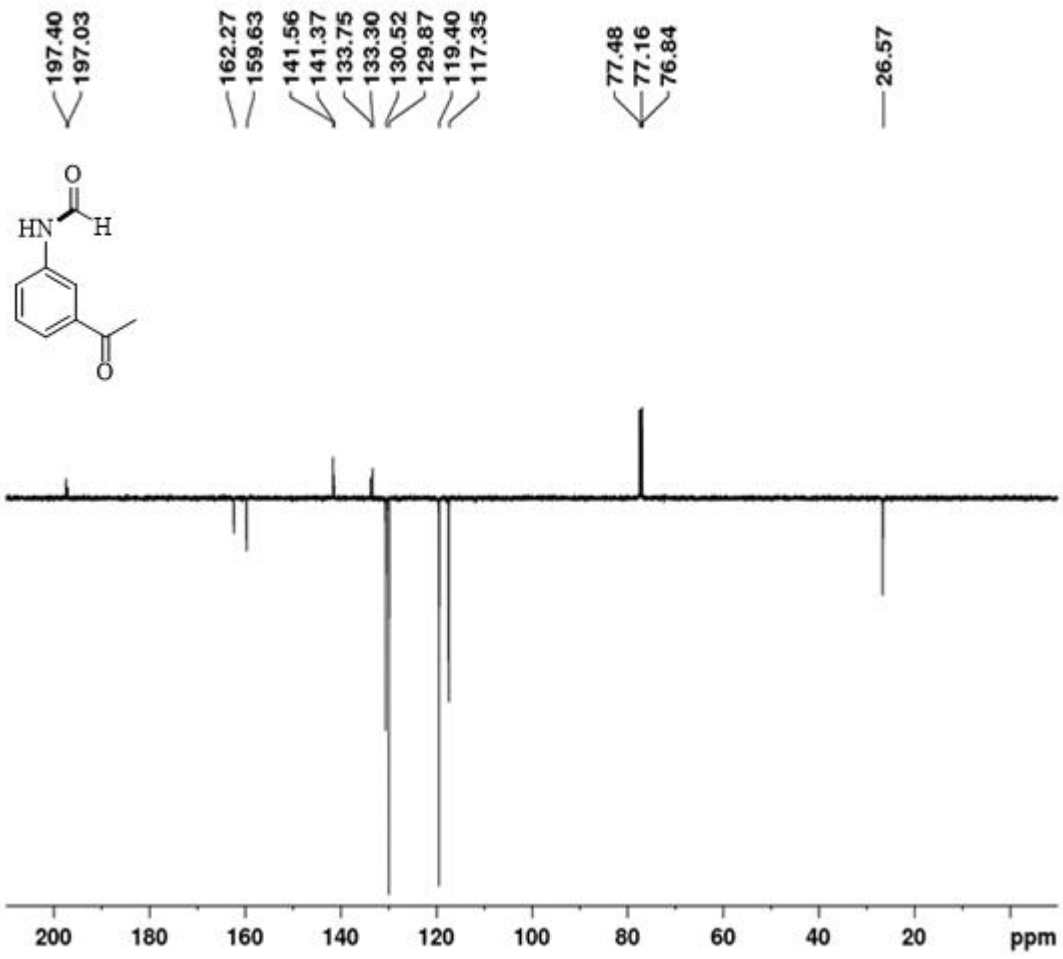

^{13}C spectrum of **3u (Chapter 6)**

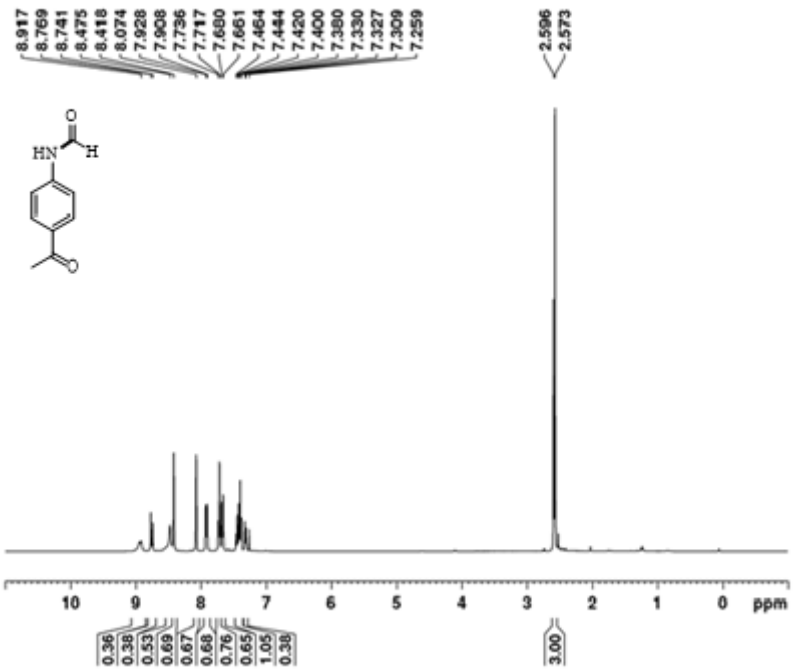

^{1}H NMR spectrum of **3v (Chapter 6)**

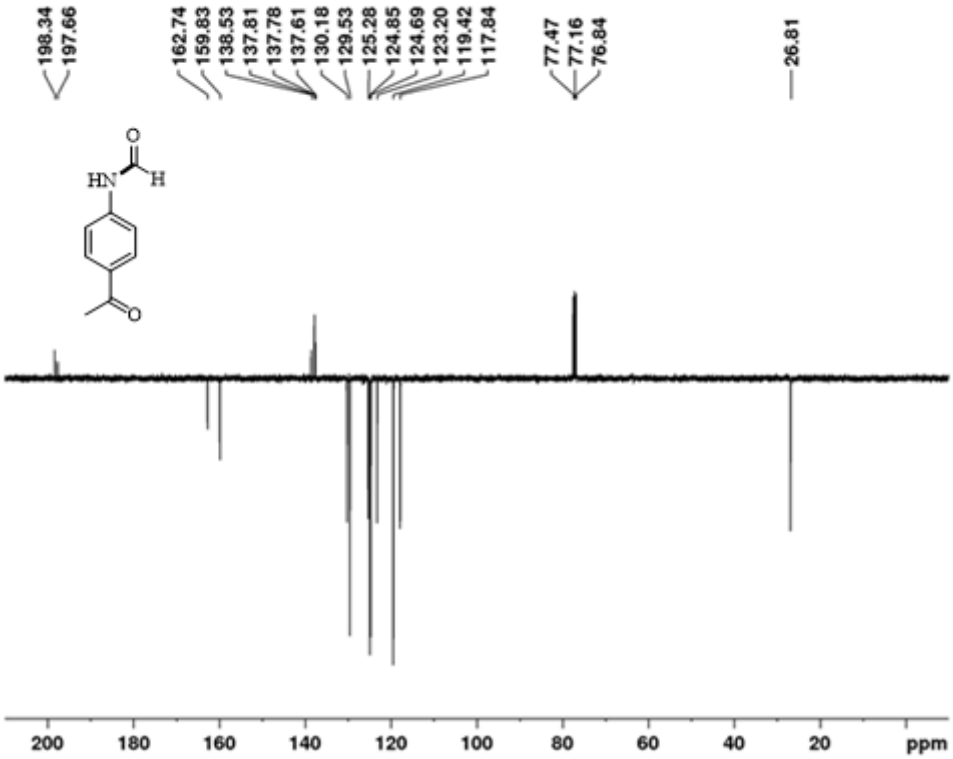

^{13}C spectrum of **3v (Chapter 6)**

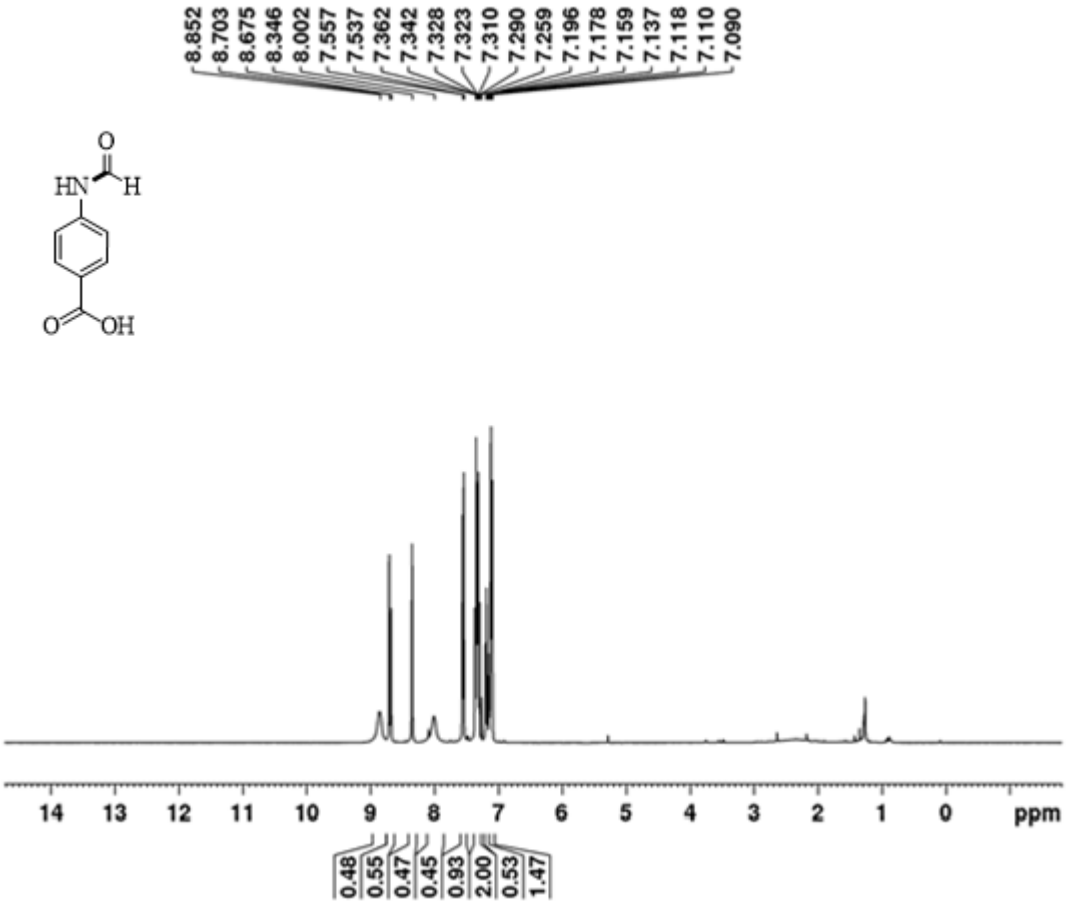

^{1}H NMR spectrum of **3w (Chapter 6)**

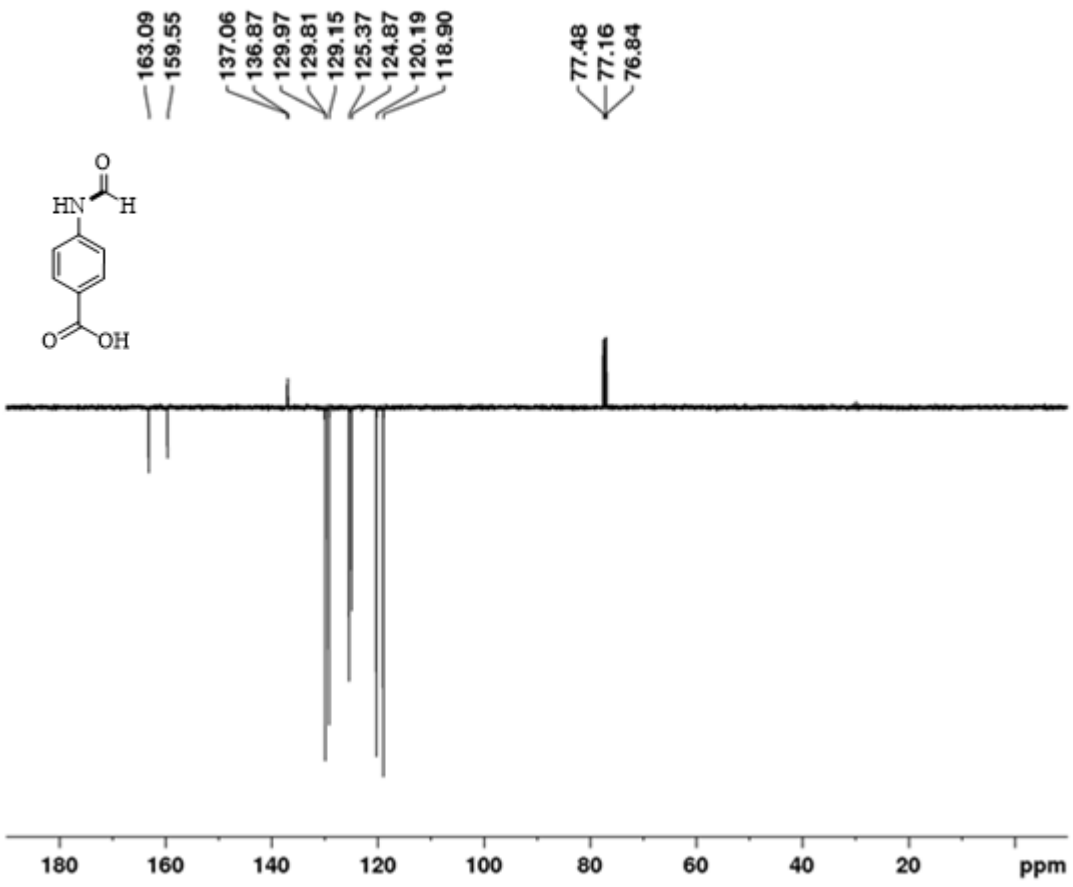

^{13}C spectrum of **3w (Chapter 6)**

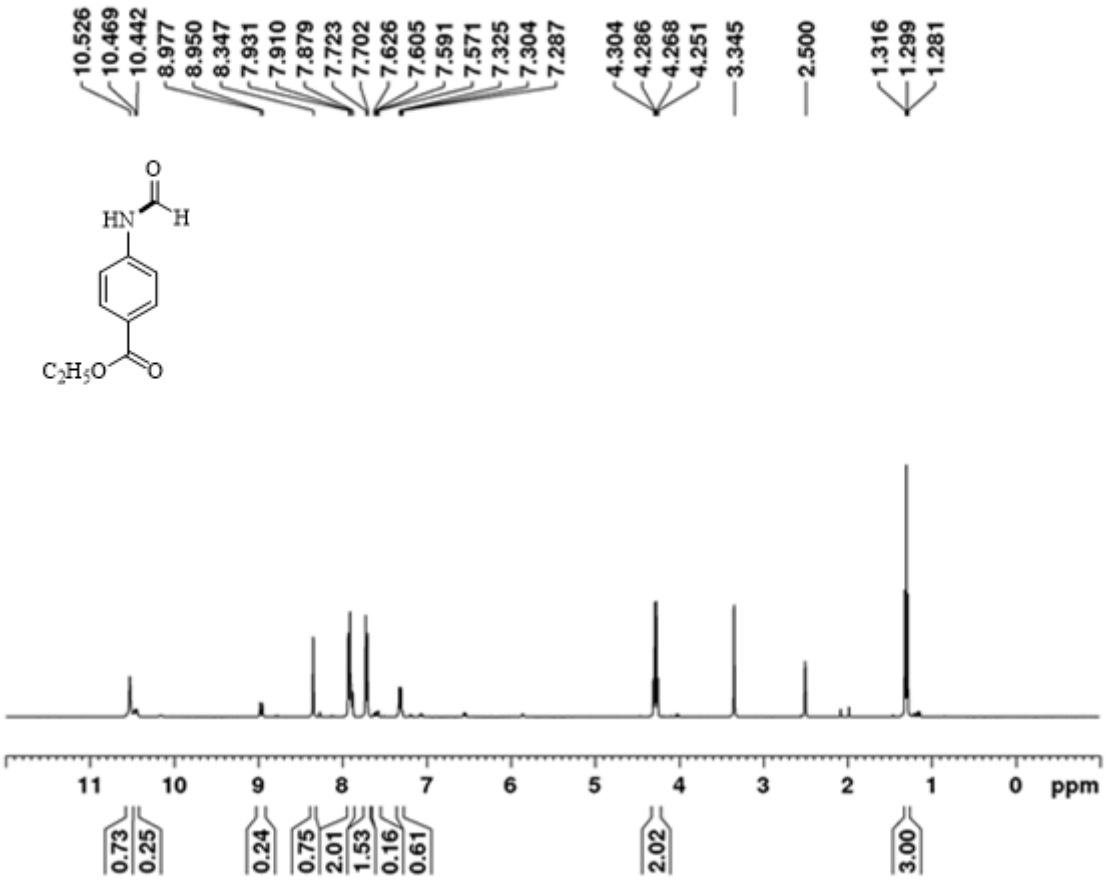

^{1}H NMR spectrum of **3x (Chapter 6)**

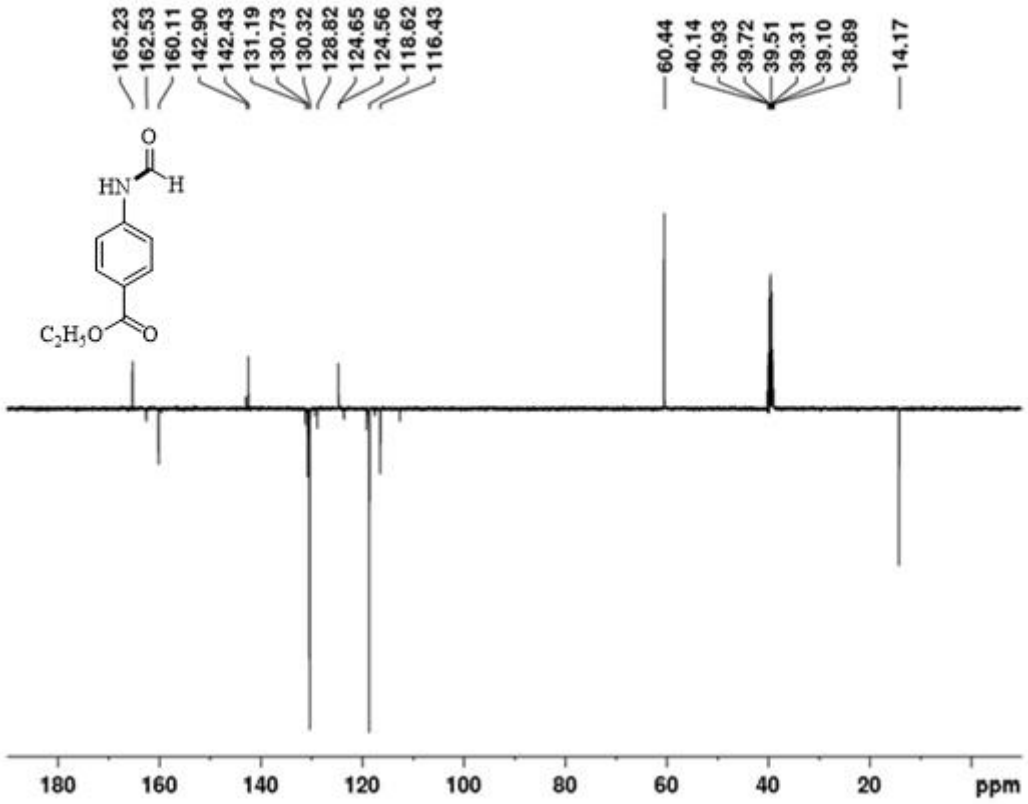

^{13}C spectrum of **3x (Chapter 6)**

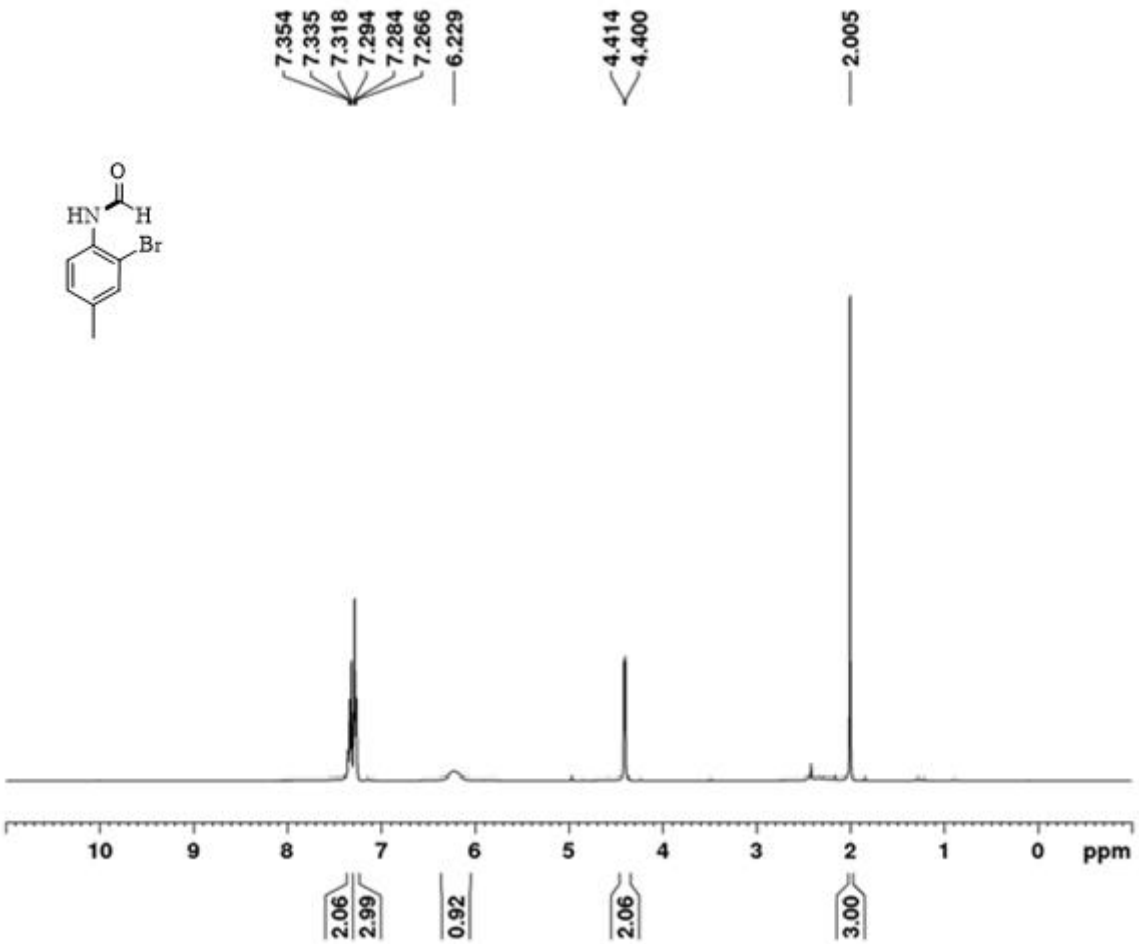

^{1}H NMR spectrum of **3y (Chapter 6)**

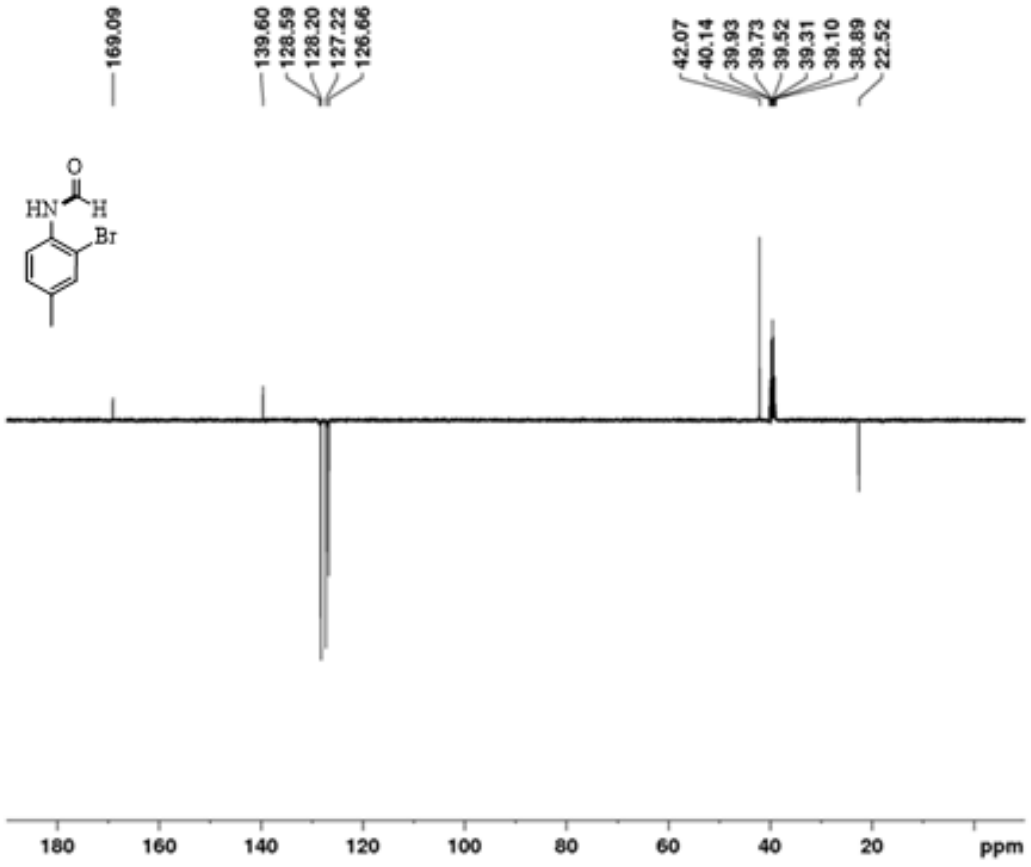

^{13}C spectrum of **3y (Chapter 6)**

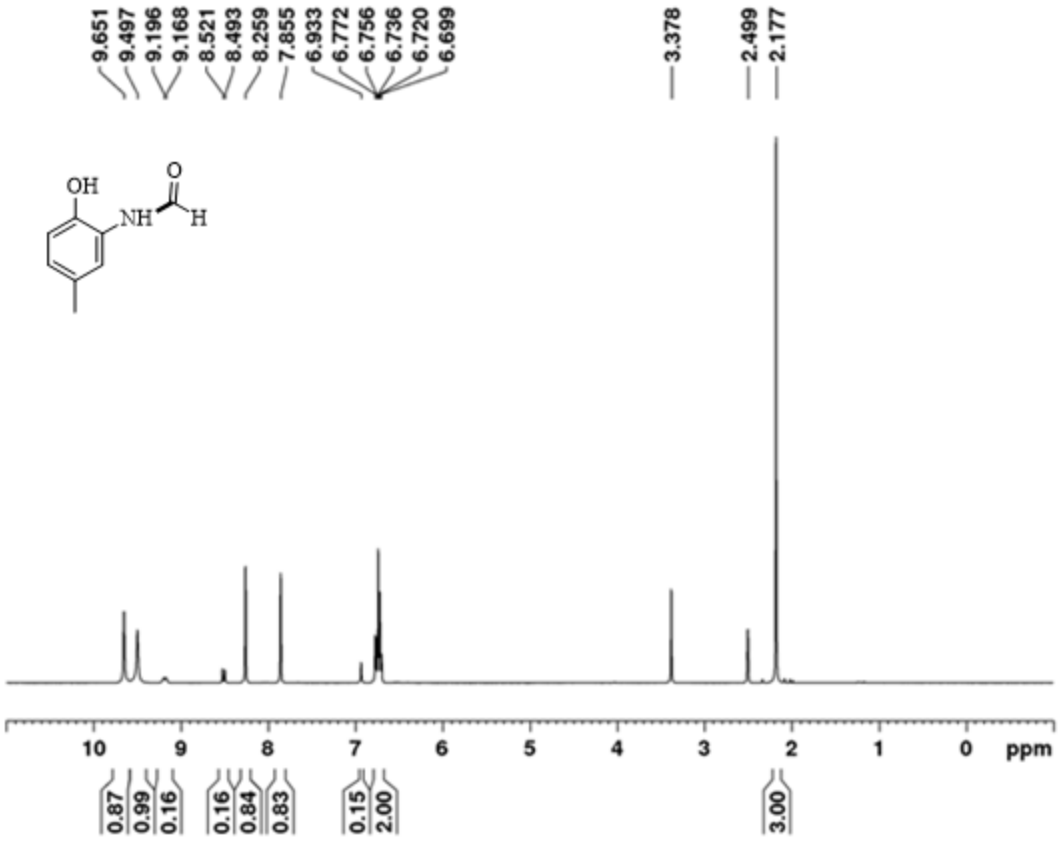

^{1}H NMR spectrum of **3aa (Chapter 6)**

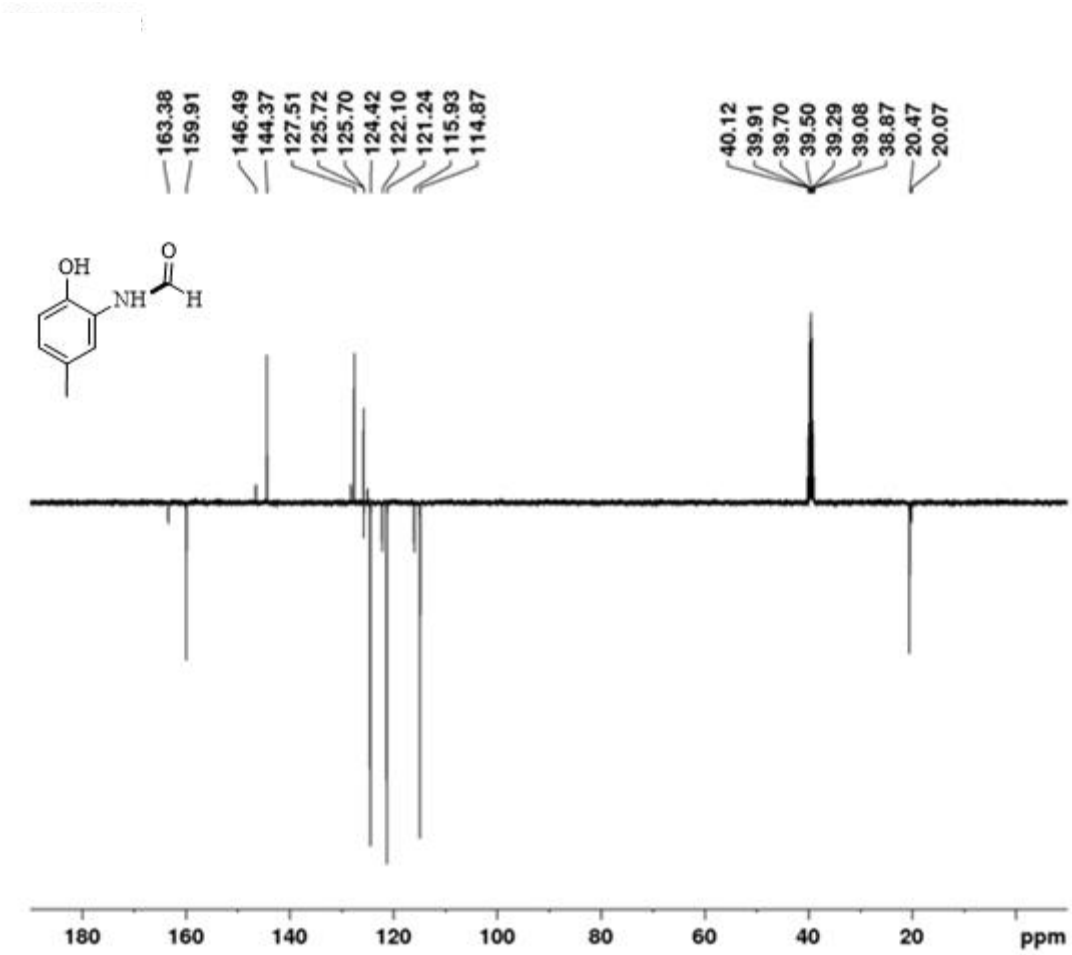

^{13}C spectrum of **3aa (Chapter 6)**

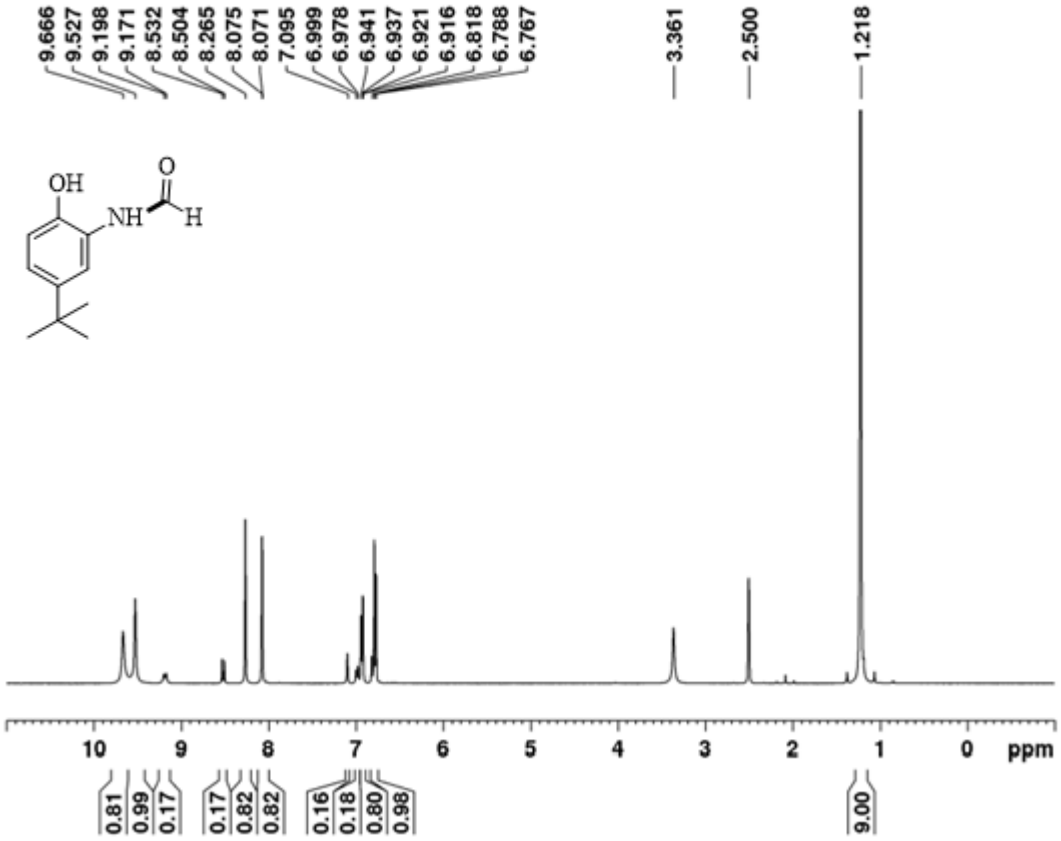

^{1}H NMR spectrum of **3ab (Chapter 6)**

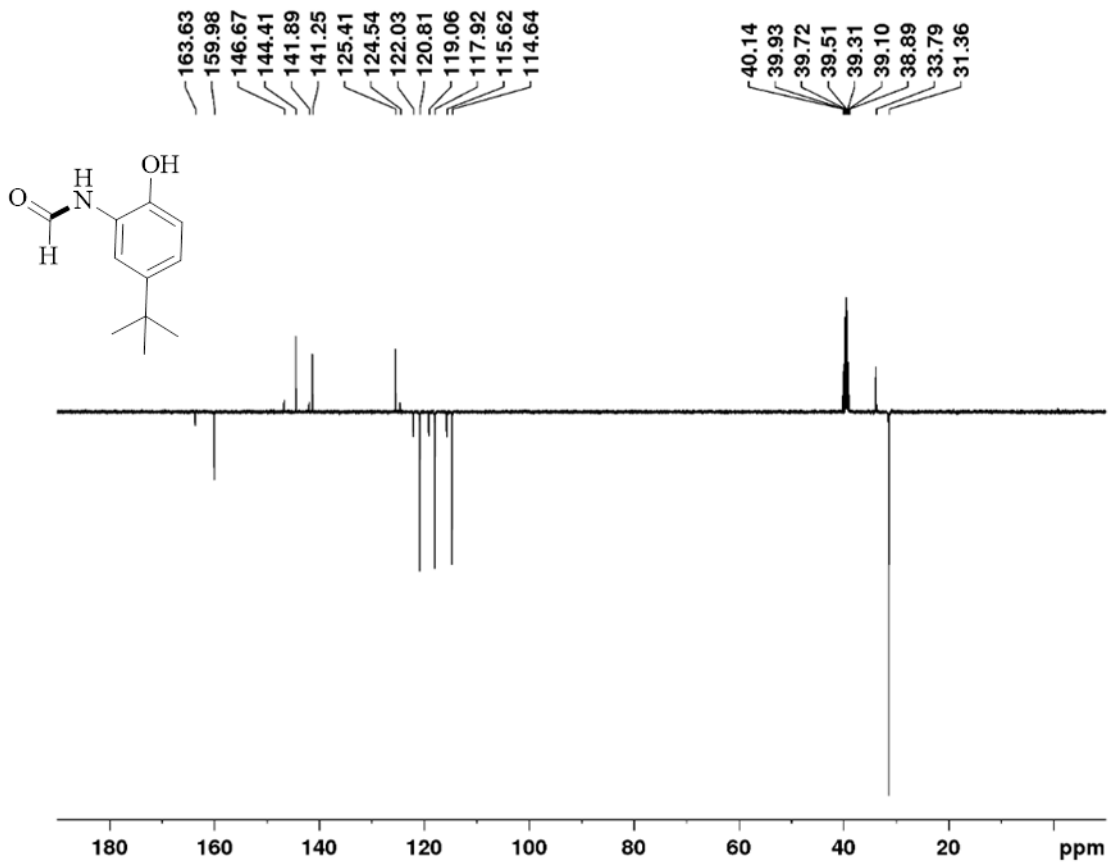

^{13}C spectrum of **3ab (Chapter 6)**

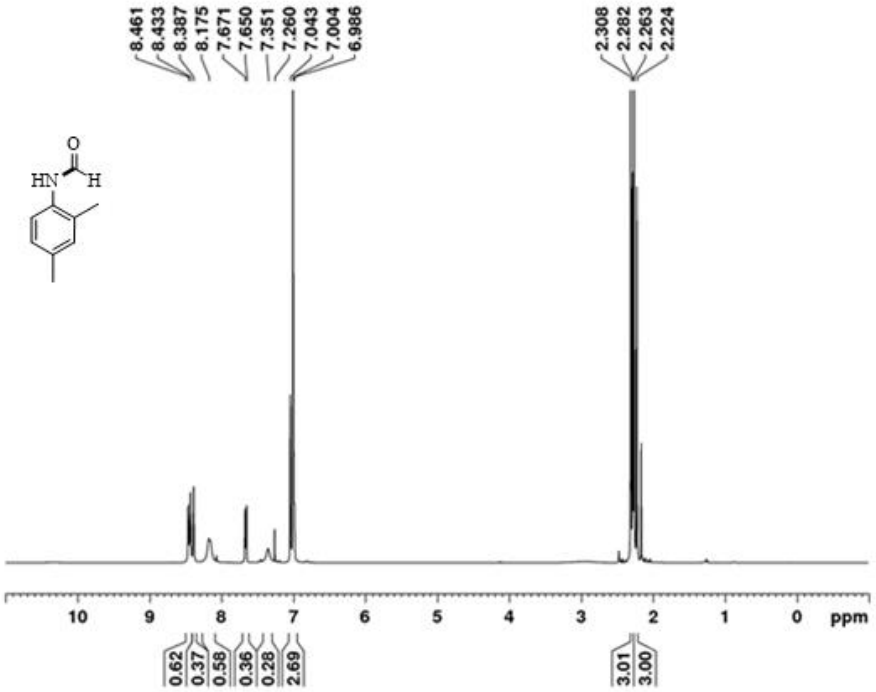

^{1}H NMR spectrum of **3ac (Chapter 6)**

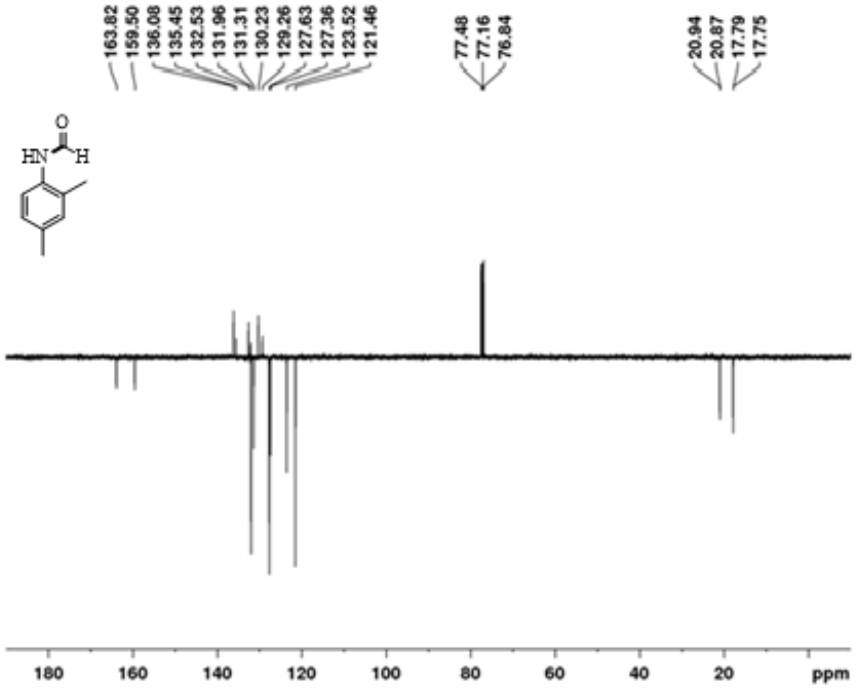

^{13}C spectrum of **3ac (Chapter 6)**

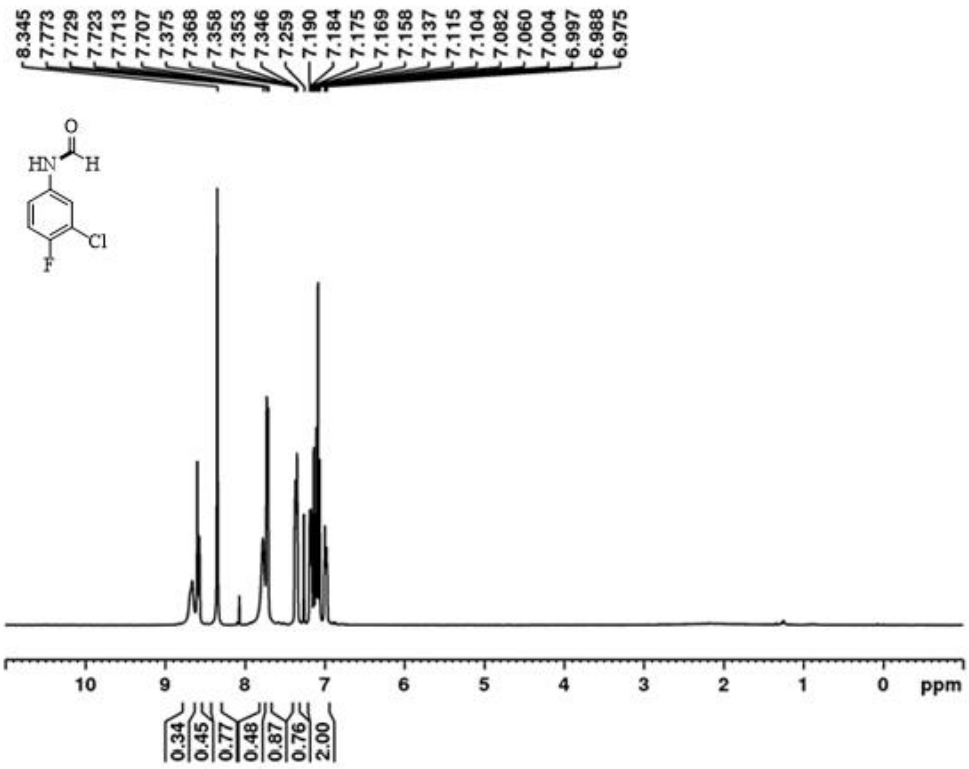

^{1}H NMR spectrum of **3ad (Chapter 6)**

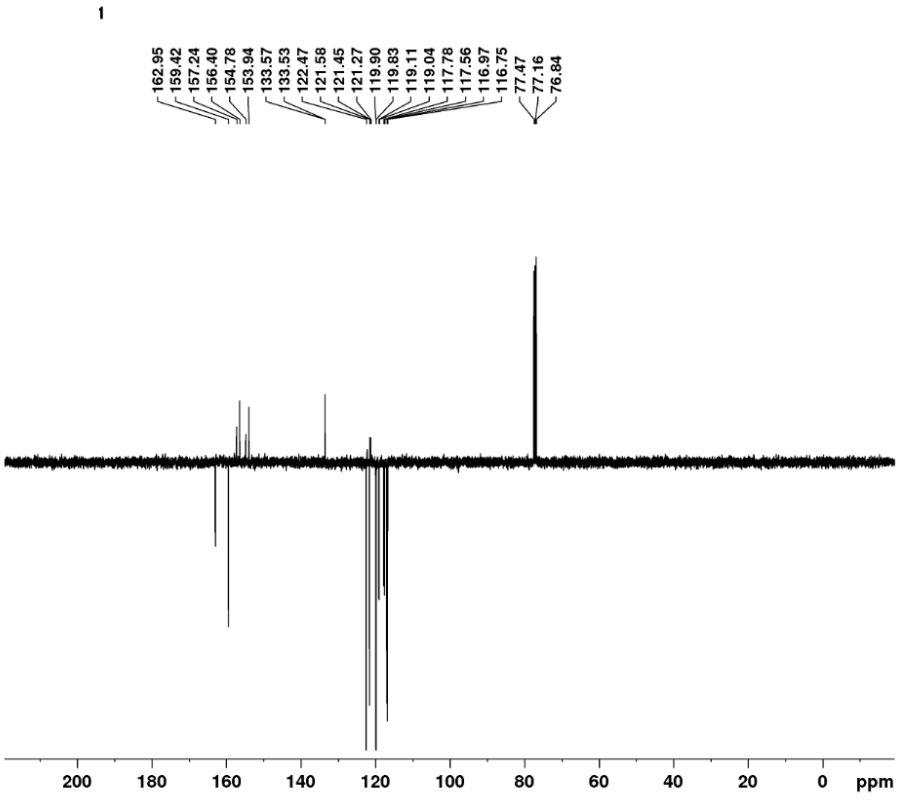

^{13}C spectrum of **3ad (Chapter 6)**

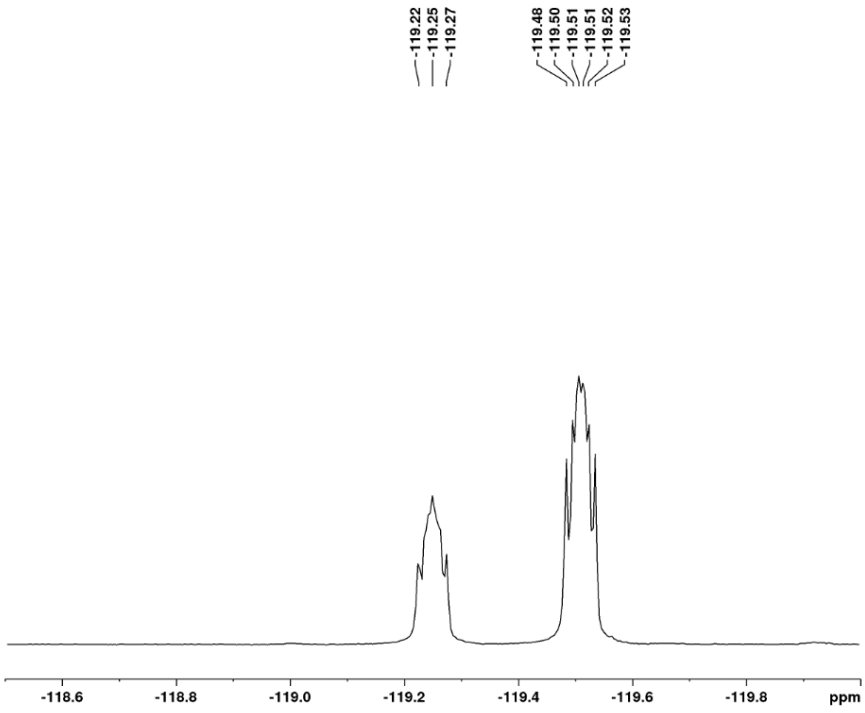

^{19}F spectrum of **3ad (Chapter 6)**

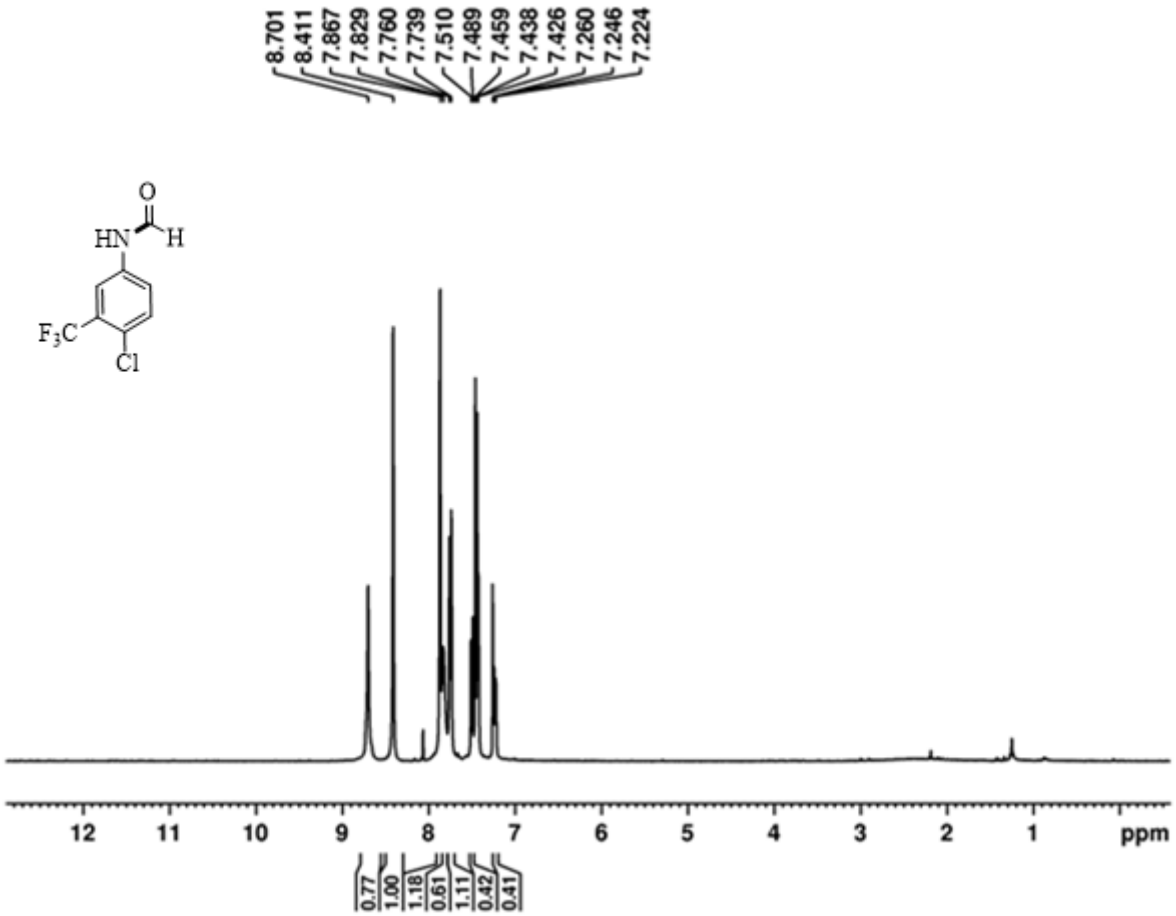

^{1}H NMR spectrum of **3ae (Chapter 6)**

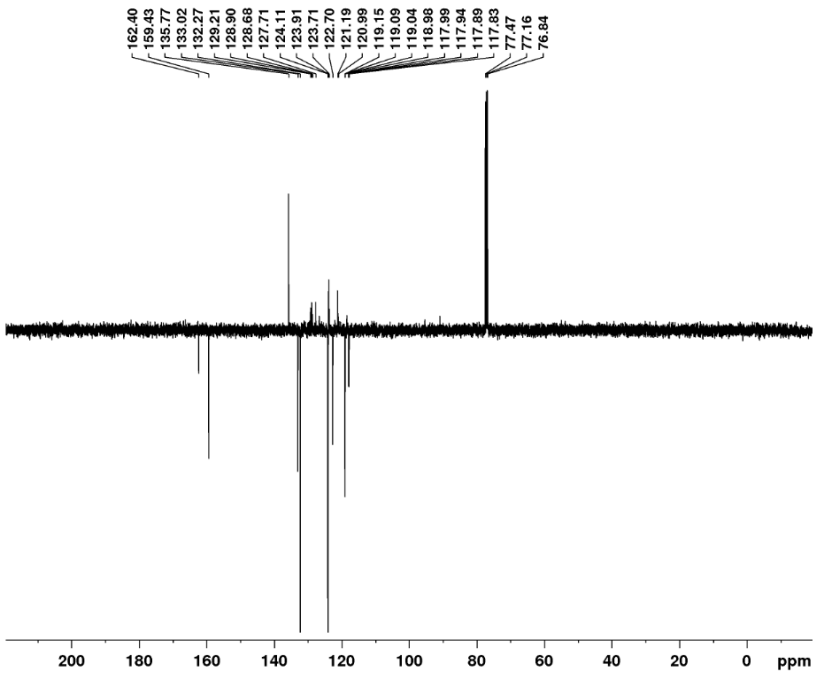

^{13}C spectrum of **3ae (Chapter 6)**

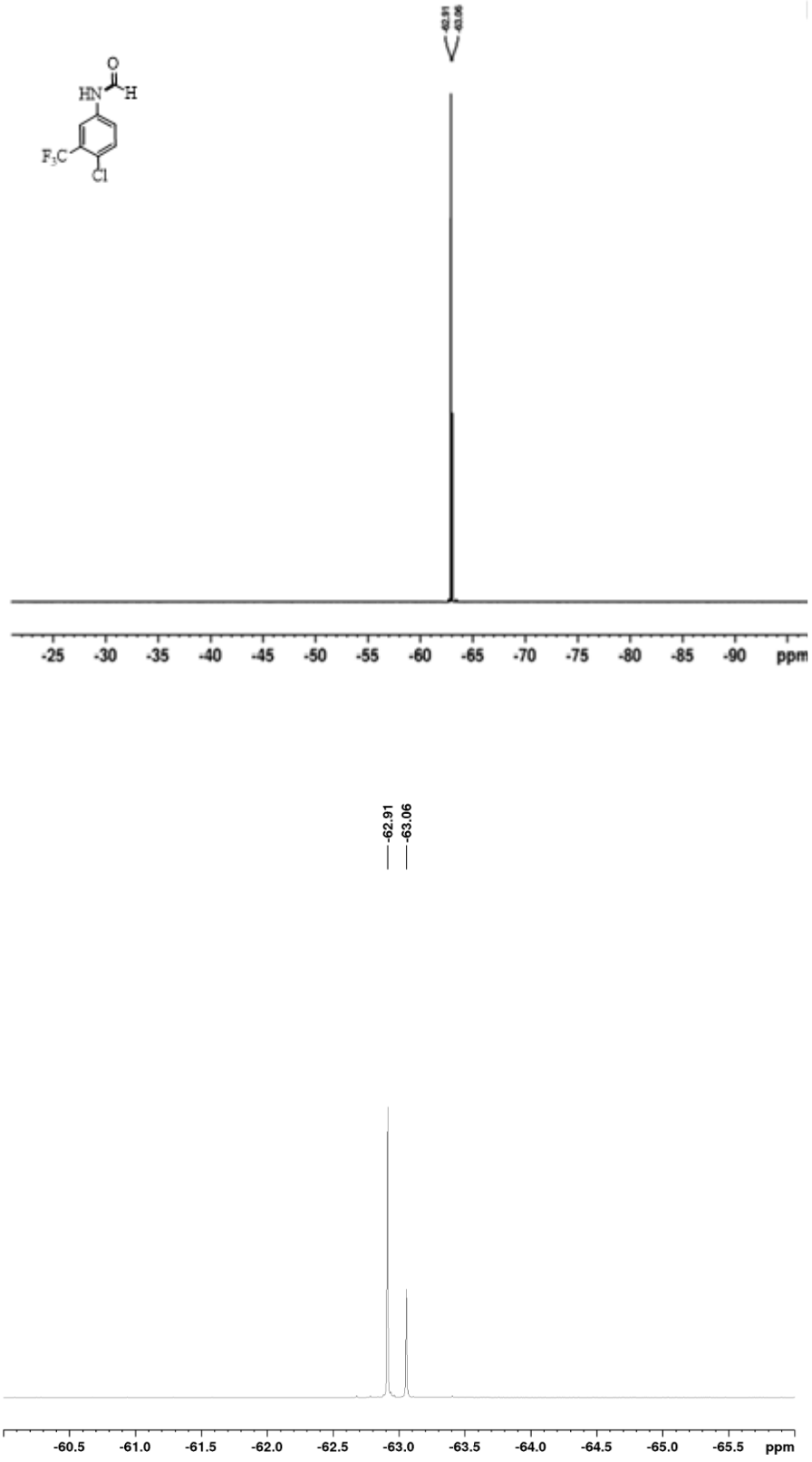

^{19}F spectrum of **3ae (Chapter 6)**

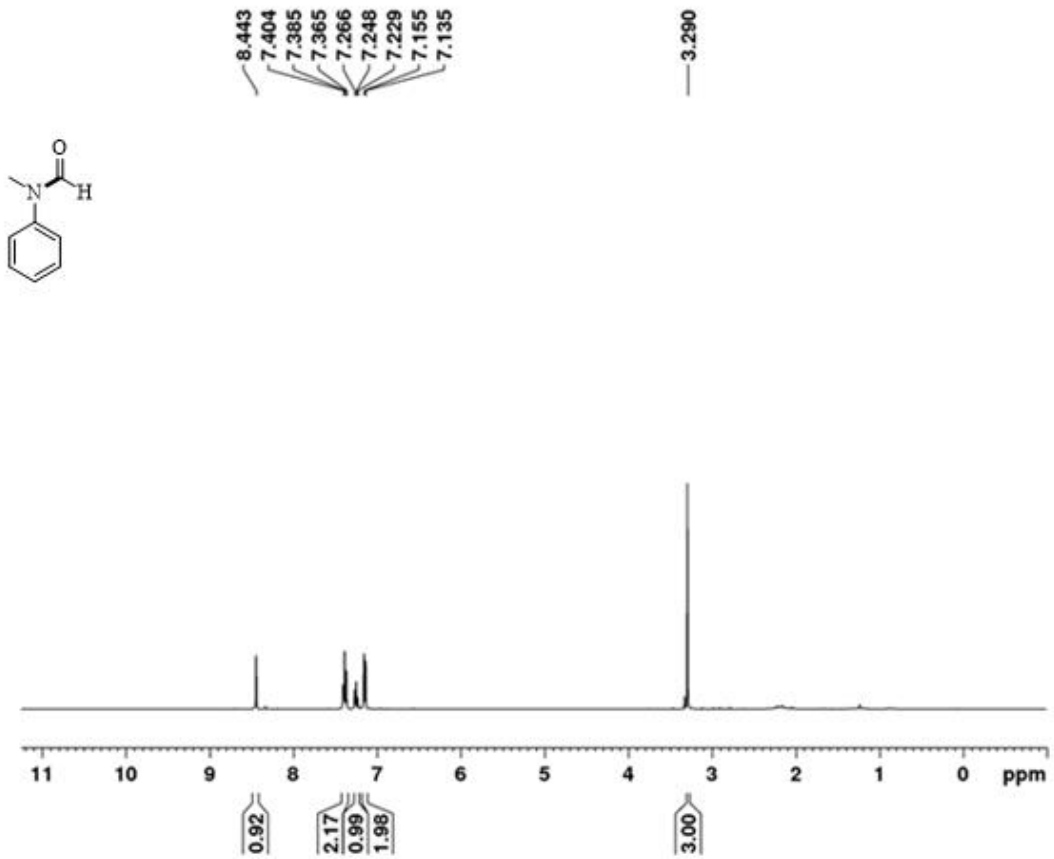

^{1}H NMR spectrum of **3af (Chapter 6)**

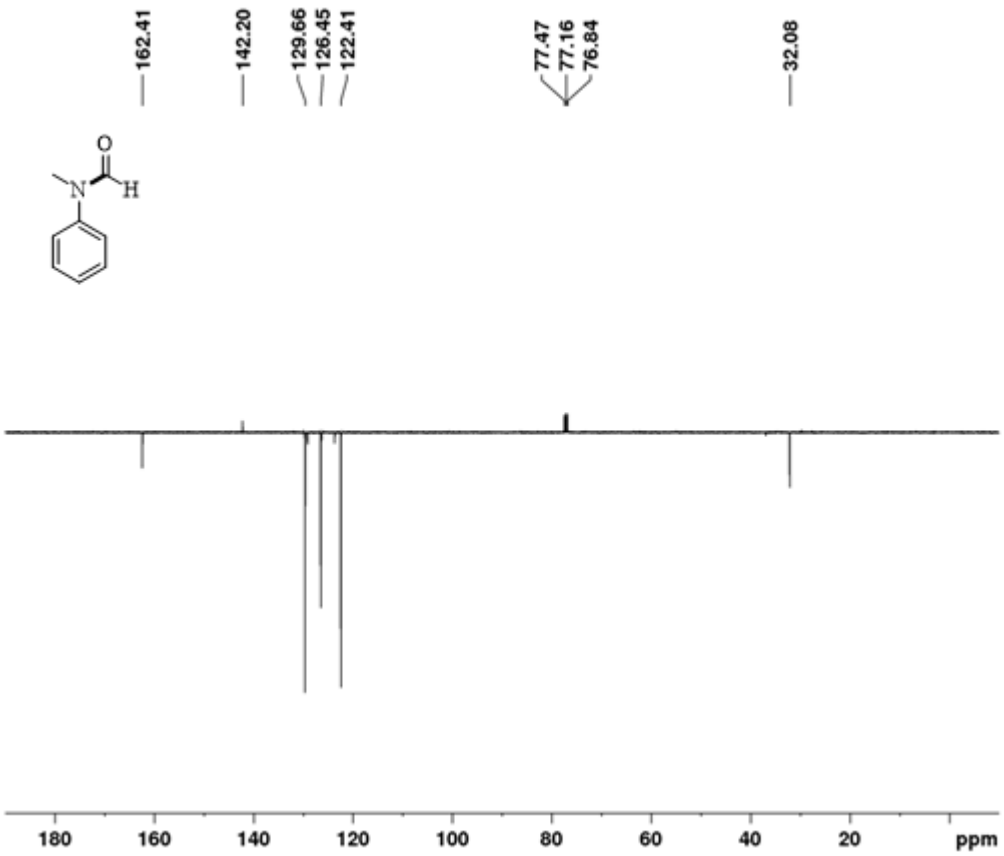

^{13}C NMR spectrum of **3af (Chapter 6)**

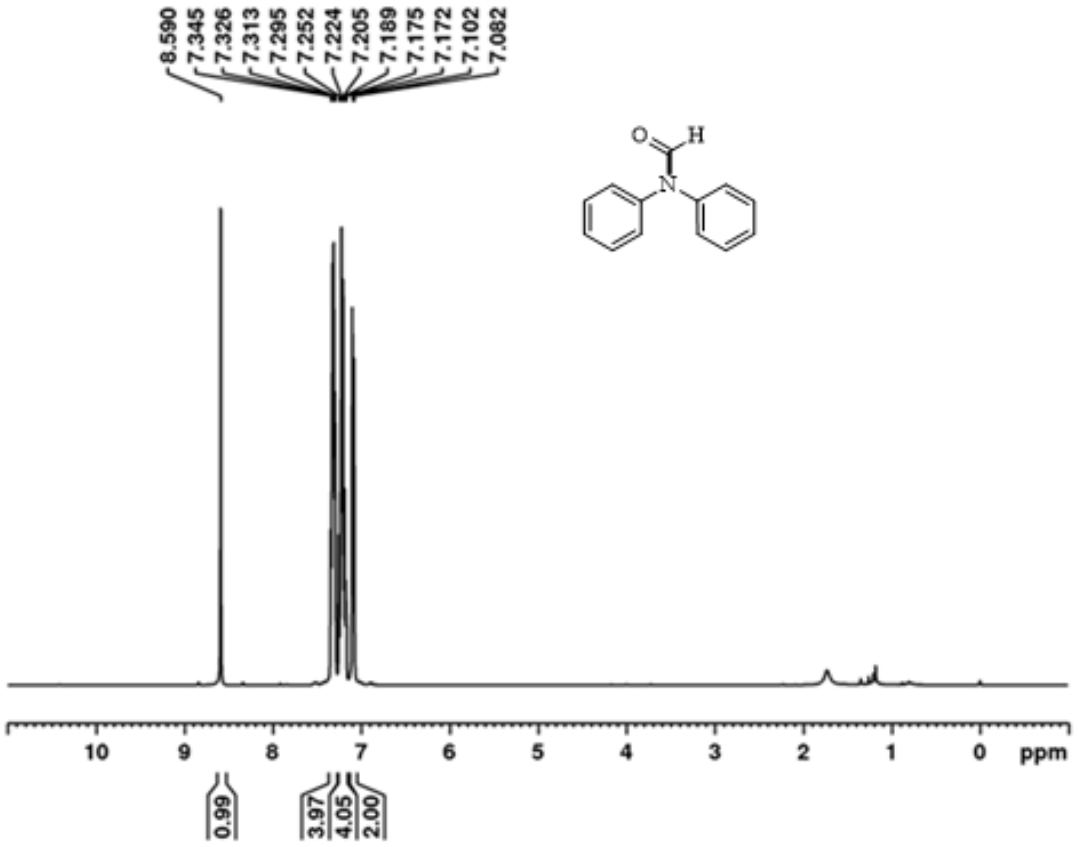

^{1}H NMR spectrum of **3ag (Chapter 6)**

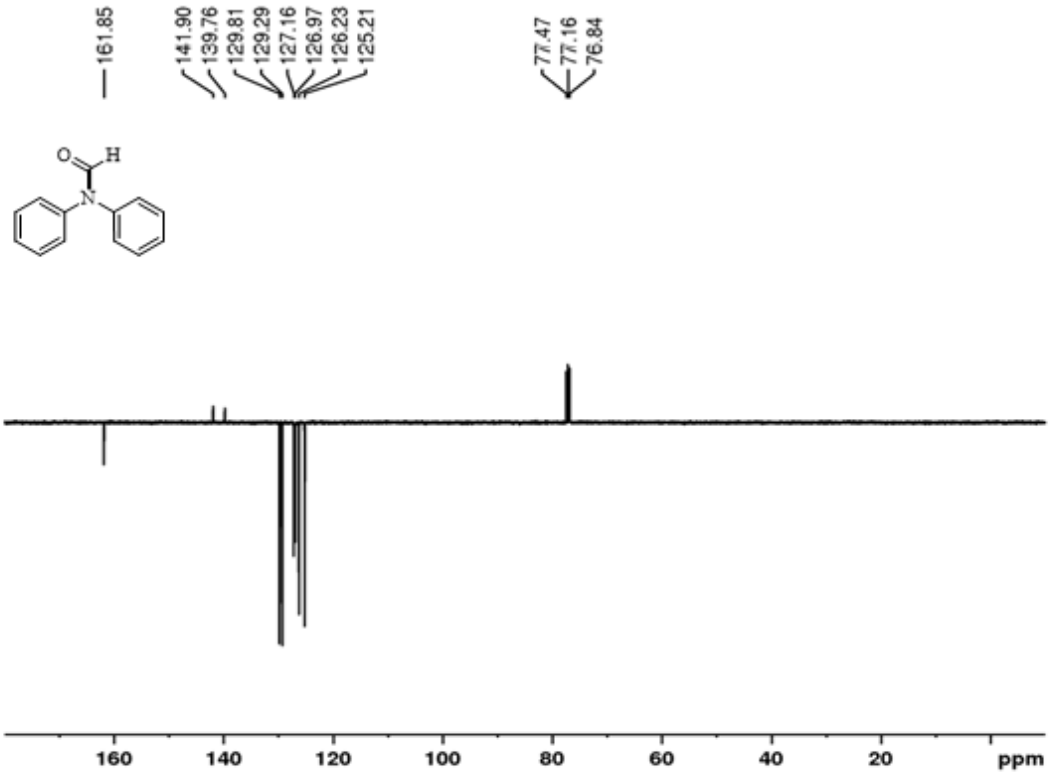

^{13}C spectrum of **3ag (Chapter 6)**

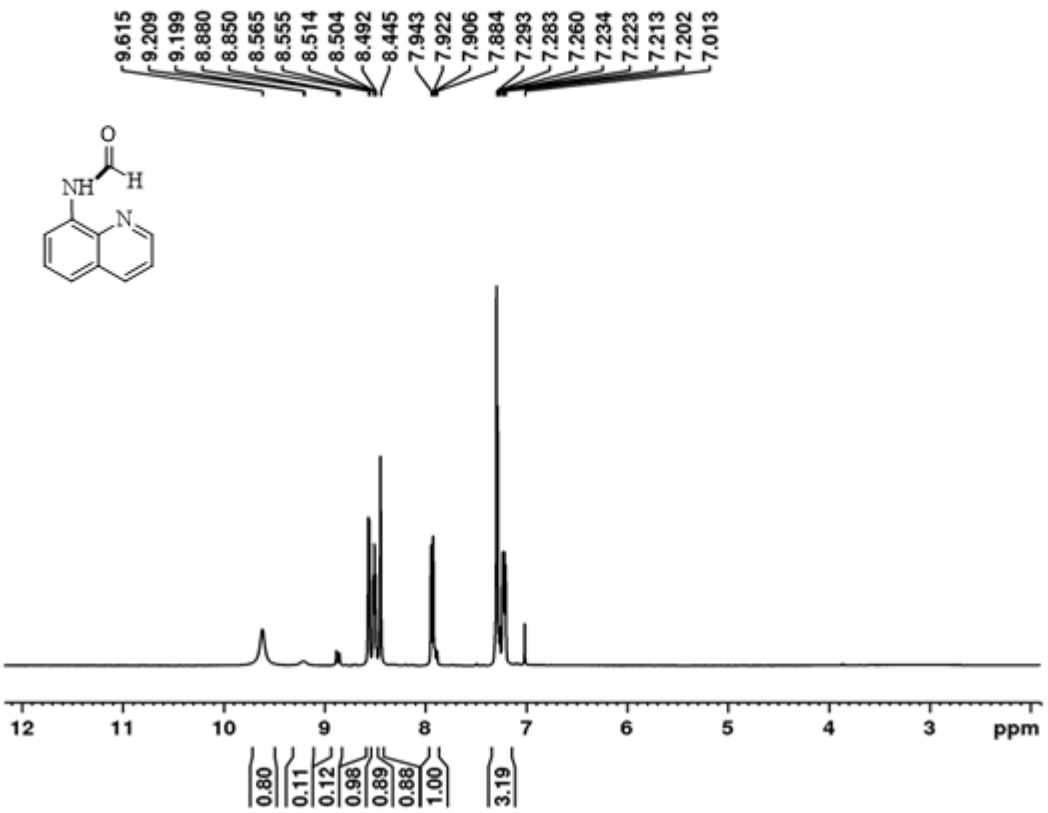

^{1}H NMR spectrum of **3ah (Chapter 6)**

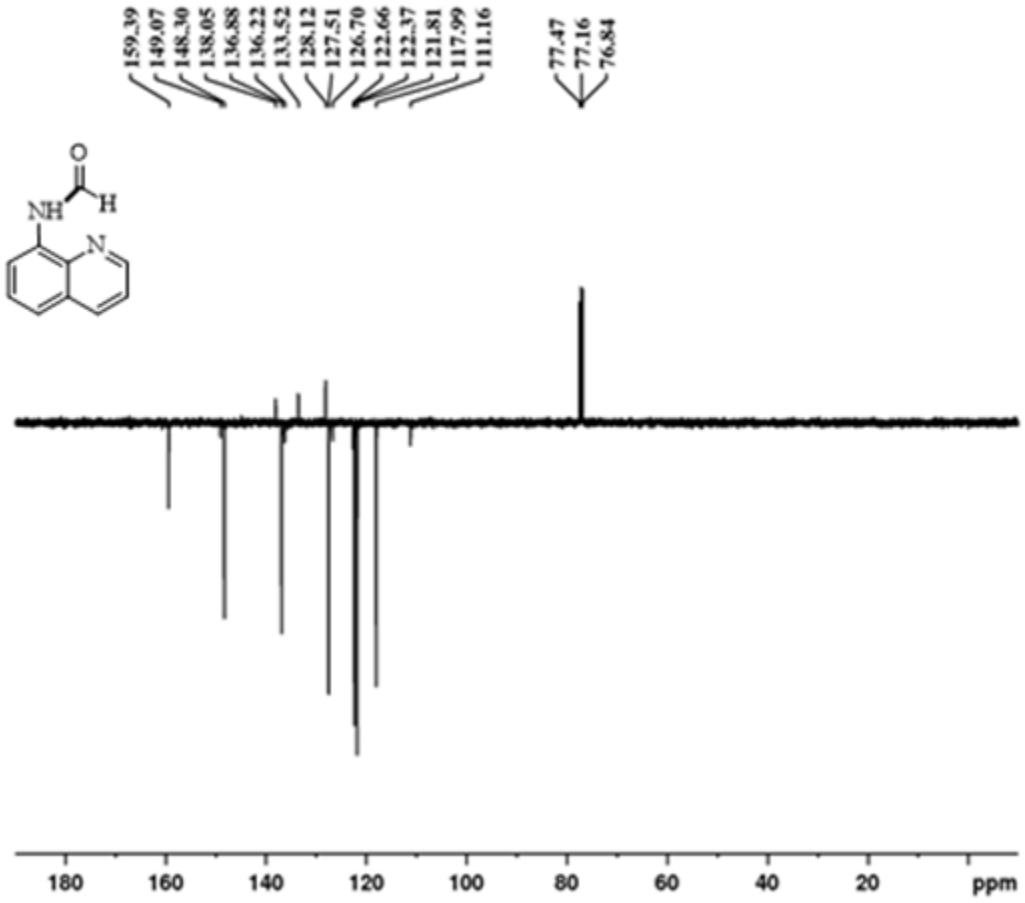

^{13}C spectrum of **3ah (Chapter 6)**

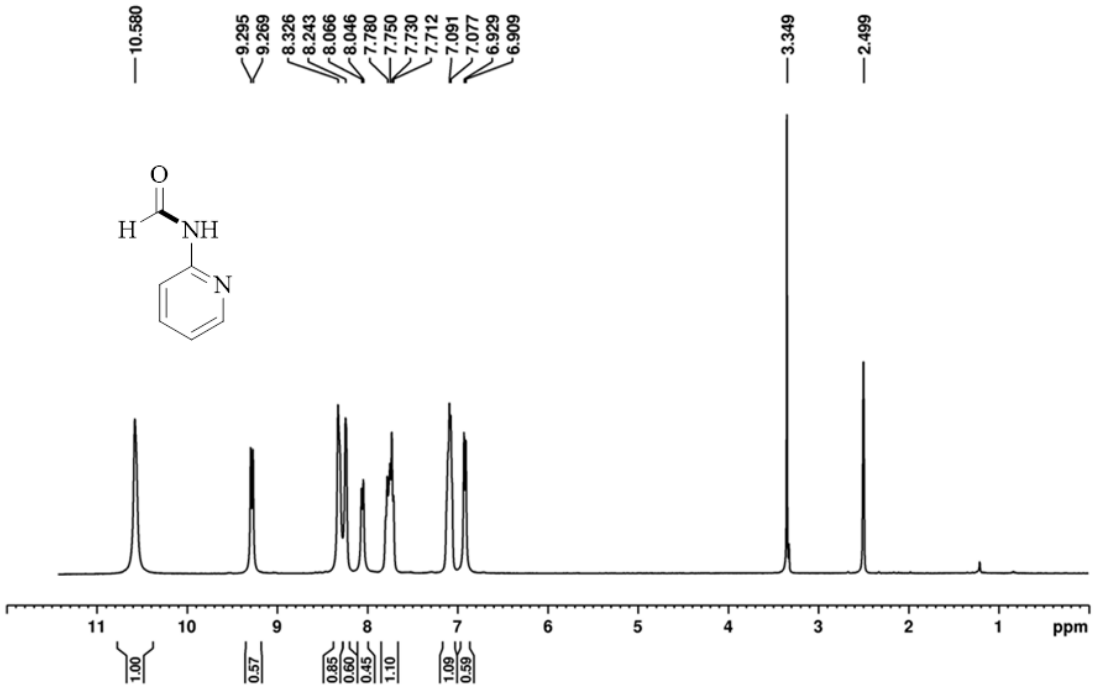

^{1}H NMR spectrum of **3ai (Chapter 6)**

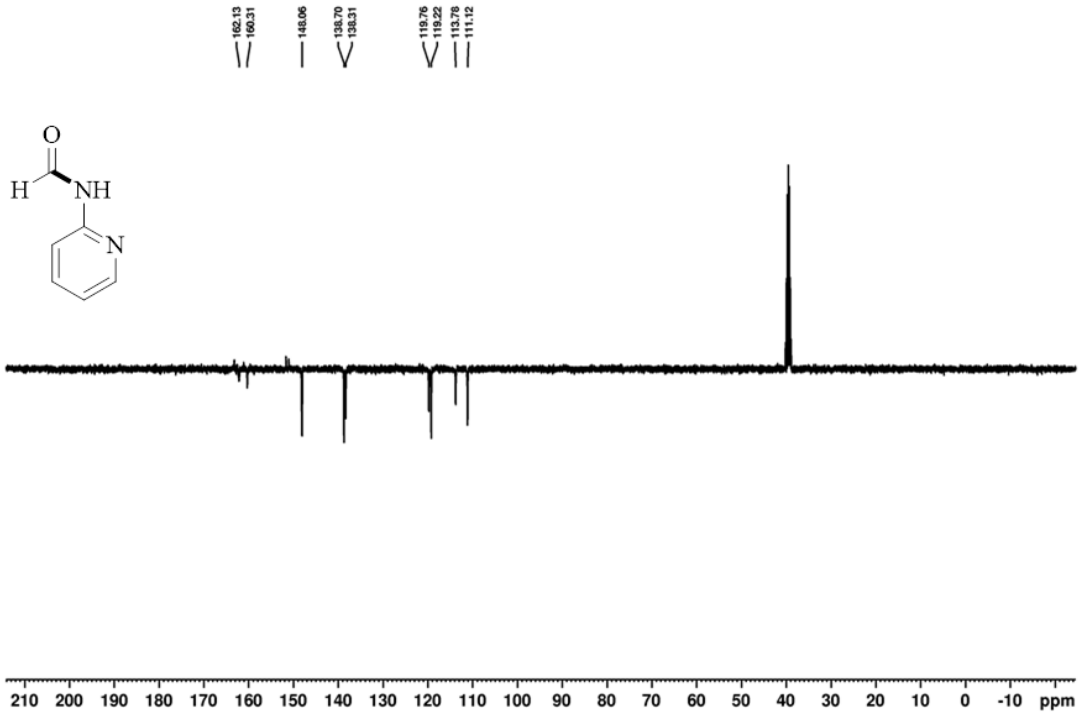

^{13}C NMR spectrum of **3ai (Chapter 6)**

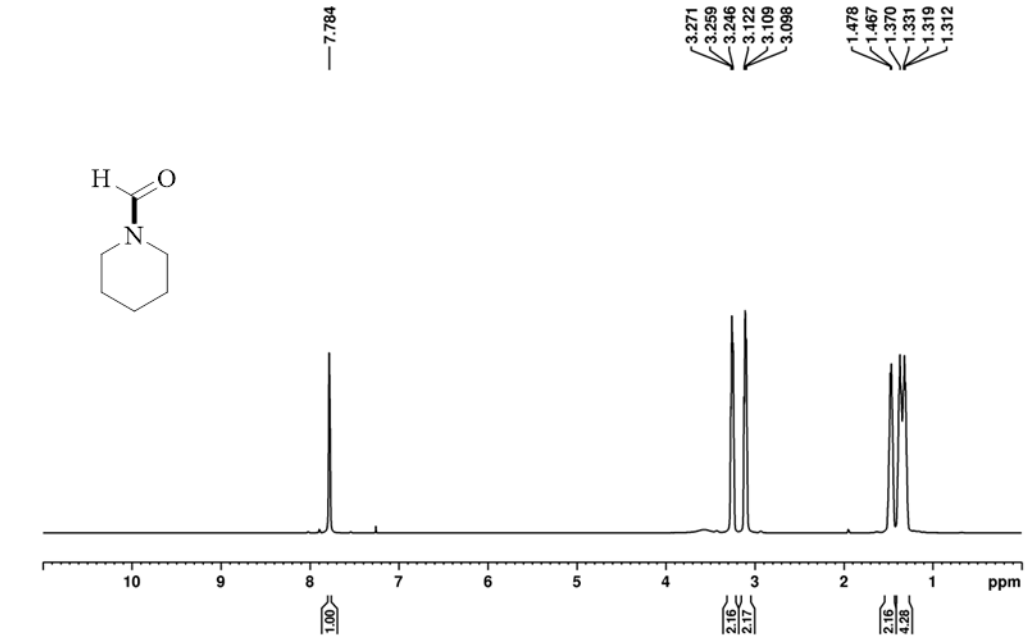

^{1}H NMR spectrum of **3aj (Chapter 6)**

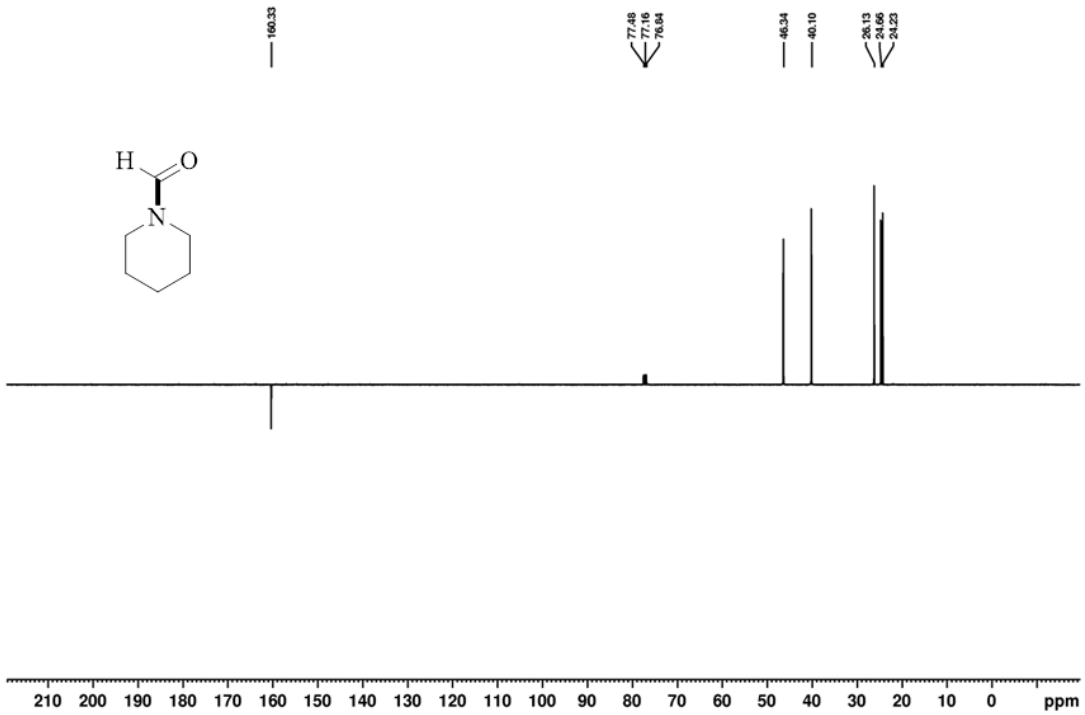

^{13}C spectrum of **3aj (Chapter 6)**

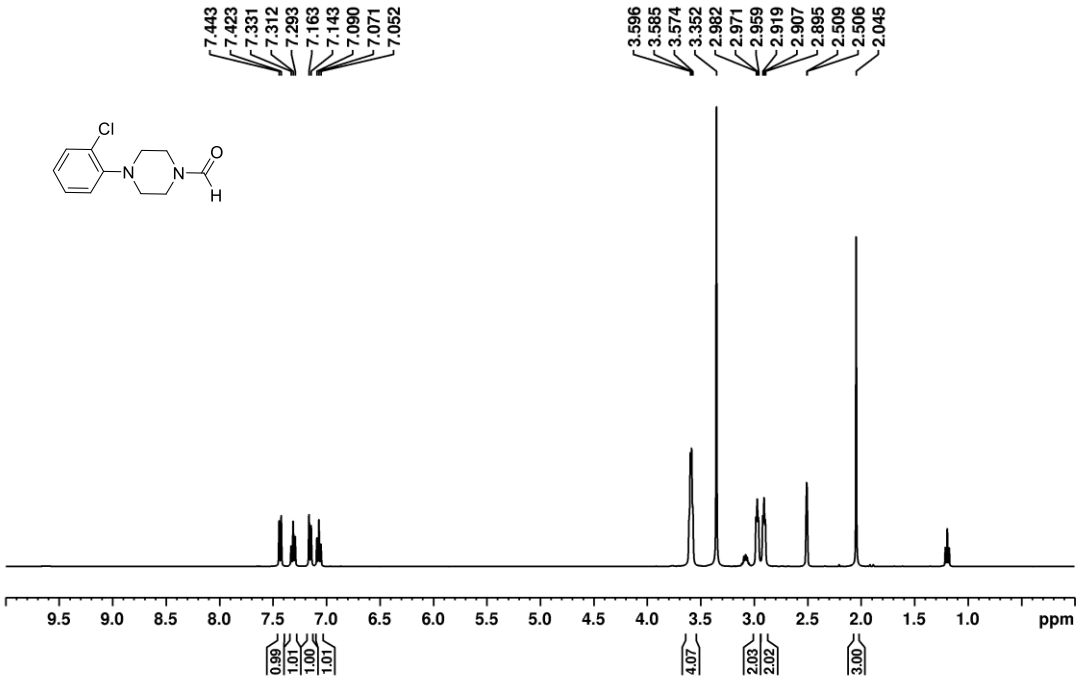

^{1}H spectrum of **3ak (Chapter 6)**

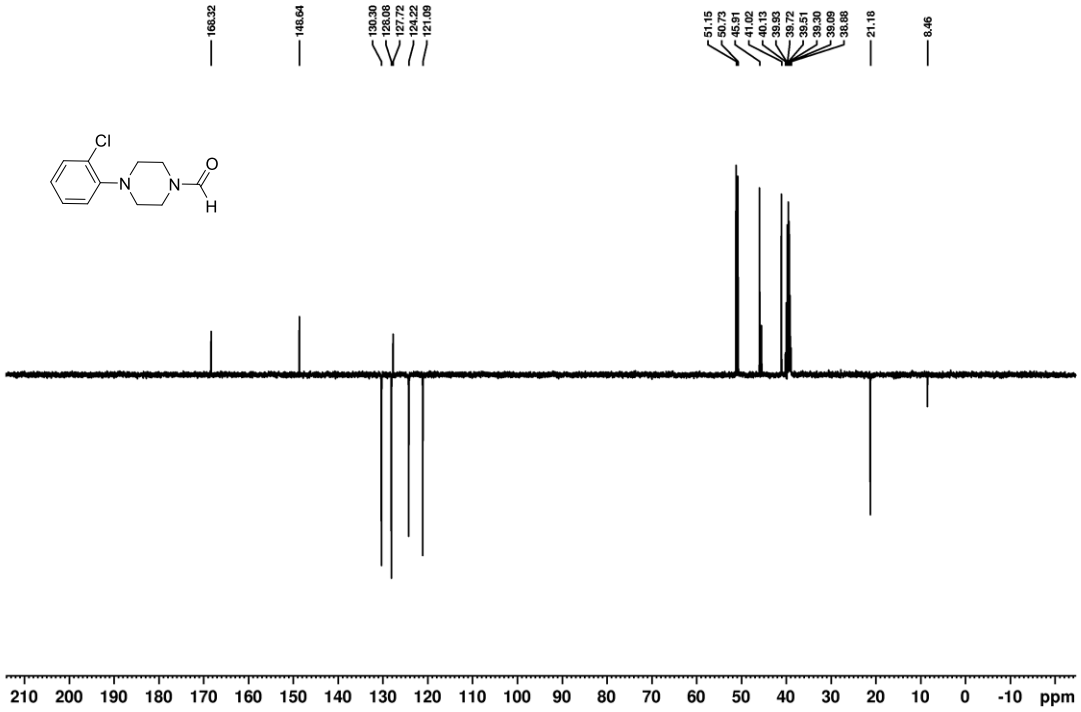

^{13}C spectrum of **3ak (Chapter 6)**

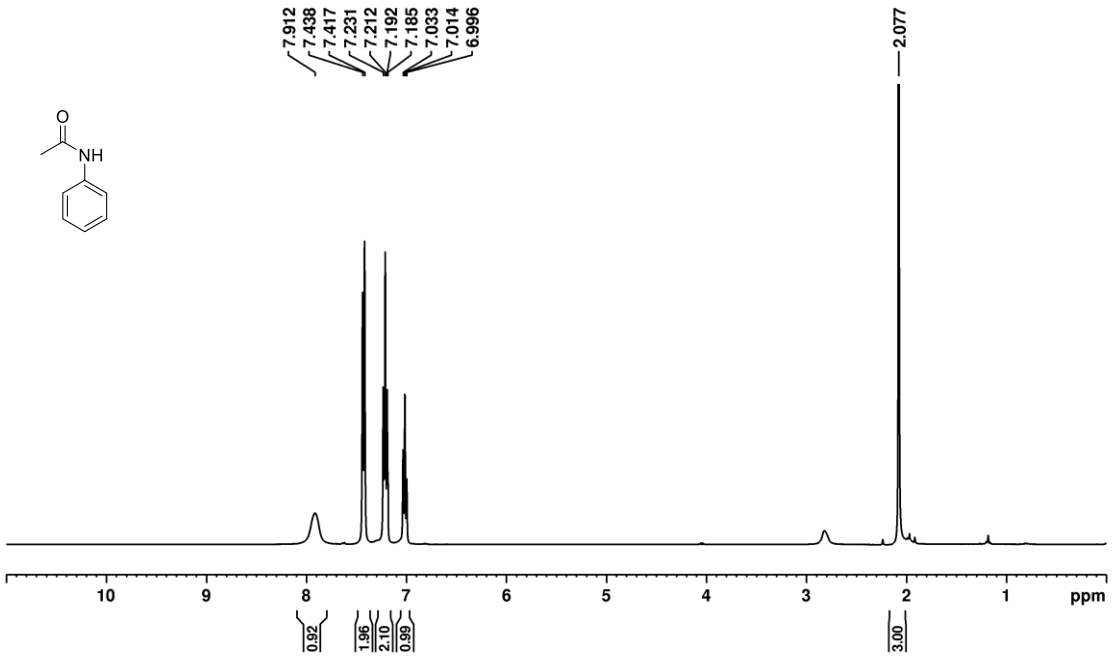

^{1}H spectrum of **3A (Chapter 6)**

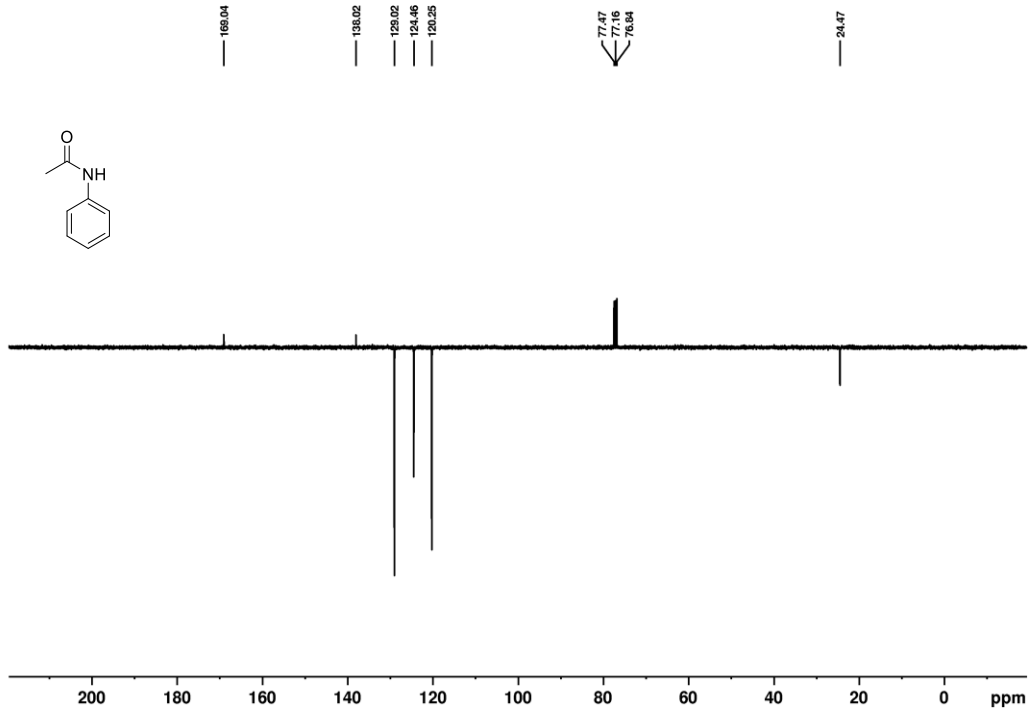

^{13}C spectrum of **3A (Chapter 6)**

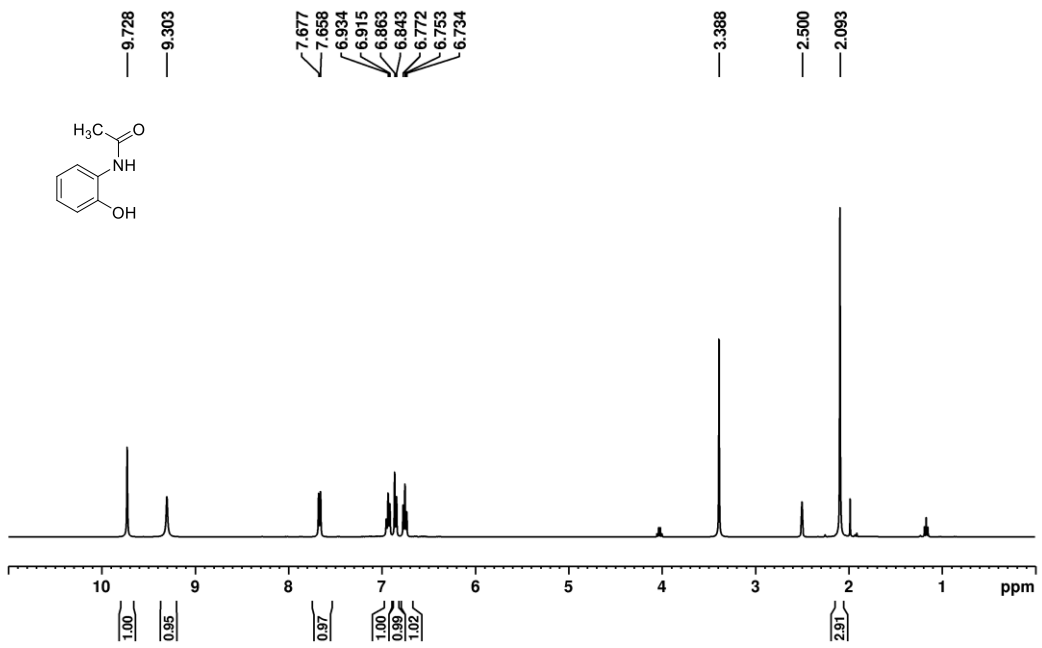

^{1}H spectrum of **3B (Chapter 6)**

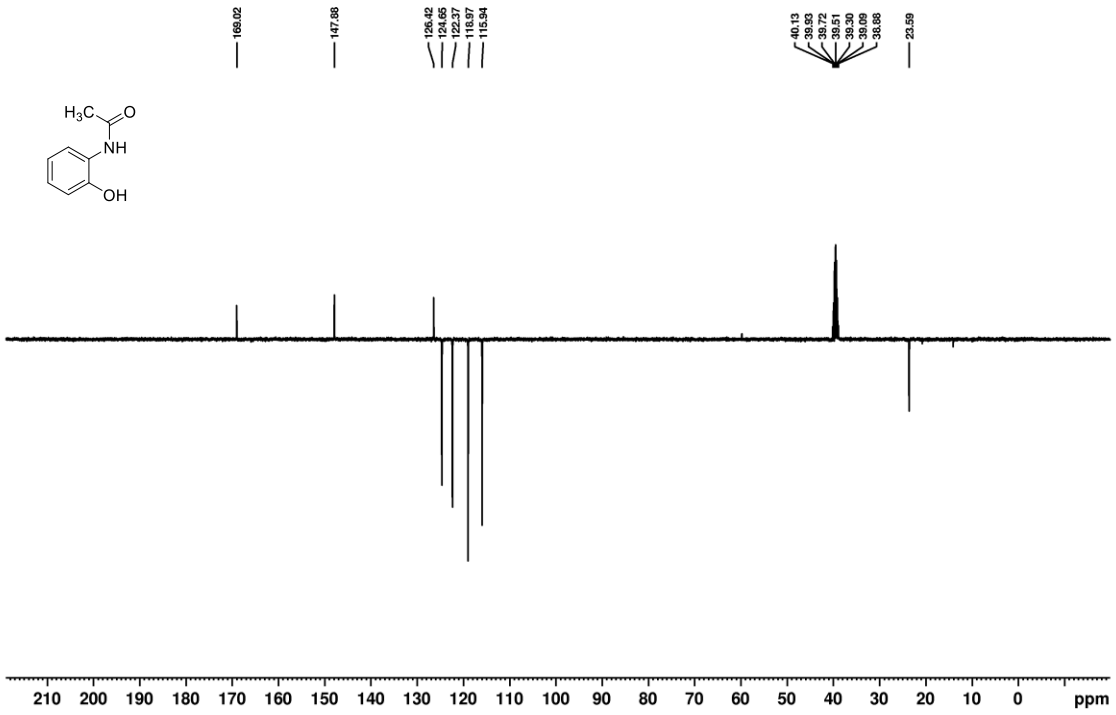

^{13}C spectrum of **3B (Chapter 6)**

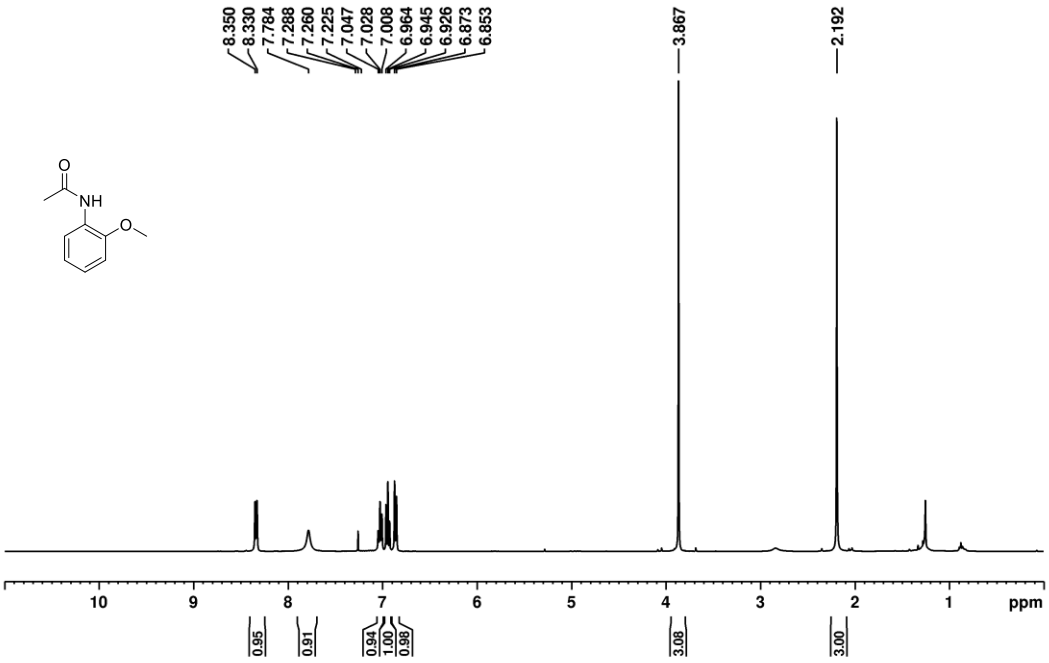

^{1}H spectrum of **3C (Chapter 6)**

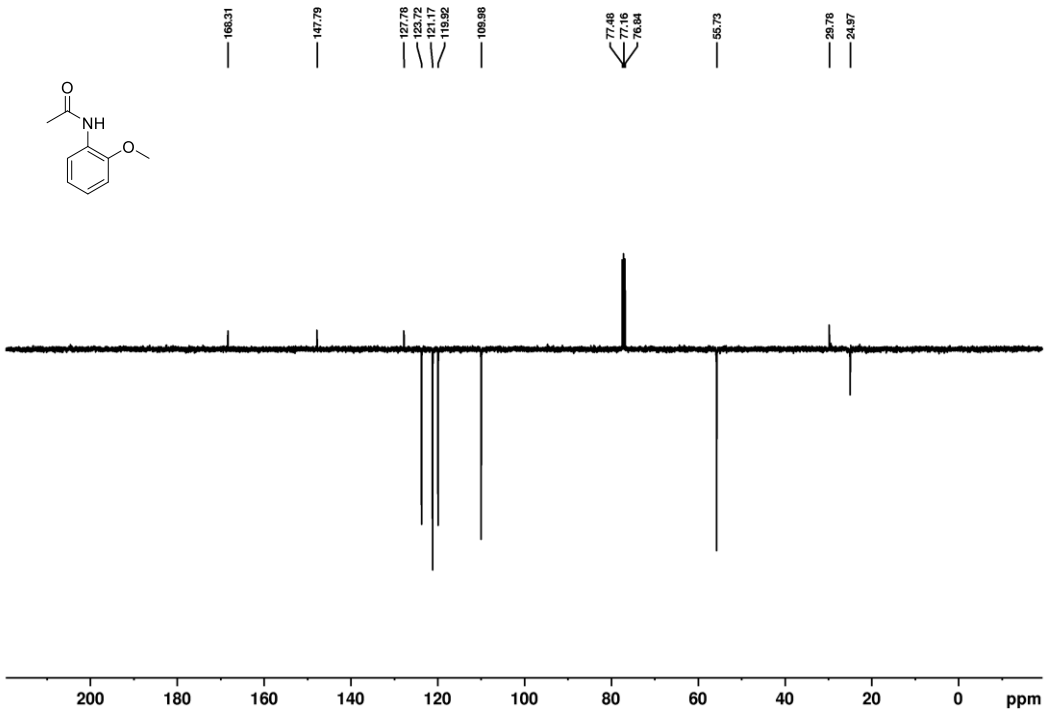

^{13}C spectrum of **3C (Chapter 6)**

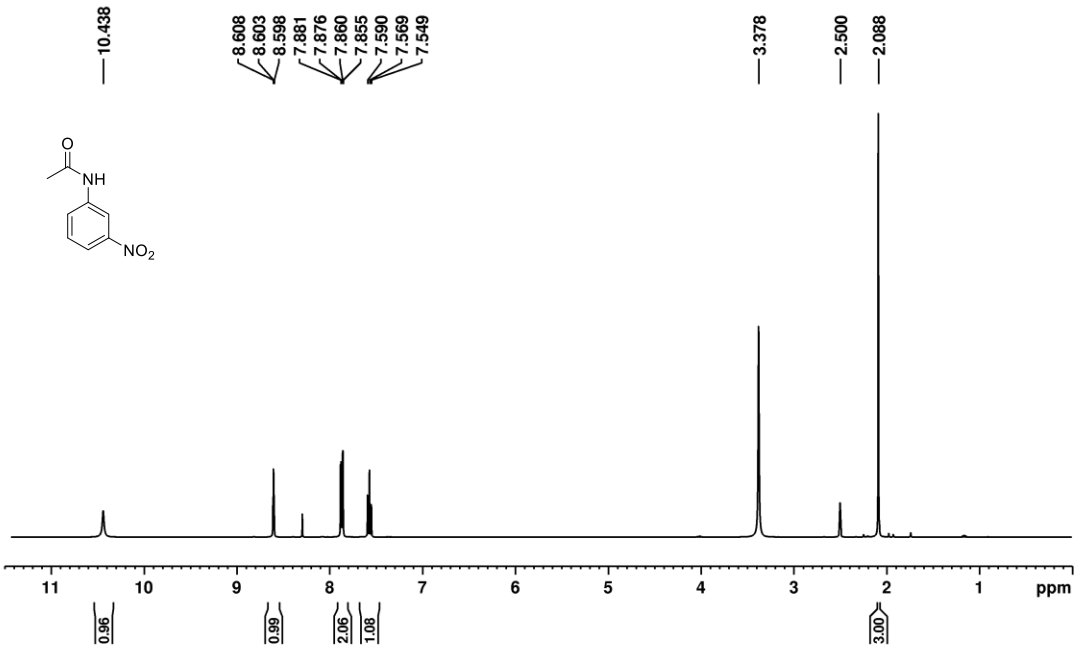

^{1}H spectrum of **3D (Chapter 6)**

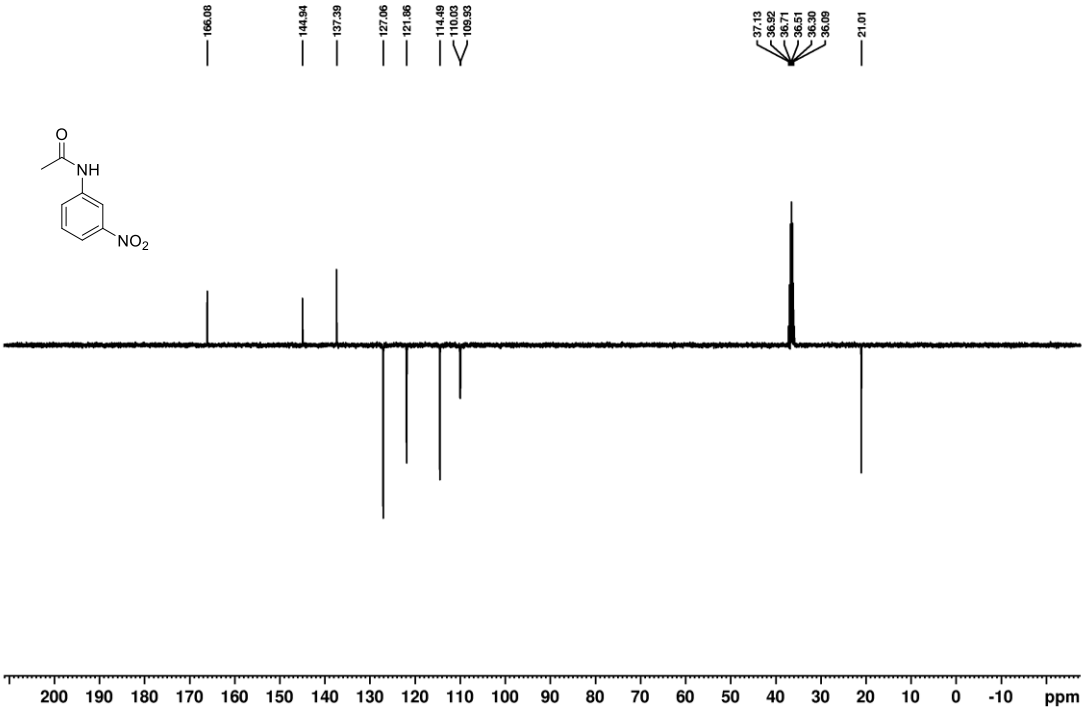

^{13}C spectrum of **3D (Chapter 6)**

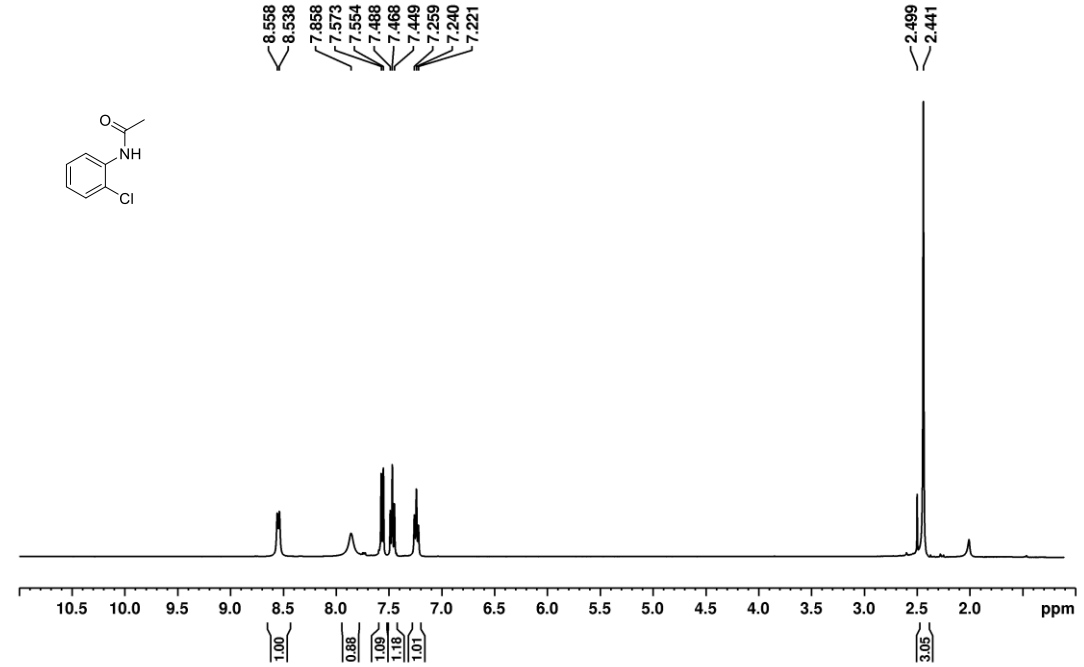

^{1}H spectrum of **3E (Chapter 6)**

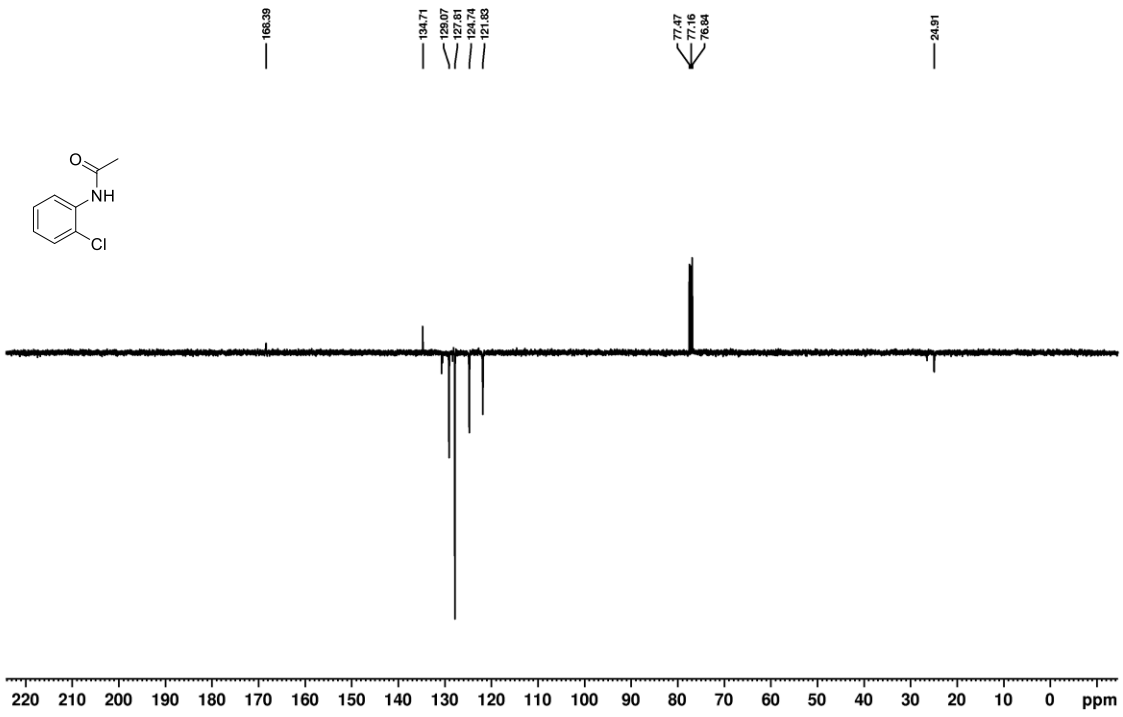

^{13}C spectrum of **3E (Chapter 6)**

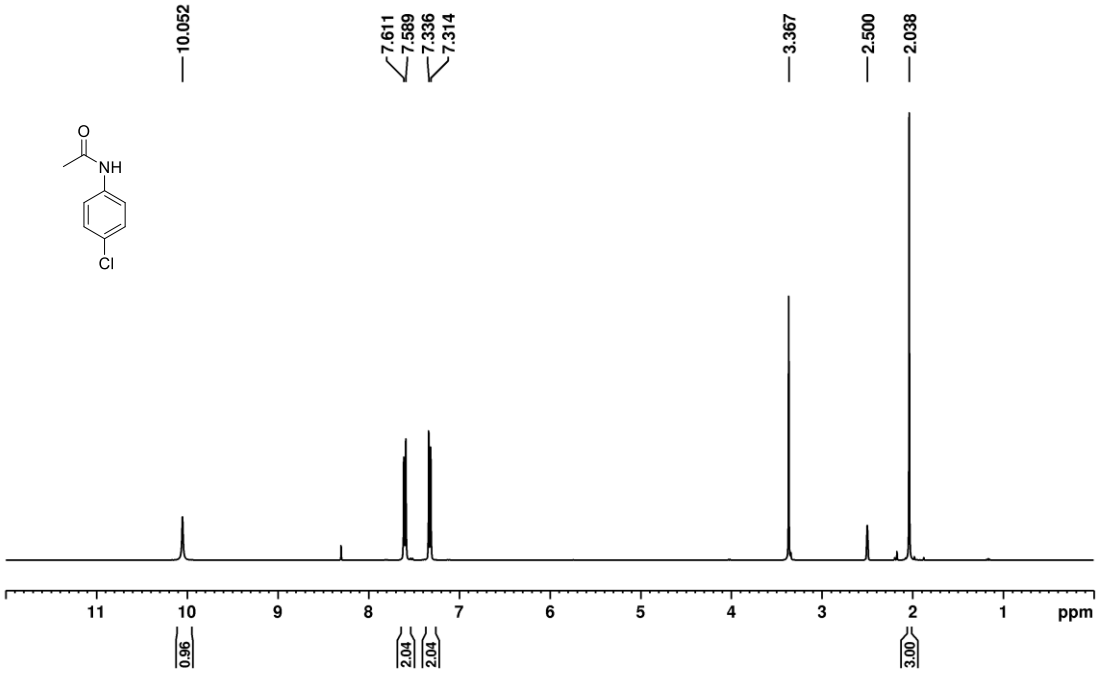

^{1}H spectrum of **3F (Chapter 6)**

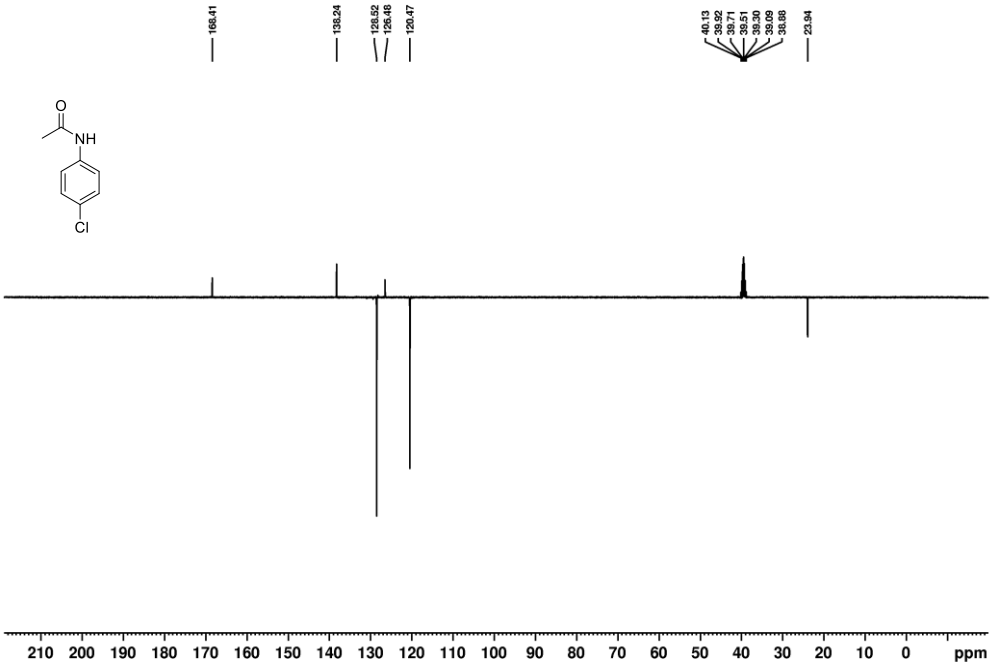

^{13}C spectrum of **3F (Chapter 6)**

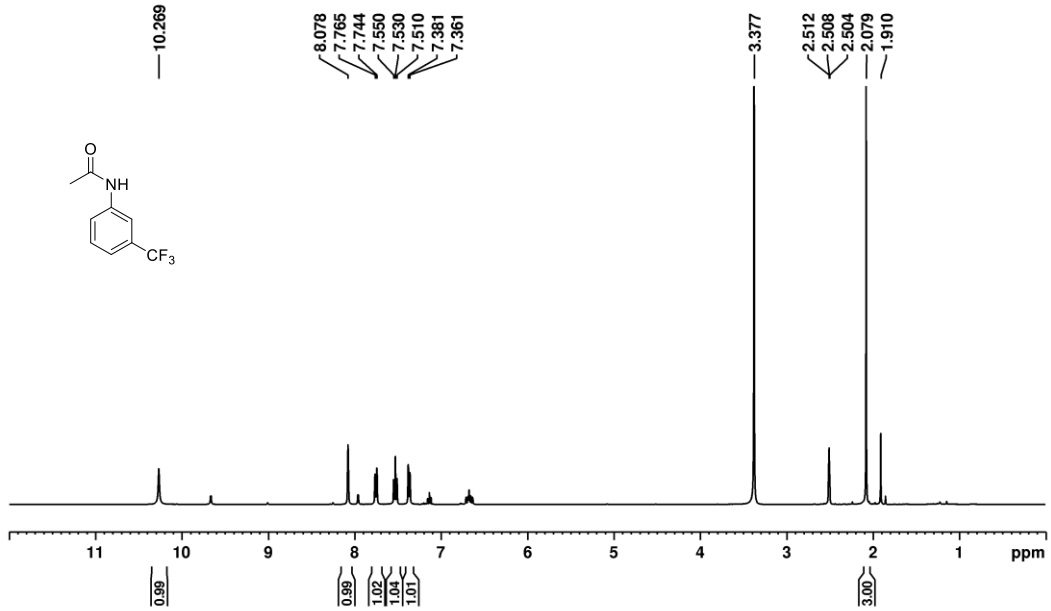

^{1}H spectrum of **3G (Chapter 6)**

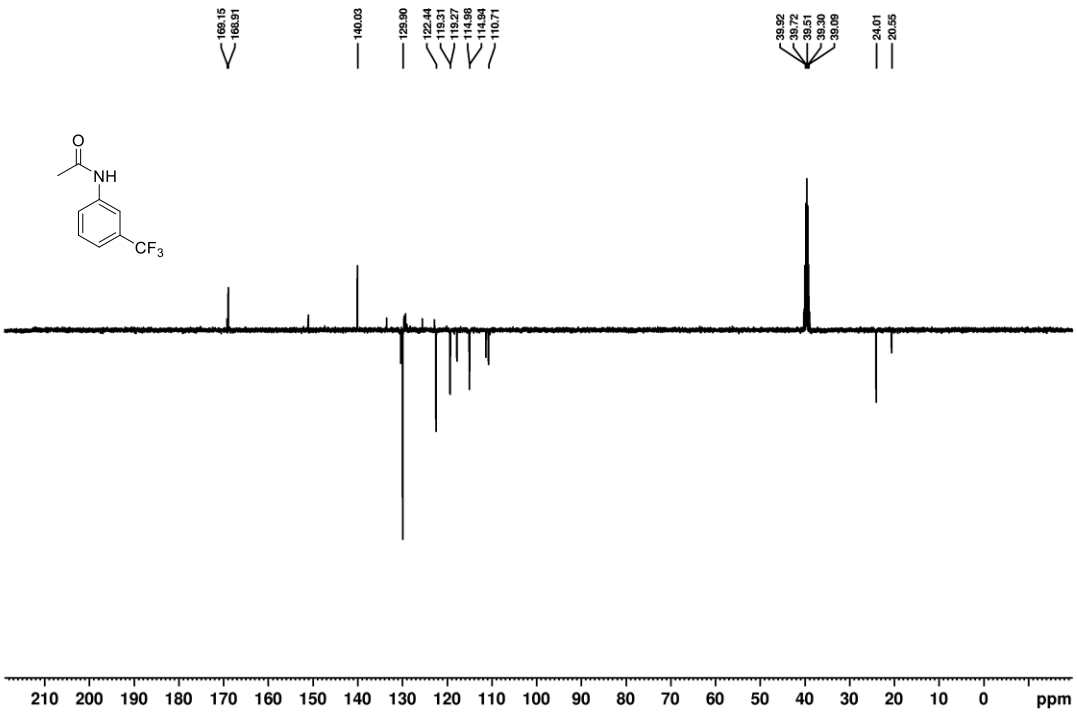

^{13}C spectrum of **3G (Chapter 6)**

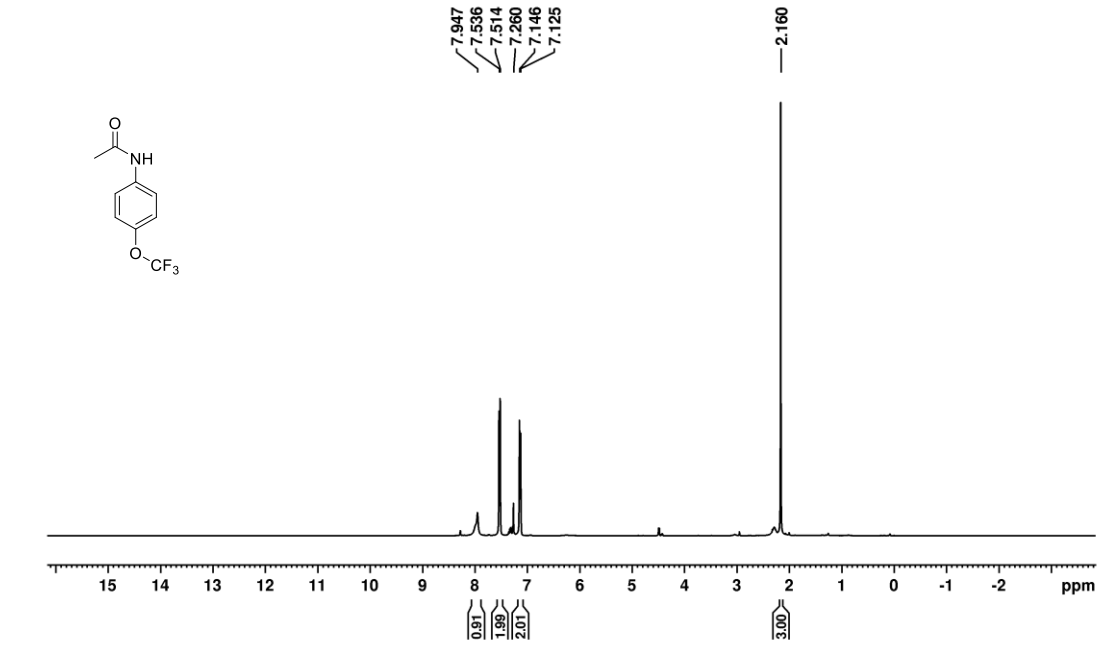

^{1}H spectrum of **3H (Chapter 6)**

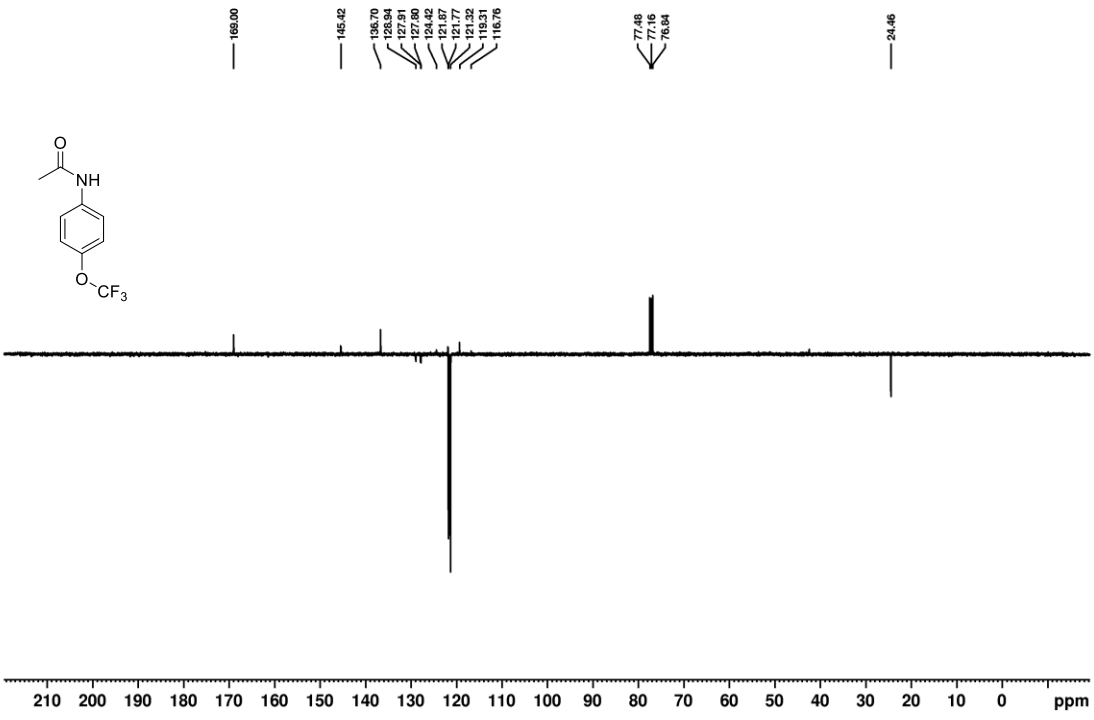

^{13}C spectrum of **3H (Chapter 6)**

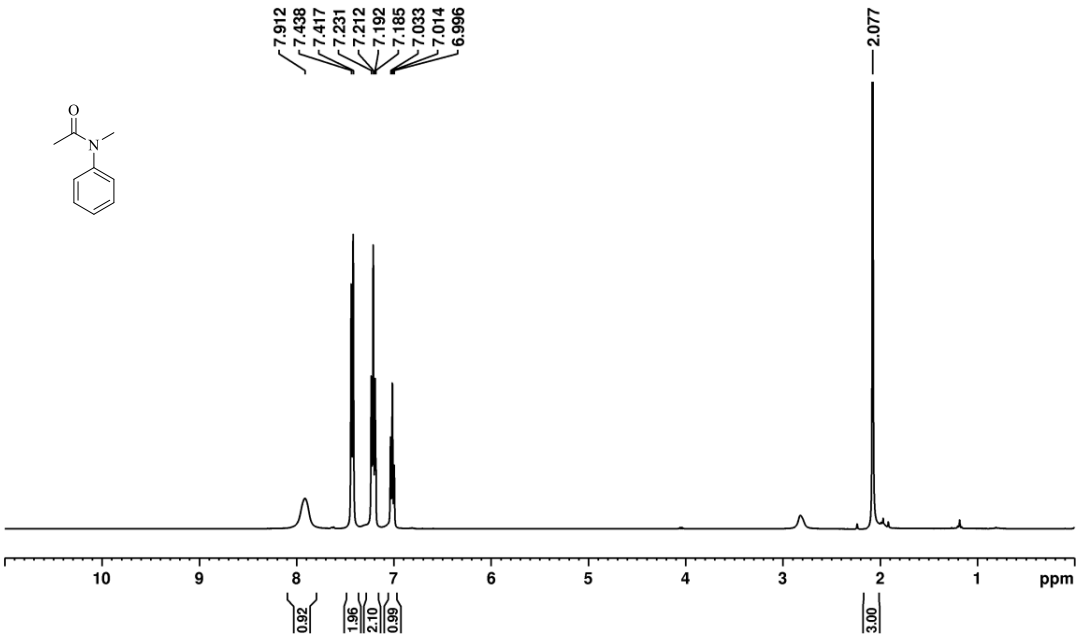

^{1}H spectrum of **3I (Chapter 6)**

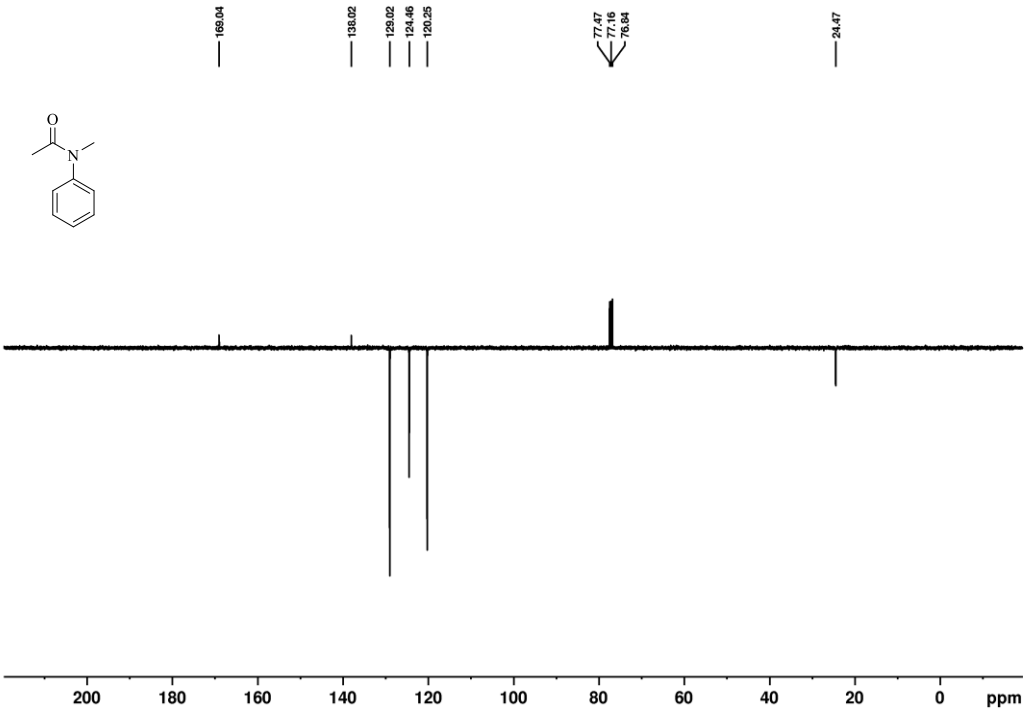

^{13}C spectrum of **3I (Chapter 6)**

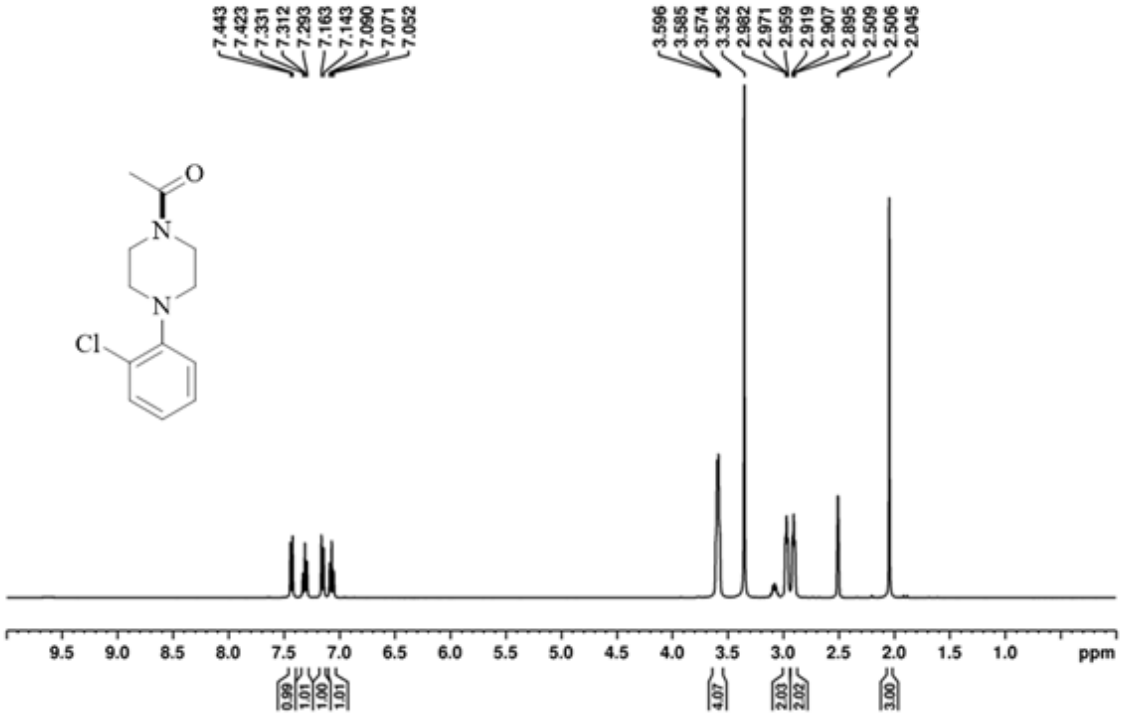

^{1}H spectrum of **3J (Chapter 6)**

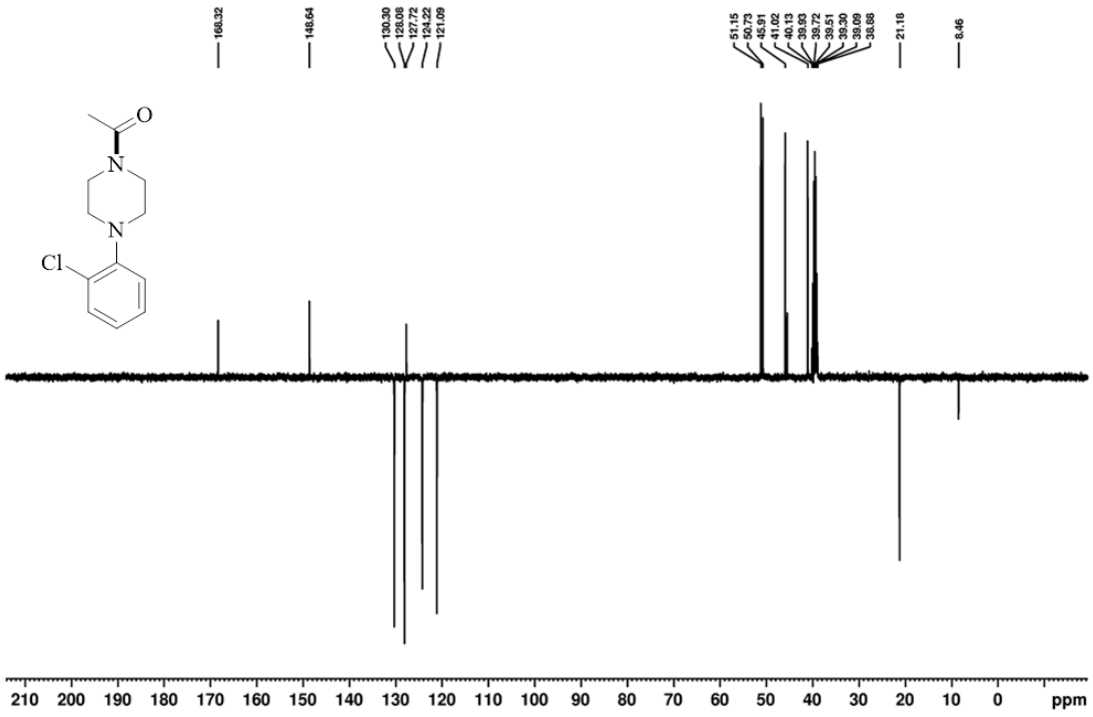

^{13}C spectrum of **3J (Chapter 6)**

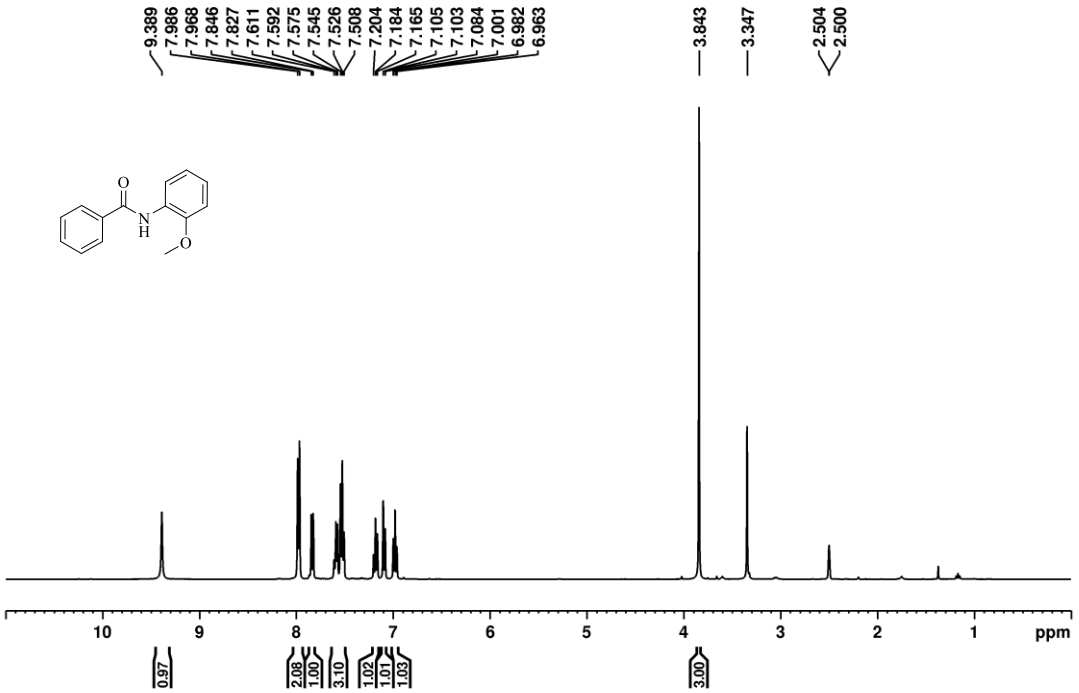

^{1}H spectrum of **3K (Chapter 6)**

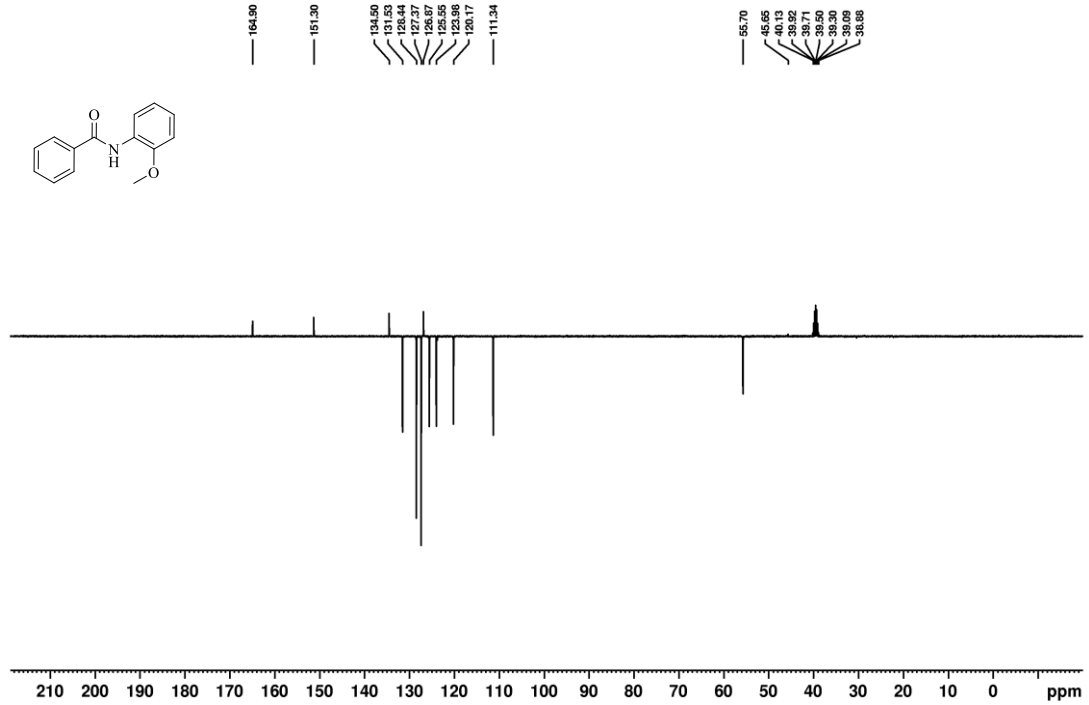

^{13}C spectrum of **3K (Chapter 6)**

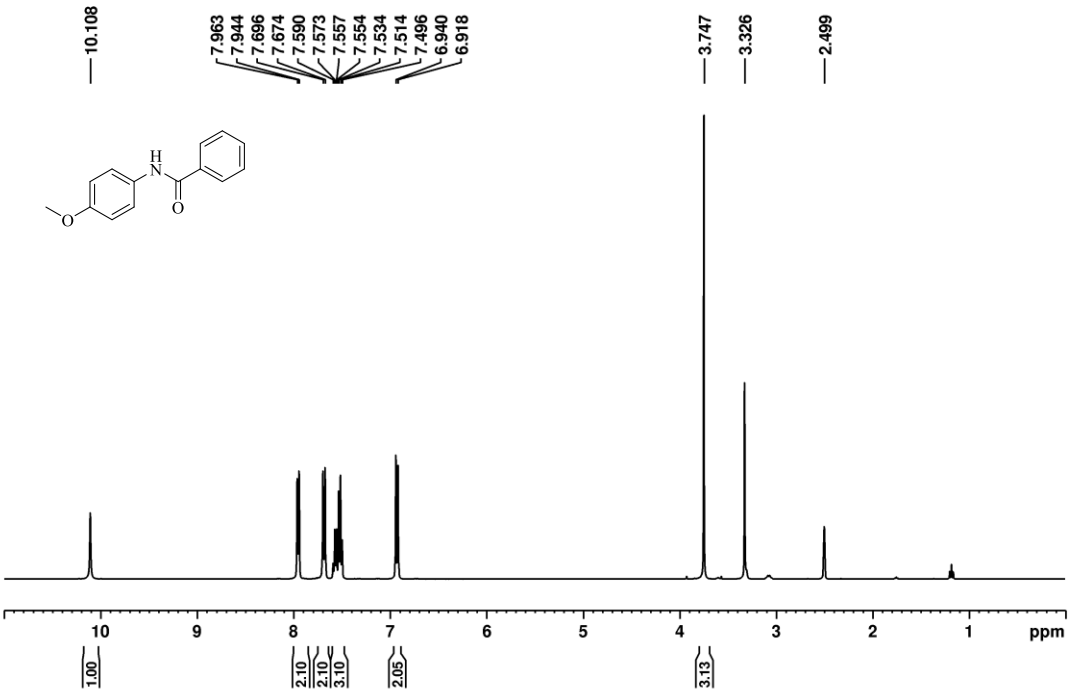

^{1}H spectrum of **3L (Chapter 6)**

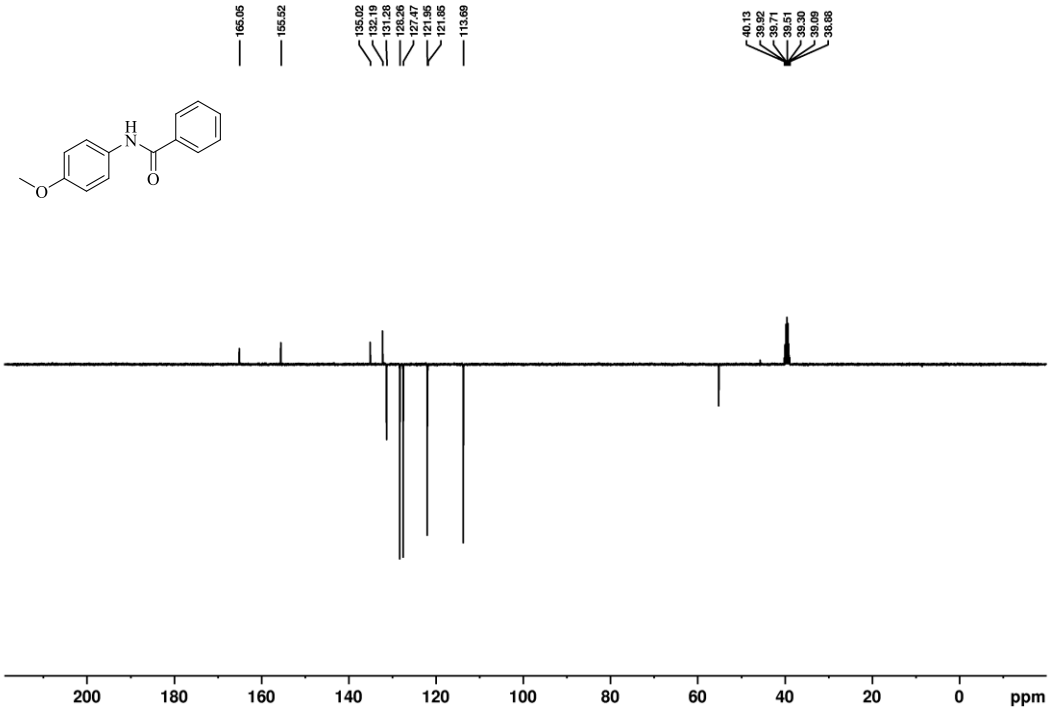

^{13}C spectrum of **3L (Chapter 6)**

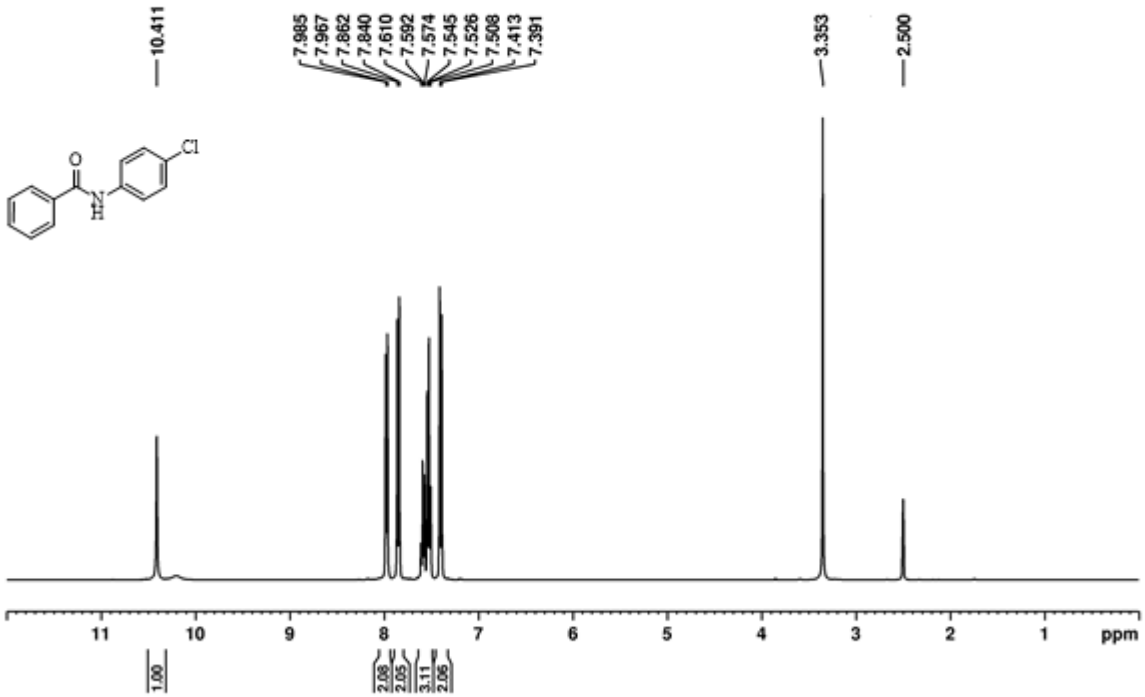

^{1}H spectrum of **3M (Chapter 6)**

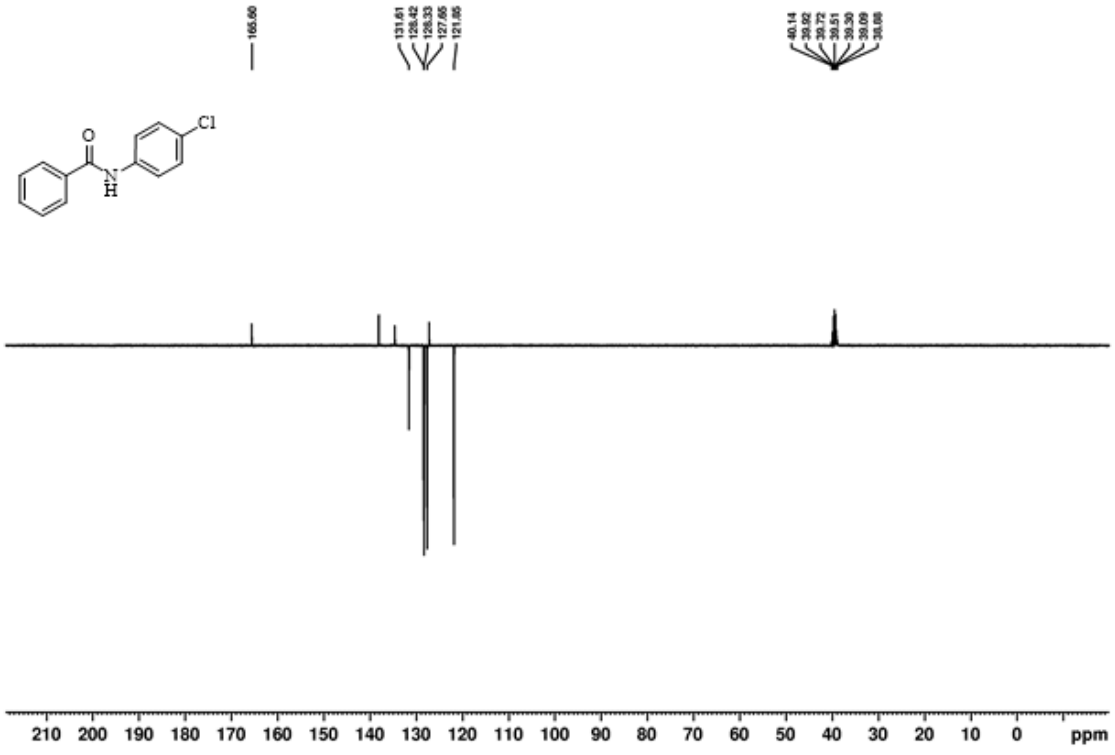

^{13}C spectrum of **3M (Chapter 6)**

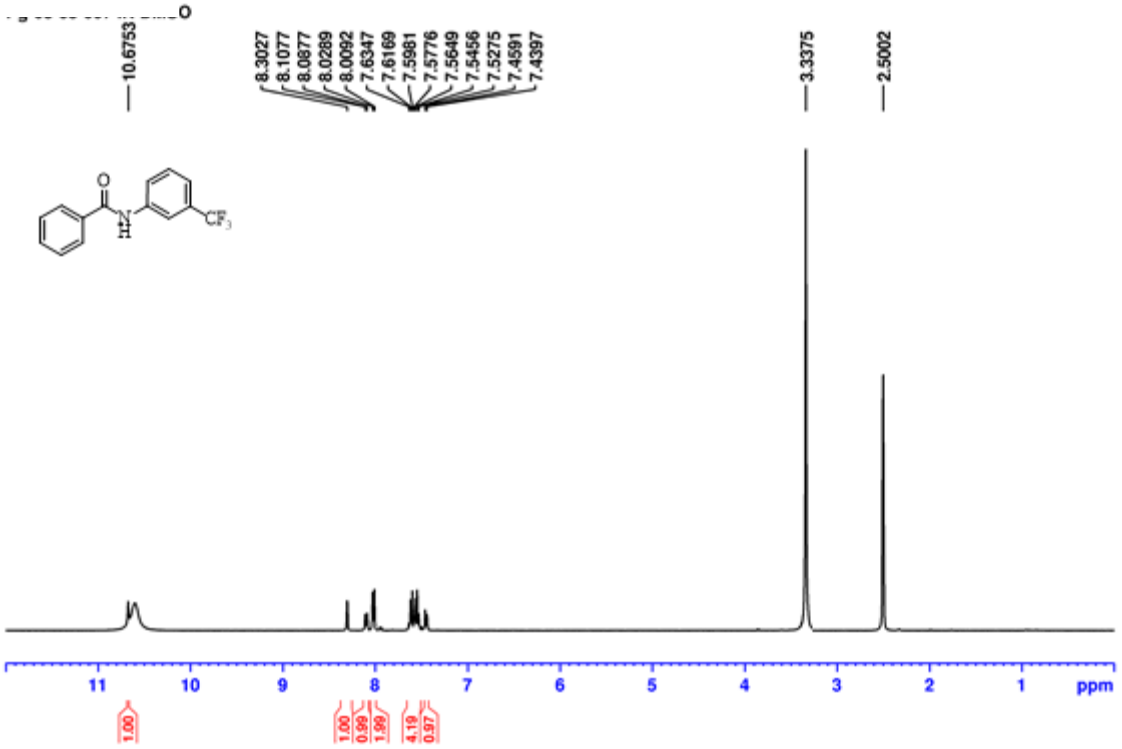

^{1}H spectrum of **3N (Chapter 6)**

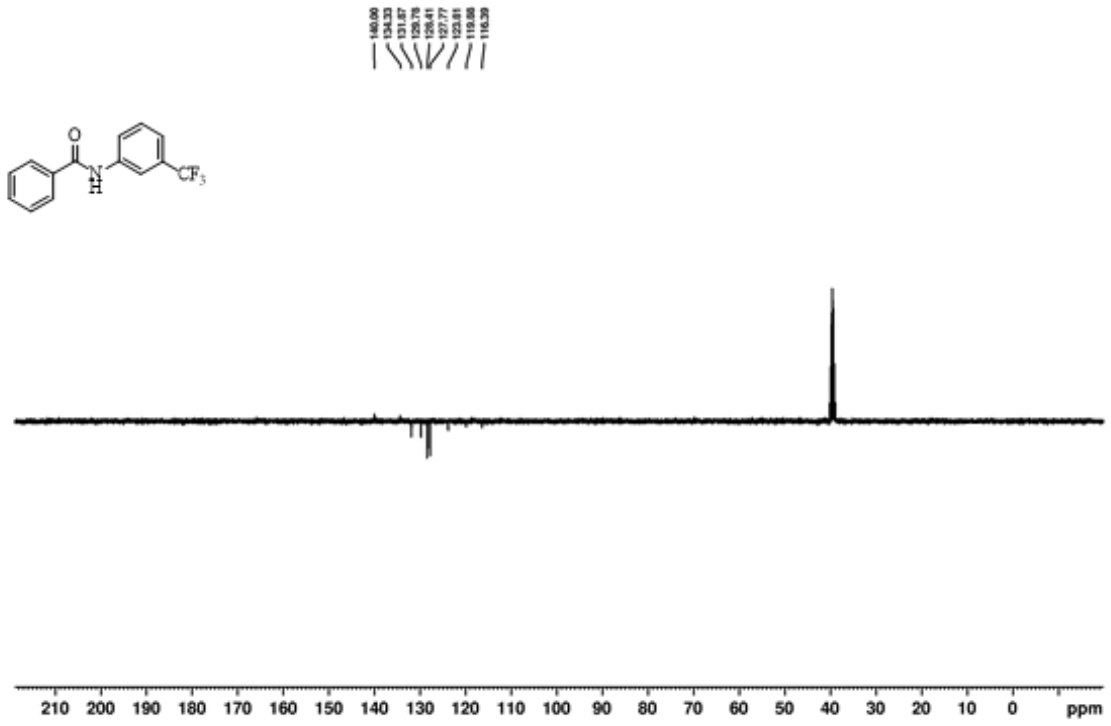

^{13}C spectrum of **3N (Chapter 6)**

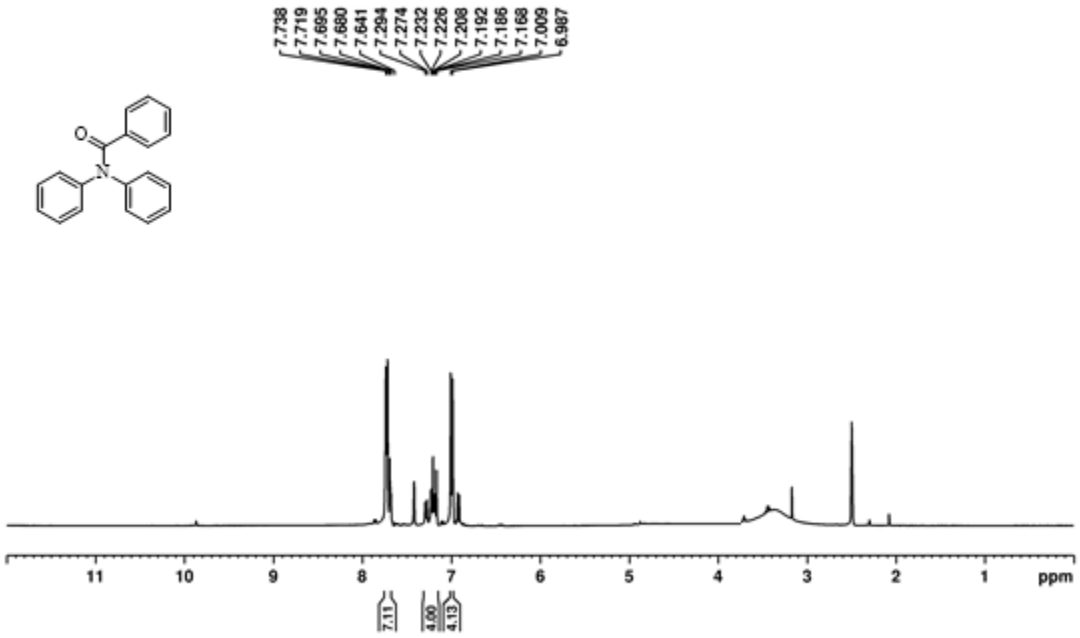

^{1}H spectrum of **3O (Chapter 6)**

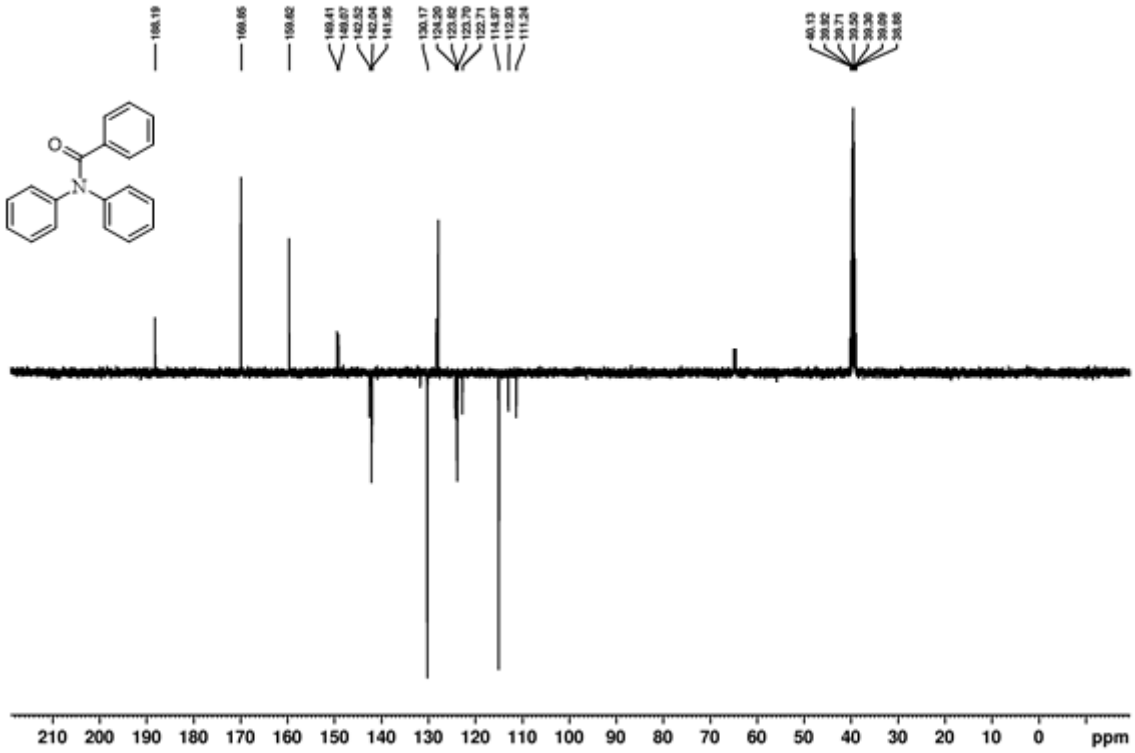

^{13}C spectrum of **3O (Chapter 6)**

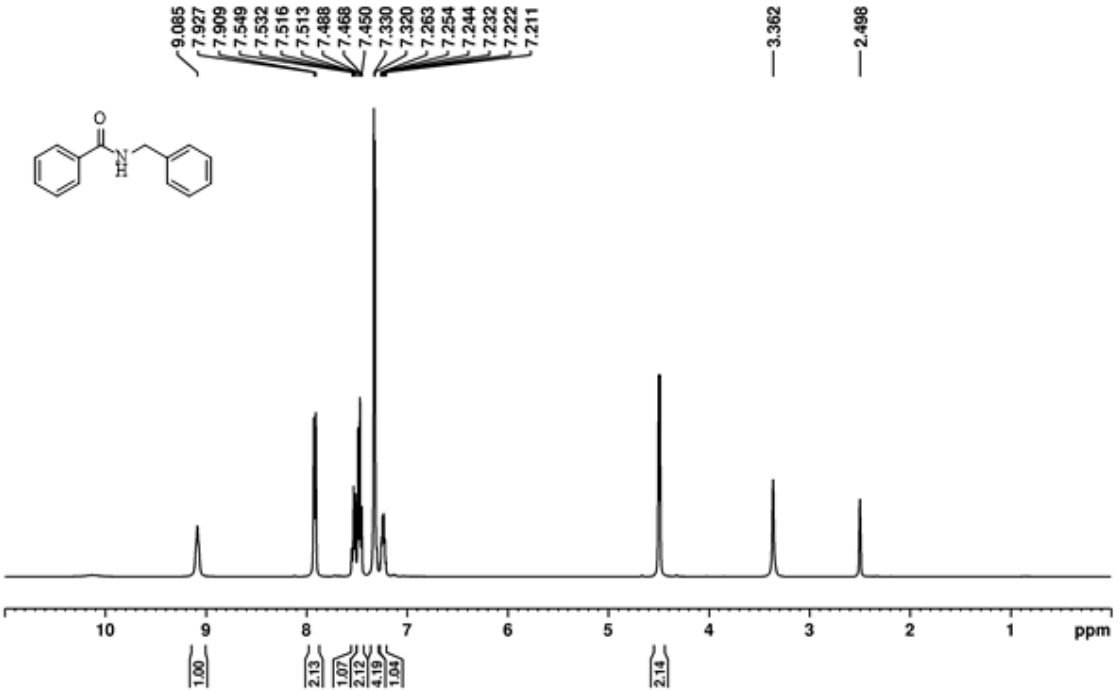

^{1}H spectrum of **3P (Chapter 6)**

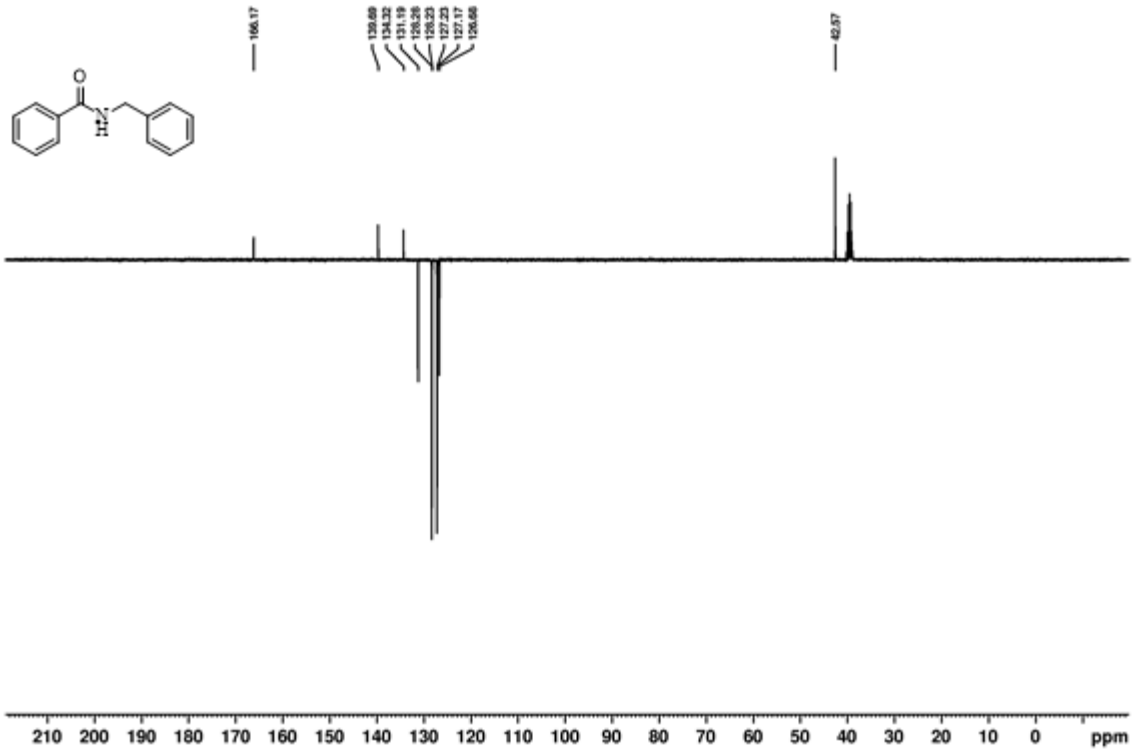

^{13}C spectrum of **3P (Chapter 6)**

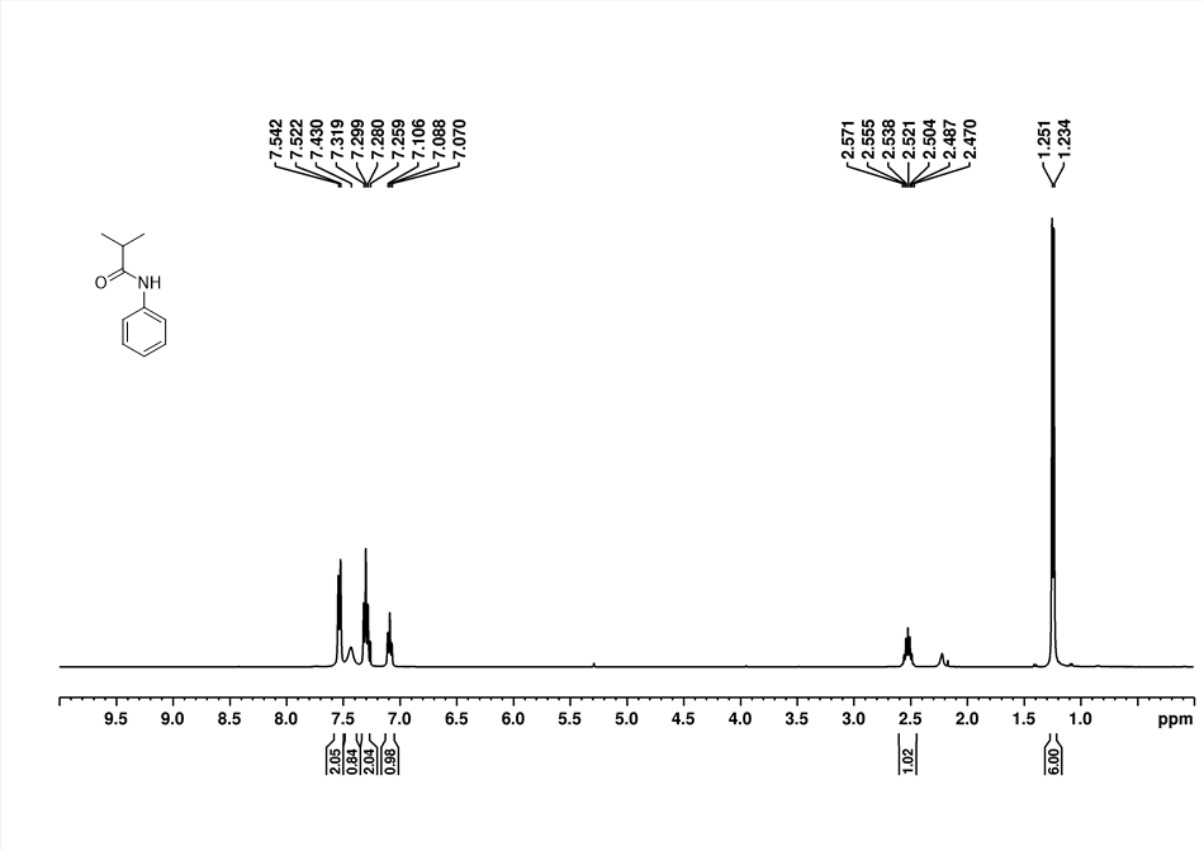

^{1}H spectrum of **3Q (Chapter 6)**

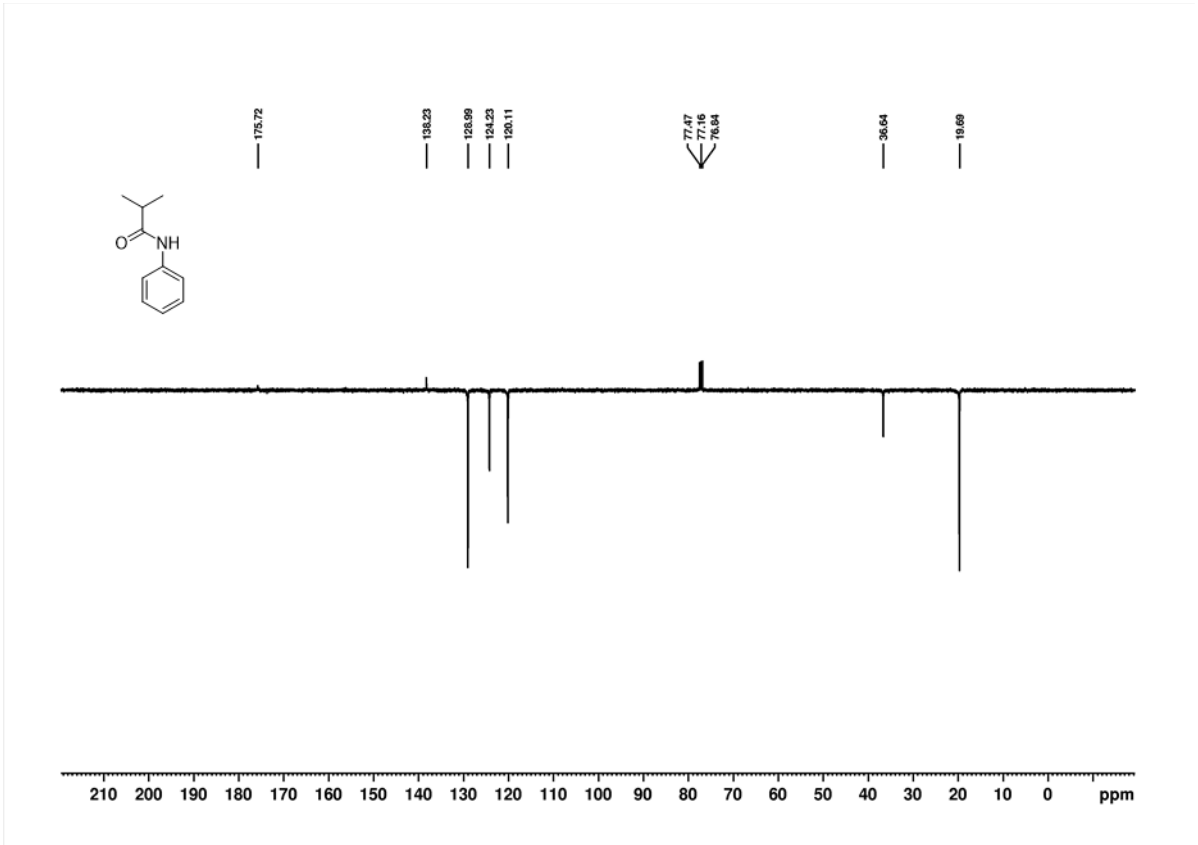

^{13}C spectrum of **3Q (Chapter 6)**

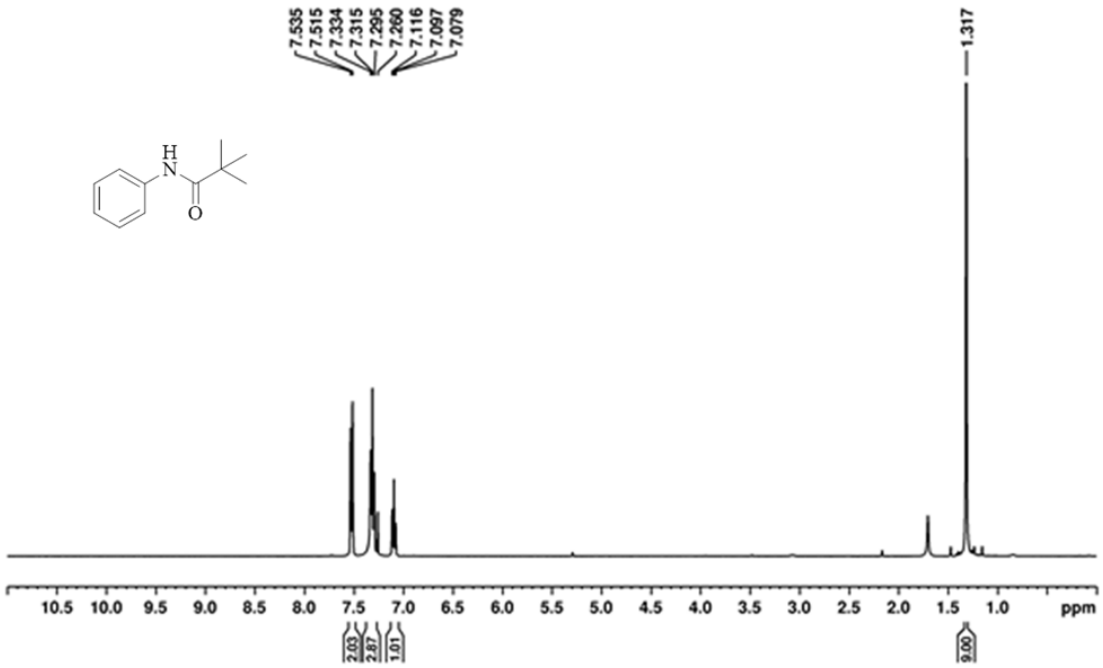

^{1}H spectrum of **3R (Chapter 6)**

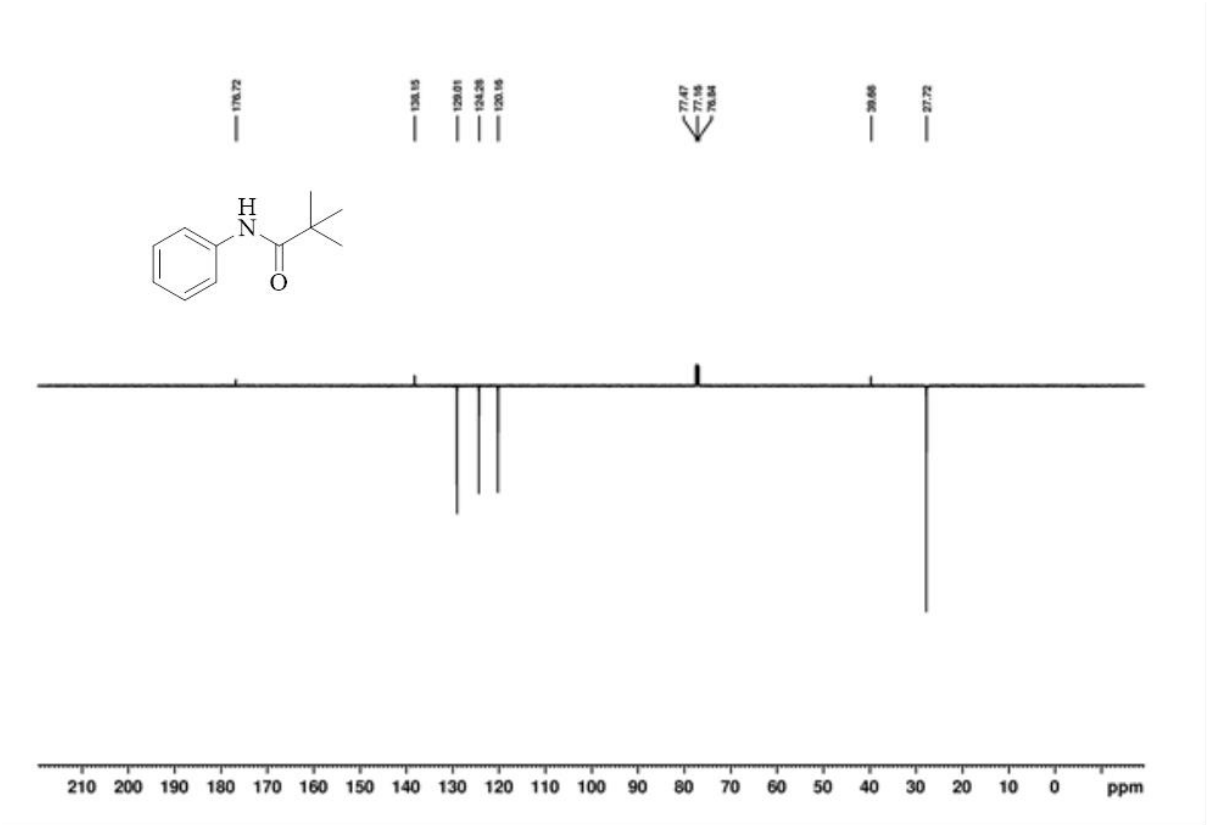

^{13}C spectrum of **3R (Chapter 6)**